

UCSF

UC San Francisco Electronic Theses and Dissertations

Title

Towards new antimalarial drug candidates from the endoperoxide class

Permalink

<https://escholarship.org/uc/item/0zn9q0rt>

Author

Klope, Matthew Thomas

Publication Date

2023

Peer reviewed|Thesis/dissertation

Towards New Antimalarial Drug Candidates from the Endoperoxide Class

by
Matthew Klope

DISSERTATION
Submitted in partial satisfaction of the requirements for degree of
DOCTOR OF PHILOSOPHY

in
Chemistry and Chemical Biology

in the
GRADUATE DIVISION
of the
UNIVERSITY OF CALIFORNIA, SAN FRANCISCO

Approved:

DocuSigned by:
Adam Renslo Adam Renslo
FBDB6299FCD244B... Chair

DocuSigned by:
Philip Rosenthal Philip Rosenthal
DocuSigned by: C4AC...

Jason Gestwicki Jason Gestwicki
4909848DBB404E5...

Committee Members

Copyright 2023

by

Matthew Klope

Acknowledgements

I owe my thanks to countless people. To Adam Renslo, for his mentorship, support, and flexibility through several uniquely challenging and unpredictable years. To Jason Gestwicki and Phil Rosenthal for their service on my thesis committee and their scientific and personal mentorship throughout my graduate study. To all members of the Renslo Lab, past and present, and particularly to Priya Jaishankar, without whom the lab would cease to function, and to Ryan Gonciarz, Jun Chen, and Juan Tapia for their scientific support and personal friendship. To the members of the Rosenthal, Sello, DeRisi, Walter, and Sullivan labs for roles many of them played in my professional and scientific development.

To my parents, Tom and Mary Jane Klope, and the innumerable ways they supported my growth and education.

To my partner of 14 years, Emily Byrne Klope, without whose support, encouragement, and companionship this journey would have never been completed.

To my daughter, Alice Grace Klope, for filling my life with immeasurable joy and purpose, and whom I love more than anything.

Contributions

Chapters 2 and 3 of this thesis are adapted from manuscripts in preparation:

Matthew T Klope, Juan A Tapia Cardona, Jenny Legac, Jun Chen, Ryan L Gonciarz, Julie Kim, Priyanka Jaishankar, Philip J Rosenthal, Adam R Renslo. “Improved trioxolane antimalarials from the carbamate class”.

Matthew T. Klope, Poulami Talukder, Brian R. Blank, Jun Chen, Priyadarshini Jaishankar, Ryan L. Gonciarz, Aswathy Vinod, Vineet Mathur, Juan Tapia, Jennifer Legac, Avani Narayan, Shaun D. Fontaine, Philip J. Rosenthal, Adam R. Renslo. “Novel Antimalarial Ozonide RLA-5764 Demonstrates Superior Drug-Like Parameters With Single Dose Cures *In Vivo* And Excellent Activity Against Artemisinin Resistant Strains.”

Abstract

Towards New Antimalarial Drugs from the Endoperoxide Class

Matthew Klope

Malaria, a disease caused by infection of protozoan parasites from genus *Plasmodium*, claims an estimated 600,000 lives annually, with the majority of these deaths in children. The utility of artemisinin and its derivatives, which constitute the foundation of modern antimalarial care, is complicated by its suboptimal pharmacological parameters and by a concerning rise in genetically driven artemisinin partial resistance phenotypes in areas of high disease burden. Following limited clinical adoption of second generation synthetic trioxolane leads arterolane and artefenomel, small molecules which retain the endoperoxide-driven antiparasitic effect of artemisinin with improved properties and streamlined synthesis, there exists an urgent and undertargeted need for improved antimalarials in this class.

Herein we report the design, synthesis, and *in vitro* and *in vivo* evaluation of a library of novel *trans*-3" substituted 1,2,4-trioxolanes. For carbamate substituted compounds in this class, we find promising antiparasitic efficacy, excellent metabolic stability, and a superior cure rate in a 2-day dosing regimen for lead compound **9d** against the rodent *P. berghei* model of malaria, motivating future advancement of **9d** into a humanized rodent malaria model (Chapter 2). We additionally report the synthesis and evaluation of *trans*-3"-aryl substituted congeners of artefenomel with a focus on carbamate-linked phenols bearing basic amine or other solubilizing functionality (Chapter 3). We find this class to broadly exhibit excellent antiparasitic efficacy and improved solubility and metabolic

stability relevant to the 2nd generation trioxolanes. We advance the lead analog **17**, which completely eliminates K13 C580Y parasites *in vitro* in the ring stage survival assay (RSA) and retains potent efficacy against high-RSA Ugandan clinical isolates. We furthermore report a stereoselective route to the (R,R)- and (S,S)- forms of **17**, observing increased solubility of the separated enantiomeric forms versus the racemate. We extensively profile **17S** as a clinical development candidate and found the compound to exhibit a protein binding and metabolic stability profile we predict should translate to extended drug exposures in human malaria patients.

We additionally explore the *P. falciparum* stress response as driven by PK4-mediated eIF2 α phosphorylation (Chapter 4). We identify dozens of drug-like kinase inhibitors from the GSK PERK kinase set with potent antiparasitic effect. We find these inhibitors phenocopy the antiparasitic effect of bona fide *Pf*PK4 inhibitor GSK-2606414 and plausibly retain the target profile of this comparator. We leverage our medium-throughput *in vitro* *P. falciparum* library screening pipeline to screen the SelleckChem antikinase library, reporting dozens of potent hits against the parasite and suggesting additional points of entry for targeting the *P. falciparum* kinome.

TABLE OF CONTENTS

	Page
Chapter 1: An Introduction to Endoperoxide Antimalarials	1
References	10
Chapter 2: Improved Trioxolane Antimalarials from the Carbamate Class	15
References	30
Chapter 3: Towards a Novel Trioxolane Antimalarial Drug Candidate	33
References	66
Chapter 4: Targeting Translation Repression in <i>P. falciparum</i>	69
References	91
Chapter S2: Supporting Information for Chapter 2	95
Chapter S3: Supporting Information for Chapter 3	231

List of Figures

	Page
Figure 1-1. Structure of artemisinin and its derivatives	3
Figure 1-2. 1,2,4 trioxolane conformational dynamics	5
Figure 1-3. Structures of antimalarial endoperoxides	6
Figure 1-4. Proposed model for K13 resistance	8
Figure 1-5. Conformational dynamics of trans-3" substitutions.....	9
Graphical Abstract	16
Figure 2-1. Stereocontrolled synthesis of (S,S) trioxolane analogues	19
Figure 2-2. Structure and <i>in vitro</i> activity of analogues 8a-8dd and 9a-9dd.....	21
Graphical Abstract	34
Figure 3-1. Stereocontrolled synthesis of 3" <i>meta</i> Artefenomel regioisomers.....	38
Figure 3-2. Synthesis of <i>ortho</i> , <i>meta</i> , and <i>para</i> 3" phenolic carbamates	41
Figure 3-3. Efficacy of selected trioxolanes against <i>P. berghei</i>	47
Figure 3-4. Plasma PK profile of 17 and artefenomel in mouse PO dosing.....	50
Figure 3-5. Iron fragmentation timecourse of 17 and artefenomel.....	51
Figure 3-6. RSA activity of selected trioxolanes against <i>P. falciparum</i>	52
Figure 3-7. Enantioselective synthesis of 17S	53
Figure 3-8. Efficacy of 17S and 17R against <i>P. berghei</i>	56
Figure 3-9. Plasma PK profile of 17 in mouse PO and IV dosing	59

Graphical Abstract	70
Figure 4-1. Artemisinin and the Synthetic Trioxolanes.....	72
Figure 4-2. Stress Response and Recrudescence in <i>P. falciparum</i>	73
Figure 4-3. Results of primary screen of GSK library against <i>P. falciparum</i>	76
Figure 4-4. Phenotypic effect of GSK hit treatment on parasite culture	76
Figure 4-5. Biochemical activity of PK4 and PERK constructs	77
Figure 4-6. DSF curve for selected hit dye	78
Figure 4-7. Attempts at confirming on-target antikinase activity	79
Figure 4-8. Compound GI ₅₀ over time of continuous exposure.....	80
Figure 4-9. Structural motifs for active and inactive library compounds	81
Figure 4-10. Selleckchem Library activity versus cultured <i>P. falciparum</i>	82
Figure 4-11. IC ₅₀ curves and structures for Selleckchem top hits	83
Figure S3-1. Stereocontrolled synthesis of 3" <i>ortho</i> Artefenomel regioisomers	232
Figure S3-2. Stereocontrolled synthesis of 3" <i>para</i> Artefenomel regioisomers	232
Figure S3-3. Artefenomel regioisomers versus artefenomel in <i>P. berghei</i>	233
Figure S3-4A. Chiral HPLC trace of 17R	233
Figure S3-4B. Chiral HPLC trace of 17S	234
Figure S3-4C. Chiral HPLC trace of 17R and 17S coinjection.....	234
Figure S3-4D. Chiral HPLC trace of 17 racemic mix	235

List of Tables

	Page
Table 2-1. Comparative <i>in vitro</i> and ADME data for selected trioxolanes	20
Table 2-2. <i>In Vitro</i> ADME data for selected analogues and controls	21
Table 2-3. Oral efficacy of selected analogues in <i>P. berghei</i> model	24
Table 3-1. Activity, metabolic stability, and solubility of 3'' artefenomel congeners.....	40
Table 3-2. Pharmacological parameters of <i>ortho</i> , <i>meta</i> , and <i>para</i> TRX carbamates.....	42
Table 3-3. Activity, metabolic stability, and solubility of <i>meta</i> analogue series	44
Table 3-4. Activity, metabolic stability, and solubility of <i>para</i> analogue series	45
Table 3-5. Divergent mouse and human liver microsome stability of 17 and OZ439	48
Table 3-6. Selected PK data from Figure 3-4.....	50
Table 3-7. Activity, metabolic stability, and solubility of 17 , 17R , and 17S	55
Table 3-8. <i>In vitro</i> efficacy of 17R and 17S against K13 mutant parasites	56
Table 3-9. ADME properties of 17 and 17S	58
Table S3-1. Aqueous solubility of 17 by column condition	236

List of Abbreviations

6414: GSK-2606414

ACT: artemisinin combination therapy

ADME: absorption, distribution, metabolism, and excretion

d.r: diastereomeric ratio

DCM: dichloromethane

DHA: dihydroartemisinin

DSF: differential scanning fluorimetry

eIF2 α : eukaryotic initiation factor 2 α

FAS: ferrous ammonium sulfate

FaSSIF: fasting state simulated intestinal fluid

FeSSIF: fed state simulated intestinal fluid

GI₅₀: concentration required to maintain growth at 50% of control

GSK: GlaxoSmithKline

HLM: human liver microsome

HPLC: high-performance liquid chromatography

IC₅₀: half maximal inhibitory concentration

IVIEWGA: in vitro evolution and whole genome analysis

K13: Kelch13

MLM: mouse liver microsome

MMV: medicines for malaria venture

NMR: nuclear magnetic resonance

OH: ohio

OZ277: arterolane

OZ439: artefenomel

PBS: phosphate buffered saline

PD₁₀₀: minimum observed fully curative oral dose

PK: pharmacokinetic
PNP: 4-nitrophenol
PO: oral dosing
RLA: renslo lab analog
RSA: ring stage survival assay
SAR: structure activity relationship
THF: tetrahydrofuran
TRX-C: carbamate substituted *trans*-3" 1,2,4-trioxolanes
TRX-P: aryl substituted *trans*-3" 1,2,4-trioxolanes
UPLC: ultra-performance liquid chromatography
UPLCMS: ultra-performance liquid chromatography-mass spectrometry
UPR: unfolded protein response
WHO: World Health Organization

Chapter 1:
An Introduction to Endoperoxide Antimalarials

MAIN

Malaria, a disease caused by infection with protozoan parasites of the genus *Plasmodium*, remains a crucial area of global concern. The disease claims an estimated 600,000 lives annually, most of them children, and persists despite the dedicated work of countless organizations and individuals pursuing a malaria-free world. Concerningly, significant gains seen in the early years of the malaria eradication campaign have recently slowed or stalled in areas of heavy disease burden, and progress in malaria treatment and prevention is threatened by declines in effectiveness of primary malaria-fighting tools.¹ Of particular concern is the rise in artemisinin partial resistance phenotypes in high-burden, high-transmission areas. Mutations in the propeller domain of the *Kelch13* (K13) protein, associated with delayed parasite clearance on artemisinin exposure and generally observed in low transmission areas in southeast Asia, have been recently detected in patient samples in Uganda^{2 3 4}, Rwanda⁵, and Eritrea⁶, a worrying development given the scope of malaria burden in east Africa and the reliance on artemisinin combination therapies (ACTs) as frontline antimalarials. The prevalence of these partial resistance mutations is likely to increase as treatment coverage increases and parasite transmission decreases, indicating an urgent need for improved antimalarials.⁷

Artemisinin is a sesquiterpene endoperoxide lactone isolated from the *Artemisia annua* plant (**Figure 1-1**). Its rapid parasitocidal action against multiple *Plasmodium* life cycle stages propelled the compound to the forefront of antimalarial care following the isolation of artemisinin by Tu Youyou 1972, buoying a struggling malaria eradication campaign that was losing ground due to growing parasite resistance to quinoline antimalarials.⁸

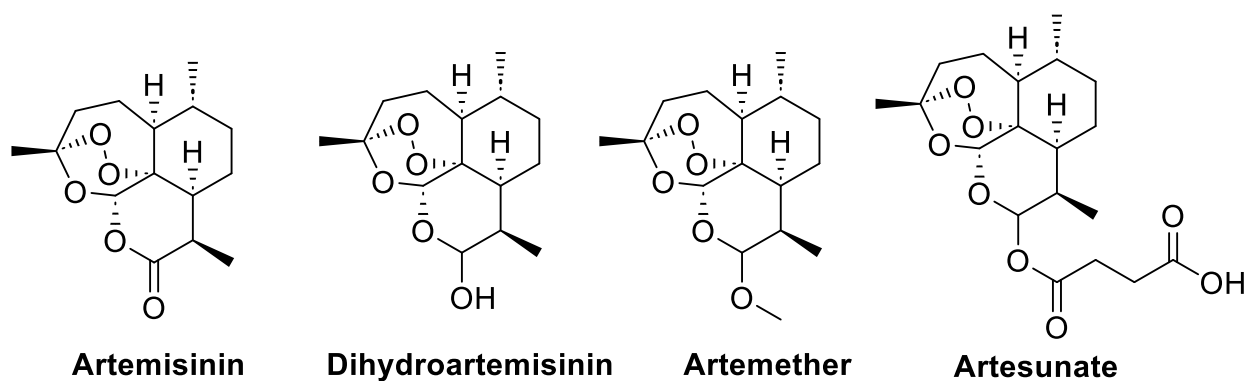


Figure 1-1. Structures of artemisinin and its derivatives.

Despite its immediate clinical advantages, it was quickly discovered that Artemisinin monotherapy results in high rates of parasite recrudescence, wherein still-susceptible parasites re-emerge following a days-long period of clinical latency.⁹ This phenomenon is attributable to Artemisinin's relatively short half-life (~4 hours), which allows small subpopulations of latent parasites to outlast treatment exposure. To circumvent this problem, Artemisinin is administered in combination with a longer-lived partner drug in clinical use.¹⁰ Artemisinin's utility is further limited by its poor bioavailability and solubility.¹¹ The challenges inherent in Artemisinin total synthesis combined with the need for affordable drug product limit the prospects for improving these properties through medicinal chemistry. Semisynthetic derivatives of Artemisinin have focused largely on modifications of the lactone ketone group (**Figure 1-1**). While these semisynthetic derivatives have achieved significant clinical utility, they represent only modest improvements to the exposure profile of artemisinin, a limitation which has motivated substantial medicinal chemistry efforts on non-artemisinin endoperoxide antimalarials.^{12 13}

Of principal importance in improving upon the limitations of the Artemisinin scaffold was determining its mechanism of action. Study toward this end indicated that artemisinin antiparasitic activity was endoperoxide dependent, inhibited by parasite iron chelation, and that accumulation of a fluorescent artemisinin probe in the parasite digestive vacuole was reduced by pre-treatment with unlabeled artemisinin.^{14 15} These and further insights led to the current understanding of artemisinin pharmacology, wherein heme catabolism in the parasite digestive vacuole leads to homolytic cleavage of the endoperoxide bridge to generate oxygen and carbon-centered free radicals that cause cytotoxic oxidative stress, likely including peroxidation of unsaturated lipids, and alkylation of protein targets in the parasite.^{16 17} The degree to which this labelling is stochastic, as well as the degree to which individual activated artemisinin radical species and individual parasite factors are most essential for driving toxicity, remains an area of active research.^{18 19 20} Regardless, such a model suggested the possibility of identifying wholly synthetic antimalarial endoperoxides not based on artemisinin structure.

Elegant work on non-artemisinin endoperoxide scaffolds by the Vennerstrom lab, most notably focused on the 1,2,4-trioxolanes, demonstrated that little structural complexity is required to achieve potent antimalarial effect with retained selectivity for heme iron activation, providing a means towards facile design and synthesis of myriad novel synthetic antimalarial endoperoxides.^{21 22} Of particular interest in these early studies were observations regarding the conformational control of endoperoxide reactivity. In dispiro-1,2,4-trioxolane systems, in which the trioxolane is flanked by spiroadamantlyl and/or spirocyclohexyl groups, the iron reactivity of the endoperoxide is influenced by conformational dynamics of the flanking moieties (**Figure 1-2A**)²³. Whereas the

conformationally locked adamantane moiety shields the endoperoxide function via 1,3-diaxial interaction with neighboring C–H bonds, chair–chair interconversion of the cyclohexane ring produces two major conformers, one (Conformer 1) where the endoperoxide is exposed for reaction with iron, and a second conformer (Conformer 2) where 1,3-diaxial interactions analogous to those in adamantane occluded the peroxide from reaction with iron. Largely empirical studies of diverse 1,2,4-trioxolane analogs revealed the utility of the dispiro adamantyl-trioxolane-cyclohexyl system in achieving a “just right” balance of iron reactivity for antiparasitic effect *in vitro*.²³

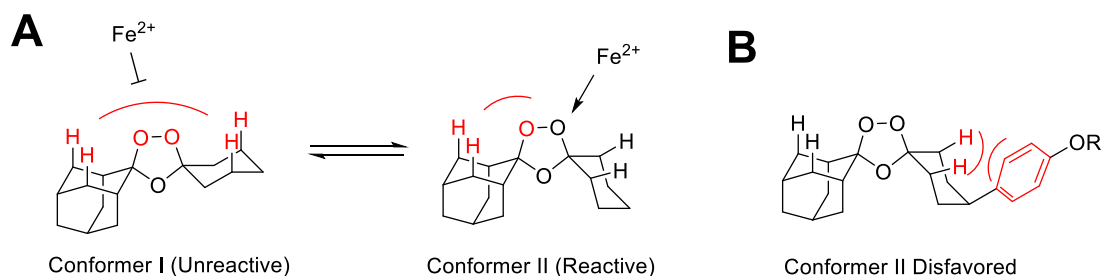


Figure 1-2. Conformational effect of cis-4” cyclohexyl substitutions on iron reactivity A) The cyclohexane ring can shield (conformer I) or expose (conformer II) the endoperoxide function for reaction with iron. B) Bulky cis-4’ substitution disfavors the iron-reactive conformer.

The structure-activity relationship of the dispiro 1,2,4 trioxolane antimalarials is thus understood as follows: the central endoperoxide functions as an iron-activable warhead, with flanking adamantyl and cyclohexyl groups providing for regioselective iron reactivity, leading to the formation of carbon-centered radicals that confer antiparasitic effects at least in part through parasite protein alkylation. Fine tuning of iron reactivity kinetics and the improvement of “drug-like” properties (bioavailability, solubility, metabolic stability) are further achieved by modification of side-chains off the cyclohexane ring, focused

historically on *cis*-4' substitution.²⁴ Thus, *cis*-4' substitution introduces severe 1,3-diaxial clashes with the neighboring axial C–H bonds in the iron-reactive conformer, shifting the conformational equilibrium toward the unreactive conformer and overall stabilizing the endoperoxide toward reaction (**Figure 1-2B**).²⁵ This fine tuning of iron reactivity and drug-like properties ultimately produced the two clinical candidates from the class, Arterolane (OZ277)²⁴ and Artefenomel (OZ439)²⁶ (**Figure 1-3**). These new synthetic antimalarials retained potent and selective antiparasitic effects *in vitro* and *in vivo*, but with improved exposure profiles in humans, as compared to the artemisinins.

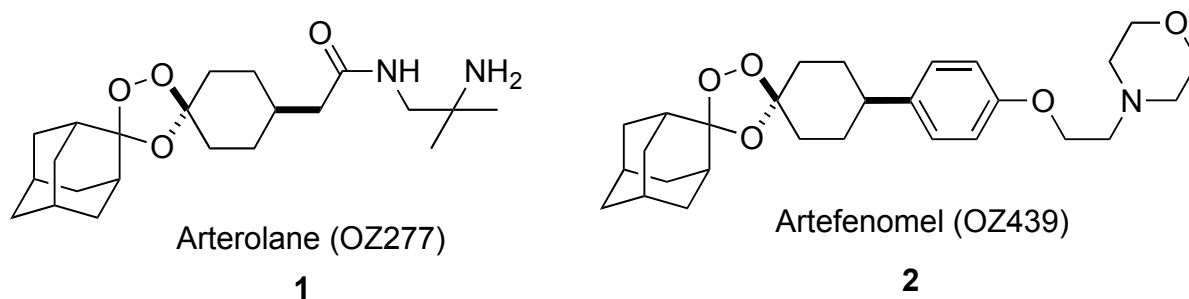


Figure 1-3. Structures of antimalarial endoperoxides.

Despite these advantages, issues encountered in clinical deployment ultimately limited their utility. Arterolane proved to be poorly stable in patients with active *Plasmodium* infection ($t_{1/2} \sim 3$ h) and subject to rapid clearance, requiring multi-day dosing paradigms and significantly restricting its clinical adoption.^{27 28} While Artefenomel demonstrated better exposure in malaria patients, difficulties in formulating the insoluble molecule with partner drugs for oral administration, and a failure to meet stringent clinical exposure benchmarks, ultimately resulted in the termination of its clinical evaluation.²⁹

The promise of synthetic endoperoxides as next-generational antimalarials remains despite the challenges noted above. Of particular interest are the effects of non-artemisinin endoperoxides on parasites with the artemisinin partial resistance phenotype. Delayed parasite clearance in the presence of artemisinin is generally associated with mutations in the propellor domain of the *Kelch13* protein. The resistance mechanism of K13 mutation is nonstandard, consistent with an understanding of artemisinin pharmacology wherein parasite toxicity is not mediated by action on a single target. The K13 partial resistance phenotype is restricted largely to ring stage parasites, is not well observed in a standard IC₅₀ assay, and carries a fitness cost relative to wild type parasites.³⁰ While the specific mechanism of resistance is an area of ongoing study, the role of *K13* in ring stage heme endocytosis^{31 32} suggests that resistance mutations may, counterintuitively, be reducing parasite hemoglobin uptake and thus limiting the pool of activating iron for artemisinin activity. Corroborating this model is the destabilizing effect of *K13* mutations and associated reduction of protein abundance levels in mutant parasites^{33 34} and the phenocopied effect of artemisinin partial resistance in digestion-deficient parasites^{35 36}. Additionally, overexpression of mutant K13 protein re-sensitizes parasites to artemisinin treatment, rather than increasing resistance.³² Thus it seems likely that destabilizing K13 mutations result in lowered rates of hemoglobin catabolism to generate a smaller pool of activating ferrous iron, reducing the activation of an endoperoxide chemotherapeutic and allowing mutant parasites to outlast treatment exposure^{37 38} (**Figure 1-4**).

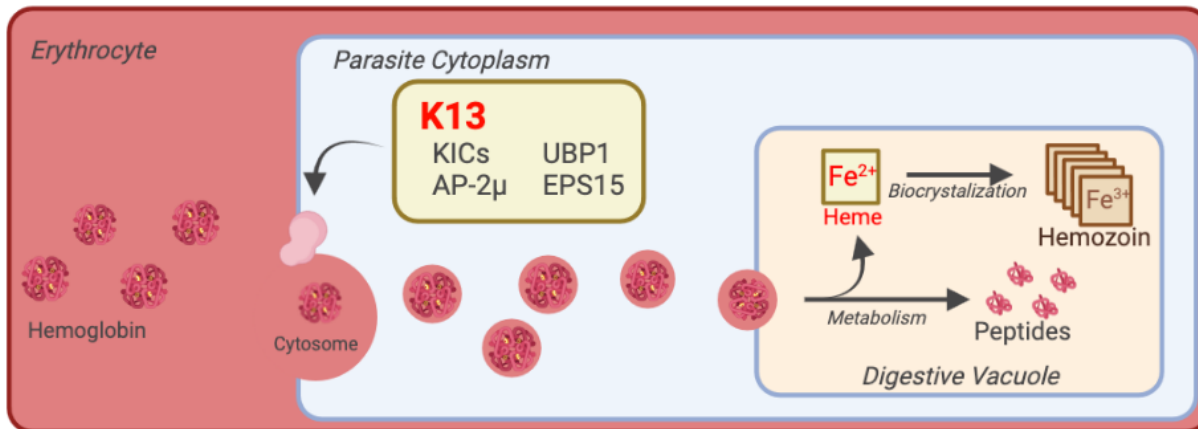


Figure 1-4. K13 likely functions in cytosome assembly and hemoglobin uptake. Destabilizing K13 mutations reduce the pool of ferrous iron heme for endoperoxide activation.

Implicit in this unusual, ring-specific mechanism of resistance is that longer-lasting endoperoxide antimalarials may overcome artemisinin partial resistance by extending the period of drug exposure to outlast the “delayed” ring stage associated with K13 mutant parasites. Indeed, it has been shown that longer-lived artefenomel significantly outperforms DHA and artemolane in the ring stage survival assay (RSA), the gold standard *in vitro* model of the K13-mediated artemisinin partial resistance phenotype.³⁰ While this effect is itself incomplete, it corroborates the claim that improved ozonides can have increased efficacy against *K13* mutant parasites and motivates further development of novel candidates in this class.

With this goal in mind, our laboratory has pioneered the synthesis and *in vivo* investigation of *trans*-3' substituted ozonide chemotypes, premised on the expectation that this substitution pattern should confer conformational effects on trioxolane reactivity analogous to canonical *cis*-4' substitution (**Figure 1-5**)²⁵. We additionally hypothesized

that the strength of the 1,3-diaxial clashes, as determined by the bulk and chemical nature of the *trans*-3' side chain, should enable conformational control over a wider range of endoperoxide reactivity. Finally, we hypothesized that the desymmetrized scaffolds produced by *trans*-3' substitution would have reduced packing energies in the solid state and might therefore exhibit improved aqueous solubilities and dissolution rates as compared to symmetrical *cis*-4' congeners.

This effort began with a systematic study of *trans*-3' analogs bearing amide or carbamate side chains inspired by that in arterolane. In relatively short order, we identified *trans*-3' analogs exhibiting improved metabolic stability and in vivo efficacy in the *P. berghei* model of malaria, including single-exposure cures at higher doses.^{39 40} Most recently, we described a four-step synthesis and extensive in vivo evaluation of an Artefenomel *trans*-3' regioisomer in the *P. berghei* model. While this specific compound exhibited in vivo efficacy that was inferior to Artefenomel, its superior solubility and metabolic stability highlights the promise of the *trans*-3'-aryl chemotype to produce differentiated drug candidates, contingent on a more exhaustive survey of structure-efficacy relationships for this chemotype.⁴¹

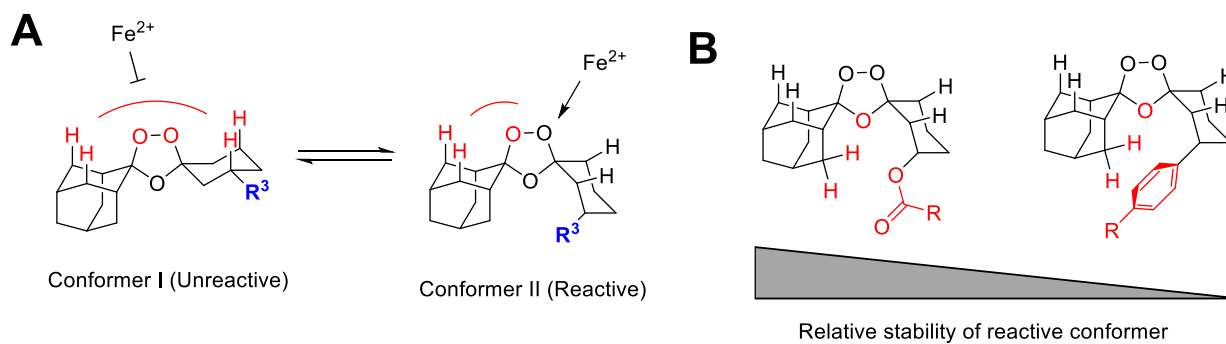


Figure 1-5. Conformational effect of *trans*-3' cyclohexyl substitutions on iron reactivity

REFERENCES

1. World Health Organization. *World malaria report 2022*. December 8, 2022
2. Tumwebaze, P. K. *et al.* Decreased susceptibility of *Plasmodium falciparum* to both dihydroartemisinin and lumefantrine in northern Uganda. *Nat. Commun.* **13**, 6353 (2022).
3. Conrad, M. D. *et al.* Evolution of Partial Resistance to Artemisinins in Malaria Parasites in Uganda. *N. Engl. J. Med.* **389**, 722–732 (2023).
4. Balikagala, B. *et al.* Evidence of Artemisinin-Resistant Malaria in Africa. *N. Engl. J. Med.* **385**, 1163–1171 (2021).
5. van Loon, W. *et al.* In Vitro Confirmation of Artemisinin Resistance in *Plasmodium falciparum* from Patient Isolates, Southern Rwanda, 2019. *Emerg. Infect. Dis.* **28**, 852–855 (2022).
6. Mihreteab, S. *et al.* Increasing Prevalence of Artemisinin-Resistant HRP2-Negative Malaria in Eritrea. *N. Engl. J. Med.* **389**, 1191–1202 (2023).
7. Conrad, M. D. & Rosenthal, P. J. Antimalarial drug resistance in Africa: the calm before the storm? *Lancet Infect. Dis.* **19**, e338–e351 (2019).
8. Miller, L. H. & Su, X. Artemisinin: Discovery from the Chinese Herbal Garden. *Cell* **146**, 855–858 (2011).
9. Li, G. Q., Arnold, K., Guo, X. B., Jian, H. X. & Fu, L. C. Randomised comparative study of mefloquine, qinghaosu, and pyrimethamine-sulfadoxine in patients with *falciparum* malaria. *Lancet Lond. Engl.* **2**, 1360–1361 (1984).
10. White, N. J. Assessment of the pharmacodynamic properties of antimalarial drugs in vivo. *Antimicrob. Agents Chemother.* **41**, 1413–1422 (1997).

11. Cumming, J. N., Ploypradith, P. & Posner, G. H. Antimalarial Activity of Artemisinin (Qinghaosu) and Related Trioxanes: Mechanism (s) of Action. in *Advances in Pharmacology* (eds. August, J. T., Anders, M. W., Murad, F. & Coyle, J. T.) vol. 37 253–297 (Academic Press, 1996).
12. Navaratnam, V. *et al.* Pharmacokinetics of Artemisinin-Type Compounds. *Clin. Pharmacokinet.* **39**, 255–270 (2000).
13. Kumari, A. *et al.* Current scenario of artemisinin and its analogues for antimalarial activity. *Eur. J. Med. Chem.* **163**, 804–829 (2019).
14. Hartwig, C. L. *et al.* Accumulation of artemisinin trioxane derivatives within neutral lipids of *Plasmodium falciparum* malaria parasites is endoperoxide-dependent. *Biochem. Pharmacol.* **77**, 322–336 (2009).
15. O'Neill, P. M. & Posner, G. H. A Medicinal Chemistry Perspective on Artemisinin and Related Endoperoxides. *J. Med. Chem.* **47**, 2945–2964 (2004).
16. Meshnick, S. R., Thomas, A., Ranz, A., Xu, C.-M. & Pan, H.-Z. Artemisinin (qinghaosu): the role of intracellular hemozoin in its mechanism of antimalarial action. *Mol. Biochem. Parasitol.* **49**, 181–189 (1991).
17. Posner, G. H. & Oh, C. H. Regiospecifically oxygen-18 labeled 1,2,4-trioxane: a simple chemical model system to probe the mechanism(s) for the antimalarial activity of artemisinin (qinghaosu). *J. Am. Chem. Soc.* **114**, 8328–8329 (1992).
18. Wang, J. *et al.* Haem-activated promiscuous targeting of artemisinin in *Plasmodium falciparum*. *Nat. Commun.* **6**, 10111 (2015).

19. Ismail, H. M. *et al.* Artemisinin activity-based probes identify multiple molecular targets within the asexual stage of the malaria parasites *Plasmodium falciparum* 3D7. *Proc. Natl. Acad. Sci.* **113**, 2080–2085 (2016).
20. O'Neill, P. M., Barton, V. E. & Ward, S. A. The molecular mechanism of action of artemisinin--the debate continues. *Mol. Basel Switz.* **15**, 1705–1721 (2010).
21. W. Jefford, C. Synthetic Peroxides as Potent Antimalarials. News and Views. *Curr. Top. Med. Chem.* **12**, 373–399 (2012).
22. Creek, D. J. *et al.* Relationship between Antimalarial Activity and Heme Alkylation for Spiro- and Dispiro-1,2,4-Trioxolane Antimalarials. *Antimicrob. Agents Chemother.* **52**, 1291–1296 (2008).
23. Dong, Y. *et al.* Spiro and Dispiro-1,2,4-trioxolanes as Antimalarial Peroxides: Charting a Workable Structure–Activity Relationship Using Simple Prototypes. *J. Med. Chem.* **48**, 4953–4961 (2005).
24. Vennerstrom, J. L. *et al.* Identification of an antimalarial synthetic trioxolane drug development candidate. *Nature* **430**, 900 (2004).
25. Creek, D. J. *et al.* Iron-mediated degradation kinetics of substituted dispiro-1,2,4-trioxolane antimalarials. *J. Pharm. Sci.* **96**, 2945–2956 (2007).
26. Charman, S. A. *et al.* Synthetic ozonide drug candidate OZ439 offers new hope for a single-dose cure of uncomplicated malaria. *Proc. Natl. Acad. Sci.* **108**, 4400–4405 (2011).
27. Kim, H. S., Hammill, J. T. & Guy, R. K. Seeking the Elusive Long-Acting Ozonide: Discovery of Artefenomel (OZ439). *J. Med. Chem.* **60**, 2651–2653 (2017).

28. White, N. J. & Nosten, F. H. SERCAP: is the perfect the enemy of the good? *Malar. J.* **20**, 281 (2021).
29. Salim, M. *et al.* Interactions of Artefenomel (OZ439) with Milk during Digestion: Insights into Digestion-Driven Solubilization and Polymorphic Transformations. *Mol. Pharm.* **15**, 3535–3544 (2018).
30. Straimer, J. *et al.* Plasmodium falciparum K13 Mutations Differentially Impact Ozonide Susceptibility and Parasite Fitness In Vitro. *mBio* **8**, 10.1128/mbio.00172-17 (2017).
31. Birnbaum, J. *et al.* A Kelch13-defined endocytosis pathway mediates artemisinin resistance in malaria parasites. *Science* **367**, 51–59 (2020).
32. Gnädig, N. F. *et al.* Insights into the intracellular localization, protein associations and artemisinin resistance properties of Plasmodium falciparum K13. *PLOS Pathog.* **16**, e1008482 (2020).
33. Siddiqui, G., Srivastava, A., Russell, A. S. & Creek, D. J. Multi-omics Based Identification of Specific Biochemical Changes Associated With PfKelch13-Mutant Artemisinin-Resistant Plasmodium falciparum. *J. Infect. Dis.* **215**, 1435–1444 (2017).
34. He, Y. *et al.* Artemisinin resistance-associated markers in Plasmodium falciparum parasites from the China-Myanmar border: predicted structural stability of K13 propeller variants detected in a low-prevalence area. *PLOS ONE* **14**, e0213686 (2019).
35. Klonis, N. *et al.* Artemisinin activity against Plasmodium falciparum requires hemoglobin uptake and digestion. *Proc. Natl. Acad. Sci.* **108**, 11405–11410 (2011).

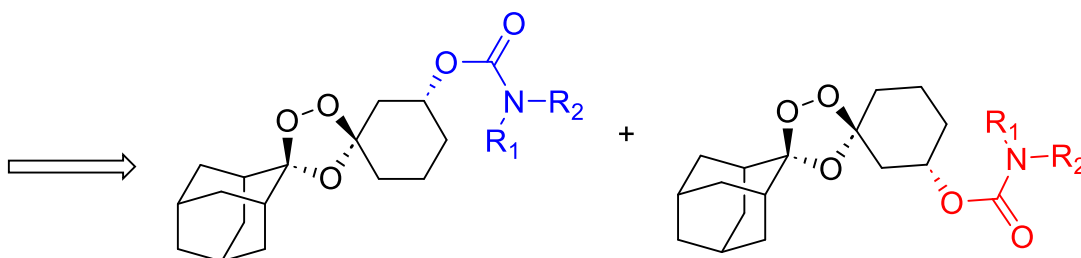
36. Xie, S. C. *et al.* Haemoglobin degradation underpins the sensitivity of early ring stage *Plasmodium falciparum* to artemisinins. *J. Cell Sci.* **129**, 406–416 (2016).
37. Behrens, H. M., Schmidt, S. & Spielmann, T. The newly discovered role of endocytosis in artemisinin resistance. *Med. Res. Rev.* **41**, 2998–3022 (2021).
38. Goldberg, D. E. & Sigala, P. A. *Plasmodium* heme biosynthesis: To be or not to be essential? *PLoS Pathog.* **13**, e1006511 (2017).
39. Blank, B. R., Gut, J., Rosenthal, P. J. & Renslo, A. R. Enantioselective Synthesis and in Vivo Evaluation of Regioisomeric Analogues of the Antimalarial Arterolane. *J. Med. Chem.* **60**, 6400–6407 (2017).
40. Blank, B. R. *et al.* Antimalarial Trioxolanes with Superior Drug-Like Properties and In Vivo Efficacy. *ACS Infect. Dis.* **6**, 1827–1835 (2020).
41. Blank, B. R., Gut, J., Rosenthal, P. J. & Renslo, A. R. Artefenomel Regioisomer RLA-3107 Is a Promising Lead for the Discovery of Next-Generation Endoperoxide Antimalarials. *ACS Med. Chem. Lett.* **14**, 493–498 (2023).

Chapter 2

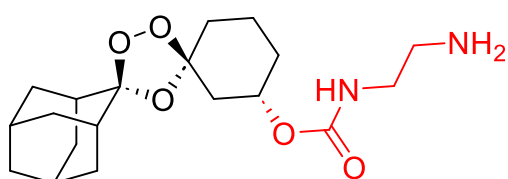
Improved trioxolane antimalarials from the carbamate class

Matthew T Klope, Juan A Tapia Cardona, Jenny Legac, Jun Chen, Ryan L Gonciarz, Julie Kim, Priyanka Jaishankar, Philip J Rosenthal, Adam R Renslo.

ABSTRACT



- Stereoselective synthesis and evaluation of (R, R) and (S, S) *trans*-3' carbamates
- Improved antiparasitic activity and drug-like properties versus class comparators



9d

P. falc. EC₅₀ (W2) = 5.0 ± 2.4 nM
HLM CL = 23.1 μL/min/mg
Solubility in PBS 7.4 = 144.0 μM

P. berghei PD₁₀₀ = 10mg/kg x 2 days

Graphical Abstract. Herein we describe the stereoselective synthesis and evaluation of novel *trans*-3' carbamate substituted 1,2,4-trioxolanes. We report **9d** as an exemplary candidate with dramatically improved *P. berghei* curative potential versus arterolane and other relevant comparators.

Emerging parasite resistance to frontline antimalarials, together with the limited clinical adoption of the second-generation synthetic trioxolanes arterolane and artefenomel, motivates the discovery of improved drug candidates in the endoperoxide class. Our lab has focused on undertargeted substitution patterns on the 1,2,4-trioxolane scaffold, previously identifying *trans*-3' carbamate substitutions as a promising chemotype for achieving potent antiparasitic effect with improved drug-like properties. Herein we describe the design, synthesis, and evaluation of novel *trans*-3' substituted carbamates bearing primary amine, alcohol, or sulfinyl functionality. We find a number of these analogues to demonstrate potent antiparasitic effect and superior metabolic stability and aqueous solubility relative to previous entries to this field. We additionally report

exemplary analogue **9d**, which completely cures mice in the *P. berghei* model at 2 doses of 10 mg/kg, a dramatically improved effect versus the curative efficacy of arterolane and similar carbamate analogues. These results indicate the enduring potential of the synthetic trioxolanes and suggest **9d** for continued evaluation in humanized mouse models.

INTRODUCTION

Refer to Chapter 1 for a comprehensive introduction to synthetic trioxolanes.

The discovery of novel, fast-acting antimalarial drugs remains an urgent public health priority. Despite the enduring work of countless contributors to the malaria eradication campaign, the timeline for the WHO global technical strategy for malaria remains significantly delayed as gains against the disease have plateaued in areas of high disease burden.¹ The exquisite antimalarial activity of frontline artemisinin antimalarials, the foundation of antimalarial care, is nonetheless limited by the poor pharmacokinetic characteristics of this class.² The low solubility, poor bioavailability, and short half-life of artemisinin requires the co-administration of artemisinin compounds with a longer-lived partner drug, a paradigm which is increasingly threatened by parasite resistance to partner drugs and, more concerningly, by an increasing incidence of a K13-driven artemisinin partial resistance phenotype observed in high-burden, high-transmission areas.^{3 4} K13-driven partial resistance is associated with a delayed clearance effect upon artemisinin exposure,⁵ achieved in K13 mutants by reducing the concentration of drug-activating heme iron in the parasite digestive vacuole.⁶ This unusual mechanism of resistance is effective due to the iron-dependent pharmacology of artemisinins and due

to the rather short half-lives of artemisinins in patients. Accordingly, extending the exposure of endoperoxides should better clear K13 mutant parasites⁷, thus motivating the search for novel endoperoxide antimalarials with significantly prolonged exposure *in vivo*.

Given the limited options for synthetic alteration of the artemisinin scaffold, previous medicinal chemistry efforts around endoperoxide antimalarials have focused on the fully synthetic 1,2,4-trioxolane and related endoperoxide scaffolds.^{8 9} Only the 1,2,4-trioxolane scaffold has so far yielded viable clinical candidates: arterolane⁹ and artefenomel.¹⁰ These promising antimalarials retain the potent antiparasitic efficacy of the Artemisinins while offering improved solubility and, for artefenomel, the potential for single-exposure cures and an improved exposure profiles relative to artemisinins in human volunteers.^{7,11} Despite its initial promise, arterolane has seen limited clinical use due to more rapid clearance in infected individuals¹², while the clinical development of artefenomel was recently terminated for failure to meet clinical pharmacokinetic benchmarks.¹³ There thus exists an urgent need to identify next-generation trioxolane antimalarials with superior solubility, metabolic stability, and *in vivo* exposure profiles to extend the clinical utility of endoperoxide antimalarials into the future.

RESULTS AND DISCUSSION

We recently reported an initial study of trioxolane analogs bearing a *trans*-3'' carbamate side chain (**Figure 2-1**).¹⁴ This chemotype can be synthesized in a fully stereocontrolled fashion, starting with a Taniaphos-mediated asymmetric borylation of cyclohexenone to prepare intermediate **2** in either the *R* or *S* form. Oxidation of boron and protection of the resulting alcohol as a TBDPS ether afforded ketone **4**, which participates in a Griesbaum co-ozonolysis with adamantan-2-one *O*-methyloxime, affording the *trans* diastereomer **5** in 12:1 diastereomeric ratio (dr) as determined by ¹H NMR analysis. Subsequent deprotection of **5** and activation as the *p*-nitrophenylcarbonate **7** allows for late-stage diversification into the desired *trans*-3''-carbamate analogs. We leveraged this route in the current study to further explore cyclic and noncyclic amine coupling partners and more fully elaborate the SAR of the *trans*-3'' carbamate scaffold.

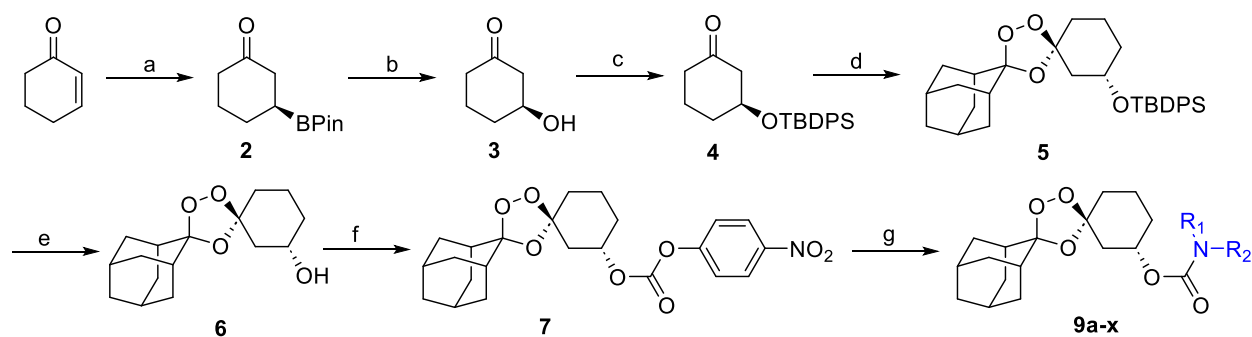
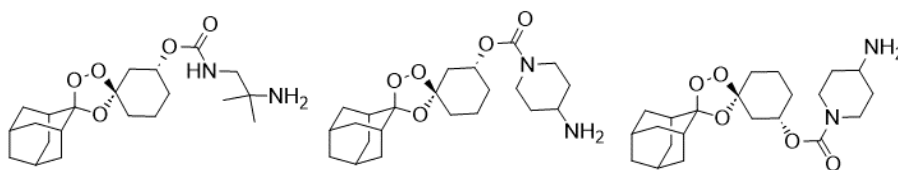


Figure 2-1. Stereocontrolled synthesis of (*S,S*)-substituted analogues as reported previously¹⁴ and employed herein. ^aReagents and conditions: (a) B₂pin₂, *t*-BuONa, CuCl. (*R*)-Taniaphos*, MeOH rt 24h (b) NaBO₃•4H₂O, THF/H₂O (3:1) rt 2.5h (c) *t*-BuPh₂SiCl, imidazole, THF 0°C to rt 16.5h (d) N-methoxyadamantan-2-imine, O₃, CCl₄ 0°C 3.5h (e) TBAF, THF 0°C to rt 3h (f) 4-NO₂PhOC(O)Cl, *i*-Pr₂Net, DMAP, CH₂Cl₂ 0°C to rt 18.5h (g) R¹(R²)NH, Et₃N, CH₂Cl₂

*The same route was used to prepare (*R,R*) analogues, using (*S*)-Taniaphos in the first step

In our lab's original study of the chemotype, we identified carbamate analogs **8a**, **8c**, and **9c** as most promising, all three compounds demonstrating comparable or superior *in vivo* efficacy as the arterolane comparator (**Table 2-1**). It was highly encouraging that with only around two dozen new analogs synthesized and evaluated, at least five were clearly superior to arterolane using repeat-dosing modalities (4 x 4 mg/kg or 4 x 2 mg/kg). Further, six of the new analogs produced cures in between 1 and 5 animals (n = 5 per group) following a single oral exposure at 40 mg/kg (artefenomel producing 5/5 cures at this dose). With this starting point, we sought to explore more diverse carbamate side chain chemotypes, inspired by the ethylamino- and aminopiperadiny carbamates of top performing analogs **8a**, **8c**, and **9c**.

Table 2-1. Comparative *in vitro* antiplasmodial, in vitro ADME, and in vivo efficacy of selected novel *trans*-3" carbamate analogs and comparators OZ277 and OZ439.¹⁴



Compound	OZ277	OZ439	8a	8c	9c
<i>P. falciparum</i> IC ₅₀ (nM)	2.5 ^a	2.15 ^a	1.8 ^a	1.7 ^a	2.4 ^a
HLM CL _{INT} (μL/min/mg)	< 7 ^b	63.7 ^b	12.8 ^a	123 ^a	11.8 ^a
PBS Solubility (μM)	504 ^b	0.181 ^c	n.d.	144.5 ^a	118 ^a
<i>P. berghei</i> PD ₁₀₀ (4 days dosing)	4 mg/kg/day ^a	n.d.	2 mg/kg/day ^a	2 mg/kg/day ^a	n.d.

^aData from our lab's report of 2020⁽¹⁴⁾ ^bData generated via Medicines for Malaria Venture

^cData from ref (16)

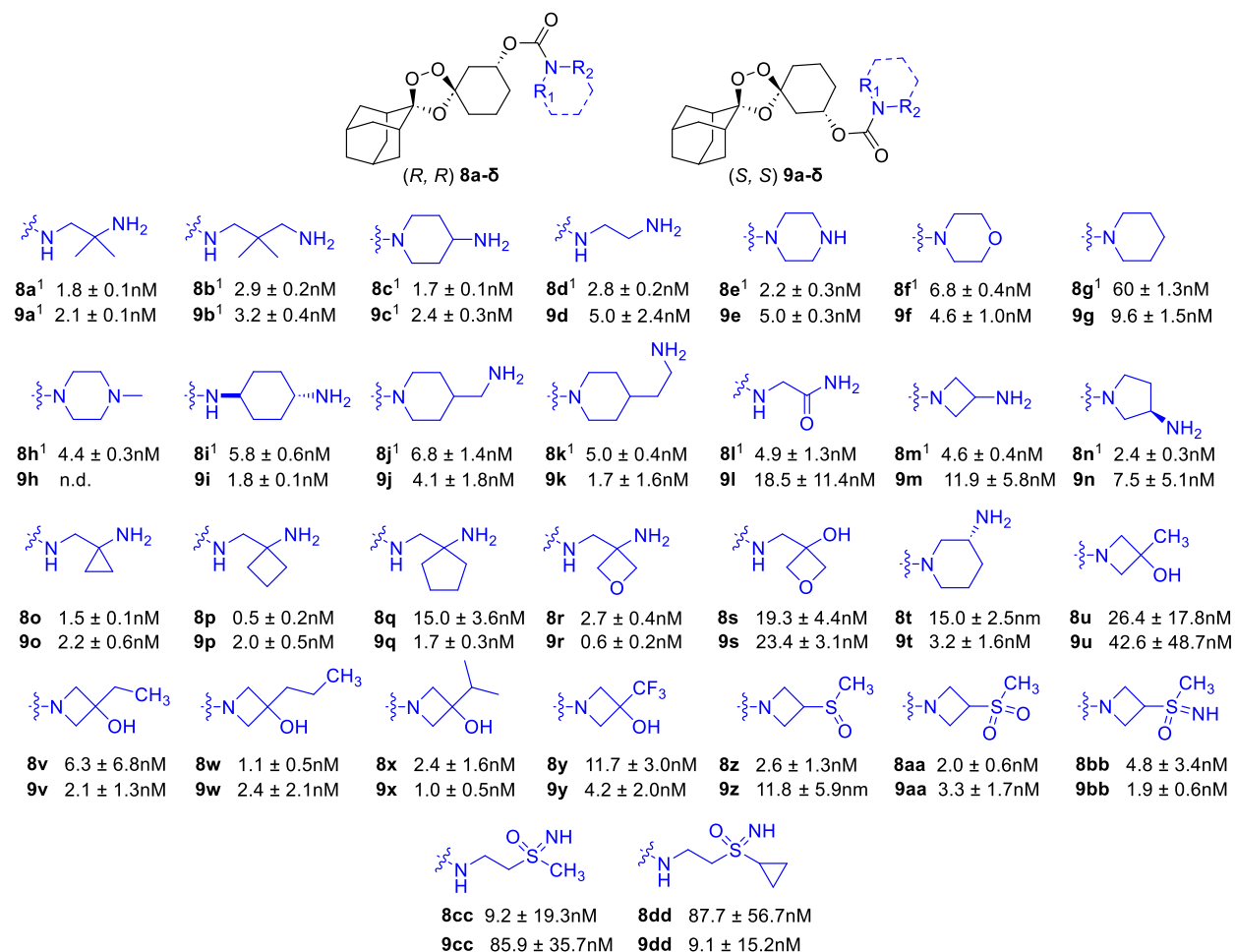


Figure 2-2. In Vitro activity of **8a-δ** and **9a-δ** against W2 *P. falciparum* parasites ($EC_{50} \pm SEM$)^a ¹Data from ref. (14) ^aReported EC_{50} values are the mean of at least 3 determinations.

Since only three analogs with (S, S) stereochemistry had been explored in our initial study, we began the new effort by synthesizing the (S, S) isomers of previously reported (R, R) analogues **8d-n** and evaluating these compounds for their antiplasmodial effects against W2 strain *P. falciparum* (**Figure 2-2, 9d-n**). Similar to their (R, R) forms, the (S, S) isomers demonstrated potent antiplasmodial effects, with EC_{50} values generally within two-fold in the enantiomeric pairs. Noting the potent antiparasitic effect and favorable solubility of analogues bearing terminal primary amines, we next explored additional (R,

R) and (*S*, *S*) pairs bearing 2-substituted ethylenediamine substitutions (**8o-8r**, **9o-9r**) and found that these analogues also retained potent, low-nM antiparasitic effects. Replacing the terminal amino function with hydroxy, as in the change from aminooxetanes **8r** and **9r** to oxetanols **8s** and **8r** resulted in a ~10 fold decrease in EC₅₀, supporting an apparent role of basic amines in promoting cellular potency of this class. Morpholine analogs **8f** & **9f** however, indicate that the low-nM potencies can also be achieved with non-basic *trans*-3" carbamate-substituted trioxolanes.

A recent report on the SAR of antimalarial benzoxaboroles described the dramatic effect of azetidine-bearing side chains on antiparasitic activity, with the effect spanning orders of magnitude.¹⁵ Since the oxaborole warhead is known to be essential for activity in this class, and was thus retained across the analogs studied, we inferred that the improved *in vivo* efficacy described for the azetidinyll analogs most likely stemmed from improved uptake, reduced efflux, and/or favorable modulation of other ADME properties arising from the azetidine side chains. With a hypothesis that similar favorable effects might be transferrable to the trioxolane pharmacophore, we synthesized *trans*-3" carbamates with various alkyl-substituted azetidine alcohols (**8u-y**, **9u-y**) as well as sulfoxide-, sulfone-, and sulfoximine-substituted azetidines (**8z-8bb**, **9z-9bb**), and also two alicyclic sulfoximine analogues (**8cc-8dd**, **9cc-9dd**). Indeed, we observed excellent antiparasitic activity across all the substituted azetidines, but not alicyclic sulfoximines **8cc-8dd** and **9cc-9dd**, which seemed to confirm the anticipated utility of the azetidinyll substitutions in targeting the parasite.

Table 2-2. In vitro ADME Data for Selected Analogues and Controls

	HLM $t_{1/2}$ (min) ^a	HLM Cl_{int} (μ L/min/mg) ^a	Solubility in PBS pH 7.4 (μ M) ^b				
				9s	4.2	332.6	111.8
				8t	31.7	43.7	74.9
				9t	26.3	52.7	128.8
arterolane	>60	<7	504	8v	2.9	480.0	58.7
artefenomel	21.8	7.7	0.181	9v	2.2	638.0	41.5
8a^c	108.4	12.8	-	8w	2.4	578.6	16.1
9a^c	>120	<11.5	173.7	9w	2.0	683.0	18.2
8b^c	96.8	14.3	-	8x	4.2	392.2	15.9
9b^c	64.8	21.4	164.1	9x	2.1	656.8	15.1
8c^c	11.3	123.0	144.5	8y	5.9	233.8	24.8
9c^c	117.4	11.8	118.0	9y	6.6	211.2	10.8
9d	60.0	23.1	144.0	8z	2.7	516.0	138.2
8e^c	35.2	39.4	157.0	9z	1.8	749.6	183.5
9e	11.5	120.0	-	8aa	2.6	526.0	66.7
9g	>120	<11.6	-	9aa	1.6	851.2	81.1
9h	-	-	109.2	8bb	5.9	233.8	267.7
9i	49.1	28.2	-	9bb	3.2	431.0	142.4
9j	19.9	69.6	112.0	8cc	5.7	243.0	127.7
9k	15.0	92.7	116.7	9cc	4.3	318.8	128.9
9m	>120	<11.6	100.6	8dd	3.2	435.0	79.3
8n	30.3	45.8	167.0	9dd	3.1	450.2	233.6
8o	33.2	41.7	-				
9o	37.1	37.4	143.0				
8p	-	-	142.2				
9p	55.6	29.9	161.9				
8q	54.7	25.3	13.4				
9q	59.3	23.4	122.4				
8r	18.2	76.2	-				
8s	5.7	244.2	-				

^aData generated for this study by Quintara Biosciences, South San Francisco CA. Verapamil is used as a positive control in the human liver microsome (HLM) assay. ^bData generated for this study by Analiza Inc, Cleveland OH. ^cData previously reported in ref. (14)

We next evaluated the ADME and physiochemical parameters of our synthesized carbamate library, with an initial focus on human liver microsome (HLM) stability and aqueous solubility in pH 7.4 PBS (**Table 2-2**). The presence of a primary amine across the studied (*R, R*) and (*S, S*) analogues resulted in excellent aqueous solubility.

Additionally, these analogues generally demonstrated good metabolic stability, with compounds **9g** (piperidiny) and **9m** (aminoazetidiny) exceeding the upper limit of the HLM assay as previously observed as well with gem-dimethyl ethylenediamine **9a**. Unfortunately, despite the encouraging antiparasitic potency of azetidine carbamates **8u-8dd** and **9u-9dd**, these groups apparently have a severe metabolic liability in the context of the trioxolane pharmacophore, as reflected in their very rapid clearance in human liver microsome incubations.

Table 2-3. Oral efficacy of selected analogues and controls in murine *P. berghei* model^a

Compound	PO Dose (days)	Cures	9q	0/5
Experiment 1		20mg/kg (1 day)	9r	0/5
artefenomel		5/5	8u	0/5
8a		0/5	8y	0/5
8c		0/5	Experiment 5 10mg/kg (2 day)	
Experiment 2		20mg/kg (1 day)	arterolane	0/5
artefenomel		5/5	9d	5/5
9a		0/5	8q	0/5
8c		0/5	8r	0/5
9c		0/5	8s	0/5
9g		0/5	9s	0/5
9m		0/5	8t	0/5
9o		0/5	9u	0/5
8r		0/5	9dd	0/5
Experiment 3		variable	^a Mice were judged cured if parasitemia was undetectable at day 3.	
artefenomel		20mg/kg (1 day)		
8c		50mg/kg (1 day)		
8c		10mg/kg (2 day)		
8c		4mg/kg (2 day)		
Experiment 4		10mg/kg (2 day)		
arterolane		0/5		
9a		3/5		
8c		0/5		
9c		0/5		
9o		0/5		
8p		0/5		

Next, we used the *P. berghei* mouse model of malaria to assess oral efficacy of selected new carbamate analogues, using arterolane or artefenomel as controls (**Table 2-3**). Briefly, female Swiss-Webster mice were infected intraperitoneally with *P. berghei*-infected murine erythrocytes, following which mice were treated via oral gavage with 100 μ L test compound or vehicle according to the dosing paradigm indicated (**Table 2-3**). Cohorts were organized with 5 animals per treatment group, Giemsa-stained blood smears were taken over time to monitor parasitemia, and subjects were considered cured if parasitemia could not be detected at day 30. All regimens were well-tolerated, with no overt signs of toxicity for any of the analogues studied.

In our prior study, we explored both repeat and single-dose regimens, and identified compounds that afforded partial cures within cohorts at 1 x 40 mg/kg. For these newer analogs we initially set a higher bar for the compounds of a single 20 mg/kg dose, since the artefenomel control can produce single-exposure cures at this low dose (**Table 2-3** Experiments 1-2). Unfortunately, we found that none of our new compounds achieved cures under this more stringent dosing regimen. Accordingly, experiment 3 was designed to evaluate additional dosing paradigms that would more fully explore the *in vivo* potential of the new compounds. Encouragingly, we found 4-aminopiperazine **8c** achieved cures in 3 of 5 animals when dosed for 2 days at 10mg/kg (i.e., the same total dose of 20 mg/kg but split over two days). Exploring this dosing schedule with additional analogues revealed a similar effect (3/5 cures) for **9a**, the (*S*, *S*) enantiomer of **8a** (**Table 2-3** Experiment 4), a promising lead from our initial report. Of note was the use of the structurally more similar drug arterolane as the positive control, and the finding that unlike **9a**, arterolane provided no cures under a 2 x 10 mg/kg dosing schedule. In a final

experiment, we were excited to find that analog **9d**, exactly analogous to **9a** but lacking the gem-dimethyl substitutions, afforded cures in all five mice with just two doses at 10 mg/kg; comparator arterolane was once again unable to cure any animals under this paradigm (**Table 2-3** Experiment 5). Compounds such as **8c** from our initial carbamate survey, and analogs **9a** and **9d** explored here, are notable in that they approach the remarkable efficacy of artefenomel in the *P. berghei* model, while possessing significantly improved human liver microsome stability and dramatically higher aqueous solubility.

CONCLUSION

Herein we described the stereocontrolled synthesis and *in vitro* and *in vivo* evaluation of novel *trans*-3" substituted 1,2,4-trioxolane carbamates, focusing on analogues with small to medium-size rings and bearing primary amine, alcohol, or sulfinyl functionality. Unexpectedly, we found that acyclic, primary amine-bearing carbamates exhibited the most promising efficacy along with the best metabolic stability in human liver microsomes. Exemplar acyclic carbamate **9d** produced consistent cures in the *P. berghei* model of mouse malaria with just two 10 mg/kg oral doses and was dramatically superior to the approved agent arterolane administered at the same dosing paradigm. Single-exposure cure is the gold-standard for new antimalarial drug candidates, but a too-narrow focus on this one criterion may, in the case of artefenomel, have led to selection of a drug candidate with other serious liabilities. The development of the humanized SCID mouse model of *P. falciparum* represents a new pre-clinical benchmark for the efficacy of antimalarial drug

candidates. The trans-3" carbamate **9d** is a promising candidate for evaluation in this more relevant and predictive *in vivo* model of human malaria.

METHODS

EC₅₀ of experimental compounds against cultured *P. falciparum* parasites

Erythrocytic cultures of *P. falciparum* strain W2 (BEI Resources) were maintained using standard methods at 2% hematocrit in RPMI 1640 medium (Invitrogen) supplemented with 0.5% AlbuMAX II (Gibco Life Technologies), 0.1mM hypoxanthine, 30ug/mL gentamicin, 24mM NaHCO₃, and 25mM HEPES pH 7.4 at 37°C in an atmosphere of 5% O₂, 5% CO₂, and 90% N₂. Infected cultures were exposed to 12 drug concentrations (12 point, 3-fold serial dilution from 10µM -> 0.06nM) or an equal volume of DMSO with tips changed between each serial dilution to minimize potential carryover of lipophilic compounds. Test plates were incubated at 37°C under the above atmosphere for 72 hours, following which erythrocytes were pelleted and fixed in 2% formaldehyde in PBS (pH 7.4) at room temperature overnight. 2% Formaldehyde PBS was removed and parasites were resuspended in permeabilization media (100mM NH₄Cl, 0.1% Triton-X, PBS pH 7.4) with freshly added 25nM YOYO-1 fluorescent dye. Plates were incubated at 4°C for a minimum of 24 hours. Parasitemia was determined from dot plots of 5x10⁴ cells acquired on a FACSCalibur flow cytometer using CELLQUEST software (Becton Dickinson), using initial gating values determined using unstained uninfected erythrocyte and stained uninfected erythrocyte controls. IC₅₀s were determined using GraphPad Prism software with 3 experimental replicates per compound.

P. berghei Mouse Malaria Model

Female Swiss Webster mice (~20 g body weight) were infected intraperitoneally with 10⁶ P. berghei-infected erythrocytes collected from a previously infected mouse.

Beginning 1 h after inoculation the mice were treated once daily by oral gavage for 1–2 days as indicated with 100 µL of solution of test compound formulated in 10% DMSO, 40% of a 20% 2-hydroxypropyl-beta-cyclodextrin solution in water, and 50% PEG400.

There were five mice in each test arm. Infections were monitored by daily microscopic evaluation of Giemsa-stained blood smears starting on day seven. Parasitemia was determined by counting the number of infected erythrocytes per 1000 erythrocytes.

Body weight was measured over the course of the treatment. Mice were euthanized when parasitemia exceeded 50% or when weight loss of more than 15% occurred.

Parasitemia, animal survival, and morbidity were closely monitored for 30 days postinfection, when experiments were terminated.

Animal Welfare

No alternative to the use of laboratory animals is available for in vivo efficacy assessments. Animals were housed and fed according to NIH and USDA regulations in the Animal Care Facility at San Francisco General Hospital. Trained animal care technicians provide routine care, and veterinary staff are readily available. Euthanasia was performed when malarial parasitemia exceeds 50%, a level that does not appear to be accompanied by distress but predicts progression to lethal disease. Euthanasia was accomplished with CO₂ followed by cervical dislocation. These methods are in accord with the recommendations of the Panel on Euthanasia of the American Veterinary

Medical Association. Our studies are approved by the UCSF Committee on Animal Research.

For experimental methods, synthetic procedures, and characterization data, please refer to Supporting Information for Chapter 2.

REFERENCES

- (1) World Health Organization. *World malaria report 2022*. December 8, 2022
- (2) Fang, J.; Song, F.; Wang, F. The Antimalarial Activity of 1,2,4-Trioxolane/Trioxane Hybrids and Dimers: A Review. *Arch. Pharm. (Weinheim)* **2022**, 355 (7), 2200077. <https://doi.org/10.1002/ardp.202200077>.
- (3) Tumwebaze, P. K.; Conrad, M. D.; Okitwi, M.; Orena, S.; Byaruhanga, O.; Katairo, T.; Legac, J.; Garg, S.; Giesbrecht, D.; Smith, S. R.; Ceja, F. G.; Nsobya, S. L.; Bailey, J. A.; Cooper, R. A.; Rosenthal, P. J. Decreased Susceptibility of *Plasmodium Falciparum* to Both Dihydroartemisinin and Lumefantrine in Northern Uganda. *Nat. Commun.* **2022**, 13 (1), 6353. <https://doi.org/10.1038/s41467-022-33873-x>.
- (4) van Loon, W.; Oliveira, R.; Bergmann, C.; Habarugira, F.; Ndoli, J.; Sendegeya, A.; Bayingana, C.; Mockenhaupt, F. P. In Vitro Confirmation of Artemisinin Resistance in *Plasmodium Falciparum* from Patient Isolates, Southern Rwanda, 2019. *Emerg. Infect. Dis.* **2022**, 28 (4), 852–855. <https://doi.org/10.3201/eid2804.212269>.
- (5) Klonis, N.; Xie, S. C.; McCaw, J. M.; Crespo-Ortiz, M. P.; Zaloumis, S. G.; Simpson, J. A.; Tilley, L. Altered Temporal Response of Malaria Parasites Determines Differential Sensitivity to Artemisinin. *Proc. Natl. Acad. Sci.* **2013**, 110 (13), 5157–5162. <https://doi.org/10.1073/pnas.1217452110>.
- (6) Behrens, H. M.; Schmidt, S.; Spielmann, T. The Newly Discovered Role of Endocytosis in Artemisinin Resistance. *Med. Res. Rev.* **2021**, 41 (6), 2998–3022. <https://doi.org/10.1002/med.21848>.
- (7) Straimer, J.; Gnädig, N. F.; Stokes, B. H.; Ehrenberger, M.; Crane, A. A.; Fidock, D. A. *Plasmodium Falciparum* K13 Mutations Differentially Impact Ozonide

- Susceptibility and Parasite Fitness In Vitro. *mBio* **2017**, 8 (2), 10.1128/mbio.00172-17. <https://doi.org/10.1128/mbio.00172-17>.
- (8) Abe, M.; Inakazu, T.; Munakata, J.; Nojima, M. 18O-Tracer Studies of Fe(II)-Induced Decomposition of 1,2,4-Trioxolanes (Ozonides) Derived from Cyclopentenones and Indenes. Inner-Sphere Electron Transfer Reduction of the Peroxide Linkage. *J. Am. Chem. Soc.* **1999**, 121 (28), 6556–6562. <https://doi.org/10.1021/ja990807v>.
- (9) Vennerstrom, J. L.; Arbe-Barnes, S.; Brun, R.; Charman, S. A.; Chiu, F. C. K.; Chollet, J.; Dong, Y.; Dorn, A.; Hunziker, D.; Matile, H.; McIntosh, K.; Padmanilayam, M.; Santo Tomas, J.; Scheurer, C.; Scorneaux, B.; Tang, Y.; Urwyler, H.; Wittlin, S.; Charman, W. N. Identification of an Antimalarial Synthetic Trioxolane Drug Development Candidate. *Nature* **2004**, 430 (7002), 900–904. <https://doi.org/10.1038/nature02779>.
- (10) Charman, S. A.; Arbe-Barnes, S.; Bathurst, I. C.; Brun, R.; Campbell, M.; Charman, W. N.; Chiu, F. C. K.; Chollet, J.; Craft, J. C.; Creek, D. J.; Dong, Y.; Matile, H.; Maurer, M.; Morizzi, J.; Nguyen, T.; Papastogiannidis, P.; Scheurer, C.; Shackleford, D. M.; Sriraghavan, K.; Stingelin, L.; Tang, Y.; Urwyler, H.; Wang, X.; White, K. L.; Wittlin, S.; Zhou, L.; Vennerstrom, J. L. Synthetic Ozonide Drug Candidate OZ439 Offers New Hope for a Single-Dose Cure of Uncomplicated Malaria. *Proc. Natl. Acad. Sci.* **2011**, 108 (11), 4400–4405. <https://doi.org/10.1073/pnas.1015762108>.
- (11) Giannangelo, C.; Fowkes, F. J. I.; Simpson, J. A.; Charman, S. A.; Creek, D. J. Ozonide Antimalarial Activity in the Context of Artemisinin-Resistant Malaria. *Trends Parasitol.* **2019**, 35 (7), 529–543. <https://doi.org/10.1016/j.pt.2019.05.002>.

- (12) Kim, H. S.; Hammill, J. T.; Guy, R. K. Seeking the Elusive Long-Acting Ozonide: Discovery of Artefenomel (OZ439). *J. Med. Chem.* **2017**, 60 (7), 2651–2653.
<https://doi.org/10.1021/acs.jmedchem.7b00299>.
- (13) Salim, M.; Khan, J.; Ramirez, G.; Clulow, A. J.; Hawley, A.; Ramachandrani, H.; Boyd, B. J. Interactions of Artefenomel (OZ439) with Milk during Digestion: Insights into Digestion-Driven Solubilization and Polymorphic Transformations. *Mol. Pharm.* **2018**, 15 (8), 3535–3544. <https://doi.org/10.1021/acs.molpharmaceut.8b00541>.
- (14) Blank, B. R.; Gonciarz, R. L.; Talukder, P.; Gut, J.; Legac, J.; Rosenthal, P. J.; Renslo, A. R. Antimalarial Trioxolanes with Superior Drug-Like Properties and In Vivo Efficacy. *ACS Infect. Dis.* **2020**, 6 (7), 1827–1835.
<https://doi.org/10.1021/acsinfecdis.0c00064>.
- (15) Zhang, Y.-K.; Plattner, J. J.; Easom, E. E.; Jacobs, R. T.; Guo, D.; Freund, Y. R.; Berry, P.; Ciaravino, V.; Erve, J. C. L.; Rosenthal, P. J.; Campo, B.; Gamo, F.-J.; Sanz, L. M.; Cao, J. Benzoxaborole Antimalarial Agents. Part 5. Lead Optimization of Novel Amide Pyrazinyloxy Benzoxaboroles and Identification of a Preclinical Candidate. *J. Med. Chem.* **2017**, 60 (13), 5889–5908.
<https://doi.org/10.1021/acs.jmedchem.7b00621>.
- (16) Charman, S. A.; Andreu, A.; Barker, H.; Blundell, S.; Campbell, A.; Campbell, M.; Chen, G.; Chiu, F. C. K.; Crighton, E.; Katneni, K.; Morizzi, J.; Patil, R.; Pham, T.; Ryan, E.; Saunders, J.; Shackelford, D. M.; White, K. L.; Almond, L.; Dickins, M.; Smith, D. A.; Moehrle, J. J.; Burrows, J. N.; Abba, N. An in Vitro Toolbox to Accelerate Anti-Malarial Drug Discovery and Development. *Malar. J.* **2020**, 19 (1), 1.
<https://doi.org/10.1186/s12936-019-3075-5>.

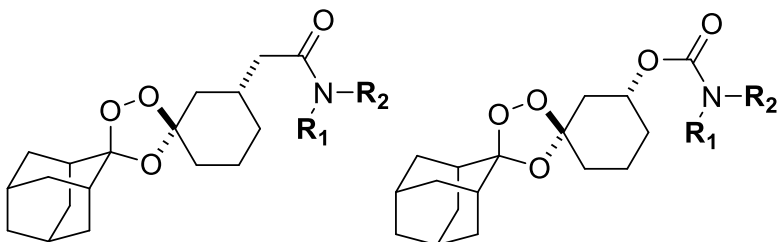
Chapter 3

Towards a Novel Trioxolane Antimalarial Drug Candidate

Matthew T. Klope, Poulami Talukder, Brian R. Blank, Jun Chen, Priyadarshini Jaishankar, Ryan L. Gonciarz, Aswathy Vinod, Vineet Mathur, Juan Tapia, Jennifer Legac, Avani Narayan, Shaun D. Fontaine, Philip J. Rosenthal, Adam R. Renslo.

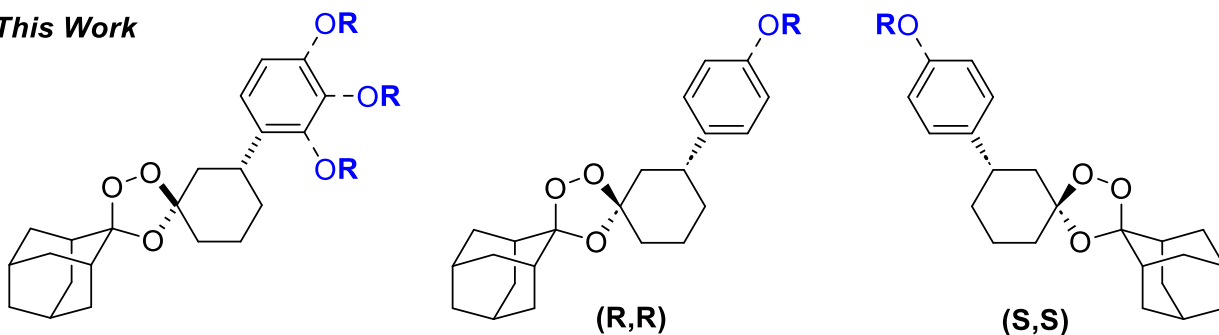
ABSTRACT

Previous work



- Exploration of *trans* 3' amide and carbamate side chains
- *in vivo* efficacy superior to artemolane for some analogs

This Work



- Evaluation of *ortho*, *meta*, and *para* substituted *trans*-3' phenolic ethers and carbamates
- Comparison of (R,R) and (S,S) enantiomeric forms of selected leads
- Improved drug-like parameters vs. previous clinical candidates

Graphical Abstract. Previous work by our laboratory^{1 2} and present report

The synthetic 1,2,4-trioxolane antimalarial artefenomel has, until recently, been viewed as the likely clinical successor to artemisinin derivatives as the fast-killing component of future first-line antimalarial combination therapies. Despite showing clinical efficacy in Phase II clinical trials when combined with piperazine³ and more recently ferroquine⁴, it was recently revealed that further clinical development of artefenomel would be

discontinued. This was due in part to formulation challenges stemming from suboptimal physiochemical properties of the molecule, and for failing to reach clinical pharmacokinetic exposure benchmarks following a single oral dose. Our group has become interested in modulating 1,2,4-trioxolane pharmacology through *trans*-3" substitutions of the cyclohexane ring, as contrasted with the *cis*-4" substitution employed in all previously described trioxolane-focused drug discovery campaigns. Here we detail our most recent and extensive efforts, which concerned artefenomel-inspired analogues bearing phenolic ethers or carbamates at the 3" position. Guided by key in vitro ADME targets, and after profiling more than forty novel TRX-C/P analogs in the *P. berghei* mouse malaria model, we identified and nominated RLA-5764 as a new antimalarial development candidate meriting further evaluation in IND-enabling pharmacokinetic and toxicological studies. RLA-5764 was stable toward hepatocytes and liver microsomes from pre-clinical and clinical species and exhibited an in vivo exposure half-life \geq 8hrs in rodents. A BCS Class I drug substance, RLA-5764 achieved cures in the *P. berghei* mouse model following a single oral dose, and at clinically achievable exposure levels. The compound exhibited potent anti-plasmodial effects against common laboratory strains of *P. falciparum*, and against field isolates currently infecting patients in Uganda, including strains that show an artemisinin partial resistance phenotype. In a Ring-Stage Assay (RSA) designed to reveal artemisinin partial resistance, RLA-5764 was notably more effective than artemisinin or artefenomel against K13 C580Y mutant *P. falciparum* parasites, while also exhibiting potent RSA values against clinical artemisinin partial-resistant strains collected from patients in Uganda in 2023. Overall, RLA-5764 is predicted to possess a human exposure profile superior to artemisinin and artefenomel,

while retaining efficacy against the K13 mutant ring stages that threaten the utility of artemisinin combination therapy in the field.

INTRODUCTION

Refer to Chapter 1 for a comprehensive introduction to synthetic trioxolanes.

Work previously reported in this report and by this lab on trans-3" substituted 1,2,4-trioxolanes has focused largely on amide and carbamate side chains most similar to that in arterolane. We reasoned on the basis of more unfavorable 1,3-diaxial interactions, that introduction of an artefenomel-like aryl ether trans-3" side chains should more dramatically disfavor the iron-reactive, peroxide exposed conformer, and thus confer greater stability towards activating ferrous iron. We further hypothesized that de-tuning iron reactivity in this way could lead to trioxolane analogs better able to persist through the 'slow ring' stage associated with K13 mutant parasites, an effect that has previously been invoked⁵ to explain the superior RSA activities of artefenomel compared to arterolane against K13 mutants. Furthermore, our initial study of a trans-3" regioisomer of artefenomel⁶ had revealed a marked improvement in aqueous solubility and liver microsome stability resulting from this desymmetrization of the artefenomel scaffold. Accordingly, we hypothesized that further exploration of 3" aryl-substituted side chains would be a fruitful route to additional analogues with improved drug-like properties.

Herein we describe a systematic study of trans-3" aryl-substituted trioxolanes bearing phenolic ether and carbamate side chains. We found that trans-3" substitution retains iron reactivity in a pharmacologically relevant regime that delivers potent antiplasmodial

effects comparable to artefenomel, but in many cases with improved aqueous solubility and human liver microsome stability. We identified RLA-4735 as an advanced lead compound that exhibits excellent in vivo pharmacokinetic and pharmacodynamic properties, while also demonstrating potent RSA activity against both laboratory strain parasites with the prevalent K13 mutation C580Y and against parasites obtained from malaria patients in Uganda in 2023. We furthermore report the enantioselective synthesis of the two enantiomeric forms of (\pm)-RLA-4735, (*R,R*)-RLA-5763 and (*S,S*)-RLA-5764, both of which produce single-exposure cures in mice, while possessing significantly improved aqueous solubility compared to the racemate. Finally, we describe extensive pre-clinical in vitro ADME assessment of (*S,S*)-RLA-5764, and nominate this molecule as a development candidate for further preclinical study and possible clinical study as a next-generation endoperoxide-class antimalarial agent.

RESULTS AND DISCUSSION

Our laboratory recently reported an efficient 4-step synthesis of RLA-3107, a direct regioisomer of artefenomel (**Figure S3-1**).⁶ We had previously shown⁷ that Griesbaum co-ozonolysis of 3-substituted cyclohexanones with adamantanone-*O*-methyl oxime proceed with high diastereomeric ratios favoring the *trans* diastereomer. In the current effort, we found that 3-aryl substituted cyclohexanones also provide Griesbaum products with high d.r. and could use this chemistry to produce key *trans*-3'' aryl-substituted intermediates with *ortho* (**Figure S3-2**) and *meta* (**compound 5, Figure 3-1**) acetate substitution, in addition to the previously reported *para* congener.

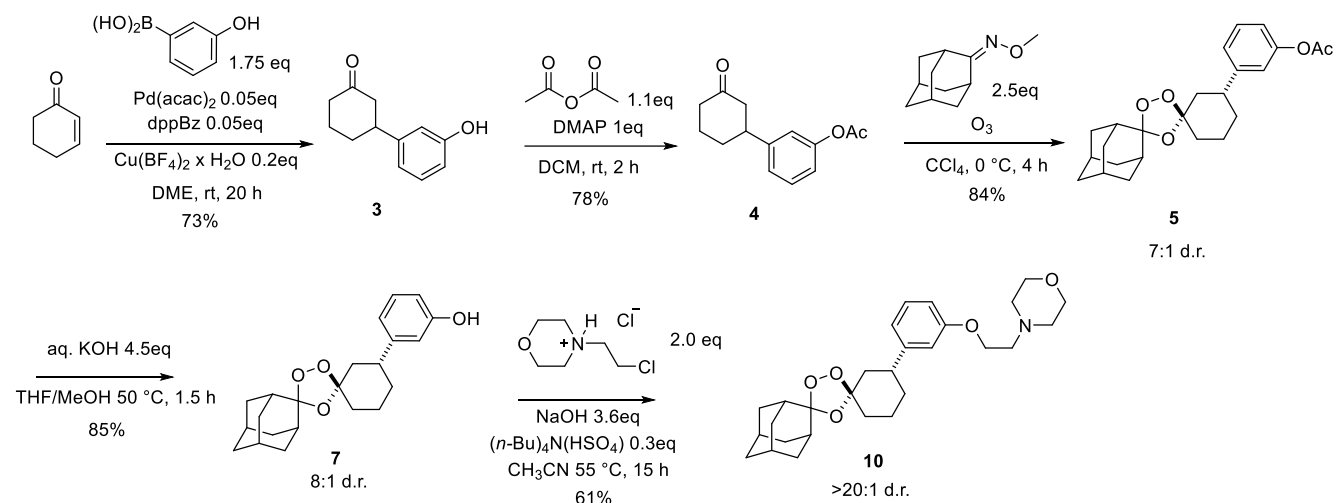


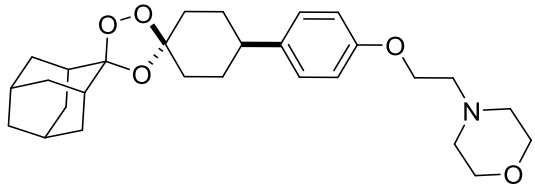
Figure 3-1. Stereocontrolled synthesis of 3'' *meta* artefenomel regioisomers **10**.

The general synthetic approach to *trans*-3'' artefenomel regioisomers is exemplified for the *meta* isomer (**Figure 3-1**) and begins with a palladium-mediated Heck reaction between a phenyl boronic acid and 2-cyclohexen-1-one catalyzed with an *in situ* generated of a palladium (II) complex obtained by mixing Pd(acac)₂, dppben, and Cu(BF₄)₂·H₂O, affording the ketone **3** in 73-91% yield. Protection of the phenol in **3** is achieved with acetic anhydride and pyridine in dichloromethane to produce ketone **4** in 78% yield. Griesbaum co-ozonolysis of **4** in the presence of adamantane-2-one and ozone at 0 °C afforded the respective *trans*-3''-aryl substituted 1,2,4-trioxolane intermediate **5** in ~80% yield, with a diastereomeric ratio of ≥7:1. Hydrolysis of the acetate function was achieved in 85-93% yield with aqueous potassium hydroxide in THF/MeOH at 50 °C to yield phenol **6**, which was then alkylated with 4-(2-chloroethyl)morpholine hydrochloride in the presence of powdered NaOH and (Bu)₄NHSO₄ at 55 °C to yield *meta* regioisomer **10** in ~60% yield and as a single diastereomer within the detection limits of ¹H NMR

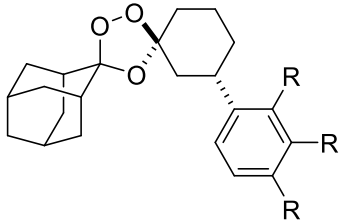
spectroscopy (>20:1 d.r.). Analogous procedures were employed to produce the other two regioisomers *ortho*-**9**, and *para*-**11**. The artefenomel congeners **9-11**, as well as the novel phenolic carbamates described later were all studied as racemic mixtures of *trans* enantiomers, with (*R,R*) and (*S,S*) configurations.

Given our hypotheses regarding the effects of *trans*-3" aryl substitution on trioxolane conformation and reactivity, we were keenly interested to evaluate the antiplasmodial activity of the three regioisomers (**Table 3-1**). We found that all three compounds retained antiplasmodial activity in the nanomolar range, but that all three were less potent than artefenomel, implying that the aryloxy morpholine side chain is more optimal for antiparasitic activity when in the *cis*-4" position. When incubated with human liver microsomes, the *ortho* isomer **9** was more rapidly metabolized than artefenomel, while the *para* and *meta* isomers **10** and **11** were superior to artefenomel. Compounds **9-11** and artefenomel as positive control were evaluated in the *P. berghei* mouse malaria model with a single oral dose of 20 mg/kg. While artefenomel cured all five animals in this study, analogs **9-11** showed variable efficacy in terms of days survival, with **10** and **11** more efficacious than **9**, but none of the new analogs produced cures at day 30 (**Figure S3-3**). On the other hand, **9-11** exhibited dramatically improved aqueous solubility compared to artefenomel, perhaps an effect of desymmetrization itself, since the lipophilicity of the regioisomers must be comparable to artefenomel. The good solubility, and reasonable *in vivo* efficacy of analogs **10** and **11**, led us to focus future work on additional analogs bearing *meta* or *para* substitutions of the aryl ring. The comparatively poor *in vivo* efficacy and *in vitro* metabolic stability of *ortho* isomer **9**, led us to deprioritize work on additional analogs with this substitution pattern.

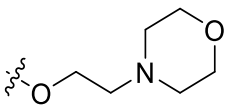
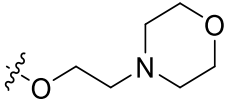
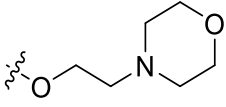
Table 3-1. Antiplasmodial Activity, Metabolic Stability, and Aqueous Solubility of Artefenomel and *trans*-3'' Aryl Congeners with Regioisomeric Side-Chain Substitution



Artefenomel



trans-R³ regioisomers

Compound	Side Chain	Position	<i>P. falciparum</i> IC ₅₀ (nM) ^a	HLM t _{1/2} (min) ^b	Aqueous Solubility (μM) ^c
artefenomel	-	-	11.2	21	0.181
9		<i>ortho</i>	53	4.9	-
10		<i>meta</i>	16	24.2	84.1
11		<i>para</i>	34	65.2	24.8

^aAverage of three determinations ± standard error in mean

^bData generated for this study by Quintara Biosciences, South San Francisco, CA. Verapamil is a positive control in the human liver microsome (HLM) assay

^cSolubility data generated for Artefenomel by MMV. Data generated for new analogues by Analiza Inc, Cleveland OH.

To explore the effect of carbamate substitutions of the 3'' aryl ring, we employed a two-step synthesis from late-stage intermediates **6-8** (**Figure 3-2**). Briefly, the phenol function was first activated as a *p*-nitrophenylcarbonate via reaction with 2-(4-nitrophenyl)acetyl chloride, DIPEA, and DMAP in dichloromethane. To this intermediate was added a reactive primary or secondary amine along with triethylamine in dichloromethane to yield the respective *meta*, *ortho*, and *para* phenolic carbamates in modest to high yield

depending on the amine reactant employed. For some analogues, a final deprotection step was required to reveal the basic amine function (Supplemental Info). This late-stage diversification approach mirrors that employed in our earlier studies of *trans*-3''-carbamates and is amenable to multigram synthesis and a wide scope of amine coupling partners.²

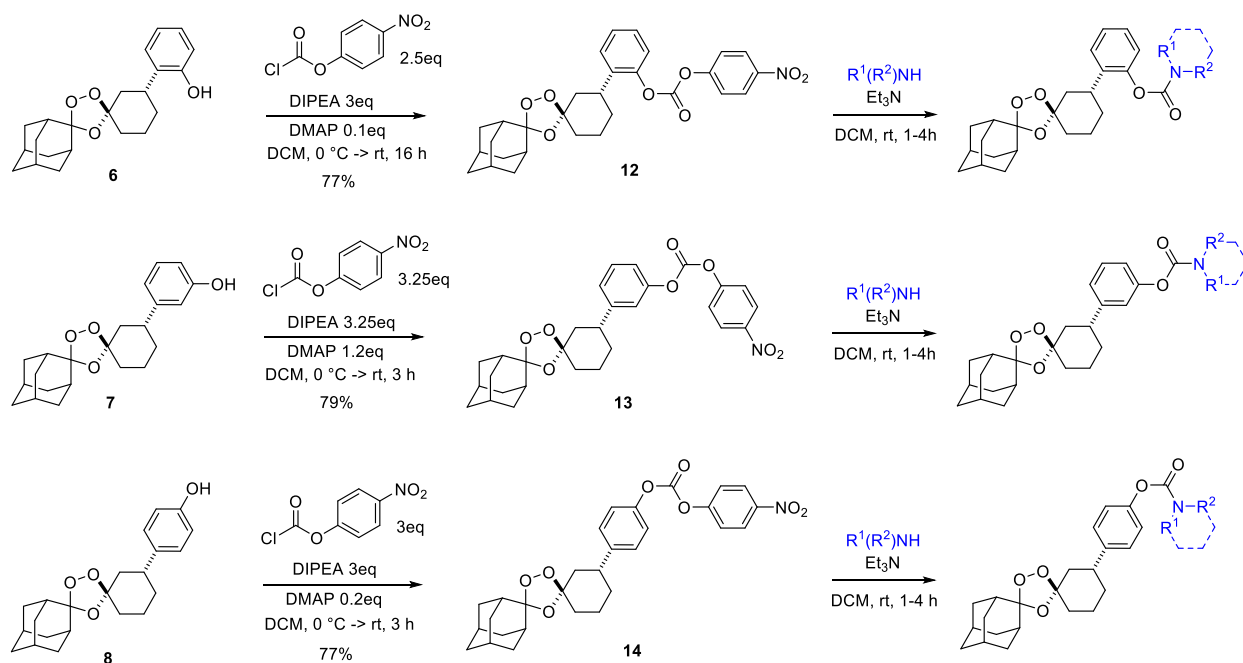
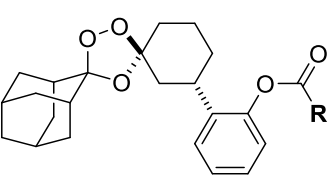


Figure 3-2. Synthesis of ortho, meta, and para- substituted 3'' phenolic carbamates.

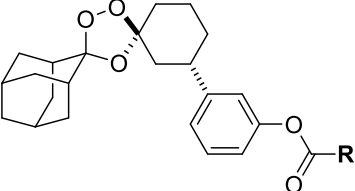
Using two favored amine building blocks from our carbamate study, we prepared the six congeneric analogs **15-20** as a means to evaluate the effect of *ortho*-, *meta*-, and *para*-aryl carbamate substitution on the antiparasitic activity, metabolic stability, and aqueous solubility (**Table 3-2**). All compounds in this initial series retained potent antiparasitic activity that was superior to aryl ethers **9-11**, while retaining the desired increase in solubility versus artefenomel. We also observed more favorable metabolic stability

profiles in the *meta*- and *para*-substituted 4-aminopiperadiny- (**16**, **17**) and 2-methyl-1,2-propanediamino- (**19**, **20**) analogues as compared to their respective *ortho* substituted stereoisomers (**15**, **18**). This further disincentivized additional work on the *ortho* substitution pattern and motivated a focus on the *meta* and *para* positions.

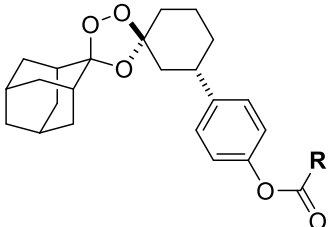
Table 3-2. Antiplasmodial Activity, Metabolic Stability, and Aqueous Solubility of *Ortho*, *Meta*, and *Para* Substituted TRX Carbamates



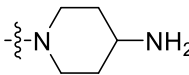
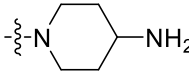
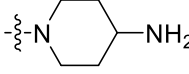
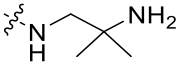
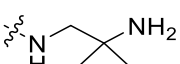
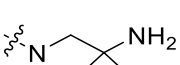
Ortho



Meta



Para

Compound	Position	Side Chain	<i>P. falciparum</i> IC ₅₀ (nM) ^a	HLM t _{1/2} (min) ^b	Aqueous Solubility (μM) ^c
15	<i>ortho</i>		17.2	33.8	54.8
16	<i>meta</i>		5.1	>120	48.7
17	<i>para</i>		6.1	>120	11.5
18	<i>ortho</i>		8.4	47.4	76.2
19	<i>meta</i>		8.8	>120	103.0
20	<i>para</i>		30.2	112.7	82.7

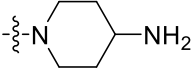
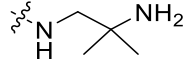
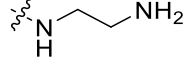
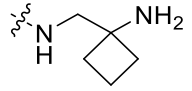
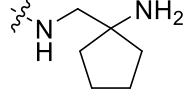
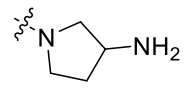
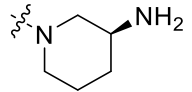
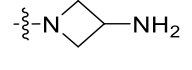
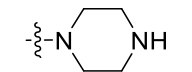
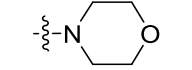
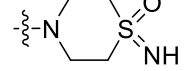
^aAverage of three determinations ± standard error in mean

^bData generated for this study by Quintara Biosciences, South San Francisco, CA. Verapamil is a positive control in the human liver microsome (HLM) assay

^cData generated for this study by Analiza Inc, Cleveland OH.

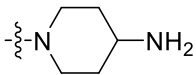
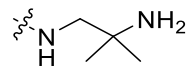
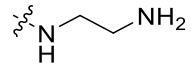
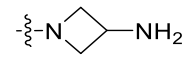
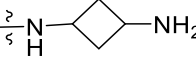
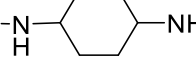
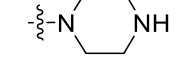
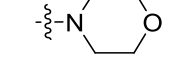
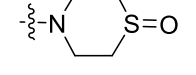
We proceeded using the synthesis described above to generate a larger selection of *meta*-aryl substituted phenolic carbamates **21-29** (Table 3-3). This series of analogs was conceived around iteration on the favored 2-methyl-1,2-propanediamino and 4-aminopiperidine aryl carbamate side chains from leads **16** and **19**. This involved deletion or cyclization of the geminal dimethyl motif (analogs **21-23**), 3-amino substitution of the piperidine ring and ring contraction to pyrrolidine and azetidine (analogs **24-26**), and finally replacement with morpholine, piperazine, and thiomorpholine sulfoximine (analogs **27-29**). Antiparasitic activities of this series of analogs was generally low to single digit nanomolar with the exception of the morpholine carbamate **28**, which exhibited only high nM activity. The presence of a primary amine in analogs **21-26**, as progenitors **16** and **19**, resulted in very favorable aqueous solubility, whereas a secondary amine in piperazine **27** or non-basic (thio)morpholine ring analogs **28** and **29** were at least 10-fold less soluble. All compounds showed generally favorable metabolic stability as judged by human liver microsome half-life, although among the new analogs only 21 was as stable as progenitors **16** and **19**. On balance of antiparasitic effect and ADME properties, meta carbamates **16**, **19**, **23**, **24**, and **26** appeared most promising.

Table 3-3. Antiplasmodial Activity, Metabolic Stability, and Aqueous Solubility of *Meta* Carbamate Series

Compound	Position	Side Chain	<i>P. falciparum</i> IC ₅₀ (nM) ^a	HLM t _{1/2} (min) ^b	Aqueous Solubility (μM) ^c
16	<i>meta</i>		5.1	>120	48.7
19	<i>meta</i>		8.8	>120	103.0
21	<i>meta</i>		44.0	>120	113.6
22	<i>meta</i>		18.8	67.1	82.5
23	<i>meta</i>		9.8	96.8	87.6
24	<i>meta</i>		2.6	75.4	24.6
25	<i>meta</i>		8.0	30.9	144.2
26	<i>meta</i>		20.0	49.0	97.7
27	<i>meta</i>		1.2	-	9.2
28	<i>meta</i>		249.1	13.5	6.1
29	<i>meta</i>		34.5	9.1	8.8

^aAverage of three determinations ± standard error in mean ^bData generated for this study by Quintara Biosciences, South San Francisco, CA. Verapamil is a positive control in the human liver microsome (HLM) assay ^cData generated for this study by Analiza Inc, Cleveland OH.

Table 3-4. Antiplasmodial Activity, Metabolic Stability, and Aqueous Solubility of *Para* Carbamate Series

Compound	Position	Side Chain	<i>P. falciparum</i> IC ₅₀ (nM) ^a	HLM t _{1/2} (min) ^b	Aqueous Solubility (μM) ^c
17	<i>para</i>		6.1	>120	11.5
20	<i>para</i>		30.2	112.7	82.7
30	<i>para</i>		41.2	82.0	78.5
31	<i>para</i>		72.8	101.1	97.7
32	<i>para</i>		4.7	>120	58.7
33	<i>para</i>		8.2	>120	6.2
34	<i>para</i>		7.0	119.6	4.7
35	<i>para</i>		42.8	61.2	< 2.1
36	<i>para</i>		119.8	11.9	47.7

^aAverage of three determinations ± standard error in mean ^bData generated for this study by Quintara Biosciences, South San Francisco, CA. Verapamil is a positive control in the human liver microsome (HLM) assay ^cData generated for this study by Analiza Inc, Cleveland OH.

We employed a similar SAR strategy in evaluating additional *para*-aryl carbamate analogues inspired by the favored side chains of **17** and **20**. These included ethylene diamine (**30**), amino-azetidine (**31**), and diamino cycloalkanes (**32** and **33**), as well as piperidine, morpholine, and thiomorpholine sulfoxide analogs **34-36** (Table 3-4).

Antiparasitic activity was in the low (**20**, **30-31**, **25**) to single-digit nM (**17**, and **32-34**) range, with the exception of thiomorpholine sulfoxide **36**. As in the *meta*-aryl series, the presence of a primary amine was generally correlated with good kinetic aqueous solubility, the exception being 4-aminocyclohexane **33**, which like morpholine (**34**) and piperazine (**35**) analogues, exhibited only low μM aqueous solubility. On the other hand, human liver microsome stability values were excellent across the *para*-aryl series, and superior overall to the *meta*-aryl series analogues. On balance of antiparasitic effect and ADME properties, *para* carbamates **17** and **32-34** appeared most promising for further study.

The *P. berghei* mouse model of malaria provides a convenient and relatively inexpensive means to evaluate the PK and PD properties of novel antimalarials. We used this model, together with the aforementioned *in vitro* human liver microsome stability and kinetic solubility data to drive our lead optimization effort, which aimed first to address the established clinical liabilities of artefenomel (poor physiochemical properties and insufficient long-term exposure in humans). In particular, we sought to identify one or more optimized analogs for progression into the humanized mouse malaria model,⁸ which employs SCID mice engrafted with human erythrocytes to enable infection by and *in vivo* efficacy assessment against the human-infective parasite *P. falciparum*.

A major caveat with the *P. berghei* model is its use of a mouse-infective plasmodium species that does not cause human disease. Additionally, the metabolic fate of our analogs in mice was unknown, since we chose to focus on human liver microsome stability as the primary gating criteria. The role of the *P. berghei* model was thus to compare the survival benefit of novel analogs following a single oral dose of 20 mg/kg,

as we described above for the initial regioisomers of artefenomel. Benchmarks for these studies were artefenomel (30 days survival) and the original *meta* and *para* artefenomel regioisomers **10** and **11** (~12 and ~15 days survival respectively). We first evaluated three carbamates from the *meta*-aryl series, including aminopiperidine **16**, and second-generation carbamates **23** and **24** (Table 3-3). Surprisingly, and despite exhibiting improved *P. falciparum* potencies and HLM stabilities compared to **10**, neither **16**, **23**, nor **24** provided any additional survival benefit over that afforded by **10** (Figure 3-3 and Figure S3-3).

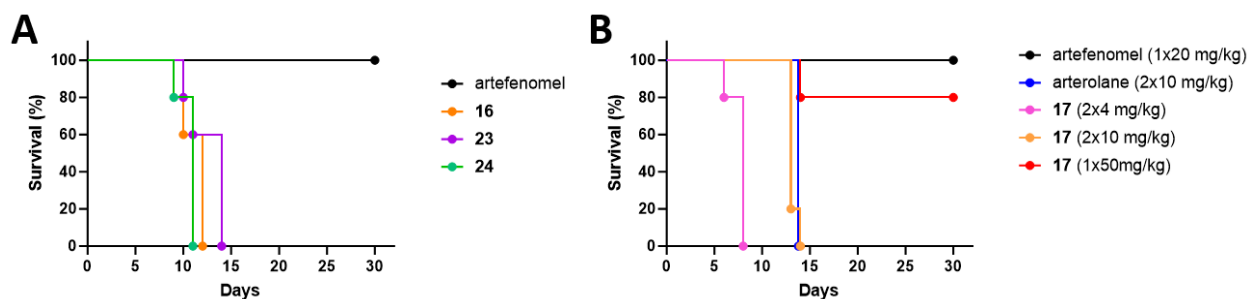


Figure 3-3. Efficacy of selected trioxolanes in rodent *P. berghei* malaria model (n=5 per group). A) 16, 23, 24 were not curative at single day 0 dose of 20mg/kg. B) **17** achieved 80% cure rate at day 0 dose of 50mg/kg.

Conceivably, this could reflect instability of the carbamate linker in mice (vs. ether in **10**), or sub-optimal PK in mice resulting from metabolism or clearance mechanisms not predicted by the human liver microsome assay employed for their selection. Ultimately, this disappointing result led us to deprioritize the *meta*-aryl carbamate series, and to focus our further in vivo studies on the *para*-aryl carbamates, which in general had exhibited superior human liver microsome stability (Table 3-4), and in the specific case of *para*-aryl ether **11**, showed superior in vivo efficacy vs. its *meta*-aryl congener **10** (Figure S3-3).

To gain insight into the properties of *para*-aryl carbamates, we selected aminopiperidine analogue **17** for more extensive in vivo study. This was due to the compound's combination of potent antiparasitic activity, excellent human liver microsome stability, and reasonable aqueous solubility that was notably superior to artefenomel if not ultimately as good as other *para*-aryl congeners (**Table 3-4**). We compared **17** to both arterolane and artefenomel, using both single-exposure and two-day dosing regimens in the *P. berghei* model (**Figure 3-3B**). Across three different regimens, we saw a clear dose dependence in the oral efficacy of **17**, with two days of daily dosing at 4 mg/kg affording little benefit over typical vehicle treated controls (<10 days survival), while two days of daily dosing at 10 mg/kg afforded improved efficacy (~14 days survival) that was comparable to arterolane at the same dose. Finally, we found that a single oral dose of **17** at 50mg/kg dose extended survival to the end of the experiment (30 days) in 4 of 5 mice, and thus was nearly as efficacious as artefenomel at a single 20 mg/kg dose (**Figure 3-3B**). Since a dose of **17** ~2.5-fold higher than artefenomel was required to achieve similar in vivo efficacy, we explored whether the exposure of artefenomel in mice was higher than **17**, as was suggested by mouse liver microsome data obtained for the two compounds (**Table 3-5**).

Table 3-5. Divergent microsome stability profile of **17** and artefenomel in human and mouse liver microsomes. Data generated by MMV.

compound	Human Microsome Clearance μL/min/mg	Mouse Microsome Clearance μL/min/mg
17	6.0	14.1
artefenomel	72.1	8.4

In a PK study sponsored by NIAID and performed at SRI International, we compared the plasma exposure of **17** and artefenomel following a single 50 mg/kg oral dose in CD-1 mice (**Figure 3-4**). Notably, artefenomel and **17** exhibited a similar and extended elimination profile with plasma concentrations at 24 hours (1.3 μ M and 0.37 μ M, respectively) that were well in excess of their respective low-nM IC₅₀ values. By comparison, three TRX-C analogs evaluated in the same study were undetectable in plasma at the 24-hour timepoint (data not shown). Despite their similar elimination profiles, however, artefenomel did exhibit a notable five-fold higher C_{max} value and three-fold higher AUC_{last} value as compared to **17** (**Table 3-6**). Thus, the extended elimination profile of these compounds likely explains their ability to achieve single-exposure cures, while the roughly three-fold higher total exposure of artefenomel is consistent with its ability to achieve cures at roughly three-fold lower dose of 20 mg/kg. The combined results from the *P. berghei* model, mouse PK study, and in vitro ADME profiling of **17** were highly encouraging. Most notably, compound **17** exhibits similar low-nM potency as artefenomel against clinically relevant *P. falciparum* parasites, while exhibiting enhanced solubility (~100-fold) and significantly improved human liver microsome stability (HLM T_{1/2} > 120 min vs. 21 min). The combined data may well predict superior drug exposure and efficacy in humans for **17**, although additional PK data as well as allometric scaling analyses will be required to confirm this prediction.

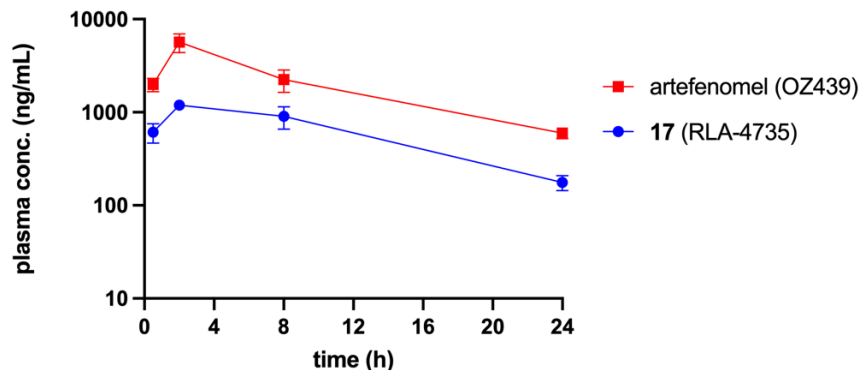


Figure 3-4. Plasma PK profile of compound **17** and artefenomel following a single oral dose of 50 mg/kg in CD-1 mice (data from SRI study B103-18, sponsored by NIAID).

Table 3-6. Selected pharmacokinetic parameters calculated from the PK study and data shown in Figure 3-4.

compound	T _{max} (hr)	C _{max} (ng/mL)	AUC _{last} (hr•ng/mL)
artefenomel	2	5660 ± 732	52600 ± 4810
17	2	1190 ± 58	16400 ± 1640

We were interested in comparing the rates of iron fragmentation for **17** and artefenomel, in light of their similar *in vitro* and *in vivo* pharmacology and our original hypothesis regarding the conformational effects of *trans*-3" aryl substitution vs. canonical *cis*-4" substitution. We previously developed and reported an *in vitro* iron fragmentation assay wherein the rate of endoperoxide fragmentation in the presence of a ferrous iron source is evaluated over time via UPLC/MS quantification of a stable ketone fragmentation product.¹⁰ We leveraged this platform to monitor the fragmentation of artefenomel (**2**) to yield ketone **2a** and of **17** to produce the analogous product **17a** in the presence of ferrous ammonium sulfate under anaerobic conditions (**Figure 3-5A**). We observed the reaction

of **17** with ferrous iron to proceed at comparable or slightly slower rates compared to **2**, as judged by UPLC analysis of the reaction course (**Figure 3-5B** and **3-5C**). These data appear to corroborate our original hypothesis that *trans*-3'' substitution would modulate iron reactivity in a regime similar to that of *cis*-4'' substitution. Moreover, both **17** and **2** were dramatically more stable towards ferrous iron than a representative TRX-C analog used for comparison ($T_{1/2}$ of minutes vs. hours, data not shown). This more dramatic difference in rates is consistent with a more severe 1,3-diaxial interaction in the iron-reactive conformation of 3''-aryl TRX-P analogs (**17** and **2**), as compared to less sterically demanding 3''-substituents present in TRX-C analogs.

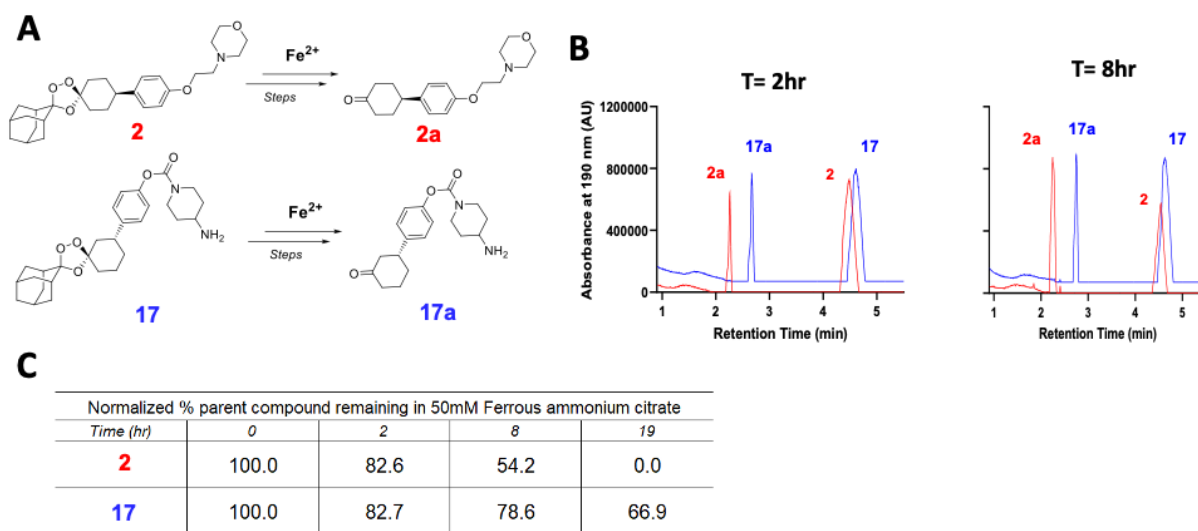


Figure 3-5. Reaction time-course of **17** and artefenomel (**2**) in 50mM ferrous ammonium sulfate under anaerobic conditions. A) Ketone products formed in the iron-promoted reactions of trioxolanes. B) Two and eight hour timepoint UPLC traces show more **17** remaining at 8 hours. C) Extended monitoring of fragmentation shows more than half of **17** parent remaining when **2** has completely reacted.

We next turned our attention to the activity of **17** against K13 mutant parasites. We employed the ring stage survival assay, the gold standard *in vitro* assay for evaluating the

artemisinin delayed-clearance phenotype.¹¹ Briefly, tightly synchronized 0-3hr post-invasion ring-stage parasites were exposed to a hyperlethal drug concentration of 700nM for 6 hours, followed by removal of media and drug pressure, and finally quantification of parasitemia after an additional 72 hours of recovery. The cited WWARN protocol was implemented with additional drug washing steps given the confounding effect of trioxolane lipophilicity in leading to residual drug concentrations under less stringent protocols.¹²

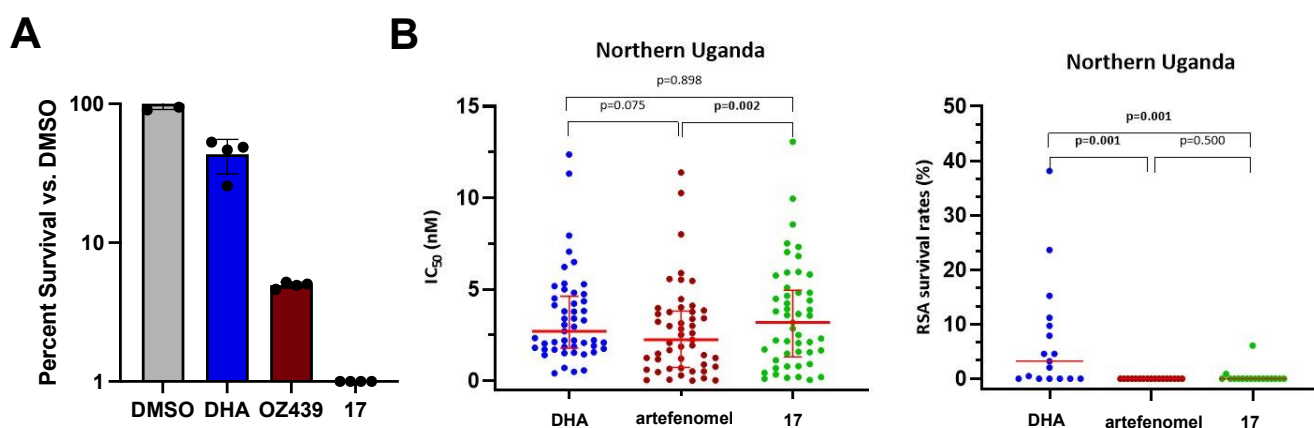


Figure 3-6. Ring Stage Survival data for DHA, artefenomel (OZ439), and **17**, wherein 0-3hr postinvasion rings are pulsed with 700nM drug pressure for 6 hours and quantified after 72hr recovery. A) K13 C580Y parasites survive DHA and artefenomel exposure but are completely eliminated by **17**. B) artefenomel and **17** activities vs. DHA against Ugandan clinical isolates of *P. falciparum* in IC₅₀ (left panel) and RSA (right panel) assays.

Against a lab-adapted K13 C580Y strain of *P. falciparum* (BEI resources), **17** demonstrated complete elimination of parasitemia (**Figure 3-6A**). Compound **17** additionally retained potent antiparasitic activity against a selection of Ugandan clinical isolates collected in 2023, including parasites with the artemisinin partial resistance phenotype (**Figure 3-6B**). These results are consistent with previous studies of

artefenomel against K13 mutant parasites¹³ and corroborate a proposed model wherein extending the cytotoxic exposure time of synthetic ozonides may directly overcome K13-driven partial artemisinin resistance^{5 14}

To further assess the potential of **17** as a development candidate, we sought to independently evaluate the (*R,R*) and (*S,S*) forms given the potential superiority of one of these enantiomers, and the strong preference in clinical development for the study of stereochemically defined and pure drug substances. We applied a stereoselective synthesis based on O'Neill's published route to enantiomerically enriched forms of the 4-aryl ketone intermediate we used in our synthesis of **17** (**Figure 3-7**).^{15 2} Setting this stereocenter would then dictate the absolute stereochemistry at the trioxolane ring carbon atom, due to the diastereoselectivity of the Griesbaum co-ozonolysis as described above.

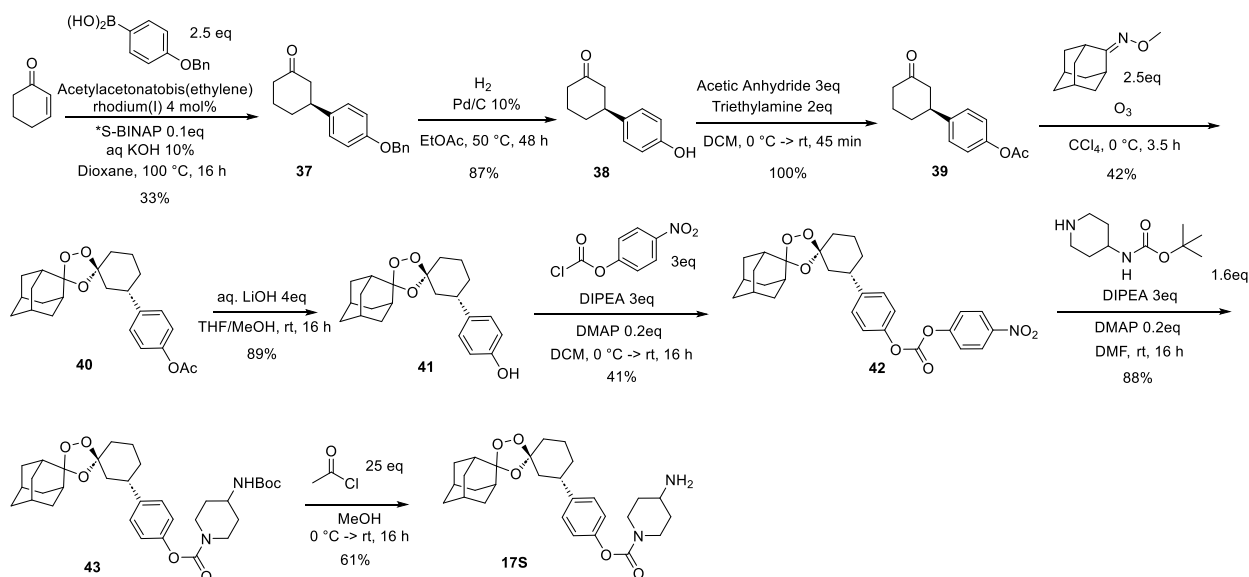


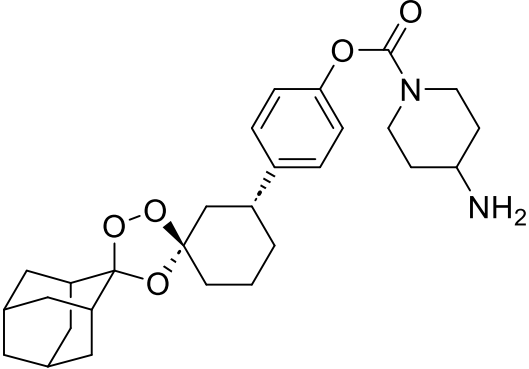
Figure 3-7. Enantioselective synthesis of (*S,S*) stereoisomer **17S**. The (*R,R*) form **17R** was synthesized analogously but with R-BINAP used in the first step.

This route employs a Rh(acac)(C₂H₄)₂-mediated conjugate addition with a chiral BINAP directing ligand and aqueous potassium hydroxide in dioxane at 100 °C to yield the (R)- or (S)-ketone **37** in modest yields. The benzyl protecting group was removed via hydrogenation over Pd/C in ethyl acetate at 50 °C, followed by acetylation with acetic anhydride and triethylamine in dichloromethane. The ketone (S)-**39** was carried through the synthesis exactly as described for (±)-**17** previously to yield (S,S)-**17** (**17S**). Synthetic **17R** and **17S** showed distinct well separated peaks by chiral UPLC analysis, when analyzed individually (**Figure S3-4A** and **S3-4B**) or as a single co-injected sample (**Figure S3-4C**) with retention times for the enantiomers that matched those of previously synthesized racemic **17** when analyzed on the same column (**Figure S3-4D**).

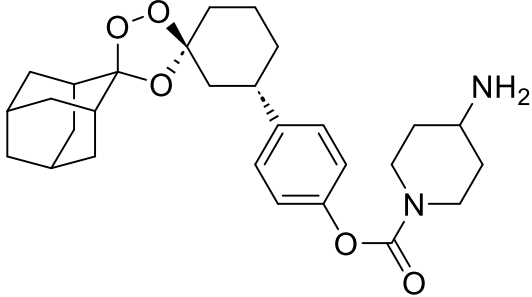
The enantiomers **17R** and **17S** retained potent antiparasitic effects that were comparable to racemic **17**, and both forms also exhibited excellent metabolic stability as evaluated in human liver microsomes (**Table 3-7**). Interestingly, the measured kinetic solubility of the enantiopure isomers **17S** and **17R** in PBS pH 7.4 was significantly higher than that for the racemic material. While we initially hypothesized that this difference could be attributable to a difference in salt form (the racemate having been originally purified in a different mobile phase than for the enantiomers), subjecting (±)-**17** to identical chromatography conditions as used for the enantiomers and did not lead to higher solubilities in a follow-up assay (**Table S3-1**). It is known that differences in crystal lattice energies can impact aqueous solubility and is therefore plausible that solid- or solution-phase intermolecular interactions of the two enantiomers present in (±)-**17** accounted for the reduced solubility of the racemate in these assays.¹⁶ Alternatively, these effects could be related to the colloidal behavior of some amphiphilic molecules, a phenomenon described already for

artefenomel, and worthy of future investigation for **17**.¹⁷ In any event, the similar antiplasmodial activities and in vitro ADME properties of **17R** and **17S** were consistent with their excellent performance in the *P. berghei* model, where both forms achieved complete cures of all animals with a single 50mg/kg dose (**Figure 3-8**).

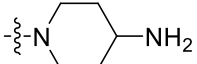
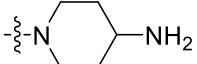
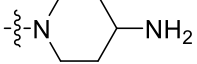
Table 3-7. Metabolic Stability, Aqueous Solubility, and Antiplasmodial Activity of artefenomel and **17** in racemic and enantiomerically pure forms.



RLA-5763 (**17R**)



RLA-5764 (**17S**)

Compound	Side Chain	Stereochem	<i>P. falciparum</i> IC ₅₀ (nM) ^a	HLM t _{1/2} (min) ^b	Aqueous Solubility (μM) ^c
artefenomel	-	-	2.15	21	0.18
17		racemic	6.1	229.7	11.5
17R		(<i>R,R</i>)	3.8	>120	163.7
17S		(<i>S,S</i>)	2.9	>120	79.7

^aAverage of three determinations ± standard error in mean ^bData generated for this study by Quintara Biosciences, South San Francisco, CA. Verapamil is a positive control in the human liver microsome (HLM) assay ^cData generated for this study by Analiza Inc, Cleveland OH.

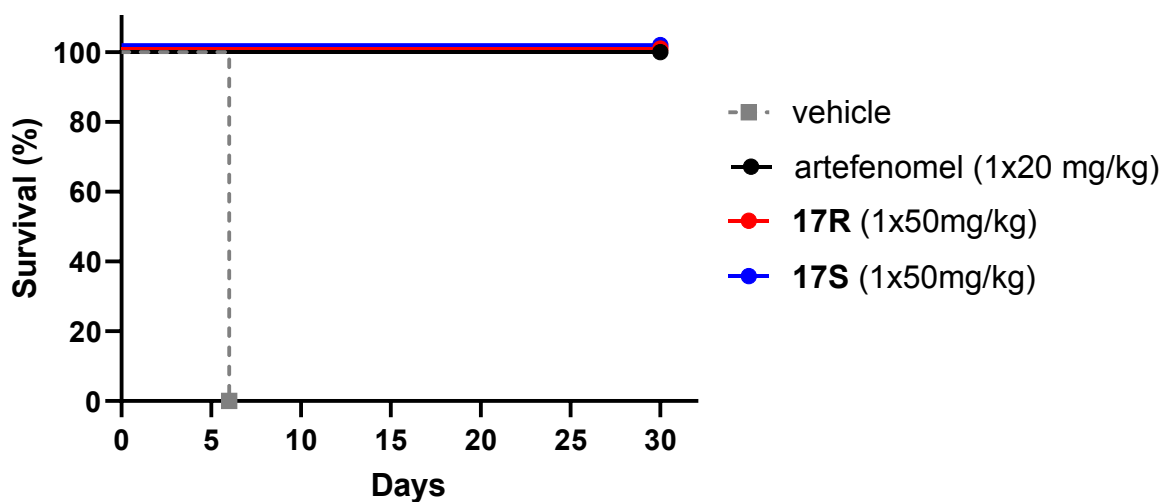


Figure 3-8. Efficacy of **17R**, **17S**, and OZ439 in the *P. berghei* mouse model of malaria. **17R** and **17S** afforded cures in 5 of 5 mice following a single dose of 50mg/kg. Artefenomel is efficacious at a single 20 mg/kg dose as previously noted.

The costs and complexity of clinical development for a small molecule therapeutic are reduced when performed on a stereochemically defined and pure drug substance. While **17R** and **17S** exhibited almost identical antiplasmodial, in vitro ADME and PK properties, we selected **17S** for further study based on its modestly but consistently superior in vitro IC₅₀ values against *P. falciparum* isolates (**Table 3-8**).

Table 3-8. *In vitro* Antiplasmodial efficacy of **17R** and **17S** against lab-adapted Ugandan clinical isolates of *P. falciparum* bearing K13 mutation and high RSA value.

Compound	<i>P. falciparum</i> K13 A578S IC ₅₀ (nM)	<i>P. falciparum</i> K13 C469Y IC ₅₀ (nM)	<i>P. falciparum</i> K13 WT, High RSA IC ₅₀ (nM)	<i>P. falciparum</i> K13 C469Y ^a IC ₅₀ (nM)	<i>P. falciparum</i> K13 C469Y ^a IC ₅₀ (nM)
17R	2.78 ± 1.46	1.34 ± 0.55	0.73 ± 0.37	1.90 ± 1.02	0.50 ± 0.18
17S	1.56 ± 0.84	0.16 ± 0.03	0.29 ± 0.07	0.76 ± 0.23	0.50 ± 0.21

^aThese indicate separate strains with identical K13 genotypes.

With input from Medicines Malaria Venture (Jeremy Burrows, personal communication) we subjected **17S** to an expanded panel of in vitro ADME assays that would establish key parameters useful for the prediction of human exposure and efficacious doses (**Table 3-9**). Thus, we found **17S** to be highly stable toward metabolism by liver microsomes and hepatocytes in rat, dog, and human, exceeding the upper limit of detection in nearly all conditions studied. We found **17S** was very highly protein bound (>99.9%) in plasma of all three species, as well as in human hepatocytes and microsomes. Despite very high protein binding, **17S** was observed to partition effectively into human red blood cells (the desired site of antimalarial action), with a blood-to-plasma ratio of 1.61 and a partitioning coefficient $K_{RBC/PL}$ of 3.55, values similar to those of the clinical antimalarial chloroquine. Also consistent with high protein binding was an orders-of-magnitude difference in thermodynamic solubility performed in fasted-state (FaSSIF) vs. fed-state (FeSSIF) simulated intestinal fluid. Taken together, these results suggest a highly protein-bound drug substance that comprises a “depot” of available drug, but with a protein off-rate sufficient to enable partitioning into the erythrocyte compartment where its efficacy can be realized. To assess intestinal absorption upon oral dosing, we performed Caco-2 permeability studies using both HBSS pH 7.4 or human plasma pH 7.4 as assay media, the latter approach previously reported to more accurately predict permeability for highly protein bound compounds.¹⁸ When the assay was performed in human plasma as media, total recovery of drug was much higher, suggesting reduced adhesion/loss of drug on the experimental apparatus. When apparent permeability was corrected for the fraction unbound in human plasma (0.06%), **17S** was found to exhibit exceptionally high

permeability rates in both the apical to basal ($1,074 \times 10^6$ cm/s) and basal to apical directions (284×10^6 cm/s).

Table 3-9. ADME Properties of **17S**, **17**, and relevant controls.^a

	Metabolic Stability							
	Microsome t1/2 By Species (min)			Hepatocyte t1/2 By Species (min)				
	Rat	Dog	Human	Rat	Dog	Human		
17S	>240	>240	>240	276.3	>480	>480		
<i>Verapamil</i>	5.1	9.1	8.0					
<i>Midazolam</i>				20.38	36.94	92.63		
	Binding and Distribution							
	Plasma Protein binding by species (%)			Human Hepatocyte Protein Binding (%)	Human Microsome Protein Binding (%)	Blood-to-Plasma Ratio	KRBC/PL	
	Rat	Dog	Human					
17S	>99.98	>99.98	>99.98	99.91	99.94	1.61	3.55	
<i>Propranolol</i>	90.65	86.74	82.75					
<i>Warfarin</i>	99.38	94.71	99.20					
<i>Chlorpromazine</i>				99.01	92.21			
<i>Chloroquine</i>						2.04	2.51	
	Solubility and Permeability							
	Thermodynamic Solubility (µg/mL)		Caco-2 apparent permeability, Papp A-B in pH 7.4 plasma (x10 ⁻⁶ cm/s)	Caco-2 apparent permeability, Papp B-A in pH 7.4 plasma (x10 ⁻⁶ cm/s)	Corrected Caco-2 permeability, Papp A-B in pH 7.4 plasma ^b (x10 ⁻⁶ cm/s)	Corrected Caco-2 permeability, Papp B-A in pH 7.4 plasma ^b (x10 ⁻⁶ cm/s)		
	FaSSIF (pH 6.5)	FeSSIF (pH 5.0)						
17S	2.3	4525.5	0.6	0.2	1074	284		
<i>Digoxin</i>			1.4	4.2				
<i>Propranolol</i>			10.5	4.2	65	26		

^aData generated for this study by Quintara Biosciences, South San Francisco, CA
^bCorrected permeability values are adjusted to account for the unbound fraction of drug as reported in ref. (18)

As expected for highly soluble and permeable drug substances, a PK study of (\pm)-**17** in mice with both oral (50 mg/kg) and IV (10 mg/kg) dosing, revealed **17** to have excellent exposure and bioavailability following an oral dose, with an extended elimination profile that was similar to that in the earlier SRI study described above (**Figure 3-9**).

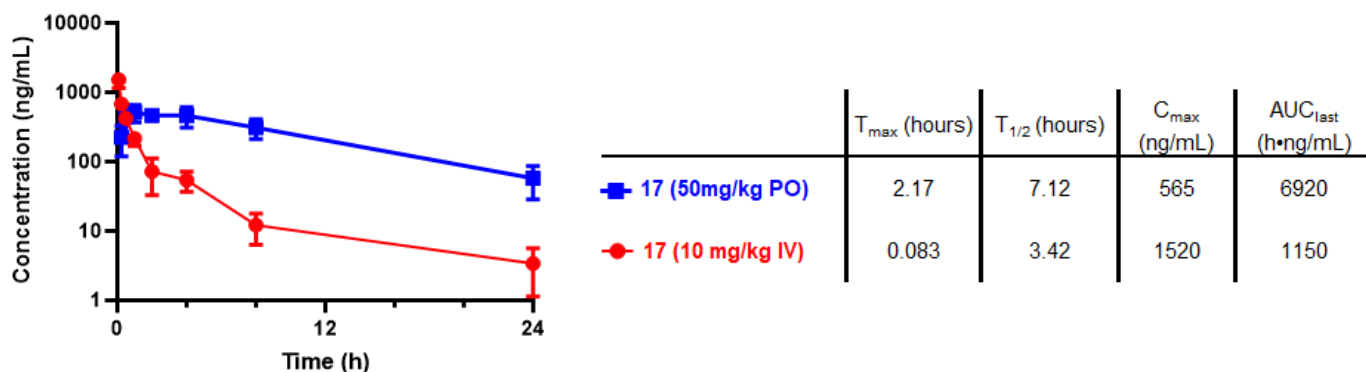


Figure 3-9. Plasma PK profile of compound **17** following PO (50 mg/kg) and IV (10 mg/kg) dosing in CD-1 mice (data from Viva Biotech and Tataru Therapeutics).

CONCLUSIONS

Here, we describe the synthesis and evaluation of *trans*-3''-aryl substituted congeners of artefenomel with a focus on carbamate-linked phenols bearing basic amine or other solubilizing functionality. We generally found this chemotype to exhibit comparable antiparasitic activity against standard lab strains as well as improved metabolic stability and solubility relative to artefenomel. We found that the optimized analog (\pm)-**17** could completely eliminate K13 C580Y *P. falciparum* parasites in the ring stage survival assay and was effective against clinical *P. falciparum* strains available at UCSF and against strains tested in the field in Northern Uganda. We furthermore report a stereoselective route to the enantiomeric forms **17R** and **17S** and observed increased solubility of the

separate enantiomers versus the racemate. Finally, we performed more extensive profiling of **17S** as a potential development candidate and found the compound to exhibit a protein binding and metabolic stability profile we predict should translate to extended drug exposures in human malaria patients. Together these results demonstrate the utility of ozonide-class antimalarials bearing *trans*-3" phenolic carbamates and present **17S** as a compelling candidate for further preclinical evaluation.

METHODS

EC₅₀ of experimental compounds against cultured *P. falciparum* parasites

Erythrocytic cultures of *P. falciparum* strain Dd2 (BEI Resources) and CamWT_C580Y (BEI Resources) were maintained using standard methods at 2% hematocrit in RPMI 1640 medium (Invitrogen) supplemented with 0.5% AlbuMAX II (Gibco Life Technologies), 0.1mM hypoxanthine, 30ug/mL gentamicin, 24mM NaHCO₃, and 25mM HEPES pH 7.4 at 37°C in an atmosphere of 5% O₂, 5% CO₂, and 90% N₂. Infected cultures were exposed to 12 drug concentrations (12 point, 3-fold serial dilution from 10µM -> 0.06nM) or an equal volume of DMSO with tips changed between each serial dilution to minimize potential carryover of lipophilic compounds. Test plates were incubated at 37°C under the above atmosphere for 72 hours, following which erythrocytes were pelleted and fixed in 2% formaldehyde in PBS (pH 7.4) at room temperature overnight. 2% Formaldehyde PBS was removed and parasites were resuspended in permeabilization media (100mM NH₄Cl, 0.1% Triton-X, PBS pH 7.4) with freshly added 25nM YOYO-1 fluorescent dye. Plates were incubated at 4°C for a minimum of 24 hours. Parasitemia was determined from dot plots of 5x10⁴ cells acquired on a FACSCalibur flow cytometer using CELLQUEST software (Becton Dickinson), using initial gating values determined using unstained uninfected erythrocyte and stained uninfected erythrocyte controls. IC₅₀s were determined using GraphPad Prism software with 3 experimental replicates per compound.

Ring Stage Survival Assay

The ring stage survival assay was performed according to protocols established by Witkowski et al. Erythrocytic cultures of *P. falciparum* strain Dd2 (BEI Resources) and CamWT_C580Y (BEI Resources) were maintained using standard methods at 2% hematocrit in RPMI 1640 medium (Invitrogen) supplemented with 0.5% AlbuMAX II (Gibco Life Technologies), 0.1mM hypoxanthine, 30ug/mL gentamicin, 24mM NaHCO₃, and 25mM HEPES pH 7.4 at 37C in an atmosphere of 5% O₂, 5% CO₂, and 90% N₂. Parasite cultures were synchronized by three 5% sorbitol treatments. Parasites at the mature schizont stage were selected using segmentation in 75% percoll to yield a highly synchronous culture which was returned to standard incubation conditions for 3 hours. Cultures were then sorbitol synchronized again to yield exclusively 0-3hr postinvasion rings (100% by stage). 0-3hr postinvasion rings at 1% parasitemia were exposed to experimental compounds at 700nM or an equal volume of DMSO for 6 hours, washed three times, and resuspended in drug-free culture medium in fresh plates at 37C for 66 hours. Giemsa-stained thin smears for each group were assessed microscopically to determine postexposure parasitemia. Four experimental replicates were completed for all drug and control groups.

***P. berghei* Mouse Malaria Model**

Female Swiss Webster mice (~20 g body weight) were infected intraperitoneally with 10⁶*P. berghei*-infected erythrocytes collected from a previously infected mouse. Beginning 1 h after inoculation the mice were treated once daily by oral gavage for 1–2 days as indicated with 100 µL of solution of test compound formulated in 10% DMSO,

40% of a 20% 2-hydroxypropyl-beta-cyclodextrin solution in water, and 50% PEG400. There were five mice in each test arm. Infections were monitored by daily microscopic evaluation of Giemsa-stained blood smears starting on day seven. Parasitemia was determined by counting the number of infected erythrocytes per 1000 erythrocytes. Body weight was measured over the course of the treatment. Mice were euthanized when parasitemia exceeded 50% or when weight loss of more than 15% occurred. Parasitemia, animal survival, and morbidity were closely monitored for 30 days postinfection, when experiments were terminated.

Animal Welfare

No alternative to the use of laboratory animals is available for in vivo efficacy assessments. Animals were housed and fed according to NIH and USDA regulations in the Animal Care Facility at San Francisco General Hospital. Trained animal care technicians provide routine care, and veterinary staff are readily available. Euthanasia was performed when malarial parasitemia exceeded 50%, a level that does not appear to be accompanied by distress but predicts progression to lethal disease. Euthanasia was accomplished with CO₂ followed by cervical dislocation. These methods are in accord with the recommendations of the Panel on Euthanasia of the American Veterinary Medical Association. Our studies are approved by the UCSF Committee on Animal Research.

Materials

All chemical reagents were obtained commercially and used without further purification unless otherwise stated. Anhydrous solvents were purchased from Sigma-Aldrich and were used without further purification. Solvents used for flash column chromatography and workup procedures were purchased from either Sigma-Aldrich or Fisher Scientific. Column chromatography was performed on Silicycle Sili-prep cartridges using a Biotage Isolera Four automated flash chromatography system.

Instrumentation

NMR spectra were recorded on a Bruker Avance III HD 400 MHz (with 5 mm BBFO Z-gradient Smart Probe), calibrated to CH(D)Cl₃ as an internal reference (7.26 and 77.00 ppm for ¹H and ¹³C NMR spectra, respectively). Data for ¹H NMR spectra are reported in terms of chemical shift (δ , ppm), multiplicity, coupling constant (Hz), and integration. Data for ¹³C NMR spectra are reported in terms of chemical shift (δ , ppm), with multiplicity and coupling constants in the case of C-F coupling. The following abbreviations are used to denote these multiplicities: s = singlet, d = doublet, t = triplet, q = quartet, m = multiplet, br = broad, app = apparent, or combinations of these. LC-MS and compound purity were determined using a Waters Micromass ZQ 4000, equipped with a Waters 2795 Separation Module, a Waters 2996 Photodiode Array Detector, and a Waters 2424 ELSD. Separations were carried out with an XBridge BEH C18, 3.5 μ m, 4.6 mm \times 20 mm column, at ambient temperature (unregulated) using a mobile phase of water-methanol containing a constant 0.10% formic acid.

For synthetic procedures and characterization data, please refer to Chapter S3 (Supporting Information for Chapter 3).

REFERENCES

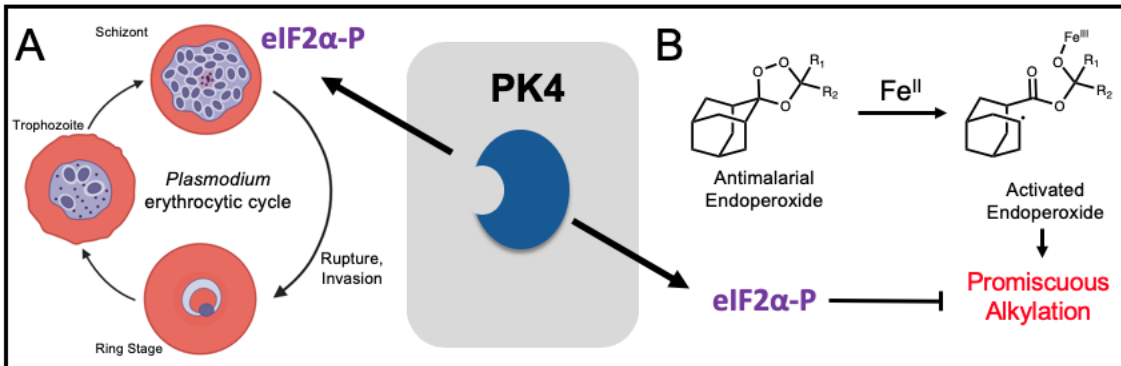
1. Blank, B. R., Gut, J., Rosenthal, P. J. & Renslo, A. R. Enantioselective Synthesis and in Vivo Evaluation of Regioisomeric Analogues of the Antimalarial Arterolane. *J. Med. Chem.* **60**, 6400–6407 (2017).
2. Blank, B. R. *et al.* Antimalarial Trioxolanes with Superior Drug-Like Properties and In Vivo Efficacy. *ACS Infect. Dis.* **6**, 1827–1835 (2020).
3. Macintyre, F. *et al.* A randomised, double-blind clinical phase II trial of the efficacy, safety, tolerability and pharmacokinetics of a single dose combination treatment with artefenomel and piperazine in adults and children with uncomplicated Plasmodium falciparum malaria. *BMC Med.* **15**, 181 (2017).
4. Sanofi. *A Randomized, Open Label, Parallel-group, Single Dose Regimen, Phase 2a Study, to Investigate the Clinical and Parasitocidal Activity and the Pharmacokinetics of 3 Dose Levels of Artefenomel (OZ439) Given in Combination With Ferroquine (FQ) and FQ Alone, in African Patients With Uncomplicated Plasmodium Falciparum Malaria.* <https://clinicaltrials.gov/study/NCT03660839> (2022).
5. Tilley, L., Straimer, J., Gnädig, N. F., Ralph, S. A. & Fidock, D. A. Artemisinin Action and Resistance in Plasmodium falciparum. *Trends Parasitol.* **32**, 682–696 (2016).
6. Blank, B. R., Gut, J., Rosenthal, P. J. & Renslo, A. R. Artefenomel Regioisomer RLA-3107 Is a Promising Lead for the Discovery of Next-Generation Endoperoxide Antimalarials. *ACS Med. Chem. Lett.* **14**, 493–498 (2023).

7. Fontaine, S. D., DiPasquale, A. G. & Renslo, A. R. Efficient and Stereocontrolled Synthesis of 1,2,4-Trioxolanes Useful for Ferrous Iron-Dependent Drug Delivery. *Org. Lett.* **16**, 5776–5779 (2014).
8. Siu, E. & Ploss, A. Modeling malaria in humanized mice: opportunities and challenges. *Ann. N. Y. Acad. Sci.* **1342**, 29–36 (2015).
9. Dong, Y. *et al.* The Structure–Activity Relationship of the Antimalarial Ozonide Arterolane (OZ277). *J. Med. Chem.* **53**, 481–491 (2010).
10. Gonciarz, R. L. *et al.* Elevated labile iron in castration–resistant prostate cancer is targetable with ferrous iron–activatable antiandrogen therapy. *Eur. J. Med. Chem.* **249**, 115110 (2023).
11. Witkowski, B., Menard, D., Amaratunga, C. & Fairhurst, R. Ring-stage Survival Assays (RSA) to evaluate the in-vitro and ex-vivo susceptibility of Plasmodium falciparum to artemisinins. *Natl. Inst. Health Proced. RSAv1* 1–16 (2013).
12. Yang, T. *et al.* Comparison of the Exposure Time Dependence of the Activities of Synthetic Ozonide Antimalarials and Dihydroartemisinin against K13 Wild-Type and Mutant Plasmodium falciparum Strains. *Antimicrob. Agents Chemother.* **60**, 4501–4510 (2016).
13. Walz, A., Leroy, D., Andenmatten, N., Mäser, P. & Wittlin, S. Anti-malarial ozonides OZ439 and OZ609 tested at clinically relevant compound exposure parameters in a novel ring-stage survival assay. *Malar. J.* **18**, 427 (2019).
14. Klonis, N. *et al.* Altered temporal response of malaria parasites determines differential sensitivity to artemisinin. *Proc. Natl. Acad. Sci.* **110**, 5157–5162 (2013).

15. Woodley, C. M. *et al.* Enantioselective Synthesis and Profiling of Potent, Nonlinear Analogues of Antimalarial Tetraoxanes E209 and N205. *ACS Med. Chem. Lett.* **12**, 1077–1085 (2021).
16. Salahinejad, M., Le, T. C. & Winkler, D. A. Aqueous Solubility Prediction: Do Crystal Lattice Interactions Help? *Mol. Pharm.* **10**, 2757–2766 (2013).
17. Clulow, A. J., Salim, M., Hawley, A., Gilbert, E. P. & Boyd, B. J. The Curious Case of the OZ439 Mesylate Salt: An Amphiphilic Antimalarial Drug with Diverse Solution and Solid State Structures. *Mol. Pharm.* **15**, 2027–2035 (2018).
18. Katneni, K. *et al.* Using Human Plasma as an Assay Medium in Caco-2 Studies Improves Mass Balance for Lipophilic Compounds. *Pharm. Res.* **35**, 210 (2018).

Chapter 4
Targeting Translation Repression in *P. falciparum*

ABSTRACT



Graphical Abstract. Proposed Model: Translation repression via PK4-mediated eIF2 α phosphorylation is (A) critical for the *Plasmodium* erythrocytic cycle and (B) functions as an adaptive response to the mechanism of action of endoperoxide antimalarials.

The *Plasmodium* genus of intracellular erythrocytic parasites, the causative agents of malaria, tightly regulate translational programs to navigate their diverse life cycle stages and to manage proteostasis and responses to cellular insult. Global translation repression via phosphorylated eukaryotic initiation factor 2 α (eIF2 α -P) is thought to mediate critical life cycle transitions and may also represent the primary parasite response to protein misfolding stress.^{1,2} This is of immediate therapeutic interest, as frontline artemisinin antimalarials and the related trioxolane endoperoxides broadly disrupt proteostasis.³ Translation repression via eIF2 α -P might conceivably play a role in the parasite response to endoperoxide-mediated cytotoxicity resulting from protein modification/alkylation in addition to its suspected role in parasite proliferation. Consistent with this notion, inhibiting the *Plasmodium* eIF2 α kinase PK4 arrests the growth of blood-stage parasites and eliminates latency in parasite sub-populations that otherwise survive artemisinin treatment.⁴ Despite the potential therapeutic benefits of inhibiting translation repression, this pathway remains untargeted by current antimalarial drugs and clinical

candidates.⁵ Rigorous validation of these drug targets has been hamstrung by a lack of potent or selective PK4 inhibitors and by incomplete evidence that phosphorylated eIF2 α (eIF2 α -P) is the primary mediator of the parasite stress response to endoperoxide exposure. Herein we describe the screening of an advanced set of drug-like inhibitors of PERK kinase, the human homolog of PK4, against *P. falciparum*, yielding several potent antiparasitic agents.

MAIN

Malaria, a mosquito-borne disease caused by the *Plasmodium* genus of eukaryotic intracellular parasites, remains a crucial public health challenge. Limited existing therapeutic options and emerging parasite resistance serve as significant obstacles to global disease eradication.^{6,7} The identification of novel and targetable parasite pathways, especially as they concern mechanisms of antimalarial resistance and treatment failure, are of principal concern. Of the disease relevant *Plasmodium* species, *P. falciparum* remains the most lethal and most common in areas of high disease burden, making *falciparum*-targeted strategies a top priority.

Among the arsenal of antimalarial therapeutics, artemisinins constitute the frontline of antimalarial care. The robust and rapid parasitocidal action of the natural product artemisinin results from Fenton-type reaction of the endoperoxide function, promoted by unbound heme, a byproduct of host hemoglobin catabolism. This activation ultimately leads to carbon-centered radicals that can alkylate heme and parasite proteins and promote lipid peroxidation, ultimately causing cellular stress and parasite death (**Figure 4-1A and 4-1B**)^{8,3,9}

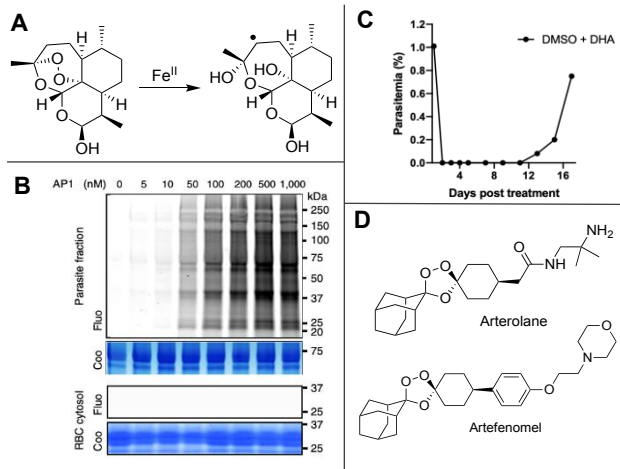


Figure 4-1: (A) Artemisinin is cleaved by heme iron to generate free radicals [8] (B) Alkyne-tagged Art (AP1) broadly labels parasite proteome [9] (C) Erythrocytic parasites recrudescence on DHA monotherapy [4] (D) Representative synthetic trioxolanes [17]

The relatively short half-life of artemisinins in malaria patients (~1 hour) allow latent parasites to survive treatment and proliferate after drug has been cleared, a phenomenon called recrudescence (**Figure 4-1C**).⁴ Recrudescence is not necessarily a

result of resistance mutations but rather of variable artemisinin susceptibility in parasite sub-populations at the time of treatment, a process conceptually similar to bacterial persister populations.¹⁰ The ability of some otherwise susceptible *Plasmodium* strains to survive artemisinin exposure (**Figure 4-1C**) may therefore reflect stochastic variations in specific stress-responsive machinery. Global translation repression through phosphorylation of the initiation factor eIF2 is implicated as a broadly relevant mechanism for inducing parasite latency upon cellular insult, but its possible role in avoiding the cytotoxic effects of artemisinin and the synthetic trioxolanes requires further investigation.¹¹

The need to address the limited exposure profile of artemisinins spurred the development of synthetic 1,2,4-trioxolanes such as artefenomel (**Figure 4-1D**), which exhibit significantly improved pharmacokinetic and pharmacodynamic properties compared to artemisinins.¹² Novel trioxolanes identified by our lab have further improved on the sub-optimal solubility of artefenomel (Chapters 2-3), but concerns regarding adaptive parasite responses to these agents remain. Longer compound half-lives will increase efficacy, but

short treatment duration does not fully explain parasite recrudescence, and wild type ring stage parasites have been shown to remain viable after extended periods of artemisinin exposure.¹³ Novel strategies that can target known liabilities of endoperoxide antimalarials could increase treatment efficacy and limit the possibility of widespread endoperoxide treatment failure. Despite evidence for an enhanced parasite stress response in artemisinin resistant parasites, this pathway remains untargeted by existing drugs and the new antimalarials currently in clinical development.¹⁴ Thus we sought to expand on foundational knowledge around the eukaryotic initiation factor 2 and its role in parasite development and response to endoperoxide therapy.

In higher-order eukaryotes, the unfolded protein response (UPR) is largely characterized by three nodes: global translation repression via PERK-mediated eIF2 α phosphorylation, transcriptional reprogramming by activation of IRE1 and ATF6, and chaperone upregulation as characterized by the Hsp70 BiP.¹⁵ *Plasmodium* species lack homologous pathways for ATF6 and IRE1, suggesting that these parasites rely primarily on eIF2 α -P-mediated translational control to manage proteostasis and response to cellular insult (Figure 4-2A).²

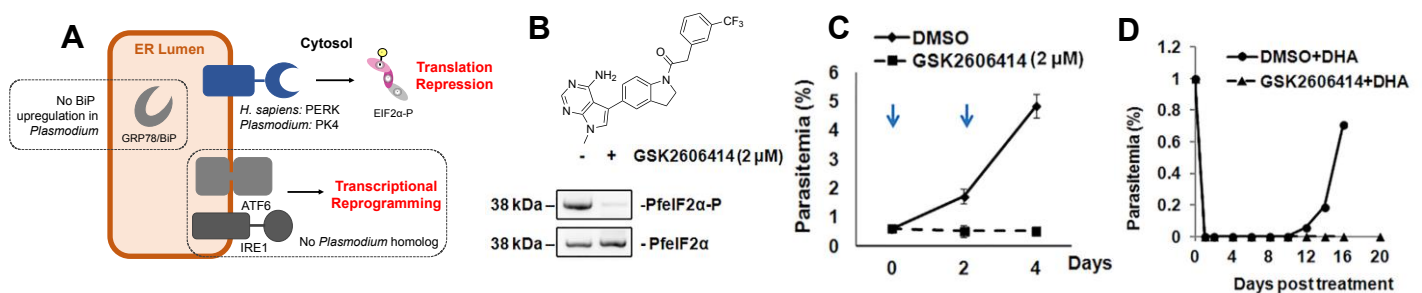


Figure 4-2: (A) *Plasmodium* species have limited protein stress responses compared to the canonical UPR (B) 6414 inhibits eIF2 α phosphorylation (C) 6414 inhibits parasite proliferation in cultured parasites (D) Erythrocytic parasites co-treated with dihydroartemisinin (DHA) and 6414 do not recrudescence. B,C,D from [4]

The eIF2 arm of the UPR is highly conserved across higher-order eukaryotes. Under normal conditions, the trimeric eIF2 catalyzes ribosome assembly and protein translation through a GTP-dependent process. In response to cellular stress, the eIF2 α subunit is phosphorylated (eIF2 α -P), converting the protein into an inhibitor of its guanine exchange factor (eIF2B) and resulting in translation repression.¹⁶

eIF2 α phosphorylation and subsequent translation repression may be more broadly relevant to the parasitic life cycle, aside from the response to artemisinin treatment. Parasite translation is tightly regulated, and a number of life cycle transitions require storage of mRNA transcripts in granules prior to conditional translational activation.¹ Inhibiting these storage events experimentally results in cell cycle arrest or premature activation of the next life cycle phase.¹⁷ The small molecule GSK-2606414 (hereafter 6414), an inhibitor of the human eIF2 α kinase PERK, also inhibits the parasite homolog PK4 and provides a window into this pathway (**Figure 4-2B and 4-2C**). It has been previously shown that incubation of cultured parasites with 6414 blocks parasite development and eliminates parasite recrudescence when co-administered with DHA (**Figure 4-2D**). Effects of the PK4 inhibitor 6414 were recapitulated by genetic PK4 disruption.¹¹ Inhibitory strategies targeted towards eIF2 α -P-mediated translation repression could therefore yield novel antimalarial therapeutics, with potentially synergistic effects towards antimalarial endoperoxides.

The utility of 6414 as a tool compound is limited by toxicity associated with on-target PERK inhibition in mammalian systems and by off-target inhibitory activity towards RIPK1 and KIT.^{18,19} This lack of selectivity across the human kinome suggests the compound is likely also promiscuous in the parasite kinome. Moreover, while 6414 is a sub-nanomolar

PERK inhibitor, its potency in *Plasmodium* parasites is only low μM , making the compound unsuitable for animal studies, though perhaps suggesting targetable divergence between PERK and PK4.¹⁹ A PK4-selective inhibitor would allow for more rigorous investigations into the role of eIF2 α -P in the parasite and would enable studies of combination drug regimens in mouse malaria models. Parallel investigations into eIF2 α -P as it applies to broad mechanisms of endoperoxide resistance would yield fundamental insight into parasite biology and inform a rational partner drug strategy for endoperoxides.

RESULTS AND DISCUSSION

We obtained from GSK a set of ~600 late-stage drug-like kinase inhibitors synthesized during the original PERK inhibitor effort that yielded 6414 (**Figure 4-3**). These compounds were evaluated against cultured erythrocytic *P. falciparum* 3D7 strain parasites (pan-sensitive) at 6 concentrations to determine preliminary IC_{50} values. From this initial screen, we identified 14 compounds with preliminary IC_{50} below $1\mu\text{M}$, representing a hit rate of 2.5% and a promising improvement in antiparasitic efficacy in comparison with the reported IC_{50} of GSK-6414 of $2\mu\text{M}$.⁴ To minimize the potential of false positives from this high-throughput screen, top performers were additionally validated with increased concentration points and replicates in an independent FACS assay utilizing unlysed RBCs and YOYO-1 dye for quantification of parasitemia (see methods). Encouragingly, 26 of 32 selected top performers maintained potent antiparasitic activity in this parallel assay, indicating a meaningful effect from compounds in this class (see methods).

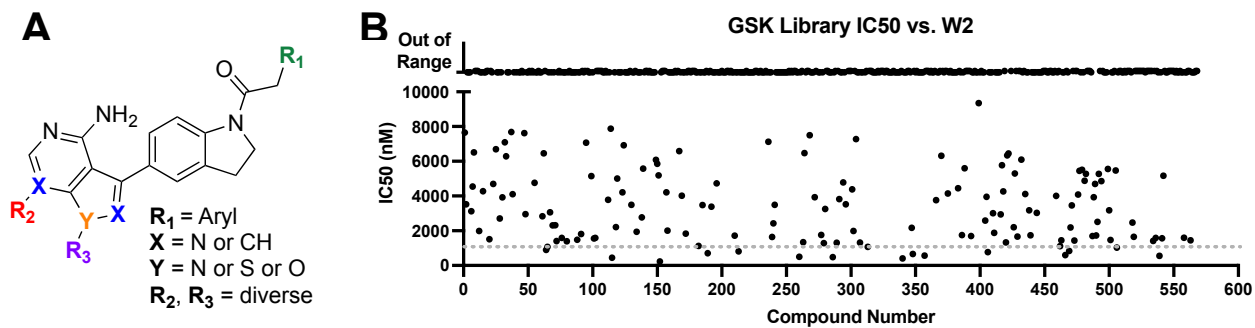


Figure 4-3. Results of primary GSK library screen in *P. falciparum*. A) Makeup of GSK antikinase set B) IC₅₀ of GSK compounds against 3D7 *P. falciparum*

It has been previously reported that GSK-2606414 exerts a parasitostatic effect by arresting parasite development at the late trophozoite/early schizont stage.⁴ We reasoned that confirming the same phenotype in the identified GSK leads could serve as an initial signature of PK4 targeting in the parasite. Indeed, upon light microscopy profiling of erythrocytic cultures exposed continuously to selected lead compounds, it was observed that the reported phenotypic effect for GSK-2606414 was also observed with selected screening hits (**Figure 4-4**)

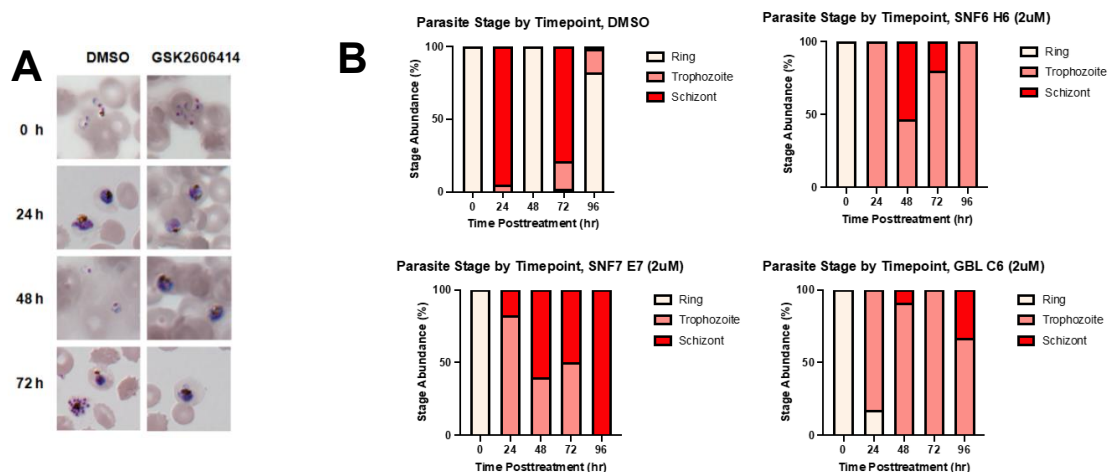


Figure 4-4. Phenotypic effect of 6414 and GSK screening hits in parasites. A) Continuous 6414 exposure results in parasite cell cycle arrest at the late trophozoite/early schizont stage. B) Exposure to selected leads demonstrates identical phenotype, suggesting target may be retained across class

To confirm this implied effect, we sought to evaluate the GSK library directly against purified recombinant PK4 in a biochemical assay. We purified a GST-tagged PK4 construct previously reported to be active and inhibitable by 6414⁴, but could not replicate the reported results in our lab. We additionally expressed alternative PK4 constructs with changes in sequence alignment and deletions as assisted by protein stability predictions from SWISS-MODEL (Expasy.org) and MODELLER (UCSF Sali Lab) and found these constructs to be inactive under the screened conditions. We additionally generated peptides isolating the 10-15 amino acid sequence immediately surrounding Ser59 of *Pfelf2α* as well as expressing murine eIF2α to test as potential alternative substrates to the originally tested *PfeIF2α* construct but could not detect kinase activity in any of the tested conditions, as was readily detectible from a similarly generated recombinant human GST-PERK construct (**Figure 4-5**). These observations persisted in both the ATP-Glo and ADP-Glo assays (Promega), which employ opposite means of detecting kinase activity and were selected to control for any potential fluorescence confounding effect from our tested compounds.

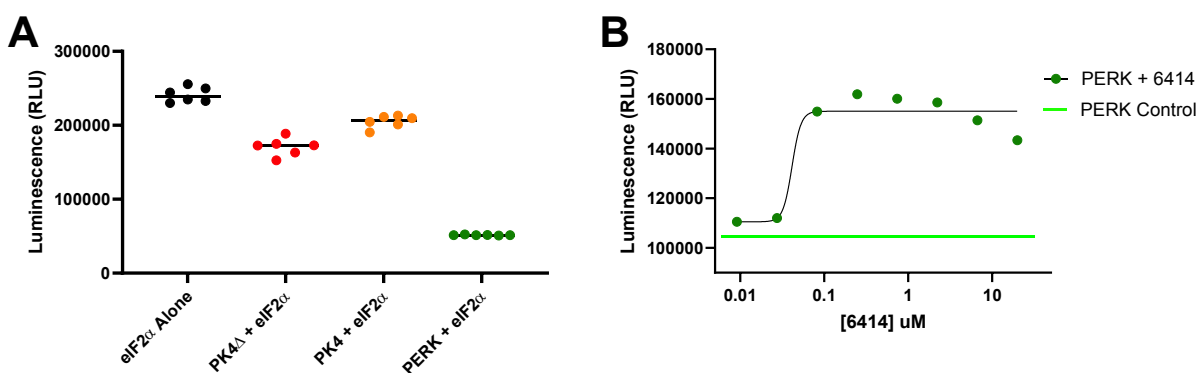


Figure 4-5. Observed *Pf*PK4 biochemical activity as compared to PERK in ATP-Glo Assay A) GST-PK4 construct significantly underperforms GST-PERK construct expressed and tested under identical conditions. B) GST-PERK activity allows for evaluation of on-target inhibitor activity, an effect not seen with any of our evaluated GST-PK4 constructs.

To better understand the reasons for the poor activity of our PK4 constructs, we evaluated the original GST-PK4 construct by differential scanning fluorimetry (DSF) to determine whether the poor activity was due to construct stability and whether DSF might serve as an alternative approach to assess binding of PK4 inhibitors. We first screened for compatible dyes using a platform made available through the UCSF Gestwicki lab.²⁰ Briefly, the GST-PK4 construct was evaluated against 312 chemically diverse dyes in a high-throughput screen to determine the most useful dyes for indicating protein T_m .

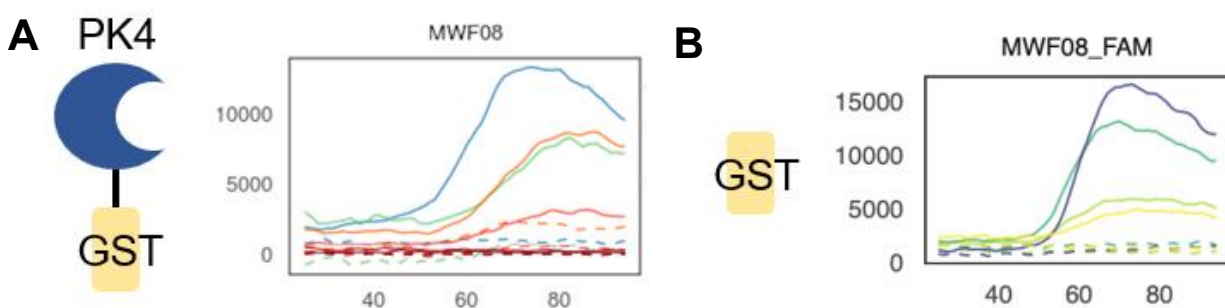


Figure 4-6. DSF curve for selected hit dye. A) Dye MWF08 detects unfolding event across several fluorescent channels (solid lines) over buffer control (dotted lines), with T_m indicated at $\sim 65^\circ\text{C}$. B) Dye MWF08 detects identical transition against GST alone, indicating kinase domain transition is not detected for full construct

While some dyes appeared initially promising, the inclusion of a control screen against GST alone suggested the detected unfolding activity was attributable to the GST tag rather than the PK4 kinase domain itself (**Figure 4-6**). This was confirmed by an identical screen of the dye library against a His-tagged PK4 kinase domain construct, from which no dyes indicated a reliable T_m curve. Taken together with previously observed poor activity from all *Pf*PK4 constructs, the results suggested that our *Pf*PK4 constructs were inherently unstable and/or poorly folded, and unlikely to serve as a useful tool for determining the on-target PK4 inhibitory activity of our library. This finding was not entirely

unexpected, given the extremely A+T rich nature of the *Plasmodium falciparum* genome²¹ and the existence of large, disordered repeats in the annotated sequence for *Pf*PK4 and across the *P. falciparum* proteome more broadly²², complicating factors for functional recombinant protein expression.

We next sought an alternative approach to confirm on-target activity of our identified hits in *P. falciparum* cultures. We observed no correlation between historical PERK IC₅₀ values (provided by GSK) and antiparasitic activity (**Figure 4-7A**). The relatively low sequence homology between PERK and PK4 (~36%) might contribute to the poor correlation but without knowledge of the corresponding PK4 IC₅₀ values or selectivity vs. other parasite kinases, no clear conclusions could be drawn. Following from these results, we explored possibly synergistic effects of DHA and 6414, as has previously been suggested⁴, via isobologram analysis, but after repeated trials could not reproduce this result. (**Figure 4-7B**). We also explored potential synergy between synthetic trioxolane RLA-4770 and the most potent screening hit GSK-13A4 in the *P. berghei* rodent model of malaria but saw no extension of survival with the combination (**Figure 4-7C**). Admittedly, without knowledge of the PK profile of 13A4 this experiment is difficult to interpret.

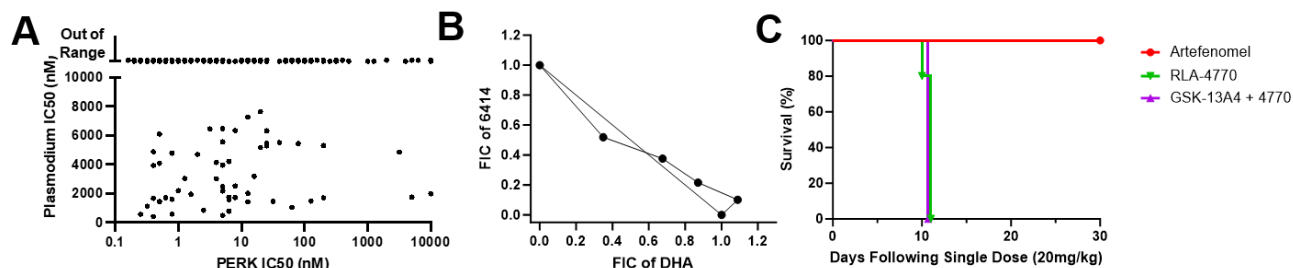


Figure 4-7. Attempts at confirming on-target PK4 activity. A) *in vitro* PERK IC₅₀ of GSK set is not correlated with *in vitro* antiplasmodial activity in *P. falciparum*. B) Isobologram analysis of 6414 and DHA does not indicate synergy. C) Hit compound GSK-13A4 does not eliminate recrudescence when co-administered with endoperoxide RLA-4770 in the rodent *P. berghei* model of malaria.

We next turned to *in vitro* resistance evolution and whole genome analysis (IVIEWGA) as the most direct method for determining the target of our identified leads. Encouragingly, the concentration of continuous drug pressure required to maintain parasite growth at 50% relative to DMSO control (GI_{50}) was observed to steadily increase as drug pressure was applied (**Figure 4-8**). While the timeline required for this experiment was ultimately incompatible with the timeline scheduled for this report, its continuation is nonetheless a promising direction for determining the targets of the selected hits.

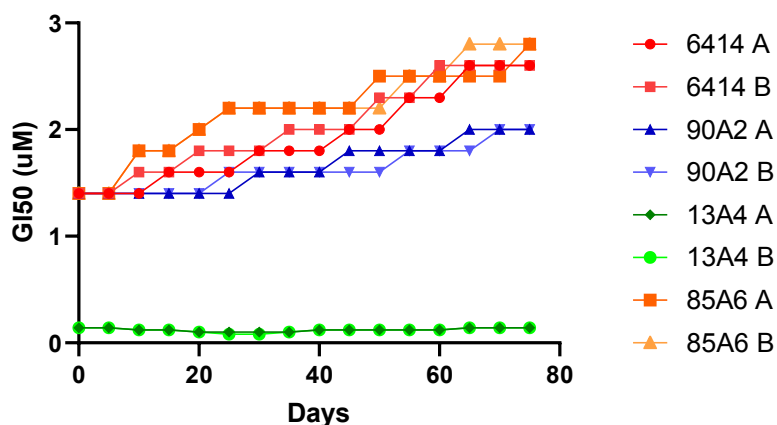


Figure 4-8. *In vitro* evolution GI_{50} concentrations over time. Parasites demonstrate increasing tolerance of continuous drug pressure.

To better understand the structural determinants of the observed activity against whole parasites, we engaged in a comparative analysis of the evaluated GSK library across two categories of compound: highly active compounds (observed IC_{50} \sim 1 μ M), and less active to inactive compounds (IC_{50} $>$ 10 μ M) (**Figure 4-9**).

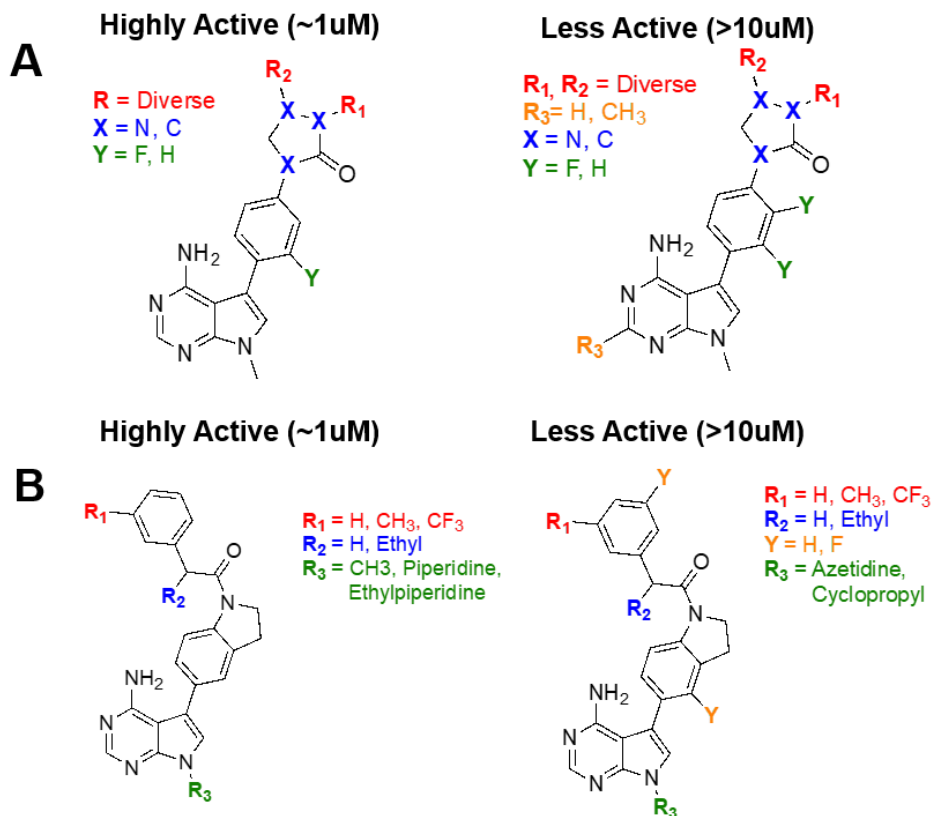


Figure 4-9. Structural motifs for active and inactive compounds for 3-aryl pyrrolopyrimidine (A) and 3-indolinopyrrolopyrimidine (B) classes. SAR for the observed antiparasitic activity remains opaque.

While the observed actives did indeed cluster into two main chemotypes, this effect was determined to be a result of enrichment of these structures within the library rather than intrinsic preference for these chemotypes within the context of antiparasitic activity. Indeed, little structural insight could be gleaned from the comparison of the actives and inactives. All three categories featured a core 4-aminopyrrolopyrimidine motif, with a *para*-substituted aryl moiety or a N-substituted indolene motif on the core ring 3 position. No immediate trends were apparent from comparison of the R groups of these compounds as related to their observed activity, and in the absence of PK4 structural data

or a plausible PK4 homology model (generation of which was attempted but could not be satisfactorily completed) additional investigation into these trends was precluded.

Given the infrastructure we had established for the high-throughput evaluation of an antikinase library, we were interested in expanding the set of small molecules evaluated against the parasite. To this end, we acquired a portion of the Selleckchem Kinase inhibitor library, a curated collection of kinase inhibitors with confirmed and annotated targets in mammalian systems (**Figure 4-10A**). From this set of 384 compounds, we observed 43 compounds with an IC₅₀ below 1μM, representing a hit rate of 11.2% (**Figure 4-10B** and **4-10C**).

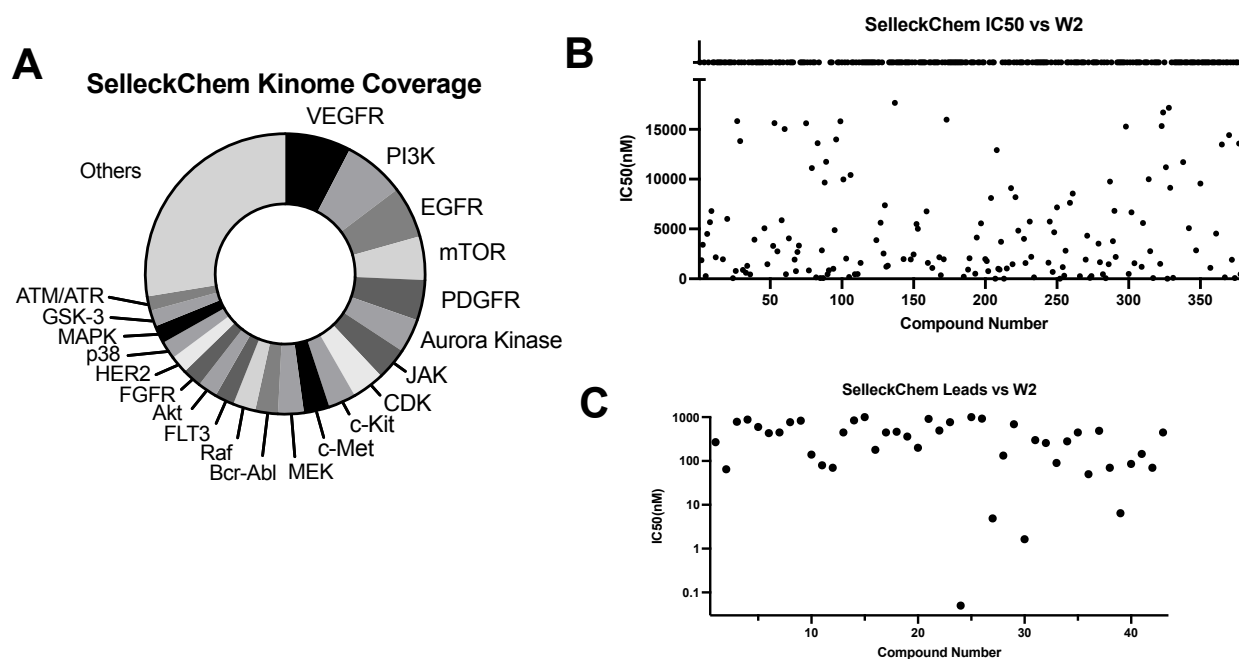


Figure 4-10. Selleckchem Library activity versus *P. falciparum*. A) Annotated targets of the Selleckchem antikinase library B) IC₅₀ of tested compounds against *P. falciparum* C) Expanded view of top 45 performers

Selecting from hits with observed IC₅₀s under 40nM, the field of annotated kinase targets in mammalian systems narrows (**Figure 4-11A**). Indeed, the majority of targets (PI3K, ATM/ATR, and mTOR) cluster in the PI3K-Related kinase family (PIKKs).²³ This shared,

limited set of mammalian targets, together with the uniquely potent antiparasitic efficacy and structural homology for these hit compounds (**Figure 4-11A**), suggests that a shared target profile may be driving the effect seen in these selected hits. Because the apicomplexan kinome is simplified relative to mammalian systems, there are fewer PIKK kinases in the *P. falciparum* kinome, simplifying the list of plausible targets. Most notably, TOR kinase is absent.²⁴ As such, we find it likely that these compounds are targeting *Pf*PI3K and, perhaps more importantly, *Pf*PI4K, the only clinically validated *Plasmodium* kinase target to date.²⁵ Indeed, hit compound VE-822 shares appreciable structural homology with advanced clinical candidate MMV0048, a *bona fide* *Pf*PI4K inhibitor (**Figure 4-11B**), as well as several other *Pf*PI4K-targeted compounds described in more recent reports.^{26 27 28} The remainder of this set may thus represent additional chemical scaffolds useful for targeting *Pf*PI4K.

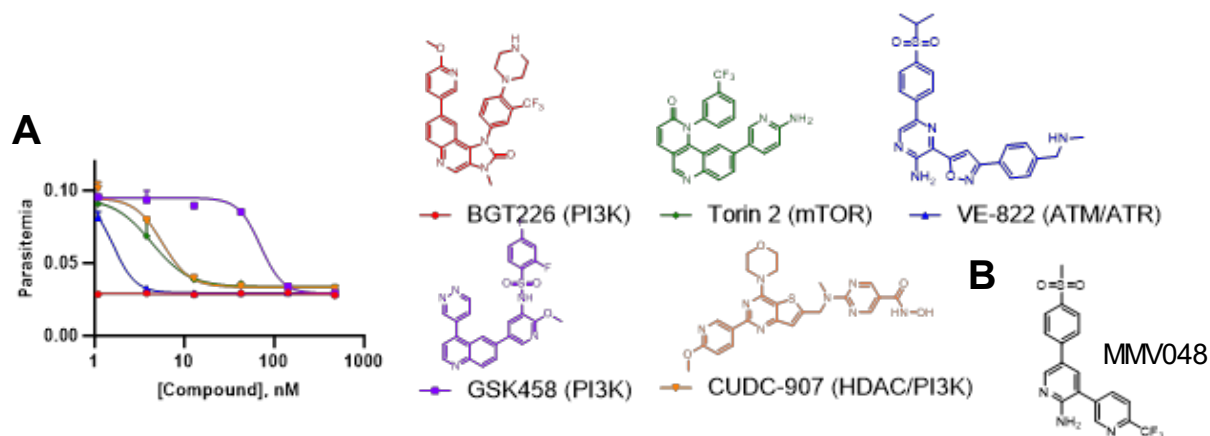


Figure 4-11. IC₅₀ curves and structures for Selleckchem top performers B) Structure of *Pf*PI4K-targeted clinical candidate MMV048.

CONCLUSIONS

The overriding goal of this project was to identify a potent and selective inhibitor of the *Plasmodium* stress kinase PK4 and to characterize the effects of inhibiting translation repression on parasite blood stages. Toward this end, we identified dozens of inhibitors with potent antiparasitic effect that plausibly target *Pf*PK4. We identified additional inhibitors from the GSK library that were structurally related to 6414 and phenocopied the compound's effects on the parasite life cycle in culture. Unfortunately, we were ultimately unable to directly confirm on-target *Pf*PK4 activity and could not reproduce many of the findings of previous studies related to PK4 inhibition, most notably the purported connection between PK4 and endoperoxide-induced latency and recrudescence. Additional work towards the end goals of this study would be best applied as follows: 1. Confirmation of on-target PK4 activity via continuation and completion of IVIEWGA. 2. Additional evaluation of endoperoxide-PK4 inhibitor synergy *in vitro* and *in vivo* with an increased sample of identified hits and experimental endoperoxides, with particular attention to the timeline of partner drug exposure in these contexts (specifically, pre-dosing of the PK4 inhibitor may be required to deplete stochastic levels of p-eIF2 α). 3. Synthesis and testing of novel small molecules based on hit compounds, with specific emphasis on increasing potency in the parasite while minimizing PERK activity.

METHODS

Compounds

GSK set compounds were donated by GlaxoSmithKline. Compounds were received as 10mM DMSO stocks in 96 well plates and kept at -20C before use. Following identification of leads, fresh compound was received in the form of lyophilized powder in glass vials and stored at 4C before use. Fresh compound was prepared for testing as a 10mM DMSO stock immediately before experimentation.

P. falciparum culture

Erythrocytic cultures of *P. falciparum* strain Dd2 (BEI Resources) and CamWT_C580Y (BEI Resources) were maintained using standard methods at 2% hematocrit in RPMI 1640 medium (Invitrogen) supplemented with 0.5% AlbuMAX II (Gibco Life Technologies), 0.1mM hypoxanthine, 30ug/mL gentamicin, 24mM NaHCO₃, and 25mM HEPES pH 7.4 (herein referred to as RPMIc) at 37°C in an atmosphere of 5% O₂, 5% CO₂, and 90% N₂. General parasitemia for culture maintenance was monitored via hand count of giemsa-stained iRBC thin smears by light microscopy. Media was changed and fresh RBC was added following a maximum period of 48 hours. Any necessary synchronization steps were completed by incubating ring-heavy iRBC pellets in 5% sorbitol at 37C for 15min.

SYBR Green IC50 Assay

Synchronized ring stage *P. falciparum* parasites maintained in RPMIc (see above) at 37C under an atmosphere of 5% O₂, 5% CO₂, and 90% N₂ were incubated with test compound at 15000, 4500, 1350, 405, 121.5, and 35.45 nM for 72 hours. Tests were

conducted in 96 well plates, each well with 200uL synchronized ring stage parasite culture at 1% parasitemia and 2% hematocrit. Following this incubation period, parasites and RBCs were lysed by repeated freeze/thaw cycles between -20C and room temperature. Following initial lysis, 100uL SYBR Green buffer was added (20mM Tris, 5mM EDTA, 0.02% saponin, 0.08% Triton-X, with 2uL 10,000X SYBR Green Nucleic Acid Gel Stain (ThermoFisher) per 10mL buffer) and wells were agitated to mix. Plate fluorescence was then recorded using a Tecan Infinite 200 Pro, Excitation = 254 Emission = 520. Plate data was graphed and IC50s quantified using GraphPad Prism 9.

YOYO-1 FACS Assay

Synchronized ring stage *P. falciparum* parasites maintained in RPMIc (see above) at 37C under an atmosphere of 5% O₂, 5% CO₂, and 90% N₂ were incubated with test compound at 17500, 5250, 1575, 1250, 937.5, 703.1, 472.5, 351.6, 175.8, 141.8, 87.9, and 42.5 nM for 72 hours. Tests were conducted in 96 well plates, each well with 200uL synchronized ring stage parasite culture at 1% parasitemia and 2% hematocrit. Following this period, RBCs were pelleted via centrifugation, media was aspirated, and RBCs were fixed by the addition of 200uL 2% formaldehyde in PBS and incubation at 37C overnight. PBS-fixed plates were stored at 4C until tested by FACS. For testing, a separate plate was populated with YOYO-1 FACS buffer (100mM NH₄Cl, 0.1% Triton-X, PBS 7.4 with freshly added 25nM YOYO-1) at 190uL per well. 10uL of the fixed formaldehyde solution from test plates was transferred from test plates to the prepared FACS plates and allowed to incubate at 4C for a minimum of 24 hours. Following this period, wells were analyzed via FACS on an Attune-NxT (ThermoFisher) using the instrument's BL1 fluorescent channel (530/30 excitation/emission) and parasitemia was quantified as a ratio of gated

iRBC “hits” versus total RBC count using ranges determined during instrument calibration as well as from internal controls. Values for each well were graphed in GraphPad Prism 9, wherein IC50 values were quantified.

Transformation of Chemically Competent *E. coli*

Previously described *P. falciparum*, *H. sapiens*, and *M. musculus* proteins were expressed using the Invitrogen pENTER Direction TOPO Cloning and Expression kits. Briefly, TOPO incorporation optimized gene fragments were ordered commercially (Integrated DNA Technologies), integrated into pENTR/SD/D-TOPO vector, and transformed into TOP10 chemically competent *E. coli* via heat shock. Transformed bacteria (selected via KAN resistance vector) were amplified and DNA was isolated via lysis and purification (Purelink HQ Mini Plasmid Purification Kit). Isolated plasmids were PCR amplified and recombined into pDEST14 entry vector for transformation into chemically competent *E. coli*, resulting in an IPTG-inducible expression system for the protein of interest.

Recombinant Expression of Proteins of Interest

Bacteria transformed as described previously were maintained at 4C on agar plates with relevant selection antibiotics. For expression, a single colony was pelleted into 10mL 2XYT broth with selection antibiotic and grown overnight at 37C with agitation. From this starter culture, 1mL was added to 2L 2XYT broth with selection antibiotic, which was maintained at 37C with agitation until reaching an OD of 0.6. Following this growth, culture growth was slowed by cooling with agitation to 4C for 30 minutes. Following cooling, IPTG was added (1X = 0.1mg/mL) and the cultures were maintained overnight

at 16C with agitation. Bacteria was then pelleted, lysed (Lysozyme in 50mM Tris, 500mM NaCl, 1% Triton-X, 10% Glycerol, EDTA-free protease inhibitor tablet, benzonuclease), and purified on an AKTA Pure protein chromatography system (Cytvia), with columns and column conditions selected based on affinity tag.

Differential Scanning Fluorimetry of Kinase Constructs

Recombinantly expressed GST-*Pf*PK4, His-*Pf*PK4, and GST alone were screened against 312 dyes according to protocols previously described by the Gestwicki lab.²⁰ 384 well “daughter plates” of the Max Weaver 312 dye library, containing 250nL of 5mM DMSO stock of each library dye, were thawed and 10uL of buffer (10mM HEPES pH 7.2, 200mM NaCl) was added to each well using an E100 ClipTip p125 Matrix Pipette (ThermoFisher) and associated tips. The resuspended daughter plate was spun down in a salad spinner for 30 seconds to remove bubbles and placed on the deck of an Opentrons OT-2 liquid handling robot at room temperature. Protein was diluted to 5X screening condition, and 2uL of this solution was dispensed into each well of an opaque white 384-well qPCR plate (Axygen) using an E100 ClipTip matrix pipette, following which the plate was spun down for 30 seconds. The plate was then added onto the deck of the Opentrons OT-2 liquid handling robot, and the OT-2 was used to transfer 8uL of the resuspended dye from the daughter plate into the prepared protein test plate, yielding 10uL of test well volume with a typical protein concentration of 1uM and typical dye concentration of 50uM. These plates were sealed with optically clear sealing film (Applied Biosystems) and spun down. The qPCR plates were placed in an Analytik Jena 384G qTower qPCR and heated from 25C to 94C in 69 increments of 1C every 30 seconds, with lid heating set to 98C to minimize condensation. Fluorescence measurements were

taken at each degree over six channels (470/520, 515/545, 535/580, 565/605, 630/670, and 660/705). Raw fluorescence readings were exported and analyzed using DSFworld.²⁹

Isobologram Analysis of Compound Synergy

Erythrocytic cultures of pan-sensitive *P. falciparum* 3D7 parasites were maintained according to the conditions above. Synchronized ring stage parasites were evaluated in a fixed-ratio Isobologram method as previously described by *Fivelman et. al.*³⁰ Briefly, IC₅₀ and IC₉₀ concentrations for DHA and GSK-6414 were determined via serial dilution in the YOYO-1 FACS assay described above. These concentrations were used to determine fixed compound combination ratios (5:0, 4:1, 3:2, 2:3, 1:4, 0:5) such that the IC₅₀ for each compound fell around the midpoint of a twofold serial dilution. This resulted in six total dose-response curves, two of which represented the two drugs alone and the remaining four representing fixed ratio pairings of the two drugs. Serial dilution curves were set up and analyzed according to procedures previously described for the YOYO-1 FACS assay. Two IC₅₀s for each drug combination were calculated separately by using the known concentration ratios of both drugs A and B, the fractional inhibitory concentration of A and B were calculated for each point, and the isobolograms were plotted and evaluated for synergy, indifference, or antagonism.

P. berghei Mouse Malaria Model

Female Swiss Webster mice (~20 g body weight) were infected intraperitoneally with 10⁶ P. berghei-infected erythrocytes collected from a previously infected mouse. Beginning 1 h after inoculation the mice were treated once daily by oral gavage for 1 day

as indicated with 100 μ L of solution of test compound formulated in 10% DMSO, 40% of a 20% 2-hydroxypropyl-beta-cyclodextrin solution in water, and 50% PEG400. There were five mice in each test arm. Infections were monitored by daily microscopic evaluation of Giemsa-stained blood smears starting on day seven. Parasitemia was determined by counting the number of infected erythrocytes per 1000 erythrocytes. Body weight was measured over the course of the treatment. Mice were euthanized when parasitemia exceeded 50% or when weight loss of more than 15% occurred. Parasitemia, animal survival, and morbidity were closely monitored for 30 days postinfection, when experiments were terminated.

In Vitro Resistance Evolution and Whole Genome Analysis

P. falciparum W2 parasites were maintained according to conditions described above. Clonal aliquots were maintained as mL cultures in 6-well plates, wherein experimental groups were assigned. Values for compound concentration resulting in 50% growth inhibition (GI_{50}) were first determined by exposing parasites to increasing doses of test compound and monitoring growth relative to DMSO control via hand count of giemsa-stained thin smears. Once GI_{50} values were determined for each test compound, parasites were exposed continuously to respective experimental compounds (or DMSO control) and actively monitored via hand count of Giemsa-stained thin smears. If growth rate in the test group accelerated relative to DMSO control, compound concentration was increased (generally by 15%) and growth rate was again monitored. This process was repeated over months, with the ultimate goal being adapted cultures with an observed GI_{50} at least 5 times higher than the initially recorded value. Parasitemia was maintained between 1-10% with cultures being diluted as necessary as growth occurred.

REFERENCES

1. Translational regulation in blood stages of the malaria parasite *Plasmodium* spp.: systems-wide studies pave the way - Vembar - 2016 - WIREs RNA - Wiley Online Library. <https://onlinelibrary.wiley.com/doi/full/10.1002/wrna.1365>.
2. Chaubey, S., Grover, M. & Tatu, U. Endoplasmic Reticulum Stress Triggers Gametocytogenesis in the Malaria Parasite. *J. Biol. Chem.* **289**, 16662–16674 (2014).
3. Wang, J. *et al.* Haem-activated promiscuous targeting of artemisinin in *Plasmodium falciparum*. *Nat. Commun.* **6**, 10111 (2015).
4. Zhang, M. *et al.* Inhibiting the Plasmodium eIF2 α Kinase PK4 Prevents Artemisinin-Induced Latency. *Cell Host Microbe* **22**, 766-776.e4 (2017).
5. Sheridan, C. M., Garcia, V. E., Ahyong, V. & DeRisi, J. L. The Plasmodium falciparum cytoplasmic translation apparatus: a promising therapeutic target not yet exploited by clinically approved anti-malarials. *Malar. J.* **17**, 465 (2018).
6. WHO. World malaria report 2019. <https://www.who.int/publications-detail/world-malaria-report-2019>.
7. Warrell, D., Cox, T. & Firth, J. *Oxford Textbook of Medicine*. Oxford Textbook of Medicine (Oxford University Press).
8. Mercer, A. E. *et al.* Evidence for the Involvement of Carbon-centered Radicals in the Induction of Apoptotic Cell Death by Artemisinin Compounds. *J. Biol. Chem.* **282**, 9372–9382 (2007).
9. Giannangelo, C. *et al.* Ozonide Antimalarials Alkylate Heme in the Malaria Parasite *Plasmodium falciparum*. *ACS Infect. Dis.* **5**, 2076–2086 (2019).

10. Ross, L. S. & Fidock, D. A. Elucidating Mechanisms of Drug-Resistant Plasmodium falciparum. *Cell Host Microbe* **26**, 35–47 (2019).
11. Zhang, M., Joyce, B. R., Sullivan, W. J. & Nussenzweig, V. Translational Control in Plasmodium and Toxoplasma Parasites. *Eukaryot. Cell* **12**, 161–167 (2013).
12. Vennerstrom, J. L. *et al.* Identification of an antimalarial synthetic trioxolane drug development candidate. *Nature* **430**, 900 (2004).
13. Teuscher, F., Chen, N., Kyle, D. E., Gatton, M. L. & Cheng, Q. Phenotypic Changes in Artemisinin-Resistant Plasmodium falciparum Lines In Vitro: Evidence for Decreased Sensitivity to Dormancy and Growth Inhibition. *Antimicrob. Agents Chemother.* **56**, 428–431 (2012).
14. Medicines for Malaria Venture. MMV-supported projects.
<https://www.mmv.org/research-development/mmv-supported-projects>.
15. Korennykh, A. & Walter, P. Structural Basis of the Unfolded Protein Response. *Annu. Rev. Cell Dev. Biol.* **28**, 251–277 (2012).
16. Pakos-Zebrucka, K. *et al.* The integrated stress response. *EMBO Rep.* **17**, 1374–1395 (2016).
17. Zhang, M. *et al.* The Plasmodium eukaryotic initiation factor-2 α kinase IK2 controls the latency of sporozoites in the mosquito salivary glands. *J. Exp. Med.* **207**, 1465–1474 (2010).
18. Rojas-Rivera, D. *et al.* When PERK inhibitors turn out to be new potent RIPK1 inhibitors: critical issues on the specificity and use of GSK2606414 and GSK2656157. *Cell Death Differ.* **24**, 1100–1110 (2017).

19. Mahameed, M. *et al.* The unfolded protein response modulators GSK2606414 and KIRA6 are potent KIT inhibitors. *Cell Death Dis.* **10**, 1–12 (2019).
20. Wu, T. *et al.* Conformationally responsive dyes enable protein-adaptive differential scanning fluorimetry. *bioRxiv* 2023.01.23.525251 (2023)
doi:10.1101/2023.01.23.525251.
21. Weber, J. L. Analysis of sequences from the extremely A + T-rich genome of *Plasmodium falciparum*. *Gene* **52**, 103–109 (1987).
22. Feng, Z.-P. *et al.* Abundance of intrinsically unstructured proteins in *P. falciparum* and other apicomplexan parasite proteomes. *Mol. Biochem. Parasitol.* **150**, 256–267 (2006).
23. Knight, Z. A. & Shokat, K. M. Chemically targeting the PI3K family. *Biochem. Soc. Trans.* **35**, 245–249 (2007).
24. McLean, K. J. & Jacobs-Lorena, M. *Plasmodium falciparum* Maf1 Confers Survival upon Amino Acid Starvation. *mBio* **8**, 10.1128/mbio.02317-16 (2017).
25. Fienberg, S. *et al.* Structural Basis for Inhibitor Potency and Selectivity of *Plasmodium falciparum* Phosphatidylinositol 4-Kinase Inhibitors. *ACS Infect. Dis.* **6**, 3048–3063 (2020).
26. Younis, Y. *et al.* 3,5-Diaryl-2-aminopyridines as a Novel Class of Orally Active Antimalarials Demonstrating Single Dose Cure in Mice and Clinical Candidate Potential. *J. Med. Chem.* **55**, 3479–3487 (2012).
27. Brunschwig, C. *et al.* UCT943, a Next-Generation *Plasmodium falciparum* PI4K Inhibitor Preclinical Candidate for the Treatment of Malaria. *Antimicrob. Agents Chemother.* **62**, (2018).

28. Liang, X. *et al.* Discovery of 6'-chloro-N-methyl-5'-(phenylsulfonamido)-[3,3'-bipyridine]-5-carboxamide (CHMFL-PI4K-127) as a novel Plasmodium falciparum PI(4)K inhibitor with potent antimalarial activity against both blood and liver stages of Plasmodium. *Eur. J. Med. Chem.* **188**, 112012 (2020).
29. Wu, T. *et al.* Three Essential Resources to Improve Differential Scanning Fluorimetry (DSF) Experiments. 2020.03.22.002543 Preprint at <https://doi.org/10.1101/2020.03.22.002543> (2020).
30. Fivelman, Q. L., Adagu, I. S. & Warhurst, D. C. Modified Fixed-Ratio Isobologram Method for Studying In Vitro Interactions between Atovaquone and Proguanil or Dihydroartemisinin against Drug-Resistant Strains of Plasmodium falciparum. *Antimicrob. Agents Chemother.* **48**, 4097–4102 (2004).

Chapter S2

Supporting Information for Chapter 2

Matthew T Klope, Juan A Tapia Cardona, Jenny Legac, Jun Chen, Ryan L Gonciarz,
Julie Kim, Priyanka Jaishankar, Philip J Rosenthal, Adam R Renslo

Synthetic Procedures

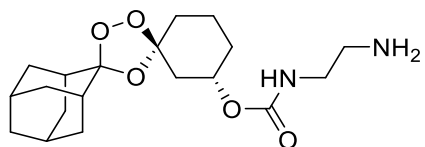
Materials

All chemical reagents were obtained commercially and used without further purification unless otherwise stated. Anhydrous solvents were purchased from Sigma-Aldrich and were used without further purification. Solvents used for flash column chromatography and workup procedures were purchased from either Sigma-Aldrich or Fisher Scientific. Column chromatography was performed on Silicycle Sili-prep cartridges using a Biotage Isolera Four automated flash chromatography system.

Instrumentation

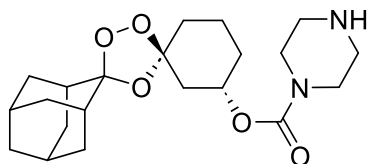
NMR spectra were recorded on a Bruker Avance III HD 400 MHz (with 5 mm BBFO Z-gradient Smart Probe), calibrated to CH(D)Cl₃ as an internal reference (7.26 and 77.00 ppm for ¹H and ¹³C NMR spectra, respectively). Data for ¹H NMR spectra are reported in terms of chemical shift (δ , ppm), multiplicity, coupling constant (Hz), and integration. Data for ¹³C NMR spectra are reported in terms of chemical shift (δ , ppm), with multiplicity and coupling constants in the case of C-F coupling. The following abbreviations are used to denote these multiplicities: s = singlet, d = doublet, t = triplet, q = quartet, m = multiplet, br = broad, app = apparent, or combinations of these. LC-MS and compound purity were determined using a Waters Micromass ZQ 4000, equipped with a Waters 2795 Separation Module, a Waters 2996 Photodiode Array Detector, and a Waters 2424 ELSD. Separations were carried out with an XBridge BEH C18, 3.5 μ m, 4.6 mm \times 20 mm column, at ambient temperature (unregulated) using a mobile phase of water-methanol containing a constant 0.10% formic acid.

Synthetic procedures for final compounds and Boc protected intermediates.



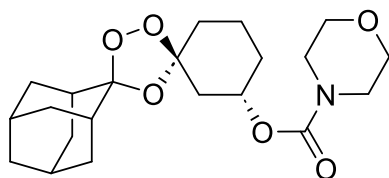
(1''S,3''S)-dispiro[adamantane-2,3'-[1,2,4]trioxolane-5',1''-cyclohexan]-3''-yl (2-aminoethyl) carbamate (9d).

To a solution of (1''S, 3''S)-dispiro[adamantane-2,3'-[1,2,4]trioxolane-5',1''-cyclohexan]-3''-yl (4-nitrophenyl) carbonate (100 mg, 0.225 mmol, 1.0 equiv.) in dichloromethane (5mL) was added triethylamine (94.1 μ L, 0.675 mmol, 3.0 equiv.), followed by ethylenediamine (75 μ L, 1.12 mmol, 5.0 equiv.) at rt. The bright yellow mixture was allowed to stir at rt for 4hr. The reaction was quenched with 1M Na₂CO₃ (10mL) and diluted with DCM (10mL). The organic phase was separated and washed with additional 1M Na₂CO₃ (4 x 10mL) until the aqueous layer was colorless (indicating that p-nitrophenol had been successfully removed from the organic layer). The combined organic layers were washed with brine (15mL), dried (MgSO₄), and concentrated under reduced pressure. The crude residue was purified using flash column chromatography (12 g silica gel cartridge, 0-20% MeOH (containing 0.7N NH₃) / CH₂Cl₂) with the desired product eluting at 15% MeOH (containing 0.7N NH₃) / CH₂Cl₂). The fractions containing the product were combined and lyophilized to give (1''S,3''S)-dispiro[adamantane-2,3'-[1,2,4]trioxolane-5',1''-cyclohexan]-3''-yl (2-aminoethyl) carbamate (62.0 mg, 0.169 mmol, 75%) as a white solid. ¹H NMR (400 MHz, MeOD) δ 4.6-4.8 (m, 1H), 3.22 (t, 2H, J=6.2 Hz), 2.80 (t, 2H, J=6.2 Hz), 2.1-2.3 (m, 1H), 2.04 (br d, 2H, J=11.9 Hz), 1.9-2.0 (m, 5H), 1.7-1.9 (m, 11H), 1.65 (dt, 1H, J=3.7, 12.7 Hz), 1.3-1.6 (m, 3H) ¹³C NMR (MeOD, 100 MHz) δ 157.2, 111.2, 108.6, 70.9, 41.6, 40.6, 39.9, 36.4, 36.4, 36.4, 34.4, 34.4, 33.3, 30.3, 27.0, 26.6, 19.4, 0.7; MS (ESI) calc for C₁₉H₃₁N₂O₅ [M+H]⁺: m/z 367.22 found 367.29



(1''S,3''S)-dispiro[adamantane-2,3'-[1,2,4]trioxolane-5',1''-cyclohexan]-3''-yl piperazine-1-carboxylate (9e).

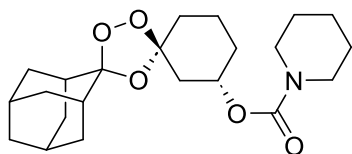
To a solution of (1''S, 3''S)-dispiro[adamantane-2,3'-[1,2,4]trioxolane-5',1''-cyclohexan]-3''-yl (4-nitrophenyl) carbonate(25 mg, 0.056 mmol, 1.0 equiv.) in dichloromethane (1.5mL) was added triethylamine (31 μ L, 0.22 mmol, 4.0 equiv.), followed by piperazine (4.8 mg, 0.056 mmol, 1.0 equiv.) at rt. The bright yellow mixture was allowed to stir at rt for 18 hours. The reaction was then quenched with DCM, washed with water, and the organic layer was extracted 3 times with 1N NaOH until the aqueous layer was colorless (indicating that p-nitrophenol had been depleted). The collected organic fractions were dried over MgSO₄, concentrated under reduced pressure. The crude residue was purified using flash column chromatography (12 g silica gel cartridge, 0-100% EtOAc:Hexanes). The fractions containing the product were combined and concentrated to yield (1''S,3''S)-dispiro[adamantane-2,3'-[1,2,4]trioxolane-5',1''-cyclohexan]-3''-yl piperazine-1-carboxylate (20.6mg, 0.053mmol, 93.9%) as a white solid. HNMR indicated the presence of grease (long-chain linear aliphatic hydrocarbon) which was carried through as an impurity. ¹H NMR (CHLOROFORM-d, 400 MHz) δ 4.84 (tt, 1H, J=4.5, 9.3 Hz), 3.4-3.6 (m, 4H), 2.89 (br s, 4H), 2.2-2.3 (m, 1H), 1.9-2.1 (m, 7H), 1.7-1.9 (m, 7H), 1.5-1.6 (m, 2H), 1.4-1.5 (m, 2H), 1.0-1.2 (m, 6H). MS (ESI) calc for C₂₁H₃₃N₂O₅ [M+H]⁺: m/z 393.24 found 393.39.



(1''S,3''S)-dispiro[adamantane-2,3'-[1,2,4]trioxolane-5',1''-cyclohexan]-3''-yl morpholine-4-carboxylate (9f).

To a solution of (1''S, 3''S)-dispiro[adamantane-2,3'-[1,2,4]trioxolane-5',1''-cyclohexan]-3''-yl (4-nitrophenyl) carbonate(25 mg, 0.056 mmol, 1.0 equiv.) in dichloromethane (1.5mL) was added triethylamine (31 μ L, 0.22 mmol, 4.0 equiv.), followed by morpholine (7.3 mg, 0.084 mmol, 1.5 equiv.) at rt. The bright yellow mixture was allowed to stir at rt

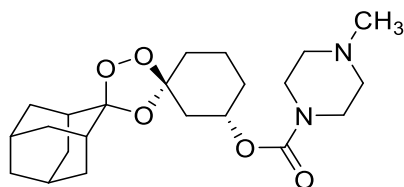
for 18 hours. The reaction was then quenched with DCM, washed with water, and the organic layer was extracted 3 times with 1N NaOH until the aqueous layer was colorless (indicating that p-nitrophenol had been depleted). The collected organic fractions were dried over MgSO₄, concentrated under reduced pressure. The crude residue was purified using flash column chromatography (12 g silica gel cartridge, 0-100% EtOAc:Hexanes). The fractions containing the product were combined and concentrated to yield (1''S,3''S)-dispiro[adamantane-2,3'-[1,2,4]trioxolane-5',1''-cyclohexan]-3''-yl morpholine-4-carboxylate (19.5mg, 0.049mmol, 88.4%) as a white solid. ¹H NMR (CHLOROFORM-d, 400 MHz) δ 4.8-4.9 (m, 1H), 3.66 (br s, 4H), 3.4-3.5 (m, 4H), 2.2-2.3 (m, 1H), 1.9-2.0 (m, 7H), 1.7-1.9 (m, 7H), 1.5-1.7 (m, 3H), 1.2-1.5 (m, 2H) MS (ESI) calc for C₂₁H₃₁NO₆Na [M+Na]⁺: m/z 416.20 found 416.20



(1''S,3''S)-dispiro[adamantane-2,3'-[1,2,4]trioxolane-5',1''-cyclohexan]-3''-yl piperidine-1-carboxylate (9g).

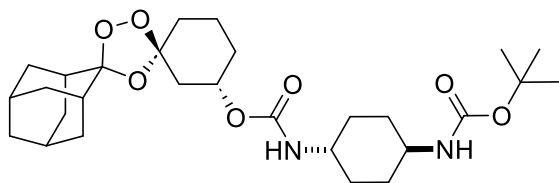
To a solution of (1''S, 3''S)-dispiro[adamantane-2,3'-[1,2,4]trioxolane-5',1''-cyclohexan]-3''-yl (4-nitrophenyl) carbonate(25 mg, 0.056 mmol, 1.0 equiv.) in dichloromethane (1.5mL) was added triethylamine (31 μL, 0.22 mmol, 4.0 equiv.), followed by piperidine (7.2 mg, 0.084 mmol, 1.5 equiv.) at rt. The bright yellow mixture was allowed to stir at rt for 18 hours. The reaction was then quenched with DCM, washed with water, and the organic layer was extracted 3 times with 1N NaOH until the aqueous layer was colorless (indicating that p-nitrophenol had been depleted). The collected organic fractions were dried over MgSO₄, concentrated under reduced pressure. The crude residue was purified using flash column chromatography (12 g silica gel cartridge, 0-100% EtOAc:Hexanes). The fractions containing the product were combined and concentrated to yield (1''S,3''S)-dispiro[adamantane-2,3'-[1,2,4]trioxolane-5',1''-cyclohexan]-3''-yl piperidine-1-carboxylate (20.6mg, 0.053mmol, 93.9%) as a white solid. ¹H NMR

(CHLOROFORM-d, 400 MHz) δ 4.8-4.9 (m, 1H), 3.42 (br d, 4H, J=5.4 Hz), 2.1-2.3 (m, 1H), 1.9-2.1 (m, 7H), 1.7-1.9 (m, 11H), 1.5-1.6 (m, 5H), 1.2-1.5 (m, 2H). MS (ESI) calc for C₂₂H₃₃NO₅Na [M+Na]⁺: m/z 414.23 found 414.25.



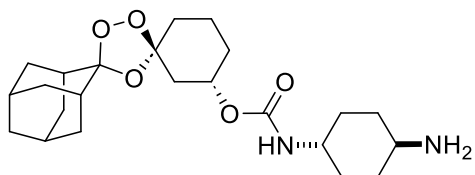
(1''S,3''S)-dispiro[adamantane-2,3'-[1,2,4]trioxolane-5',1''-cyclohexan]-3''-yl 4-methylpiperazine-1-carboxylate (9h).

To a solution of (1''S, 3''S)-dispiro[adamantane-2,3'-[1,2,4]trioxolane-5',1''-cyclohexan]-3''-yl (4-nitrophenyl) carbonate (100 mg, 0.225 mmol, 1.0 equiv.) in dichloromethane (5mL) was added triethylamine (78.2 μ L, 0.561 mmol, 2.5 equiv.), followed by 1-methylpiperazine (78.2 μ L, 0.561 mmol, 2.5 equiv.) at rt. The bright yellow mixture was allowed to stir at rt for 16hr. The reaction was quenched with 1M Na₂CO₃ (10mL) and diluted with DCM (10mL). The organic phase was separated and washed with additional 1M Na₂CO₃ (4 x 10mL) until the aqueous layer was colorless (indicating that p-nitrophenol had been successfully removed from the organic layer). The combined organic layers were washed with brine (15mL), dried (MgSO₄), and concentrated under reduced pressure. The crude residue was purified using flash column chromatography (12 g silica gel cartridge, 0-20% MeOH (containing 0.7N NH₃) / CH₂Cl₂) with the desired product eluting at 5% MeOH (containing 0.7N NH₃) / CH₂Cl₂). The fractions containing the product were combined and lyophilized to give (1''S,3''S)-dispiro[adamantane-2,3'-[1,2,4]trioxolane-5',1''-cyclohexan]-3''-yl 4-methylpiperazine-1-carboxylate (62.0 mg, 0.169 mmol, 75%) as a white solid. ¹H NMR (400 MHz, MeOD) δ 4.8-4.9 (m, 1H), 3.4-3.6 (m, 4H), 2.2-2.4 (m, 6H), 1.9-2.0 (m, 8H), 1.7-1.9 (m, 12H), 1.5-1.6 (m, 1H), 1.2-1.5 (m, 2H); ¹³C NMR (MeOD, 100 MHz) δ 154.6, 111.7, 108.6, 71.2, 54.7, 46.2, 39.8, 36.8, 36.3, 36.2, 35.0, 34.8, 34.7, 34.6, 34.2, 30.6, 26.9, 26.5, 19.5; MS (ESI) calc for C₂₂H₃₅N₂O₅ [M+H]⁺: m/z 407.25 found 407.38



(1''S,3''S)-dispiro[adamantane-2,3'-[1,2,4]trioxolane-5',1''-cyclohexan]-3''-yl [(trans)-4-(tert-butoxycarbonylamino)cyclohexyl]carbamate

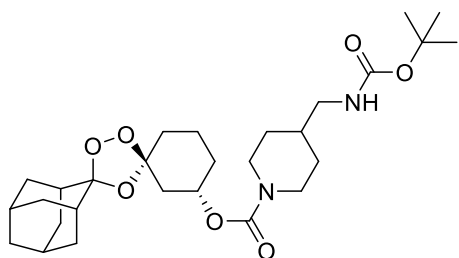
To a solution of (1''S, 3''S)-dispiro[adamantane-2,3'-[1,2,4]trioxolane-5',1''-cyclohexan]-3''-yl (4-nitrophenyl) carbonate (25 mg, 0.056 mmol) in N,N-dimethylformamide (2 mL), was added *tert*-butyl ((1*r*,4*r*)-4-aminocyclohexyl)carbamate (18 mg, 0.084 mmol), and triethylamine (23 μ L, 0.17 mmol). After stirring at room temperature for 18 h, the reaction mixture was then diluted with ethyl acetate and washed with thrice with 1M aqueous sodium hydroxide solution. The organic layer was then washed with brine, dried over magnesium sulfate, filtered, and concentrated under reduced pressure. The residue was then purified by flash column chromatography (0-100% ethyl acetate/hexanes) to yield 24 mg (82%) of (1''S,3''S)-dispiro[adamantane-2,3'-[1,2,4]trioxolane-5',1''-cyclohexan]-3''-yl [(trans)-4-(tert-butoxycarbonylamino)cyclohex-yl]carbamate as a white solid. ^1H NMR (CHLOROFORM-*d*, 400 MHz) δ 4.73 (br s, 1H), 4.40-4.49 (m, 2H), 3.43 (br s, 2H), 2.22-2.26 (m, 1H), 1.53-2.06 (m, 25H), 1.45 (s, 9H), 1.19-1.30 (m, 4H).



(1''S,3''S)-dispiro[adamantane-2,3'-[1,2,4]trioxolane-5',1''-cyclohexan]-3''-yl [(trans)-4-aminocyclohexyl]carbamate (9i)

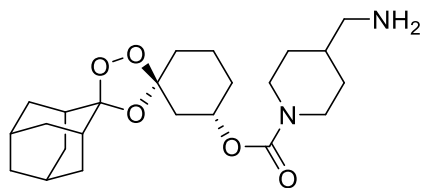
To a cooled (0° C) solution of (1''S,3''S)-dispiro[adamantane-2,3'-[1,2,4]trioxolane-5',1''-cyclohexan]-3''-yl [(trans)-4-(tert-butoxycarbonylamino)cyclohexyl]carbamate (24 mg, 0.046 mmol) in methanol (5 mL), was added acetyl chloride (150 μ L, 2.1 mmol). The

reaction was then allowed to stir at room temperature for 18 h. The reaction mixture was concentrated and purified by flash column chromatography (0-15% 0.7N ammonia in Methanol/dichloromethane) to yield 12 mg (62%) of (1''S,3''S)-dispiro[adamantane-2,3'-[1,2,4]trioxolane-5',1''-cyclohexan]-3''-yl [(trans)-4-aminocyclohexyl]carbamate as a white solid. ¹H NMR (METHANOL-d₄, 400 MHz) δ 4.63 (br s, 1H), 3.35-3.37 (m, 1H), 2.79 (br s, 1H), 2.18-2.21 (m, 1H), 1.31-2.05 (m, 29H). MS (ESI) calculated for C₂₃H₃₇N₂O₅ [M + H]⁺ *m/z* 421.26, found 421.30.



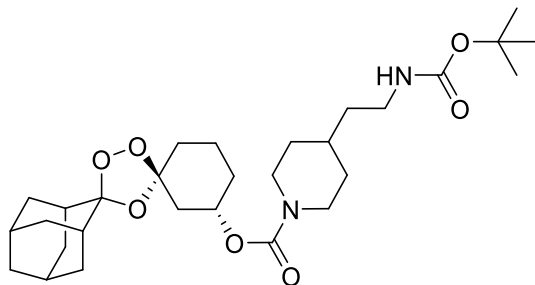
(1''S,3''S)- dispiro[adamantane-2,3'-[1,2,4]trioxolane-5',1''-cyclohexan]-3''-yl 4-[(tert-butoxycarbonylamino)methyl]-1-piperidinecarboxylate.

To a solution of (1''S, 3''S)-dispiro[adamantane-2,3'-[1,2,4]trioxolane-5',1''-cyclohexan]-3''-yl (4-nitrophenyl) carbonate (100 mg, 0.224 mmol, 1.0 equiv.) in dichloromethane (5mL) was added triethylamine (62.6 μL, 0.449 mmol, 2 equiv.), followed by tert-butyl (piperidin-4-ylmethyl)carbamate (96.2 mg, 0.449 mmol, 2 equiv.) at rt. The bright yellow mixture was allowed to stir at rt for 4.5hr. The reaction was quenched with 1M Na₂CO₃ (10mL) and diluted with DCM (10mL). The organic phase was separated and washed with additional 1M Na₂CO₃ (4 x 10mL) until the aqueous layer was colorless (indicating that p-nitrophenol had been successfully removed from the organic layer). The combined organic layers were washed with brine (15mL), dried (MgSO₄), and concentrated under reduced pressure. The crude residue was purified using flash column chromatography (12 g silica gel cartridge, 0-50% EtOAc:Hexanes) with the desired product eluting at 35% EtOAc. The fractions containing the product were combined and lyophilized to give (1''S,3''S)- dispiro[adamantane-2,3'-[1,2,4]trioxolane-5',1''-cyclohexan]-3''-yl 4-[(tert-butoxycarbonylamino)methyl]-1-piperidinecarboxylate (117mg, 0.224 mmol, 100%) as a white solid. MS (ESI) calc for C₂₈H₄₄N₂O₇Na [M+Na]⁺: *m/z* 543.30 found 543.19.



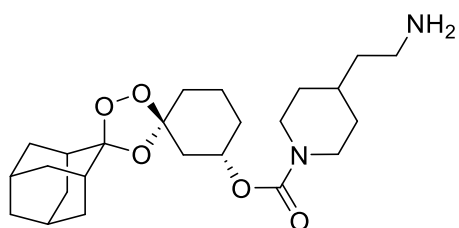
(1''S,3'S)-dispiro[adamantane-2,3'-[1,2,4]trioxolane-5',1''-cyclohexan]-3''-yl 4-(aminomethyl)-1-piperidinecarboxylate (9j).

To a solution of (1''S,3'S)-dispiro[adamantane-2,3'-[1,2,4]trioxolane-5',1''-cyclohexan]-3''-yl 4-[(tert-butoxycarbonylamino)methyl]-1-piperidinecarboxylate (117mg, 0.224 mmol, 1 equiv) in MeOH (5mL) cooled to 0 °C was added acetyl chloride (160uL, 2.24 mmol, 10 equiv) dropwise via microsyringe. The reaction was stirred at 0 °C for 5 minutes before being allowed to return to room temperature. After 4.5 hours, the reaction was quenched with 10 mL 1M Na₂CO₃ (10mL) and diluted with DCM (15mL). The organic phase was separated and washed with additional 1M Na₂CO₃ (2 x 10mL), followed by brine (10mL). The combined organic layers were dried (MgSO₄) and concentrated under reduced pressure. The crude residue was purified using flash column chromatography (12 g silica gel cartridge, 0-20% MeOH (containing 0.7N NH₃) / CH₂Cl₂) with the desired product eluting at 15% MeOH (containing 0.7N NH₃) / CH₂Cl₂). The fractions containing the product were combined and lyophilized to give (1''S,3'S)-dispiro[adamantane-2,3'-[1,2,4]trioxolane-5',1''-cyclohexan]-3''-yl 4-(aminomethyl)-1-piperidinecarboxylate (35 mg, 0.083 mmol, 37%) as a white solid. ¹H NMR (CDCl₃, 400 MHz) δ 4.8-4.9 (m, 1H), 4.1-4.3 (m, 2H), 2.6-2.8 (m, 4H), 2.2-2.3 (m, 1H), 1.9-2.1 (m, 7H), 1.5-1.9 (m, 16H), 1.39 (br d, 1H, J=9.0 Hz), 1.27 (s, 2H), 1.1-1.2 (m, 2H); ¹³C NMR (CDCl₃, 400 MHz) δ 154.7, 111.6, 108.7, 71.1, 43.7, 39.8, 36.8, 36.3, 36.3, 35.0, 34.8, 34.7, 34.6, 34.1, 30.7, 29.7, 26.9, 26.5, 19.6; MS (ESI) calc for C₂₃H₃₇N₂O₅ [M+H]⁺: m/z 421.27 found 421.20



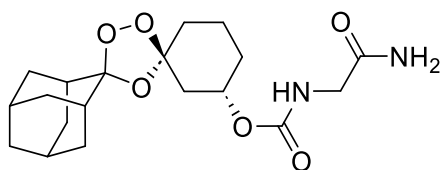
(1''S,3''S)-Dispiro[adamantane-2,3'-[1,2,4]trioxolane-5',1''-cyclohexan]-3''-yl 4-[2-(tert-butoxycarbonylamino)ethyl]-1-piperidinecarboxylate.

To a solution of (1''S, 3''S)-dispiro[adamantane-2,3'-[1,2,4]trioxolane-5',1''-cyclohexan]-3''-yl (4-nitrophenyl) carbonate (100 mg, 0.224 mmol, 1.0 equiv.) in dichloromethane (5mL) was added triethylamine (62.6 μ L, 0.449 mmol, 2 equiv.), followed by tert-butyl N-[2-(piperidin-4-yl)ethyl]carbamate (103 mg, 0.449 mmol, 2 equiv.) at rt. The bright yellow mixture was allowed to stir at rt for 4.5hr. The reaction was quenched with 1M Na₂CO₃ (10mL) and diluted with DCM (10mL). The organic phase was separated and washed with additional 1M Na₂CO₃ (4 x 10mL) until the aqueous layer was colorless (indicating that p-nitrophenol had been successfully removed from the organic layer). The combined organic layers were washed with brine (15mL), dried (MgSO₄), and concentrated under reduced pressure. The crude residue was purified using flash column chromatography (12 g silica gel cartridge, 0-50% EtOAc:Hexanes) with the desired product eluting at 35% EtOAc. The fractions containing the product were combined and lyophilized to give (1''S,3''S)-Dispiro[adamantane-2,3'-[1,2,4]trioxolane-5',1''-cyclohexan]-3''-yl 4-[2-(tert-butoxycarbonylamino)ethyl]-1-piperidinecarboxylate (74.5mg, 0.139 mmol, 62%) as a white solid. MS (ESI) calc for C₂₉H₄₆N₂O₇Na [M+Na]⁺: m/z 557.32 found 557.70.



(1''S,3''S)-Dispiro[adamantane-2,3'-[1,2,4]trioxolane-5',1''-cyclohexan]-3''-yl 4-(2-aminoethyl)-1-piperidinecarboxylate (9k).

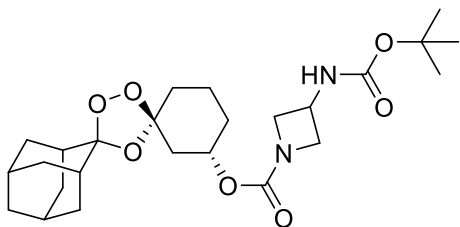
To a solution of (1''S,3''S)-Dispiro[adamantane-2,3'-[1,2,4]trioxolane-5',1''-cyclohexan]-3''-yl 4-[2-(tert-butoxycarbonylamino)ethyl]-1-piperidinecarboxylate (74.5 mg, 0.139 mmol, 1 equiv) in MeOH (5mL) cooled to 0 °C was added acetyl chloride (99.1uL, 1.39 mmol, 10 equiv) dropwise via microsyringe. The reaction was stirred at 0 °C for 5 minutes before being allowed to return to room temperature. After 16 hours, the reaction was quenched with 10 mL 1M Na₂CO₃ (10mL) and diluted with DCM (15mL). The organic phase was separated and washed with additional 1M Na₂CO₃ (2 x 10mL), followed by brine (10mL). The combined organic layers were dried (MgSO₄) and concentrated under reduced pressure. The crude residue was purified using flash column chromatography (12 g silica gel cartridge, 0-20% MeOH (containing 0.7N NH₃) / CH₂Cl₂) with the desired product eluting at 15% MeOH (containing 0.7N NH₃) / CH₂Cl₂). The fractions containing the product were combined and lyophilized to give (1''S,3''S)-Dispiro[adamantane-2,3'-[1,2,4]trioxolane-5',1''-cyclohexan]-3''-yl 4-(2-aminoethyl)-1-piperidinecarboxylate (27.3 mg, 0.062 mmol, 45%) as a white solid. ¹H NMR (CDCl₃, 400 MHz) δ 4.7-4.9 (m, 1H), 4.0-4.2 (m, 2H), 2.8-3.0 (m, 4H), 2.74 (br t, 4H, J=11.9 Hz), 2.1-2.3 (m, 1H), 2.02 (br s, 2H), 1.9-2.0 (m, 5H), 1.7-1.9 (m, 6H), 1.7-2.1 (m, 4H), 1.3-1.6 (m, 5H), 1.28 (s, 1H), 1.14 (br d, 2H, J=8.0 Hz); ¹³C NMR (CDCl₃, 100 MHz) δ 154.7, 111.6, 108.7, 77.2, 71.1, 43.9, 39.9, 38.6, 37.7, 36.8, 36.3, 36.3, 35.0, 34.8, 34.7, 34.6, 34.1, 33.4, 31.9, 30.7, 26.9, 26.5, 19.6; MS (ESI) calc for C₂₄H₃₉N₂O₅ [M+H]⁺: m/z 435.29 found 435.64



(1''S,3''S)-Dispiro[adamantane-2,3'-[1,2,4]trioxolane-5',1''-cyclohexan]-3''-yl (2-amino-2-oxoethyl)carbamate (9l)

To a solution of (1''S, 3''S)-dispiro[adamantane-2,3'-[1,2,4]trioxolane-5',1''-cyclohexan]-3''-yl (4-nitrophenyl) carbonate(25 mg, 0.056 mmol) in N,N-dimethylformamide (2 mL),

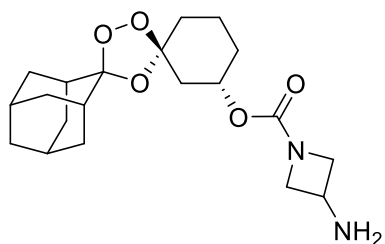
was added glycine hydrochloride (9.3 mg, 0.084 mmol), and triethylamine (23 μ L, 0.17 mmol). After stirring at room temperature for 18 h, the reaction mixture was then diluted with ethyl acetate and washed with thrice with 1M aqueous sodium hydroxide solution. The organic layer was then washed with brine, dried over magnesium sulfate, filtered, and concentrated under reduced pressure. The residue was then purified by flash column chromatography (0-10% methanol/dichloromethane) to yield 14.6 mg (69%) of (1''S,3''S)-Dispiro[adamantane-2,3'-[1,2,4]trioxolane-5',1''-cyclohexan]-3''-yl (2-amino-2-oxoethyl)carbamate as a colorless oil. $^1\text{H NMR}$ (METHANOL- d_4 , 400 MHz) δ 4.64-4.71 (m, 1H), 3.75 (s, 1H), 2.23-2.27 (m, 1H), 1.62-2.04 (m, 19H), 1.31-1.51 (m, 2H).



(1''S,3''S)-dispiro[adamantane-2,3'-[1,2,4]trioxolane-5',1''-cyclohexan]-3''-yl 3-(tert-butoxycarbonylamino)-1-azetidinecarboxylate.

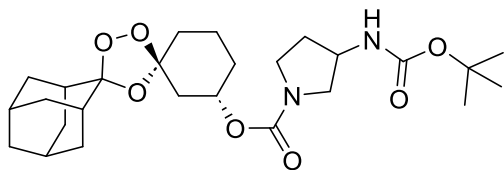
To a solution of (1''S, 3''S)-dispiro[adamantane-2,3'-[1,2,4]trioxolane-5',1''-cyclohexan]-3''-yl (4-nitrophenyl) carbonate (100 mg, 0.224 mmol, 1.0 equiv.) in dichloromethane (5mL) was added triethylamine (78.2 μ L, 0.561 mmol, 2.5 equiv.), followed by tert-butyl N-[(azetidin-3-yl)methyl]carbamate (96.7 mg, 0.561 mmol, 2.5 equiv.) at rt. The bright yellow mixture was allowed to stir at rt for 4.5hr. The reaction was quenched with 1M Na_2CO_3 (10mL) and diluted with DCM (10mL). The organic phase was separated and washed with additional 1M Na_2CO_3 (4 x 10mL) until the aqueous layer was colorless (indicating that p-nitrophenol had been successfully removed from the organic layer). The combined organic layers were washed with brine (15mL), dried (MgSO_4), and concentrated under reduced pressure. The crude residue was purified using flash column chromatography (12 g silica gel cartridge, 0-50% EtOAc:Hexanes) with the desired product eluting at 35% EtOAc. The fractions containing the product were combined and lyophilized to give (1''S,3''S)-dispiro[adamantane-2,3'-[1,2,4]trioxolane-5',1''-cyclohexan]-

3"-yl 3-(tert-butoxycarbonylamino)-1-azetidincarboxylate (104.0mg, 0.217 mmol, 97%) as a white solid. MS (ESI) calc for C₂₅H₃₈N₂O₇Na [M+Na]⁺: m/z 501.26 found 501.27.



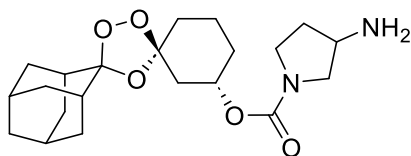
(1''S,3''S)-Dispiro[adamantane-2,3'-[1,2,4]trioxolane-5',1''-cyclohexan]-3''-yl 3-amino-1-azetidincarboxylate (9m).

To a solution of (1''S,3''S)-dispiro[adamantane-2,3'-[1,2,4]trioxolane-5',1''-cyclohexan]-3''-yl 3-(tert-butoxycarbonylamino)-1-azetidincarboxylate (51.4 mg, 0.107 mmol, 1 equiv) in MeOH (5mL) cooled to 0 °C was added acetyl chloride (76.4uL, 2.17 mmol, 10 equiv) dropwise via microsyringe. The reaction was stirred at 0 °C for 5 minutes before being allowed to return to room temperature. After 16 hours, the reaction was quenched with 10 mL 1M Na₂CO₃ (10mL) and diluted with DCM (15mL). The organic phase was separated and washed with additional 1M Na₂CO₃ (2 x 10mL), followed by brine (10mL). The combined organic layers were dried (MgSO₄) and concentrated under reduced pressure. The crude residue was purified using flash column chromatography (12 g silica gel cartridge, 0-20% MeOH (containing 0.7N NH₃) / CH₂Cl₂) with the desired product eluting at 15% MeOH (containing 0.7N NH₃) / CH₂Cl₂). The fractions containing the product were combined and lyophilized to give (1''S,3''S)-Dispiro[adamantane-2,3'-[1,2,4]trioxolane-5',1''-cyclohexan]-3''-yl 3-amino-1-azetidincarboxylate (15 mg, 0.040 mmol, 37%) as a white solid. ¹H NMR (CHLOROFORM-d, 400 MHz) Shift 4.6-4.9 (m, 1H), 4.1-4.4 (m, 3H), 3.8-4.0 (m, 1H), 2.3-2.4 (m, 1H), 2.1-2.3 (m, 3H), 1.9-2.1 (m, 4H), 1.91 (br s, 1H), 1.7-1.9 (m, 5H), 1.6-1.7 (m, 1H), 1.5-1.6 (m, 1H), 1.3-1.5 (m, 1H), 1.3-1.3 (m, 5H), 0.9-0.9 (m, 1H) ¹³C NMR (CHLOROFORM-d, 100 MHz) Shift 111.6, 100.0, 77.2, 71.5, 42.4, 39.9, 36.8, 36.3, 34.7, 33.9, 33.3, 31.9, 30.6, 29.7, 29.5, 29.4, 29.3, 26.9, 26.4, 24.8, 22.7, 19.6, 14.1 MS (ESI) calc for C₂₀H₃₀N₂O₅Na [M+Na]⁺: m/z 401.21 found 401.50



(1''S,3''S)- dispiro[adamantane-2,3'-[1,2,4]trioxolane-5',1''-cyclohexan]-3''-yl 3-(tert-butoxycarbonylamino)-1-pyrrolidinecarboxylate.

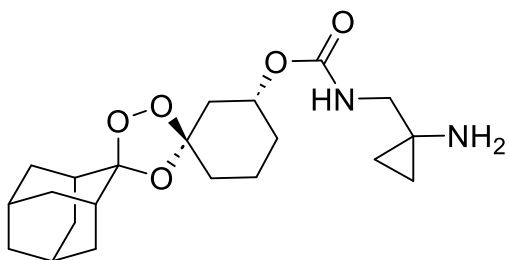
To a solution of (1''S, 3''S)-dispiro[adamantane-2,3'-[1,2,4]trioxolane-5',1''-cyclohexan]-3''-yl (4-nitrophenyl) carbonate (25 mg, 0.056 mmol) in N,N-dimethylformamide (1 mL), was added 3-(Boc-amino)-pyrrolidine (15.6 mg, 0.084 mmol), and triethylamine (23 μ L, 0.17 mmol). After stirring at room temperature for 18 h, the reaction mixture was then diluted with ethyl acetate and washed with thrice with 1M aqueous sodium hydroxide solution. The organic layer was then washed with brine, dried over magnesium sulfate, filtered, and concentrated under reduced pressure. The residue was then purified by flash column chromatography (0-10% methanol/dichloromethane) to yield 25.4 mg (92%) of (1''S,3''S)- dispiro[adamantane-2,3'-[1,2,4]trioxolane-5',1''-cyclohexan]-3''-yl 3-(tert-butoxycarbonylamino)-1-pyrrolidinecarboxylate as a colorless oil. ^1H NMR (CHLOROFORM-d, 400 MHz) δ 4.78-4.82 (m, 1H), 4.62 (br s, 1H), 4.20 (br s, 1H), 3.64 (dd, 1H, $J=6.1, 11.2$ Hz), 3.46 (br s, 2H), 3.21 (br s, 1H), 2.20-2.25 (m, 1H), 1.34-2.16 (m, 32H).



(1''S,3''S)-Dispiro[adamantane-2,3'-[1,2,4]trioxolane-5',1''-cyclohexan]-3''-yl 3-amino-1-pyrrolidinecarboxylate (9n)

To a cooled (0° C) solution of (1''S,3''S)- dispiro[adamantane-2,3'-[1,2,4]trioxolane-5',1''-cyclohexan]-3''-yl 3-(tert-butoxycarbonylamino)-1-pyrrolidinecarboxylate (25.4 mg, 0.051 mmol) in methanol (2 mL), was added acetyl chloride (164 μ L, 2.32 mmol). The reaction

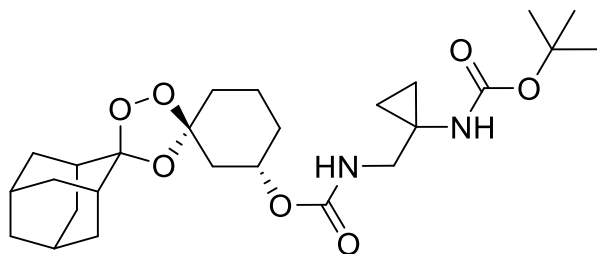
was then allowed to stir at room temperature for 18 h. The reaction mixture was concentrated and purified by flash column chromatography (0-15% 0.7N ammonia in Methanol/dichloromethane) to yield 2.3 mg (12%) of (1''S,3''S)-Dispiro[adamantane-2,3'-[1,2,4]trioxolane-5',1''-cyclohexan]-3''-yl 3 amino-1-pyrrolidinecarboxylate as a white solid. ¹H NMR (METHANOL-d₄, 400 MHz) δ 4.51-5.52 (m, 1H), 3.67-3.68 (m, 2H), 2.71 (s, 2H), 2.10-2.15 (m, 4H), 2.00-2.03 (m, 3H), 1.90-1.93 (m, 4H), 1.76-1.83 (m, 6H), 1.40 (br s, 4H), 1.31 (br s, 4H). MS (ESI) calculated for C₂₁H₃₃N₂O₅ [M + H]⁺ *m/z* 393.23, found 393.17.



(1''R,3''R)-dispiro[adamantane-2,3'-[1,2,4]trioxolane-5',1''-cyclohexan]-3''-yl N-[(1-aminocyclopropyl)methyl]carbamate (8o).

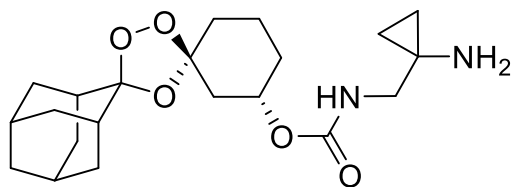
To a solution of (1''R, 3''R)-dispiro[adamantane-2,3'-[1,2,4]trioxolane-5',1''-cyclohexan]-3''-yl (4-nitrophenyl) carbonate (50 mg, 0.11 mmol, 1.0 equiv.) in dichloromethane (1.5 mL) was added triethylamine (47 μL, 0.34 mmol, 3.0 equiv.), followed by 1-(aminomethyl)cyclopropan-1-amine, 2HCl (27 mg, 0.17 mmol, 1.5 equiv.) at rt. The bright yellow mixture was allowed to stir at rt for 16 hours. The reaction was then quenched with DCM, washed with water, and the organic layer was extracted 3 times with saturated NaHCO₃ until the aqueous layer was colorless (indicating that p-nitrophenol had been depleted). The collected organic fractions were dried over MgSO₄, concentrated under reduced pressure. The crude residue was purified using flash column chromatography (12 g silica gel cartridge, 0-20% methanol (with 0.8N ammonia) in DCM). The fractions containing the product were combined and concentrated to yield (1''R,3''R)-dispiro[adamantane-2,3'-[1,2,4]trioxolane-5',1''-cyclohexan]-3''-yl N-[(1-aminocyclopropyl)methyl]carbamate (33.9 mg, 0.086 mmol, 78.5%) as a white solid. ¹H NMR (400 MHz,

MeOD) δ 4.6-4.8 (m, 1H), 3.15 (s, 2H), 2.1-2.3 (m, 1H), 2.0-2.1 (m, 3H), 1.7-2.0 (m, 16H), 1.65 (dt, 1H, $J=3.7, 12.7$ Hz), 1.3-1.5 (m, 3H), 0.58 (br d, 4H, $J=6.3$ Hz) ^{13}C NMR (100 MHz, MeOD) δ 157.4, 111.2, 108.6, 70.8, 48.9, 39.9, 36.4, 36.4, 36.4, 34.4, 33.8, 33.4, 30.3, 27.0, 26.6, 19.4, 11.2 MS (ESI) calc for $\text{C}_{21}\text{H}_{33}\text{N}_2\text{O}_5$ $[\text{M}+\text{H}]^+$: m/z 393.24 found 393.32



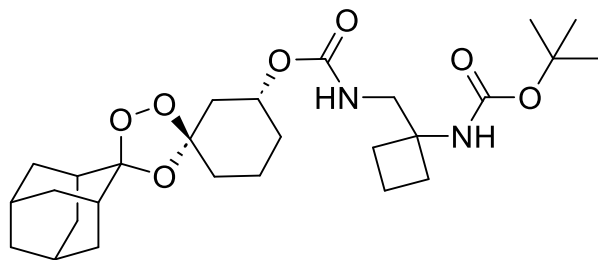
(1''S,3''S)-dispiro[adamantane-2,3'-[1,2,4]trioxolane-5',1''-cyclohexan]-3''-yl N-[(1-((tert-butoxy)carbonyl)amino)cyclopropyl)methyl]carbamate.

To a solution of (1''S, 3''S)-dispiro[adamantane-2,3'-[1,2,4]trioxolane-5',1''-cyclohexan]-3''-yl (4-nitrophenyl) carbonate (100 mg, 0.224 mmol, 1.0 equiv.) in dichloromethane (5mL) was added triethylamine (62.6 μL , 0.449 mmol, 2.0 equiv.), followed by tert-butyl (1-(aminomethyl)cyclopropyl)carbamate (83.6 mg, 0.449 mmol, 2.0 equiv.) at rt. The bright yellow mixture was allowed to stir at rt for 16hr. The reaction was quenched with 1M Na_2CO_3 (10mL) and diluted with DCM (10mL). The organic phase was separated and washed with additional 1M Na_2CO_3 (4 x 10mL) until the aqueous layer was colorless (indicating that p-nitrophenol had been successfully removed from the organic layer). The combined organic layers were washed with brine (15mL), dried (MgSO_4), and concentrated under reduced pressure. The crude residue was purified using flash column chromatography (12 g silica gel cartridge, 0-50% EtOAc:Hexanes) with the desired product eluting at 30% EtOAc. The fractions containing the product were combined and lyophilized to give (1''S,3''S)-dispiro[adamantane-2,3'-[1,2,4]trioxolane-5',1''-cyclohexan]-3''-yl N-[(1-((tert-butoxy)carbonyl)amino)cyclopropyl)methyl]carbamate (80.6 mg, 0.164 mmol, 72.9%) as a white solid. MS (ESI) calc for $\text{C}_{26}\text{H}_{40}\text{N}_2\text{O}_7\text{Na}$ $[\text{M}+\text{Na}]^+$: m/z 515.27 found 515.48.



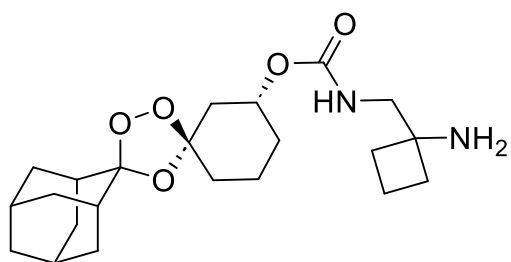
(1''S,3''S)-dispiro[adamantane-2,3'-[1,2,4]trioxolane-5',1''-cyclohexan]-3''-yl N-[(1-aminocyclopropyl)methyl]carbamate (9o).

To a solution of (1''S,3''S)-dispiro[adamantane-2,3'-[1,2,4]trioxolane-5',1''-cyclohexan]-3''-yl N-[(1-[(tert-butoxy)carbonyl]amino)cyclopropyl)methyl]carbamate (80.6 mg, 0.164 mmol, 1 equiv) in MeOH (5mL) cooled to 0 °C was added acetyl chloride (116 uL, 1.64 mmol, 10 equiv) dropwise via microsyringe. The reaction was stirred at 0 °C for 5 minutes before being allowed to return to room temperature. After 16 hours, the reaction was quenched with 10 mL 1M Na₂CO₃ (10mL) and diluted with DCM (15mL). The organic phase was separated and washed with additional 1M Na₂CO₃ (2 x 10mL), followed by brine (10mL). The combined organic layers were dried (MgSO₄) and concentrated under reduced pressure. The crude residue was purified using flash column chromatography (12 g silica gel cartridge, 0-20% MeOH (containing 0.7N NH₃) / CH₂Cl₂) with the desired product eluting at 10% MeOH (containing 0.7N NH₃) / CH₂Cl₂). The fractions containing the product were combined and lyophilized to give (1''S,3''S)-dispiro[adamantane-2,3'-[1,2,4]trioxolane-5',1''-cyclohexan]-3''-yl N-[(1-aminocyclopropyl)methyl]carbamate (50.5 mg, 0.129 mmol, 78.6%) as a white solid. ¹H NMR (CHLOROFORM-d, 400 MHz) δ 5.01 (br t, 1H, J=5.7 Hz), 4.76 (br s, 1H), 3.19 (br d, 2H, J=5.7 Hz), 2.2-2.4 (m, 2H), 2.13 (br s, 3H), 1.9-2.1 (m, 9H), 1.7-1.9 (m, 8H), 1.4-1.7 (m, 3H), 1.2-1.4 (m, 2H), 0.5-0.7 (m, 4H), ¹³C NMR (CHLOROFORM-d, 100 MHz) δ 156.2, 111.6, 108.7, 71.1, 50.0, 40.3, 36.8, 36.3, 34.9, 34.8, 34.7, 34.7, 34.5, 33.8, 30.7, 26.9, 26.5, 19.7, 13.0, MS (ESI) calc for C₂₁H₃₃N₂O₅ [M+H]⁺: m/z 393.24 found 393.37



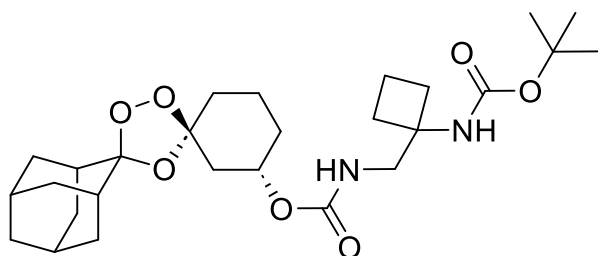
(1''R,3''R)-dispiro[adamantane-2,3'-[1,2,4]trioxolane-5',1''-cyclohexan]-3''-yl N-[(1-[(tert-butoxy)carbonyl]amino)cyclobutyl)methyl]carbamate.

To a solution of (1''R, 3''R)-dispiro[adamantane-2,3'-[1,2,4]trioxolane-5',1''-cyclohexan]-3''-yl (4-nitrophenyl) carbonate (100 mg, 0.224 mmol, 1.0 equiv.) in dichloromethane (5mL) was added triethylamine (78.2 μ L, 0.561 mmol, 2.5 equiv.), followed by tert-butyl (R)-piperidin-3-ylcarbamate (112.0 mg, 0.561 mmol, 2.5 equiv.) at rt. The bright yellow mixture was allowed to stir at rt for 16hr. The reaction was quenched with 1M Na₂CO₃ (10mL) and diluted with DCM (10mL). The organic phase was separated and washed with additional 1M Na₂CO₃ (4 x 10mL) until the aqueous layer was colorless (indicating that p-nitrophenol had been successfully removed from the organic layer). The combined organic layers were washed with brine (15mL), dried (MgSO₄), and concentrated under reduced pressure. The crude residue was purified using flash column chromatography (12 g silica gel cartridge, 0-50% EtOAc:Hexanes) with the desired product eluting at 30% EtOAc. The fractions containing the product were combined and lyophilized to yield (1''R,3''R)-dispiro[adamantane-2,3'-[1,2,4]trioxolane-5',1''-cyclohexan]-3''-yl N-[(1-[(tert-butoxy)carbonyl]amino)cyclobutyl)methyl]carbamate (114 mg, 0.224 mmol, 100%) as a white solid. MS (ESI) calc for C₂₇H₄₂N₂O₇Na [M+Na]⁺: m/z 529.29 found 529.28.



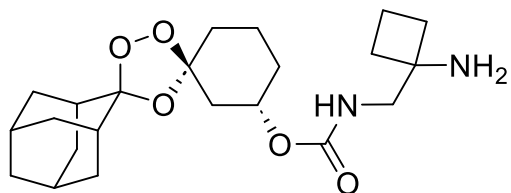
(1''R,3''R)-dispiro[adamantane-2,3'-[1,2,4]trioxolane-5',1''-cyclohexan]-3''-yl N-[(1-amino-cyclobutyl)methyl]carbamate (8p).

To a solution of (1''R,3''R)-dispiro[adamantane-2,3'-[1,2,4]trioxolane-5',1''-cyclohexan]-3''-yl N-[(1-[[tert-butoxy]carbonyl]amino)cyclobutyl)methyl]carbamate (114 mg, 0.224 mmol, 1 equiv) in MeOH (5mL) cooled to 0 °C was added acetyl chloride (161 uL, 2.27mmol, 10 equiv) dropwise via microsyringe. The reaction was stirred at 0 °C for 5 minutes before being allowed to return to room temperature. After 16 hours, the reaction was quenched with 10 mL 1M Na₂CO₃ (10mL) and diluted with DCM (15mL). The organic phase was separated and washed with additional 1M Na₂CO₃ (2 x 10mL), followed by brine (10mL). The combined organic layers were dried (MgSO₄) and concentrated under reduced pressure. The crude residue was purified using flash column chromatography (12 g silica gel cartridge, 0-20% MeOH (containing 0.7N NH₃) / CH₂Cl₂) with the desired product eluting at 10% MeOH (containing 0.7N NH₃) / CH₂Cl₂). The fractions containing the product were combined and lyophilized to give (1''R,3''R)-dispiro[adamantane-2,3'-[1,2,4]trioxolane-5',1''-cyclohexan]-3''-yl N-[(1-amino-cyclobutyl)methyl]carbamate (84.8 mg, 0.209 mmol, 93.3%) as a white solid. ¹H NMR (CHLOROFORM-d, 400 MHz) δ 5.3-5.5 (m, 1H), 4.7-4.9 (m, 1H), 3.2-3.4 (m, 2H), 2.98 (br s, 3H), 2.2-2.4 (m, 1H), 1.9-2.1 (m, 12H), 1.7-1.9 (m, 9H), 1.5-1.7 (m, 3H), 1.2-1.4 (m, 2H) ¹³C NMR (CHLOROFORM-d, 100 MHz) δ 156.1, 111.5, 108.8, 71.0, 56.0, 48.1, 40.3, 36.8, 36.3, 34.9, 34.8, 34.7, 33.8, 33.3, 30.7, 26.9, 26.5, 19.8, 12.9 MS (ESI) calc for C₂₂H₃₅N₂O₅ [M+H]⁺: m/z calc 407.25 found 407.43



(1''S,3''S)-dispiro[adamantane-2,3'-[1,2,4]trioxolane-5',1''-cyclohexan]-3''-yl N-[(1-[[tert-butoxy]carbonyl]amino)cyclobutyl)methyl]carbamate.

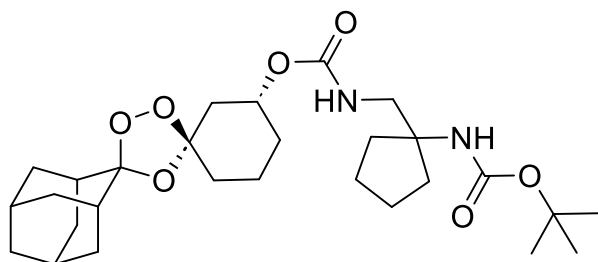
To a solution of (1''S, 3''S)-dispiro[adamantane-2,3'-[1,2,4]trioxolane-5',1''-cyclohexan]-3''-yl (4-nitrophenyl) carbonate(100 mg, 0.224 mmol, 1.0 equiv.) in dichloromethane (5mL) was added triethylamine (62.6 μ L, 0.449 mmol, 2.0 equiv.), followed by tert-butyl (1-(aminomethyl)cyclobutyl)carbamate (83.6 mg, 0.449 mmol, 2.0 equiv.) at rt. The bright yellow mixture was allowed to stir at rt for 16hr. The reaction was quenched with 1M Na₂CO₃ (10mL) and diluted with DCM (10mL). The organic phase was separated and washed with additional 1M Na₂CO₃ (4 x 10mL) until the aqueous layer was colorless (indicating that p-nitrophenol had been successfully removed from the organic layer). The combined organic layers were washed with brine (15mL), dried (MgSO₄), and concentrated under reduced pressure. The crude residue was purified using flash column chromatography (12 g silica gel cartridge, 0-50% EtOAc:Hexanes) with the desired product eluting at 30% EtOAc. The fractions containing the product were combined and lyophilized to give (1''S,3''S)-dispiro[adamantane-2,3'-[1,2,4]trioxolane-5',1''-cyclohexan]-3''-yl N-[(1-[(tert-butoxy)carbonyl]amino)cyclobutyl)methyl]carbamate (84.8 mg, 0.167 mmol, 75%) as a white solid. MS (ESI) calc for C₂₇H₄₂N₂O₇Na [M+Na]⁺: m/z 529.29 found 529.18.



(1''S,3''S)-dispiro[adamantane-2,3'-[1,2,4]trioxolane-5',1''-cyclohexan]-3''-yl N-[(1-amino-cyclobutyl)methyl]carbamate (9p).

To a solution of (1''S,3''S)-dispiro[adamantane-2,3'-[1,2,4]trioxolane-5',1''-cyclohexan]-3''-yl N-[(1-[(tert-butoxy)carbonyl]amino)cyclobutyl)methyl]carbamate (84.8 mg, 0.167 mmol, 1 equiv) in MeOH (5mL) cooled to 0 °C was added acetyl chloride (119 μ L, 1.67 mmol, 10 equiv) dropwise via microsyringe. The reaction was stirred at 0 °C for 5 minutes before being allowed to return to room temperature. After 16 hours, the reaction was quenched with 10 mL 1M Na₂CO₃ (10mL) and diluted with DCM (15mL). The organic phase was separated and washed with additional 1M Na₂CO₃ (2 x 10mL), followed by

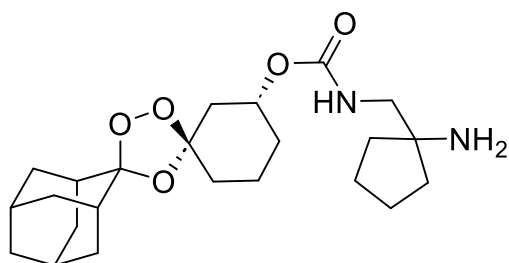
brine (10mL). The combined organic layers were dried (MgSO₄) and concentrated under reduced pressure. The crude residue was purified using flash column chromatography (12 g silica gel cartridge, 0-20% MeOH (containing 0.7N NH₃) / CH₂Cl₂) with the desired product eluting at 10% MeOH (containing 0.7N NH₃) / CH₂Cl₂). The fractions containing the product were combined and lyophilized to give (1''S,3''S)-dispiro[adamantane-2,3'-[1,2,4]trioxolane-5',1''-cyclohexan]-3''-yl N-[(1-amino-cyclobutyl)methyl]carbamate (46.9 mg, 0.115 mmol, 69%) as a white solid. ¹H NMR (CHLOROFORM-d, 400 MHz) δ 5.31 (br s, 1H), 4.7-4.9 (m, 1H), 3.2-3.4 (m, 2H), 2.73 (br s, 4H), 2.2-2.4 (m, 1H), 1.9-2.1 (m, 11H), 1.7-1.9 (m, 8H), 1.5-1.7 (m, 3H), 1.2-1.4 (m, 2H) ¹³C NMR (CHLOROFORM-d, 100 MHz) δ 156.6, 111.5, 108.8, 77.2, 71.0, 56.0, 48.1, 40.3, 36.8, 36.3, 34.9, 34.8, 34.7, 33.8, 33.3, 30.7, 26.9, 26.5, 19.8, 12.9 MS (ESI) calc for C₂₂H₃₅N₂O₅ [M+H]⁺: m/z 407.25 found 407.38



(1''R,3''R)-dispiro[adamantane-2,3'-[1,2,4]trioxolane-5',1''-cyclohexan]-3''-yl N-[[[(tert-butoxy)carbonyl]amino}cyclopentyl)methyl]carbamate.

To a solution of (1''R, 3''R)-dispiro[adamantane-2,3'-[1,2,4]trioxolane-5',1''-cyclohexan]-3''-yl (4-nitrophenyl) carbonate (100 mg, 0.224 mmol, 1.0 equiv.) in dichloromethane (5mL) was added triethylamine (78.2μL, 0.561 mmol, 2.5 equiv.), followed by tert-butyl (1-(aminomethyl)cyclopentyl)carbamate (120.0 mg, 0.561 mmol, 2.5 equiv.) at rt. The bright yellow mixture was allowed to stir at rt for 16hr. The reaction was quenched with 1M Na₂CO₃ (10mL) and diluted with DCM (10mL). The organic phase was separated and washed with additional 1M Na₂CO₃ (4 x 10mL) until the aqueous layer was colorless (indicating that p-nitrophenol had been successfully removed from the organic layer). The combined organic layers were washed with brine (15mL), dried (MgSO₄), and

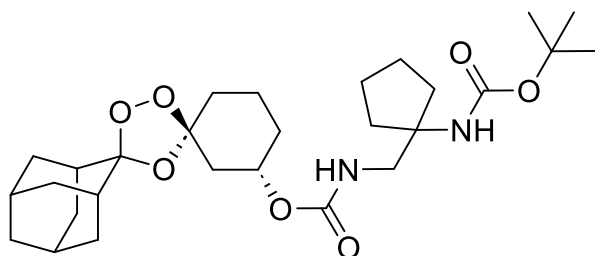
concentrated under reduced pressure. The crude residue was purified using flash column chromatography (12 g silica gel cartridge, 0-50% EtOAc:Hexanes) with the desired product eluting at 30% EtOAc. The fractions containing the product were combined and lyophilized to give (1''R,3''R)-dispiro[adamantane-2,3'-[1,2,4]trioxolane-5',1''-cyclohexan]-3''-yl N-[(1-[[[(tert-butoxy)carbonyl]amino]cyclopentyl)methyl]-carbamate (117.0 mg, 0.224 mmol, 100%) as a white solid. MS (ESI) calc for C₂₈H₄₄N₂O₇ [M+H]⁺: m/z 543.30 found 543.44.



(1''R,3''R)-dispiro[adamantane-2,3'-[1,2,4]trioxolane-5',1''-cyclohexan]-3''-yl N-[(1-aminocyclopentyl)methyl]carbamate (8q).

To a solution of (1''R,3''R)-dispiro[adamantane-2,3'-[1,2,4]trioxolane-5',1''-cyclohexan]-3''-yl N-[(1-[[[(tert-butoxy)carbonyl]amino]cyclopentyl)methyl]carbamate (117 mg, 0.225 mmol, 1 equiv) in MeOH (5mL) cooled to 0 °C was added acetyl chloride (160 uL, 2.25mmol, 10 equiv) dropwise via microsyringe. The reaction was stirred at 0 °C for 5 minutes before being allowed to return to room temperature. After 16 hours, the reaction was quenched with 10 mL 1M Na₂CO₃ (10mL) and diluted with DCM (15mL). The organic phase was separated and washed with additional 1M Na₂CO₃ (2 x 10mL), followed by brine (10mL). The combined organic layers were dried (MgSO₄) and concentrated under reduced pressure. The crude residue was purified using flash column chromatography (12 g silica gel cartridge, 0-20% MeOH (containing 0.7N NH₃) / CH₂Cl₂) with the desired product eluting at 10% MeOH (containing 0.7N NH₃) / CH₂Cl₂). The fractions containing the product were combined and lyophilized to give (1''R,3''R)-dispiro[adamantane-2,3'-[1,2,4]trioxolane-5',1''-cyclohexan]-3''-yl N-[(1-aminocyclopentyl)methyl]carbamate (86.3 mg, 0.205 mmol, 91.3%) as a white solid. ¹H NMR

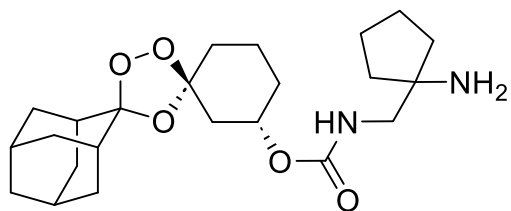
(CHLOROFORM-d, 400 MHz) δ 5.36 (br s, 1H), 4.7-4.9 (m, 1H), 3.1-3.4 (m, 2H), 2.83 (br s, 2H), 2.28 (br dd, 1H, J=2.2, 12.7 Hz), 1.99 (br d, 5H, J=13.9 Hz), 1.92 (br s, 2H), 1.7-1.9 (m, 8H), 1.6-1.7 (m, 3H), 1.5-1.6 (m, 4H), 1.2-1.4 (m, 2H) ¹³C NMR (CHLOROFORM-d, 100 MHz) δ 156.5, 111.5, 108.8, 71.0, 59.0, 49.5, 40.3, 37.8, 36.8, 36.3, 34.9, 34.8, 34.7, 33.8, 30.8, 26.9, 26.5, 24.0, 19.8 MS (ESI) calc for C₂₃H₃₇N₂O₅ [M+H]⁺: m/z 421.27 found 421.53



(1''S,3''S)-dispiro[adamantane-2,3'-[1,2,4]trioxolane-5',1''-cyclohexan]-3''-yl N-[(1-((tert-butoxy)carbonyl)amino)cyclopentyl)methyl]carbamate.

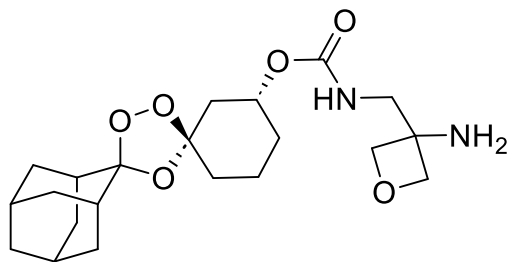
To a solution of (1''S, 3''S)-dispiro[adamantane-2,3'-[1,2,4]trioxolane-5',1''-cyclohexan]-3''-yl (4-nitrophenyl) carbonate (100 mg, 0.224 mmol, 1.0 equiv.) in dichloromethane (5mL) was added triethylamine (62.6 μ L, 0.449 mmol, 2.0 equiv.), followed by tert-butyl N-[1-(aminomethyl)cyclopentyl]carbamate (96.2 mg, 0.449 mmol, 2.0 equiv.) at rt. The bright yellow mixture was allowed to stir at rt for 16hr. The reaction was quenched with 1M Na₂CO₃ (10mL) and diluted with DCM (10mL). The organic phase was separated and washed with additional 1M Na₂CO₃ (4 x 10mL) until the aqueous layer was colorless (indicating that p-nitrophenol had been successfully removed from the organic layer). The combined organic layers were washed with brine (15mL), dried (MgSO₄), and concentrated under reduced pressure. The crude residue was purified using flash column chromatography (12 g silica gel cartridge, 0-50% EtOAc:Hexanes) with the desired product eluting at 30% EtOAc. The fractions containing the product were combined and lyophilized to give (1''S,3''S)-dispiro[adamantane-2,3'-[1,2,4]trioxolane-5',1''-cyclohexan]-3''-yl N-[(1-((tert-butoxy)carbonyl)amino)cyclopentyl)methyl]carbamate (97.3 mg, 0.186

mmol, 83%) as a white solid. Product was confirmed using TLC and used immediately in the next reaction.



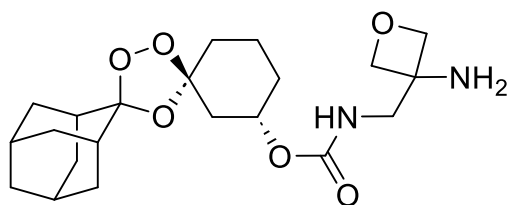
(1''S,3''S)-dispiro[adamantane-2,3'-[1,2,4]trioxolane-5',1''-cyclohexan]-3''-yl N-[(1-amino-cyclopentyl)methyl]carbamate (9q).

To a solution of (1''S,3''S)-dispiro[adamantane-2,3'-[1,2,4]trioxolane-5',1''-cyclohexan]-3''-yl N-[(1-[(tert-butoxy)carbonyl]amino)cyclopentyl)methyl]carbamate (97.3 mg, 0.186 mmol, 1 equiv) in MeOH (5mL) cooled to 0 °C was added acetyl chloride (133 uL, 1.86 mmol, 10 equiv) dropwise via microsyringe. The reaction was stirred at 0 °C for 5 minutes before being allowed to return to room temperature. After 16 hours, the reaction was quenched with 10 mL 1M Na₂CO₃ (10mL) and diluted with DCM (15mL). The organic phase was separated and washed with additional 1M Na₂CO₃ (2 x 10mL), followed by brine (10mL). The combined organic layers were dried (MgSO₄) and concentrated under reduced pressure. The crude residue was purified using flash column chromatography (12 g silica gel cartridge, 0-20% MeOH (containing 0.7N NH₃) / CH₂Cl₂) with the desired product eluting at 10% MeOH (containing 0.7N NH₃) / CH₂Cl₂). The fractions containing the product were combined and lyophilized to give (1''S,3''S)-dispiro[adamantane-2,3'-[1,2,4]trioxolane-5',1''-cyclohexan]-3''-yl N-[(1-amino-cyclopentyl)methyl]carbamate (41.6 mg, 0.098 mmol, 53.2%) as a white solid. HNMR indicated the presence of some residual PNP, which was carried through as an impurity. ¹H NMR (CHLOROFORM-d, 400 MHz) δ 4.6-4.8 (m, 1H), 3.51 (s, 2H), 2.2-2.4 (m, 1H), 1.9-2.1 (m, 8H), 1.76 (br s, 16H), 1.28 (s, 5H), 0.9-1.0 (m, 1H) ¹³C NMR (CHLOROFORM-d, 100 MHz) δ 111.6, 77.2, 60.8, 60.8, 36.8, 36.3, 34.8, 33.8, 30.7, 29.7, 29.4, 29.3, 26.9, 26.5, 23.9, 22.9, 22.7, 19.9 MS (ESI) calc for C₂₃H₃₇N₂O₅ [M+H]⁺: m/z 421.27 found 421.53



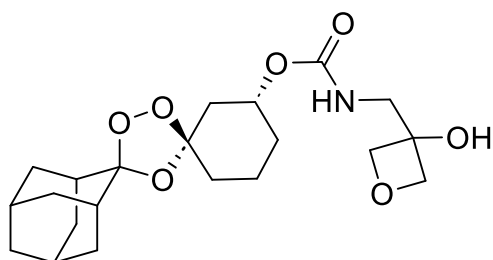
(1''S,3''S)-dispiro[adamantane-2,3'-[1,2,4]trioxolane-5',1''-cyclohexan]-3''-yl N-[(3-aminooxetan-3-yl)methyl]carbamate (8r).

To a solution of RR-TRX-PNP (50 mg, 0.11 mmol, 1.0 equiv.) in dichloromethane (1.5mL) was added triethylamine (47 μ L, 0.34 mmol, 3.0 equiv.), followed by 3-(aminomethyl)oxetan-3-amine, Oxalic acid (32 mg, 0.17 mmol, 1.5 equiv.) at rt. The bright yellow mixture was allowed to stir at rt for 16 hours. The reaction was then quenched with DCM, washed with water, and the organic layer was extracted 3 times with saturated NaHCO₃ until the aqueous layer was colorless (indicating that p-nitrophenol had been depleted). The collected organic fractions were dried over MgSO₄, concentrated under reduced pressure. The crude residue was purified using flash column chromatography (12 g silica gel cartridge, 0-20% methanol (with 0.8N ammonia) in DCM). The fractions containing the product were combined and concentrated to yield (1''S,3''S)-dispiro[adamantane-2,3'-[1,2,4]trioxolane-5',1''-cyclohexan]-3''-yl N-[(3-aminooxetan-3-yl)methyl]carbamate (34.7mg, 0.085mmol, 77.3%) as a white solid. ¹H NMR (400 MHz, MeOD) δ 4.6-4.7 (m, 1H), 4.4-4.5 (m, 3H), 3.4-3.6 (m, 2H), 2.1-2.3 (m, 1H), 2.0-2.1 (m, 2H), 1.7-2.0 (m, 14H), 1.65 (dt, 1H, J=3.8, 12.6 Hz), 1.3-1.6 (m, 4H) ¹³C NMR (100 MHz, MeOD) δ 157.6, 111.2, 108.6, 81.3, 71.0, 56.2, 48.1, 47.9, 46.4, 39.9, 36.4, 36.4, 36.4, 34.4, 34.4, 33.3, 30.3, 27.0, 26.6, 19.4 MS (ESI) calc for C₂₁H₃₃N₂O₆ [M+H]⁺: m/z 409.23 found 409.38



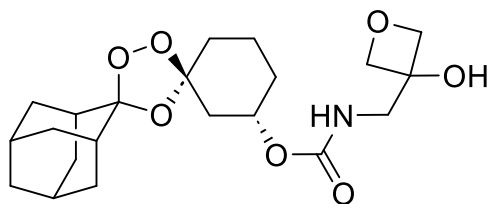
(1''S,3''S)-dispiro[adamantane-2,3'-[1,2,4]trioxolane-5',1''-cyclohexan]-3''-yl N-[(3-aminooxetan-3-yl)methyl]carbamate (9r).

To a solution of (1''S, 3''S)-dispiro[adamantane-2,3'-[1,2,4]trioxolane-5',1''-cyclohexan]-3''-yl (4-nitrophenyl) carbonate(100 mg, 0.225 mmol, 1.0 equiv.) in dichloromethane (5mL) was added triethylamine (440.0 μ L, 3.16 mmol, 14.1 equiv.), followed by 3-(ammoniomethyl)oxetan-3-aminium oxalate (200 mg, 1.04 mmol, 4.64 equiv.) at rt. The bright yellow mixture was allowed to stir at rt for 16hr. The reaction was quenched with 1M Na₂CO₃ (10mL) and diluted with DCM (10mL). The organic phase was separated and washed with additional 1M Na₂CO₃ (4 x 10mL) until the aqueous layer was colorless (indicating that p-nitrophenol had been successfully removed from the organic layer). The combined organic layers were washed with brine (15mL), dried (MgSO₄), and concentrated under reduced pressure. The crude residue was purified using flash column chromatography (12 g silica gel cartridge, 0-20% MeOH (containing 0.7N NH₃) / CH₂Cl₂) with the desired product eluting at 5% MeOH (containing 0.7N NH₃) / CH₂Cl₂). The fractions containing the product were combined and lyophilized to give (1''S,3''S)-dispiro[adamantane-2,3'-[1,2,4]trioxolane-5',1''-cyclohexan]-3''-yl N-[(3-aminooxetan-3-yl)methyl]carbamate (84.8 mg, 0.208 mmol, 92.5%) as a white solid. NMR and UPLC/MS indicated the presence of an unknown impurity which was carried through initial compound evaluation. ¹H NMR (400 MHz, CDCl₃) δ 4.7-4.8 (m, 1H), 4.50 (br d, 2H, J=6.3 Hz), 4.43 (d, 2H, J=6.6 Hz), 3.52 (br s, 1H), 2.60 (br s, 1H), 2.2-2.3 (m, 1H), 1.8-2.0 (m, 14H), 1.7-1.8 (m, 7H), 1.5-1.6 (m, 3H), 1.2-1.3 (m, 9H) ¹³C NMR (CDCl₃, 100 MHz) δ 156.4, 111.6, 108.7, 82.3, 71.3, 56.5, 40.2, 36.7, 36.3, 35.8, 34.8, 34.8, 33.8, 31.9, 30.9, 30.7, 29.7, 29.4, 26.9, 26.4, 25.8, 22.7, 19.7, 14.1 MS (ESI) calc for C₂₁H₃₃N₂O₆ [M+H]⁺: m/z 409.23 found 409.48



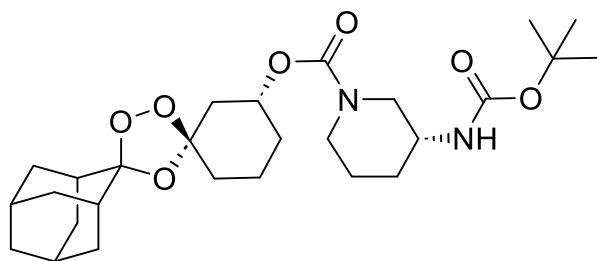
(1''R,3''R)-dispiro[adamantane-2,3'-[1,2,4]trioxolane-5',1''-cyclohexan]-3''-yl N-[(3-hydroxyoxetan-3-yl)methyl]carbamate (8s).

To a solution of (1''R, 3''R)-dispiro[adamantane-2,3'-[1,2,4]trioxolane-5',1''-cyclohexan]-3''-yl (4-nitrophenyl) carbonate(100 mg, 0.225 mmol, 1.0 equiv.) in dichloromethane (5mL) was added triethylamine (78.2 μ L, 0.561 mmol, 2.5 equiv.), followed by 3-(aminomethyl)oxetan-3-ol (57.9mg, 0.561 mmol, 2.5 equiv.) at rt. The bright yellow mixture was allowed to stir at rt for 16hr. The reaction was quenched with 1M Na₂CO₃ (10mL) and diluted with DCM (10mL). The organic phase was separated and washed with additional 1M Na₂CO₃ (4 x 10mL) until the aqueous layer was colorless (indicating that p-nitrophenol had been successfully removed from the organic layer). The combined organic layers were washed with brine (15mL), dried (MgSO₄), and concentrated under reduced pressure. The crude residue was purified using flash column chromatography (12 g silica gel cartridge, 0-20% MeOH (containing 0.7N NH₃) / CH₂Cl₂) with the desired product eluting at 5% MeOH (containing 0.7N NH₃) / CH₂Cl₂). The fractions containing the product were combined and lyophilized to give (1''R,3''R)-dispiro[adamantane-2,3'-[1,2,4]trioxolane-5',1''-cyclohexan]-3''-yl N-[(3-hydroxyoxetan-3-yl)methyl]carbamate (92.1 mg, 0.225 mmol, 100%) as a white solid. ¹H NMR (400 MHz, CDCl₃) δ 5.21 (br s, 1H), 4.7-4.8 (m, 1H), 4.62 (d, 2H, J=7.1 Hz), 4.44 (d, 2H, J=6.8 Hz), 3.63 (d, 2H, J=5.8 Hz), 2.2-2.4 (m, 1H), 1.9-2.0 (m, 7H), 1.7-1.9 (m, 8H), 1.7-1.7 (m, 1H), 1.4-1.7 (m, 2H), 1.2-1.4 (m, 2H) ¹³C NMR (CDCl₃, 100 MHz) δ 158.2, 111.7, 108.6, 81.7, 72.1, 47.5, 40.1, 36.8, 36.3, 36.3, 34.8, 34.7, 33.7, 30.6, 26.9, 26.4, 19.7 MS (ESI) calc for C₂₁H₃₂NO₇ [M+H]⁺: m/z 410.22 found 410.43



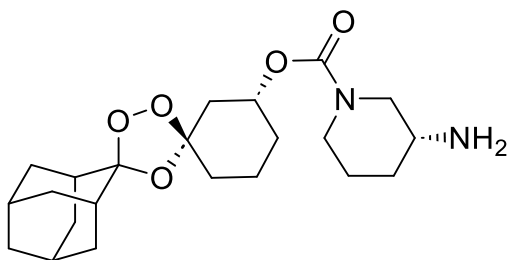
(1''S,3''S)-dispiro[adamantane-2,3'-[1,2,4]trioxolane-5',1''-cyclohexan]-3''-yl N-[(3-hydroxyoxetan-3-yl)methyl]carbamate (9s).

To a solution of (1''S, 3''S)-dispiro[adamantane-2,3'-[1,2,4]trioxolane-5',1''-cyclohexan]-3''-yl (4-nitrophenyl) carbonate(100 mg, 0.225 mmol, 1.0 equiv.) in dichloromethane (5mL) was added triethylamine (78.2 μ L, 0.561 mmol, 2.5 equiv.), followed by 3-(aminomethyl)oxetan-3-ol (57.9mg, 0.561 mmol, 2.5 equiv.) at rt. The bright yellow mixture was allowed to stir at rt for 16hr. The reaction was quenched with 1M Na₂CO₃ (10mL) and diluted with DCM (10mL). The organic phase was separated and washed with additional 1M Na₂CO₃ (4 x 10mL) until the aqueous layer was colorless (indicating that p-nitrophenol had been successfully removed from the organic layer). The combined organic layers were washed with brine (15mL), dried (MgSO₄), and concentrated under reduced pressure. The crude residue was purified using flash column chromatography (12 g silica gel cartridge, 0-20% MeOH (containing 0.7N NH₃) / CH₂Cl₂) with the desired product eluting at 5% MeOH (containing 0.7N NH₃) / CH₂Cl₂). The fractions containing the product were combined and lyophilized to give (1''S,3''S)-dispiro[adamantane-2,3'-[1,2,4]trioxolane-5',1''-cyclohexan]-3''-yl N-[(3-hydroxyoxetan-3-yl)methyl]carbamate (51.8 mg, 0.127 mmol, 56.4%) as a white solid. ¹H NMR (400 MHz, CDCl₃) δ 5.23 (br s, 1H), 4.7-4.9 (m, 1H), 4.62 (d, 2H, J=6.8 Hz), 4.44 (d, 2H, J=7.1 Hz), 4.37 (br s, 1H), 3.62 (d, 2H, J=5.8 Hz), 2.2-2.3 (m, 1H), 1.99 (br d, 5H, J=7.8 Hz), 1.7-1.9 (m, 9H), 1.7-1.7 (m, 3H), 1.4-1.7 (m, 2H), 1.2-1.4 (m, 2H) ¹³C NMR (CDCl₃, 100 MHz) δ 158.0, 111.7, 108.6, 81.7, 72.1, 47.5, 40.1, 36.8, 36.3, 36.3, 34.8, 34.7, 33.7, 30.6, 29.7, 26.9, 26.4, 19.7 MS (ESI) calc for C₂₁H₃₂NO₇ [M+H]⁺: m/z 410.22 found 410.38



(1''R,3''R)-dispiro[adamantane-2,3'-[1,2,4]trioxolane-5',1''-cyclohexan]-3''-yl (3R)-3-[[tert-butoxy]carbonyl]amino]piperidine-1-carboxylate.

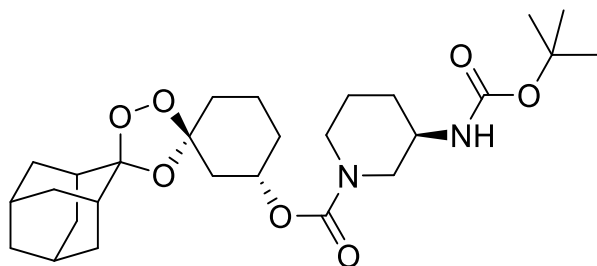
To a solution of (1''R, 3''R)-dispiro[adamantane-2,3'-[1,2,4]trioxolane-5',1''-cyclohexan]-3''-yl (4-nitrophenyl) carbonate(100 mg, 0.224 mmol, 1.0 equiv.) in dichloromethane (5mL) was added triethylamine (78.2µL, 0.561 mmol, 2.5 equiv.), followed by tert-butyl (R)-piperidin-3-ylcarbamate (112.0 mg, 0.561 mmol, 2.5 equiv.) at rt. The bright yellow mixture was allowed to stir at rt for 16hr. The reaction was quenched with 1M Na₂CO₃ (10mL) and diluted with DCM (10mL). The organic phase was separated and washed with additional 1M Na₂CO₃ (4 x 10mL) until the aqueous layer was colorless (indicating that p-nitrophenol had been successfully removed from the organic layer). The combined organic layers were washed with brine (15mL), dried (MgSO₄), and concentrated under reduced pressure. The crude residue was purified using flash column chromatography (12 g silica gel cartridge, 0-50% EtOAc:Hexanes) with the desired product eluting at 30% EtOAc. The fractions containing the product were combined and lyophilized to give (1''R,3''R)-dispiro[adamantane-2,3'-[1,2,4]trioxolane-5',1''-cyclohexan]-3''-yl (3R)-3-[[tert-butoxy)carbonyl]amino}piperidine-1-carboxylate (114.0 mg, 0.224 mmol, 100%) as a white solid. MS (ESI) calc for C₂₇H₄₂N₂O₇Na [M+Na]⁺: m/z 529.29 found 529.08.



(1''R,3''R)-dispiro[adamantane-2,3'-[1,2,4]trioxolane-5',1''-cyclohexan]-3''-yl (3R)-3-aminopiperidine-1-carboxylate (8t).

To a solution of (1''R,3''R)-dispiro[adamantane-2,3'-[1,2,4]trioxolane-5',1''-cyclohexan]-3''-yl (3R)-3-[[tert-butoxy)carbonyl]amino}piperidine-1-carboxylate (114 mg, 0.225 mmol, 1 equiv) in MeOH (5mL) cooled to 0 °C was added acetyl chloride (160 µL, 2.25mmol, 10 equiv) dropwise via microsyringe. The reaction was stirred at 0 °C for 5 minutes before being allowed to return to room temperature. After 16 hours, the reaction was quenched with 10 mL 1M Na₂CO₃ (10mL) and diluted with DCM (15mL). The organic phase was

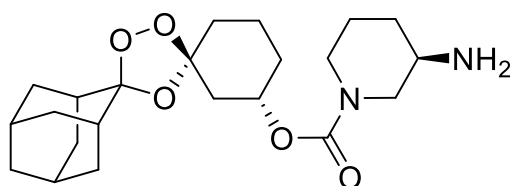
separated and washed with additional 1M Na₂CO₃ (2 x 10mL), followed by brine (10mL). The combined organic layers were dried (MgSO₄) and concentrated under reduced pressure. The crude residue was purified using flash column chromatography (12 g silica gel cartridge, 0-20% MeOH (containing 0.7N NH₃) / CH₂Cl₂) with the desired product eluting at 10% MeOH (containing 0.7N NH₃) / CH₂Cl₂). The fractions containing the product were combined and lyophilized to give (1''R,3''R)-dispiro[adamantane-2,3'-[1,2,4]trioxolane-5',1''-cyclohexan]-3''-yl (3R)-3-aminopiperidine-1-carboxylate (71.3 mg, 0.175 mmol, 77.9%) as a white solid. ¹H NMR (CHLOROFORM-d, 400 MHz) δ 4.7-4.9 (m, 1H), 3.97 (br d, 1H, J=11.0 Hz), 3.77 (br s, 1H), 2.88 (br s, 2H), 2.47 (br s, 4H), 2.1-2.4 (m, 1H), 1.9-2.0 (m, 8H), 1.7-1.9 (m, 8H), 1.6-1.7 (m, 2H), 1.3-1.6 (m, 4H), 1.27 (s, 1H) ¹³C NMR (CHLOROFORM-d, 100 MHz) δ 158.6, 111.6, 108.7, 71.4, 47.5, 43.8, 39.9, 36.8, 36.3, 36.3, 34.9, 34.8, 34.7, 34.6, 34.1, 30.6, 29.7, 26.9, 26.5, 23.3, 19.6 MS (ESI) calc for C₂₂H₃₅N₂O₅ [M+H]⁺: m/z calc 407.25 found 407.43



(1''S,3''S)-dispiro[adamantane-2,3'-[1,2,4]trioxolane-5',1''-cyclohexan]-3''-yl (3R)-3-[(tert-butoxy)carbonyl]amino)piperidine-1-carboxylate.

To a solution of (1''S, 3''S)-dispiro[adamantane-2,3'-[1,2,4]trioxolane-5',1''-cyclohexan]-3''-yl (4-nitrophenyl) carbonate(100 mg, 0.224 mmol, 1.0 equiv.) in dichloromethane (5mL) was added triethylamine (78.2 μL, 0.561 mmol, 2.5 equiv.), followed by tert-butyl (R)-piperidin-3-ylcarbamate (112 mg, 0.561 mmol, 2.5 equiv.) at rt. The bright yellow mixture was allowed to stir at rt for 16hr. The reaction was quenched with 1M Na₂CO₃ (10mL) and diluted with DCM (10mL). The organic phase was separated and washed with additional 1M Na₂CO₃ (4 x 10mL) until the aqueous layer was colorless (indicating that p-nitrophenol had been successfully removed from the organic layer). The combined

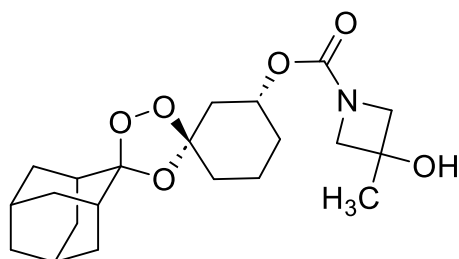
organic layers were washed with brine (15mL), dried (MgSO₄), and concentrated under reduced pressure. The crude residue was purified using flash column chromatography (12 g silica gel cartridge, 0-50% EtOAc:Hexanes) with the desired product eluting at 30% EtOAc. The fractions containing the product were combined and lyophilized to give (1''S,3''S)-dispiro[adamantane-2,3'-[1,2,4]trioxolane-5',1''-cyclohexan]-3''-yl (3R)-3-[[tert-butoxy)carbonyl]amino]piperidine-1-carboxylate (88.7mg, 0.175 mmol, 78%) as a white solid. MS (ESI) calc for C₂₇H₄₂N₂O₇ [M+H]⁺: m/z 529.29 found 529.24.



(1''S,3''S)-dispiro[adamantane-2,3'-[1,2,4]trioxolane-5',1''-cyclohexan]-3''-yl (3R)-3-aminopiperidine-1-carboxylate (9t).

To a solution of (1''S,3''S)-dispiro[adamantane-2,3'-[1,2,4]trioxolane-5',1''-cyclohexan]-3''-yl (3R)-3-[[tert-butoxy)carbonyl]amino]piperidine-1-carboxylate (88.7 mg, 0.175 mmol, 1 equiv) in MeOH (5mL) cooled to 0 °C was added acetyl chloride (124 μ L, 1.75 mmol, 10 equiv) dropwise via microsyringe. The reaction was stirred at 0 °C for 5 minutes before being allowed to return to room temperature. After 16 hours, the reaction was quenched with 10 mL 1M Na₂CO₃ (10mL) and diluted with DCM (15mL). The organic phase was separated and washed with additional 1M Na₂CO₃ (2 x 10mL), followed by brine (10mL). The combined organic layers were dried (MgSO₄) and concentrated under reduced pressure. The crude residue was purified using flash column chromatography (12 g silica gel cartridge, 0-20% MeOH (containing 0.7N NH₃) / CH₂Cl₂) with the desired product eluting at 15% MeOH (containing 0.7N NH₃) / CH₂Cl₂). The fractions containing the product were combined and lyophilized to give (1''S,3''S)-dispiro[adamantane-2,3'-[1,2,4]trioxolane-5',1''-cyclohexan]-3''-yl (3R)-3-aminopiperidine-1-carboxylate (15 mg, 0.040 mmol, 15%) as a white solid. ¹H NMR (400 MHz, MeOD) δ 4.7-4.8 (m, 1H), 3.98 (br d, 1H, J=10.2 Hz), 3.83 (br s, 1H), 2.7-3.1 (m, 5H), 2.2-2.3 (m, 1H), 1.9-2.1 (m, 7H), 1.6-1.9 (m, 12H), 1.3-1.6 (m, 4H), 1.27 (s, 2H); ¹³C NMR (MeOD, 100 MHz) δ 154.3,

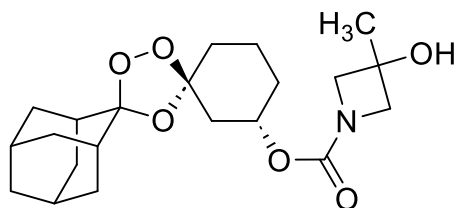
111.6, 108.7, 71.4, 47.4, 43.9, 39.9, 36.8, 36.3, 34.9, 34.8, 34.7, 34.7, 34.1, 31.9, 30.7, 29.7, 26.9, 26.5, 23.4, 22.7, 19.6; MS (ESI) calc for C₂₂H₃₅N₂O₅ [M+H]⁺: m/z 407.25 found 407.38



(1''R,3''R)-dispiro[adamantane-2,3'-[1,2,4]trioxolane-5',1''-cyclohexan]-3''-yl 3-hydroxy-3-methylazetidine-1-carboxylate (8u).

To a solution of (1''R, 3''R)-dispiro[adamantane-2,3'-[1,2,4]trioxolane-5',1''-cyclohexan]-3''-yl (4-nitrophenyl) carbonate(100 mg, 0.224 mmol, 1.0 equiv.) in dichloromethane (5mL) was added triethylamine (78.2 μ L, 0.561 mmol, 2.5 equiv.), followed by 3-methylazetidin-3-ol (48.9 mg, 0.561 mmol, 2.5 equiv.) at rt. The bright yellow mixture was allowed to stir at rt for 16hr. The reaction was quenched with 1M Na₂CO₃ (10mL) and diluted with DCM (10mL). The organic phase was separated and washed with additional 1M Na₂CO₃ (4 x 10mL) until the aqueous layer was colorless (indicating that p-nitrophenol had been successfully removed from the organic layer). The combined organic layers were washed with brine (15mL), dried (MgSO₄), and concentrated under reduced pressure. The crude residue was purified using flash column chromatography (12 g silica gel cartridge, 10-100% EtOAc:Hexanes) with the desired product eluting at 35% EtOAc. The fractions containing the product were combined and lyophilized to give (1''R,3''R)-dispiro[adamantane-2,3'-[1,2,4]trioxolane-5',1''-cyclohexan]-3''-yl 3-hydroxy-3-methylazetidine-1-carboxylate (88.3 mg, 0.224 mmol, 100%) as a white solid. ¹H NMR (CHLOROFORM-d, 400 MHz) δ 4.7-4.8 (m, 1H), 3.8-4.1 (m, 4H), 2.2-2.3 (m, 1H), 1.9-2.1 (m, 7H), 1.7-1.9 (m, 5H), 1.4-1.7 (m, 9H), 1.2-1.4 (m, 3H) ¹³C NMR (CHLOROFORM-d, 100 MHz) δ 156.2, 111.6, 108.7, 71.2, 68.5, 63.4, 40.1, 36.8, 36.3, 34.9, 34.8, 34.7, 33.9,

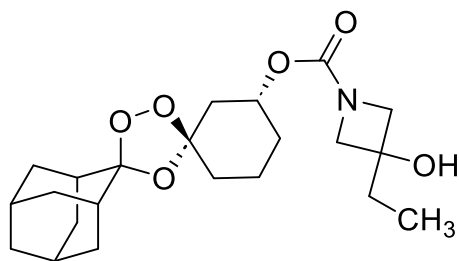
30.7, 29.7, 26.9, 26.4, 26.2, 19.6 MS (ESI) calc for C₂₁H₃₁NO₆Na [M+Na]⁺: m/z 416.20
found 416.43



(1''S,3''S)-dispiro[adamantane-2,3'-[1,2,4]trioxolane-5',1''-cyclohexan]-3''-yl 3-hydroxy-3-methylazetidide-1-carboxylate (9u).

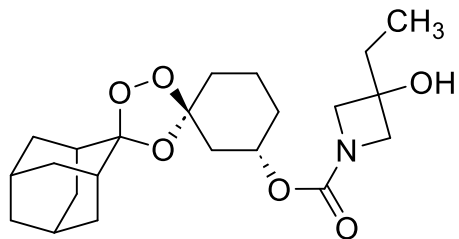
To a solution of (1''S, 3''S)-dispiro[adamantane-2,3'-[1,2,4]trioxolane-5',1''-cyclohexan]-3''-yl (4-nitrophenyl) carbonate (100 mg, 0.224 mmol, 1.0 equiv.) in dichloromethane (5mL) was added triethylamine (78.2μL, 0.561 mmol, 2.5 equiv.), followed by 3-methylazetidide-3-ol (48.9 mg, 0.561 mmol, 2.5 equiv.) at rt. The bright yellow mixture was allowed to stir at rt for 16hr. The reaction was quenched with 1M Na₂CO₃ (10mL) and diluted with DCM (10mL). The organic phase was separated and washed with additional 1M Na₂CO₃ (4 x 10mL) until the aqueous layer was colorless (indicating that p-nitrophenol had been successfully removed from the organic layer). The combined organic layers were washed with brine (15mL), dried (MgSO₄), and concentrated under reduced pressure. The crude residue was purified using flash column chromatography (12 g silica gel cartridge, 10-100% EtOAc:Hexanes) with the desired product eluting at 35% EtOAc. The fractions containing the product were combined and lyophilized to yield (1''S,3''S)-dispiro[adamantane-2,3'-[1,2,4]trioxolane-5',1''-cyclohexan]-3''-yl 3-hydroxy-3-methylazetidide-1-carboxylate

(77.0 mg, 0.196 mmol, 87.2%) as a white solid. ¹H NMR (CHLOROFORM-d, 400 MHz) δ 4.7-4.8 (m, 1H), 3.8-4.0 (m, 4H), 2.50 (br s, 1H), 2.2-2.3 (m, 1H), 1.9-2.1 (m, 7H), 1.7-1.9 (m, 6H), 1.5-1.7 (m, 10H), 1.2-1.4 (m, 2H) ¹³C NMR (CHLOROFORM-d, 100 MHz) δ 156.2, 111.6, 108.7, 71.2, 68.5, 63.4, 40.1, 36.8, 36.3, 36.3, 34.9, 34.8, 34.7, 33.9, 30.7, 29.7, 26.9, 26.4, 26.2, 19.6 MS (ESI) calc for C₂₁H₃₁NO₆Na [M+Na]⁺: m/z 416.20 found 416.33



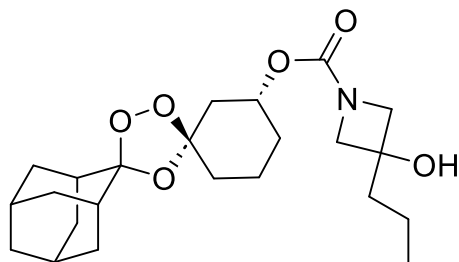
(1''R,3''R)-dispiro[adamantane-2,3'-[1,2,4]trioxolane-5',1''-cyclohexan]-3''-yl 3-ethyl-3-hydroxyazetidinoate (8v).

To a solution of (1''R, 3''R)-dispiro[adamantane-2,3'-[1,2,4]trioxolane-5',1''-cyclohexan]-3''-yl (4-nitrophenyl) carbonate (100 mg, 0.224 mmol, 1.0 equiv.) in dichloromethane (5mL) was added triethylamine (110 μ L, 0.786 mmol, 3.5 equiv.), followed by 3-ethylazetidino-3-ol (79.5 mg, 0.786 mmol, 3.5 equiv.) at rt. The bright yellow mixture was allowed to stir at rt for 16hr. The reaction was quenched with 1M Na₂CO₃ (10mL) and diluted with DCM (10mL). The organic phase was separated and washed with additional 1M Na₂CO₃ (4 x 10mL) until the aqueous layer was colorless (indicating that p-nitrophenol had been successfully removed from the organic layer). The combined organic layers were washed with brine (15mL), dried (MgSO₄), and concentrated under reduced pressure. The crude residue was purified using flash column chromatography (12 g silica gel cartridge, 0-60% EtOAc:Hexanes) with the desired product eluting at 30% EtOAc. The fractions containing the product were combined and lyophilized to yield (1''R,3''R)-dispiro[adamantane-2,3'-[1,2,4]trioxolane-5',1''-cyclohexan]-3''-yl 3-ethyl-3-hydroxyazetidinoate (67.2 mg, 0.165 mmol, 73.5%) as a white solid. ¹H NMR (CHLOROFORM-d, 400 MHz) δ 4.7-4.8 (m, 1H), 3.87 (q, 4H, J=9.2 Hz), 2.2-2.3 (m, 1H), 2.08 (br d, 1H, J=11.2 Hz), 1.9-2.0 (m, 7H), 1.7-1.9 (m, 9H), 1.4-1.7 (m, 3H), 1.2-1.4 (m, 2H), 0.99 (t, 3H, J=7.4 Hz) ¹³C NMR (CHLOROFORM-d, 100 MHz) δ 156.2, 111.6, 108.7, 71.4, 71.2, 61.6, 40.0, 36.8, 36.3, 34.9, 34.8, 34.7, 33.9, 31.6, 30.7, 26.9, 26.5, 19.6, 7.4 MS (ESI) calc for C₂₂H₃₃NO₆Na [M+Na]⁺: m/z 430.22 found 430.34



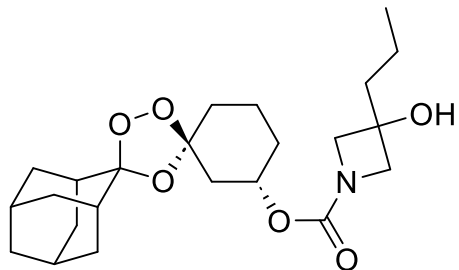
(1''S,3''S)-dispiro[adamantane-2,3'-[1,2,4]trioxolane-5',1''-cyclohexan]-3''-yl 3-ethyl-3-hydroxyazetid-1-carboxylate (9v).

To a solution of (1''S, 3''S)-dispiro[adamantane-2,3'-[1,2,4]trioxolane-5',1''-cyclohexan]-3''-yl (4-nitrophenyl) carbonate (100 mg, 0.224 mmol, 1.0 equiv.) in dichloromethane (5mL) was added triethylamine (110 μ L, 0.786 mmol, 3.5 equiv.), followed by 3-methylazetid-3-ol (79.5 mg, 0.786 mmol, 3.5 equiv.) at rt. The bright yellow mixture was allowed to stir at rt for 16hr. The reaction was quenched with 1M Na₂CO₃ (10mL) and diluted with DCM (10mL). The organic phase was separated and washed with additional 1M Na₂CO₃ (4 x 10mL) until the aqueous layer was colorless (indicating that p-nitrophenol had been successfully removed from the organic layer). The combined organic layers were washed with brine (15mL), dried (MgSO₄), and concentrated under reduced pressure. The crude residue was purified using flash column chromatography (12 g silica gel cartridge, 0-60% EtOAc:Hexanes) with the desired product eluting at 30% EtOAc. The fractions containing the product were combined and lyophilized to yield (1''S,3''S)-dispiro[adamantane-2,3'-[1,2,4]trioxolane-5',1''-cyclohexan]-3''-yl 3-ethyl-3-hydroxyazetid-1-carboxylate (71.4 mg, 0.175 mmol, 78.1%) as a white solid. ¹H NMR (CHLOROFORM-d, 400 MHz) δ 4.7-4.8 (m, 1H), 3.8-3.9 (m, 4H), 2.1-2.3 (m, 1H), 2.06 (s, 1H), 1.9-2.0 (m, 8H), 1.7-1.9 (m, 9H), 1.4-1.7 (m, 3H), 1.2-1.4 (m, 2H), 0.99 (t, 3H, J=7.4 Hz) ¹³C NMR (CHLOROFORM-d, 100 MHz) δ 156.1, 111.6, 108.7, 71.4, 71.1, 61.6, 40.0, 36.8, 36.3, 36.3, 34.9, 34.8, 34.7, 33.9, 31.6, 30.7, 26.9, 26.5, 19.6, 7.4 MS (ESI) calc for C₂₂H₃₃NO₆Na [M+Na]⁺: m/z 430.22 found 430.29



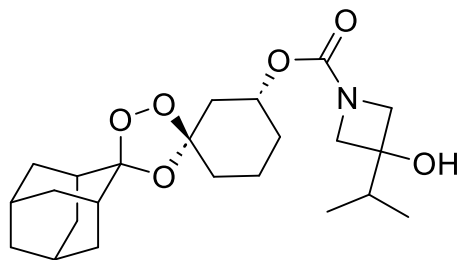
(1''R,3''R)-dispiro[adamantane-2,3'-[1,2,4]trioxolane-5',1''-cyclohexan]-3''-yl 3-hydroxy-3-propylazetidide-1-carboxylate (8w).

To a solution of (1''R, 3''R)-dispiro[adamantane-2,3'-[1,2,4]trioxolane-5',1''-cyclohexan]-3''-yl (4-nitrophenyl) carbonate (100 mg, 0.224 mmol, 1.0 equiv.) in dichloromethane (5mL) was added triethylamine (93.9 μ L, 0.673 mmol, 3 equiv.), followed by 3-propylazetidide-3-ol (79.5 mg, 0.673 mmol, 3 equiv.) at rt. The bright yellow mixture was allowed to stir at rt for 16hr. The reaction was quenched with 1M Na₂CO₃ (10mL) and diluted with DCM (10mL). The organic phase was separated and washed with additional 1M Na₂CO₃ (4 x 10mL) until the aqueous layer was colorless (indicating that p-nitrophenol had been successfully removed from the organic layer). The combined organic layers were washed with brine (15mL), dried (MgSO₄), and concentrated under reduced pressure. The crude residue was purified using flash column chromatography (12 g silica gel cartridge, 0-60% EtOAc:Hexanes) with the desired product eluting at 20% EtOAc. The fractions containing the product were combined and lyophilized to yield (1''R,3''R)-dispiro[adamantane-2,3'-[1,2,4]trioxolane-5',1''-cyclohexan]-3''-yl 3-hydroxy-3-propylazetidide-1-carboxylate (94.6mg, 0.224 mmol, 100%) as a white solid. ¹H NMR (CHLOROFORM-d, 400 MHz) δ 4.7-4.8 (m, 1H), 3.8-3.9 (m, 4H), 2.2-2.3 (m, 1H), 2.14 (br s, 1H), 1.9-2.0 (m, 7H), 1.7-1.9 (m, 12H), 1.6-1.7 (m, 1H), 1.4-1.6 (m, 3H), 1.3-1.4 (m, 1H), 0.99 (t, 3H, J=7.4 Hz) ¹³C NMR (CHLOROFORM-d, 100 MHz) δ 156.1, 111.6, 108.7, 71.1, 71.0, 62.1, 41.0, 40.1, 36.8, 36.3, 36.3, 34.9, 34.8, 34.7, 33.9, 30.7, 26.9, 26.5, 19.6, 16.7, 14.2 MS (ESI) calc for C₂₃H₃₅NO₆Na [M+Na]⁺: m/z 444.24 found 444.35



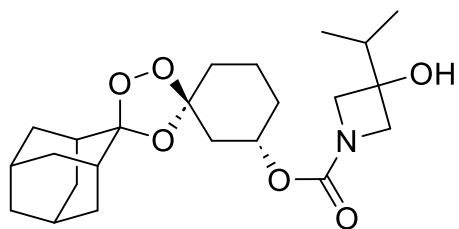
(1''S,3''S)-dispiro[adamantane-2,3'-[1,2,4]trioxolane-5',1''-cyclohexan]-3''-yl 3-hydroxy-3-propylazetidide-1-carboxylate (9w).

To a solution of (1''S, 3''S)-dispiro[adamantane-2,3'-[1,2,4]trioxolane-5',1''-cyclohexan]-3''-yl (4-nitrophenyl) carbonate (100 mg, 0.224 mmol, 1.0 equiv.) in dichloromethane (5mL) was added triethylamine (110 μ L, 0.786 mmol, 3.5 equiv.), followed by 3-propylazetidide-3-ol (90.5 mg, 0.786 mmol, 3.5 equiv.) at rt. The bright yellow mixture was allowed to stir at rt for 16hr. The reaction was quenched with 1M Na₂CO₃ (10mL) and diluted with DCM (10mL). The organic phase was separated and washed with additional 1M Na₂CO₃ (4 x 10mL) until the aqueous layer was colorless (indicating that p-nitrophenol had been successfully removed from the organic layer). The combined organic layers were washed with brine (15mL), dried (MgSO₄), and concentrated under reduced pressure. The crude residue was purified using flash column chromatography (12 g silica gel cartridge, 0-60% EtOAc:Hexanes) with the desired product eluting at 20% EtOAc. The fractions containing the product were combined and lyophilized to yield (1''S,3''S)-dispiro[adamantane-2,3'-[1,2,4]trioxolane-5',1''-cyclohexan]-3''-yl 3-hydroxy-3-propylazetidide-1-carboxylate (94.6 mg, 0.224 mmol, 100%) as a white solid. ¹H NMR (CHLOROFORM-d, 400 MHz) δ 4.7-4.8 (m, 1H), 3.8-3.9 (m, 4H), 2.2-2.3 (m, 1H), 2.13 (br s, 1H), 1.9-2.0 (m, 7H), 1.7-1.9 (m, 12H), 1.6-1.7 (m, 1H), 1.4-1.6 (m, 3H), 1.3-1.4 (m, 1H), 0.99 (t, 3H, J=7.3 Hz) ¹³C NMR (CHLOROFORM-d, 100 MHz) δ 156.1, 111.6, 108.7, 71.1, 71.0, 62.1, 41.0, 40.1, 36.8, 36.3, 36.3, 34.9, 34.8, 34.7, 33.9, 30.7, 26.9, 26.5, 19.6, 16.7, 14.2 MS (ESI) calc for C₂₃H₃₅NO₆Na [M+Na]⁺: m/z 444.24 found 444.30



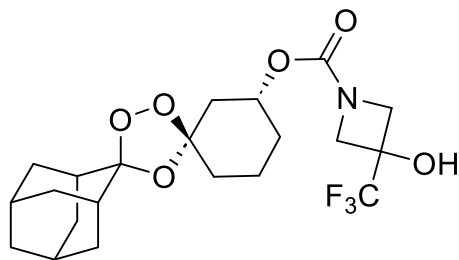
(1''R,3''R)-dispiro[adamantane-2,3'-[1,2,4]trioxolane-5',1''-cyclohexan]-3''-yl 3-hydroxy-3-(propan-2-yl)azetidine-1-carboxylate (8x).

To a solution of (1''R, 3''R)-dispiro[adamantane-2,3'-[1,2,4]trioxolane-5',1''-cyclohexan]-3''-yl (4-nitrophenyl) carbonate (100 mg, 0.224 mmol, 1.0 equiv.) in dichloromethane (5mL) was added triethylamine (93.9 μ L, 0.673 mmol, 3 equiv.), followed by 3-isopropylazetidin-3-ol (77.6 mg, 0.673 mmol, 3 equiv.) at rt. The bright yellow mixture was allowed to stir at rt for 16hr. The reaction was quenched with 1M Na₂CO₃ (10mL) and diluted with DCM (10mL). The organic phase was separated and washed with additional 1M Na₂CO₃ (4 x 10mL) until the aqueous layer was colorless (indicating that p-nitrophenol had been successfully removed from the organic layer). The combined organic layers were washed with brine (15mL), dried (MgSO₄), and concentrated under reduced pressure. The crude residue was purified using flash column chromatography (12 g silica gel cartridge, 0-60% EtOAc:Hexanes) with the desired product eluting at 40% EtOAc. The fractions containing the product were combined and lyophilized to yield (1''R,3''R)-dispiro[adamantane-2,3'-[1,2,4]trioxolane-5',1''-cyclohexan]-3''-yl 3-hydroxy-3-(propan-2-yl)azetidine-1-carboxylate (94.6 mg, 0.224 mmol, 100%) as a white solid. ¹H NMR (CHLOROFORM-d, 400 MHz) δ 4.7-4.8 (m, 1H), 3.8-4.0 (m, 4H), 2.2-2.3 (m, 1H), 2.12 (br s, 1H), 1.9-2.0 (m, 8H), 1.7-1.9 (m, 7H), 1.4-1.7 (m, 3H), 1.3-1.4 (m, 1H), 0.95 (d, 6H, J=6.8 Hz) ¹³C NMR (CHLOROFORM-d, 100 MHz) δ 156.1, 111.6, 108.7, 73.8, 71.1, 60.7, 40.0, 36.8, 36.3, 36.3, 34.9, 34.8, 34.8, 34.7, 33.9, 30.7, 26.9, 26.5, 19.6, 15.5 MS (ESI) calc for C₂₃H₃₅NO₆Na [M+Na]⁺: m/z 444.24 found 444.30



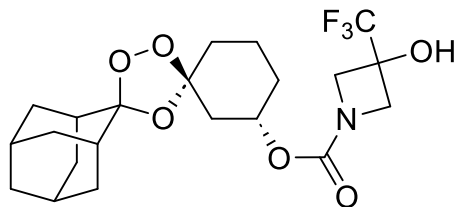
(1''S,3''S)-dispiro[adamantane-2,3'-[1,2,4]trioxolane-5',1''-cyclohexan]-3''-yl 3-hydroxy-3-(propan-2-yl)azetidine-1-carboxylate (9x).

To a solution of (1''S, 3''S)-dispiro[adamantane-2,3'-[1,2,4]trioxolane-5',1''-cyclohexan]-3''-yl (4-nitrophenyl) carbonate (100 mg, 0.224 mmol, 1.0 equiv.) in dichloromethane (5mL) was added triethylamine (110 μ L, 0.786 mmol, 3.5 equiv.), followed by 3-isopropylazetidin-3-ol (90.5 mg, 0.786 mmol, 3.5 equiv.) at rt. The bright yellow mixture was allowed to stir at rt for 16hr. The reaction was quenched with 1M Na₂CO₃ (10mL) and diluted with DCM (10mL). The organic phase was separated and washed with additional 1M Na₂CO₃ (4 x 10mL) until the aqueous layer was colorless (indicating that p-nitrophenol had been successfully removed from the organic layer). The combined organic layers were washed with brine (15mL), dried (MgSO₄), and concentrated under reduced pressure. The crude residue was purified using flash column chromatography (12 g silica gel cartridge, 0-60% EtOAc:Hexanes) with the desired product eluting at 40% EtOAc. The fractions containing the product were combined and lyophilized to yield (1''S,3''S)-dispiro[adamantane-2,3'-[1,2,4]trioxolane-5',1''-cyclohexan]-3''-yl 3-hydroxy-3-(propan-2-yl)azetidine-1-carboxylate (97.8 mg, 0.232 mmol, Quant.) as a white solid. ¹H NMR (CHLOROFORM-d, 400 MHz) δ 4.7-4.8 (m, 1H), 3.8-4.0 (m, 4H), 2.1-2.3 (m, 1H), 1.9-2.0 (m, 9H), 1.7-1.9 (m, 6H), 1.4-1.7 (m, 7H), 1.2-1.4 (m, 1H), 0.95 (d, 6H, J=6.8 Hz) ¹³C NMR (CHLOROFORM-d, 100 MHz) δ 156.1, 111.6, 108.7, 73.9, 71.1, 60.7, 40.0, 36.8, 36.3, 36.3, 34.9, 34.8, 34.7, 34.7, 33.9, 30.7, 26.9, 26.5, 19.6, 15.5 MS (ESI) calc for C₂₃H₃₅NO₆Na [M+Na]⁺: m/z 444.24 found 444.40



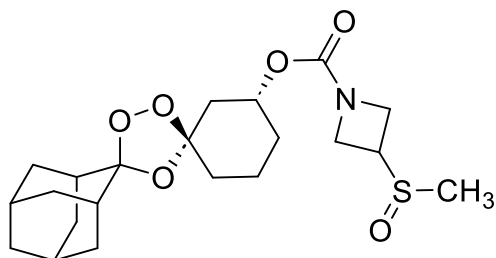
(1''R,3''R)-dispiro[adamantane-2,3'-[1,2,4]trioxolane-5',1''-cyclohexan]-3''-yl 3-hydroxy-3-(trifluoromethyl)azetidine-1-carboxylate (8y).

To a solution of (1''R, 3''R)-dispiro[adamantane-2,3'-[1,2,4]trioxolane-5',1''-cyclohexan]-3''-yl (4-nitrophenyl) carbonate (100 mg, 0.224 mmol, 1.0 equiv.) in dichloromethane (5mL) was added triethylamine (78.2 μ L, 0.561 mmol, 2.5 equiv.), followed by 3-(trifluoromethyl)azetidine-3-ol (79.2 mg, 0.561 mmol, 2.5 equiv.) at rt. The bright yellow mixture was allowed to stir at rt for 16hr. The reaction was quenched with 1M Na₂CO₃ (10mL) and diluted with DCM (10mL). The organic phase was separated and washed with additional 1M Na₂CO₃ (4 x 10mL) until the aqueous layer was colorless (indicating that p-nitrophenol had been successfully removed from the organic layer). The combined organic layers were washed with brine (15mL), dried (MgSO₄), and concentrated under reduced pressure. The crude residue was purified using flash column chromatography (12 g silica gel cartridge, 0-20% Methanol (with 0.8N NH₃):DCM) with the desired product eluting at 8% MeOH. The fractions containing the product were combined and lyophilized to yield (1''R,3''R)-dispiro[adamantane-2,3'-[1,2,4]trioxolane-5',1''-cyclohexan]-3''-yl 3-hydroxy-3-(trifluoromethyl)azetidine-1-carboxylate (56.0 mg, 0.125 mmol, 55.8%) as a white solid. ¹H NMR (CHLOROFORM-d, 400 MHz) δ 4.7-4.8 (m, 1H), 4.25 (d, 2H, J=10.0 Hz), 4.00 (br d, 2H, J=10.0 Hz), 3.67 (br s, 1H), 2.2-2.3 (m, 1H), 1.9-2.1 (m, 7H), 1.7-1.9 (m, 7H), 1.4-1.7 (m, 3H), 1.2-1.4 (m, 2H) ¹³C NMR (CHLOROFORM-d, 100 MHz) δ 155.8, 129.7, 127.4, 125.7, 122.9, 127.2, 127.5, 111.8, 108.6, 72.0, 69.4, 57.2, 56.7, 39.9, 36.7, 36.3, 34.9, 34.8, 34.7, 33.8, 30.5, 29.7, 26.8, 26.4, 19.5 MS (ESI) calc for C₂₁H₂₇F₃NO₆ [M-H]⁻ m/z 446.18 found 446.29



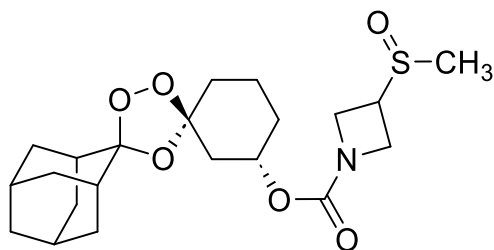
(1''S,3''S)-dispiro[adamantane-2,3'-[1,2,4]trioxolane-5',1''-cyclohexan]-3''-yl 3-hydroxy-3-(trifluoromethyl)azetidine-1-carboxylate (9y).

To a solution of (1''S, 3''S)-dispiro[adamantane-2,3'-[1,2,4]trioxolane-5',1''-cyclohexan]-3''-yl (4-nitrophenyl) carbonate (100 mg, 0.224 mmol, 1.0 equiv.) in dichloromethane (5mL) was added triethylamine (78.2 μ L, 0.561 mmol, 2.5 equiv.), followed by 3-(trifluoromethyl)azetidine-3-ol (79.2 mg, 0.561 mmol, 2.5 equiv.) at rt. The bright yellow mixture was allowed to stir at rt for 16hr. The reaction was quenched with 1M Na₂CO₃ (10mL) and diluted with DCM (10mL). The organic phase was separated and washed with additional 1M Na₂CO₃ (4 x 10mL) until the aqueous layer was colorless (indicating that p-nitrophenol had been successfully removed from the organic layer). The combined organic layers were washed with brine (15mL), dried (MgSO₄), and concentrated under reduced pressure. The crude residue was purified using flash column chromatography (12 g silica gel cartridge, 0-20% Methanol (with 0.8N NH₃):DCM) with the desired product eluting at 8% MeOH. The fractions containing the product were combined and lyophilized to yield (1''S,3''S)-dispiro[adamantane-2,3'-[1,2,4]trioxolane-5',1''-cyclohexan]-3''-yl 3-hydroxy-3-(trifluoromethyl)azetidine-1-carboxylate (73.9 mg, 0.165 mmol, 73.6%) as a white solid. ¹H NMR (CHLOROFORM-d, 400 MHz) δ 4.7-4.8 (m, 1H), 4.23 (d, 2H, J=10.0 Hz), 3.99 (br d, 2H, J=9.7 Hz), 2.2-2.4 (m, 2H), 1.9-2.1 (m, 8H), 1.7-1.9 (m, 7H), 1.5-1.7 (m, 3H), 1.3-1.4 (m, 1H) ¹³C NMR (CHLOROFORM-d, 100 MHz) δ 155.9, 126.4, 111.8, 108.5, 72.1, 69.3, 57.0, 56.7, 39.9, 36.7, 36.3, 34.8, 34.8, 34.7, 34.7, 33.8, 30.5, 26.8, 26.4, 19.5 MS (ESI) calc for C₂₁H₂₇F₃NO₆ [M-H]⁻ m/z 446.18 found 446.39



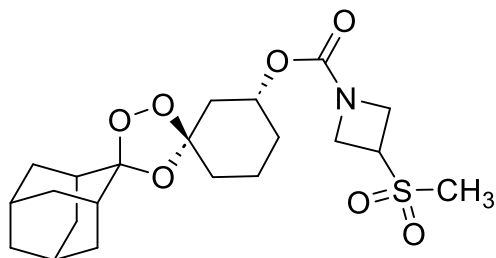
(1''R,3''R)-dispiro[adamantane-2,3'-[1,2,4]trioxolane-5',1''-cyclohexan]-3''-yl 3-methanesulfinylazetidine-1-carboxylate (8z).

To a solution of (1''R, 3''R)-dispiro[adamantane-2,3'-[1,2,4]trioxolane-5',1''-cyclohexan]-3''-yl (4-nitrophenyl) carbonate(100 mg, 0.224 mmol, 1.0 equiv.) in dichloromethane (5mL) was added triethylamine (110 μ L, 0.786 mmol, 3.5 equiv.), followed by 3-(methanesulfinyl)azetidine (93.6 mg, 0.786 mmol, 3.5 equiv.) at rt. The bright yellow mixture was allowed to stir at rt for 16hr. The reaction was quenched with 1M Na₂CO₃ (10mL) and diluted with DCM (10mL). The organic phase was separated and washed with additional 1M Na₂CO₃ (4 x 10mL) until the aqueous layer was colorless (indicating that p-nitrophenol had been successfully removed from the organic layer). The combined organic layers were washed with brine (15mL), dried (MgSO₄), and concentrated under reduced pressure. The crude residue was purified using flash column chromatography (12 g silica gel cartridge, 0-20% Methanol (with 0.8N NH₃):DCM) with the desired product eluting at 8% MeOH. The fractions containing the product were combined and lyophilized to yield (1''R,3''R)-dispiro[adamantane-2,3'-[1,2,4]trioxolane-5',1''-cyclohexan]-3''-yl 3-methanesulfinylazetidine-1-carboxylate (79.3 mg, 0.186 mmol, 83%) as a white solid. ¹H NMR (CHLOROFORM-d, 400 MHz) δ 4.7-4.8 (m, 1H), 4.4-4.6 (m, 1H), 4.0-4.3 (m, 3H), 3.56 (tt, 1H, J=5.6, 8.3 Hz), 2.48 (s, 3H), 2.2-2.4 (m, 1H), 2.08 (br s, 1H), 1.98 (br d, 5H, J=13.6 Hz), 1.90 (br s, 2H), 1.7-1.9 (m, 10H), 1.4-1.6 (m, 2H), 1.2-1.4 (m, 1H) ¹³C NMR (CHLOROFORM-d, 100 MHz) δ 155.6, 111.6, 108.6, 100.0, 71.6, 49.2, 48.5, 40.0, 36.8, 36.3, 35.7, 34.9, 34.8, 34.7, 34.7, 33.8, 30.6, 26.9, 26.4, 19.6 MS (ESI) calc for C₂₁H₃₁NO₆SNa [M+Na]⁺ m/z 448.18 found 448.25



(1''S,3''S)-dispiro[adamantane-2,3'-[1,2,4]trioxolane-5',1''-cyclohexan]-3''-yl 3-methanesulfinylazetidine-1-carboxylate (9z).

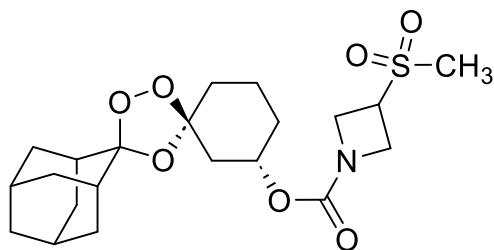
To a solution of (1''S, 3''S)-dispiro[adamantane-2,3'-[1,2,4]trioxolane-5',1''-cyclohexan]-3''-yl (4-nitrophenyl) carbonate(100 mg, 0.224 mmol, 1.0 equiv.) in dichloromethane (5mL) was added triethylamine (110μL, 0.786 mmol, 3.5 equiv.), followed by 3-(methanesulfinyl)azetidine (93.6 mg, 0.786 mmol, 3.5 equiv.) at rt. The bright yellow mixture was allowed to stir at rt for 16hr. The reaction was quenched with 1M Na₂CO₃ (10mL) and diluted with DCM (10mL). The organic phase was separated and washed with additional 1M Na₂CO₃ (4 x 10mL) until the aqueous layer was colorless (indicating that p-nitrophenol had been successfully removed from the organic layer). The combined organic layers were washed with brine (15mL), dried (MgSO₄), and concentrated under reduced pressure. The crude residue was purified using flash column chromatography (12 g silica gel cartridge, 0-20% Methanol (with 0.8N NH₃):DCM) with the desired product eluting at 8% MeOH. The fractions containing the product were combined and lyophilized to yield (1''S,3''S)-dispiro[adamantane-2,3'-[1,2,4]trioxolane-5',1''-cyclohexan]-3''-yl 3-methanesulfinylazetidine-1-carboxylate (72.8 mg, 0.171 mmol, 76.2%) as a white solid. ¹H NMR (CHLOROFORM-d, 400 MHz) δ 4.73 (td, 1H, J=5.3, 10.2 Hz), 4.4-4.5 (m, 1H), 4.2-4.3 (m, 2H), 4.0-4.1 (m, 1H), 3.56 (tt, 1H, J=5.6, 8.2 Hz), 2.48 (s, 3H), 2.2-2.3 (m, 1H), 2.0-2.2 (m, 1H), 1.98 (br d, 6H, J=13.4 Hz), 1.90 (br s, 2H), 1.6-1.9 (m, 12H), 1.2-1.4 (m, 2H) ¹³C NMR (CHLOROFORM-d, 100 MHz) δ 155.6, 111.6, 108.6, 71.6, 49.1, 48.5, 40.0, 36.8, 36.3, 35.7, 34.9, 34.8, 34.7, 34.7, 33.8, 30.6, 26.9, 26.4, 19.6 MS (ESI) calc for C₂₁H₃₁NO₆SNa [M+Na]⁺ m/z 448.18 found 448.35



(1''R,3''R)-dispiro[adamantane-2,3'-[1,2,4]trioxolane-5',1''-cyclohexan]-3''-yl 3-methanesulfonylazetidine-1-carboxylate (8aa).

To a solution of (1''R, 3''R)-dispiro[adamantane-2,3'-[1,2,4]trioxolane-5',1''-cyclohexan]-3''-yl (4-nitrophenyl) carbonate(100 mg, 0.224 mmol, 1.0 equiv.) in dichloromethane (5mL) was added triethylamine (110μL, 0.786 mmol, 3.5 equiv.), followed by 3-

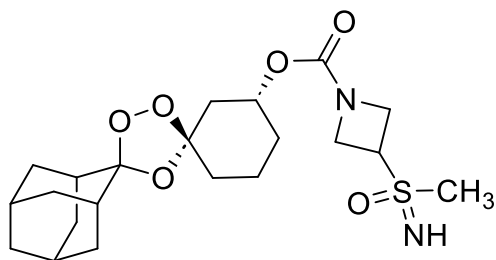
(methylsulfonyl)azetidine (106.0 mg, 0.786 mmol, 3.5 equiv.) at rt. The bright yellow mixture was allowed to stir at rt for 16hr. The reaction was quenched with 1M Na₂CO₃ (10mL) and diluted with DCM (10mL). The organic phase was separated and washed with additional 1M Na₂CO₃ (4 x 10mL) until the aqueous layer was colorless (indicating that p-nitrophenol had been successfully removed from the organic layer). The combined organic layers were washed with brine (15mL), dried (MgSO₄), and concentrated under reduced pressure. The crude residue was purified using flash column chromatography (12 g silica gel cartridge, 0-20% Methanol (with 0.8N NH₃):DCM) with the desired product eluting at 8% MeOH. The fractions containing the product were combined and lyophilized to yield (1''R,3''R)-dispiro[adamantane-2,3'-[1,2,4]trioxolane-5',1''-cyclohexan]-3''-yl 3-methanesulfonylazetidine-1-carboxylate (10.8 mg, 0.224 mmol, 10.9%) as a white solid. ¹H NMR (CHLOROFORM-d, 400 MHz) δ 4.7-4.8 (m, 1H), 4.2-4.4 (m, 4H), 3.8-4.1 (m, 1H), 2.9-3.0 (m, 3H), 2.2-2.3 (m, 1H), 1.9-2.1 (m, 7H), 1.91 (br s, 2H), 1.7-1.9 (m, 8H), 1.5-1.7 (m, 7H), 1.2-1.4 (m, 5H), 0.8-1.0 (m, 1H) ¹³C NMR (CHLOROFORM-d, 100 MHz) δ 155.1, 111.7, 108.6, 71.9, 50.1, 49.5, 40.0, 38.4, 36.8, 36.3, 34.9, 34.8, 34.7, 34.7, 33.8, 31.9, 30.6, 29.7, 26.9, 26.4, 19.6 MS (ESI) calc for C₂₁H₃₁NO₇SNa [M+Na]⁺ m/z 464.17 found 464.40



(1''S,3''S)-dispiro[adamantane-2,3'-[1,2,4]trioxolane-5',1''-cyclohexan]-3''-yl 3-methanesulfonylazetidine-1-carboxylate (9aa).

To a solution of (1''S, 3''S)-dispiro[adamantane-2,3'-[1,2,4]trioxolane-5',1''-cyclohexan]-3''-yl (4-nitrophenyl) carbonate(100 mg, 0.224 mmol, 1.0 equiv.) in dichloromethane (5mL) was added triethylamine (110μL, 0.786 mmol, 3.5 equiv.), followed by 3-(methylsulfonyl)azetidine (106.0 mg, 0.786 mmol, 3.5 equiv.) at rt. The bright yellow mixture was allowed to stir at rt for 16hr. The reaction was quenched with 1M Na₂CO₃ (10mL) and diluted with DCM (10mL). The organic phase was separated and washed

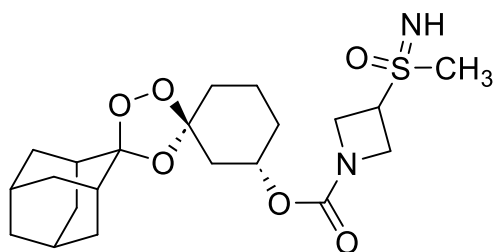
with additional 1M Na₂CO₃ (4 x 10mL) until the aqueous layer was colorless (indicating that p-nitrophenol had been successfully removed from the organic layer). The combined organic layers were washed with brine (15mL), dried (MgSO₄), and concentrated under reduced pressure. The crude residue was purified using flash column chromatography (12 g silica gel cartridge, 0-20% Methanol (with 0.8N NH₃):DCM) with the desired product eluting at 8% MeOH. The fractions containing the product were combined and lyophilized to yield (1''S,3''S)-dispiro[adamantane-2,3'-[1,2,4]trioxolane-5',1''-cyclohexan]-3''-yl 3-methanesulfonylazetidine-1-carboxylate (15.3 mg, 0.035 mmol, 15.4%) as a white solid. ¹H NMR (CHLOROFORM-d, 400 MHz) δ 4.7-4.8 (m, 1H), 4.2-4.4 (m, 4H), 3.8-4.1 (m, 1H), 2.9-3.0 (m, 3H), 2.2-2.3 (m, 1H), 1.9-2.1 (m, 7H), 1.7-1.9 (m, 10H), 1.4-1.7 (m, 3H), 1.2-1.4 (m, 4H), 0.8-1.0 (m, 1H) ¹³C NMR (CHLOROFORM-d, 100 MHz) δ 155.5, 111.7, 108.6, 71.9, 50.1, 49.5, 40.0, 38.4, 36.8, 36.3, 35.8, 34.9, 34.8, 34.7, 34.7, 33.8, 30.6, 29.7, 26.9, 26.4, 19.6 MS (ESI) calc for C₂₁H₃₁NO₇SNa [M+Na]⁺ m/z 464.17 found 464.35



(1''R,3''R)-dispiro[adamantane-2,3'-[1,2,4]trioxolane-5',1''-cyclohexan]-3''-yl 3-[(imino(methyl)oxo-lambda6-sulfanyl)azetidine-1-carboxylate (8bb).

To a solution of (1''R, 3''R)-dispiro[adamantane-2,3'-[1,2,4]trioxolane-5',1''-cyclohexan]-3''-yl (4-nitrophenyl) carbonate(100 mg, 0.224 mmol, 1.0 equiv.) in dichloromethane (5mL) was added triethylamine (110μL, 0.786 mmol, 3.5 equiv.), followed by azetidine-3-yl(imino)(methyl)-l6-sulfanone (105 mg, 0.786 mmol, 3.5 equiv.) at rt. The bright yellow mixture was allowed to stir at rt for 16hr. The reaction was quenched with 1M Na₂CO₃ (10mL) and diluted with DCM (10mL). The organic phase was separated and washed with additional 1M Na₂CO₃ (4 x 10mL) until the aqueous layer was colorless (indicating that p-nitrophenol had been successfully removed from the organic layer). The combined organic layers were washed with brine (15mL), dried (MgSO₄), and concentrated under

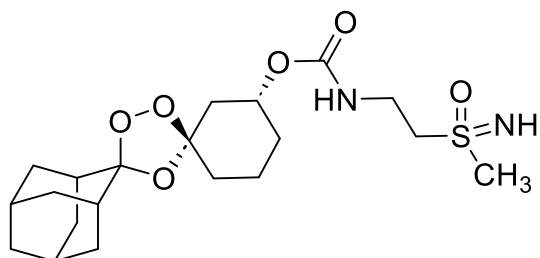
reduced pressure. The crude residue was purified using flash column chromatography (12 g silica gel cartridge, 0-20% Methanol (with 0.8N NH₃):DCM) with the desired product eluting at 8% MeOH. The fractions containing the product were combined and lyophilized to yield (1''R,3''R)-dispiro[adamantane-2,3'-[1,2,4]trioxolane-5',1''-cyclohexan]-3''-yl 3-[imino(methyl)oxo-lambda6-sulfanyl]azetidide-1-carboxylate (61.5 mg, 0.140 mmol, 62.2%) as a white solid. ¹H NMR (CHLOROFORM-d, 400 MHz) δ 4.5-4.8 (m, 1H), 4.1-4.3 (m, 4H), 3.02 (s, 2H), 2.85 (br s, 2H), 2.24 (br d, 1H, J=11.4 Hz), 1.9-2.0 (m, 6H), 1.7-1.9 (m, 6H), 1.4-1.7 (m, 3H), 1.2-1.4 (m, 1H) ¹³C NMR (CHLOROFORM-d, 100 MHz) δ 155.6, 111.7, 108.6, 71.9, 52.0, 40.2, 40.0, 36.7, 36.3, 34.8, 34.8, 34.7, 34.7, 33.8, 30.6, 29.7, 26.9, 26.4, 19.6 MS (ESI) calc for C₂₁H₃₃N₂O₆S [M+H]⁺ m/z 441.21 found 441.34



(1''S,3''S)-dispiro[adamantane-2,3'-[1,2,4]trioxolane-5',1''-cyclohexan]-3''-yl 3-[imino(methyl)oxo-lambda6-sulfanyl]azetidide-1-carboxylate (9bb).

To a solution of (1''R, 3''R)-dispiro[adamantane-2,3'-[1,2,4]trioxolane-5',1''-cyclohexan]-3''-yl (4-nitrophenyl) carbonate(100 mg, 0.224 mmol, 1.0 equiv.) in dichloromethane (5mL) was added triethylamine (110μL, 0.786 mmol, 3.5 equiv.), followed by azetidide-3-yl(imino)(methyl)-l6-sulfanone (105 mg, 0.786 mmol, 3.5 equiv.) at rt. The bright yellow mixture was allowed to stir at rt for 16hr. The reaction was quenched with 1M Na₂CO₃ (10mL) and diluted with DCM (10mL). The organic phase was separated and washed with additional 1M Na₂CO₃ (4 x 10mL) until the aqueous layer was colorless (indicating that p-nitrophenol had been successfully removed from the organic layer). The combined organic layers were washed with brine (15mL), dried (MgSO₄), and concentrated under reduced pressure. The crude residue was purified using flash column chromatography (12 g silica gel cartridge, 0-20% Methanol (with 0.8N NH₃):DCM) with the desired product eluting at 8% MeOH. The fractions containing the product were combined and lyophilized to yield (1''S,3''S)-dispiro[adamantane-2,3'-[1,2,4]trioxolane-5',1''-cyclohexan]-3''-yl 3-

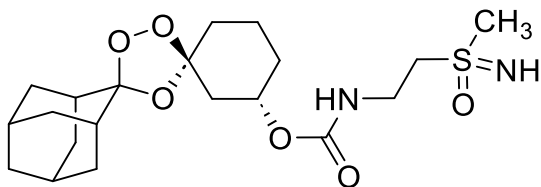
[imino(methyl)oxo-lambda6-sulfanyl]azetidone-1-carboxylate (22.0 mg, 0.050 mmol, 22.2%) as a white solid. ¹H NMR (CHLOROFORM-d, 400 MHz) δ 4.7-4.8 (m, 1H), 4.3-4.4 (m, 4H), 4.1-4.3 (m, 1H), 3.27 (br d, 2H, J=16.1 Hz), 3.15 (br s, 2H), 2.2-2.4 (m, 1H), 1.9-2.1 (m, 8H), 1.7-1.9 (m, 7H), 1.4-1.7 (m, 2H), 1.2-1.4 (m, 3H) ¹³C NMR (CHLOROFORM-d, 100 MHz) δ 155.6, 111.7, 108.6, 100.0, 72.0, 52.0, 40.1, 36.7, 36.3, 34.8, 34.8, 33.8, 30.6, 29.7, 26.9, 26.4, 19.6 MS (ESI) calc for C₂₁H₃₂N₂O₆SNa [M+Na]⁺ m/z 463.19 found 463.70



(1''R,3''R)-dispiro[adamantane-2,3'-[1,2,4]trioxolane-5',1''-cyclohexan]-3''-yl N-{2-[imino(methyl)oxo-lambda6-sulfanyl]ethyl}carbamate (8cc).

To a solution of (1''R, 3''R)-dispiro[adamantane-2,3'-[1,2,4]trioxolane-5',1''-cyclohexan]-3''-yl (4-nitrophenyl) carbonate (100 mg, 0.224 mmol, 1.0 equiv.) in dichloromethane (5mL) was added triethylamine (110μL, 0.786 mmol, 3.5 equiv.), followed by (2-aminoethyl)(imino)(methyl)-l6-sulfanone (96.0 mg, 0.786 mmol, 3.5 equiv.) at rt. The bright yellow mixture was allowed to stir at rt for 16hr. The reaction was quenched with 1M Na₂CO₃ (10mL) and diluted with DCM (10mL). The organic phase was separated and washed with additional 1M Na₂CO₃ (4 x 10mL) until the aqueous layer was colorless (indicating that p-nitrophenol had been successfully removed from the organic layer). The combined organic layers were washed with brine (15mL), dried (MgSO₄), and concentrated under reduced pressure. The crude residue was purified using flash column chromatography (12 g silica gel cartridge, 0-20% Methanol (with 0.8N NH₃):DCM) with the desired product eluting at 8% MeOH. The fractions containing the product were combined and lyophilized to yield (1''R,3''R)-dispiro[adamantane-2,3'-[1,2,4]trioxolane-5',1''-cyclohexan]-3''-yl N-{2-[imino(methyl)oxo-lambda6-sulfanyl]ethyl}carbamate (22.3 mg, 0.052 mmol, 23.2%) as a white solid. ¹H NMR (CHLOROFORM-d, 400 MHz) δ 4.6-4.8 (m, 1H), 3.7-3.8 (m, 2H), 3.4-3.6 (m, 2H), 3.2-3.4 (m, 4H), 2.1-2.4 (m, 1H), 1.9-2.0 (m,

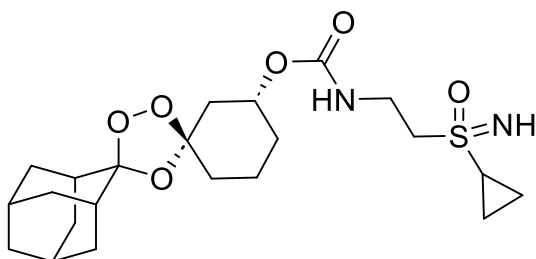
7H), 1.7-1.9 (m, 6H), 1.4-1.6 (m, 2H), 1.2-1.4 (m, 3H) ¹³C NMR (CHLOROFORM-d, 100 MHz) Shift 155.9, 111.6, 108.7, 77.3, 71.6, 55.6, 43.2, 40.2, 36.8, 36.3, 36.3, 35.5, 34.8, 34.8, 33.7, 30.7, 29.7, 26.9, 26.4, 19.8 MS (ESI) calc for C₂₀H₃₃N₂O₆S [M+H]⁺ m/z 429.21 found 429.39



(1''S,3''S)-dispiro[adamantane-2,3'-[1,2,4]trioxolane-5',1''-cyclohexan]-3''-yl N-{2-[imino(methyl)oxo-lambda6-sulfanyl]ethyl}carbamate (9cc).

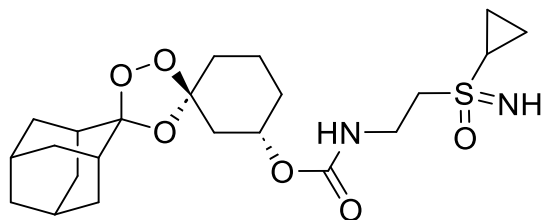
To a solution of (1''S, 3''S)-dispiro[adamantane-2,3'-[1,2,4]trioxolane-5',1''-cyclohexan]-3''-yl (4-nitrophenyl) carbonate (100 mg, 0.224 mmol, 1.0 equiv.) in dichloromethane (5mL) was added triethylamine (110μL, 0.786 mmol, 3.5 equiv.), followed by (2-aminoethyl)(imino)(methyl)-l6-sulfanone (96.0 mg, 0.786 mmol, 3.5 equiv.) at rt. The bright yellow mixture was allowed to stir at rt for 16hr. The reaction was quenched with 1M Na₂CO₃ (10mL) and diluted with DCM (10mL). The organic phase was separated and washed with additional 1M Na₂CO₃ (4 x 10mL) until the aqueous layer was colorless (indicating that p-nitrophenol had been successfully removed from the organic layer). The combined organic layers were washed with brine (15mL), dried (MgSO₄), and concentrated under reduced pressure. The crude residue was purified using flash column chromatography (12 g silica gel cartridge, 0-20% Methanol (with 0.8N NH₃):DCM) with the desired product eluting at 8% MeOH. The fractions containing the product were combined and lyophilized to yield (1''S,3''S)-dispiro[adamantane-2,3'-[1,2,4]trioxolane-5',1''-cyclohexan]-3''-yl N-{2-[imino(methyl)oxo-lambda6-sulfanyl]ethyl}-carbamate (8.4 mg, 0.020 mmol, 8.7%) as a white solid. NMR and UPLC/MS indicated some impurity (~10%) which was carried through downstream analysis. ¹H NMR (CHLOROFORM-d, 400 MHz) δ 4.72 (br s, 1H), 3.81 (br s, 2H), 3.47 (br s, 2H), 3.2-3.4 (m, 2H), 2.2-2.4 (m, 2H), 1.9-2.1 (m, 9H), 1.85 (br s, 2H), 1.7-1.8 (m, 6H), 1.6-1.7 (m, 2H), 1.51 (br s, 1H), 1.4-1.5 (m, 1H), 1.27 (s, 9H), 1.0-1.2 (m, 1H) ¹³C NMR (CHLOROFORM-d, 100 MHz) δ 155.9, 111.7, 108.7, 77.2, 71.7, 55.1, 42.3, 40.2, 36.8, 36.3, 35.3, 34.8, 33.7, 31.9, 30.7,

29.7, 29.7, 29.6, 29.5, 29.4, 29.3, 29.1, 26.9, 26.8, 26.5, 24.8, 22.7, 19.8, 14.1 MS (ESI)
calc for C₂₀H₃₃N₂O₆S [M+H]⁺ m/z 429.21 found 429.34



(1''R,3''R)-dispiro[adamantane-2,3'-[1,2,4]trioxolane-5',1''-cyclohexan]-3''-yl N-{2-[cyclopropyl(imino)oxo-lambda6-sulfanyl]ethyl}carbamate (8dd).

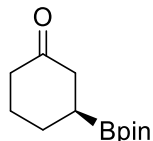
To a solution of (1''R, 3''R)-dispiro[adamantane-2,3'-[1,2,4]trioxolane-5',1''-cyclohexan]-3''-yl (4-nitrophenyl) carbonate (100 mg, 0.224 mmol, 1.0 equiv.) in dichloromethane (5mL) was added triethylamine (110µL, 0.786 mmol, 3.5 equiv.), followed by (2-aminoethyl)(cyclopropyl)(imino)-l6-sulfanone (116.0 mg, 0.786 mmol, 3.5 equiv.) at rt. The bright yellow mixture was allowed to stir at rt for 16hr. The reaction was quenched with 1M Na₂CO₃ (10mL) and diluted with DCM (10mL). The organic phase was separated and washed with additional 1M Na₂CO₃ (4 x 10mL) until the aqueous layer was colorless (indicating that p-nitrophenol had been successfully removed from the organic layer). The combined organic layers were washed with brine (15mL), dried (MgSO₄), and concentrated under reduced pressure. The crude residue was purified using flash column chromatography (12 g silica gel cartridge, 0-20% Methanol (with 0.8N NH₃):DCM) with the desired product eluting at 8% MeOH. The fractions containing the product were combined and lyophilized to yield (1''R,3''R)-dispiro[adamantane-2,3'-[1,2,4]trioxolane-5',1''-cyclohexan]-3''-yl N-{2-[cyclopropyl(imino)oxo-lambda6-sulfanyl]ethyl}carbamate (18.4 mg, 0.041 mmol, 18.0%) as a white solid. ¹H NMR (CHLOROFORM-d, 400 MHz) δ 5.89 (br s, 1H), 4.7-4.8 (m, 1H), 3.7-3.9 (m, 2H), 3.4-3.6 (m, 2H), 3.23 (br s, 2H), 2.6-2.8 (m, 1H), 2.26 (td, 1H, J=2.2, 12.9 Hz), 1.9-2.0 (m, 7H), 1.7-1.9 (m, 6H), 1.4-1.7 (m, 3H), 1.1-1.4 (m, 5H) ¹³C NMR (CHLOROFORM-d, 100 MHz) δ 153.8, 111.6, 108.7, 71.6, 40.2, 37.1, 36.8, 36.3, 34.8, 33.7, 32.8, 31.9, 30.7, 30.0, 29.7, 26.9, 26.5, 25.9, 19.8, 14.1, 5.8, 5.2 MS (ESI) calc for C₂₂H₃₅N₂O₆S [M+H]⁺ m/z 455.22 found 455.44



(1''S,3''S)-dispiro[adamantane-2,3'-[1,2,4]trioxolane-5',1''-cyclohexan]-3''-yl N-{2-[cyclopropyl(imino)oxo-lambda6-sulfanyl]ethyl}carbamate (9dd).

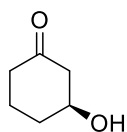
To a solution of (1''R, 3''R)-dispiro[adamantane-2,3'-[1,2,4]trioxolane-5',1''-cyclohexan]-3''-yl (4-nitrophenyl) carbonate (100 mg, 0.224 mmol, 1.0 equiv.) in dichloromethane (5mL) was added triethylamine (110µL, 0.786 mmol, 3.5 equiv.), followed by (2-aminoethyl)(cyclopropyl)(imino)-l6-sulfanone (116.0 mg, 0.786 mmol, 3.5 equiv.) at rt. The bright yellow mixture was allowed to stir at rt for 16hr. The reaction was quenched with 1M Na₂CO₃ (10mL) and diluted with DCM (10mL). The organic phase was separated and washed with additional 1M Na₂CO₃ (4 x 10mL) until the aqueous layer was colorless (indicating that p-nitrophenol had been successfully removed from the organic layer). The combined organic layers were washed with brine (15mL), dried (MgSO₄), and concentrated under reduced pressure. The crude residue was purified using flash column chromatography (12 g silica gel cartridge, 0-20% Methanol (with 0.8N NH₃):DCM) with the desired product eluting at 8% MeOH. The fractions containing the product were combined and lyophilized to yield (1''S,3''S)-dispiro[adamantane-2,3'-[1,2,4]trioxolane-5',1''-cyclohexan]-3''-yl N-{2-[cyclopropyl(imino)oxo-lambda6-sulfanyl]ethyl}carbamate (35.0 mg, 0.077 mmol, 34.3%) as a white solid. ¹H NMR (CHLOROFORM-d, 400 MHz) δ 4.7-4.8 (m, 1H), 3.8-3.9 (m, 1H), 3.74 (br d, 1H, J=1.5 Hz), 3.55 (br d, 2H, J=4.9 Hz), 2.2-2.4 (m, 1H), 1.9-2.0 (m, 7H), 1.86 (br s, 2H), 1.7-1.8 (m, 5H), 1.4-1.7 (m, 7H), 1.37 (br s, 2H), 1.0-1.1 (m, 4H) ¹³C NMR (CHLOROFORM-d, 100 MHz) δ 155.8, 111.6, 108.7, 100.0, 48.1, 36.8, 36.3, 34.8, 34.7, 33.7, 30.7, 30.1, 29.7, 26.9, 26.5, 19.7, 14.1, 5.5, 4.8 MS (ESI) calc for C₂₂H₃₅N₂O₆S [M+H]⁺ m/z 455.22 found 455.49

Synthesis of (S,S) Intermediates



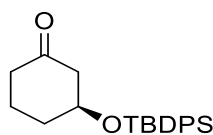
(S)-3-(4,4,5,5-tetramethyl-1,3,2-dioxaborolan-2-yl)cyclohexan-1-one (2).

A heat-gun dried, two-necked 50-mL round bottom flask equipped with an Ar(g) inlet, stirbar and rubber septum, was charged with copper(I)chloride (16.2 mg, 0.164 mmol, 0.02 equiv), sodium tert-butoxide (23.6 mg, 0.246 mmol, 0.03 equiv) and (R)-(+)-[(R)-2-diphenylphosphinoferrocenyl](N,N-dimethylamino)(2-diphenylphosphinophenyl)methane (R,R-Taniaphos) (225 mg, 0.328 mmol, 0.04 equiv) followed by anhydrous THF (15 mL). The homogenous orange solution was stirred at rt for 30 min before a solution of bis(pinacolato)diboron (2.288 g, 9.01 mmol, 1.1 equiv) in anhydrous THF (11 mL) was added. The reaction mixture was stirred for 10 mins at rt before 2-cyclohexen-1-one (0.793 mL, 8.192 mmol, 1.0 equiv) was added via syringe, followed by anhydrous MeOH (663 μ L, 16.383 mmol, 2.0 equiv) and anhydrous THF (11 mL). The reaction was stirred at rt for 24 hrs before being judged complete by TLC (1:3, EtOAc–Hexanes with CAM staining, product Rf 0.40). The reaction mixture was then filtered through celite and the pad washed with EtOAc (100 mL), the filtrate was then concentrated under reduced pressure to a crude orange oil (3.85 g). Purification via flash column chromatography (120 g silica gel cartridge, 0-25% EtOAc–Hexanes) afforded pinacol ester (S)-2 (1.77 g, 7.88 mmol, 93%) as a colorless oil. ^1H NMR (400 MHz, CDCl_3) δ 2.23–2.45 (m, 4H), 2.01–2.12 (m, 1H), 1.83–1.94 (m, 1H), 1.67–1.81 (m, 1H), 1.56–1.68 (m, 1H), 1.38–1.52 (m, 1H), 1.20–1.27 (m, 12H); ^{13}C NMR (100 MHz, CDCl_3) δ 212.3, 83.5, 83.4, 42.6, 41.9, 28.4, 26.5, 25.0, 24.7, 24.7; MS (ESI) calcd for $\text{C}_{12}\text{H}_{22}\text{BO}_3$ $[\text{M} + \text{H}]^+$: m/z 225.17, found: 225.06.



(S)-3-hydroxycyclohexan-1-one (3).

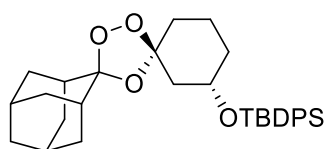
To a 150-mL round bottom flask equipped with a stirbar, rubber septum and Ar(g) inlet was added pinacol ester (S)-2 (1.82 g, 8.12 mmols, 1.0 equiv) followed by THF (14 mL) and DI H₂O (5 mL). Sodium perborate (5.00 g, 32.5 mmols, 4.0 equiv) was added to the reaction in one portion to give a colorless suspension that was stirred at rt for 3 hr. TLC indicated that the reaction was complete (1:1, EtOAc–Hexanes with CAM staining, product R_f 0.31) so the mixture was filtered through a glass frit with EtOAc (100 mL) to wash the funnel. The filtrate was transferred to a separating funnel and brine (11 mL) was added, the layers were separated and the aqueous layer was back-extracted with EtOAc (3 × 30 mL) until only pinacol remained in the aqueous layer by TLC. The combined organic layers were concentrated under reduced pressure to a crude colorless oil (1.90 g). Purification via flash column chromatography (220 g silica gel cartridge, 0–80% EtOAc–Hexanes) afforded alcohol (S)-3 (794 mg, 6.96 mmol, 83%) as a colorless oil. ¹H NMR (400 MHz, CDCl₃) δ 4.14–4.22 (m, 1H), 2.79 (br s, 1H), 2.63 (dd, J = 14.1, 4.1 Hz, 1H), 2.40 (dd, J = 14.1, 7.5 Hz, 1H), 2.30 (t, J = 6.6 Hz, 1H), 1.96–2.12 (m, 2H), 1.64–1.81 (m, 2H); MS (ESI) calcd for C₆H₁₁O₂ [M + H]⁺: m/z 115.08, found 115.15.



(S)-3-((tert-butyldiphenylsilyl)oxy)cyclohexan-1-one (4).

To a 100-mL round bottom flask equipped with a stirbar, rubber septum and Ar(g) inlet was added alcohol (S)-3 (794 mg, 6.96 mmol, 1.0 equiv), anhydrous N,N-dimethylformamide (19 mL), and imidazole (947 mg, 13.91 mmol, 2.0 equiv). The mixture was cooled to 0 °C while tert-butyl(chloro)diphenyl silane (1.81 mL, 6.96 mmol, 1.0 equiv) was added dropwise via syringe and the reaction was warmed gradually to rt over 16 hr. The following day, the reaction mixture was diluted with EtOAc (100 mL) and DI H₂O (100 mL) and the layers were separated. The organic phase was washed with brine (2 × 50 mL), dried (MgSO₄), filtered and concentrated to a crude colorless oil (1.90 g). Purification via flash column chromatography (220 g silica gel cartridge, 0–9% EtOAc–Hexanes, product elutes during 6% EtOAc–Hexanes) afforded ketone (S)-4

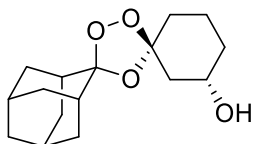
(contaminated with 13% by weight t-BuPh₂SiOH, 2.74 g, 7.77 mmol) as a colorless oil that was used in the next step without further purification. ¹H NMR (400 MHz, CDCl₃) δ 7.65–7.72 (m, 4H), 7.38–7.49 (m, 6H), 4.22 (app quin, J = 4.9 Hz, 1H), 2.46 (d, J = 4.9 Hz, 2H) 2.34–2.42 (m, 1H), 2.23–2.32 (m, 1H), 2.11–2.21 (m, 1H), 1.75–1.84 (m, 2H), 1.67 (dt, J = 12.5, 6.3 Hz, 1H), 1.09 (s, 9H); ¹³C NMR (100 MHz, CDCl₃) δ 209.9, 135.8, 135.7, 134.8, 133.9, 133.6, 129.8, 129.8, 127.7, 127.7, 71.1, 50.4, 41.2, 32.9, 29.7, 26.9, 20.6, 19.2; MS (ESI) calcd for C₂₂H₂₈O₂SiNa [M + Na]⁺: m/z 375.18, found: 374.98.



(1''S,3''S)-tert-butyl((dispiro[adamantane-2,3'-[1,2,4]trioxolane-5',1''-cyclohexan]-3''-yl)oxy) diphenylsilane (5).

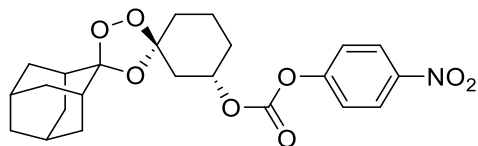
To a 200-mL recovery flask equipped with a stir bar was added ketone (S)-4 (2.74 g, 7.77 mmol, 1.0 equiv), CCl₄ (114 mL), and O-methyl 2-adamantanone oxime (2.09 g, 11.66 mmol, 1.5 equiv). The solution was cooled to 0 °C and sparged with O₂ for 10 minutes. The reaction was maintained at 0 °C while ozone was bubbled through the solution (2 L/min, 40% power). After stirring for 100 min, the reaction was deemed to be incomplete based on TLC and LCMS analysis. Additional oxime (348 mg, 1.94 mmol, 0.25 equiv) was added in a single portion to the reaction with CCl₄ (30 mL) and ozone was bubbled through the reaction for a further 2 hr. Additional oxime (348 mg, 1.94 mmol, 0.25 equiv) was added in a single portion and ozone was bubbled through the reaction for a further 40 min until TLC and LCMS showed consumption of ketone starting material. The solution was then sparged with O₂ for 10 min, sparged with Ar(g) for 10 min and concentrated under reduced pressure to a crude semi-solid (5.95 g). Purification via flash column chromatography (220 g silica gel cartridge, 0-5% EtOAc–Hexanes, product eluted during 4% EtOAc–Hexanes) afforded trioxolane (S,S)-5 (2.82 g, 5.44 mmol, 67% over 2-steps from 3) as a colorless solid. The diastereoselectivity of the Griesbaum co-ozonolysis was determined to be 92:8 in favor of the trans diastereomer. ¹H NMR (400 MHz, CDCl₃) δ

7.65–7.72 (m, 4H), 7.35–7.46 (m, 6H), 3.88–3.97 (m, 1H), 3.74–3.87 (m, 1H), 1.91–2.11 (m, 3H), 1.63–1.80 (m, 12H), 1.45–1.62 (m, 3H), 1.15–1.44 (m, 3H), 1.07 (s, 9H); ¹³C NMR (100 MHz, CDCl₃) δ 135.8, 135.7, 134.5 (minor diastereomer), 134.4 (minor diastereomer), 129.5, 129.5, 127.6, 127.5, 112.8, 111.2, 110.2 (minor diastereomer), 109.2, 109.0 (minor diastereomer), 77.2, 69.8, 43.8, 37.1, 37.0, 36.9, 36.8, 36.3, 36.2, 34.9, 34.9, 34.7, 34.7, 34.6, 34.4, 34.2, 34.0, 33.8, 33.6, 33.2, 31.5, 27.1, 27.1, 27.0 (app d, J = 1.5 Hz), 26.9, 26.5, 26.1 (app d, J = 1.5 Hz), 19.9, 19.2, 14.2; MS (ESI) calcd for C₃₂H₄₂O₄Si [M + Na]⁺: m/z 541.28, found: 541.08.



(1''S,3''S)-dispiro[adamantane-2,3'-[1,2,4]trioxolane-5',1''-cyclohexan]-3''-ol (6).

To a stirred solution of trioxolane (S,S)-5 (2.85 g, 5.49 mmol, 1.0 equiv) in anhydrous THF (30 mL) at 0 °C was added a solution of tetrabutylammonium fluoride (1.0 M in THF, 27.5 mL, 27.5 mmol, 5.0 equiv). The reaction mixture was allowed to warm to rt and stirred for 12 hr until deemed complete by LCMS and TLC (1:9, EtOAc–Hexanes with CAM staining, product R_f 0.08). The reaction was then diluted with DI H₂O (30 mL) and extracted with EtOAc (1 × 30 mL). The aqueous layer was back-extracted with EtOAc (3 × 30 mL) and the combined organic phases were washed with brine (1 × 50 mL), dried (MgSO₄), filtered and concentrated under reduced pressure to a crude colorless oil (4.87 g). Purification via flash column chromatography (220 g silica gel cartridge, 0–29% EtOAc–Hexanes, product eluted during 20% EtOAc–Hexanes) afforded alcohol (S,S)-6 (1.37 g, 4.87 mmol, 89%) as a colorless oil. ¹H NMR (400 MHz, CDCl₃) δ 3.91–4.01 (m, 1H), 2.56 (br s, 1H), 1.99–2.10 (m, 3H), 1.87–1.99 (m, 5H), 1.73–1.87 (m, 6H), 1.66–1.73 (m, 6H), 1.36–1.63 (m, 2H); ¹³C NMR (100 MHz, CDCl₃) δ 112.2, 112.0, 109.0, 68.2, 41.6, 37.2, 36.7, 36.2, 36.2, 35.0, 34.9, 34.8, 33.7, 33.7, 33.0, 31.2, 29.7, 27.1, 26.8, 26.4, 19.1; MS (ESI) calcd for C₁₆H₂₄O₄Na [M + Na]⁺: m/z 303.16, found 303.13.

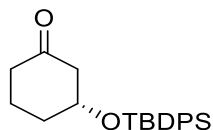


(1''S,3''S)-dispiro[adamantane-2,3'-[1,2,4]trioxolane-5',1''-cyclohexan]-3''-yl (4-nitrophenyl) carbonate (7).

To an oven-dried 250-mL round bottom flask equipped with a stirbar, Ar(g) inlet and rubber septum was added alcohol (S,S)-6 (1.30 g, 4.64 mmol, 1.0 equiv) followed by anhydrous dichloromethane (93 mL) and N,N-diisopropylethylamine (2.63 mL, 15.1 mmol, 3.25 equiv). 4-Dimethylaminopyridine (680 mg, 5.56 mmol, 1.2 equiv) was added and the reaction was cooled to 0 °C before 4-nitrophenylchloroformate (3.04 g, 15.1 mmol, 3.25 equiv) was added in two portions. The cloudy yellow solution was stirred at rt for 3 hr before LCMS and TLC (1:5, EtOAc–Hexanes, product Rf 0.50) indicated that the reaction was complete. The reaction was then diluted with DI H₂O (60 mL) and extracted with dichloromethane (1 × 60 mL). The aqueous layer was back-extracted with dichloromethane (3 × 50 mL) and the combined organic phases were washed repeatedly with 1M aq Na₂CO₃ solution until the aqueous layer was visibly less yellow (meaning that significant quantities of p-nitrophenol had been removed from the organic layer). The organic phase was then dried (MgSO₄), filtered and concentrated under reduced pressure to a crude yellow oil (2.48 g). Purification via flash column chromatography (220 g silica gel cartridge, 0-20% EtOAc–Hexanes, product eluted during 10% EtOAc–Hexanes) afforded carbonate (S,S)-7 (1.03 g, 2.31 mmol, 50%) as a colorless solid (9:1 dr in favor of the trans diastereomer). ¹H NMR (400 MHz, CDCl₃) δ 8.29 (d, J = 8.8 Hz, 2H), 7.40 (d, J = 8.8 Hz, 2H), 4.93–5.01 (m, 1H, minor diastereomer), 4.82–4.90 (m, 1H), 2.41 (dt, J = 12.8, 1.9 Hz, 1H), 2.08–2.15 (m, 1H), 1.97–2.07 (m, 6H), 1.65–1.96 (m, 17H), 1.41–1.64 (m, 3H), 1.19–1.37 (m, 1H), 0.80–0.93 (m, 1H); ¹³C NMR (100 MHz, CDCl₃) δ 155.6, 151.8 (minor diastereomer), 151.6, 145.3, 125.3, 121.9 (minor diastereomer), 121.7, 112.2 (minor diastereomer), 112.0, 108.3, 108.1 (minor diastereomer), 76.2, 47.0, 39.7 (minor diastereomer), 39.6, 39.3, 36.7, 36.4, 36.3 (minor diastereomer), 36.3, 35.0 (minor diastereomer), 34.9, 34.8, 34.7, 34.7, 33.5, 33.4 (minor diastereomer), 30.2 (minor

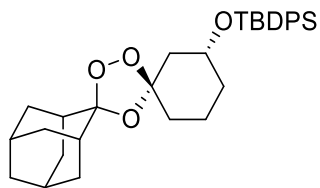
diastereomer), 30.1, 29.7, 27.5, 26.8, 26.4, 19.6 (minor diastereomer), 19.6; MS (ESI) calcd for C₂₃H₂₇NO₈Na [M + Na]⁺: m/z 468.16, found 467.97.

Synthesis of (R,R) Intermediates



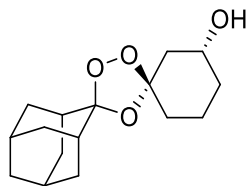
(R)-3-((tert-Butyldiphenylsilyloxy)cyclohexan-1-one.

A 200 mL round-bottom flask equipped with a stirbar, rubber septum, and argon inlet was charged with (R)-3-hydroxycyclohexan-1-one (2.1 g, 18.4 mmol, 1.0 equiv), N,N-dimethylformamide (40 mL), and imidazole (2.51 g, 36.8 mmol, 2.0 equiv). The mixture was cooled at 0 °C while tert-butyl(chloro)diphenyl silane (5.3 mL, 20.2 mmol, 1.1 equiv) was added dropwise via syringe. The reaction mixture was allowed to slowly warm to room temperature (rt). After stirring for 16 h, the reaction was judged complete based on TLC and LC/MS analysis. The reaction mixture was then diluted with EtOAc (100 mL) and DI H₂O (100 mL). The organic phase was separated and washed with brine (2 × 50 mL), dried (MgSO₄), filtered, and concentrated to afford a colorless oil. The crude material was purified using flash column chromatography (330 g silica gel cartridge, 0–20% EtOAc–Hexanes, product eluted during 8% EtOAc–Hex) to give the desired ketone 4 (6.01 g, 17.05 mmol, 93%) as a colorless oil. ¹H NMR (400 MHz, CDCl₃): δ 7.68–7.72 (m, 4 H), 7.39–7.49 (m, 6 H), 4.23 (t, J = 4.9 Hz, 1 H), 2.47 (d, J = 5.0 Hz, 2 H), 2.35–2.42 (m, 1 H), 2.25–2.32 (m, 1 H), 2.17 (br dd, J = 8.5, 5.8 Hz, 1 H), 1.78–1.83 (m, 2 H), 1.64–1.71 (m, 1 H), 1.08–1.12 (s, 9 H). ¹³C NMR (100 MHz, CDCl₃): δ 210.0, 135.8, 135.7, 134.9, 133.9, 133.6, 129.9, 129.8, 127.7, 127.7, 71.1, 50.4, 41.2, 32.9, 26.9, 26.6, 20.6, 19.2. MS (ESI) calcd for C₂₂H₂₉O₂Si [M + H]⁺: m/z 353.19, found 353.46.



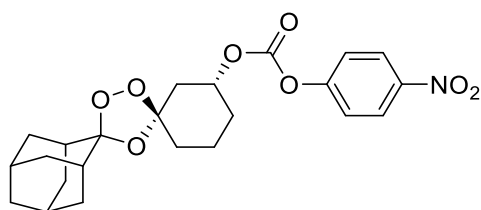
(1''R,3''R)-tert-Butyl((dispiro[adamantane-2,3'-[1,2,4]trioxolane-5',1''-cyclohexan]-3''-yl)oxy) diphenylsilane.

A 200 mL recovery flask was charged with ketone (R)-4 (1.51 g, 4.28 mmol, ca. 1 equiv), carbon tetrachloride (100 mL), and O-methyl 2-adamantanone oxime (768 mg, 4.28 mmol, 1.0 equiv). The solution was cooled to 0 °C and sparged with O₂ for 10 min. The reaction was maintained at 0 °C while ozone was bubbled (2 L/min, 40% power) through the solution. After stirring for 90 min, the reaction was judged to be incomplete based on TLC and LC/MS analysis, so additional oxime (0.386 g, 2.14 mmol, 0.5 equiv) was added in a single portion to the reaction mixture followed by additional carbon tetrachloride (50 mL). Ozone was bubbled through the reaction mixture for another 45 min, after which a third portion of oxime (0.386 g, 2.14 mmol, 0.5 equiv) was added and ozone again was bubbled through the reaction for a final 45 min. The solution was then sparged with O₂ for 10 min to remove any dissolved ozone, followed by sparging with argon gas for 10 min to remove any dissolved oxygen. The solution was then concentrated under reduced pressure to provide a viscous oil. The crude material was purified using flash column chromatography (120 g silica gel cartridge, 0–20% EtOAc–Hexanes, product eluted during 5% EtOAc–Hex) to give the desired trioxolane product 5 (2.01 g, 3.87 mmol, 91%, 12:1 dr) as a colorless semisolid. ¹H NMR (400 MHz, CDCl₃): δ 7.69 (td, J = 7.7, 1.5 Hz, 4 H), 7.36–7.46 (m, 6 H), 3.89–3.96 (m, 1 H), 3.78–3.85 (m, 1 H), 1.95–2.05 (m, 3 H), 1.65–1.84 (m, 12 H), 1.46–1.65 (m, 3 H), 1.19–1.36 (m, 3 H), 1.08 (s, 9 H). ¹³C NMR (100 MHz, CDCl₃): δ 135.8, 135.8, 134.5, 134.4, 129.6, 129.5, 127.6, 127.5, 111.2, 109.2, 69.8, 43.8, 36.8, 36.3, 36.2, 34.8, 34.4, 33.8, 33.2, 27.0, 26.9, 26.5, 19.9, 19.2. MS (ESI) calcd for C₃₂H₄₂NaO₄Si [M + Na]⁺: m/z 541.28, found 541.56.



(1''R,3''R)-Dispiro[adamantane-2,3'-[1,2,4]trioxolane-5',1''-cyclohexan]-3''-ol.

To a stirred solution of 5 (2.0 g, 3.86 mmol, 1.0 equiv) in THF (20 mL) was added a solution of tetrabutylammonium fluoride (1.0 M in THF, 19.2 mL, 19.3 mmol, 5.0 equiv) dropwise while stirring at 0 °C. The reaction mixture was allowed to slowly warm to rt and was stirred for 12 h, at which point conversion was determined to be complete based on TLC and LC/MS analysis. The reaction was then diluted with brine (100 mL) and extracted with EtOAc (2 × 100 mL). The organic layer was then dried (Na₂SO₄), filtered, and concentrated under reduced pressure to afford a yellow oil. The crude material was purified using flash column chromatography (80 g silica gel cartridge, 0–50% EtOAc–Hexanes, product eluted during 20% EtOAc–Hex) to yield the desired product 6 (1.01 g, 3.60 mmol, 93%) as a colorless solid. ¹H NMR (400 MHz, CDCl₃): δ 3.94–4.14 (m, 1 H), 2.47 (br s, 1 H), 2.07 (d, J = 4.0 Hz, 1 H), 1.90–2.05 (m, 7 H), 1.69–1.88 (m, 12 H), 1.47–1.63 (m, 2 H). ¹³C NMR (100 MHz, CDCl₃): δ 111.9, 109.1, 67.9, 41.7, 36.7, 36.2, 36.2, 34.9, 34.9, 34.8, 34.7, 33.8, 33.1, 26.8, 26.4, 19.1. MS (ESI) calcd for C₁₆H₂₄O₄ [M + H]⁺: m/z 281.17, found 281.51.

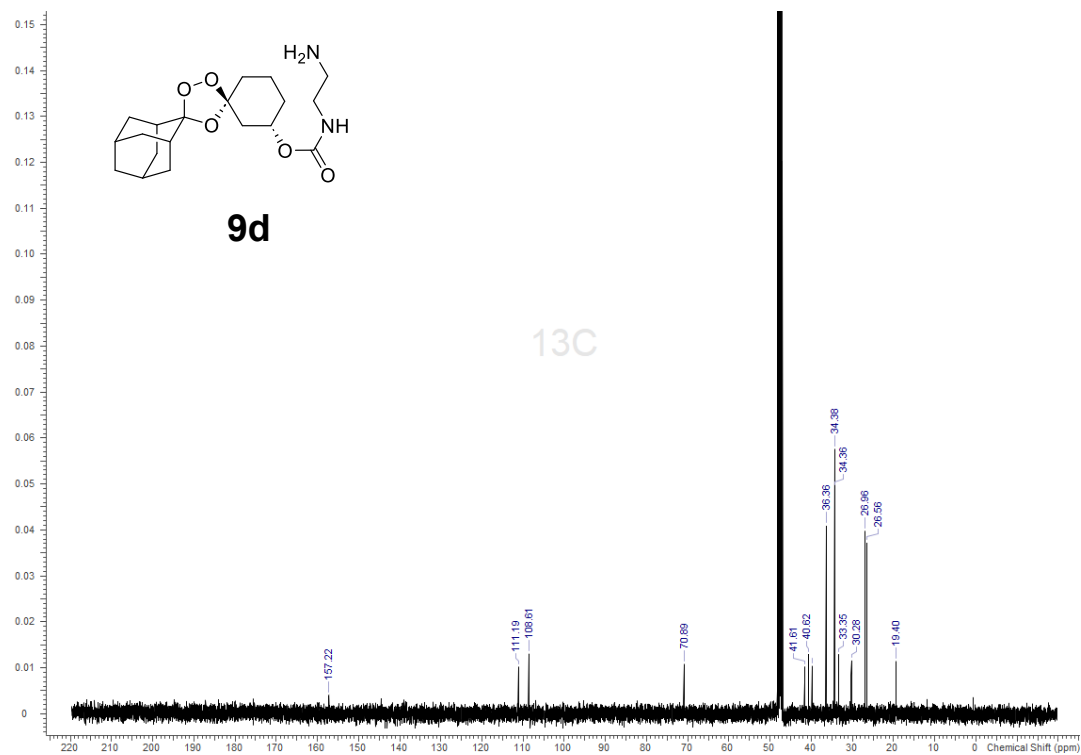
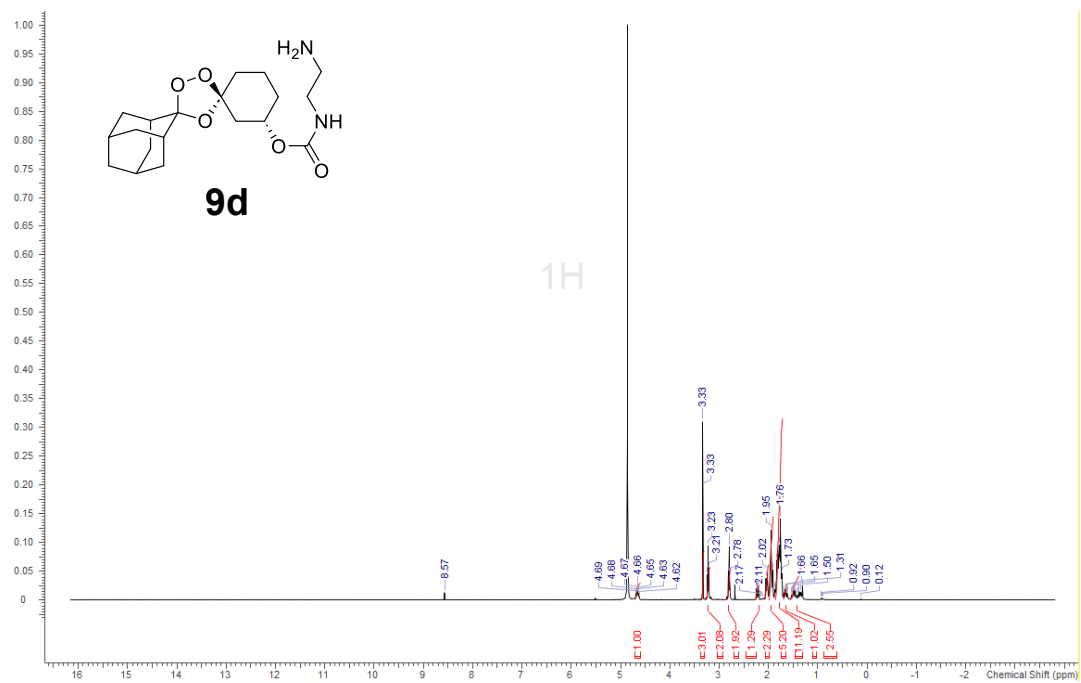


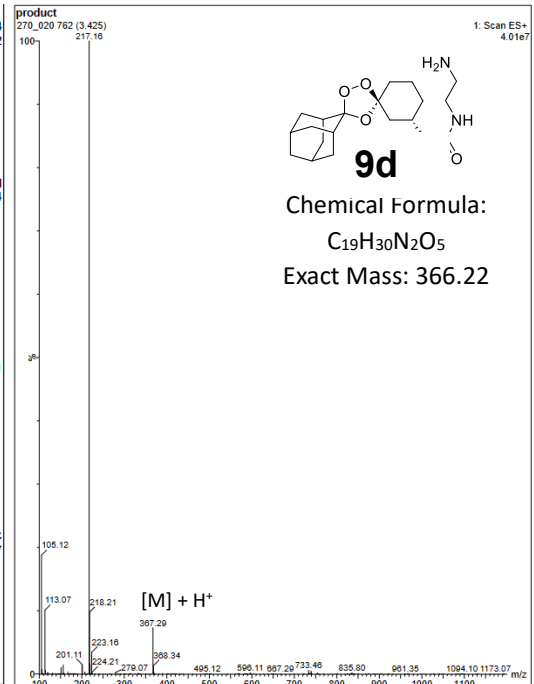
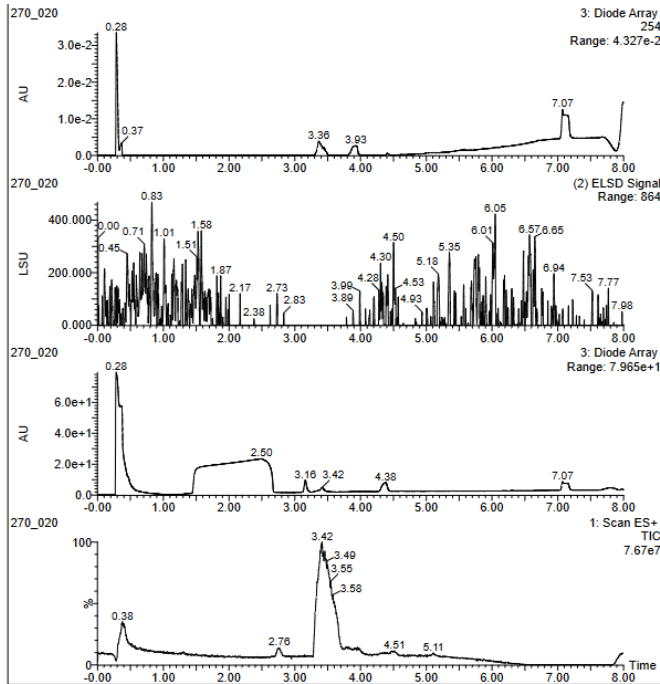
(1''R,3''R)-Dispiro[adamantane-2,3'-[1,2,4]trioxolane-5',1''-cyclohexan]-3''-yl (4-nitrophenyl) carbonate.

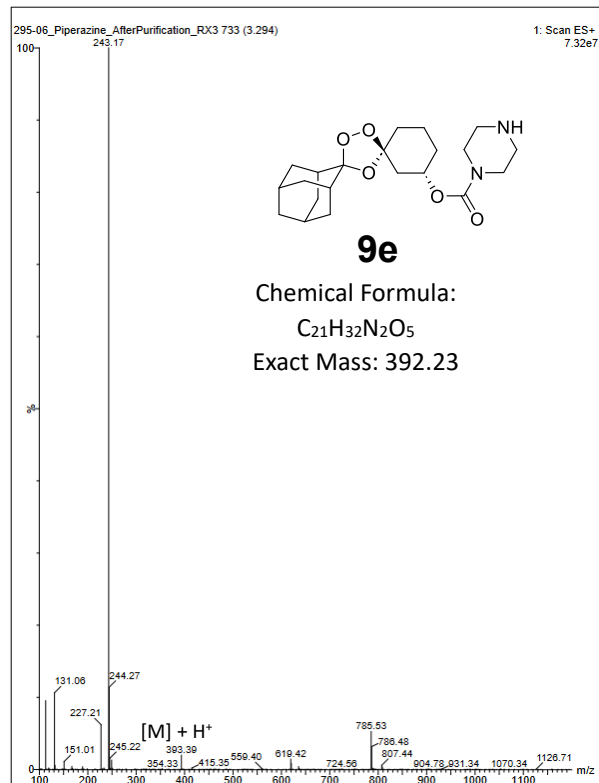
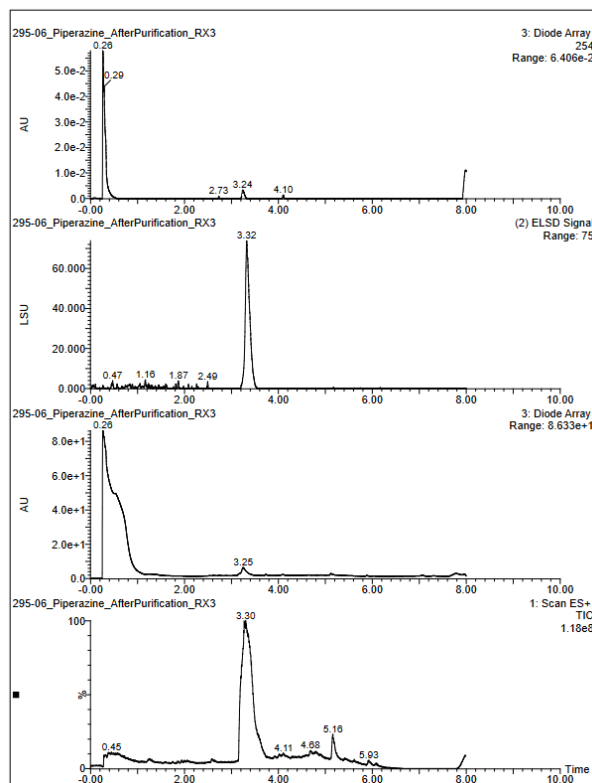
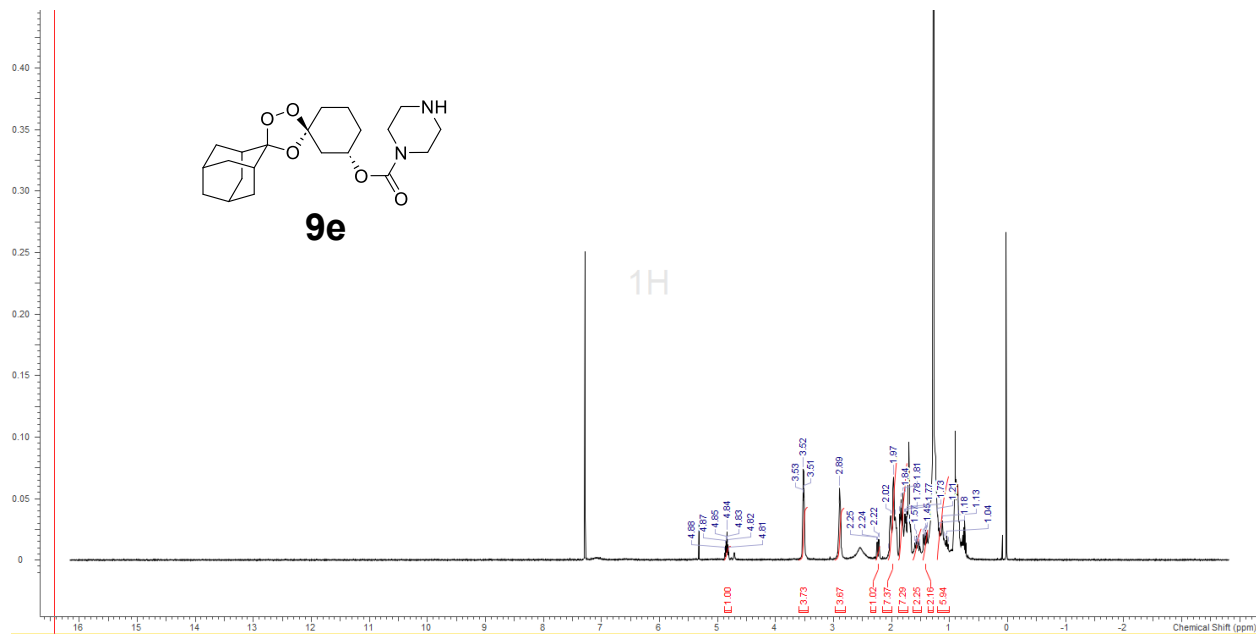
To an oven-dried round-bottom flask containing a magnetic stir bar under an Ar (g) atmosphere was added alcohol 6 (0.150 mg, 0.54 mmol, 1.0 equiv), dichloromethane (10 mL), N,N-diisopropylethylamine (0.30 mL, 1.74 mmol, 3.25 equiv), and 4-

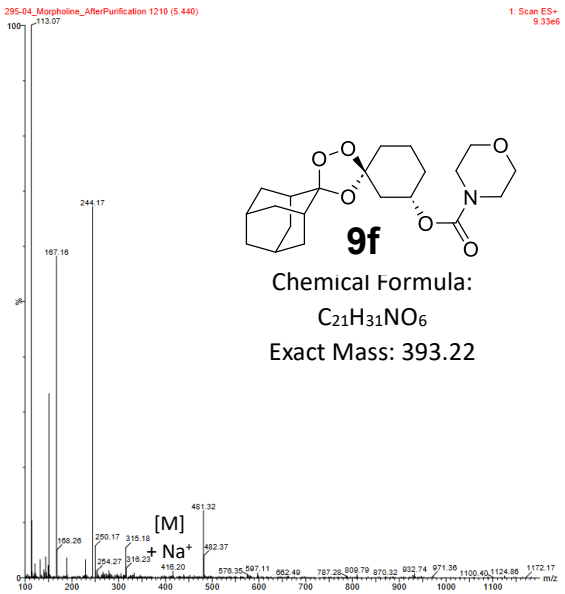
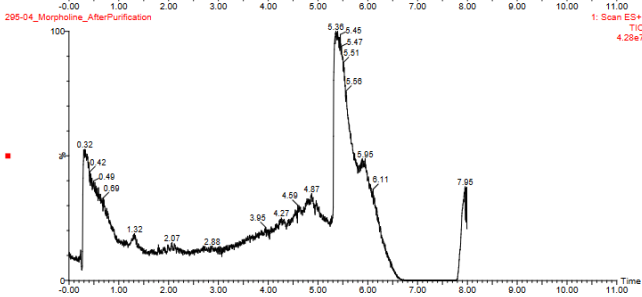
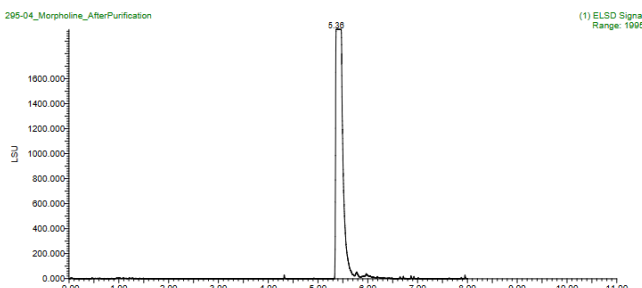
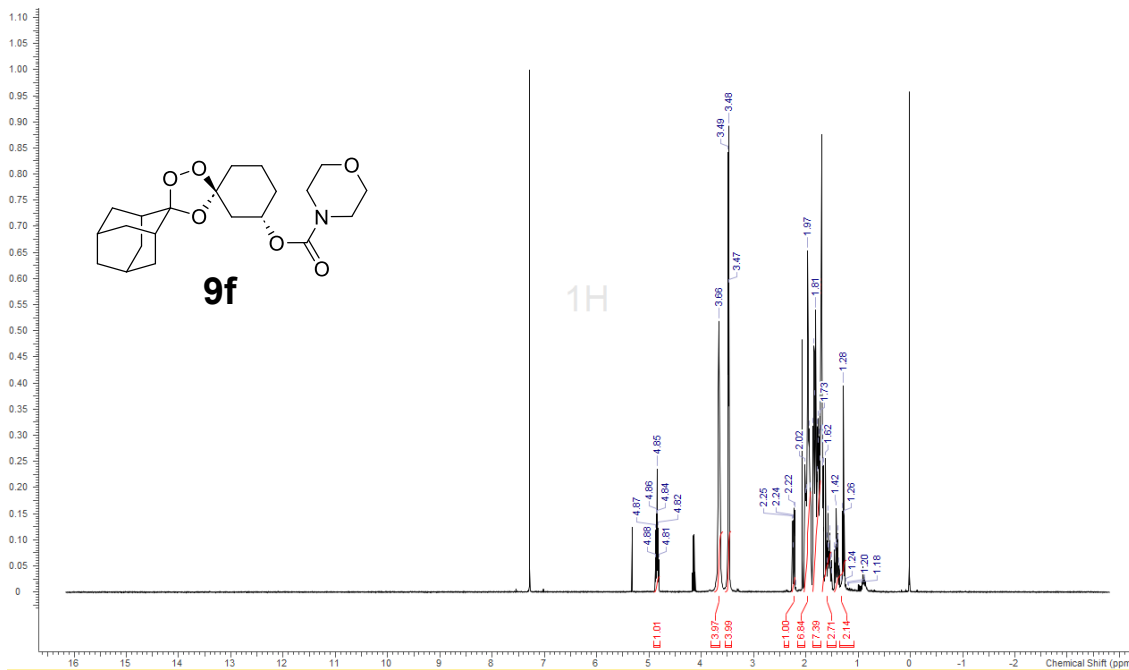
dimethylaminopyridine (0.078 g, 0.64 mmol, 1.2 equiv). The mixture was cooled to 0 °C while 4-nitrophenyl chloroformate (0.350 g, 1.74 mmol, 3.25 equiv) was added as a solid in two portions. The reaction mixture was allowed to warm to rt and was stirred for 3 h. The reaction was diluted with DI H₂O (100 mL) and extracted with EtOAc (1 × 100 mL). The organic layer was washed repeatedly with 1 M aq K₂CO₃ solution until the aqueous layer was colorless and no longer yellow (indicating that most of the p-nitrophenol had been successfully removed from the organic layer). The organic layer was then dried (Na₂SO₄), filtered, and concentrated under reduced pressure to yield a viscous yellow oil. The crude material was purified using flash column chromatography (80 g silica gel cartridge, 0–25% EtOAc–Hexanes, product eluted during 10% EtOAc–Hex) to yield the desired product 7 (208 mg, 0.467 mmol, 87%) as a pale yellow oil (93:7 d.r.). ¹H NMR (400 MHz, CDCl₃): δ 8.26 (d, J = 9.1 Hz, 2 H), 7.38 (br d, J = 9.1 Hz, 2 H), 4.94 (td, J = 9.2, 4.5 Hz, 1 H, minor diastereomer), 4.79–4.88 (m, 1 H), 2.32–2.42 (m, 1 H), 2.10 (br d, J = 8.8 Hz, 1 H), 1.69–2.00 (m, 1 H), 1.64–2.01 (m, 17 H), 1.40–1.64 (m, 3 H), 1.20–1.28 (m, 1 H), 0.83–0.96 (m, 1 H). ¹³C NMR (100 MHz, CDCl₃): δ 155.5, 151.6, 145.3, 125.3, 121.9, 121.7, 111.9, 108.3, 76.2, 39.5, 36.7, 36.3, 36.3, 34.8, 34.7, 34.7, 34.7, 33.5, 30.0, 26.8, 26.4, 19.5. MS (ESI) calcd for C₂₃H₂₇NNaO₈ [M + Na]⁺: m/z 468.16, found 467.99.

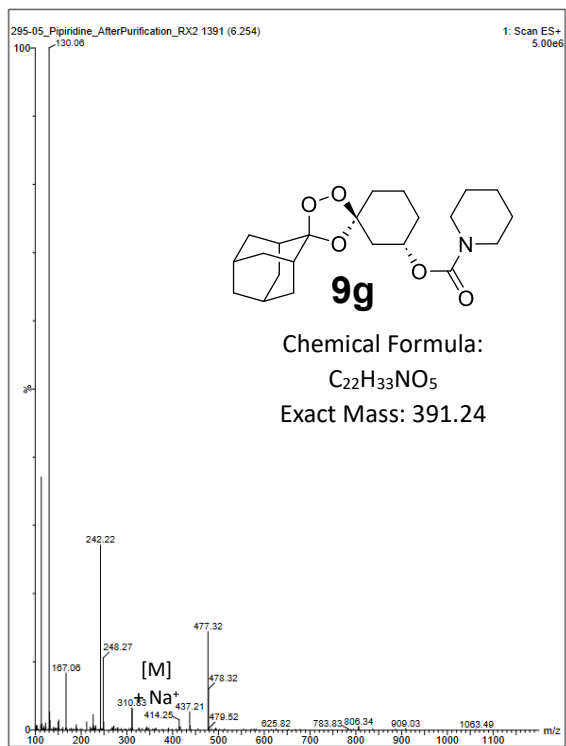
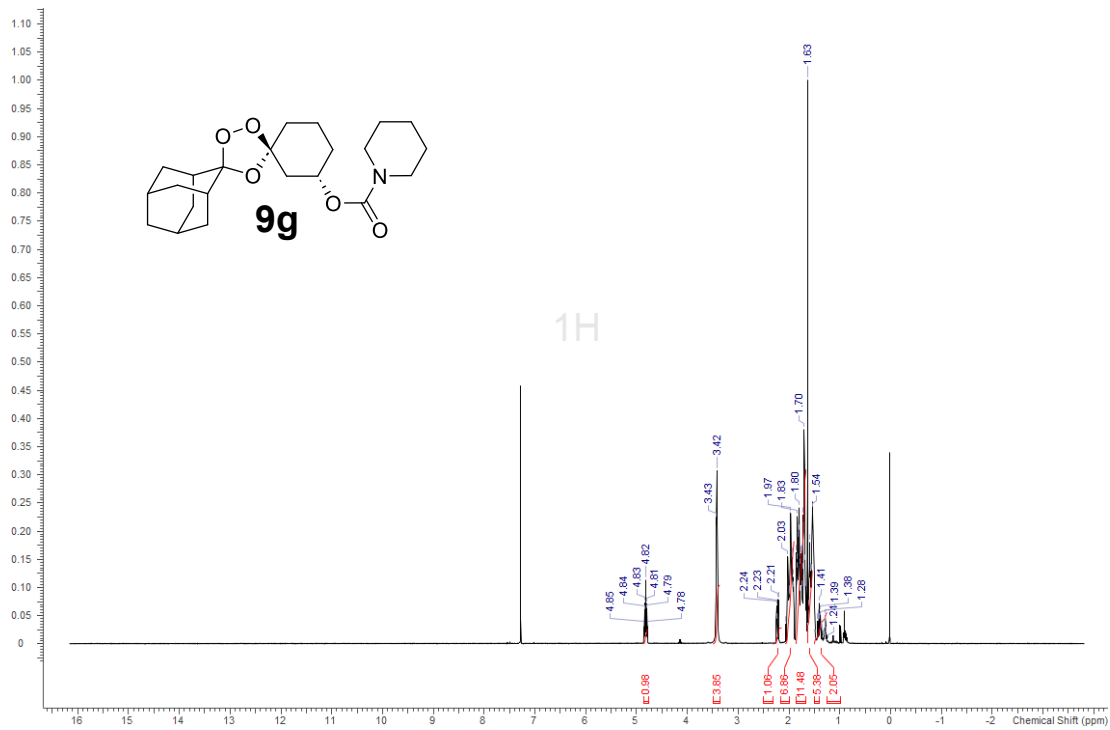
¹H and ¹³C NMR spectra and LCMS chromatograms for final compounds

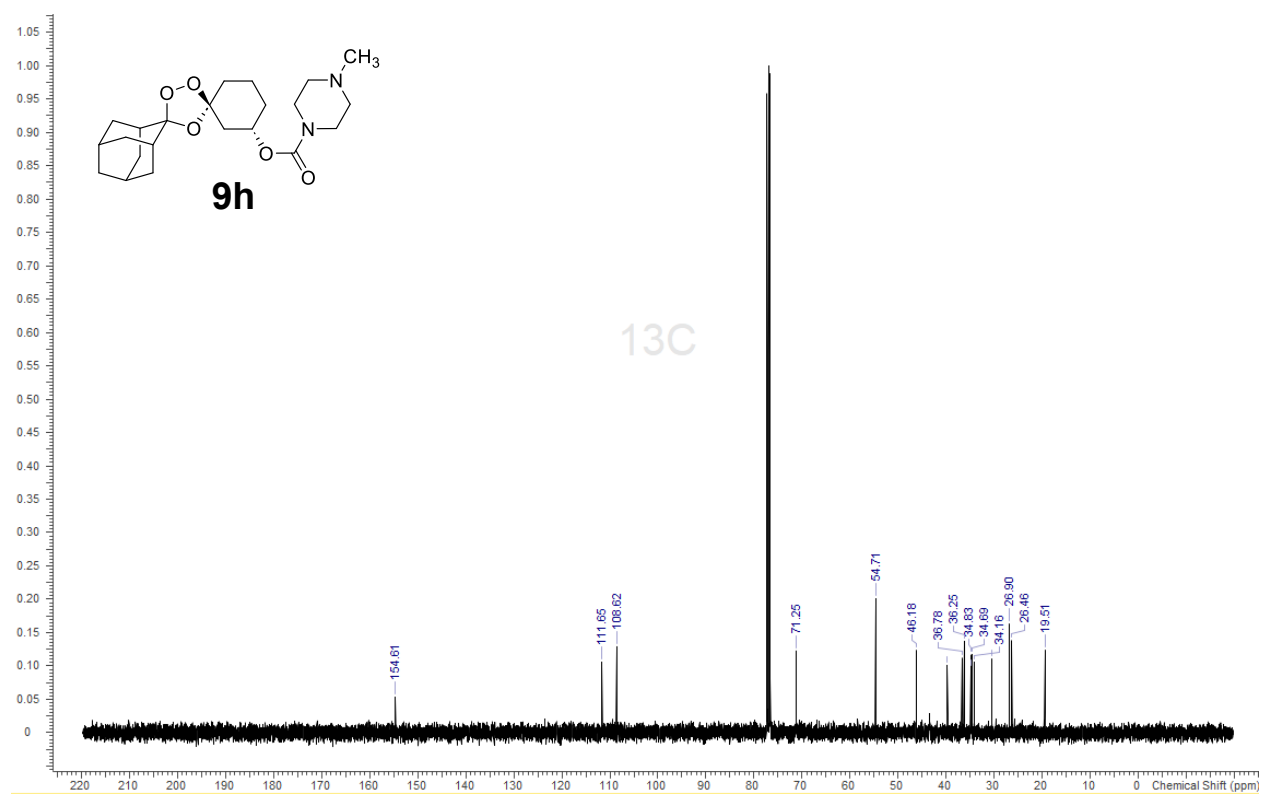
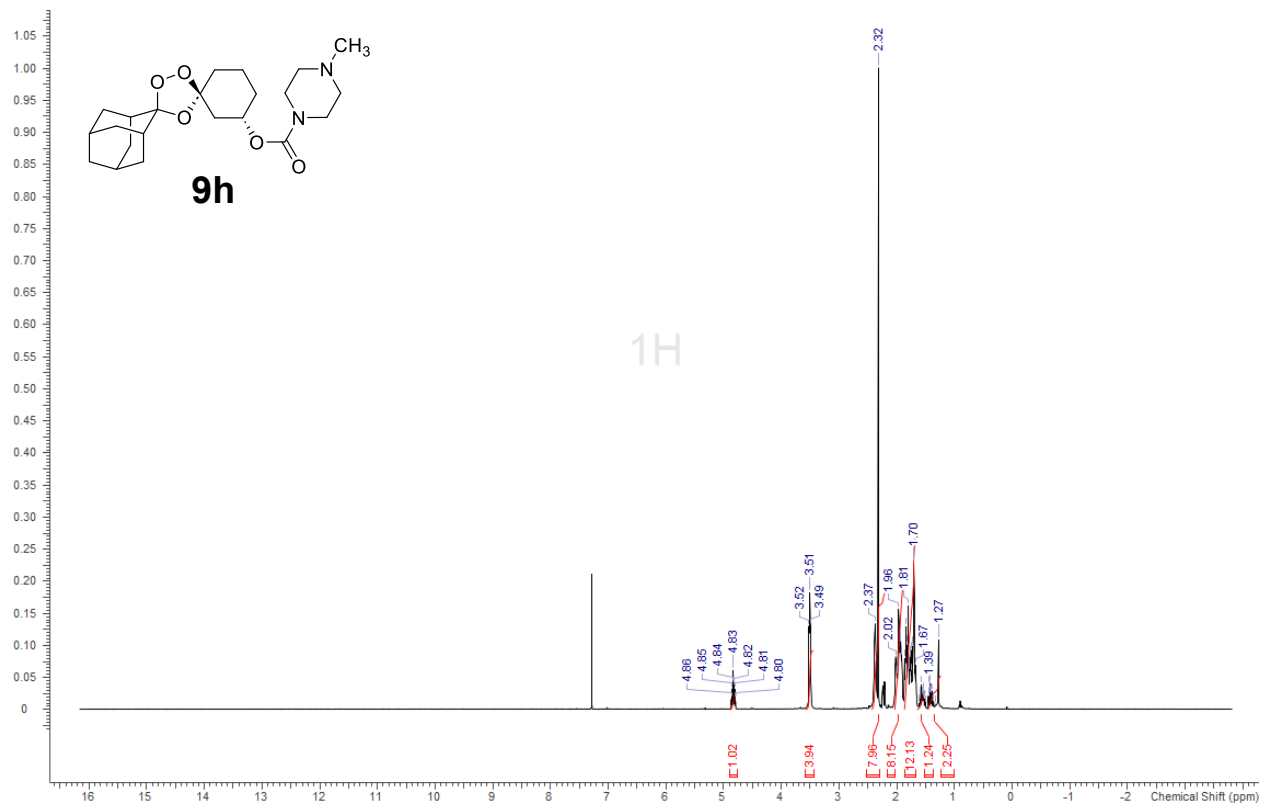


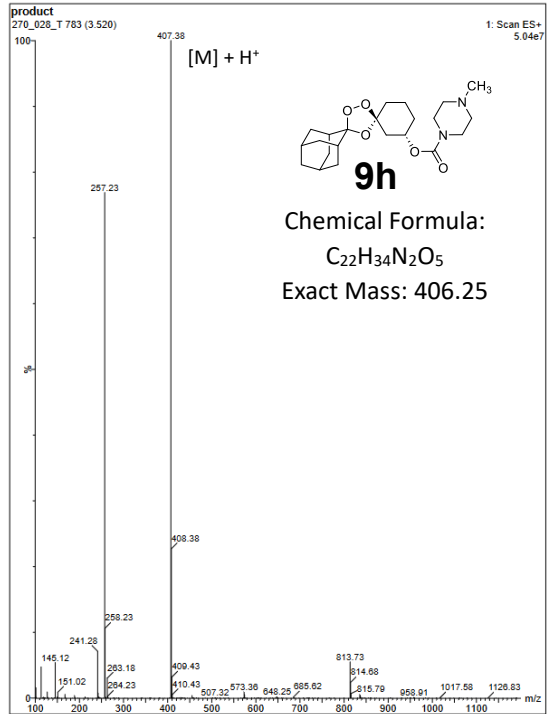
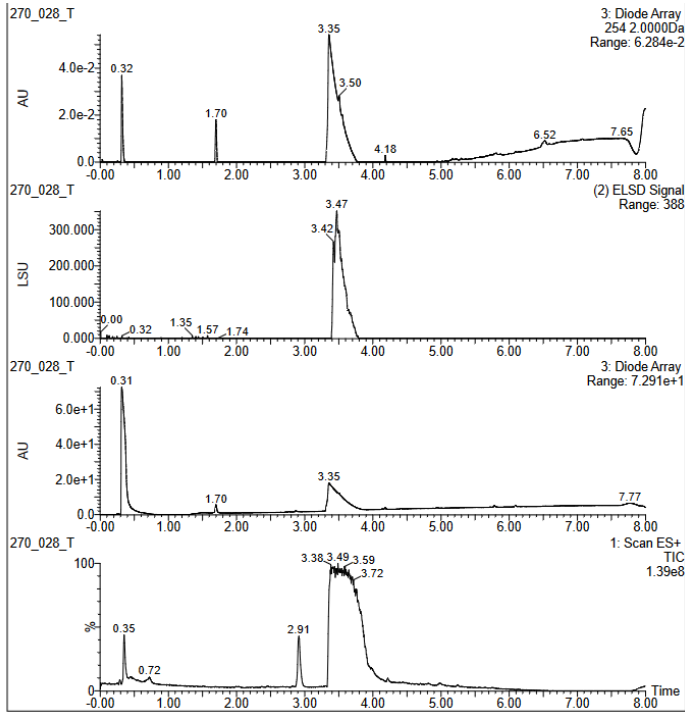


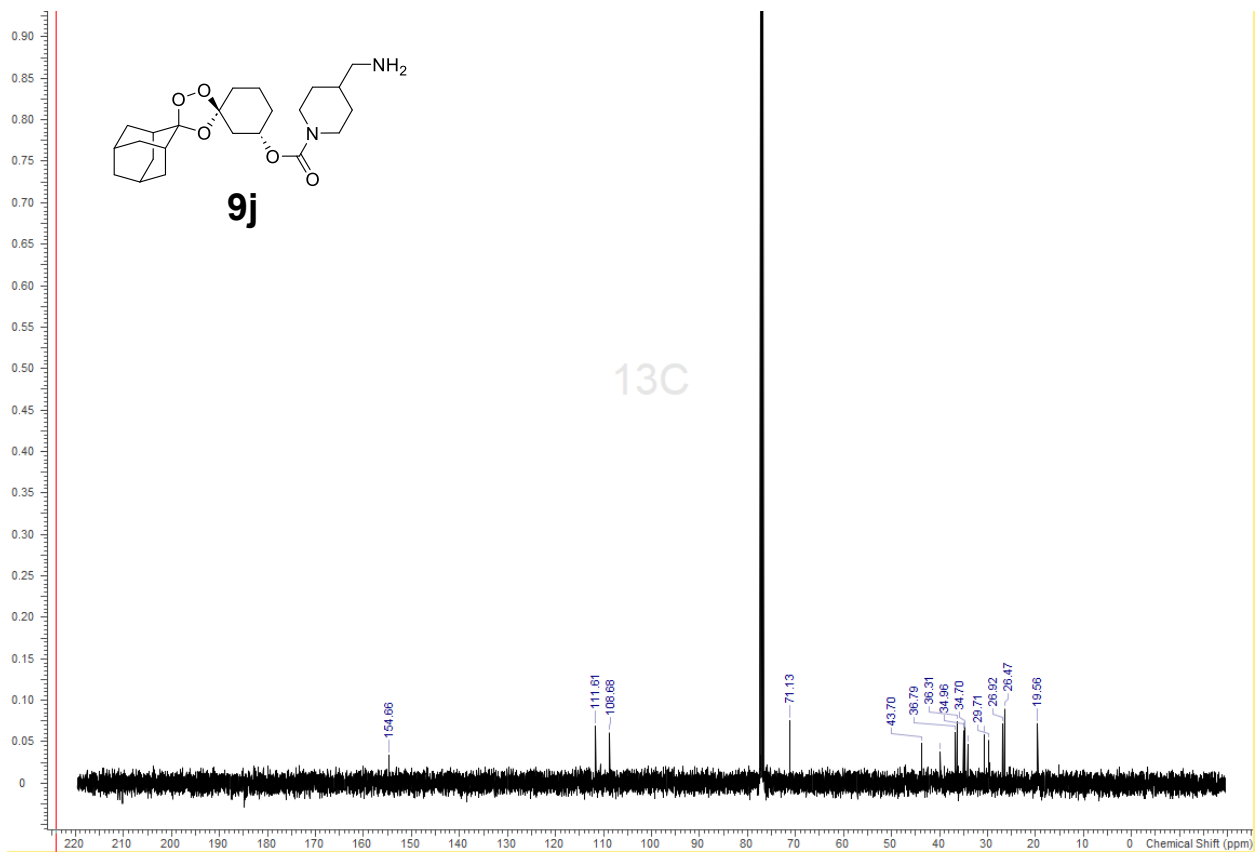
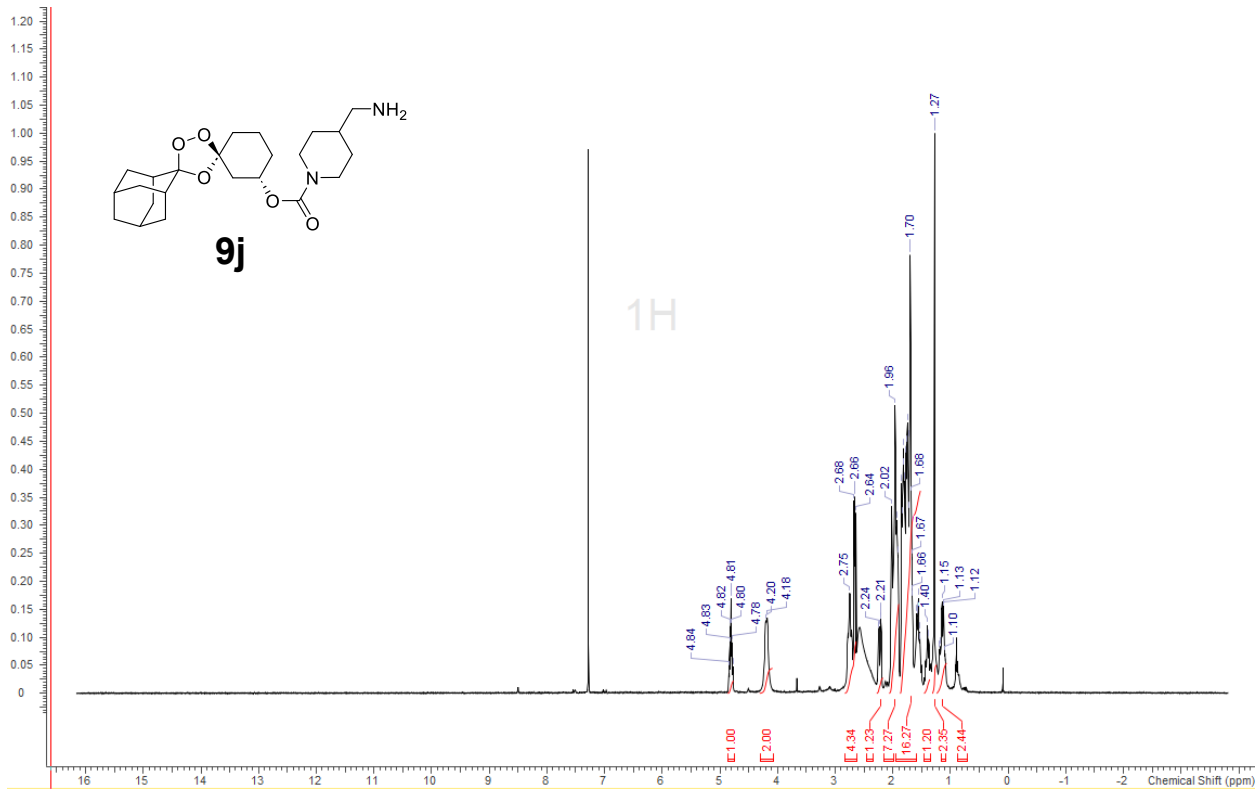


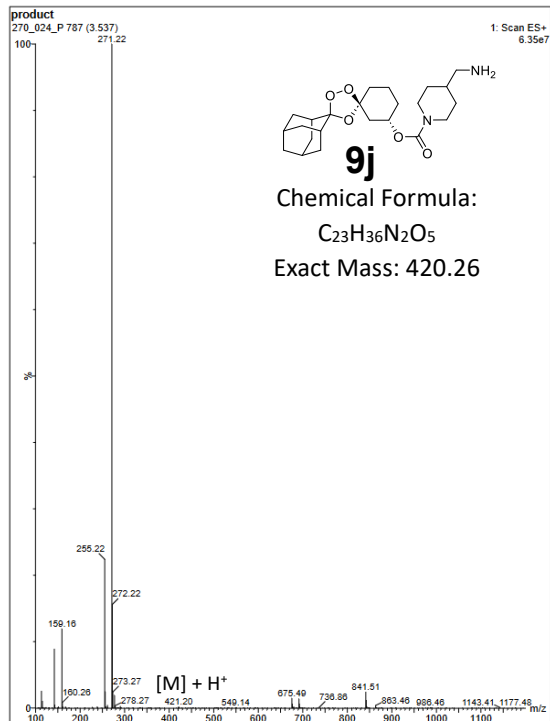
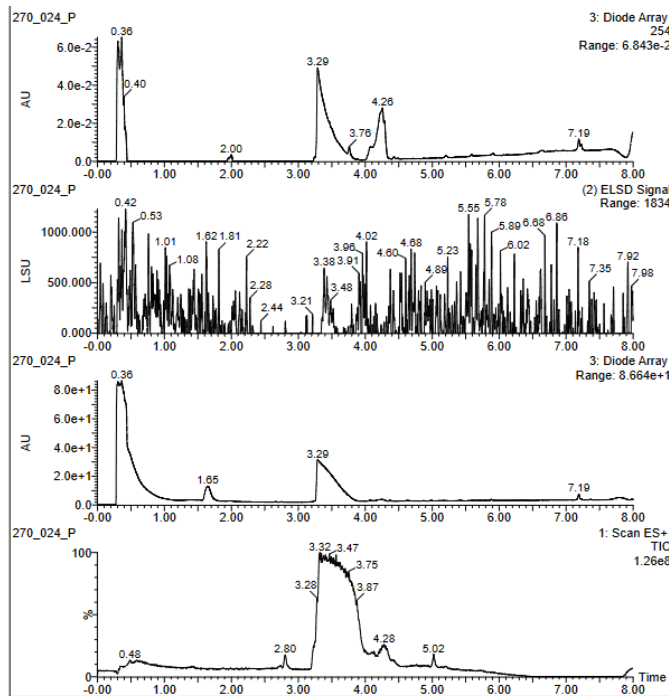


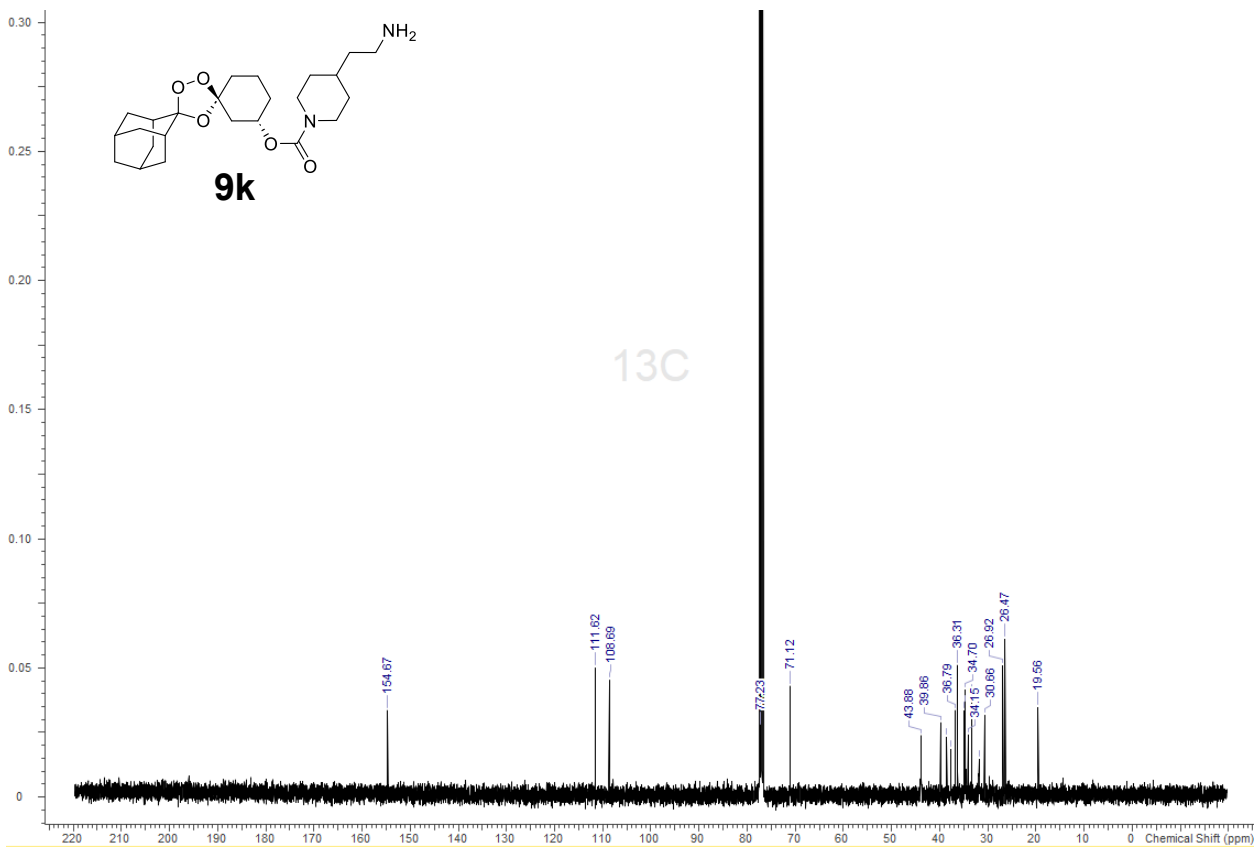
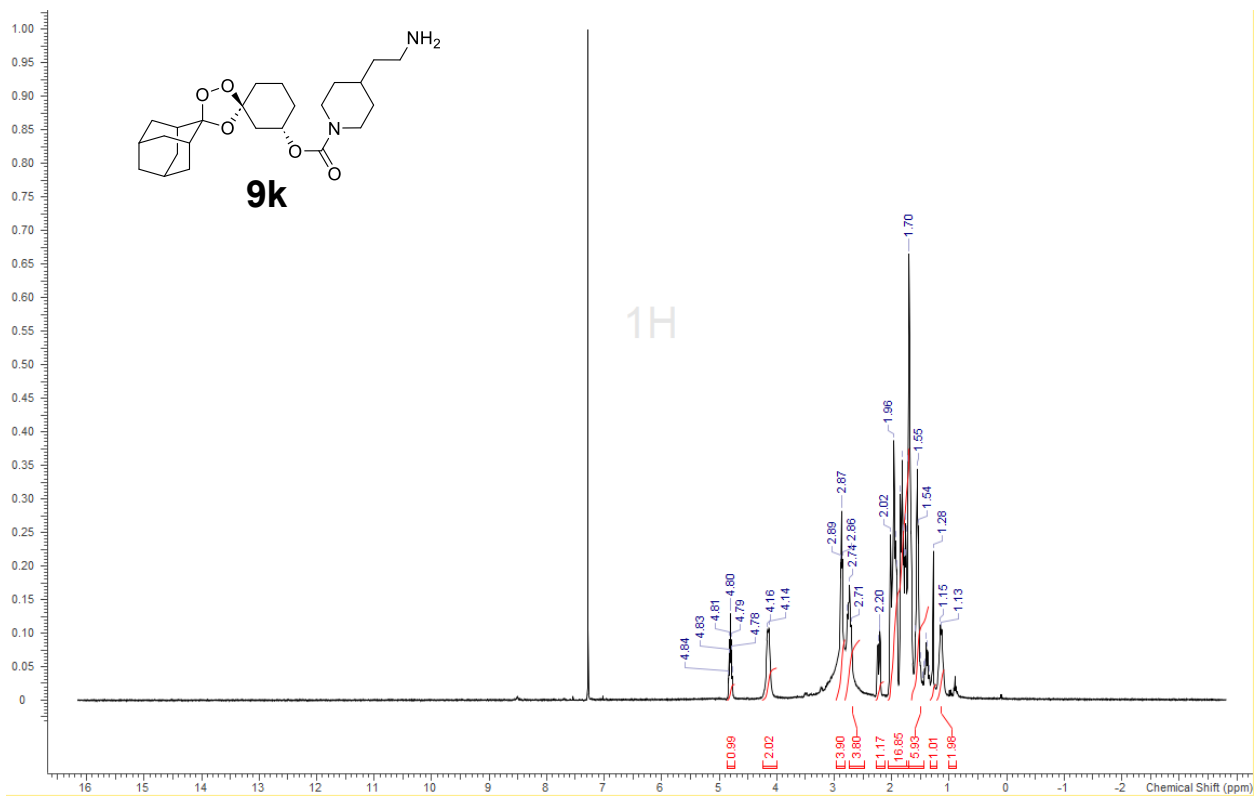


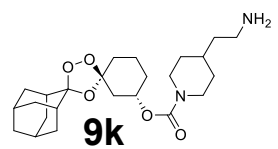
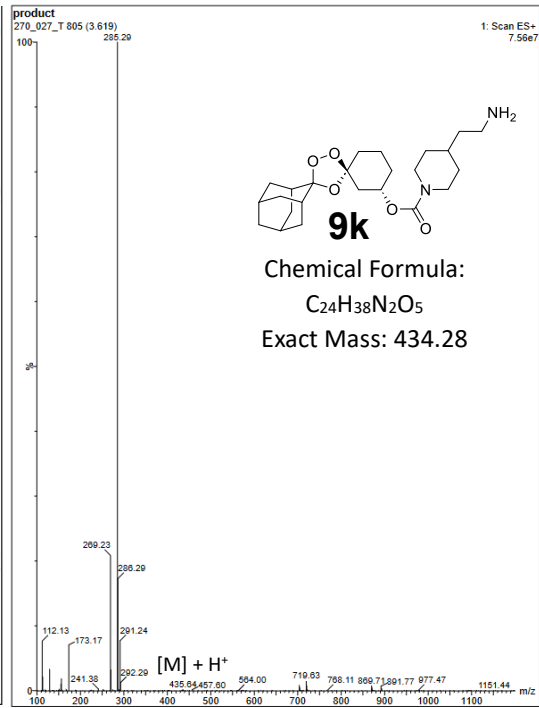
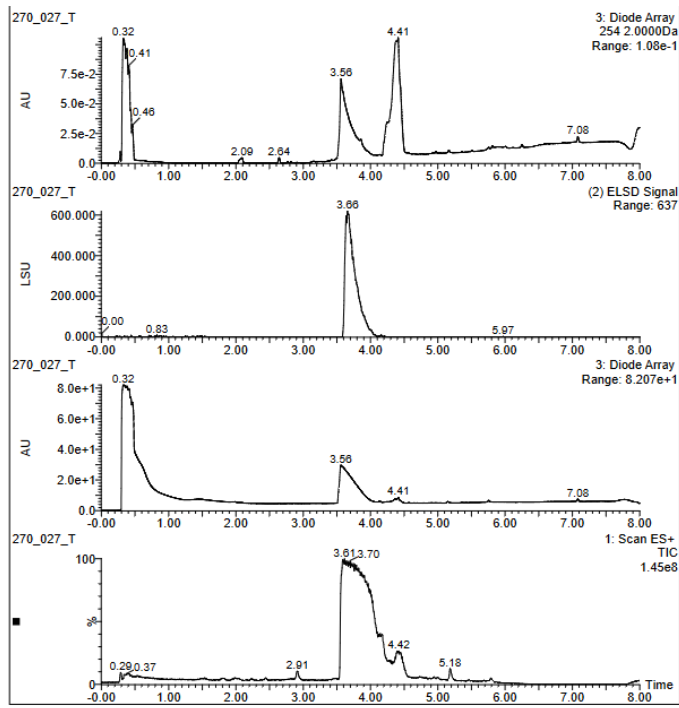




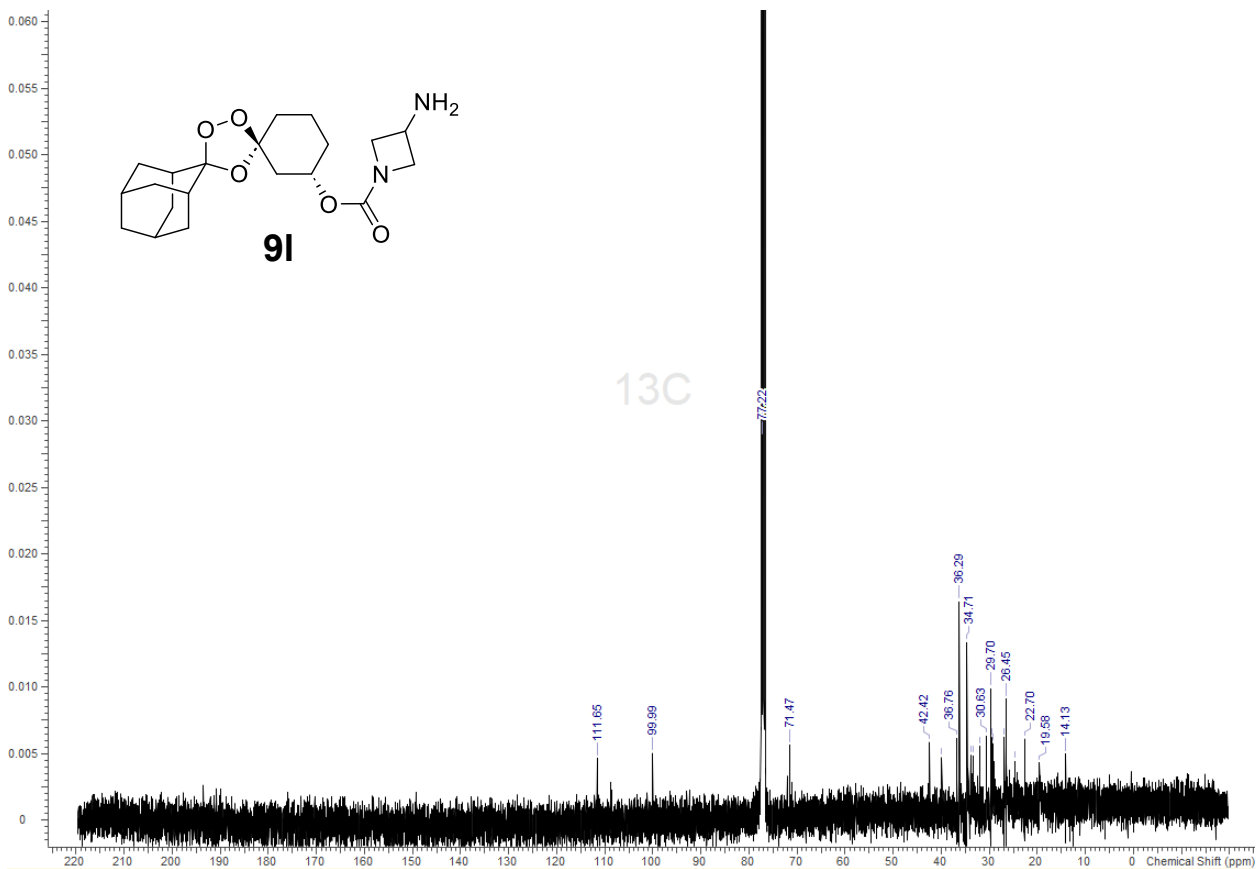
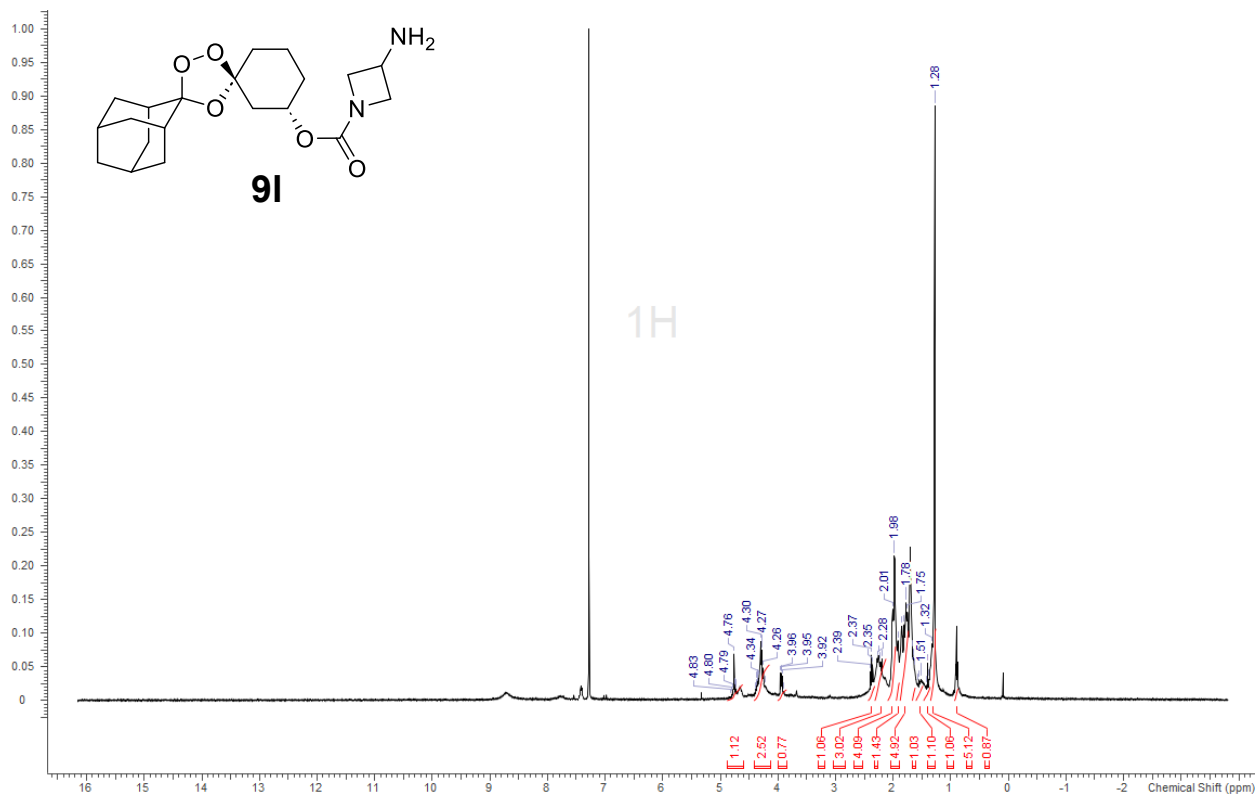


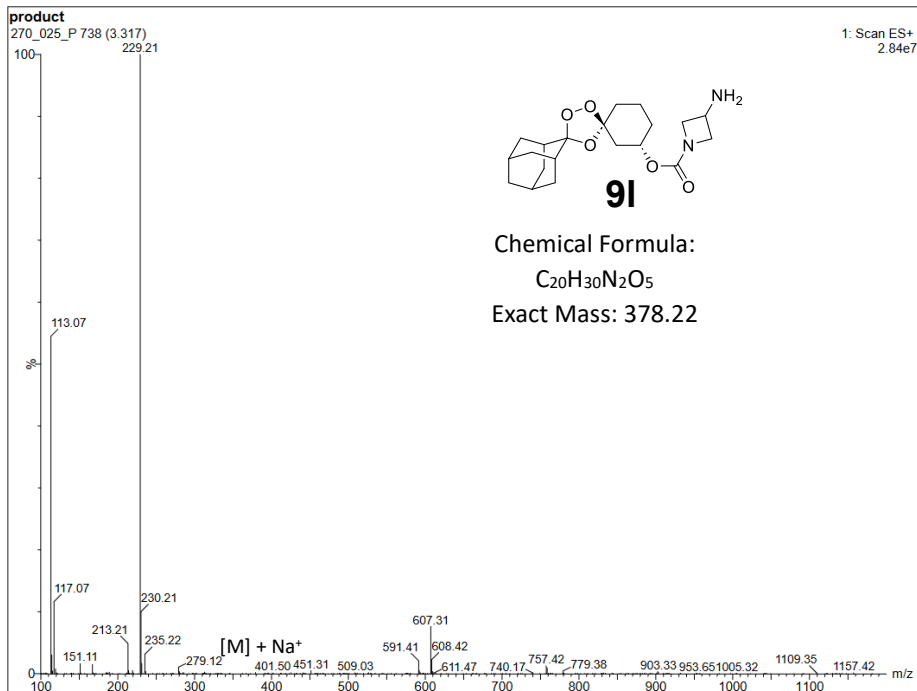
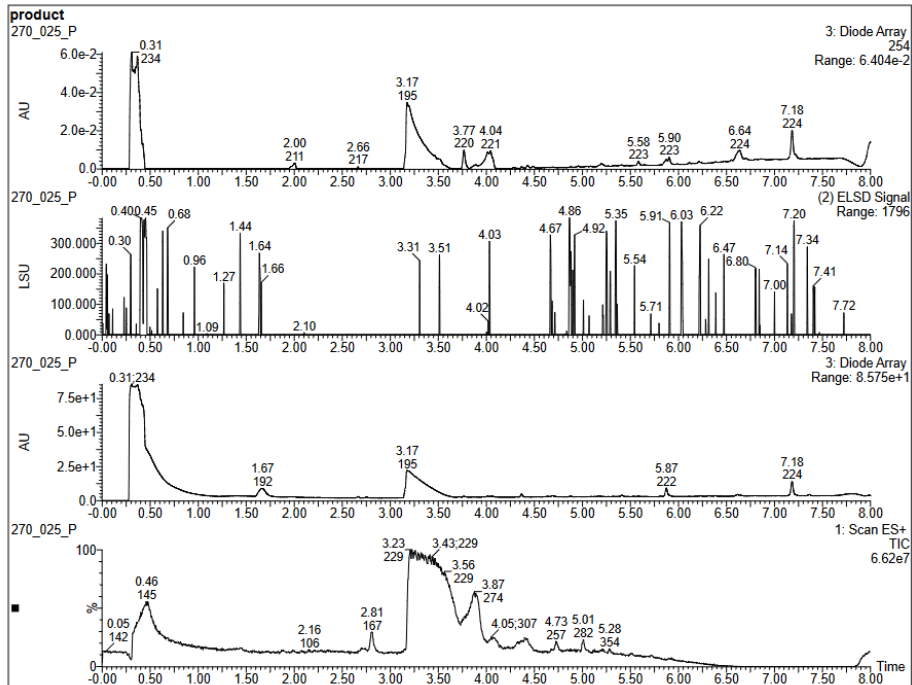


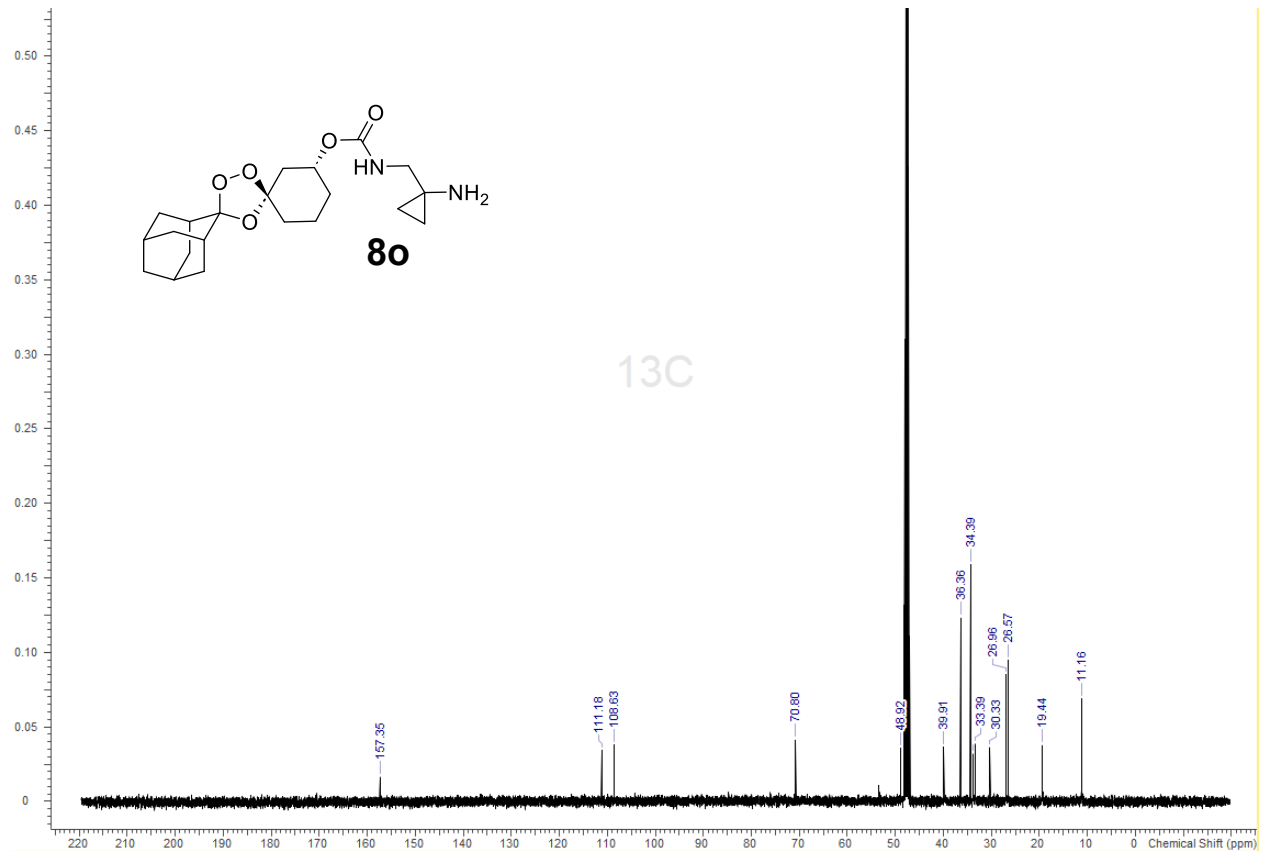
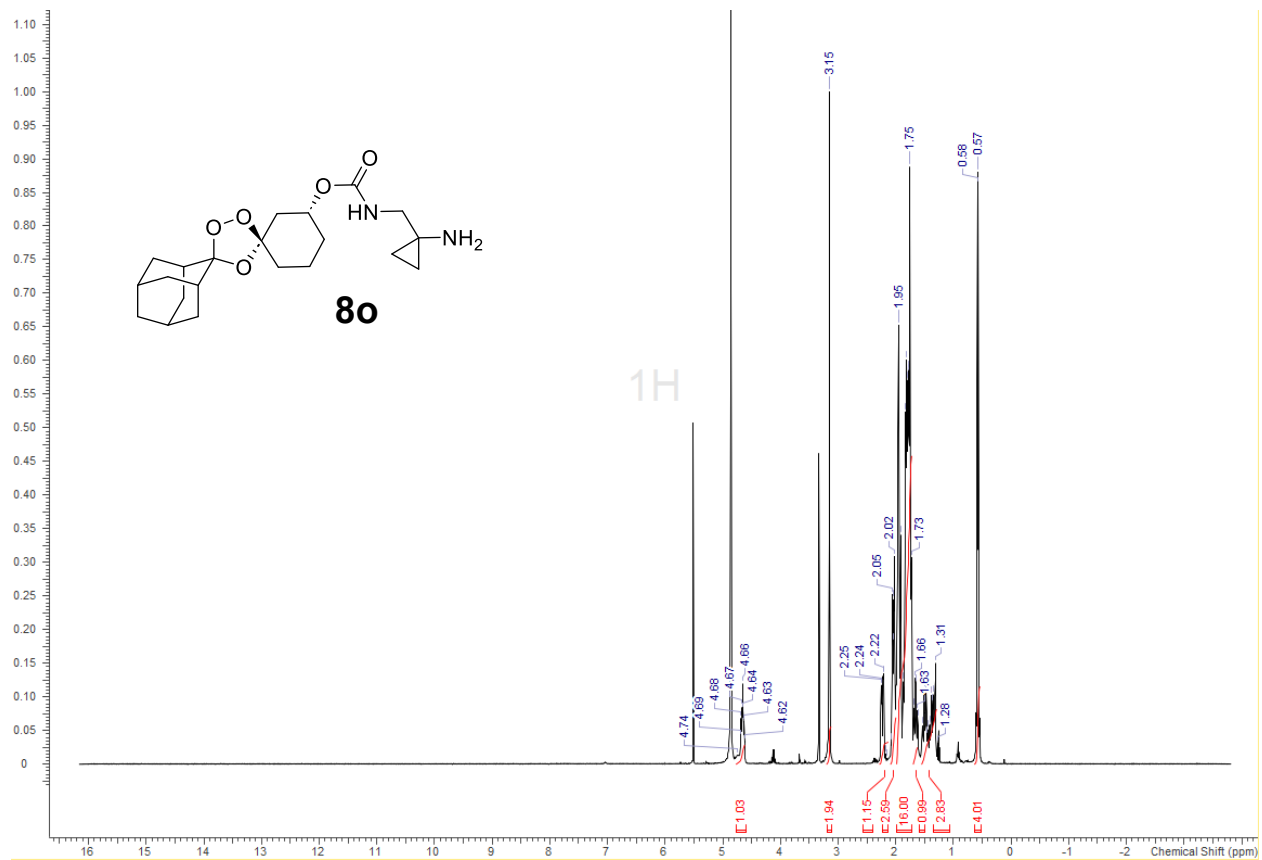


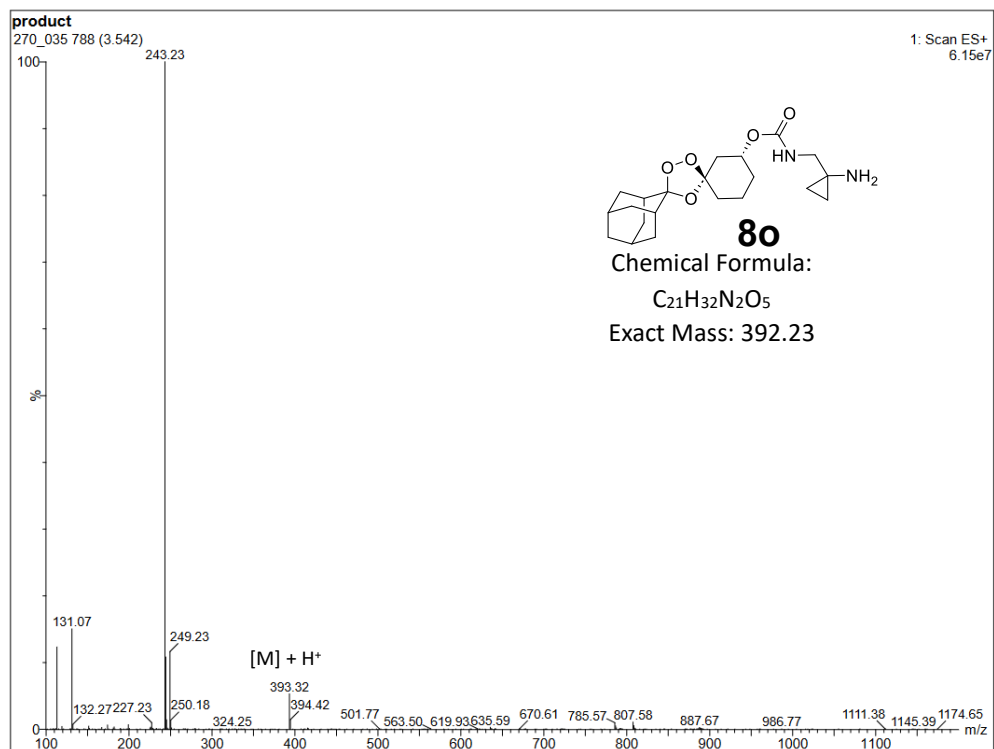
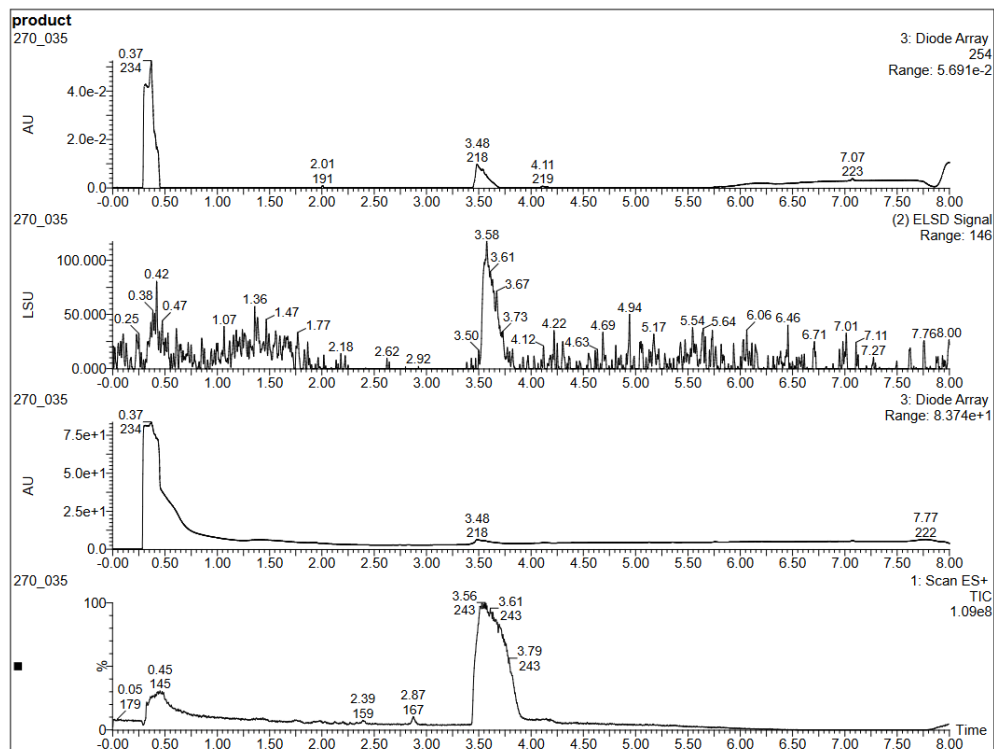


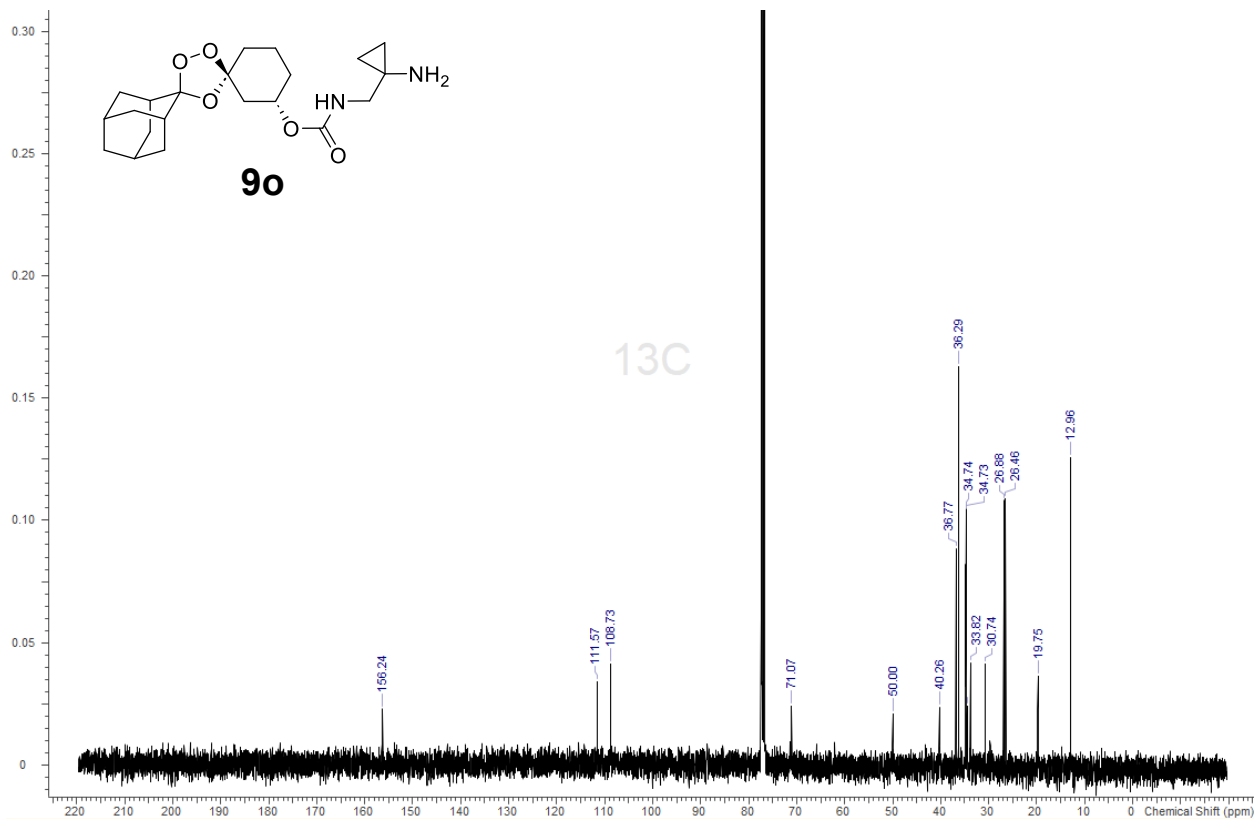
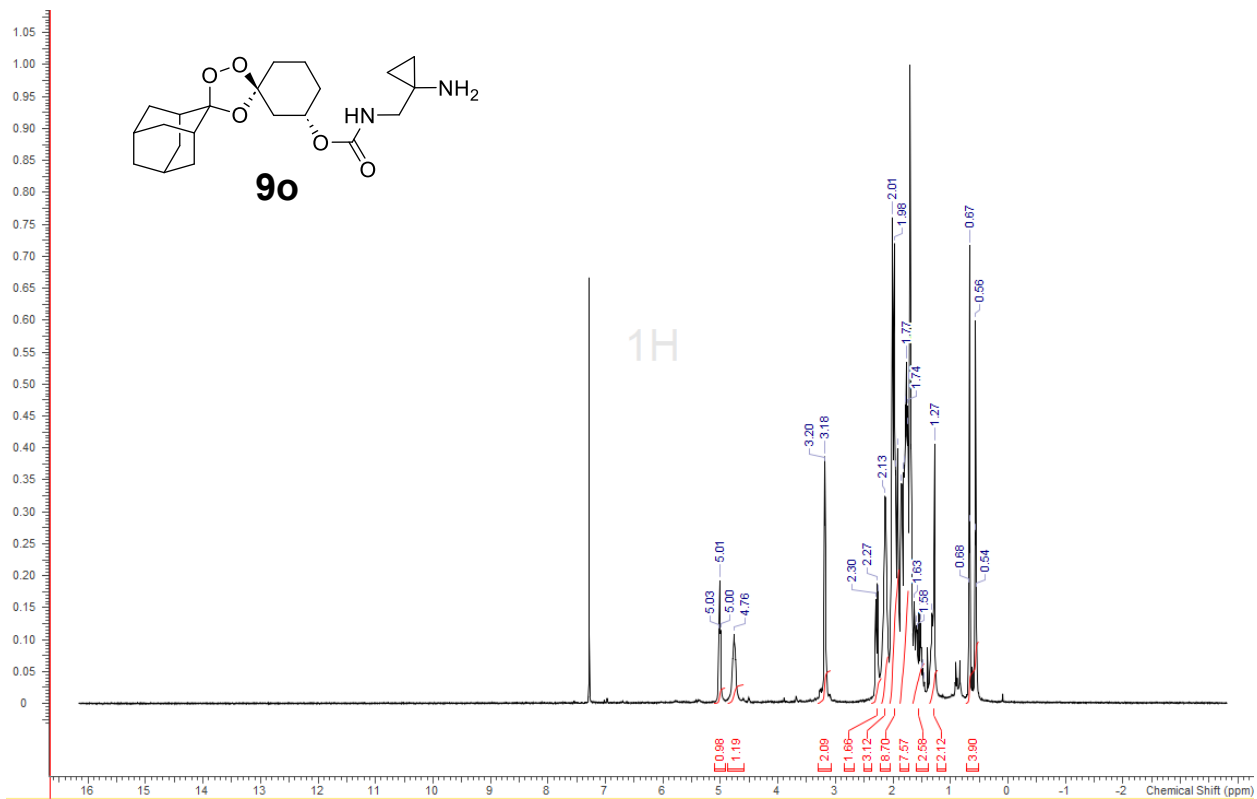
Chemical Formula:
C₂₄H₃₈N₂O₅
Exact Mass: 434.28

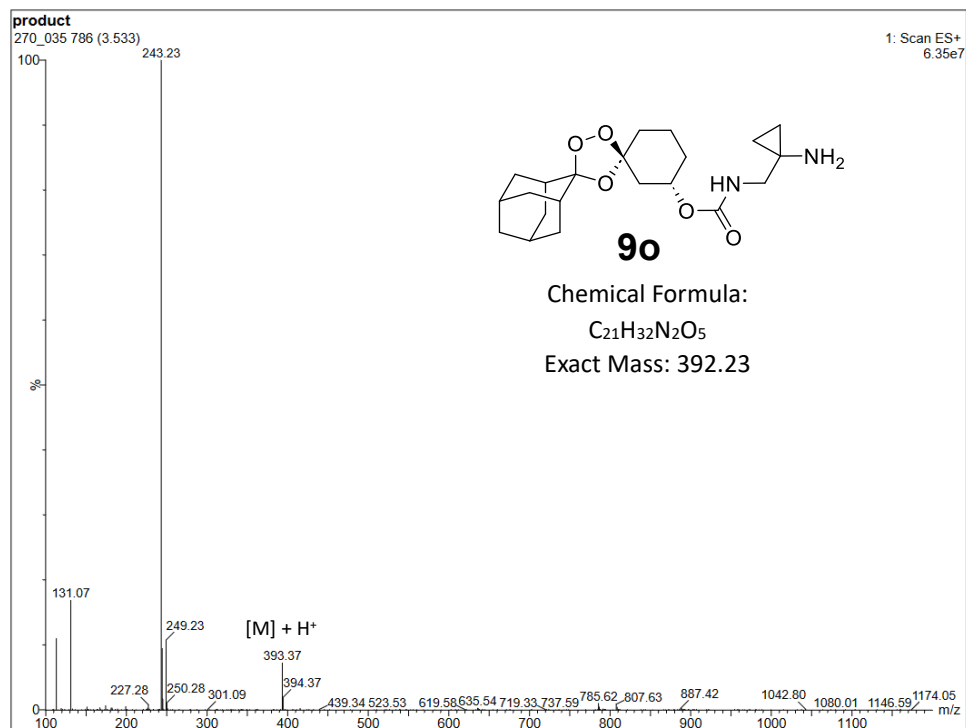
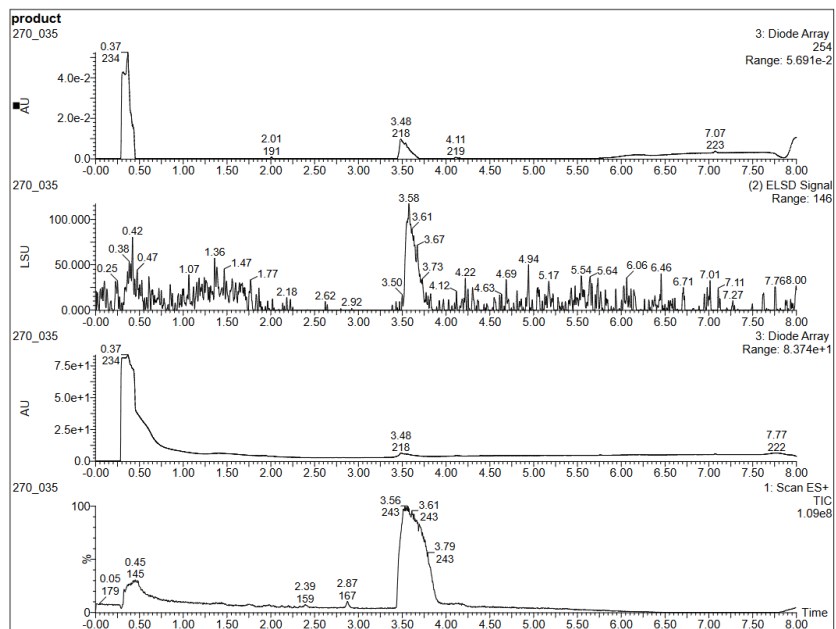


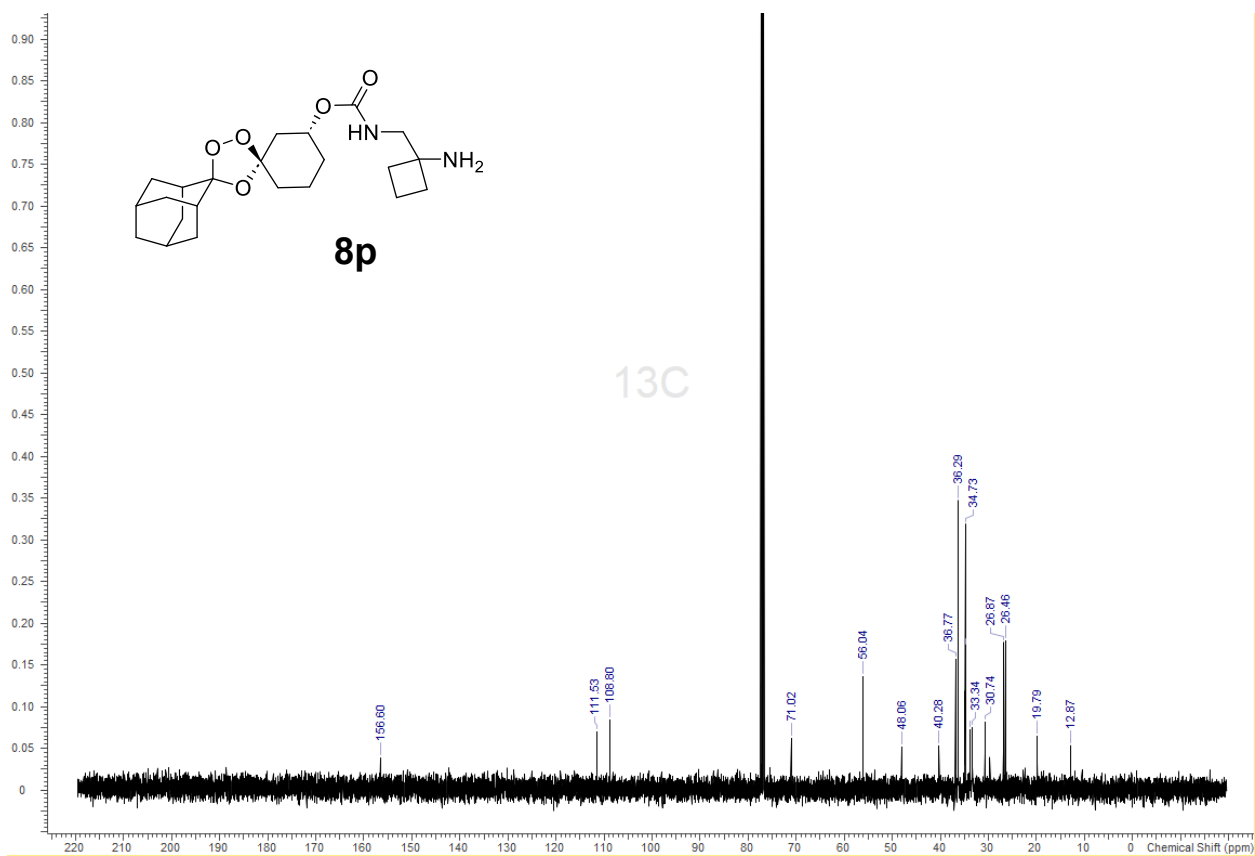
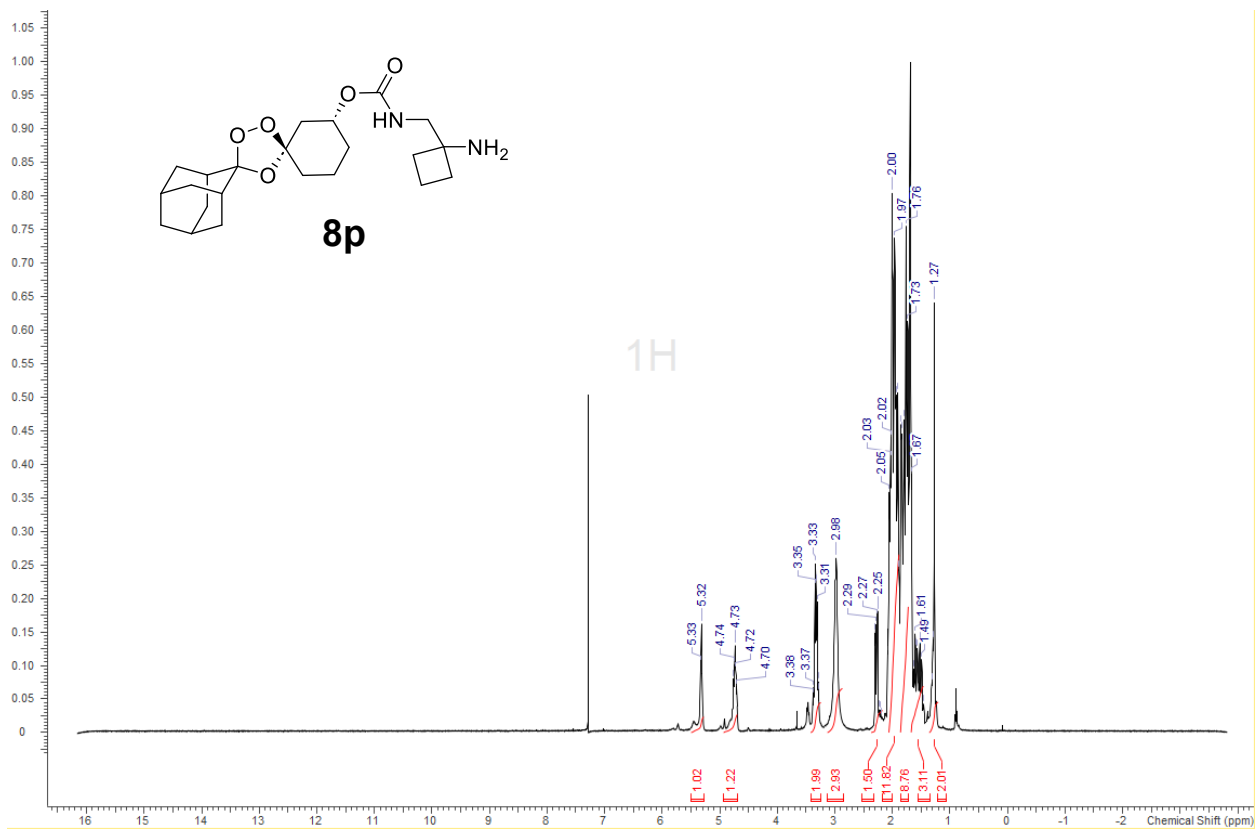


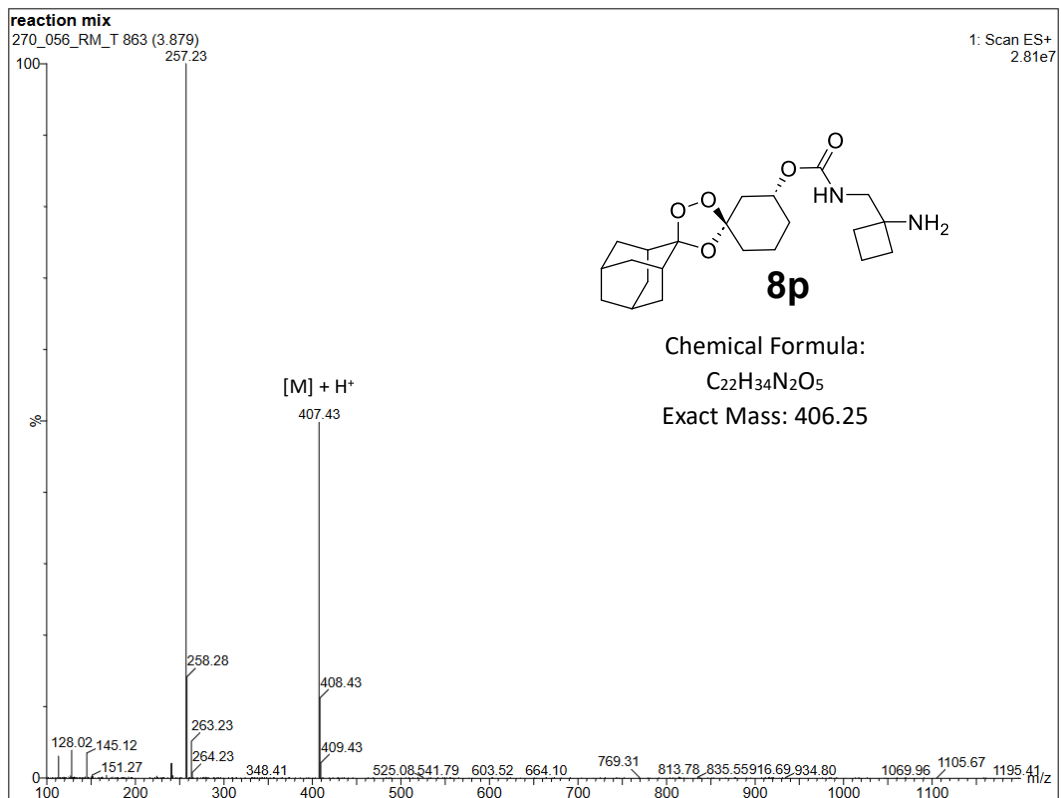
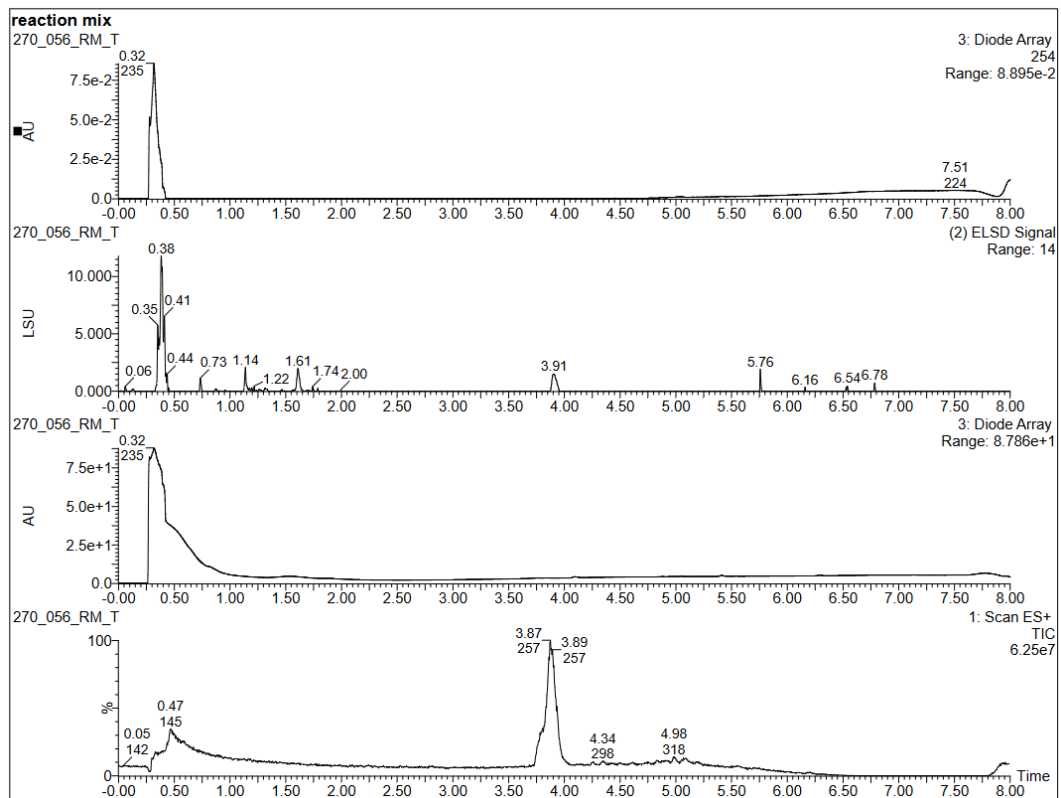


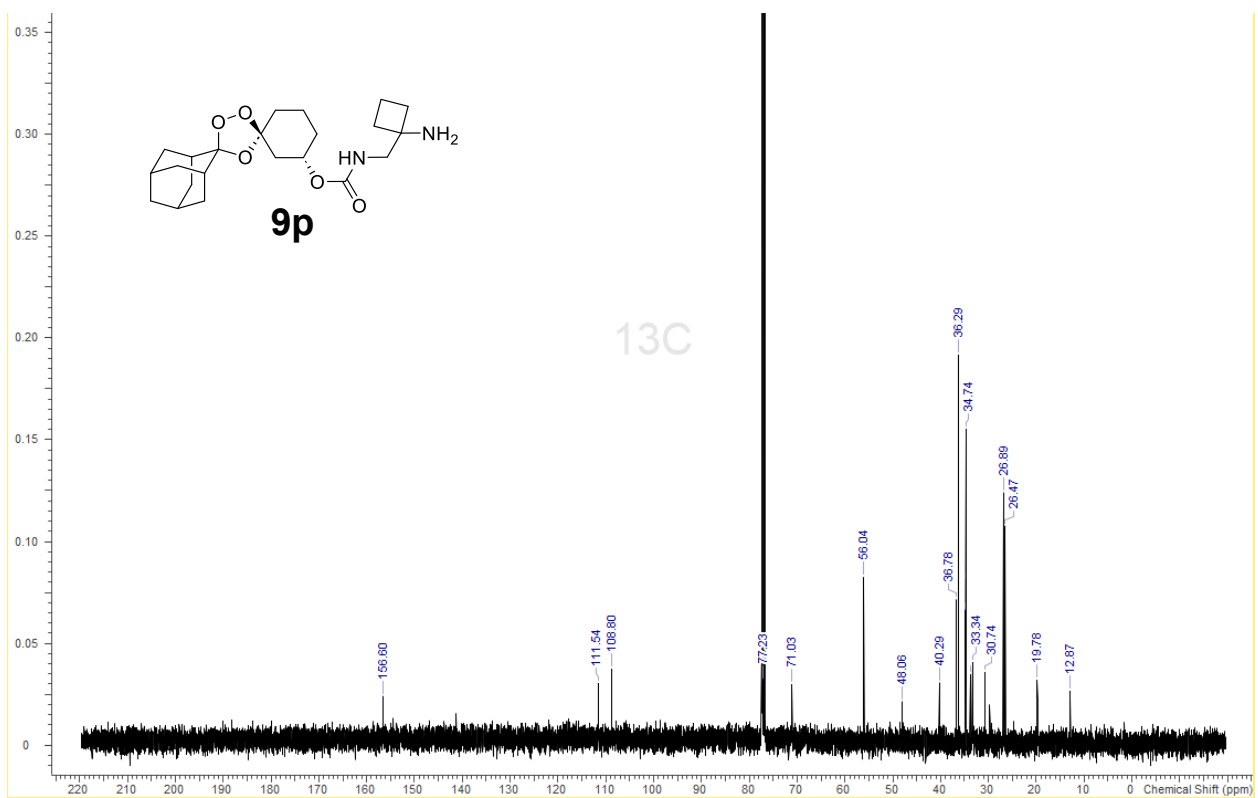
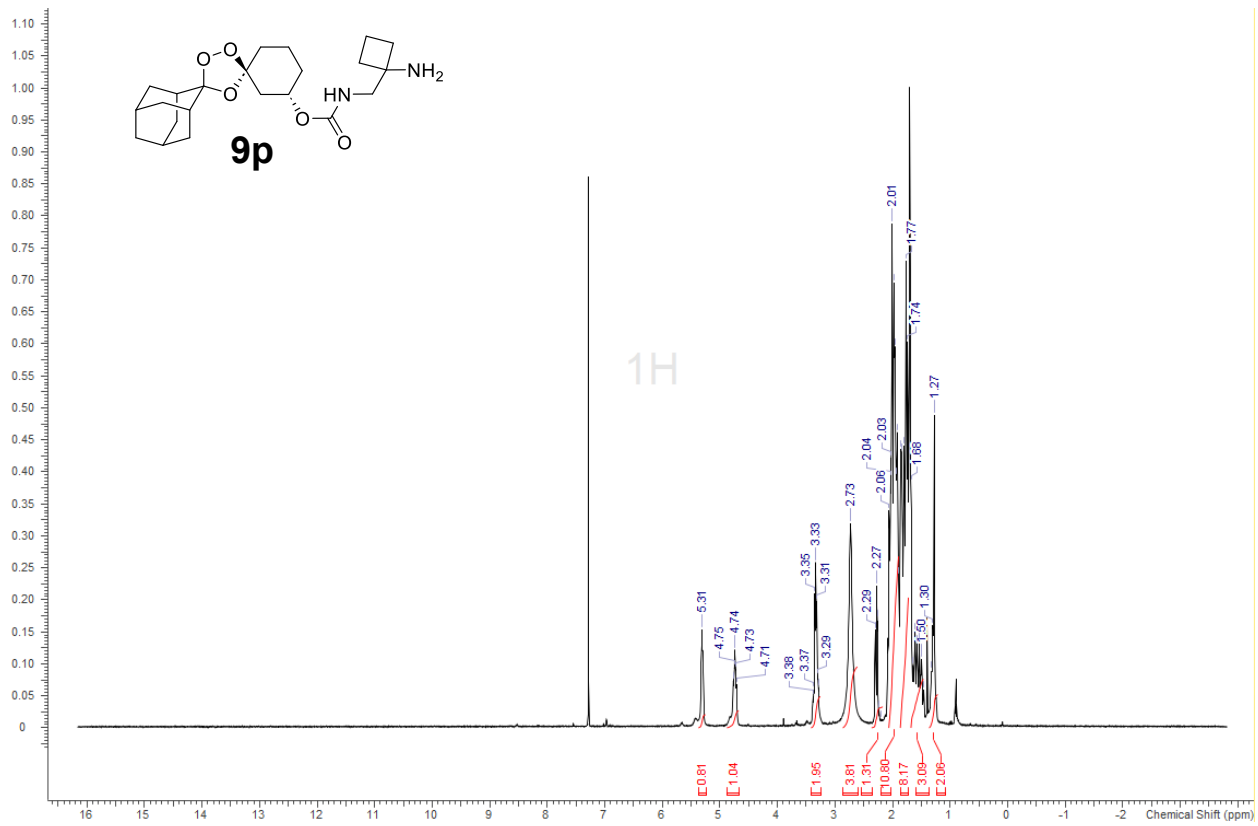


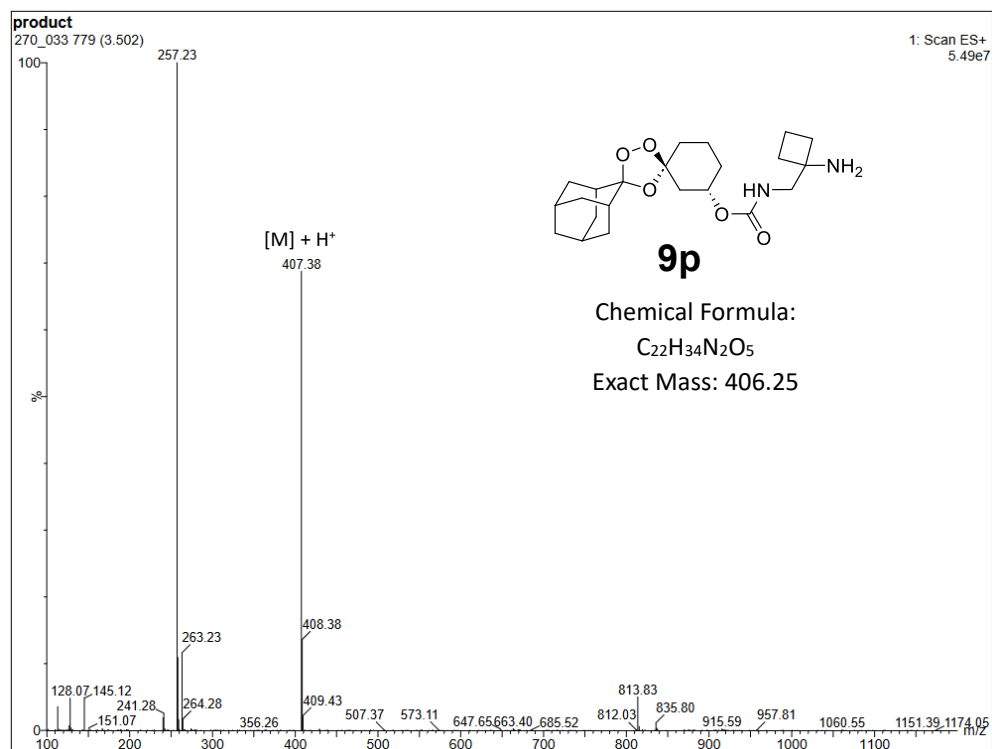
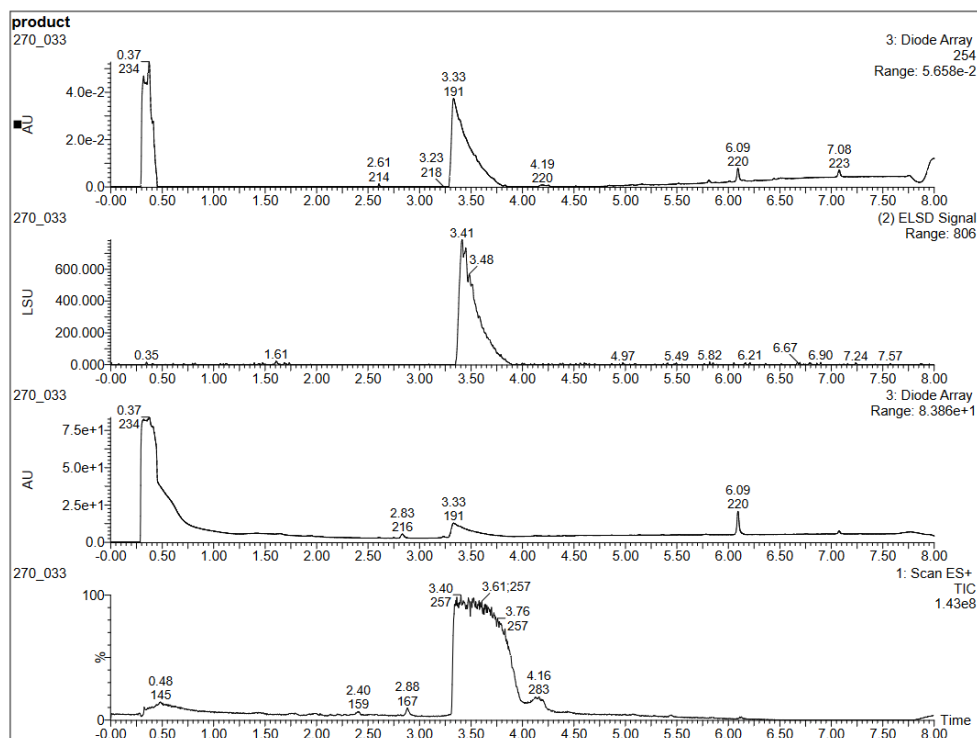


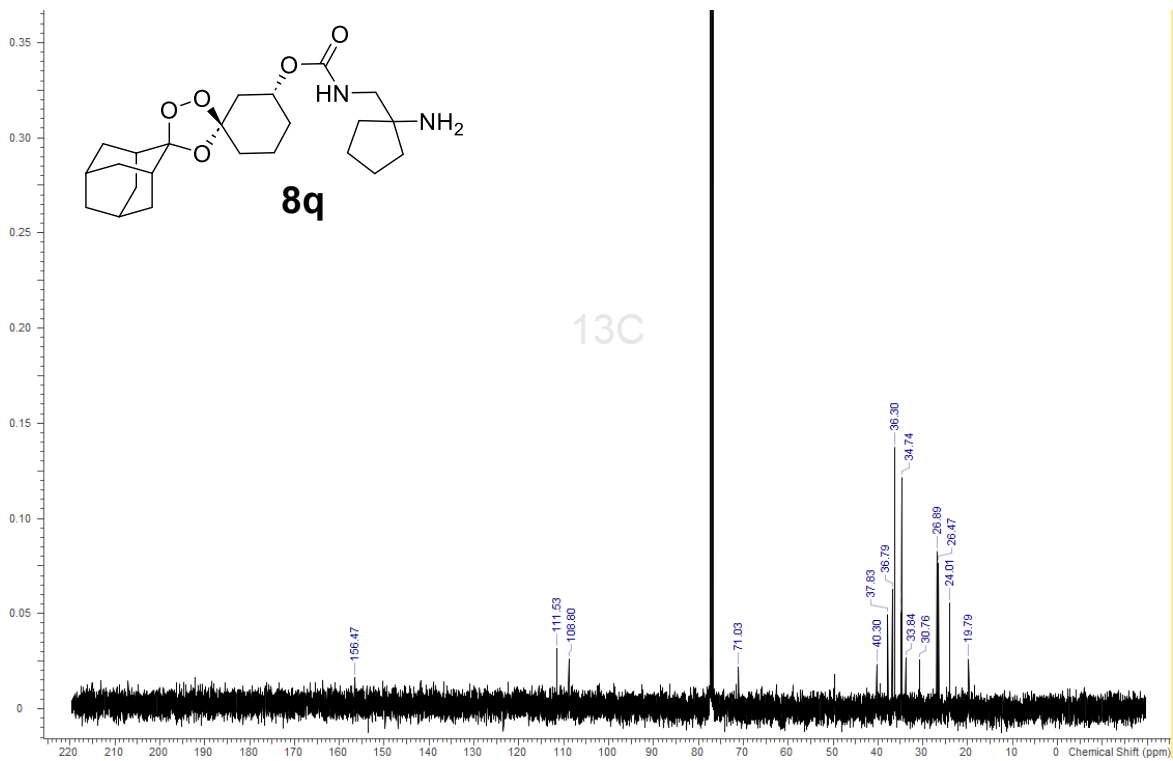
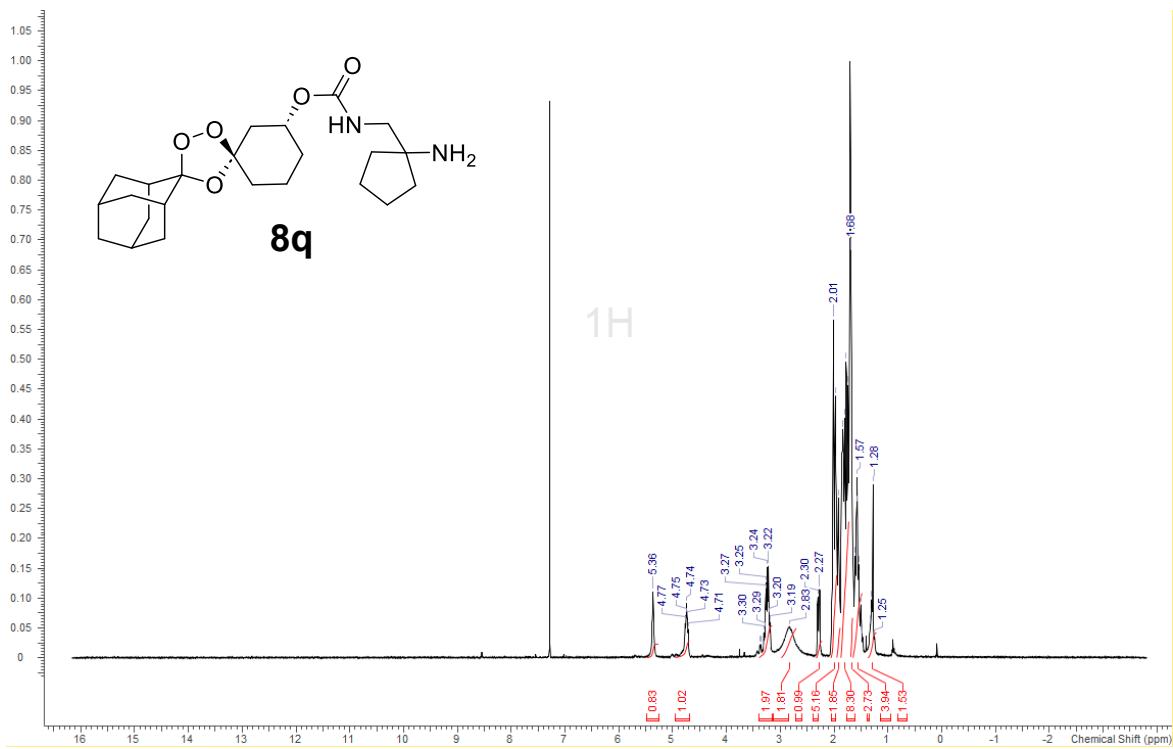


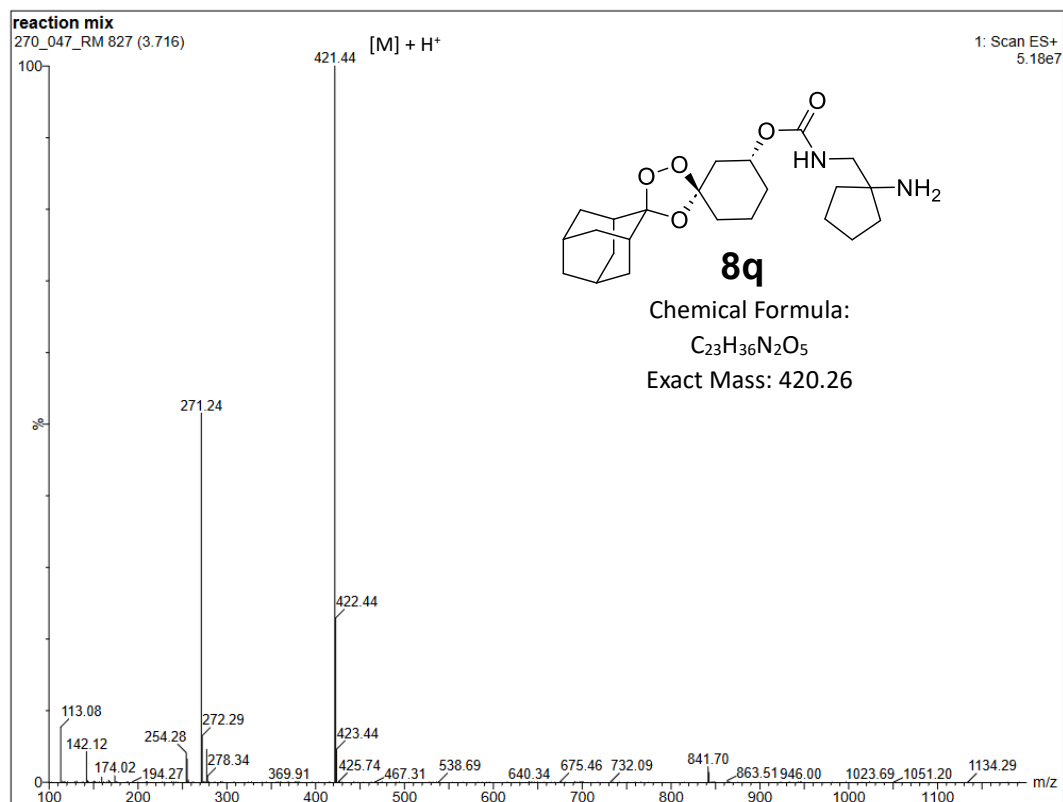
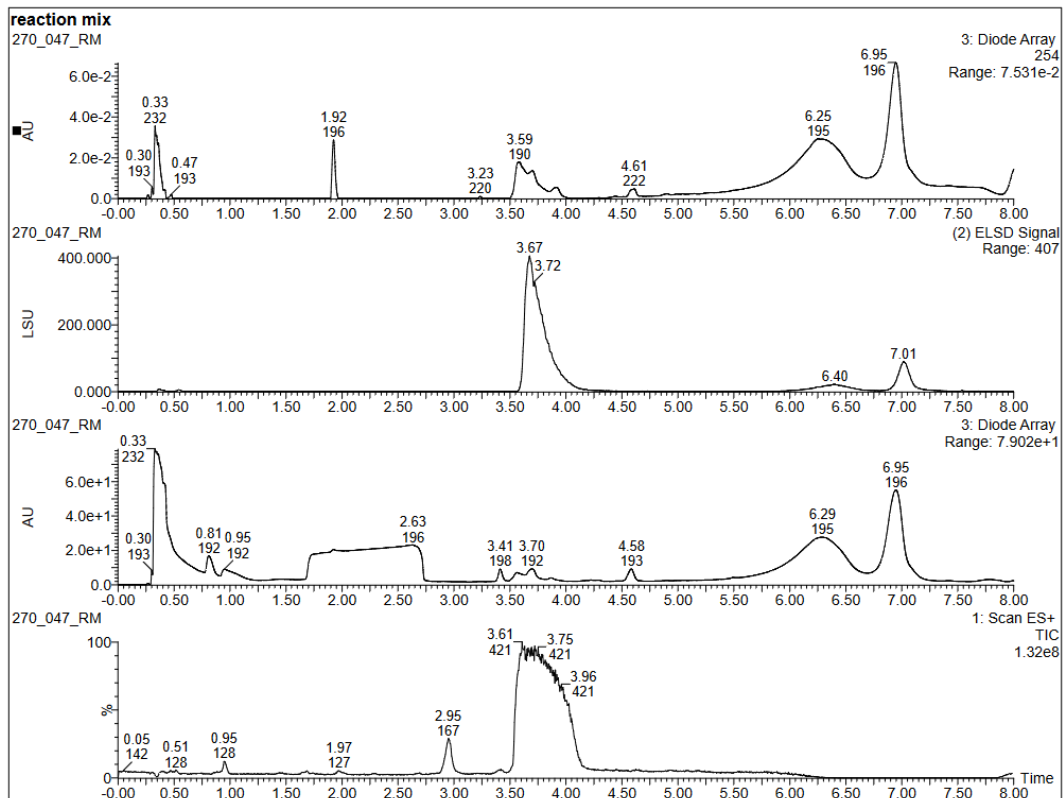


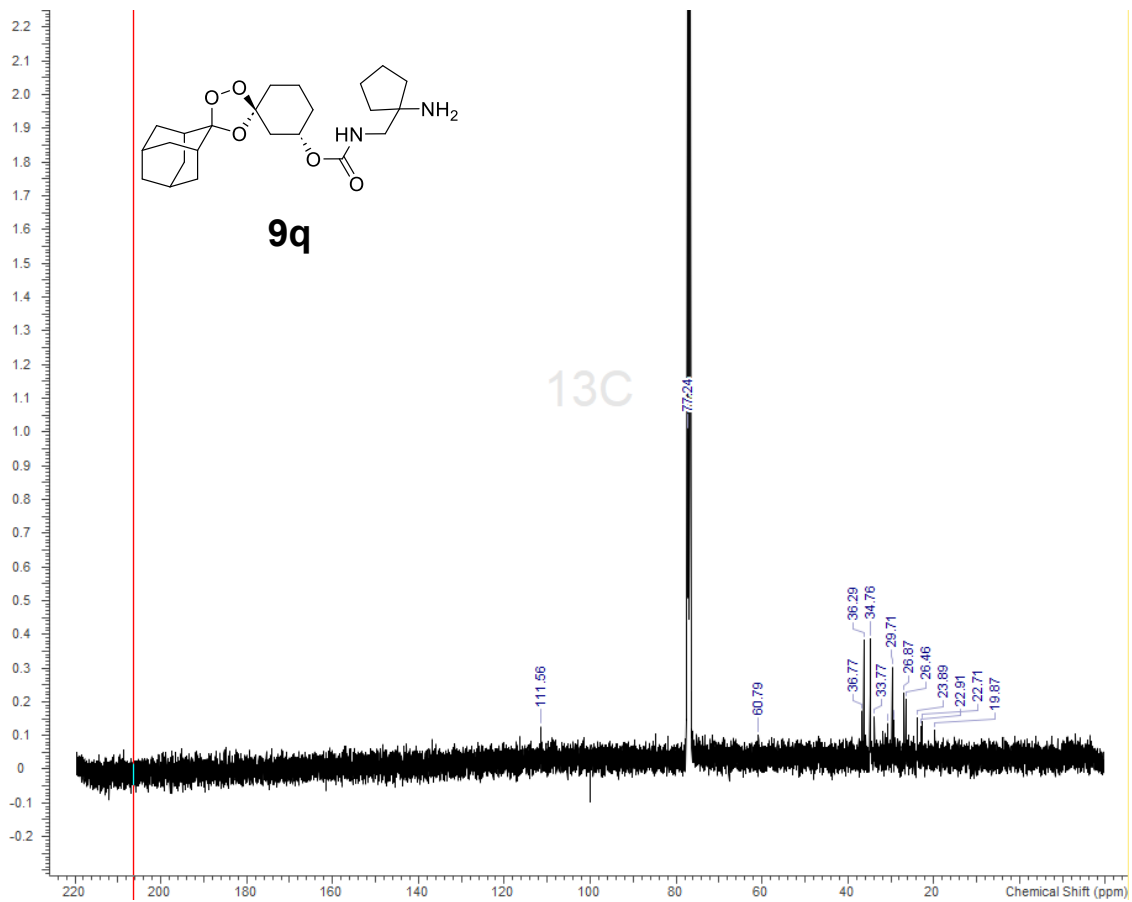
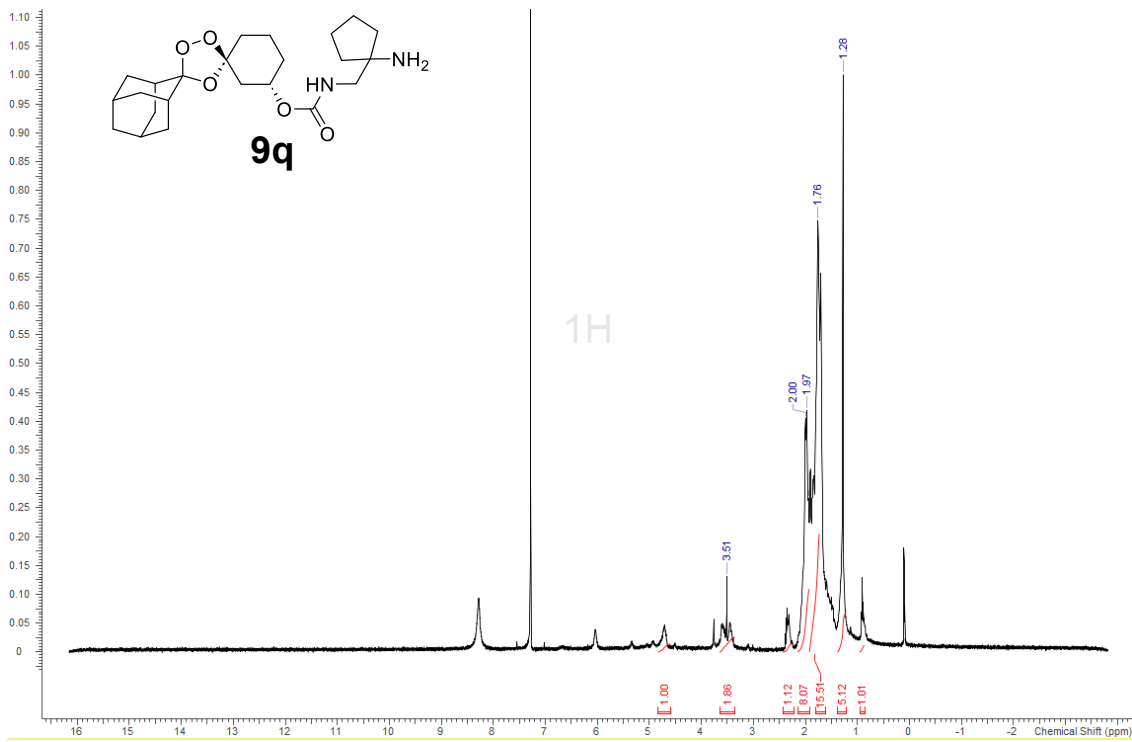


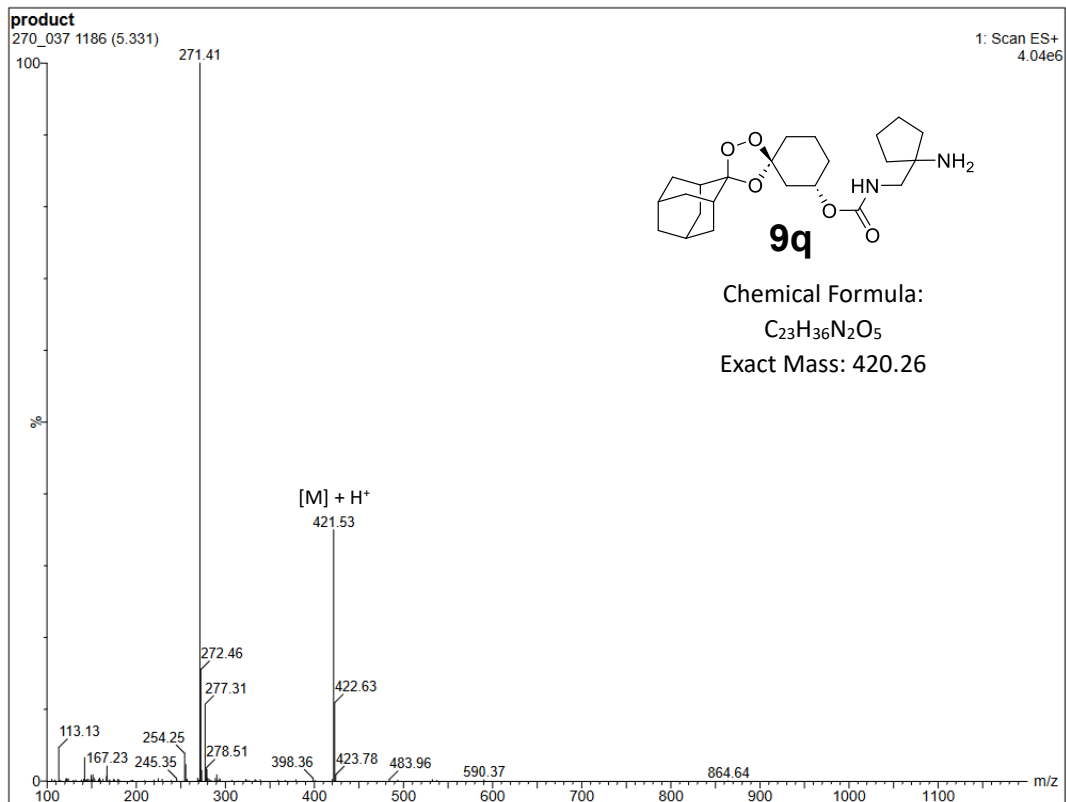
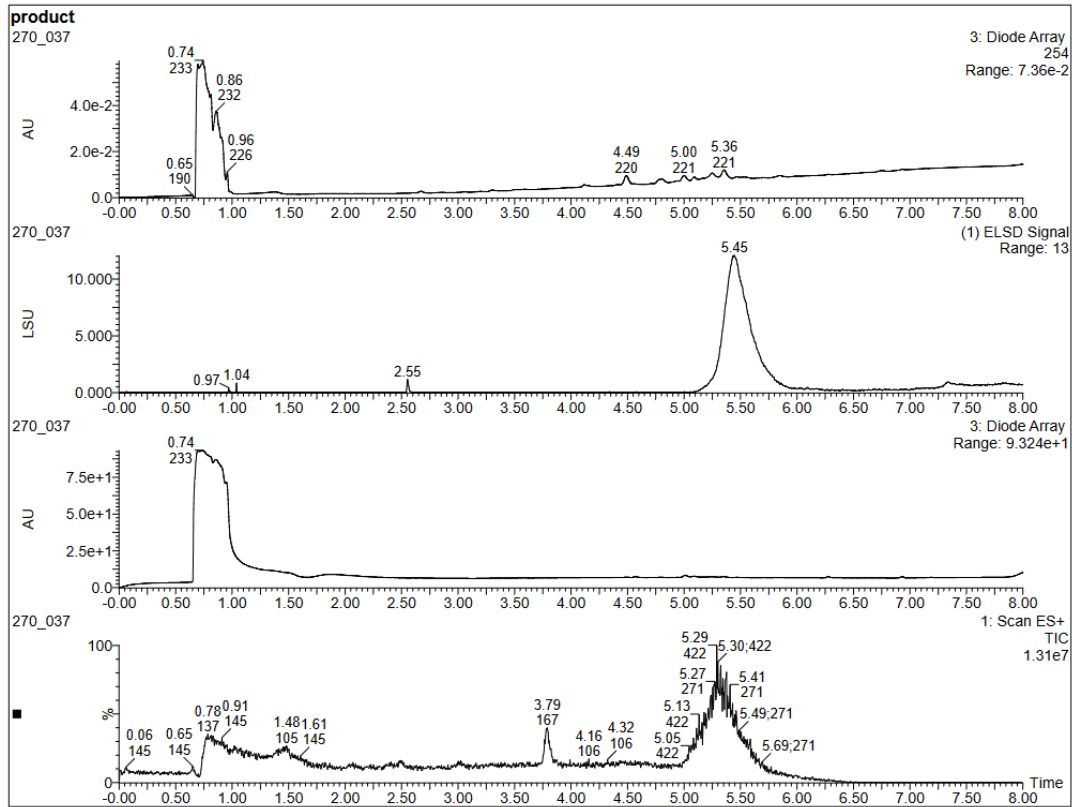


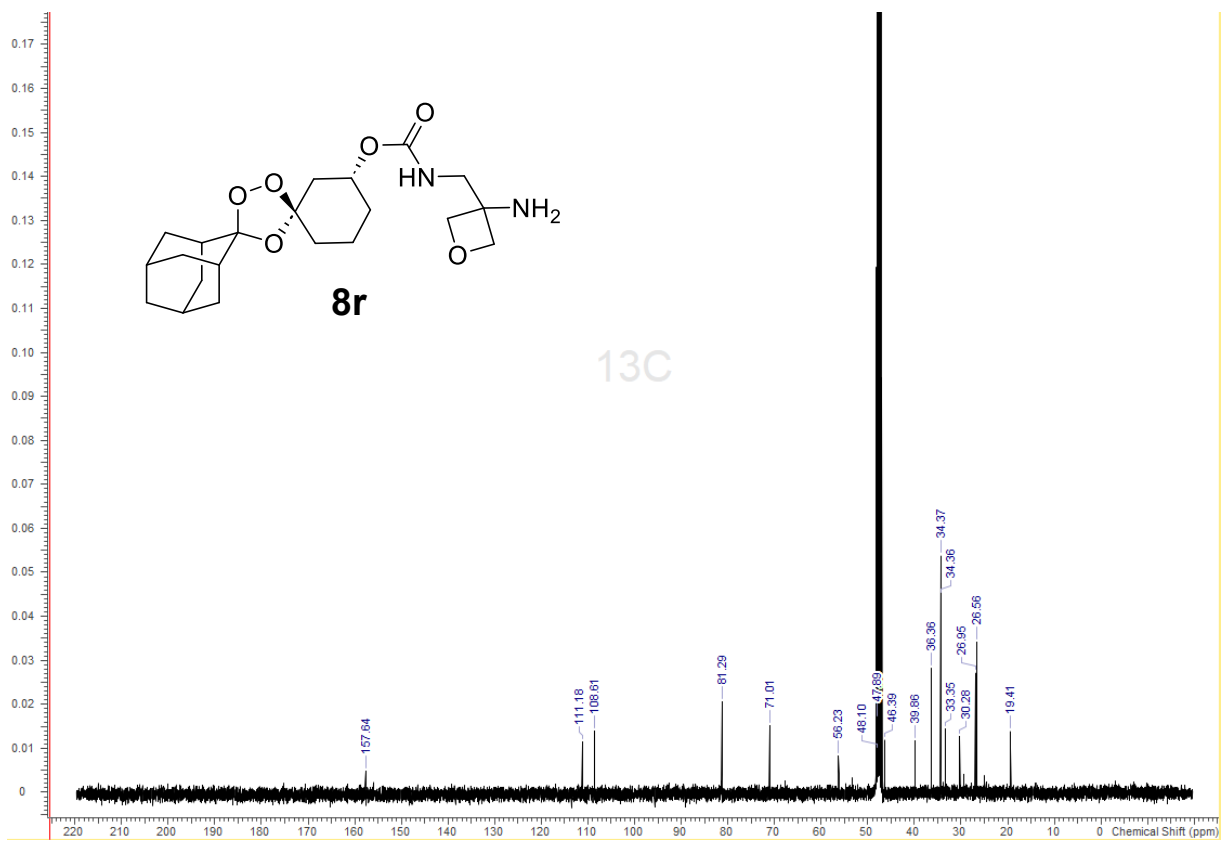
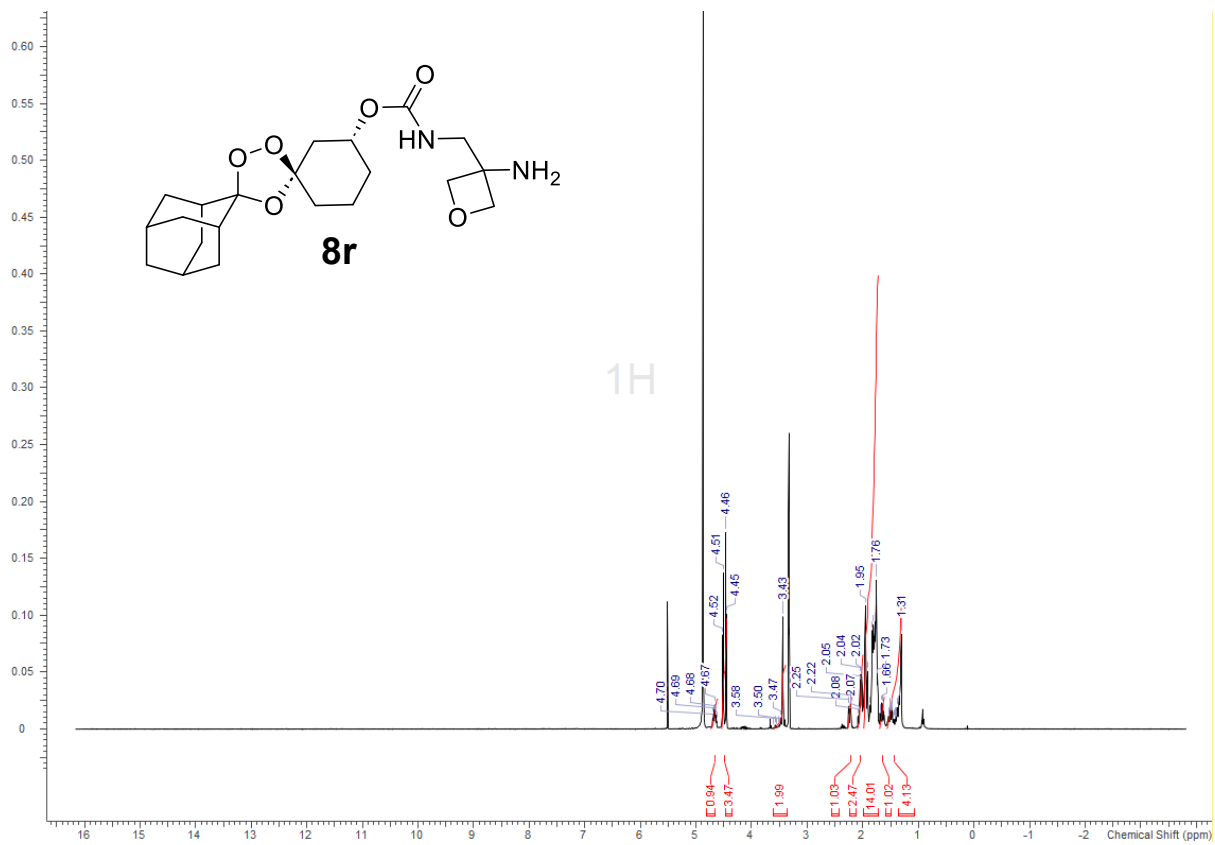


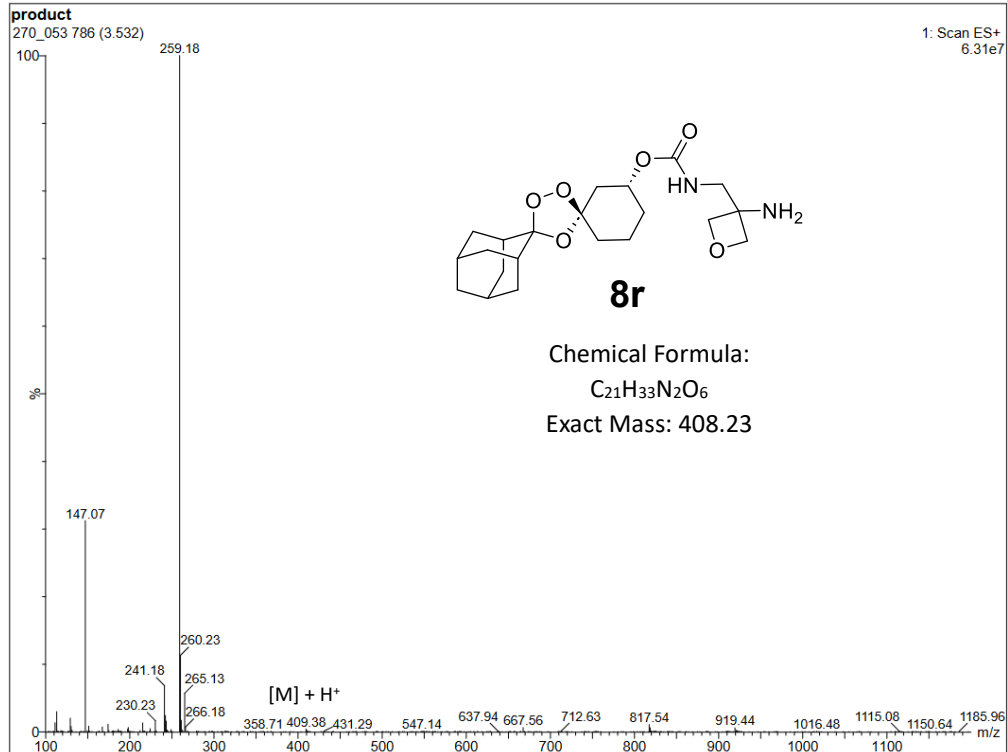
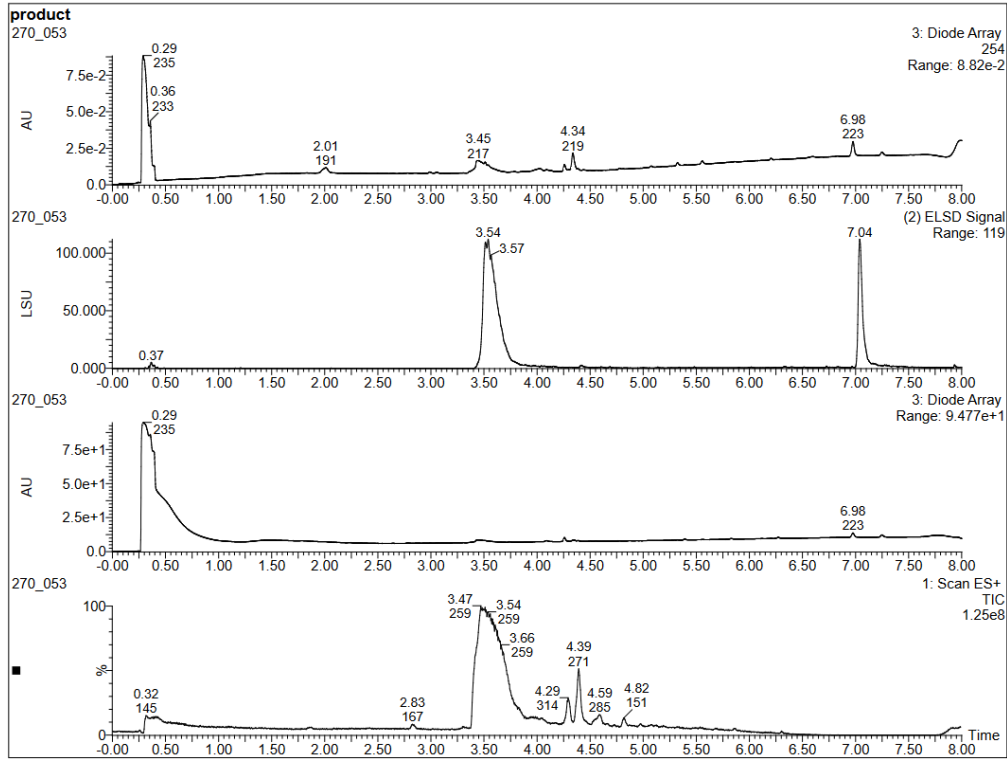


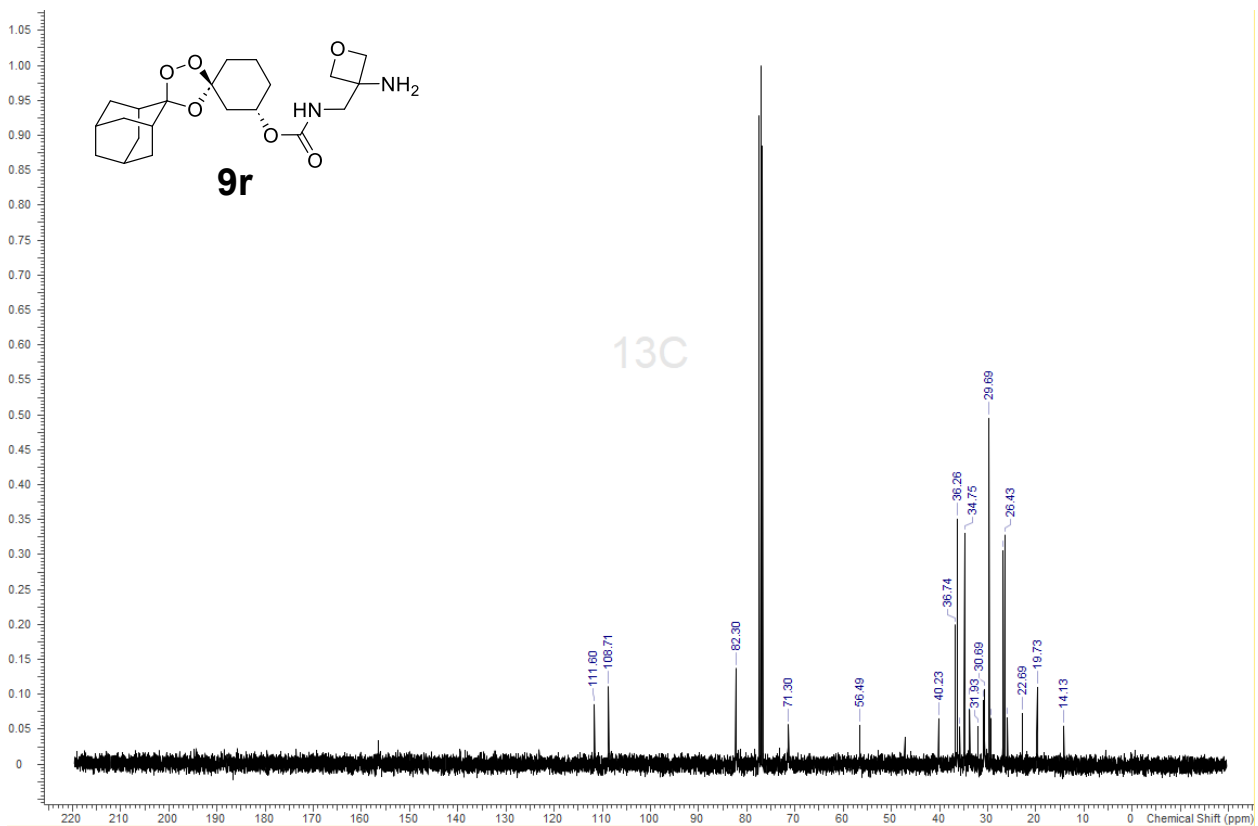
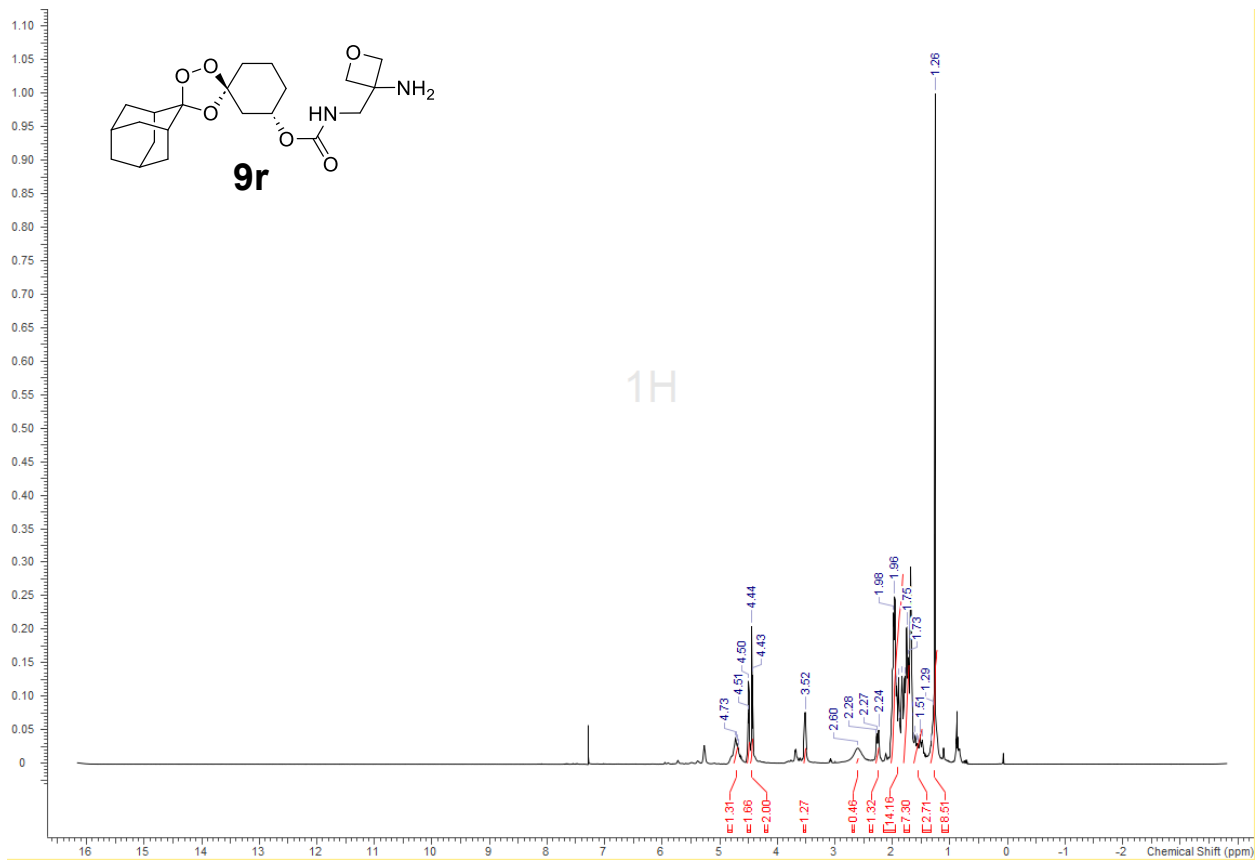


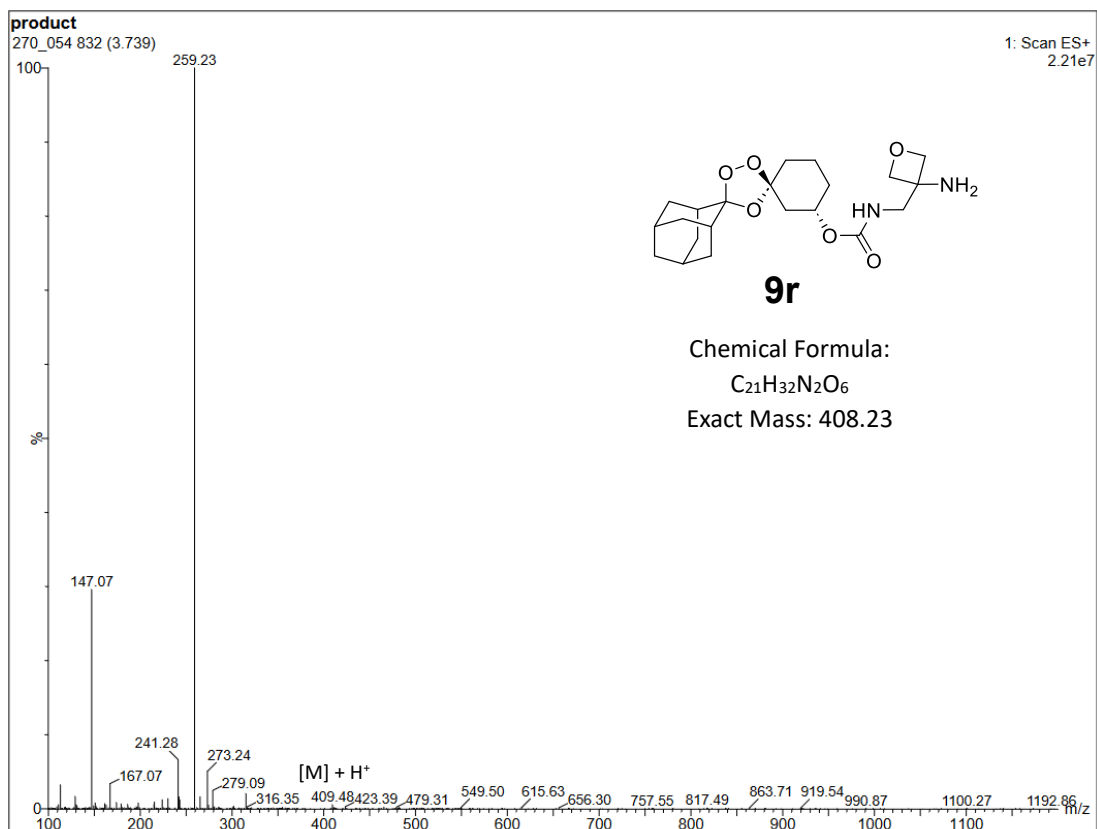
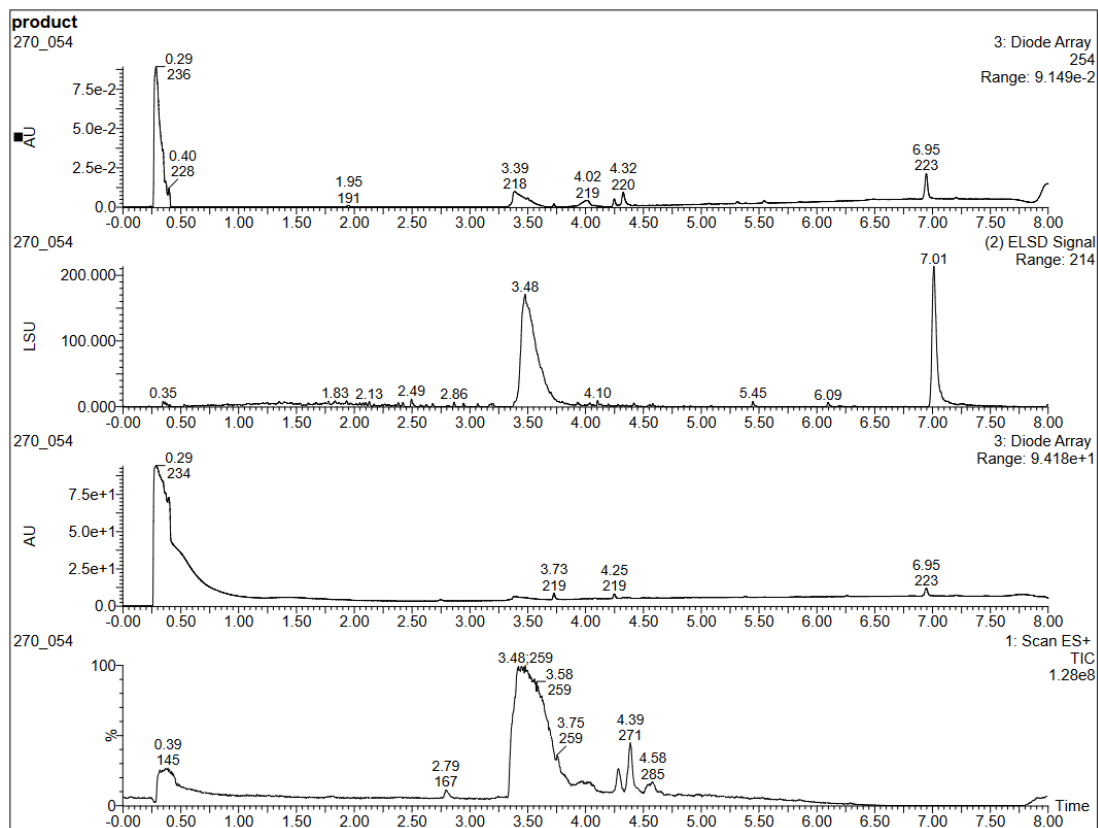


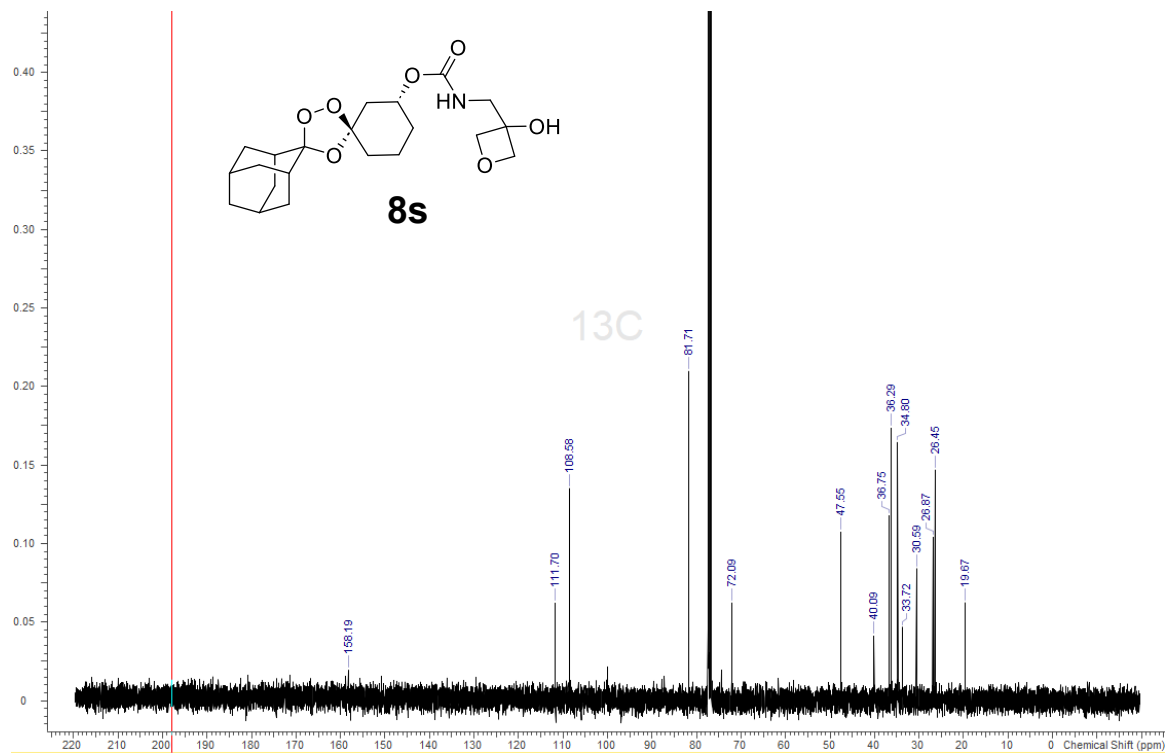
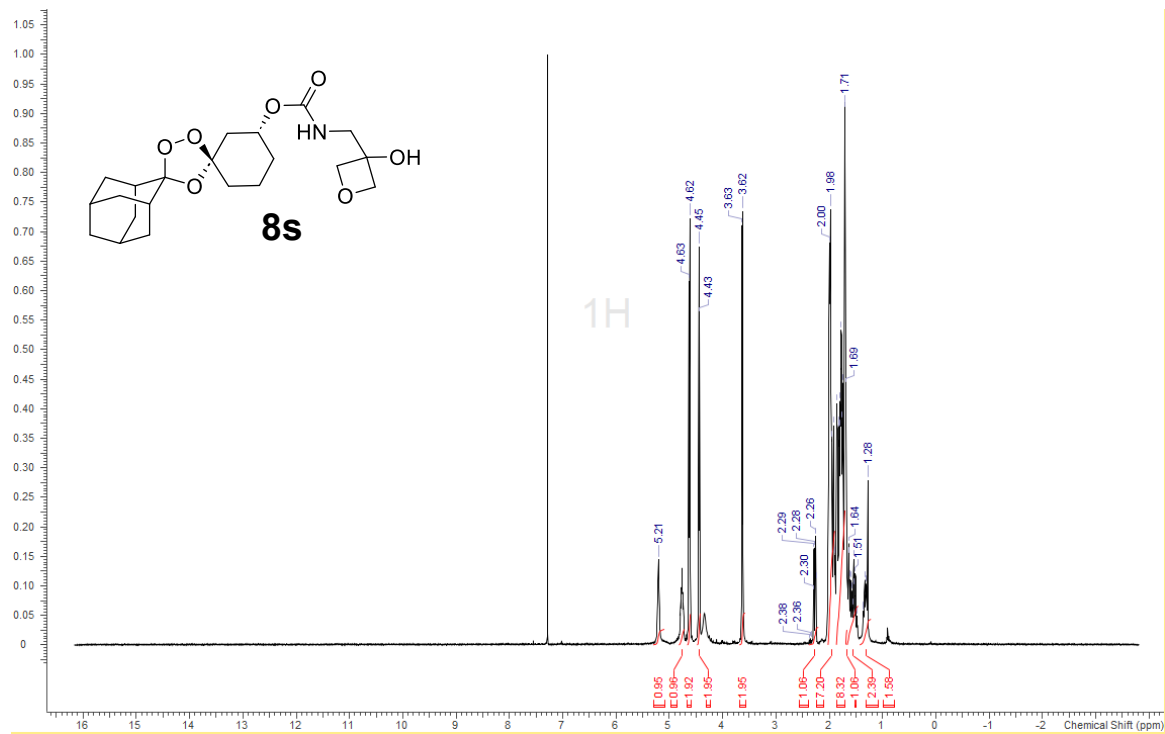


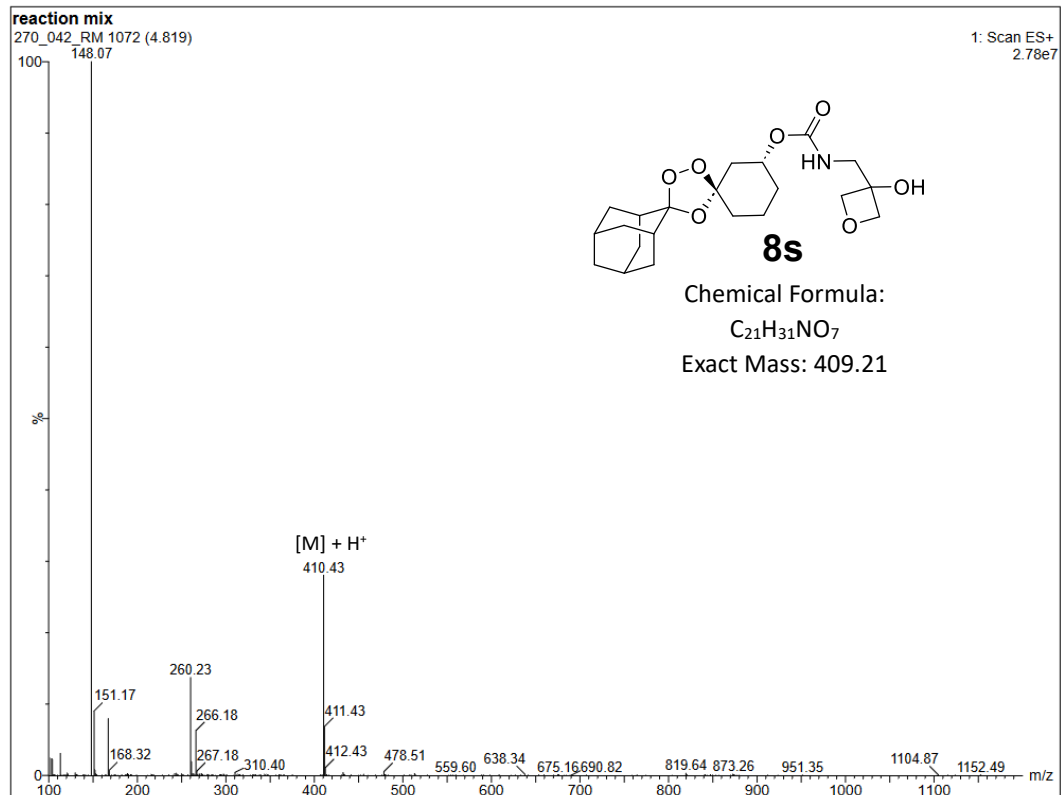
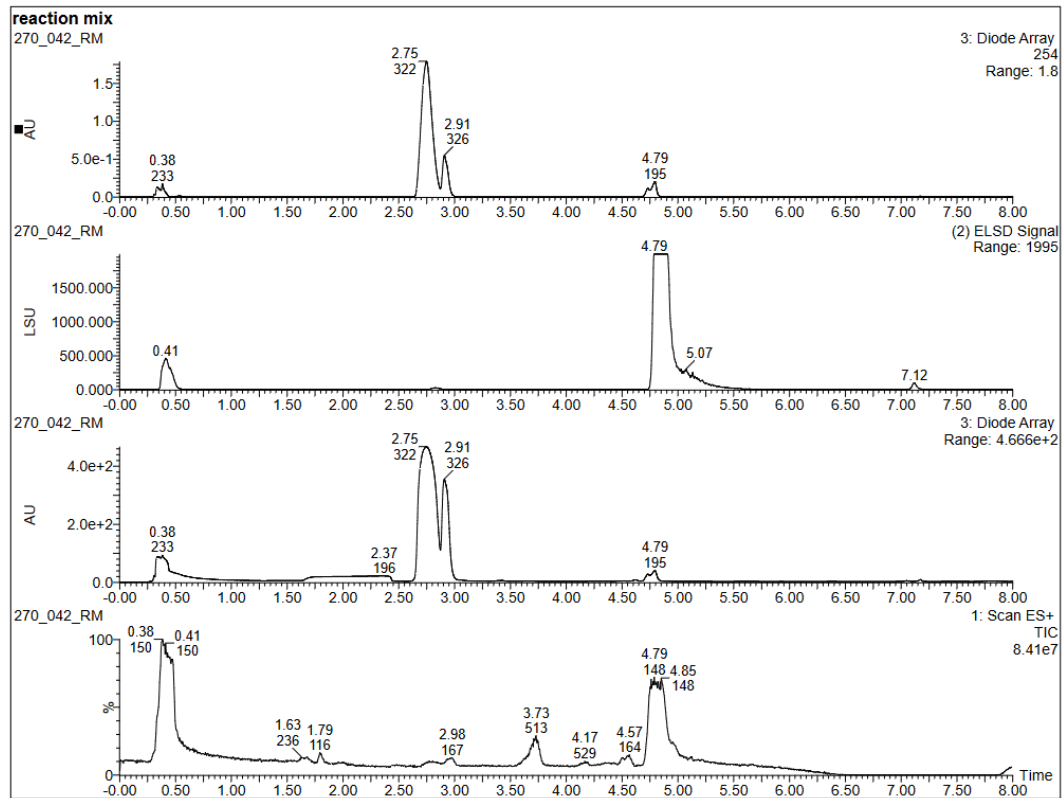


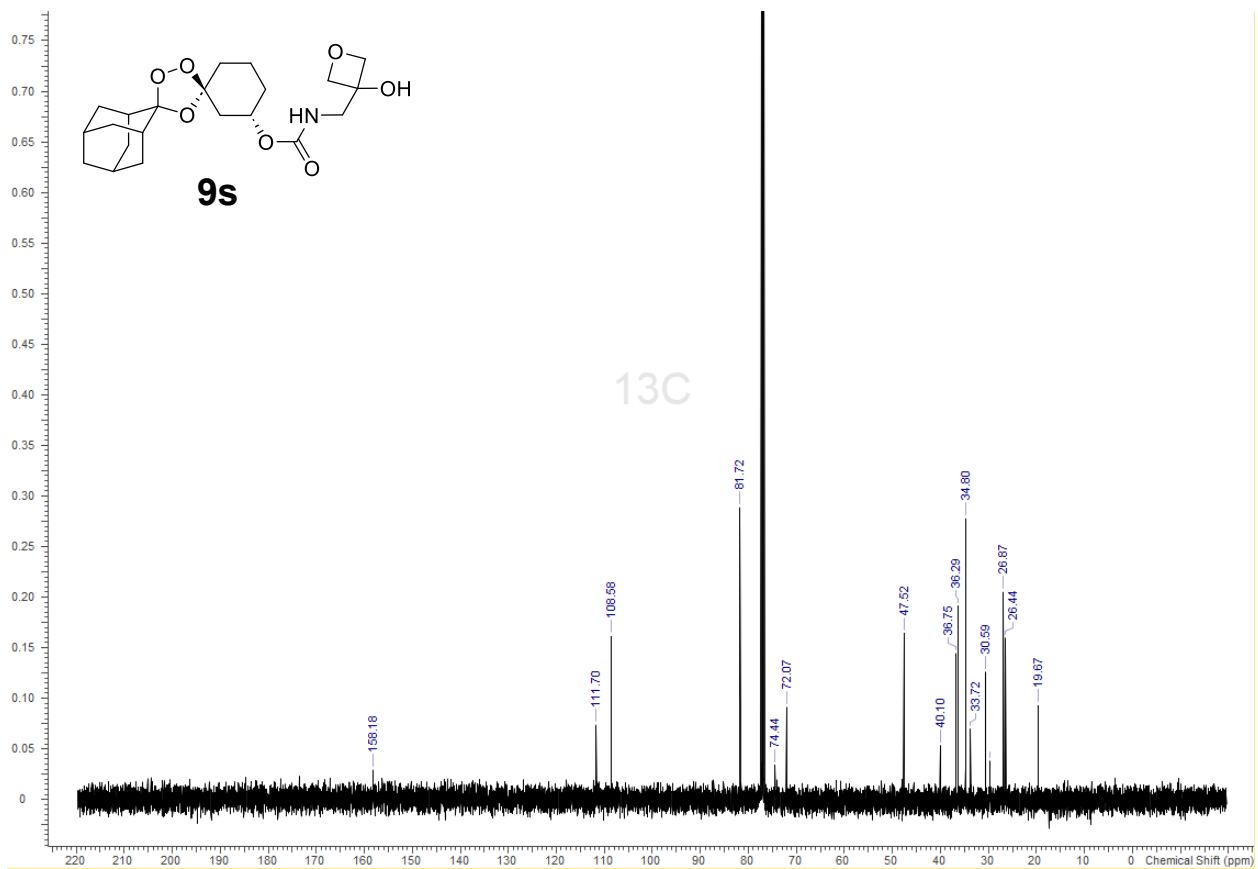
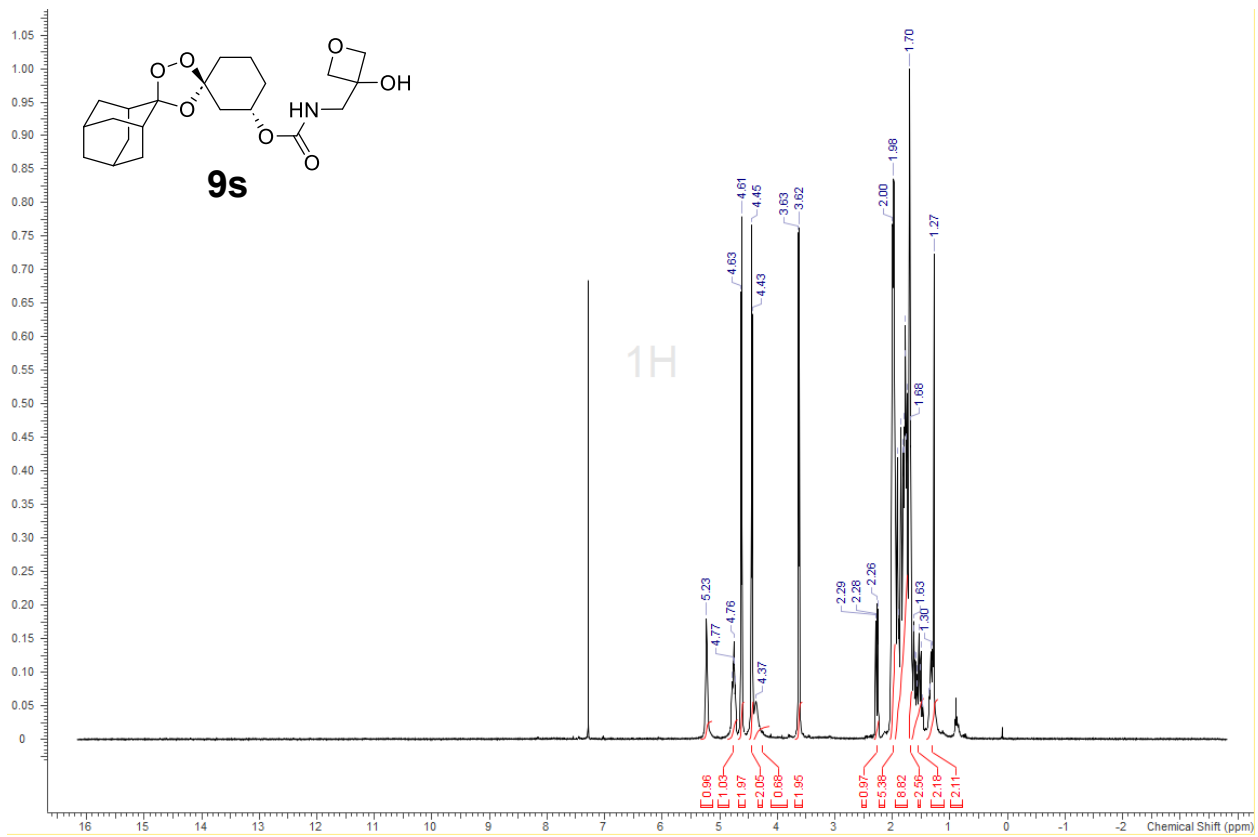


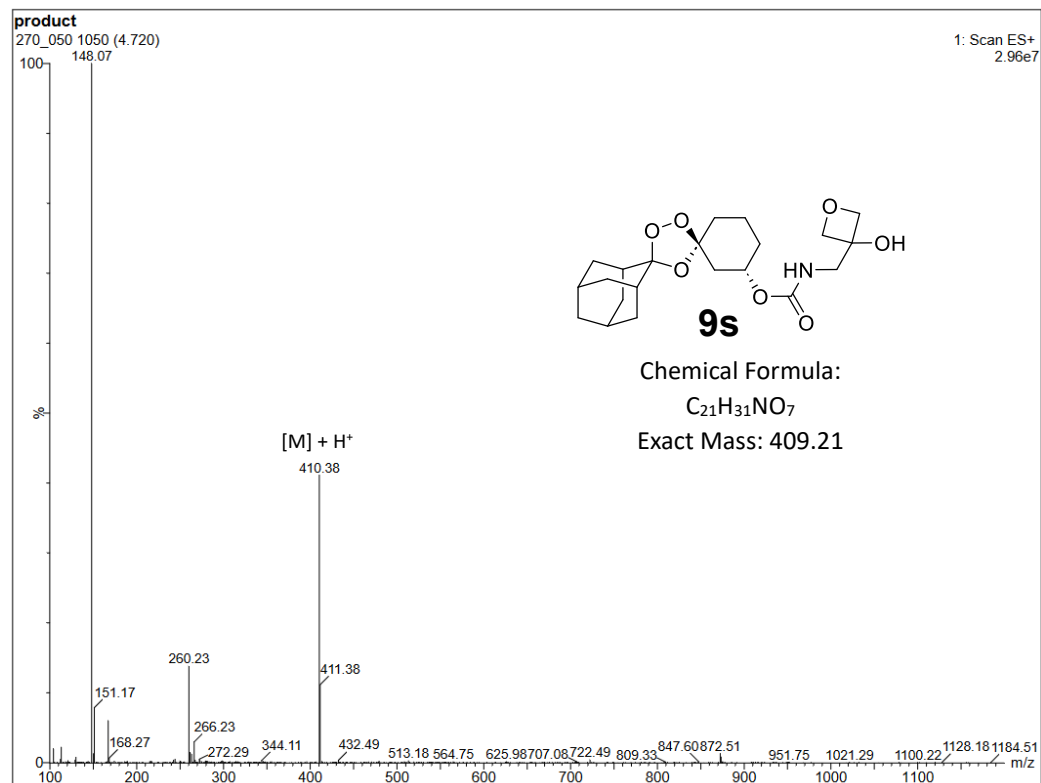
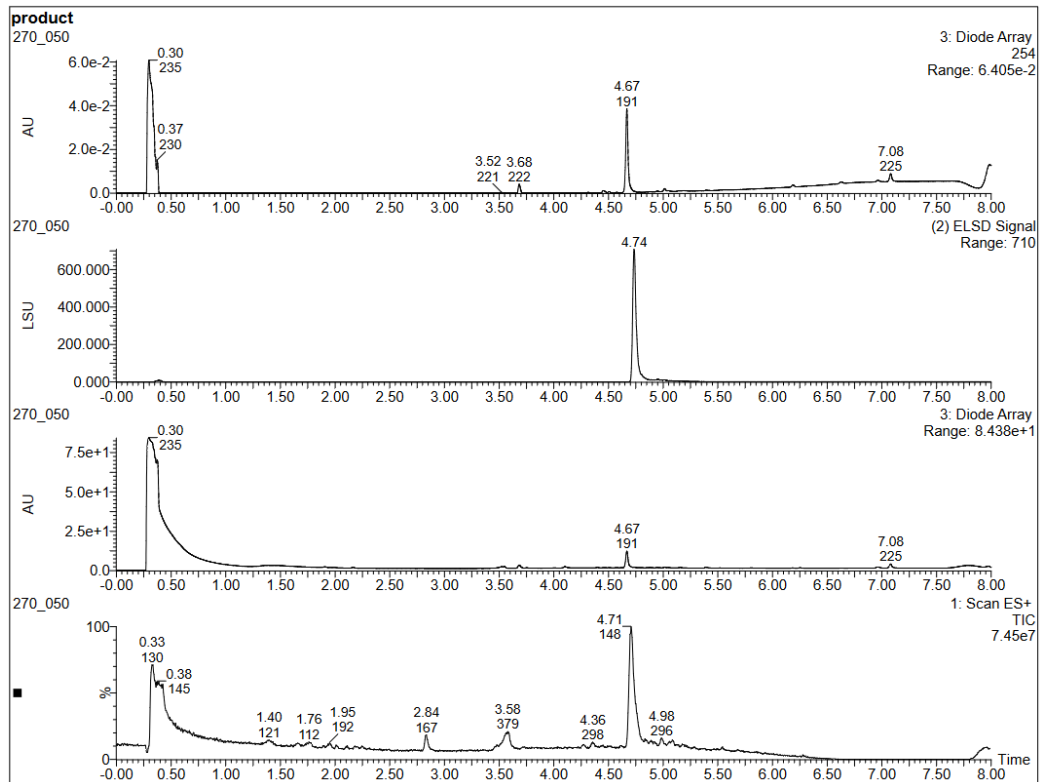


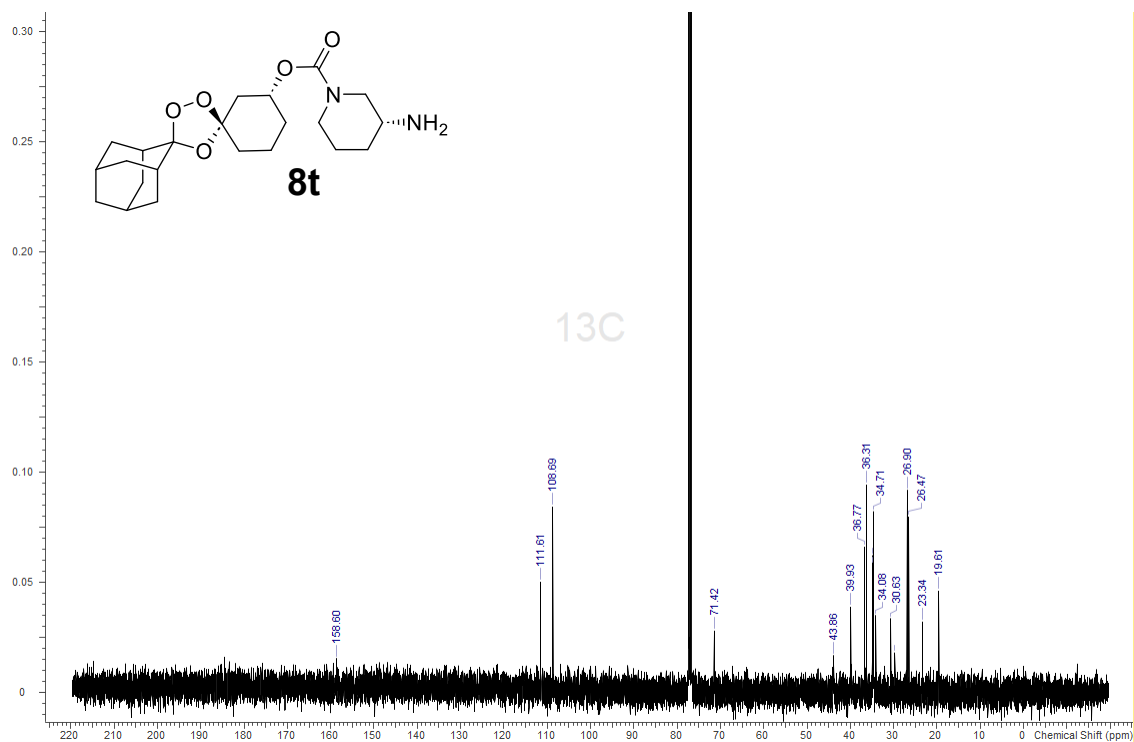
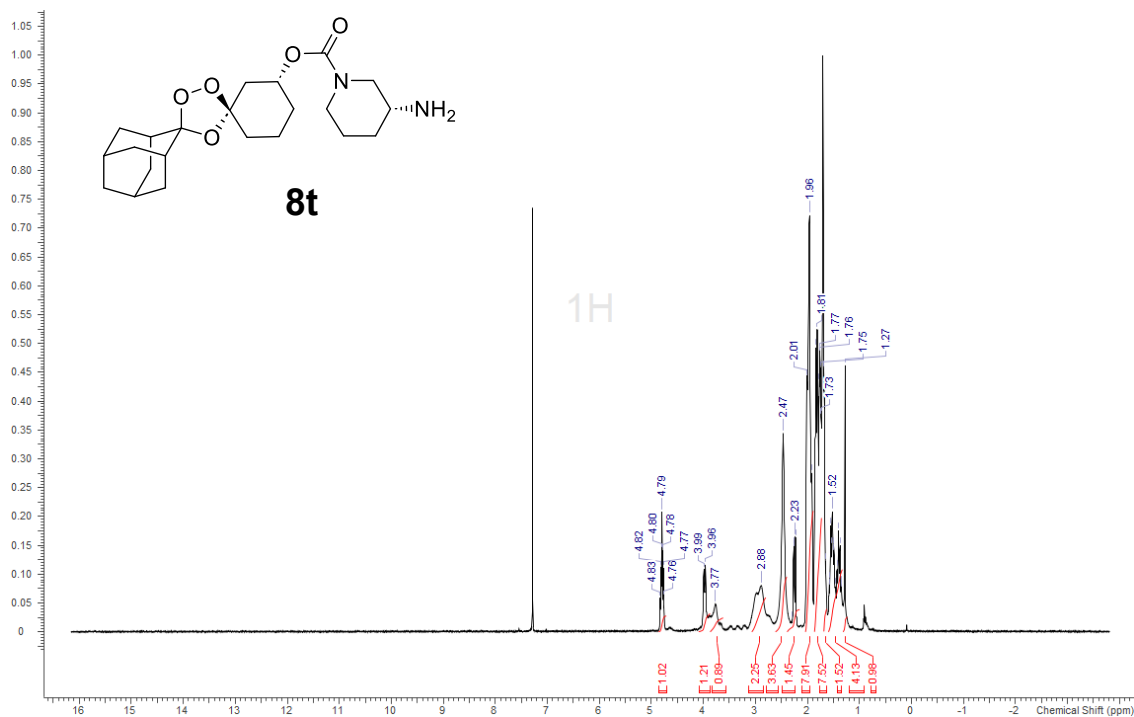


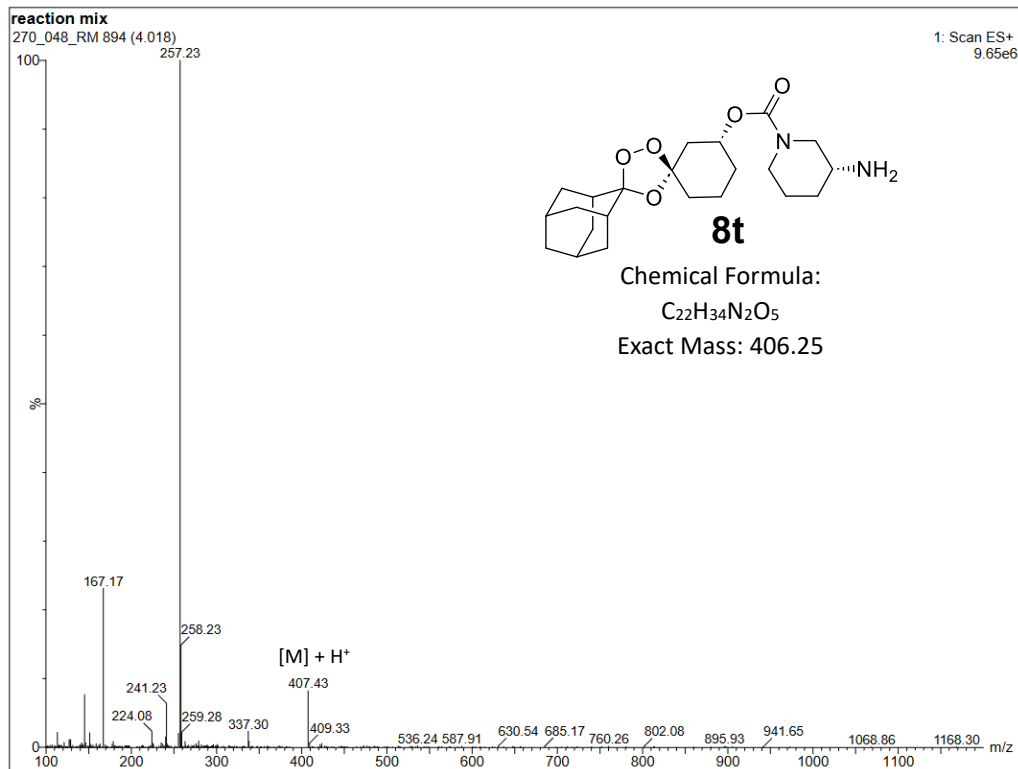
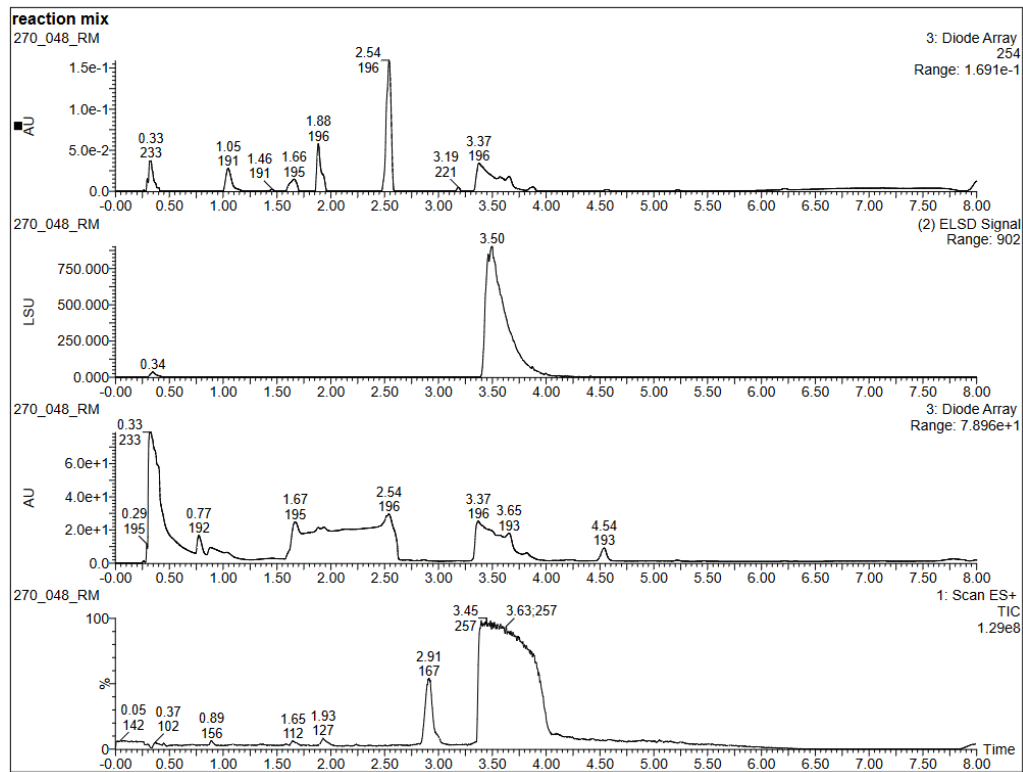


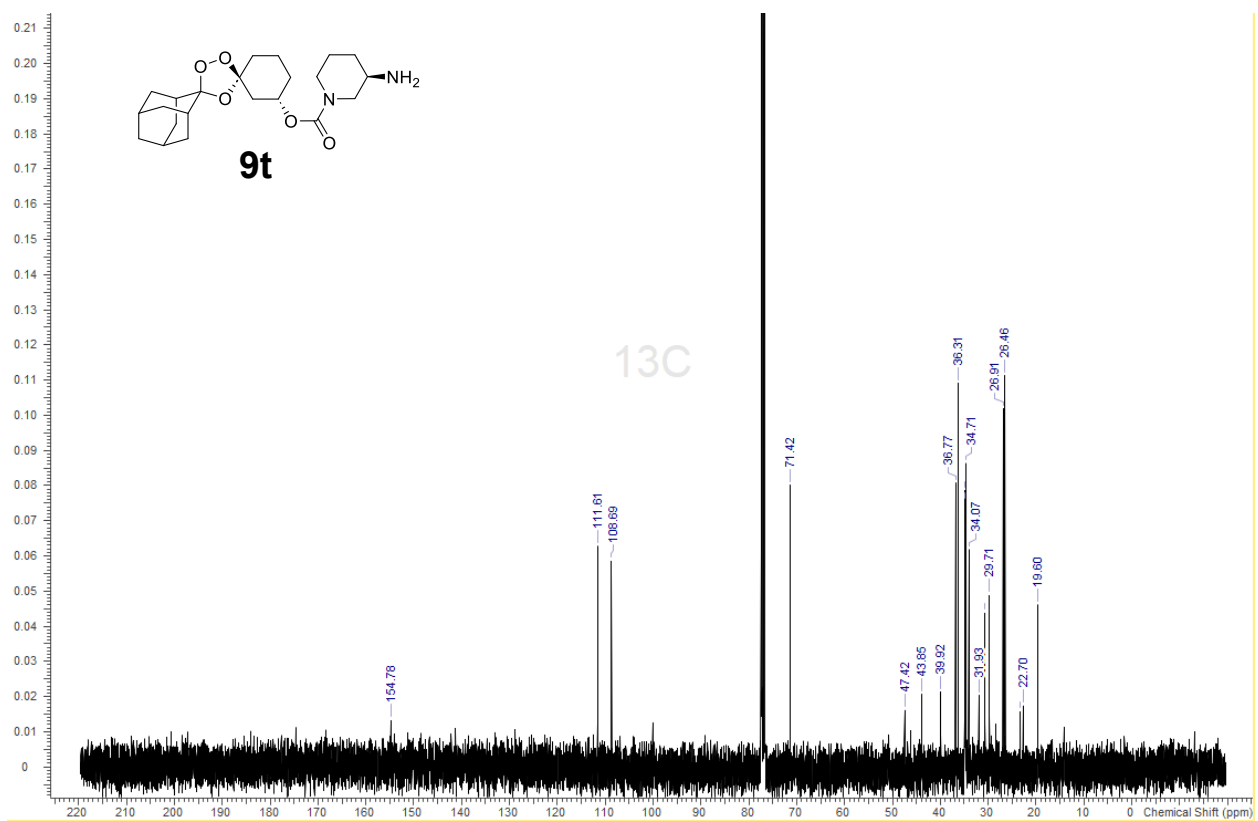
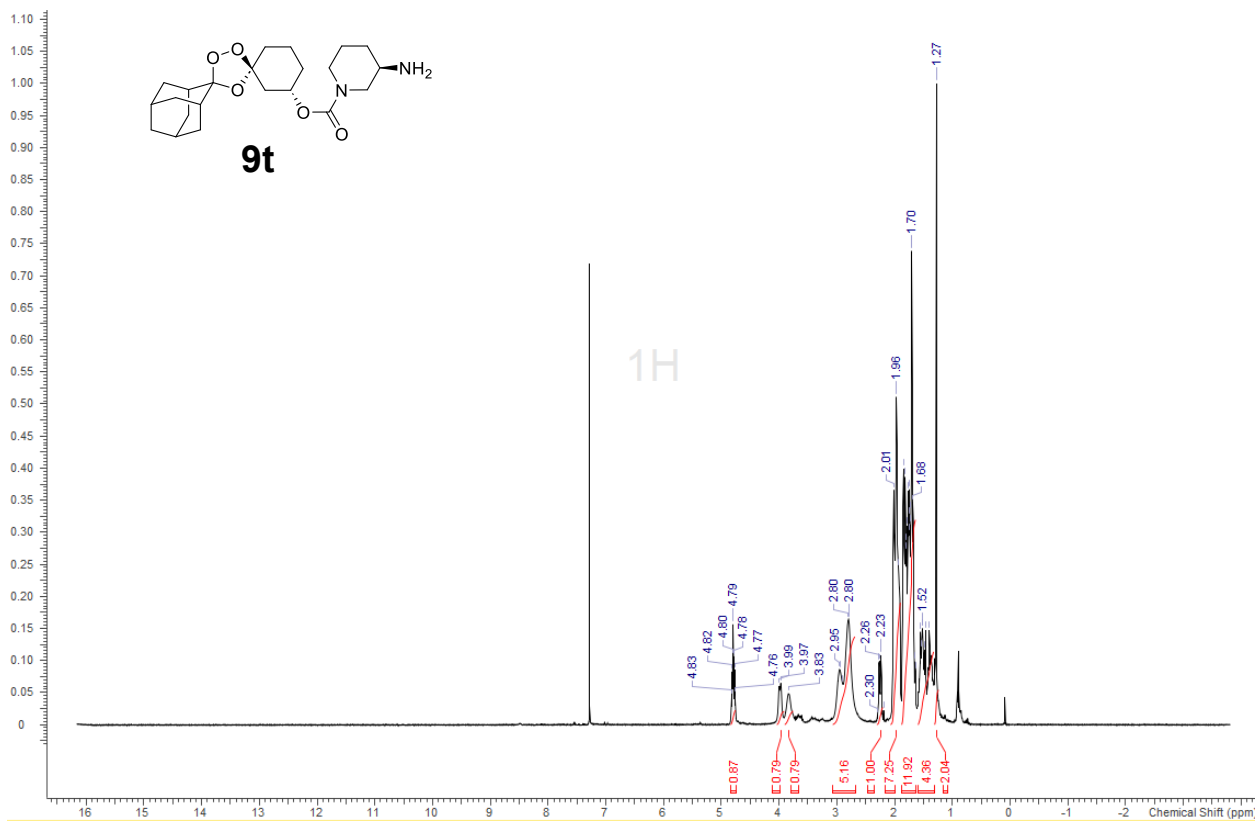


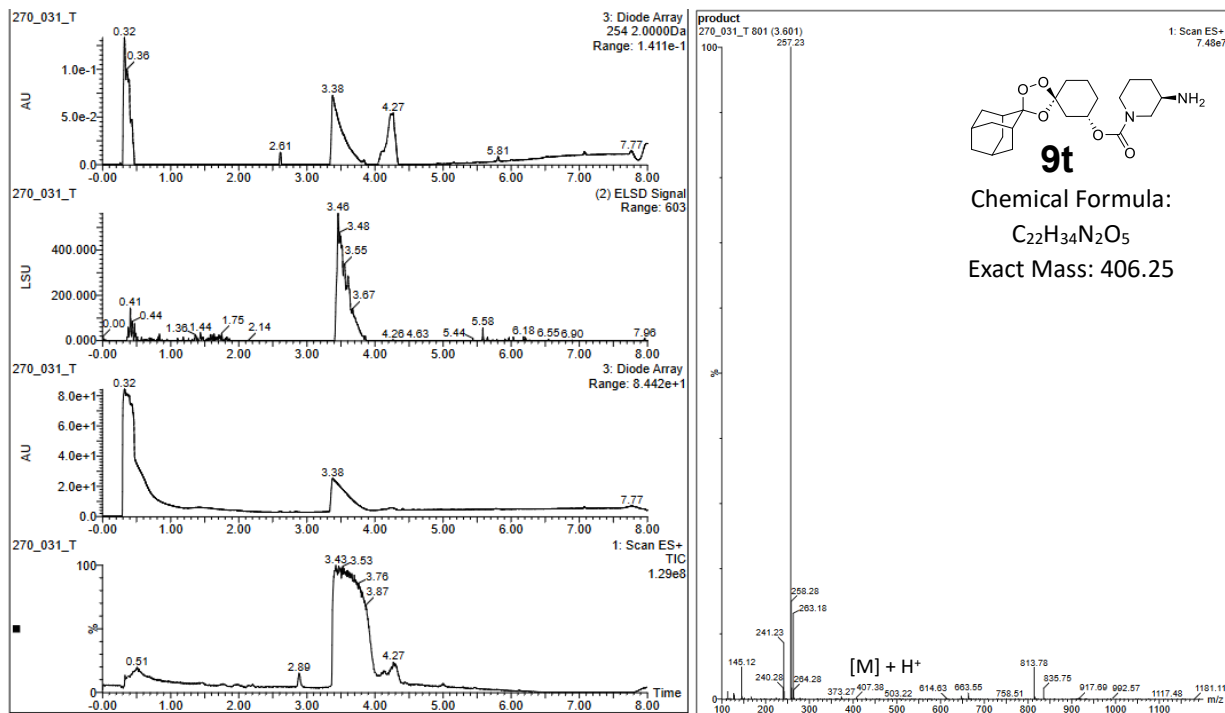


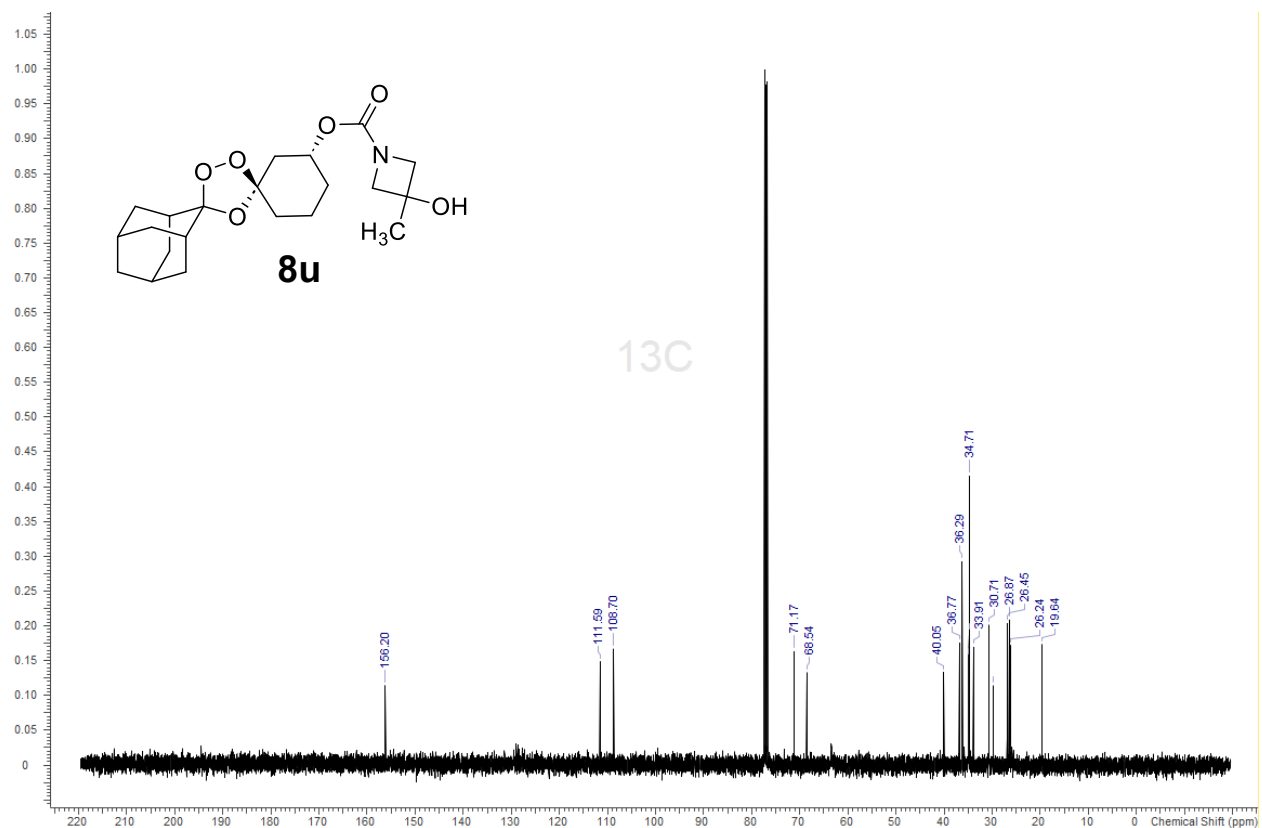
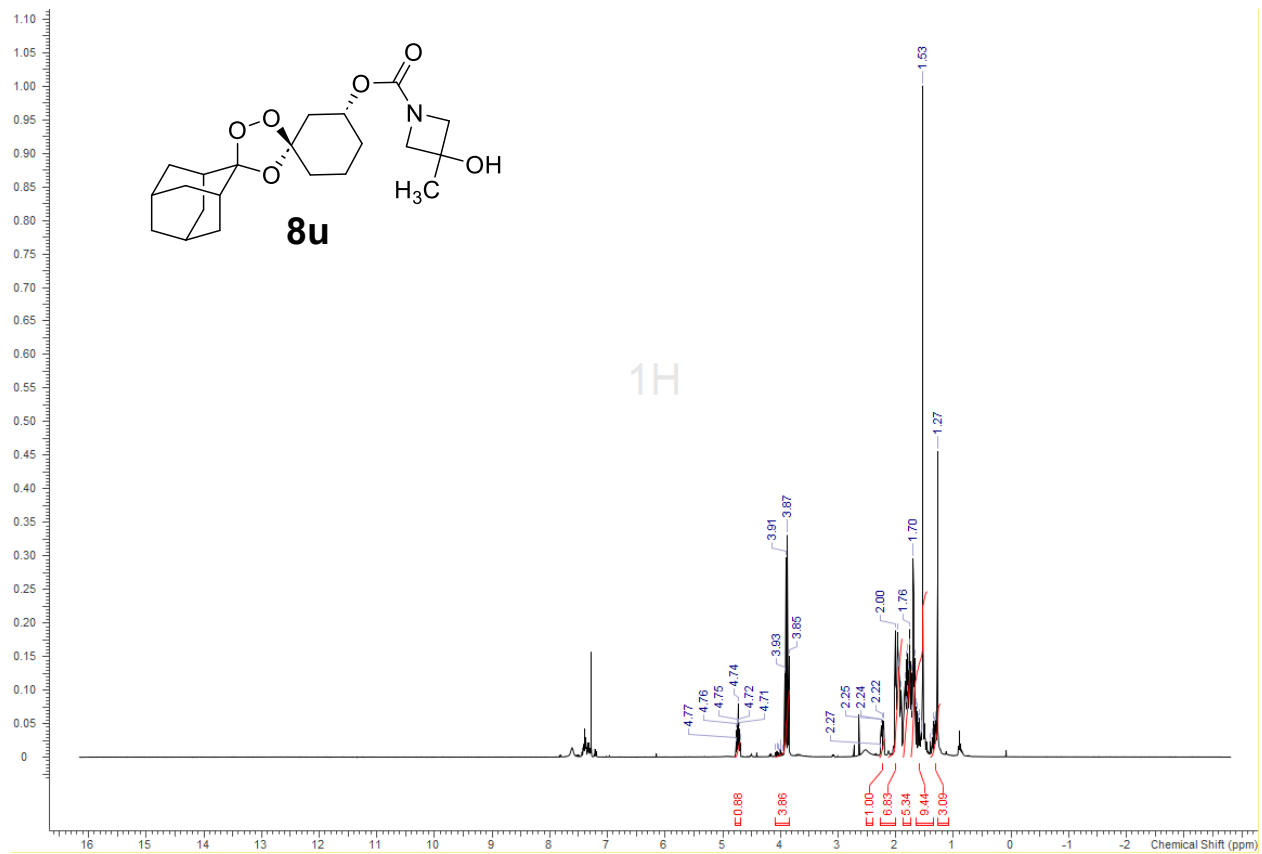


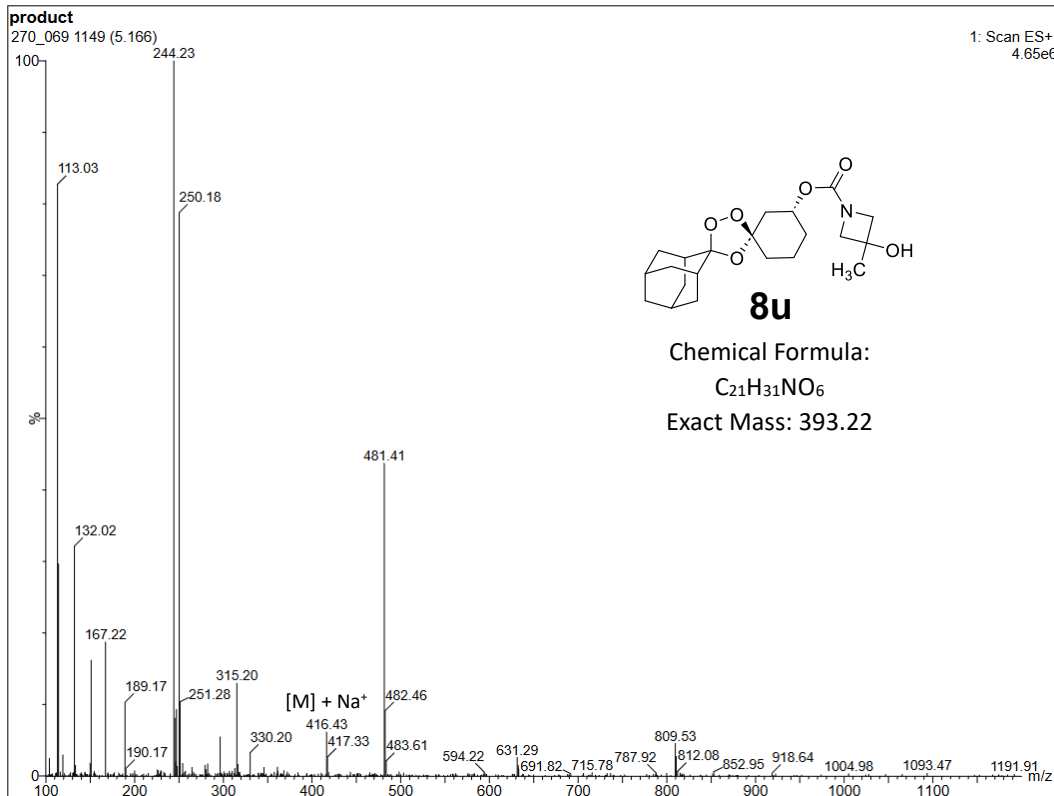
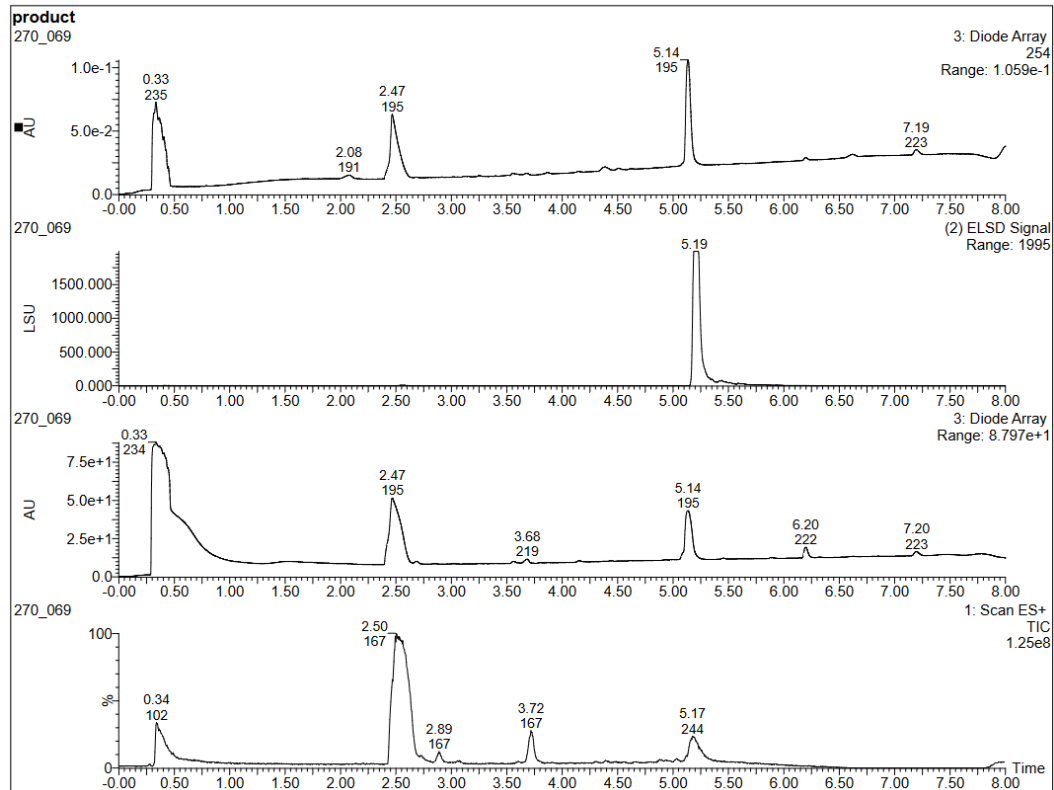


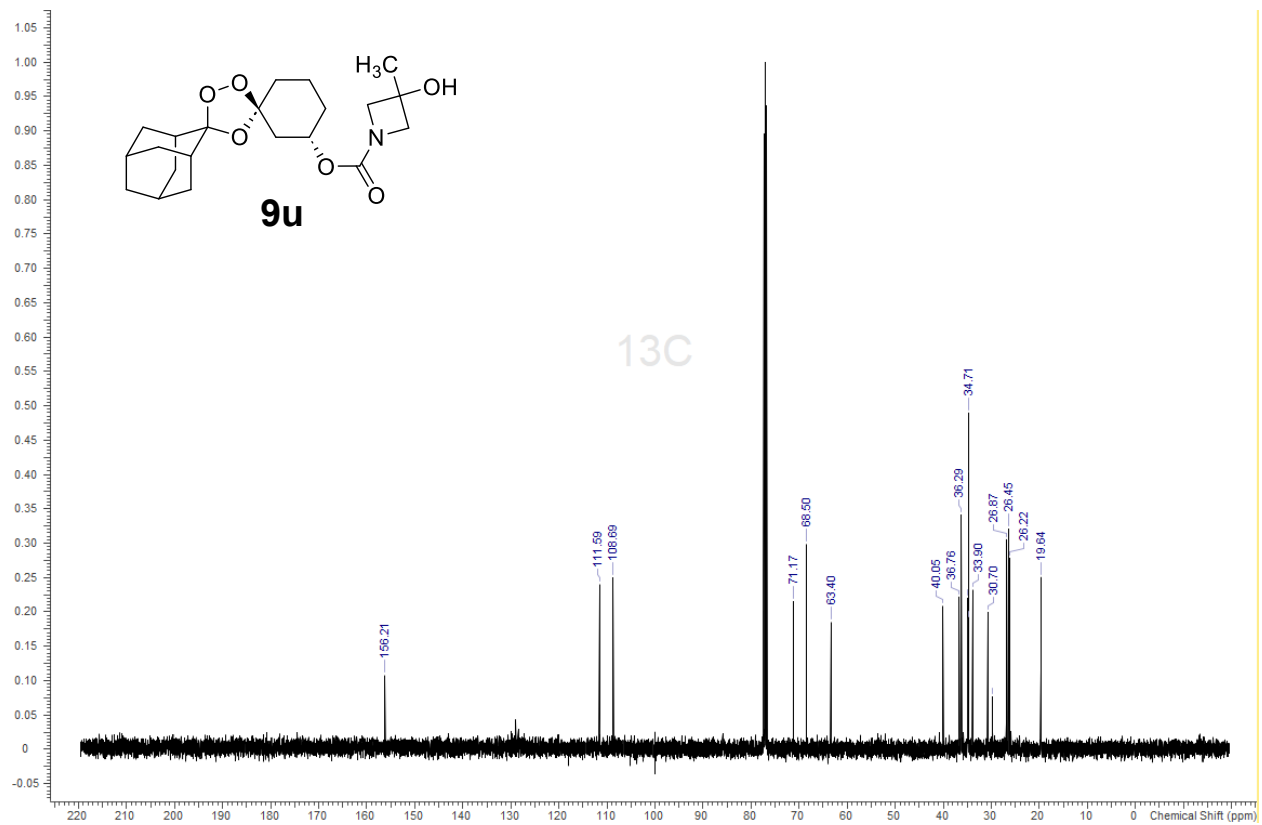
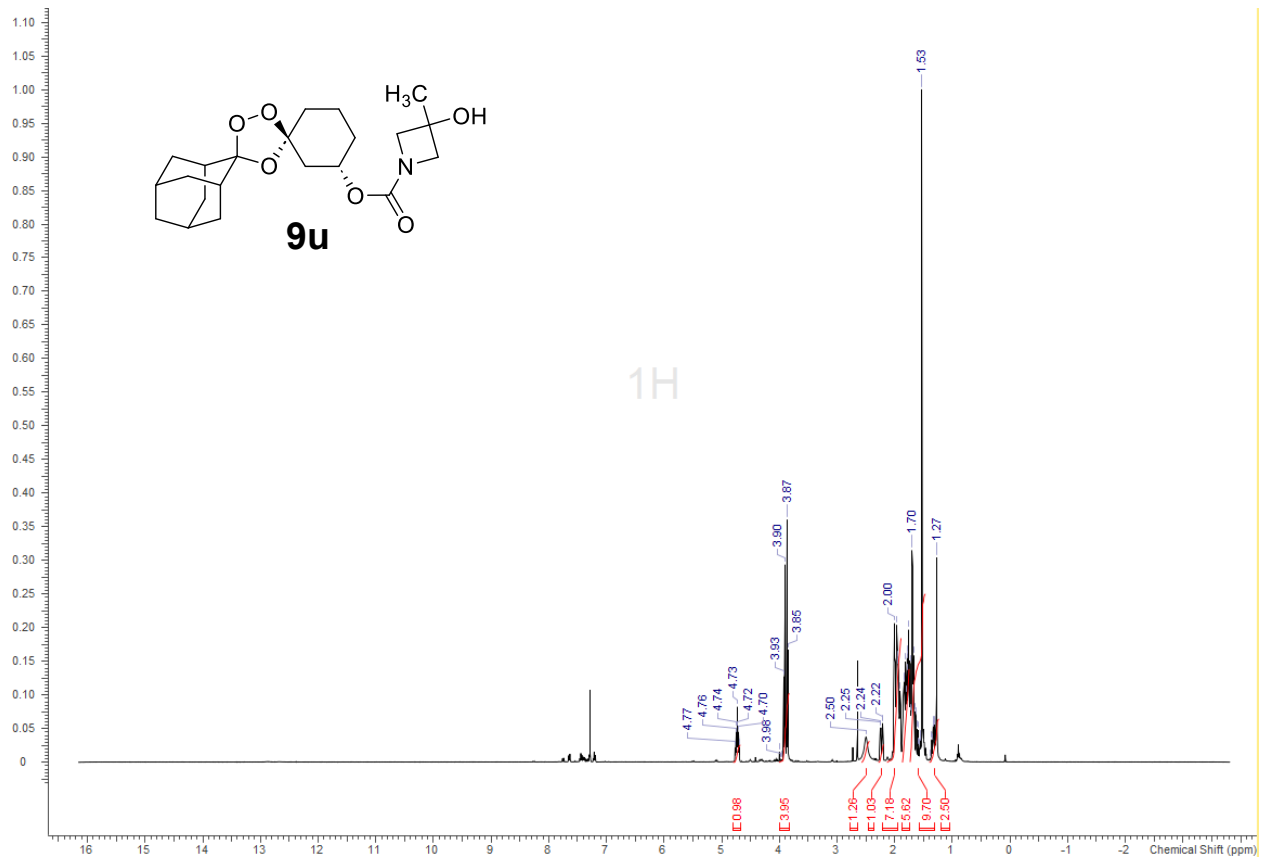


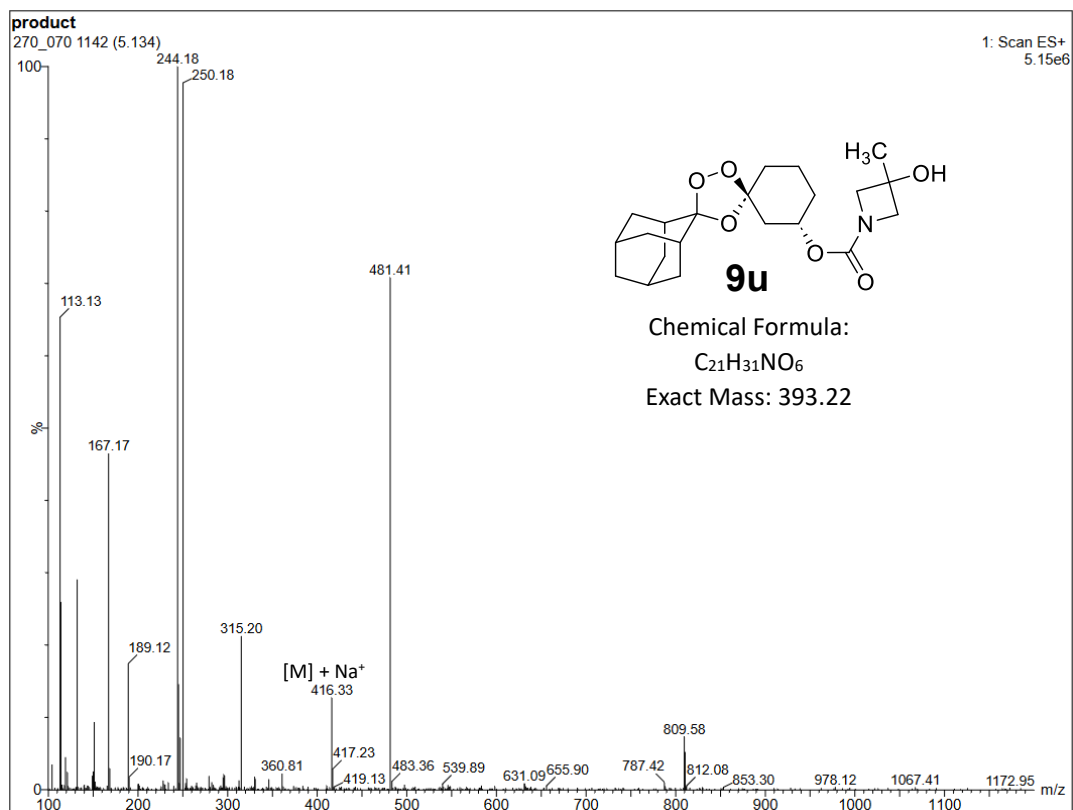
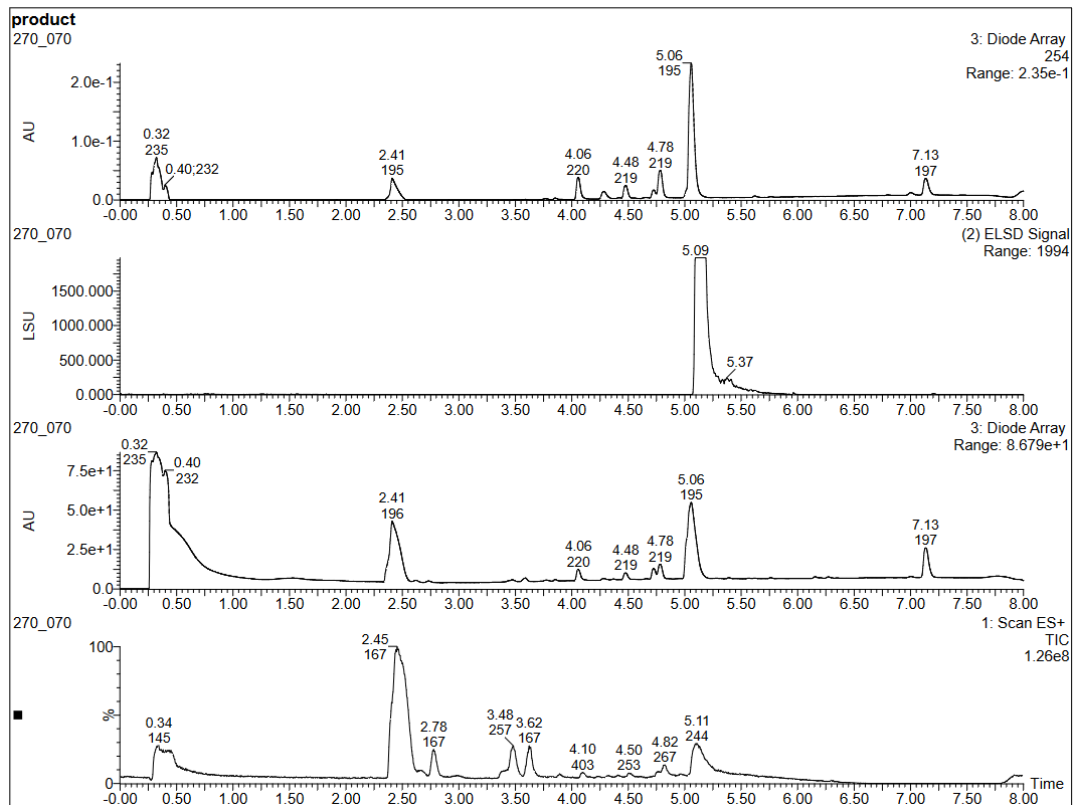


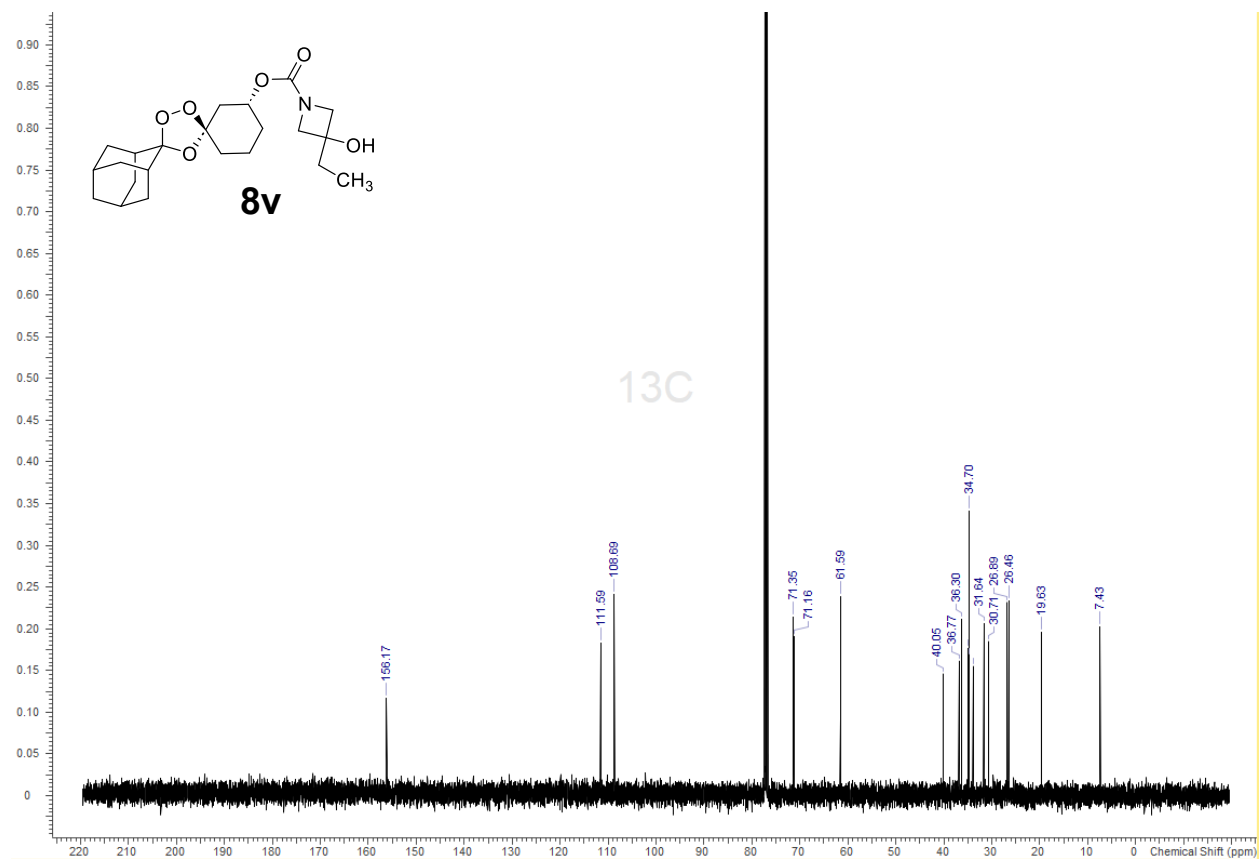
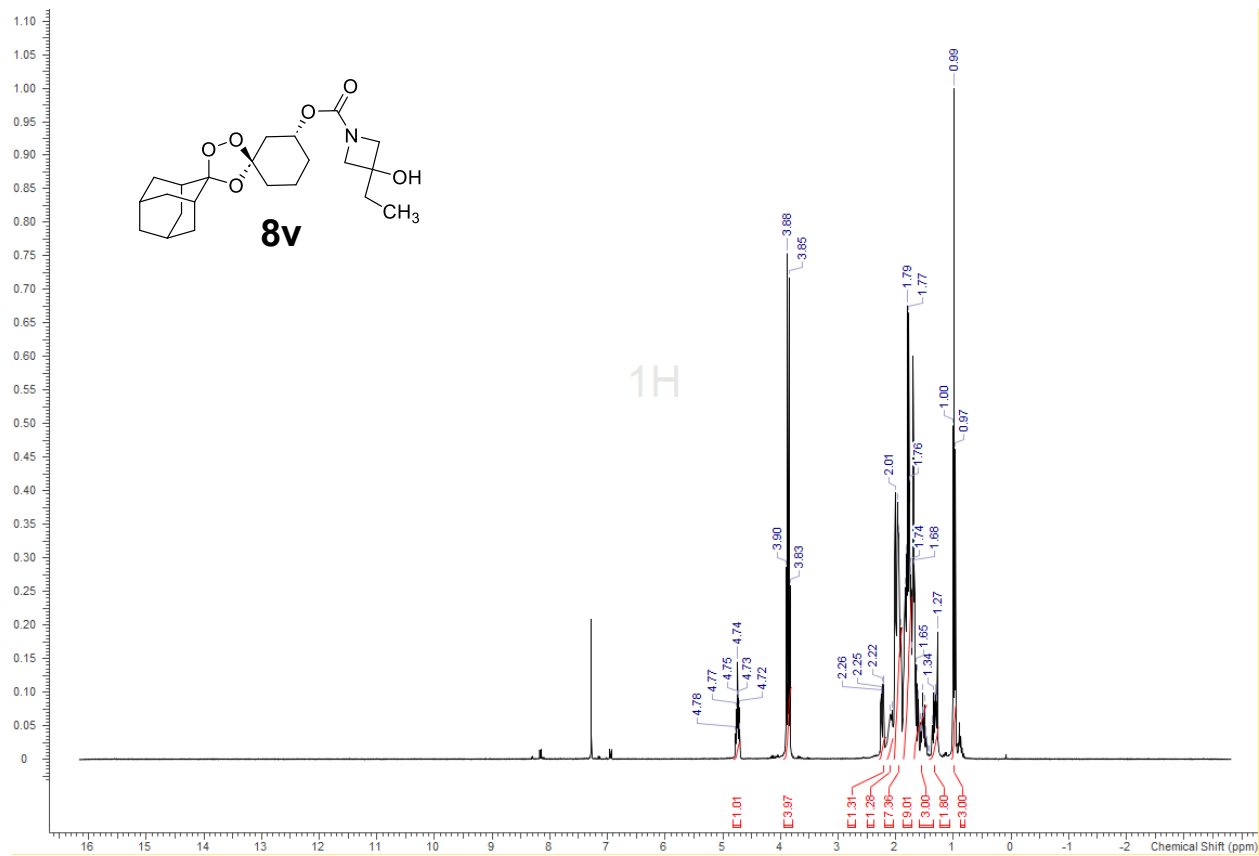


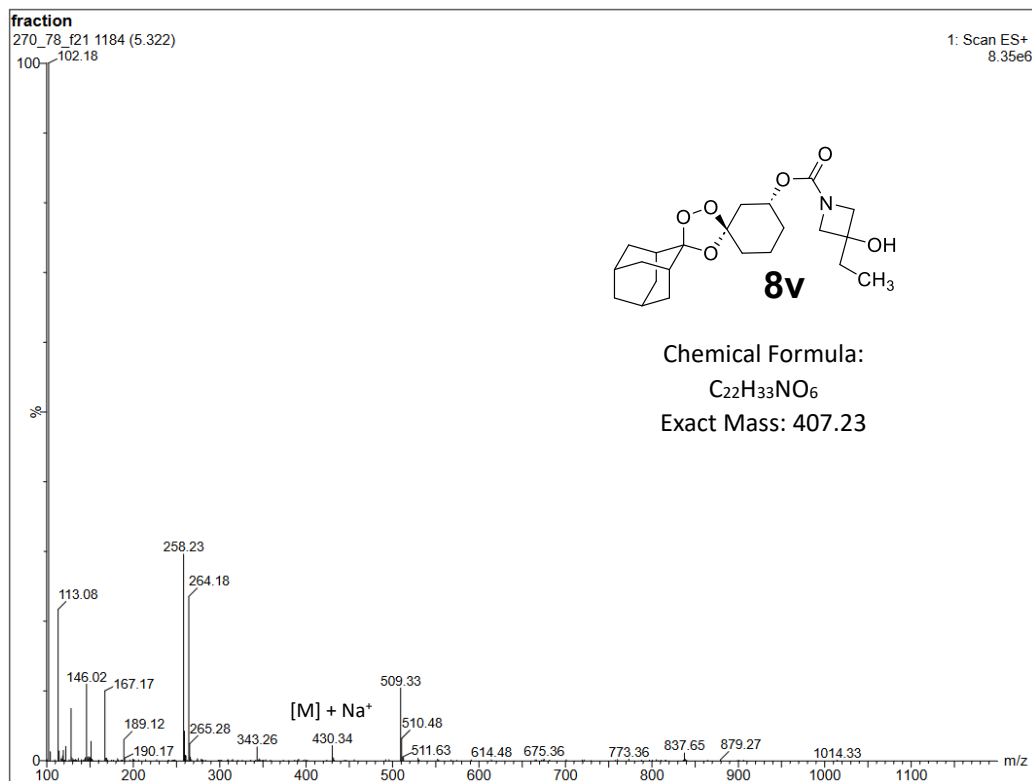
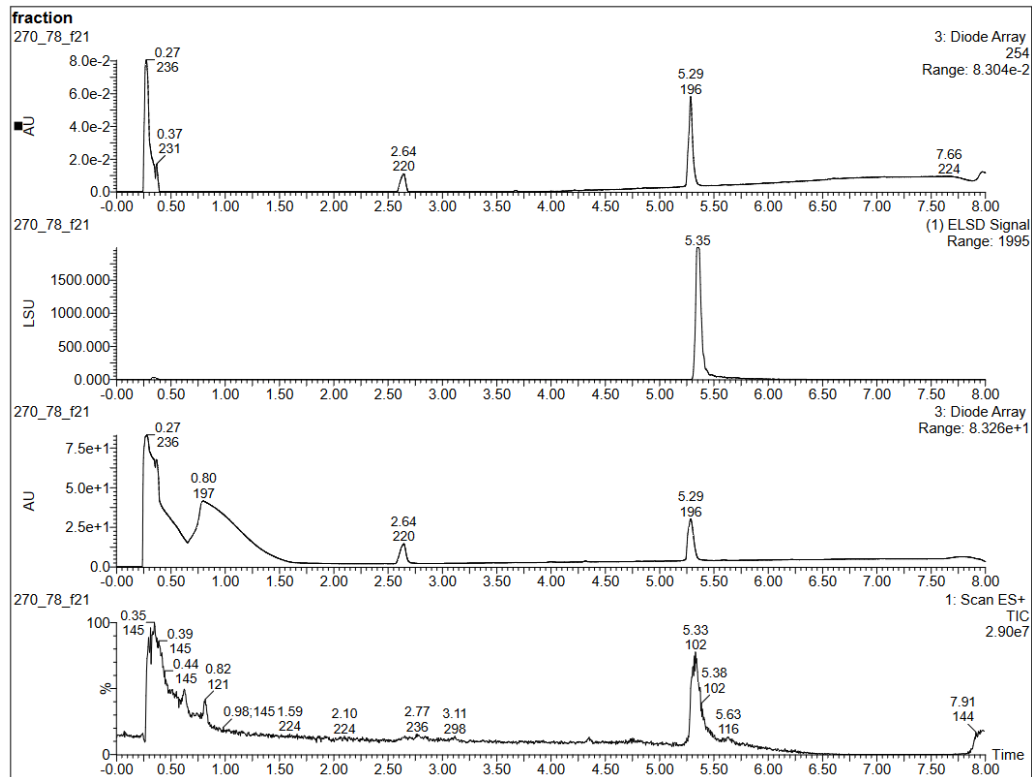


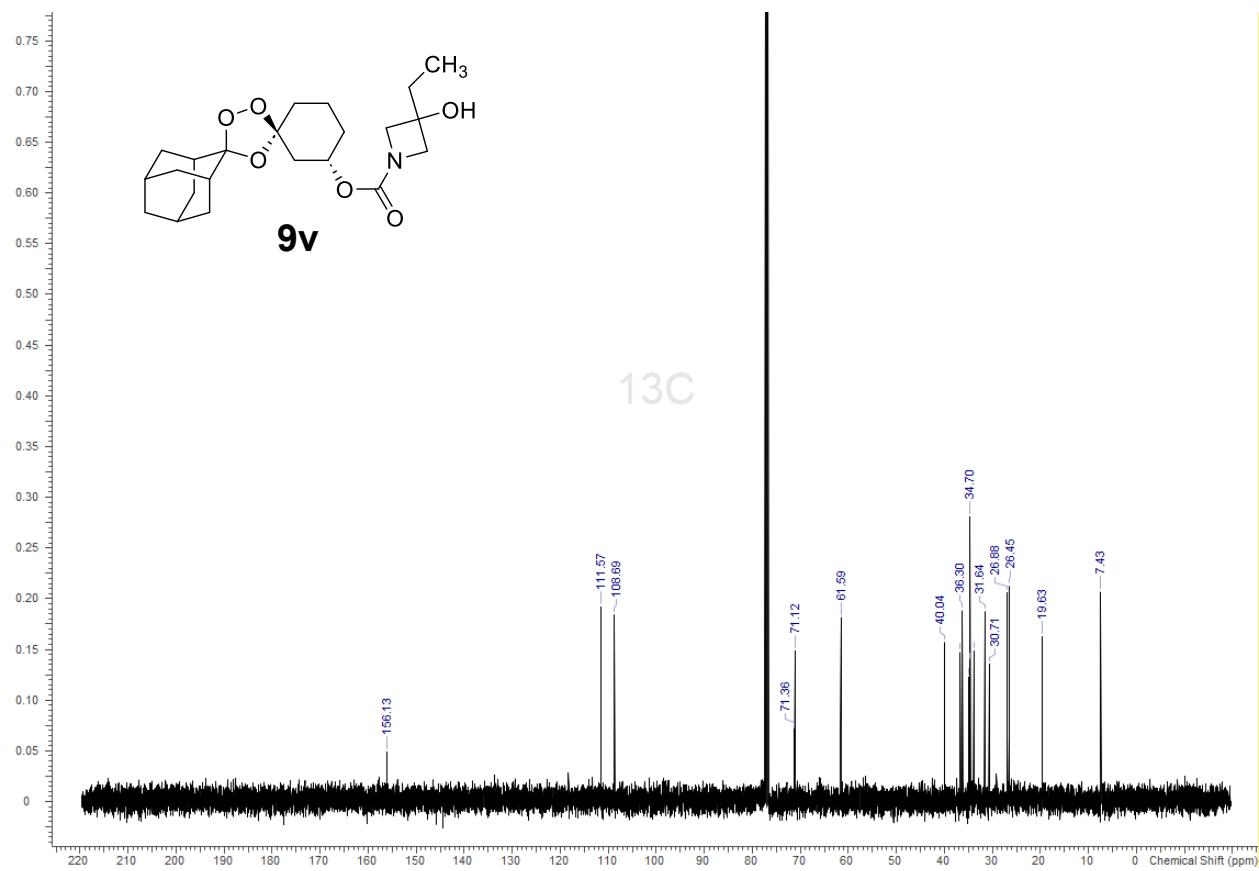
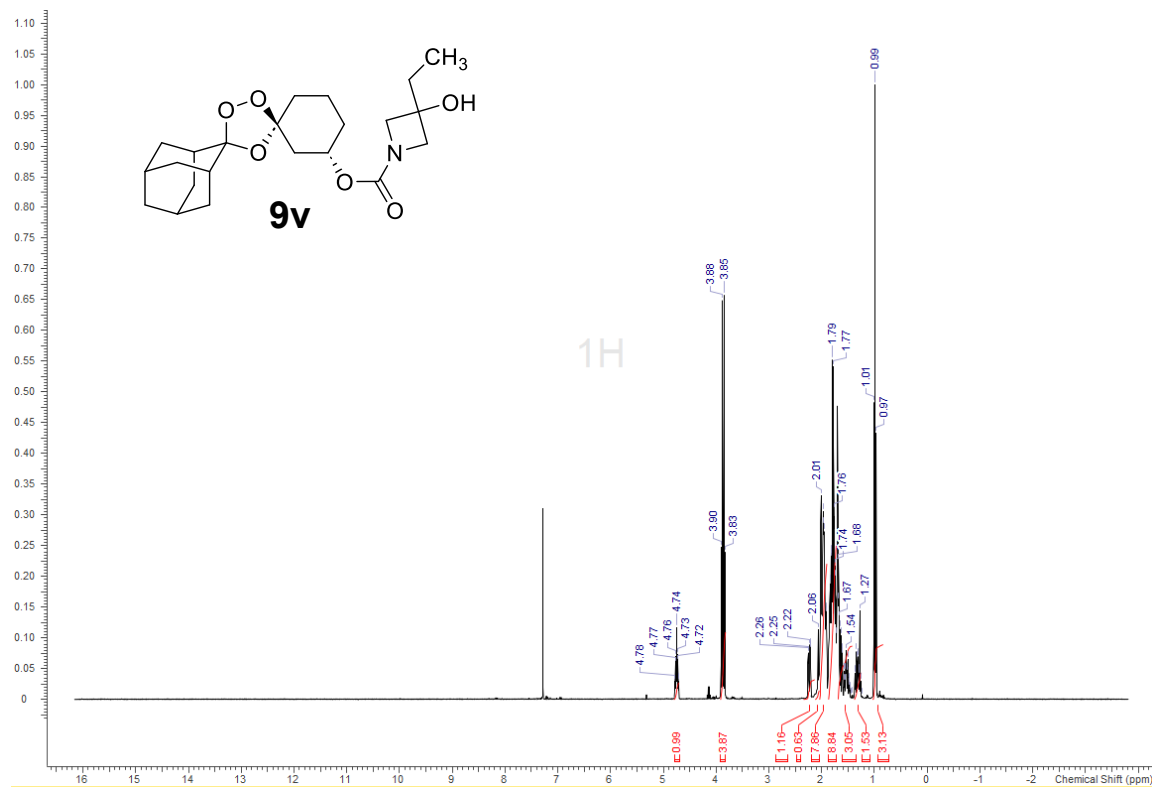


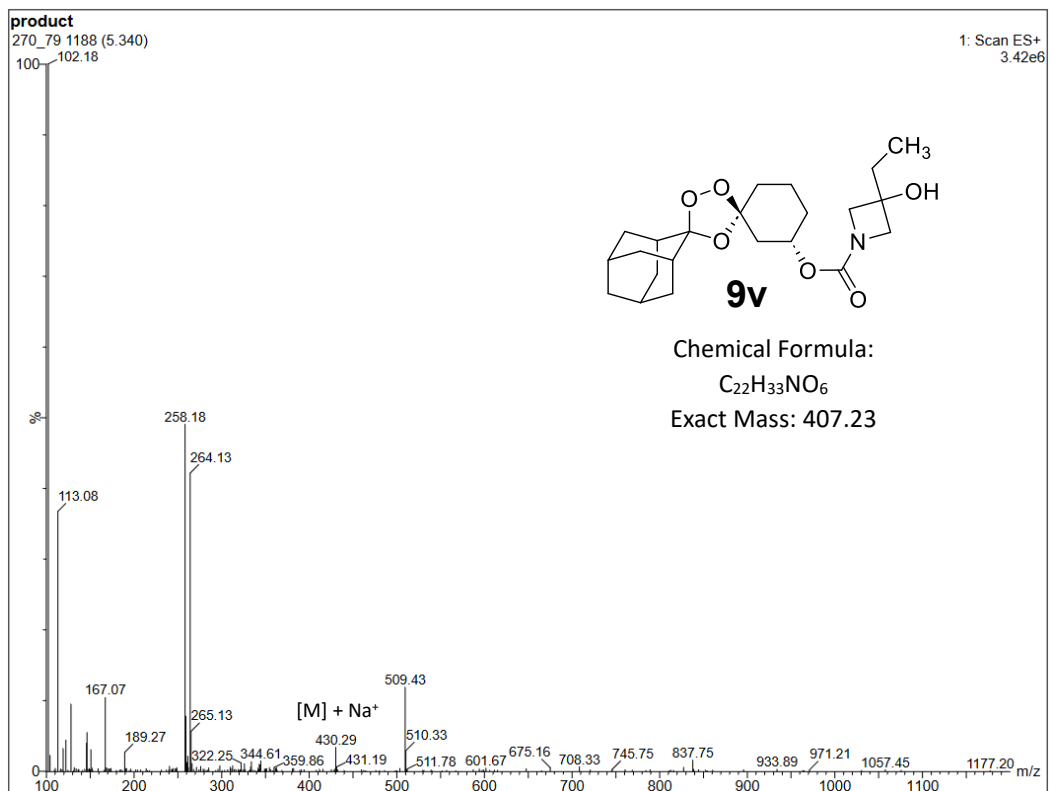
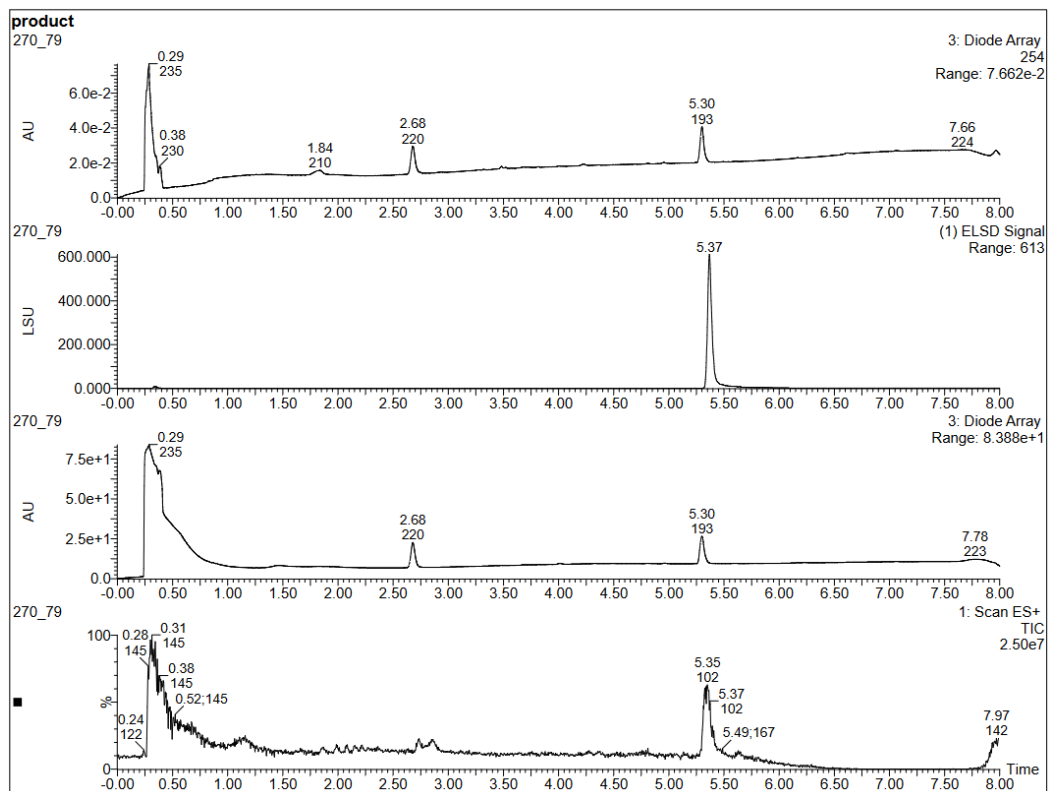


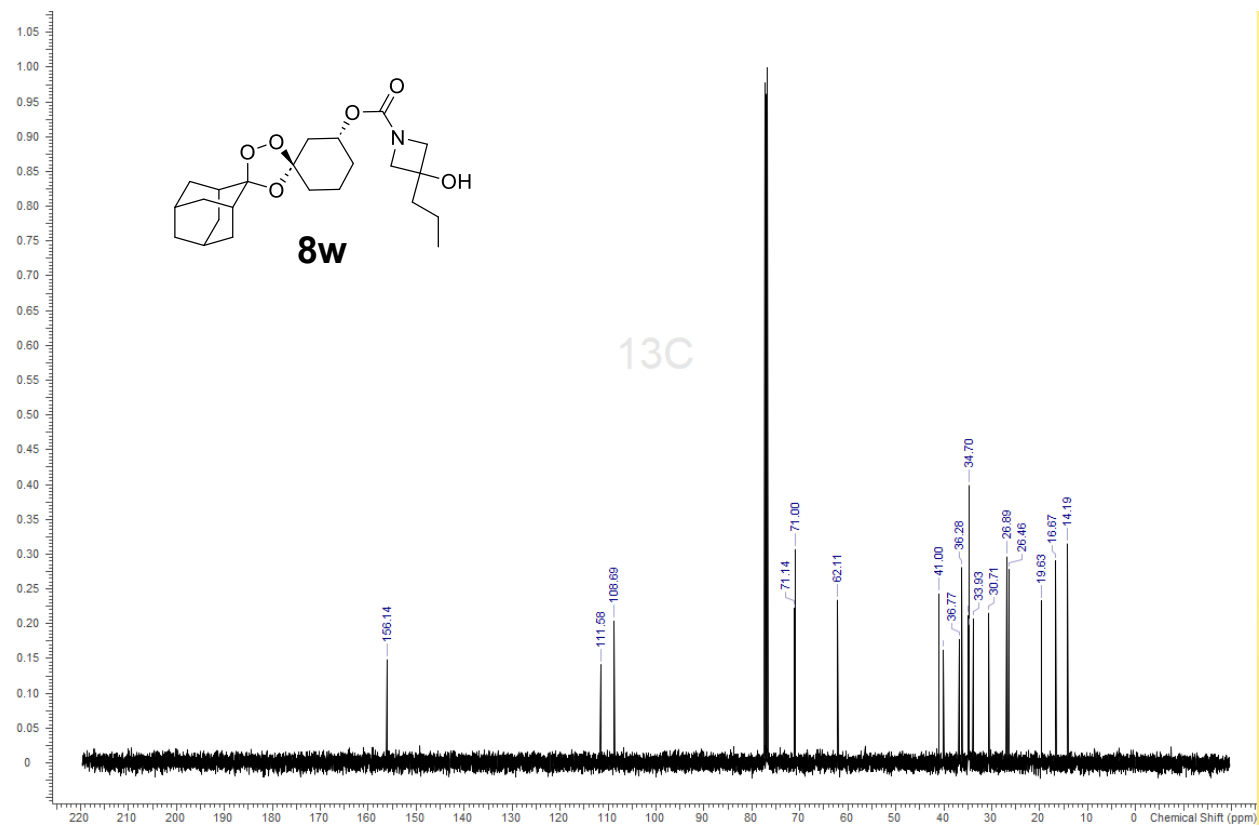
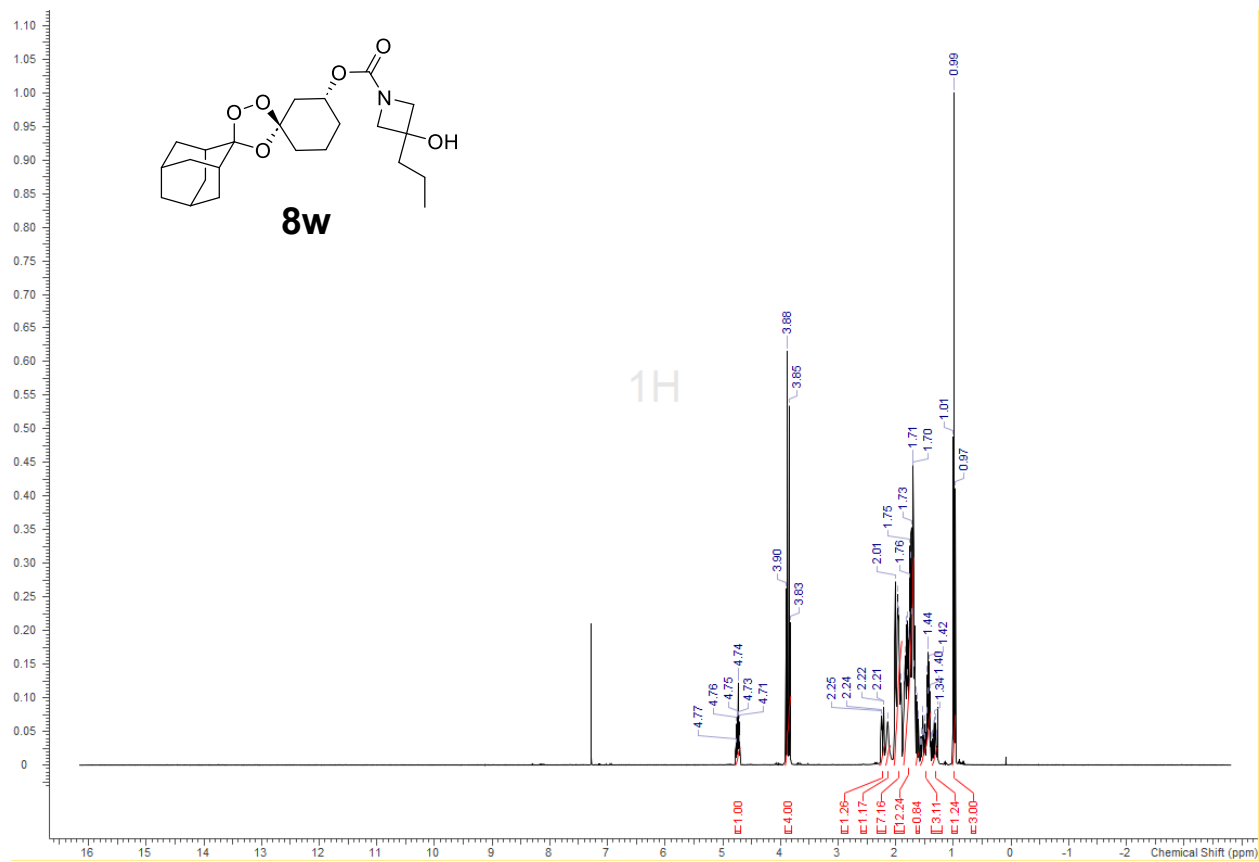


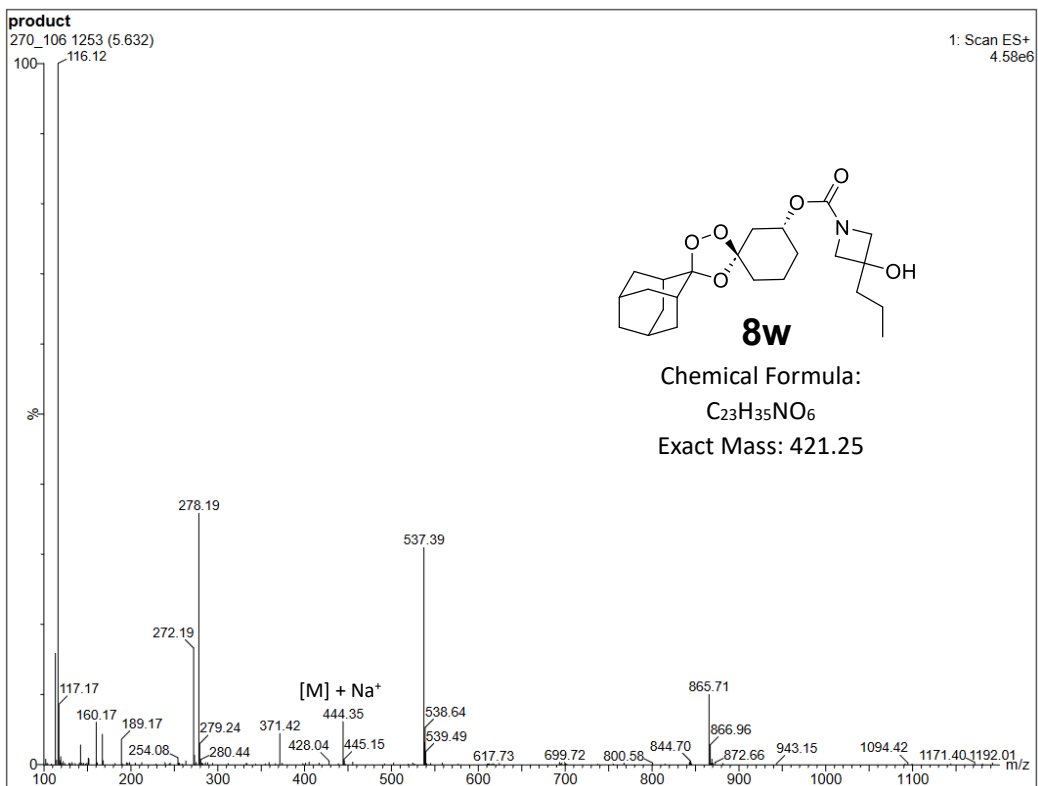
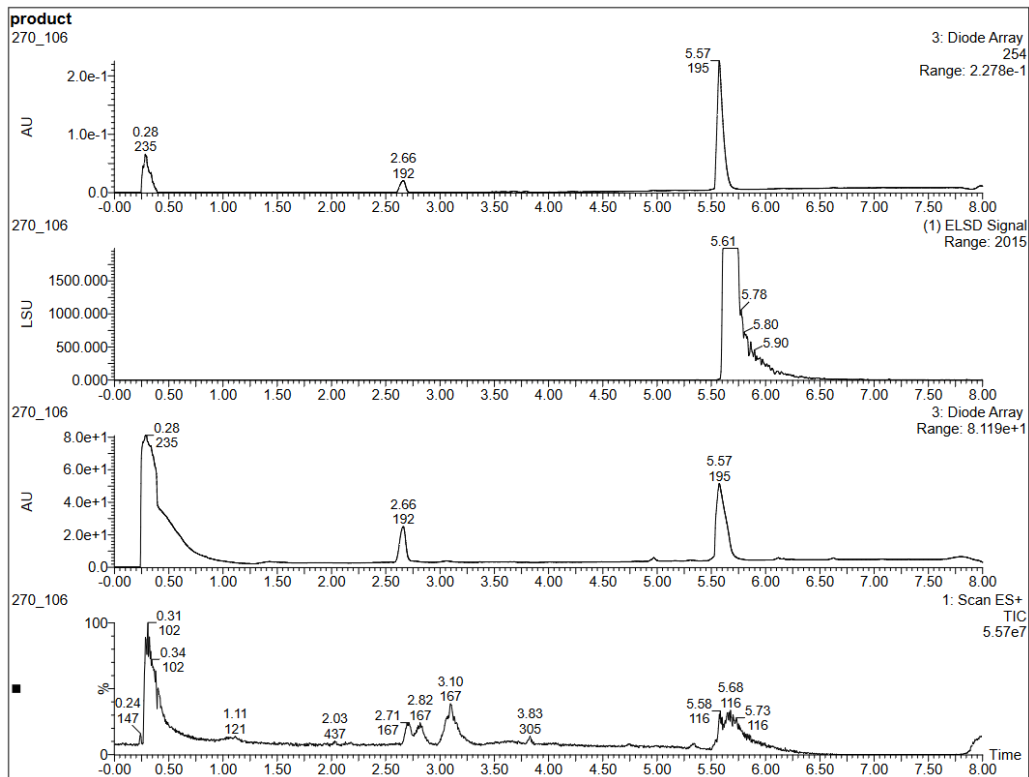


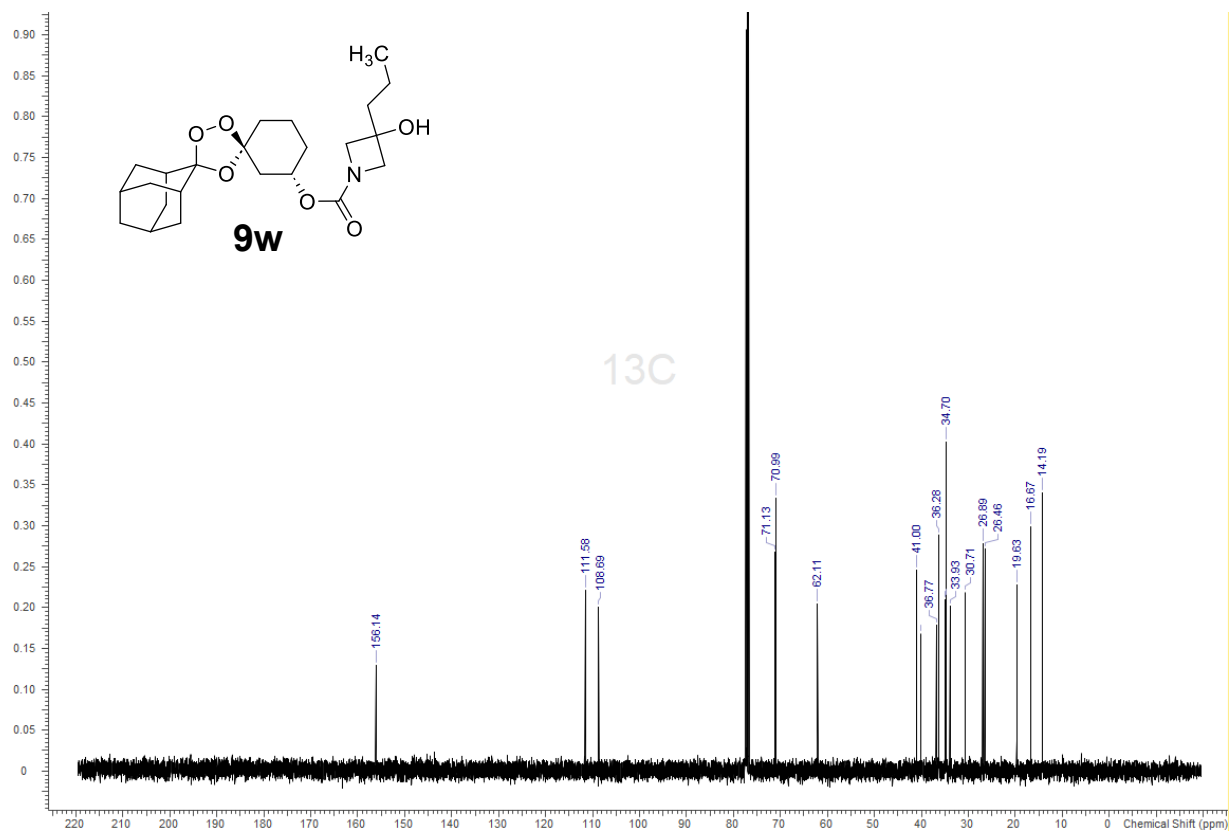
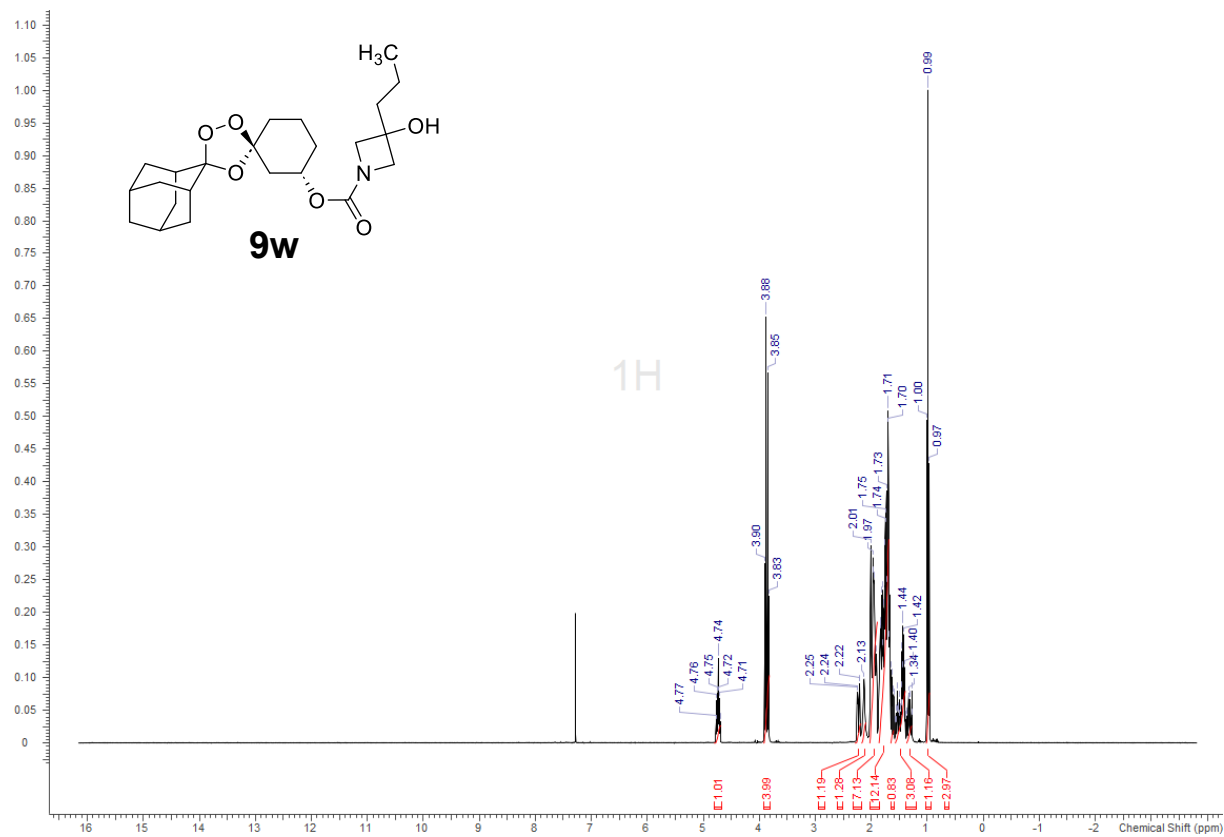


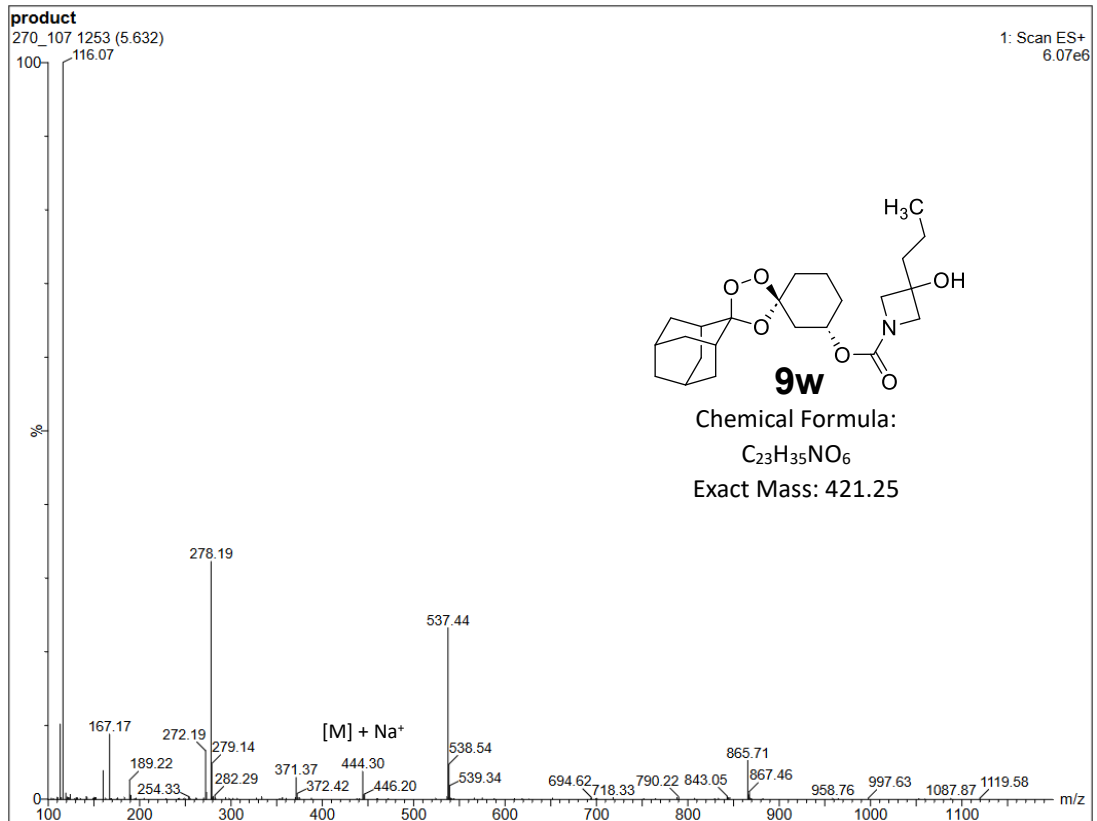
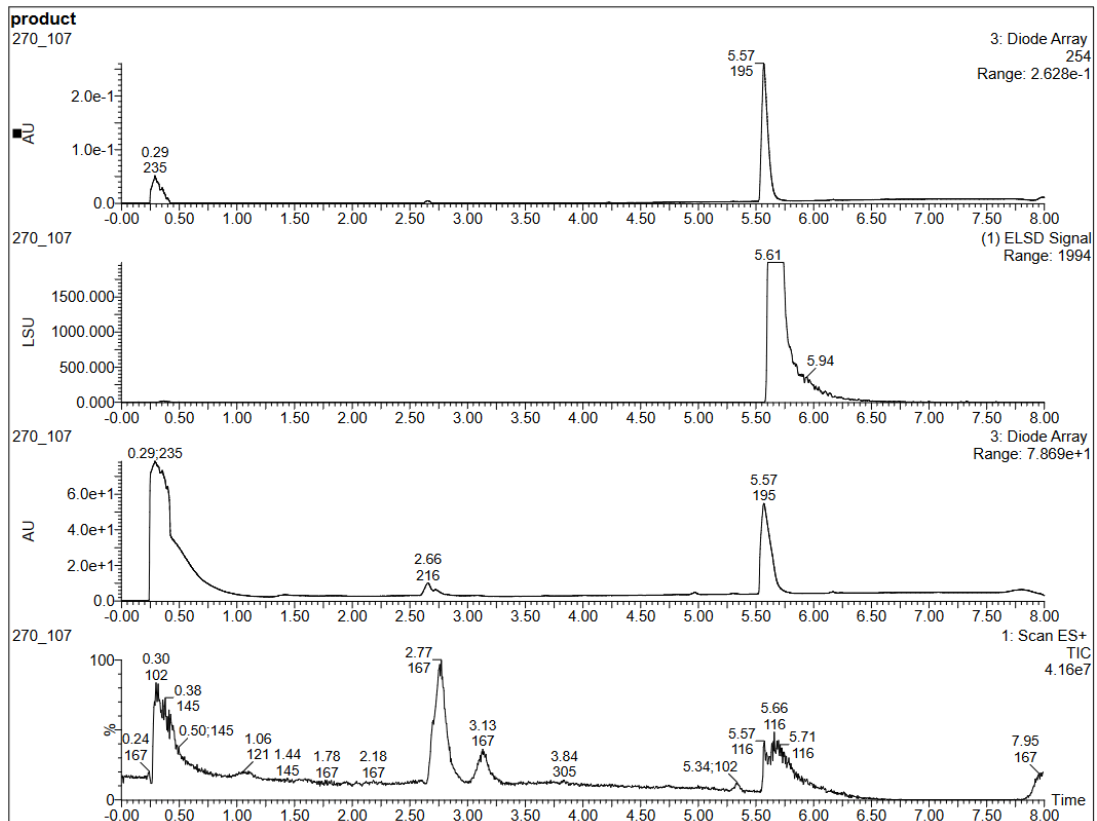


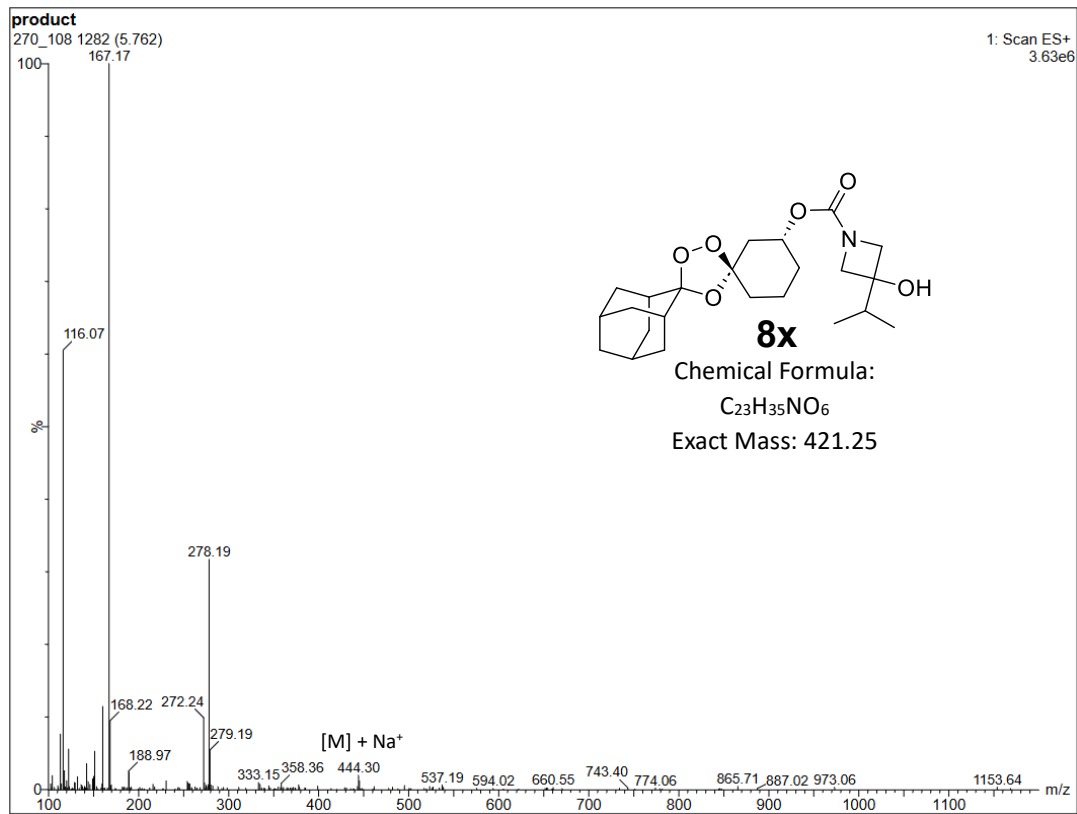
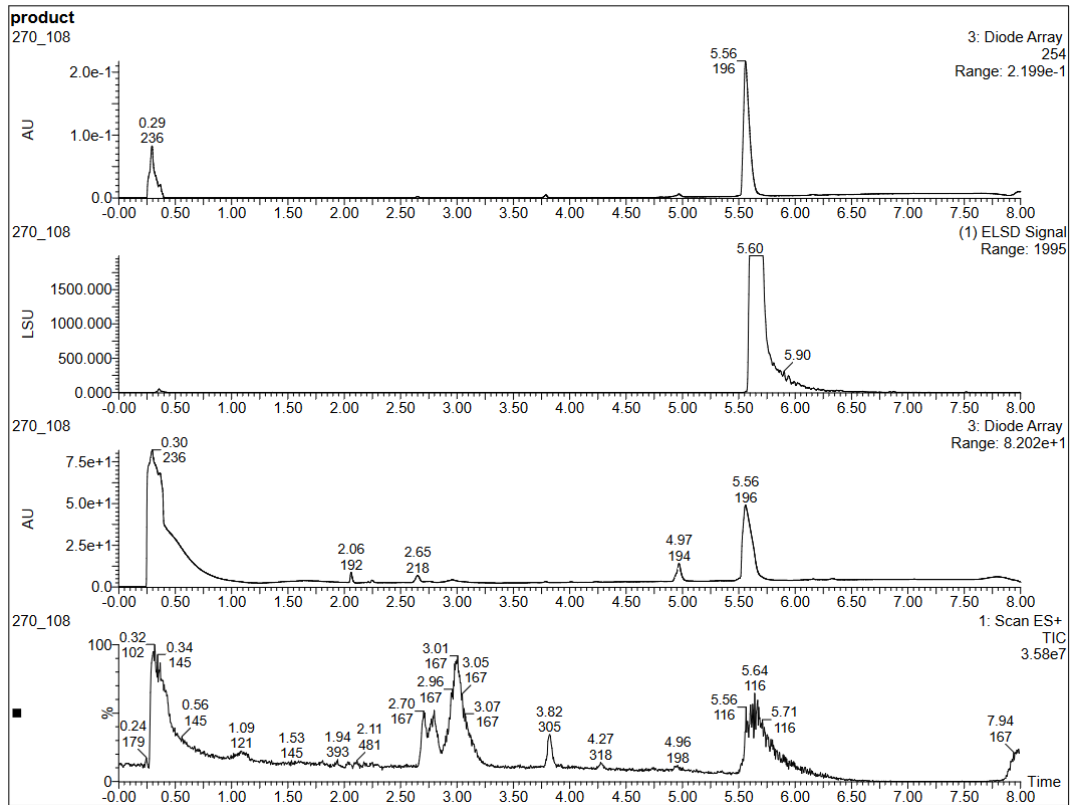


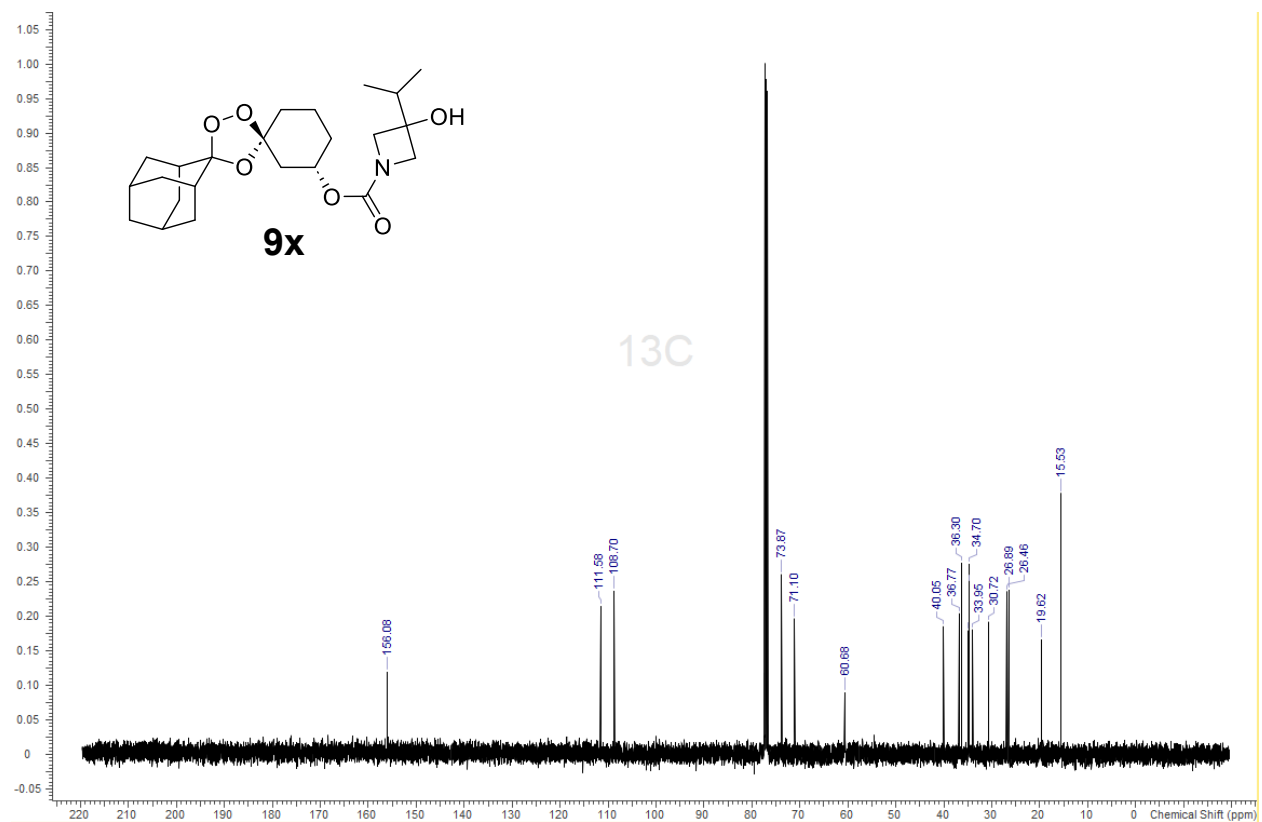
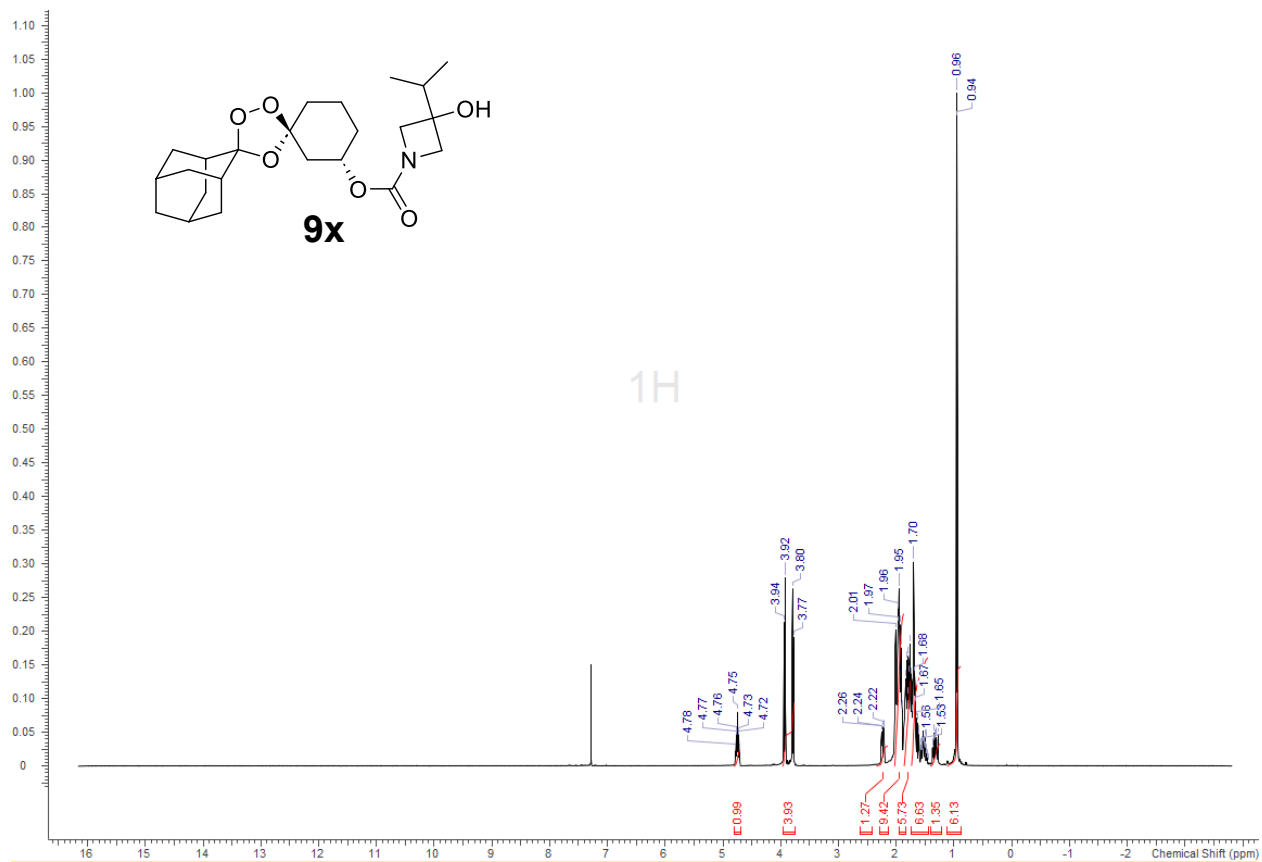


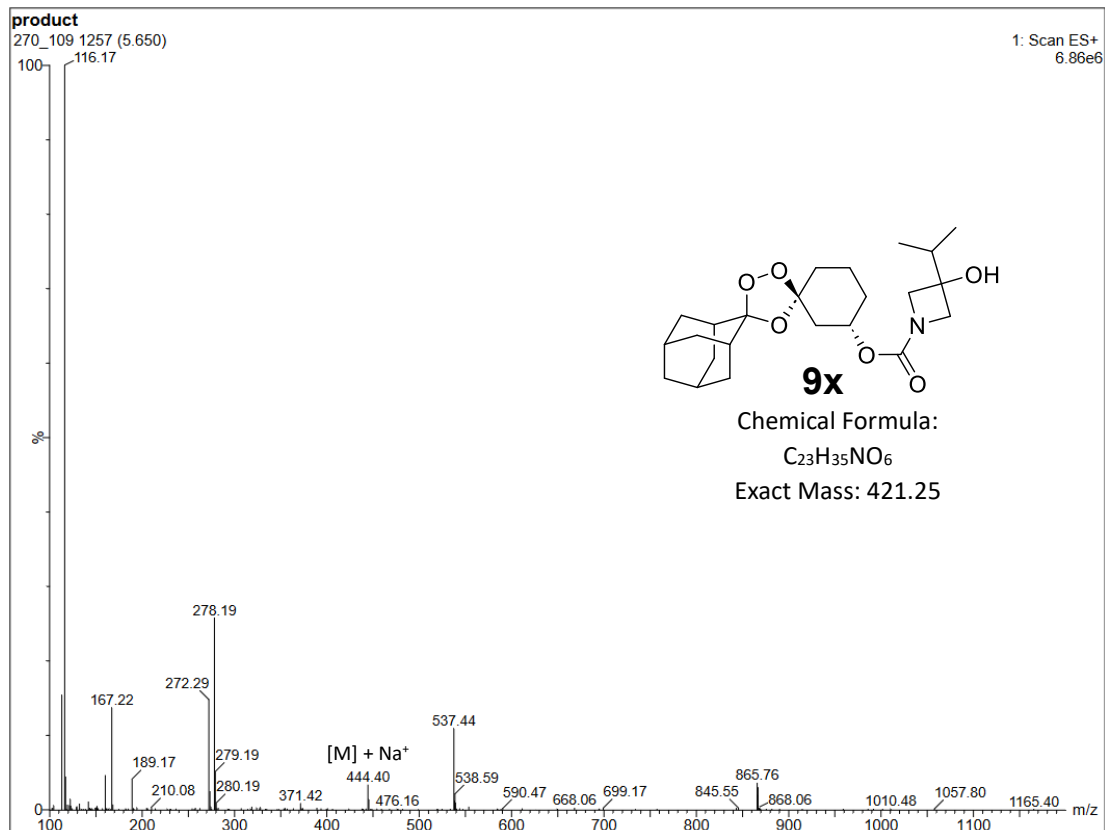
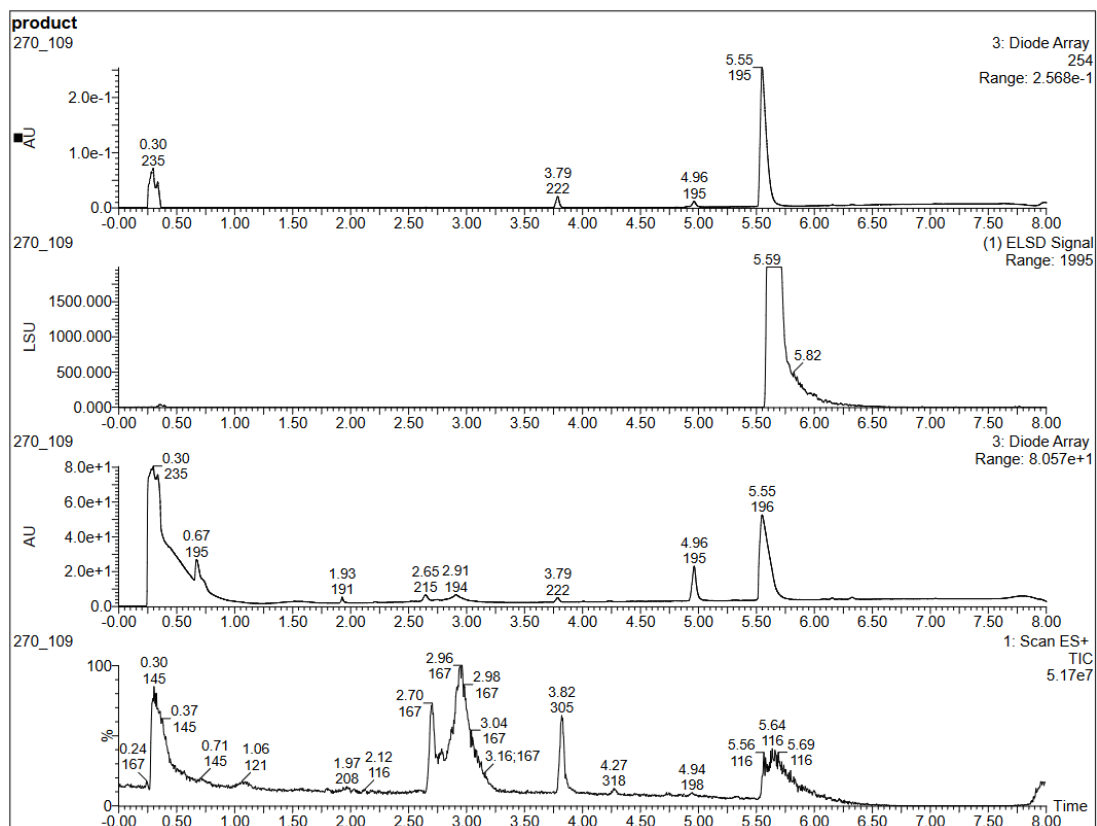


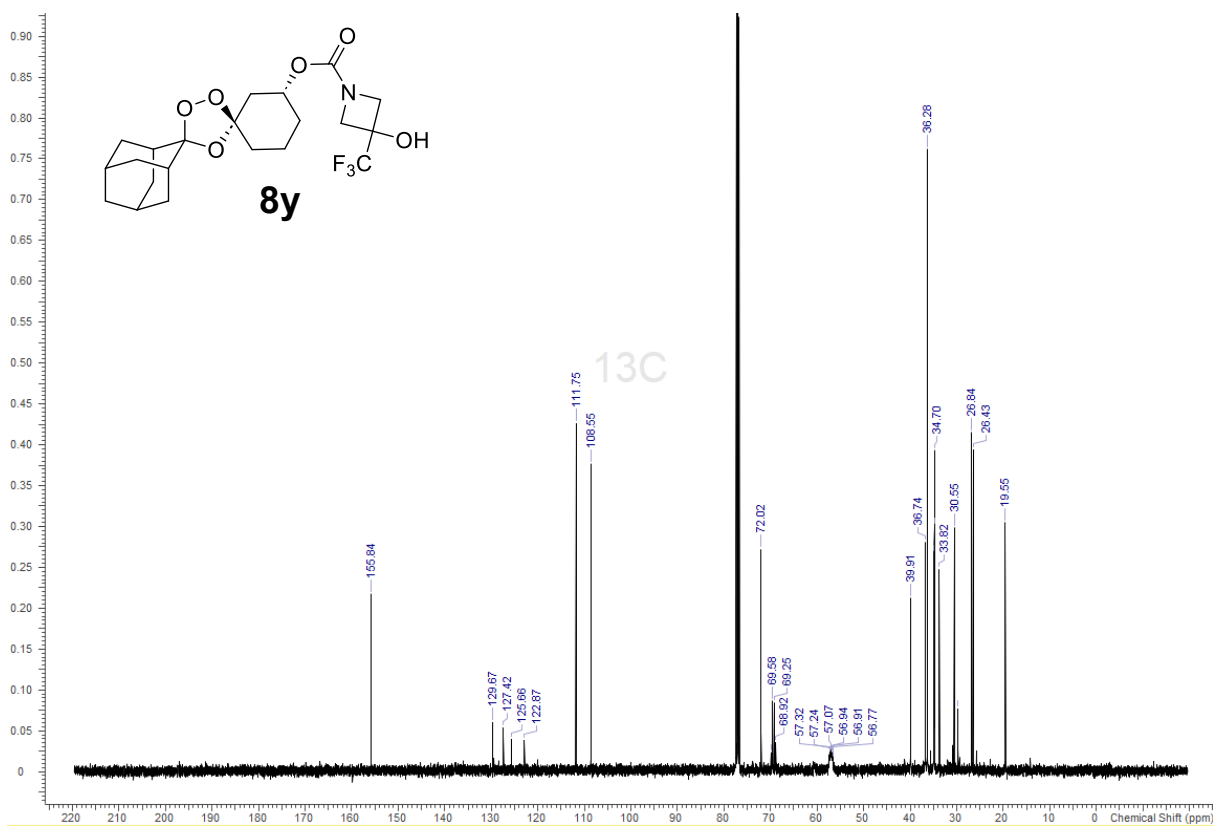
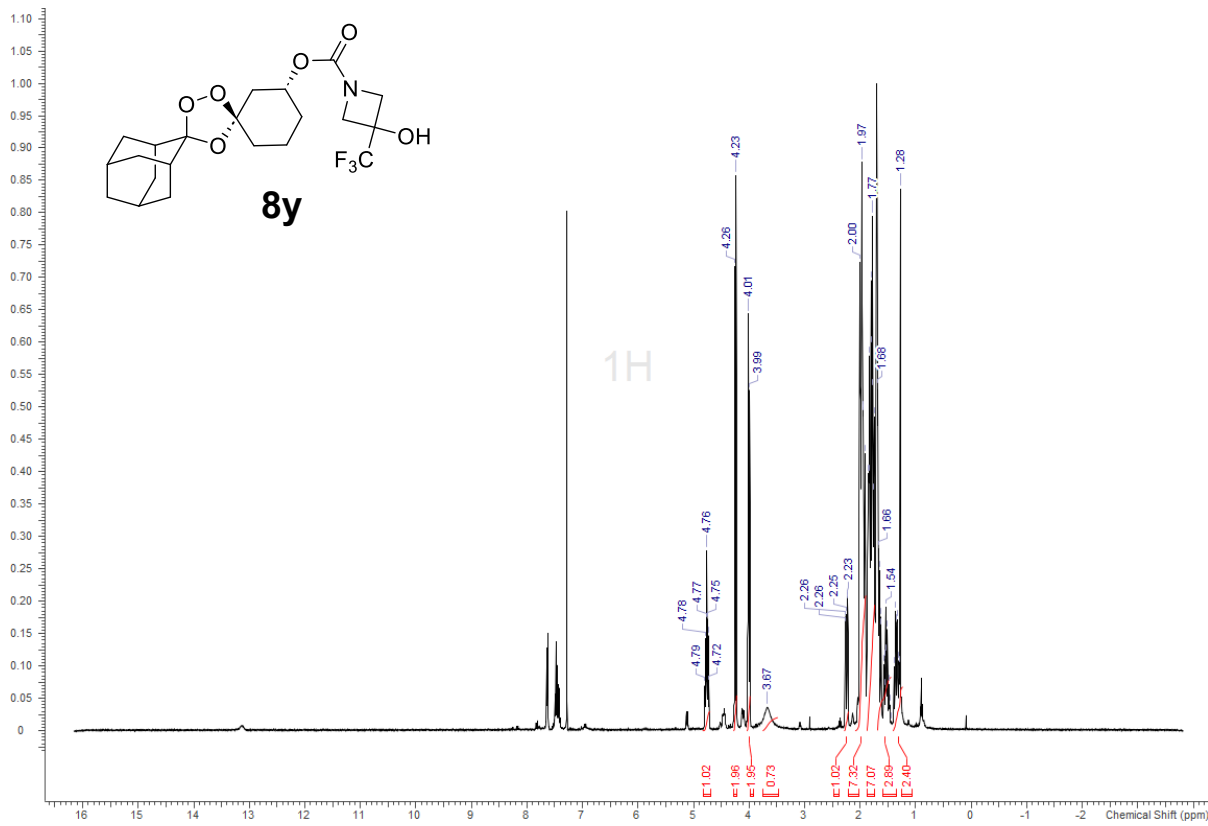


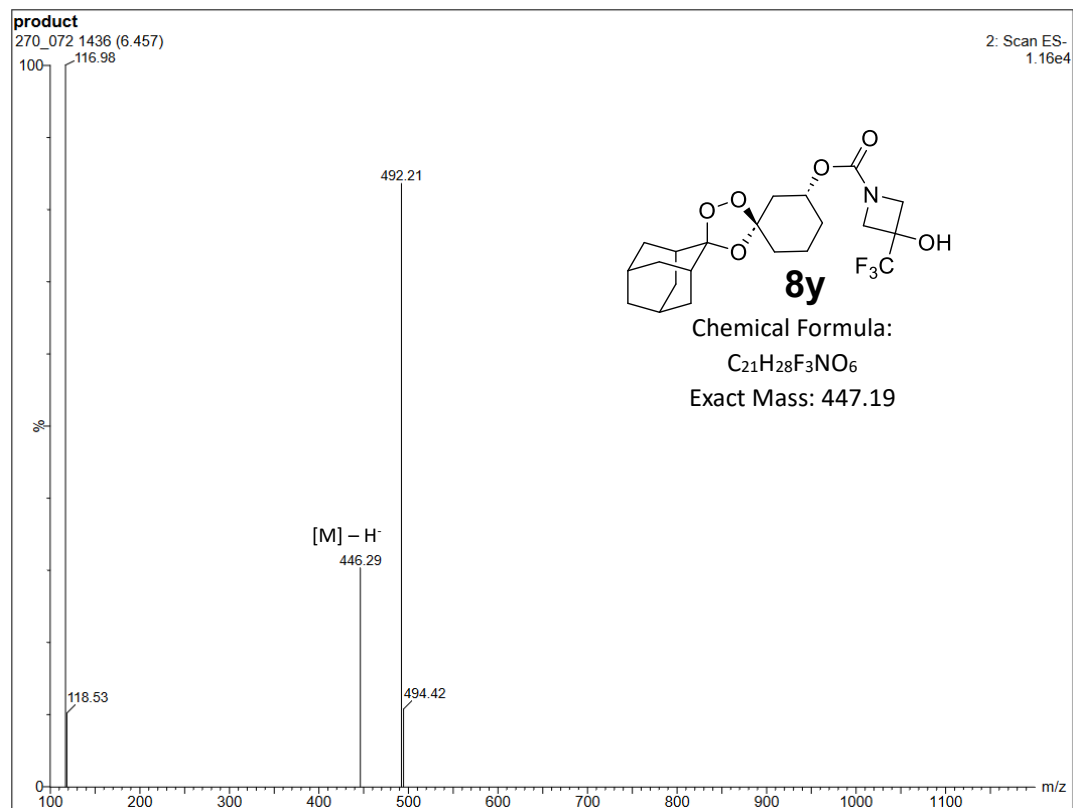
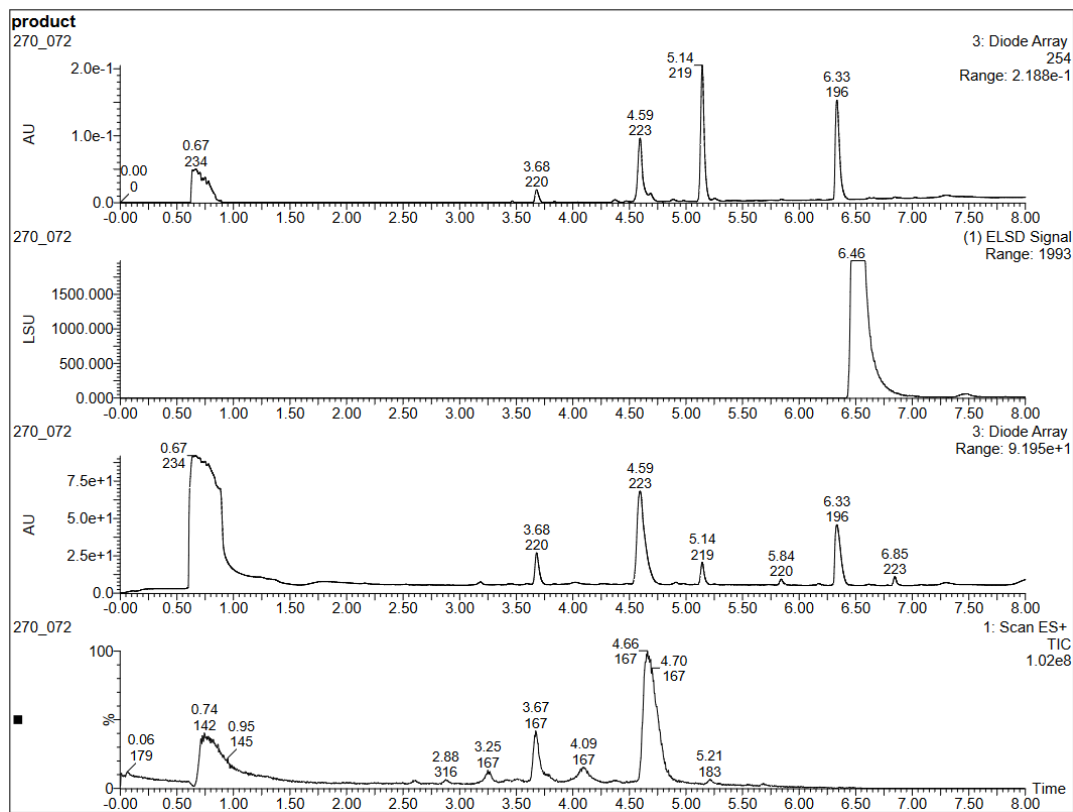


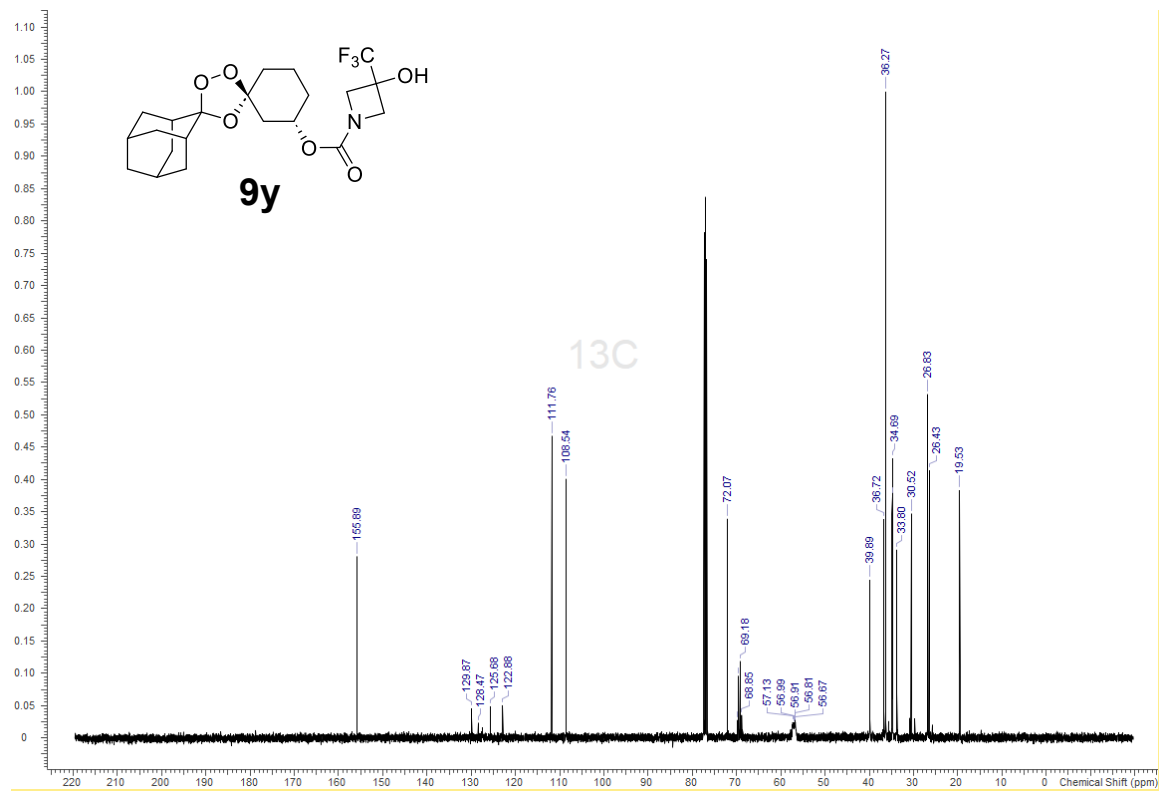
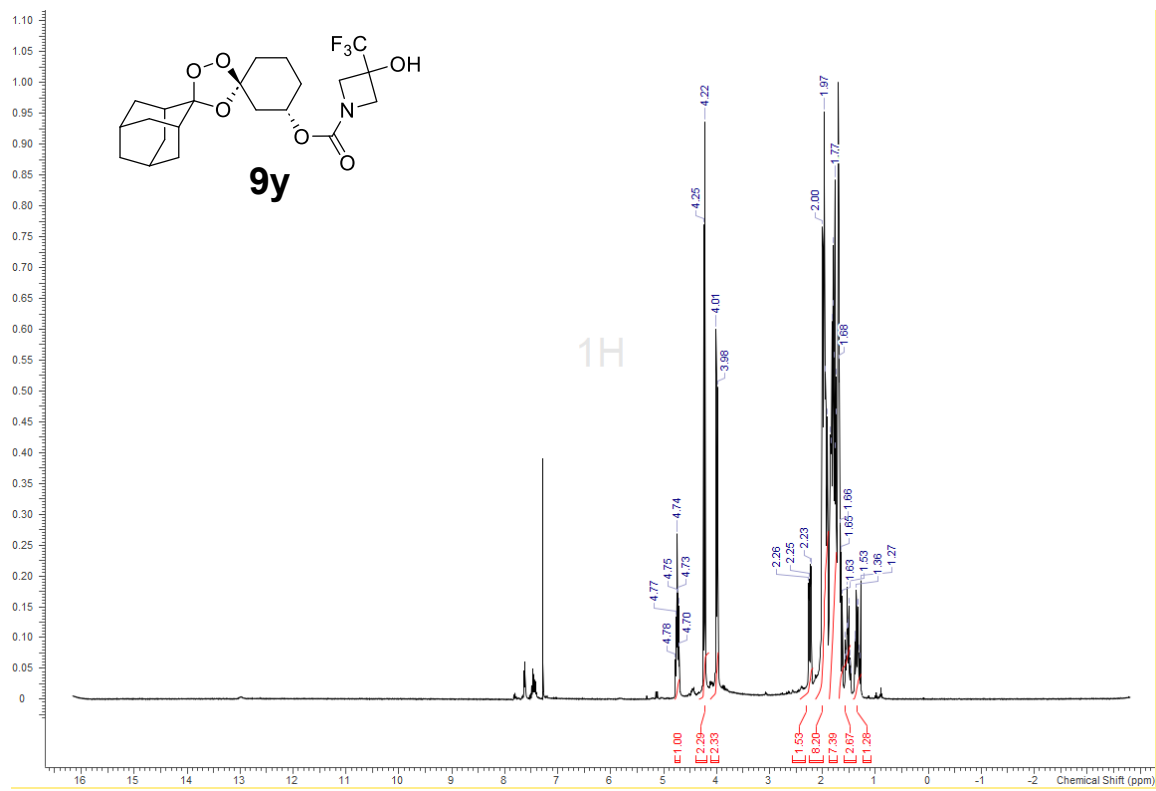


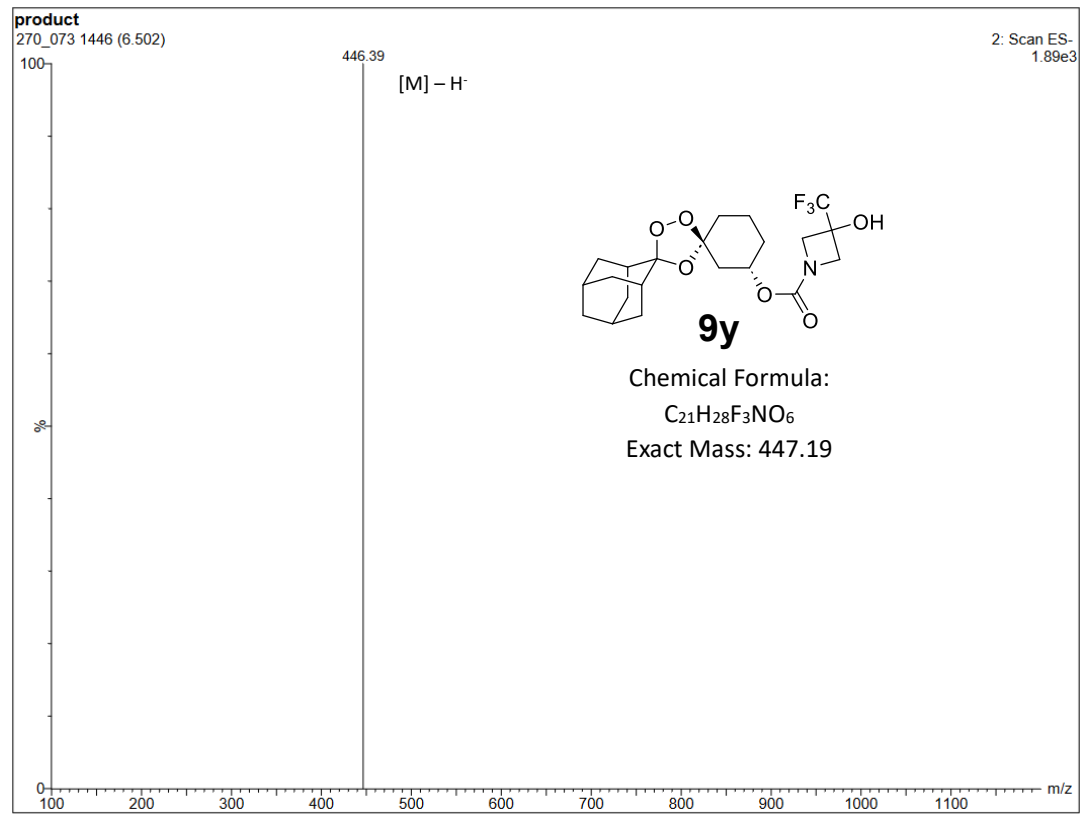
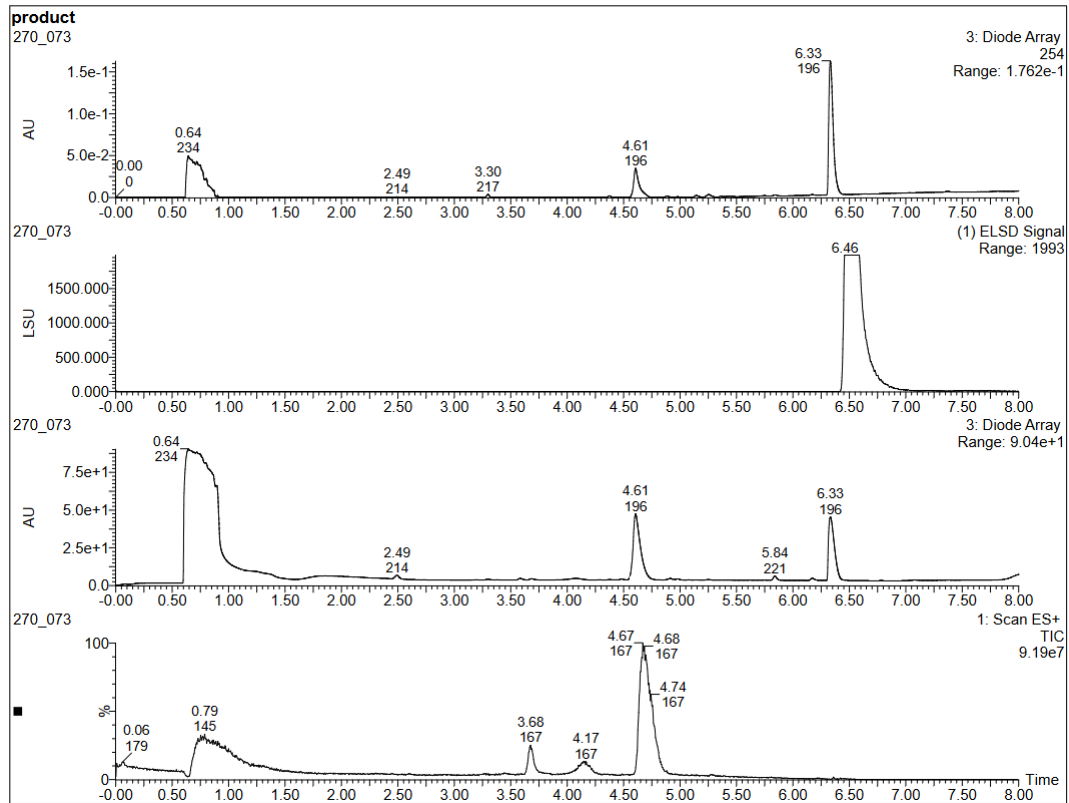


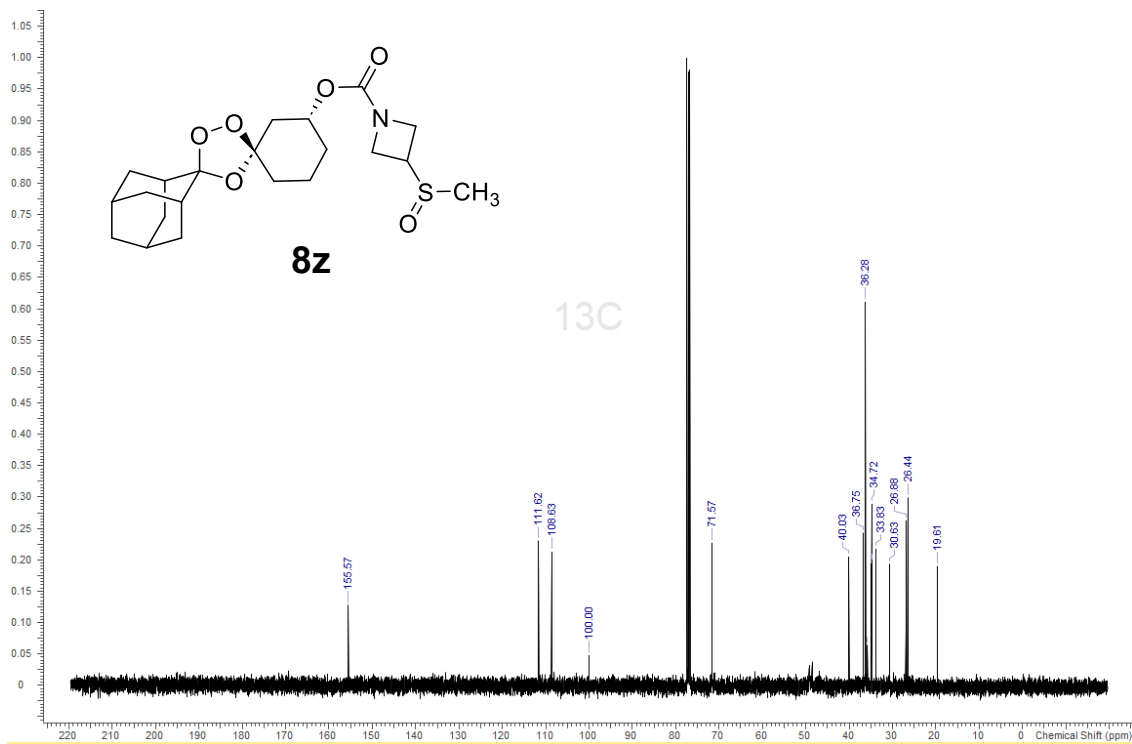
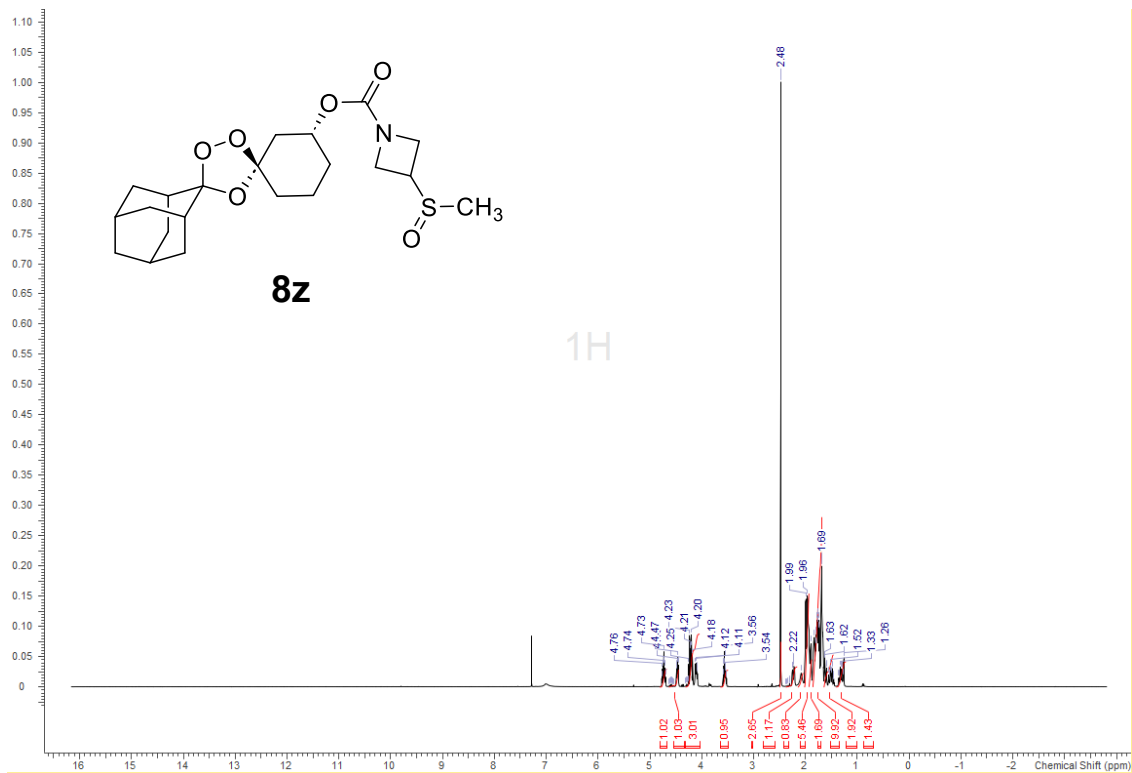


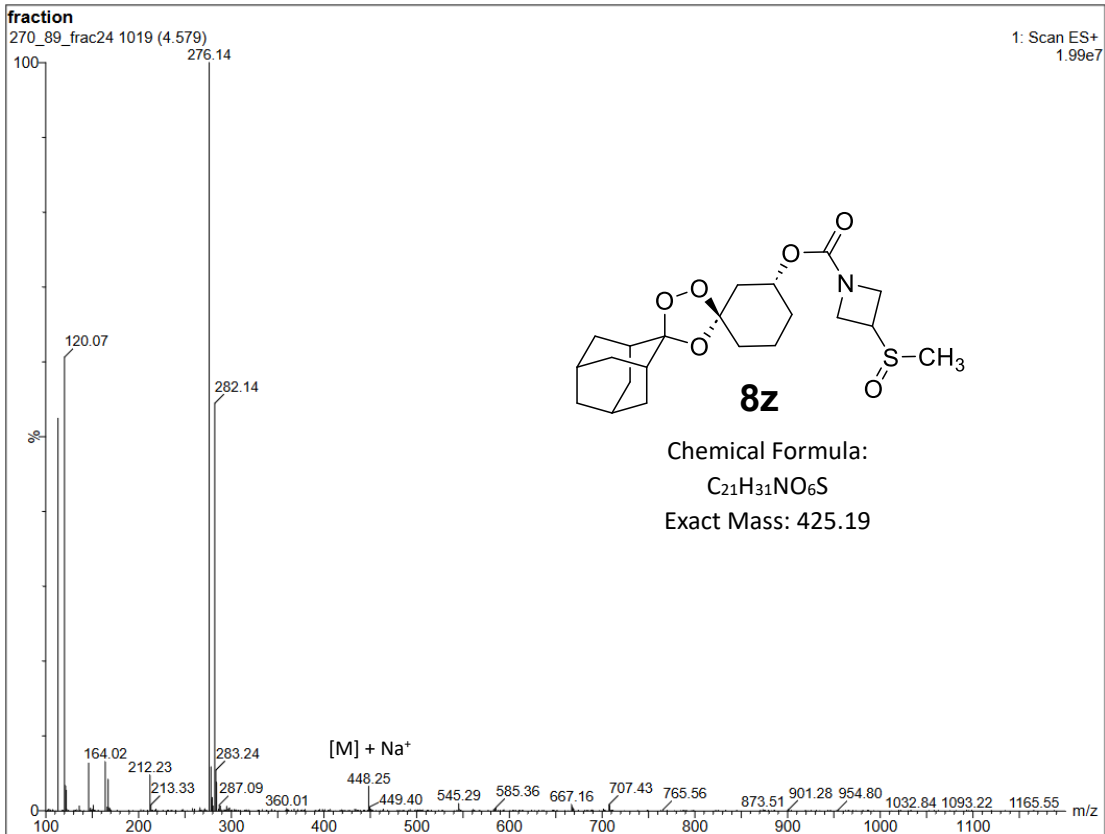
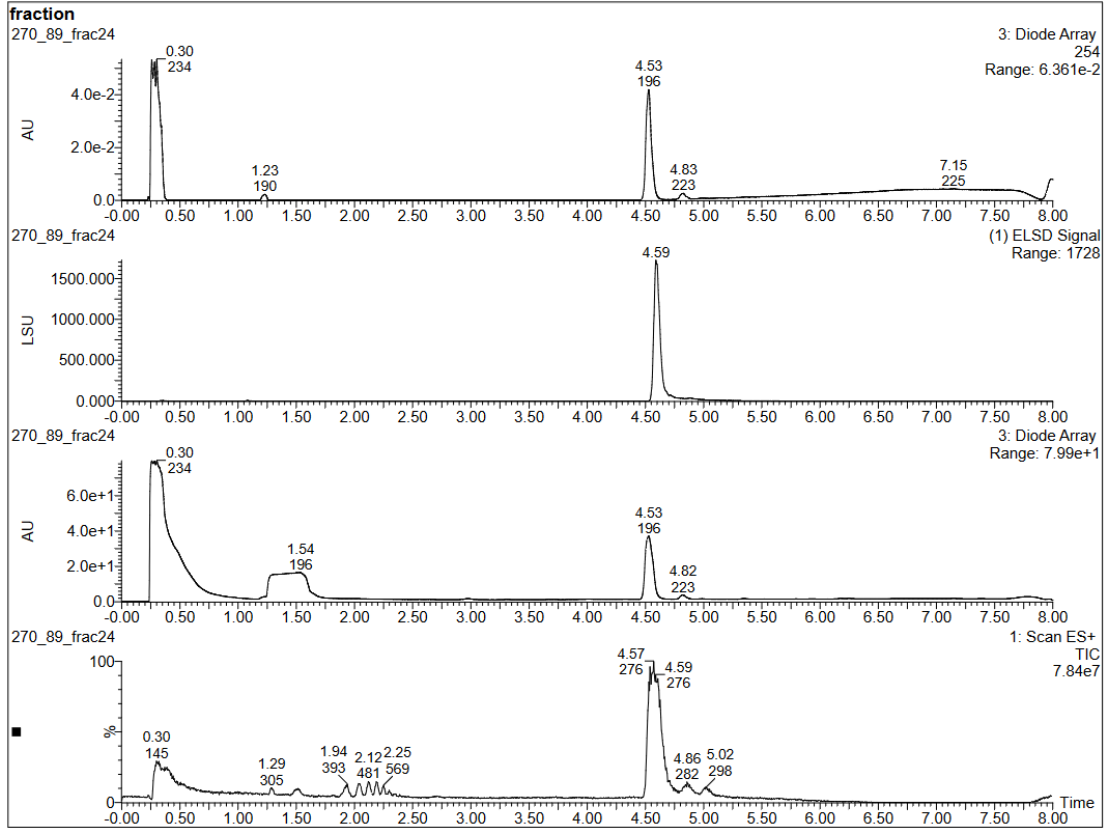


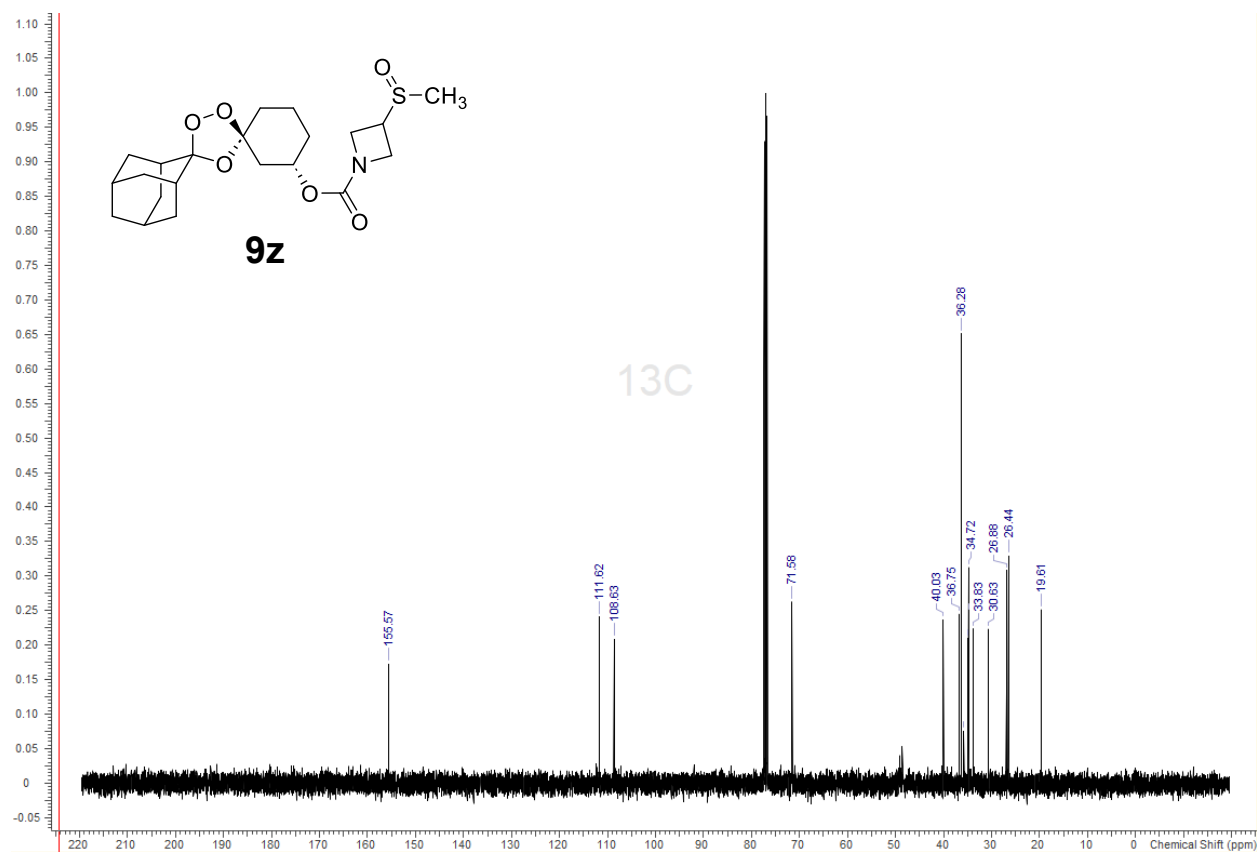
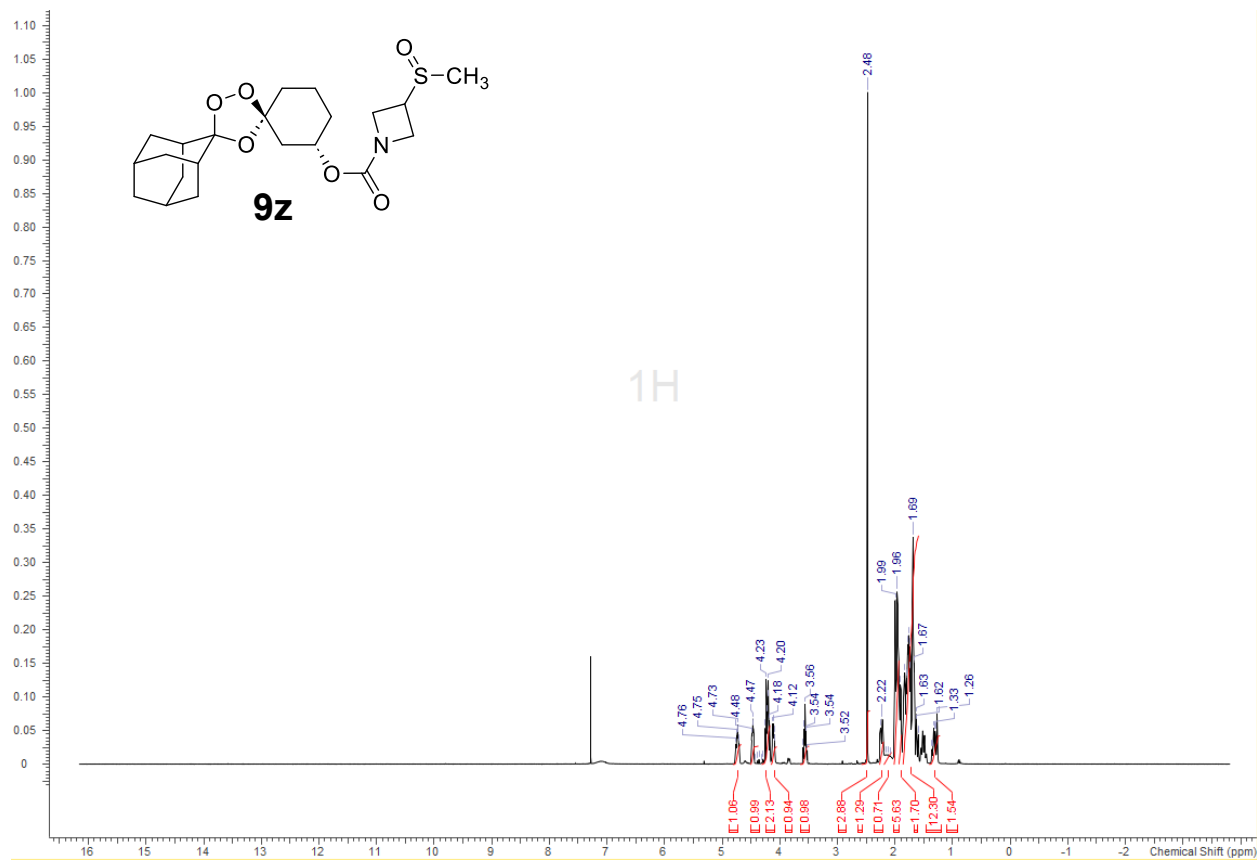


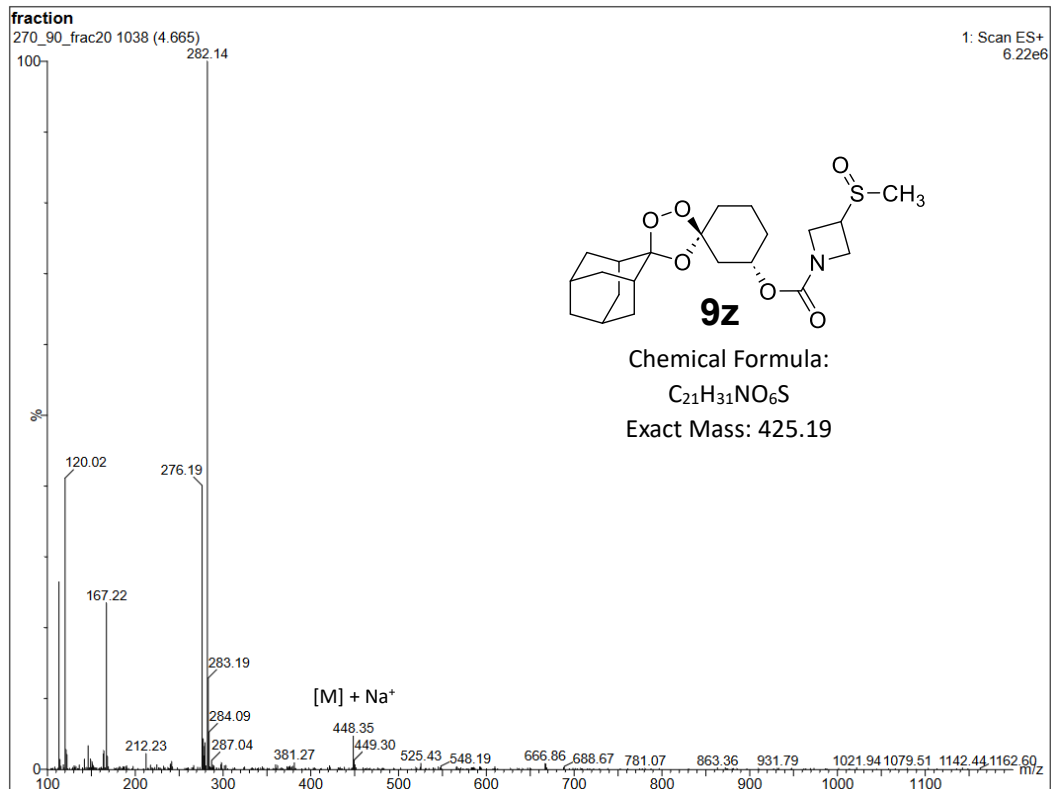
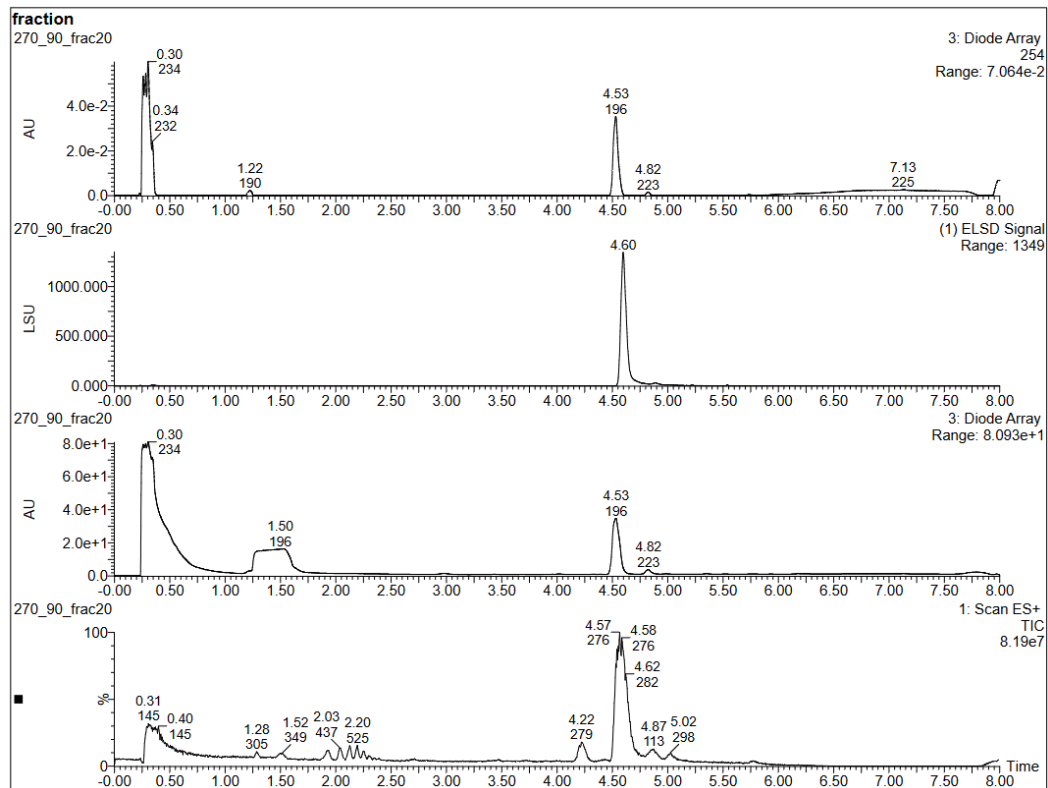


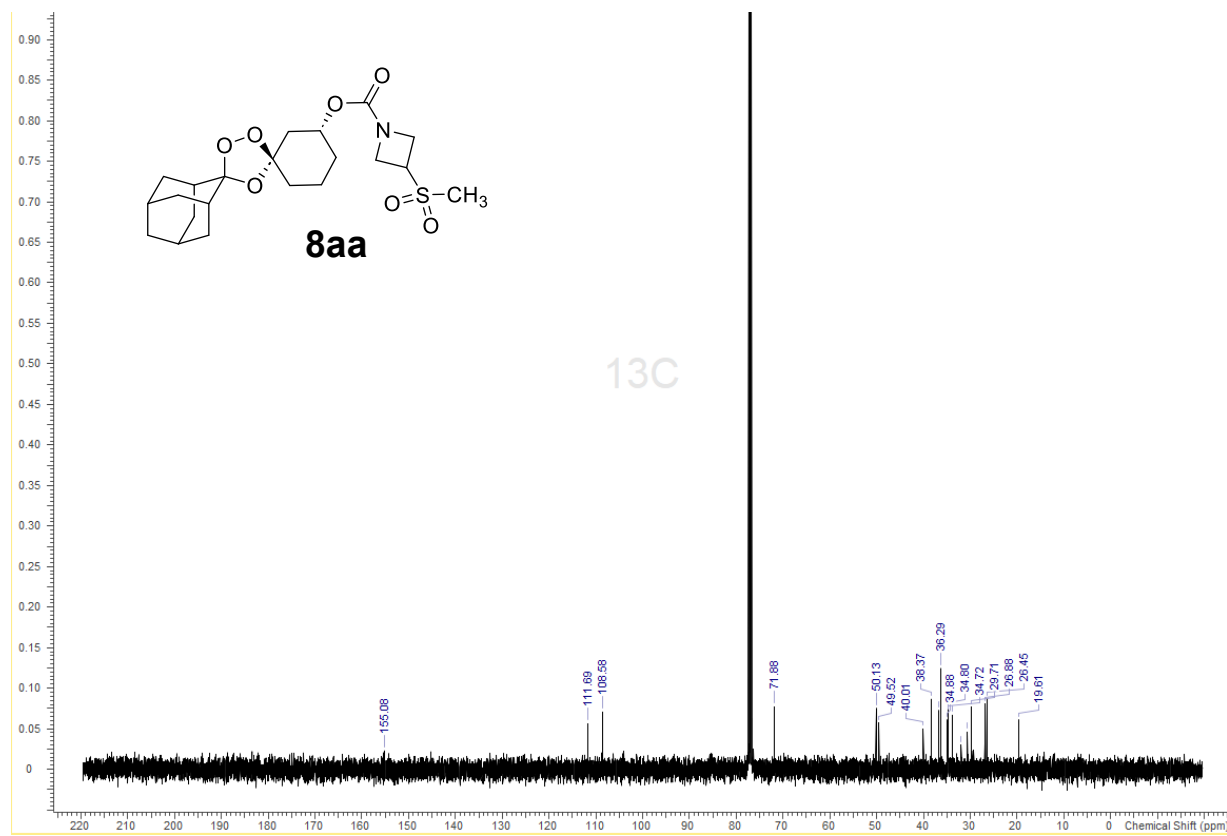
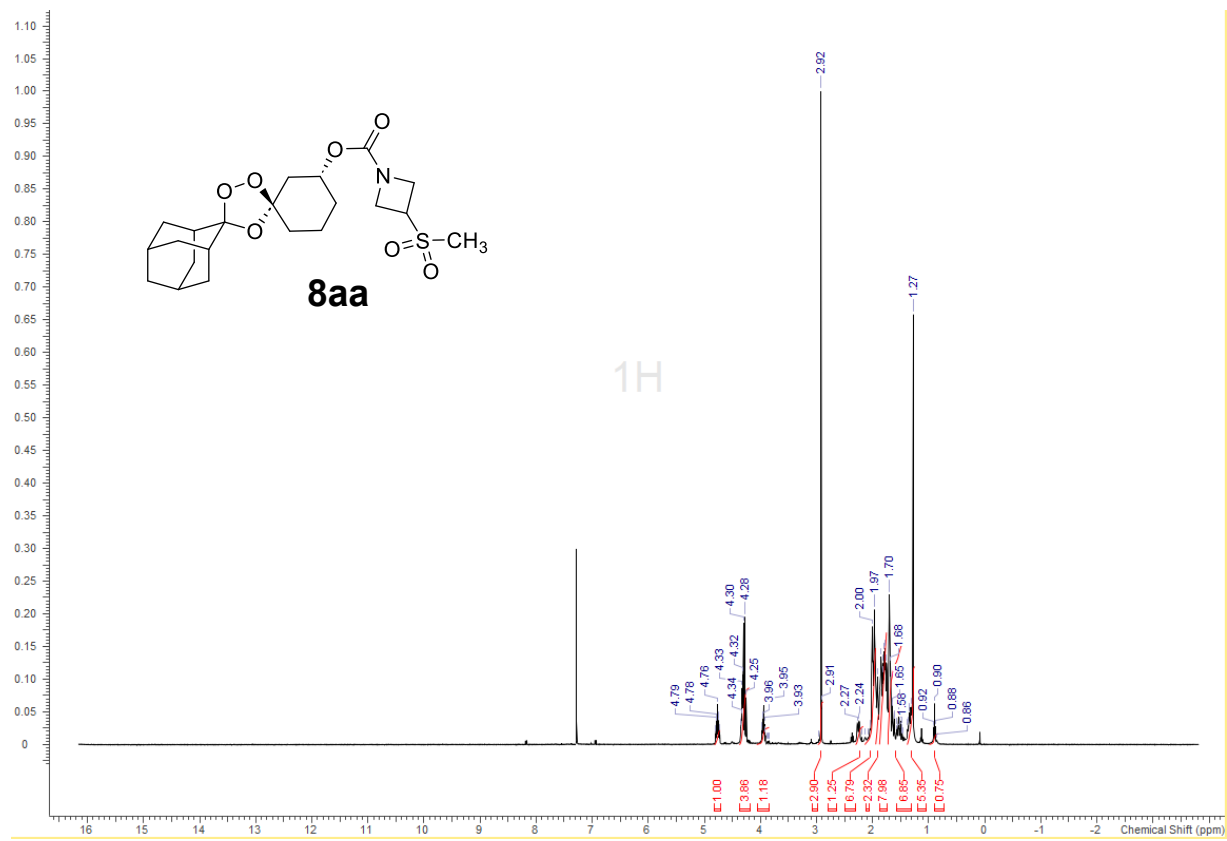


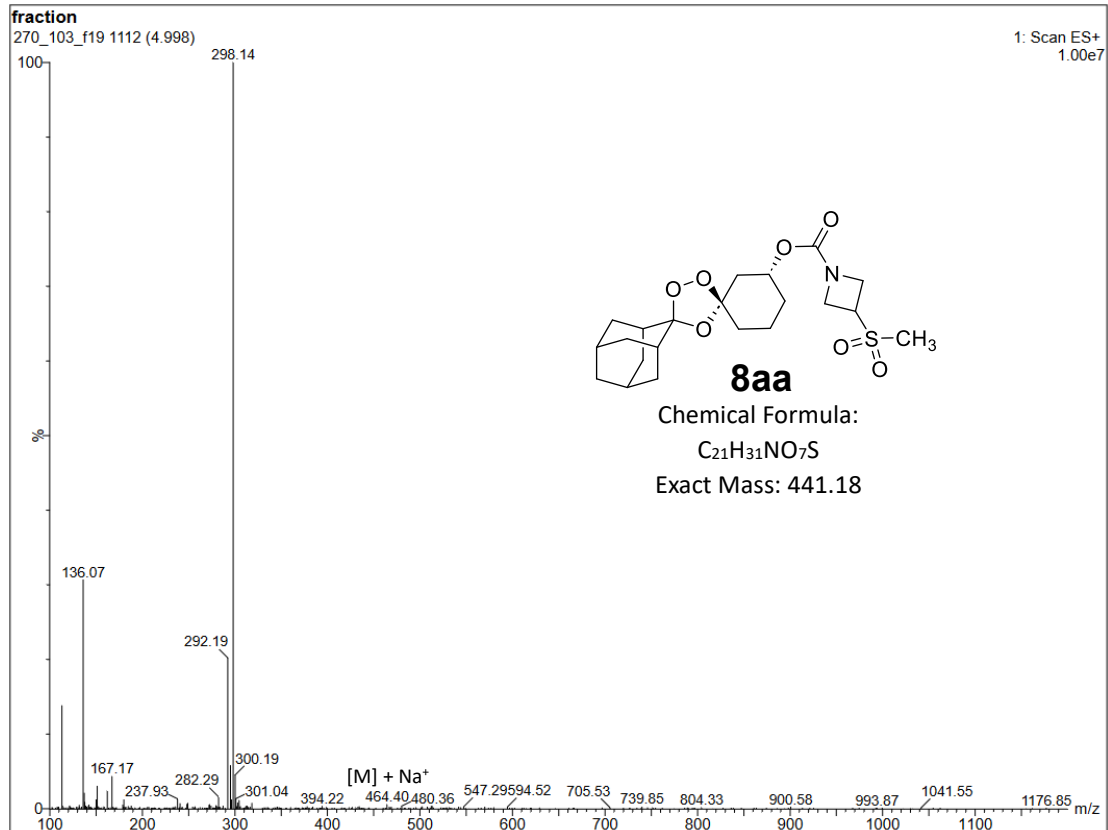
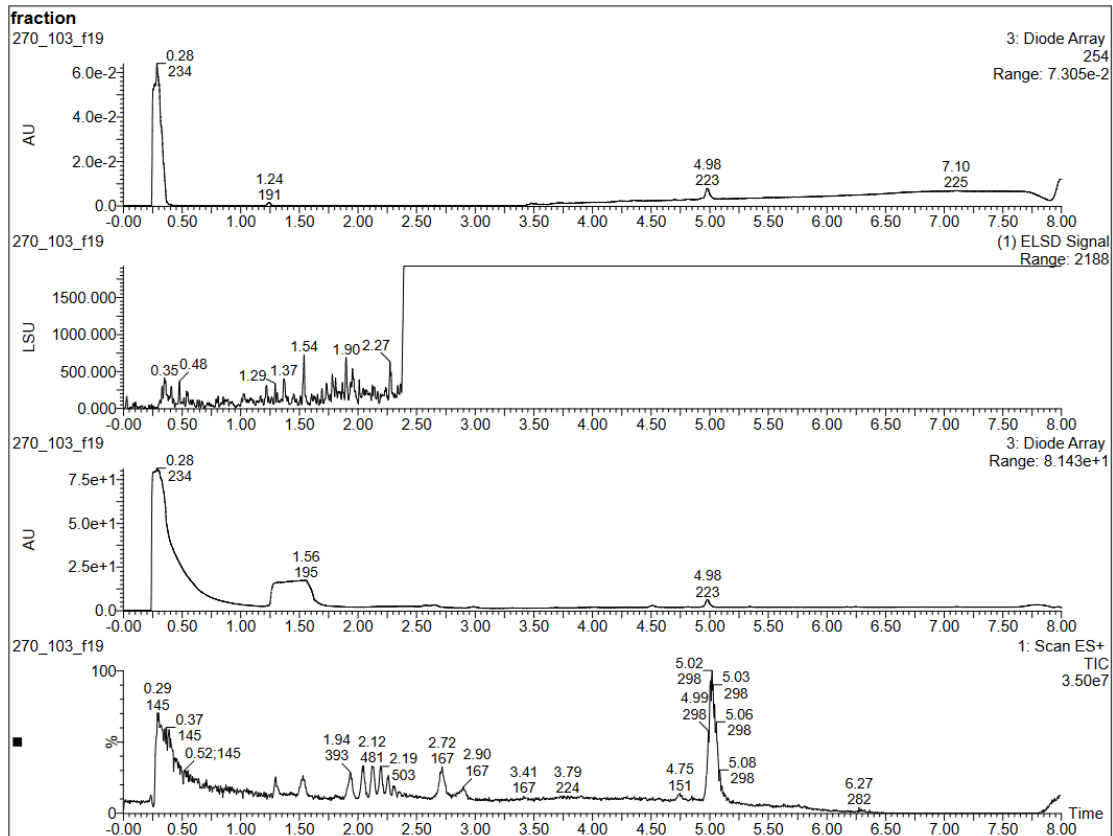


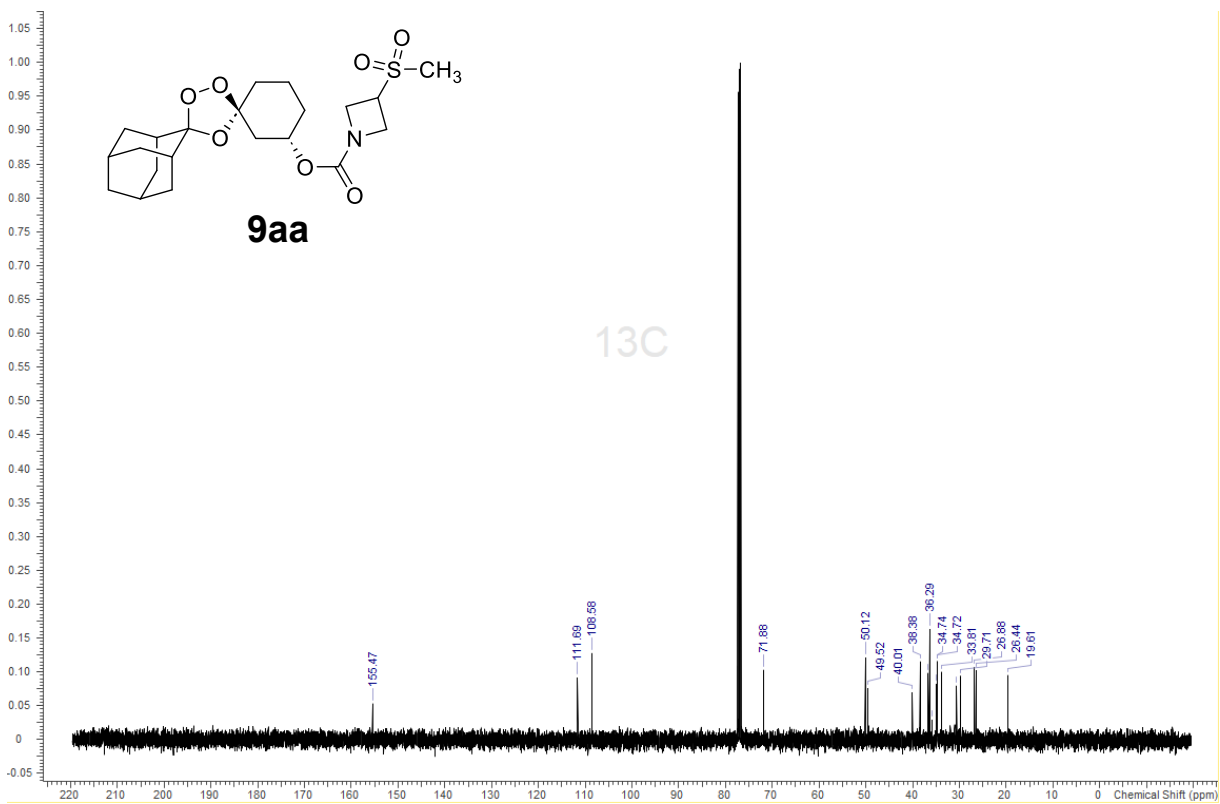
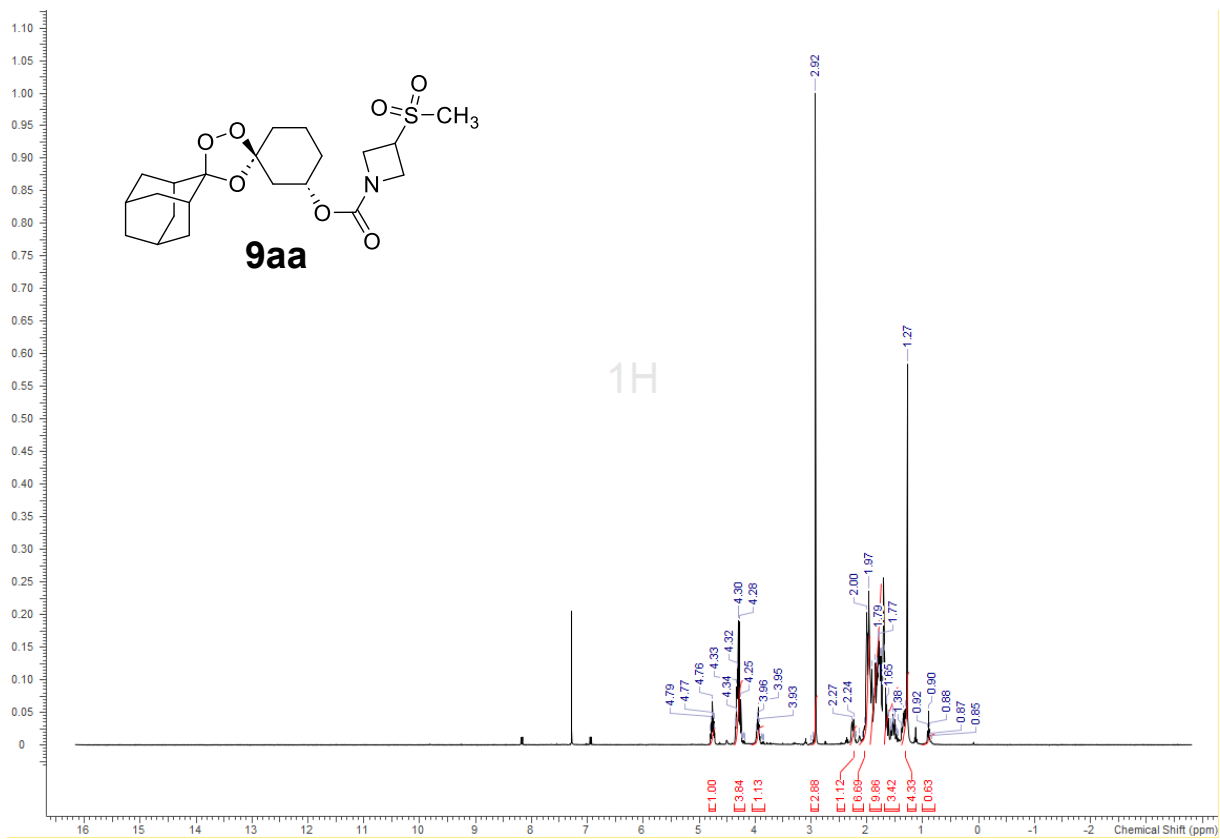


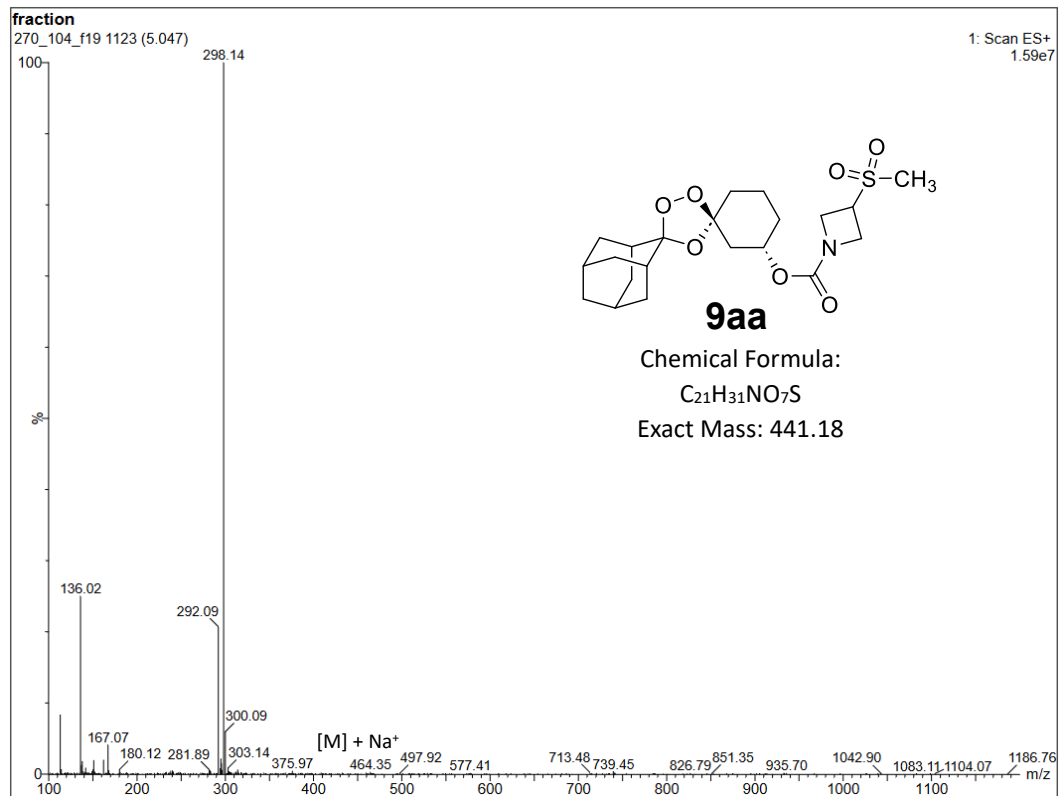
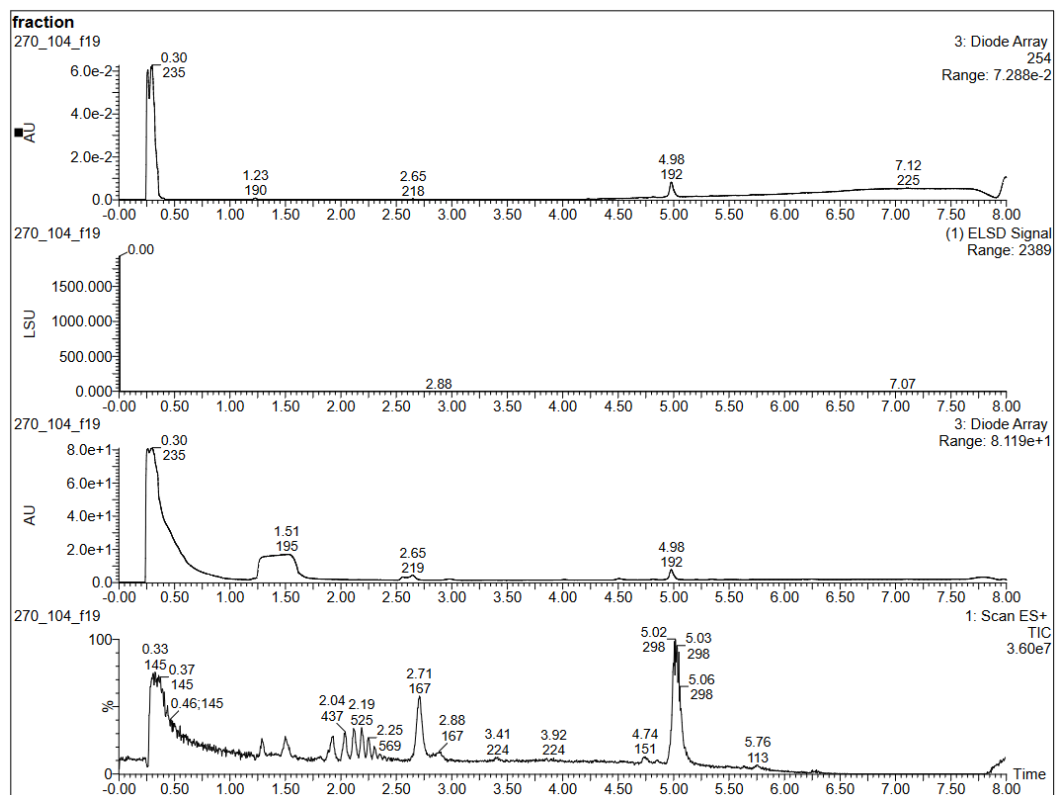


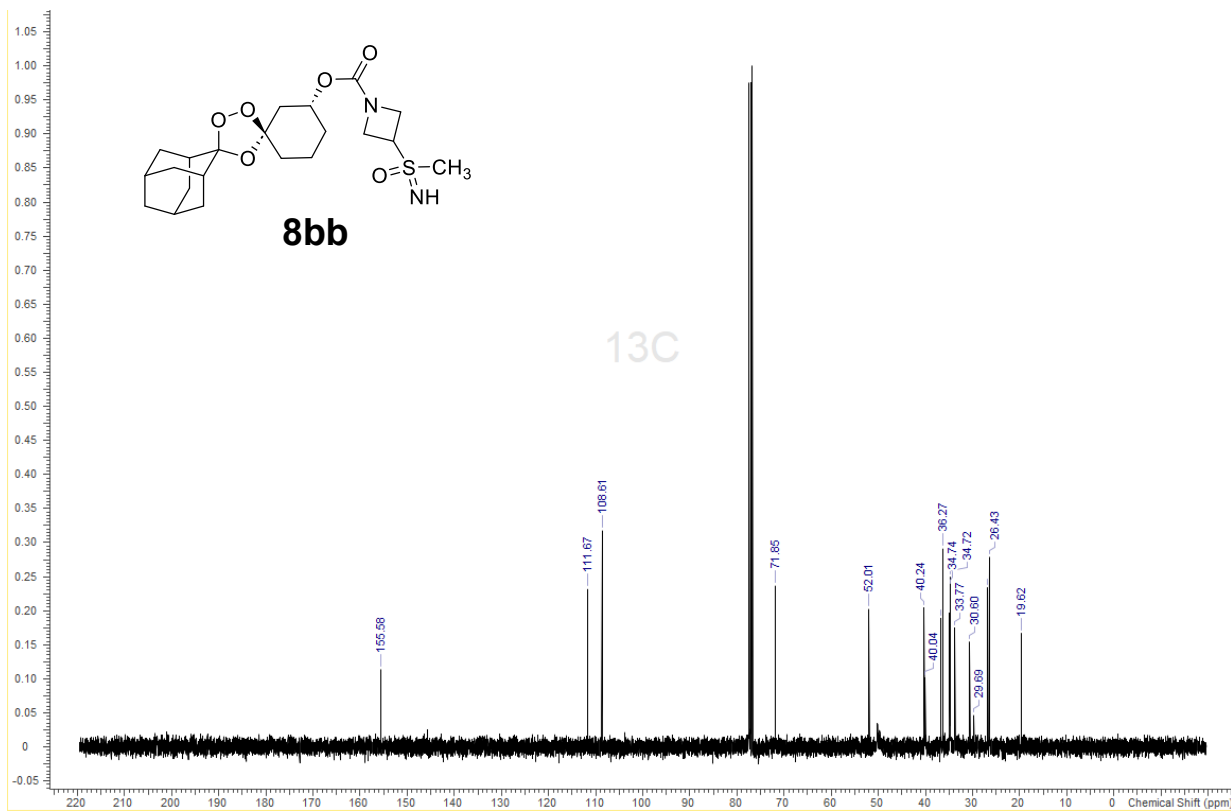
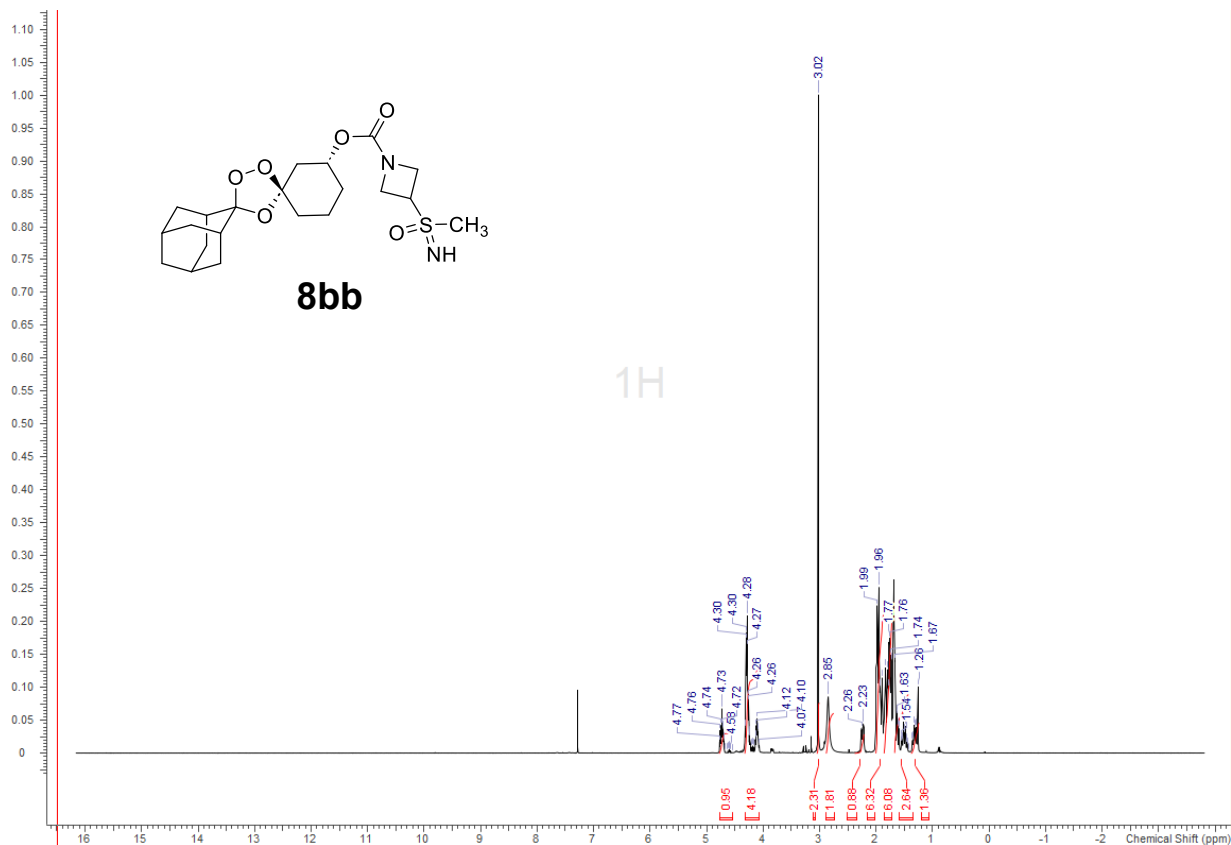


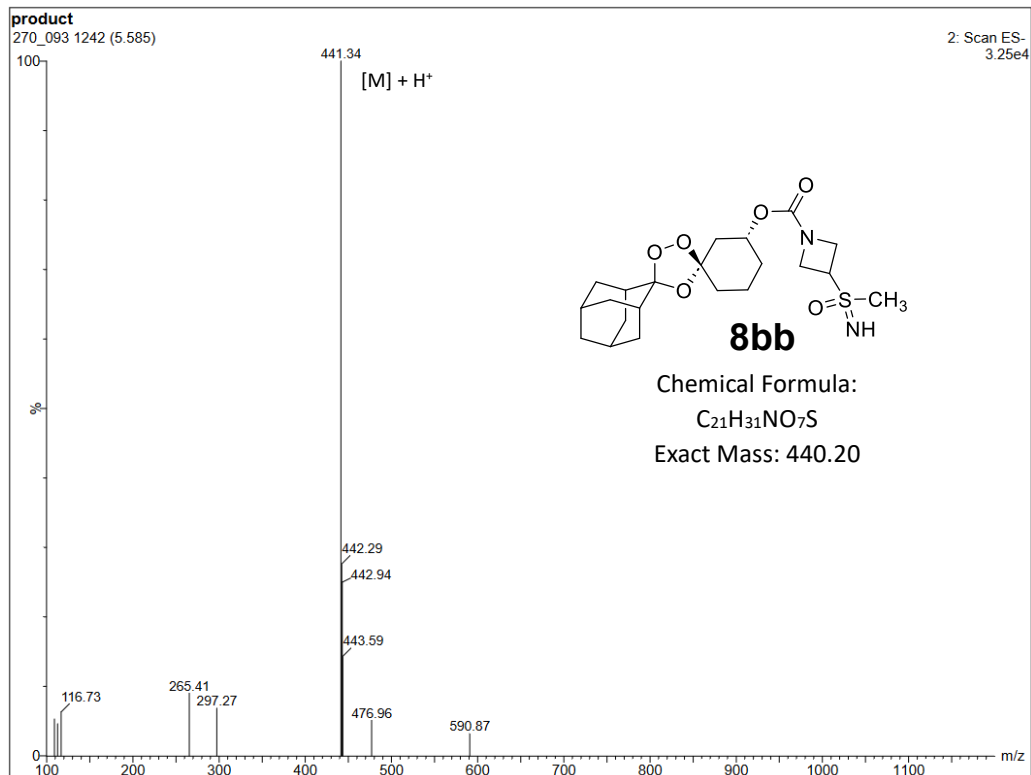
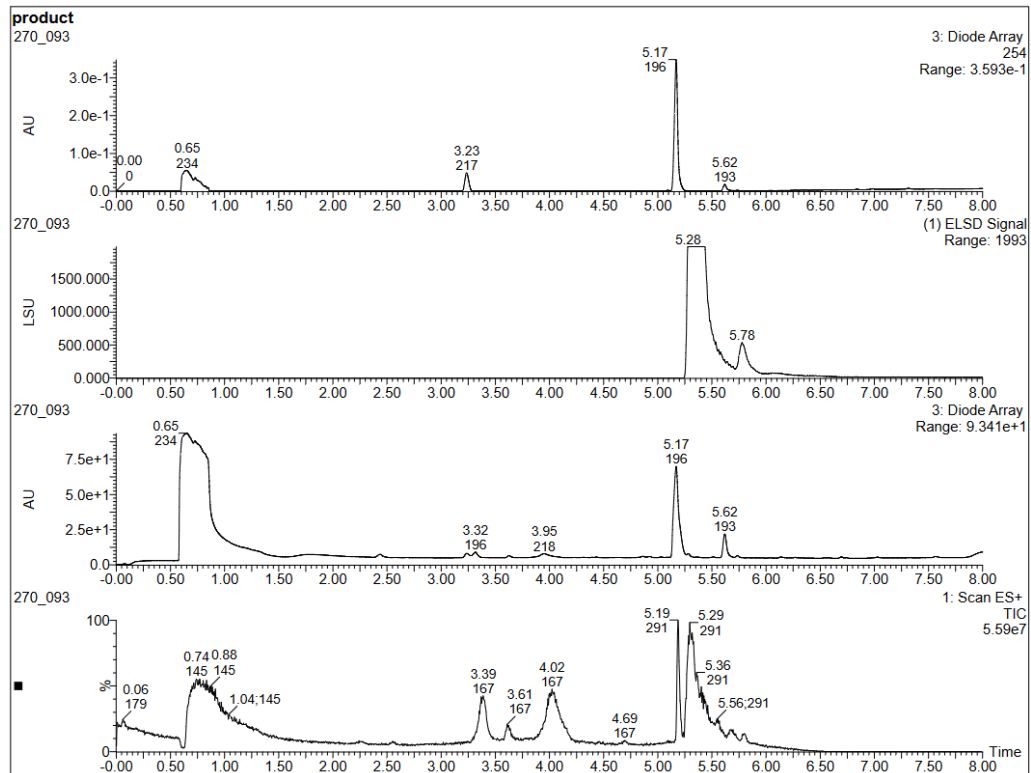


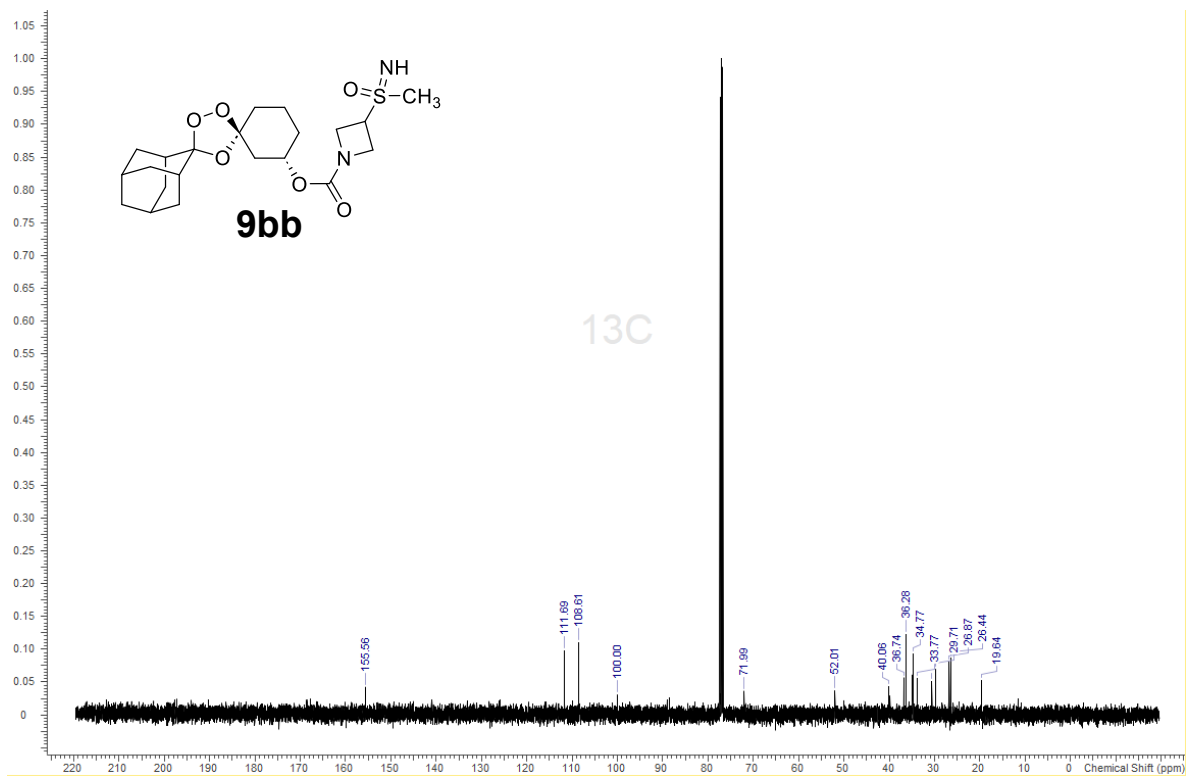
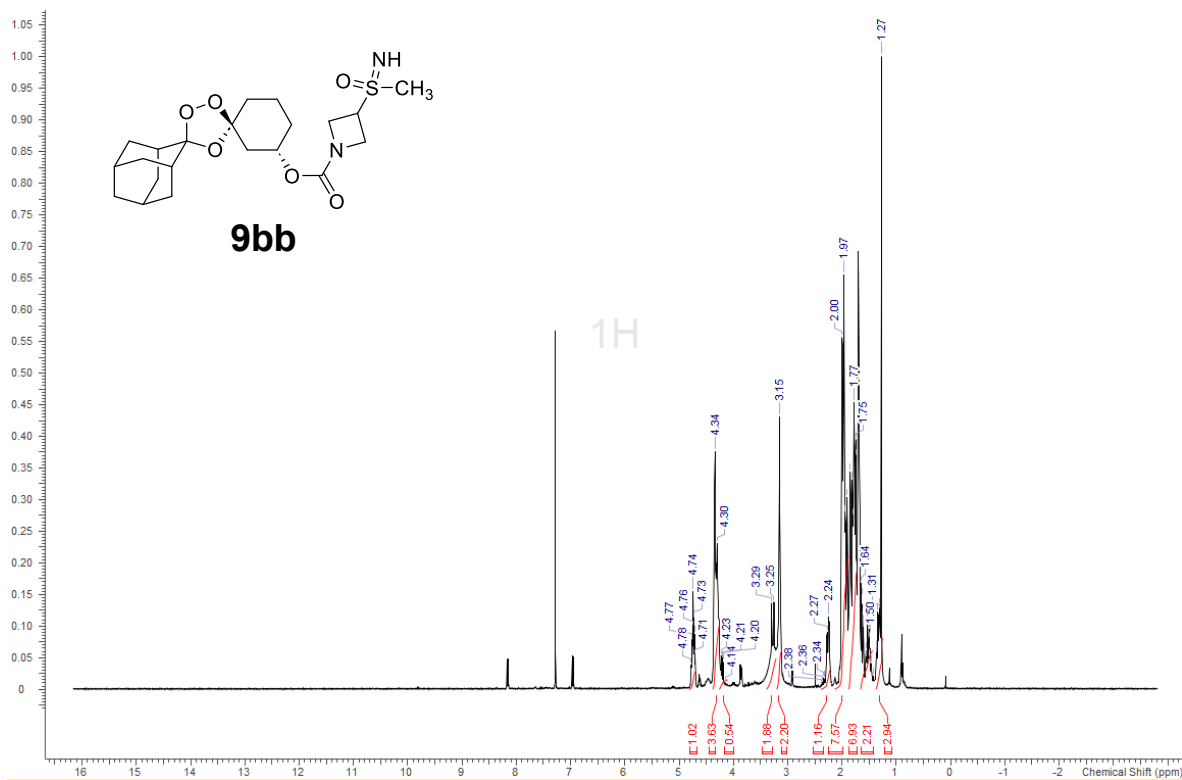


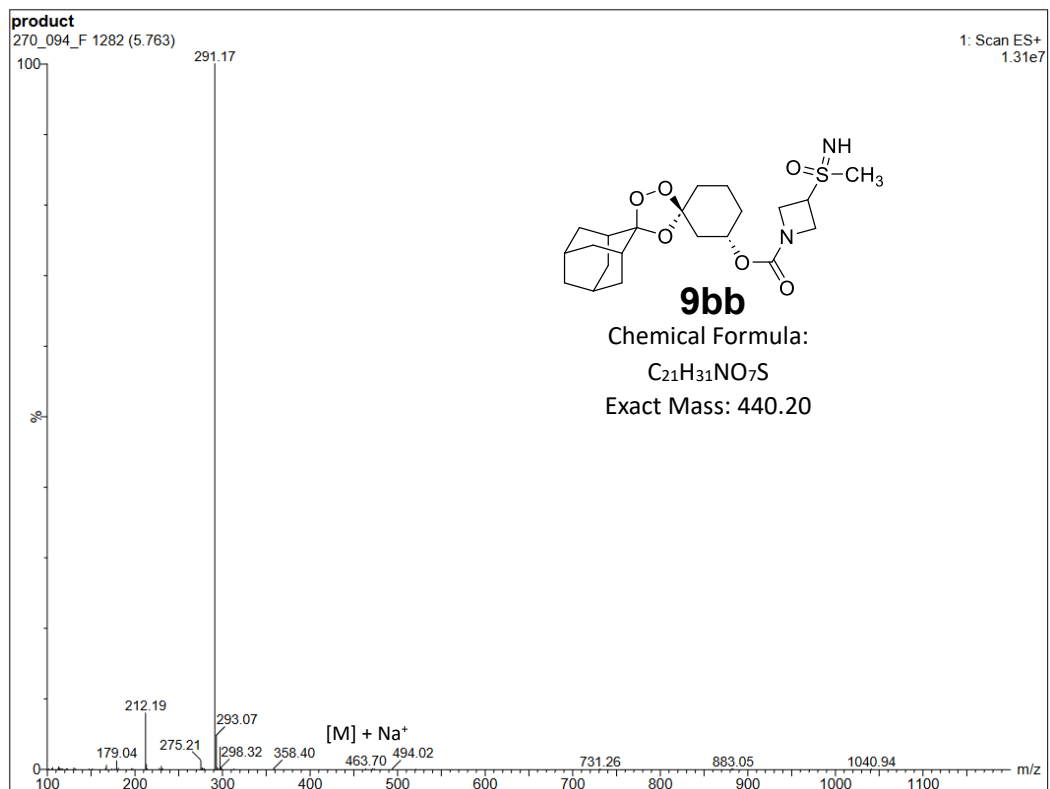
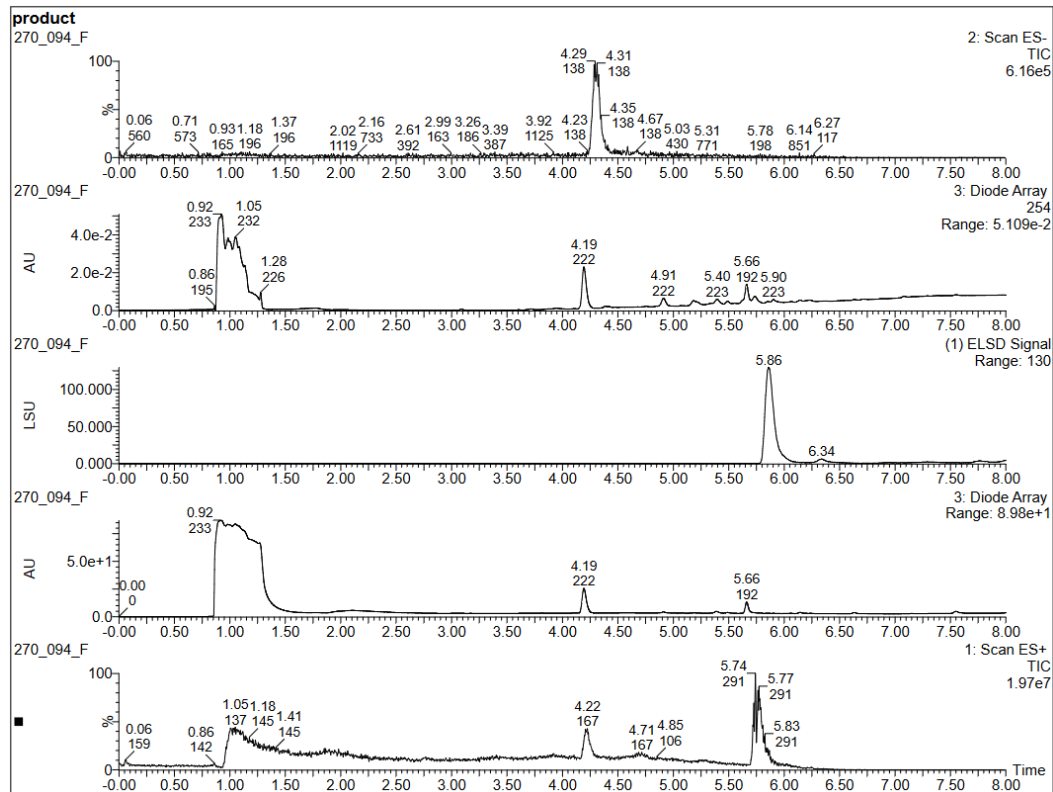


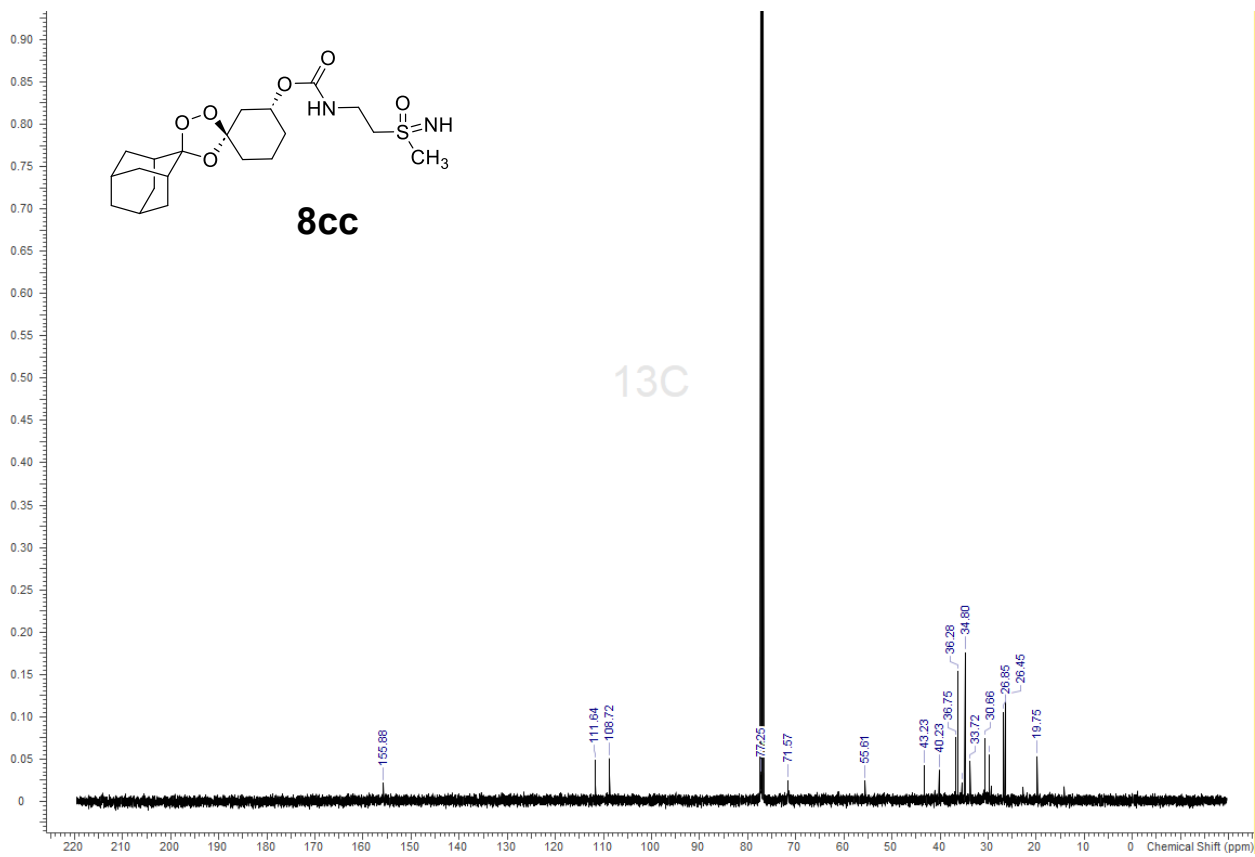
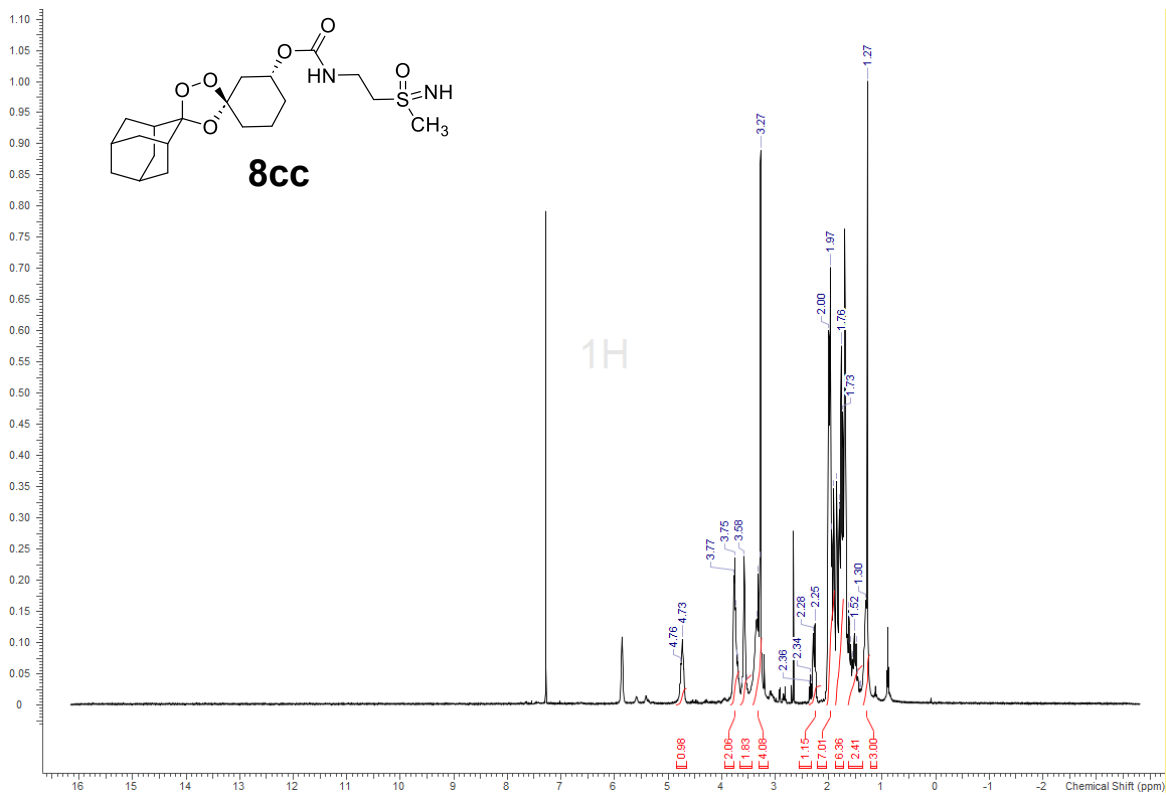


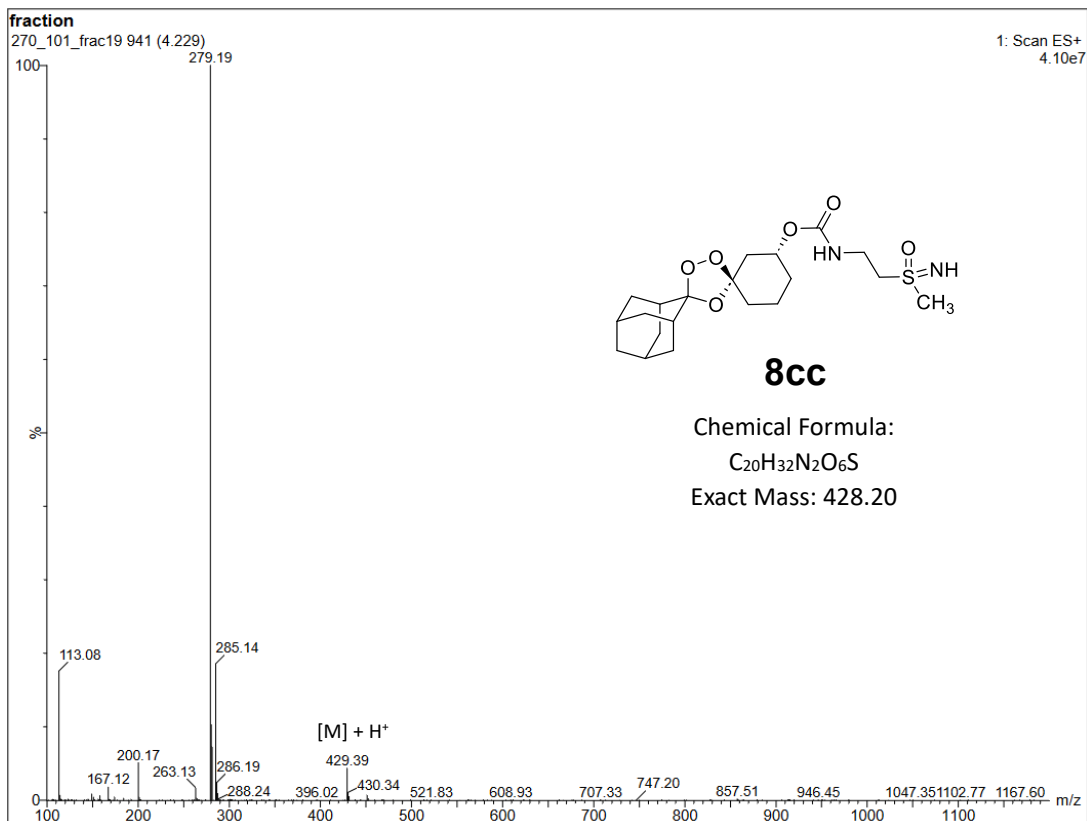
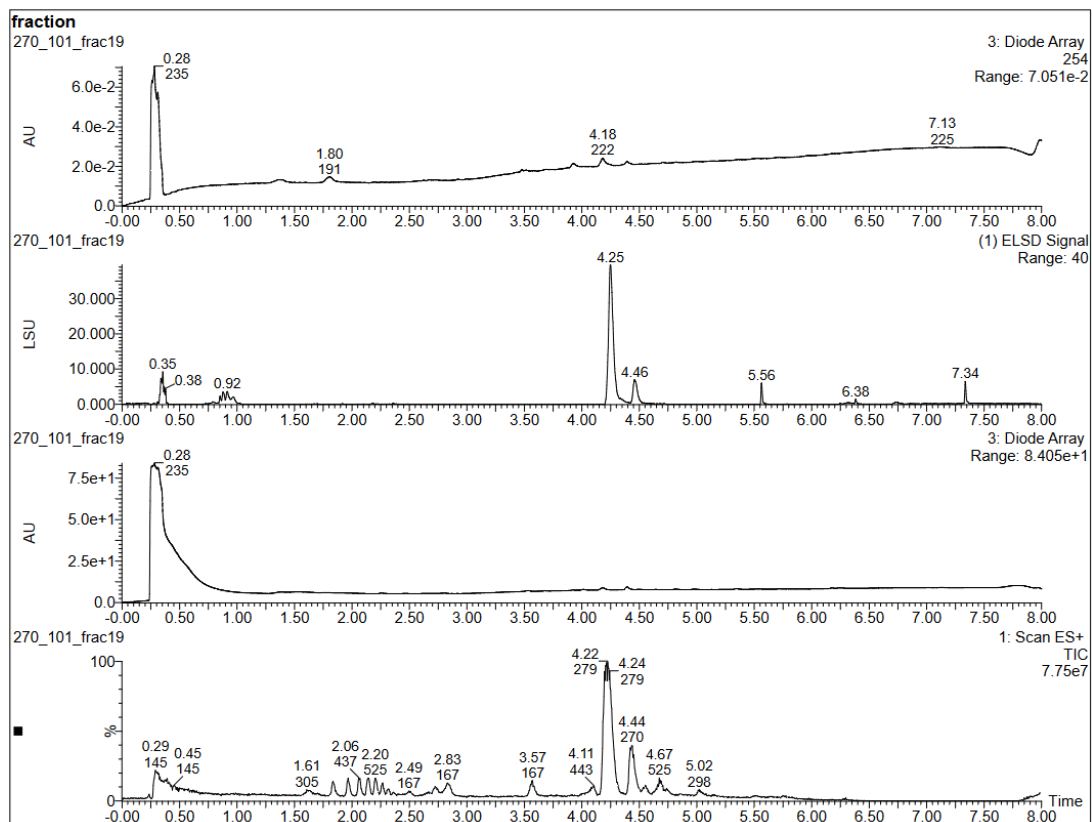


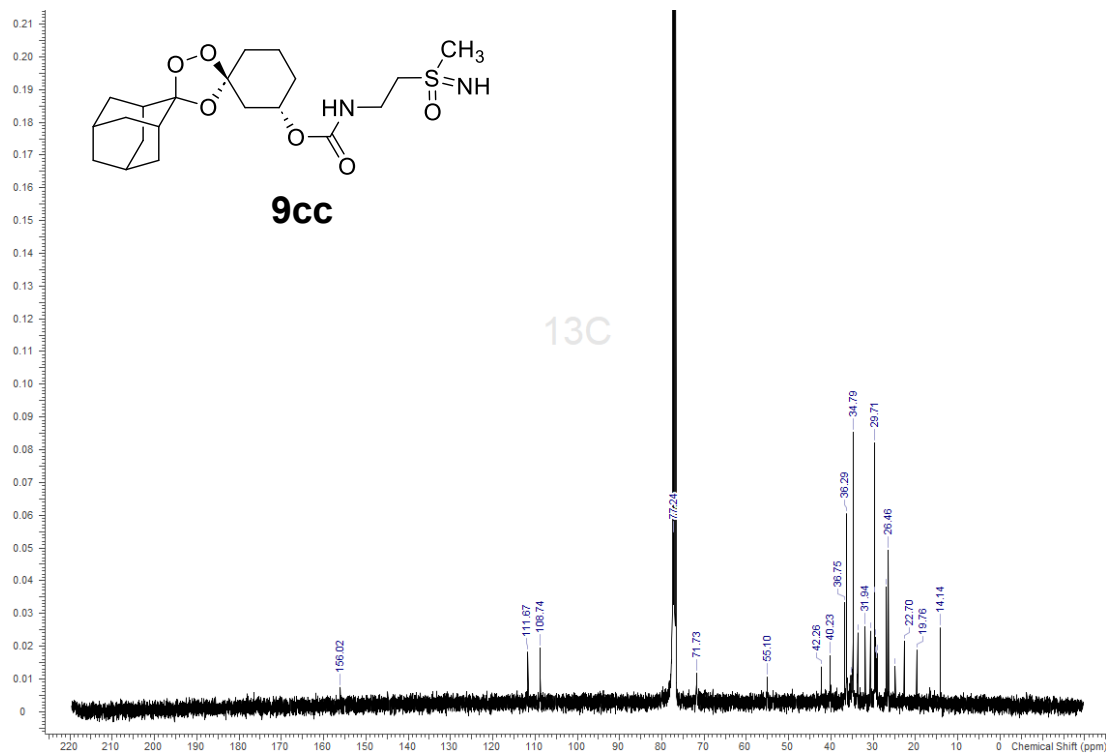
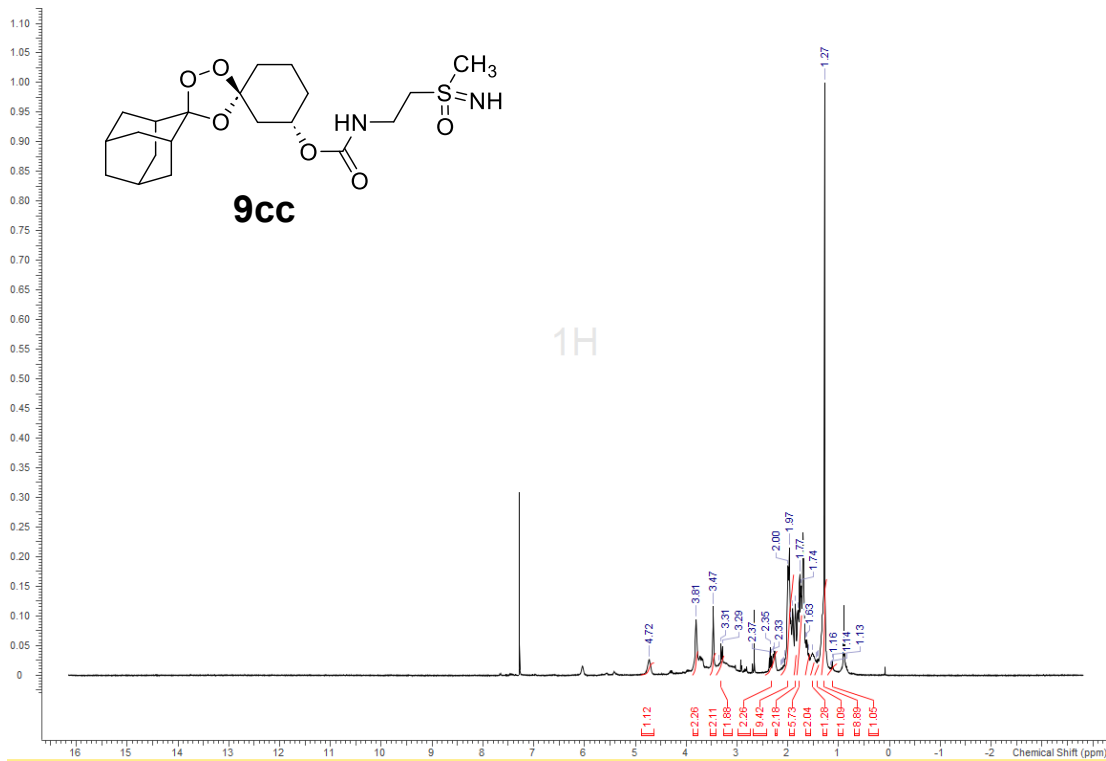


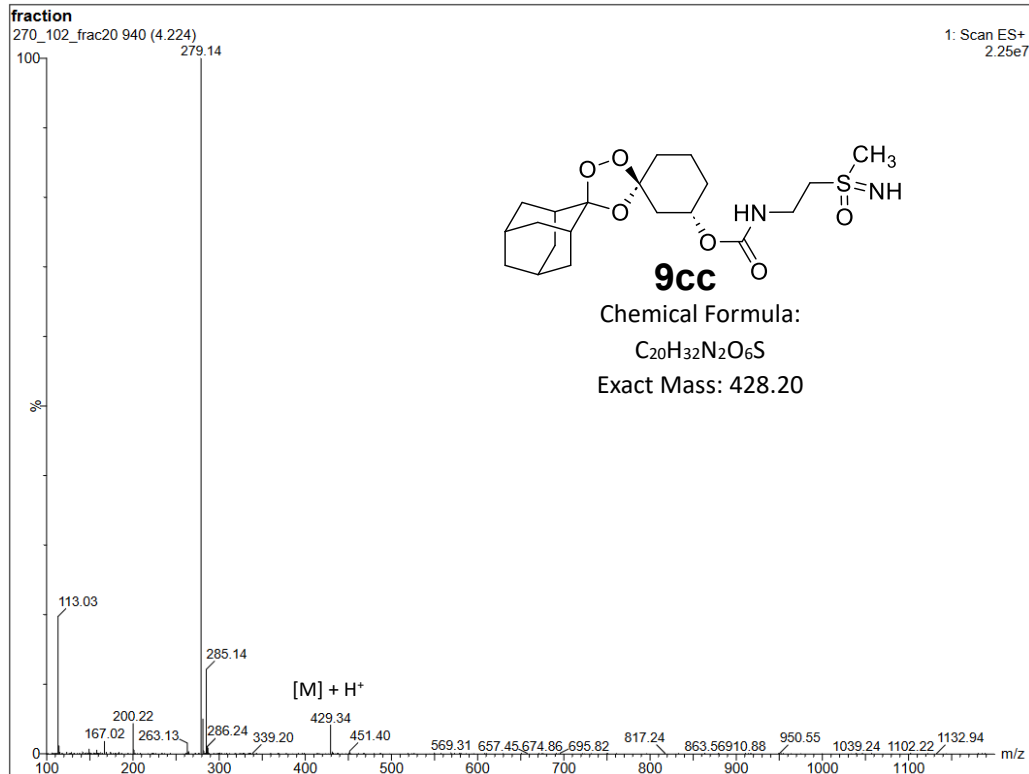
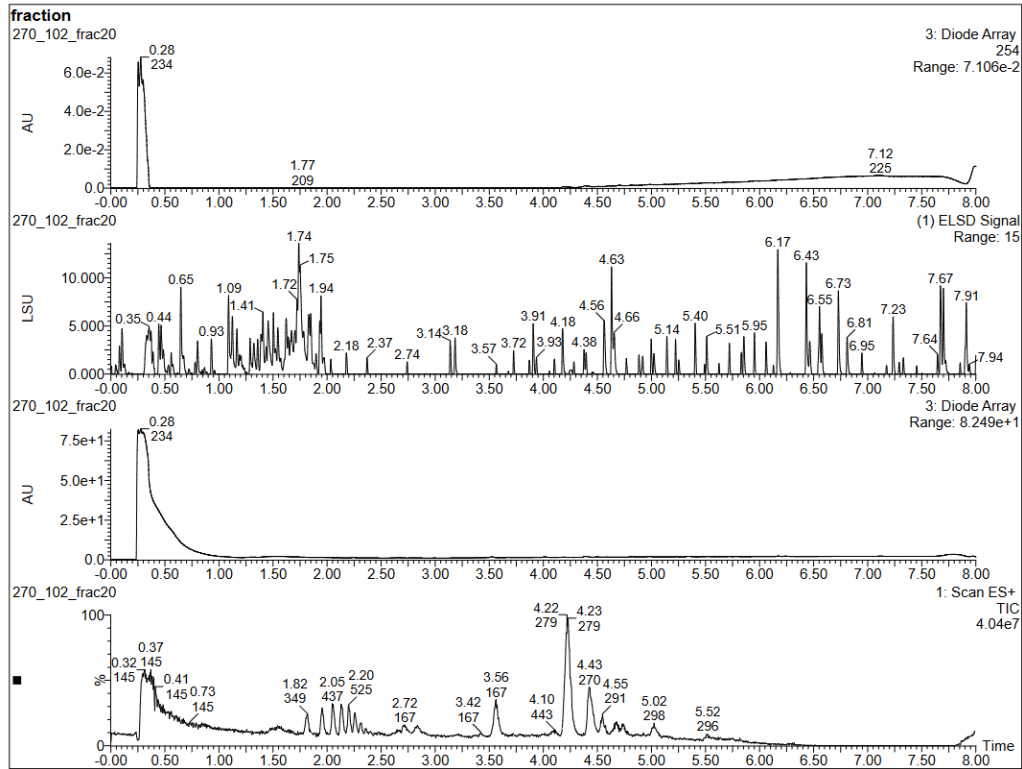


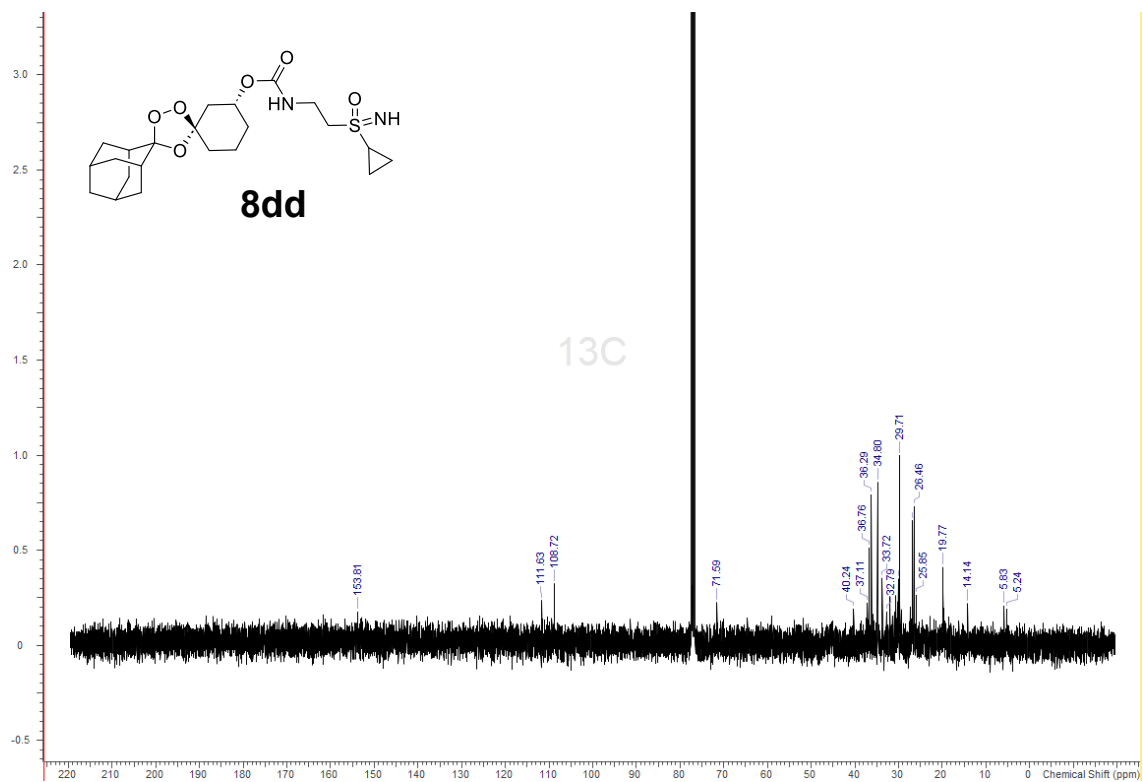
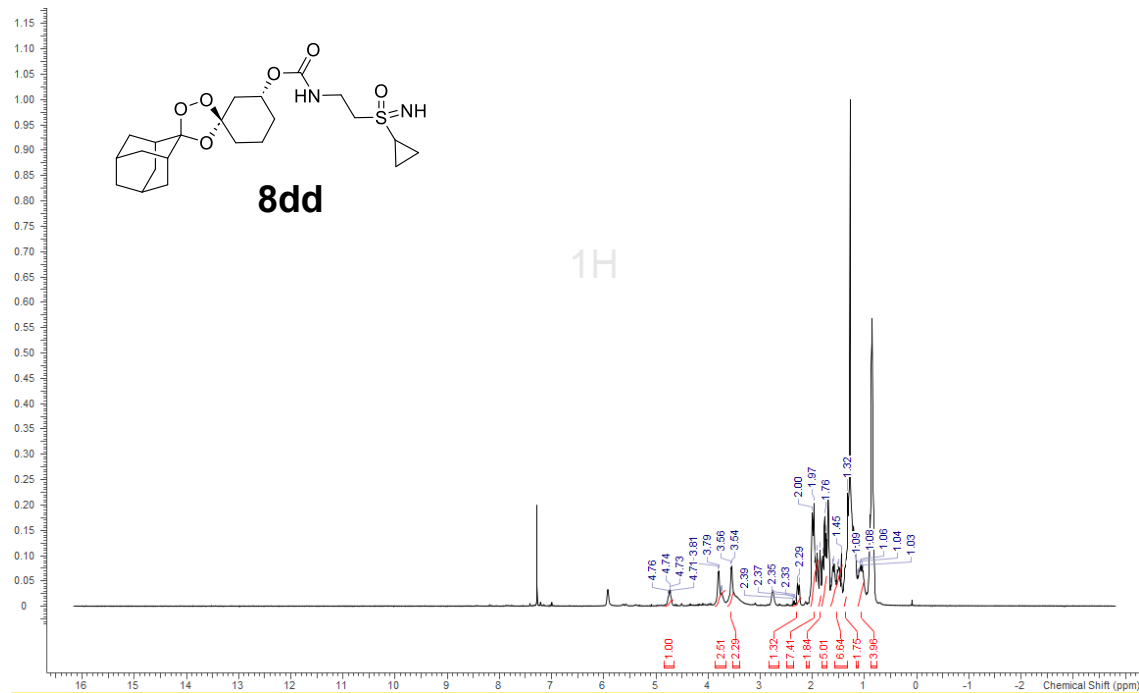


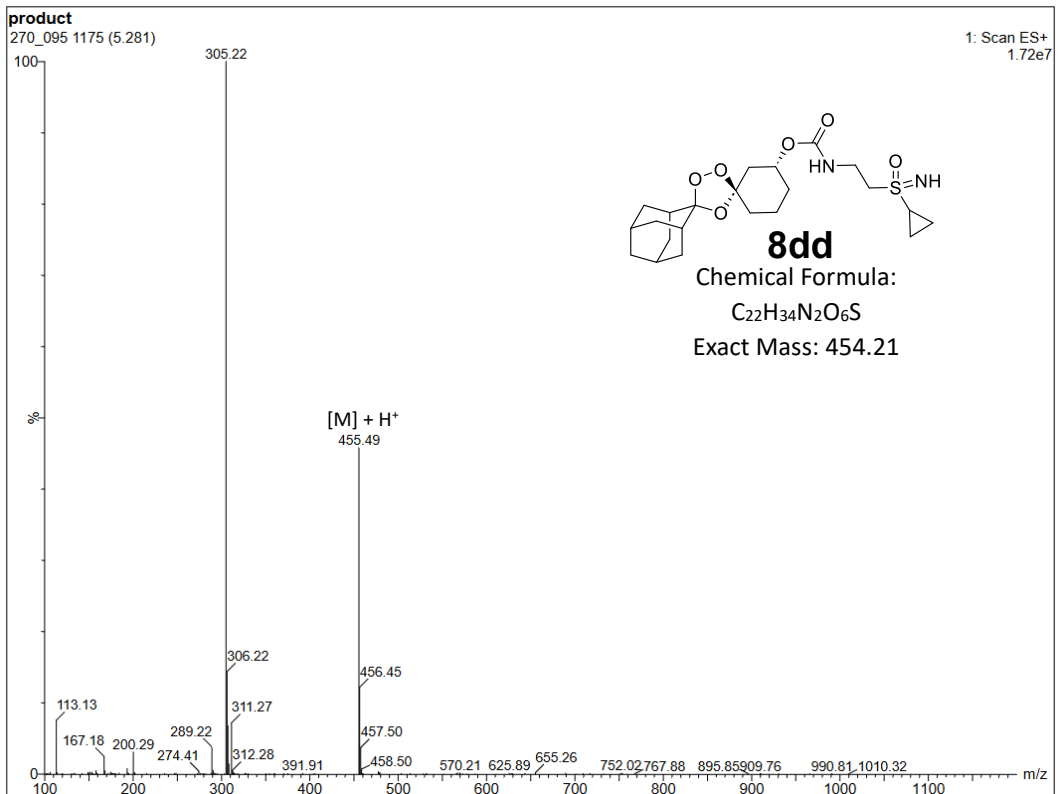
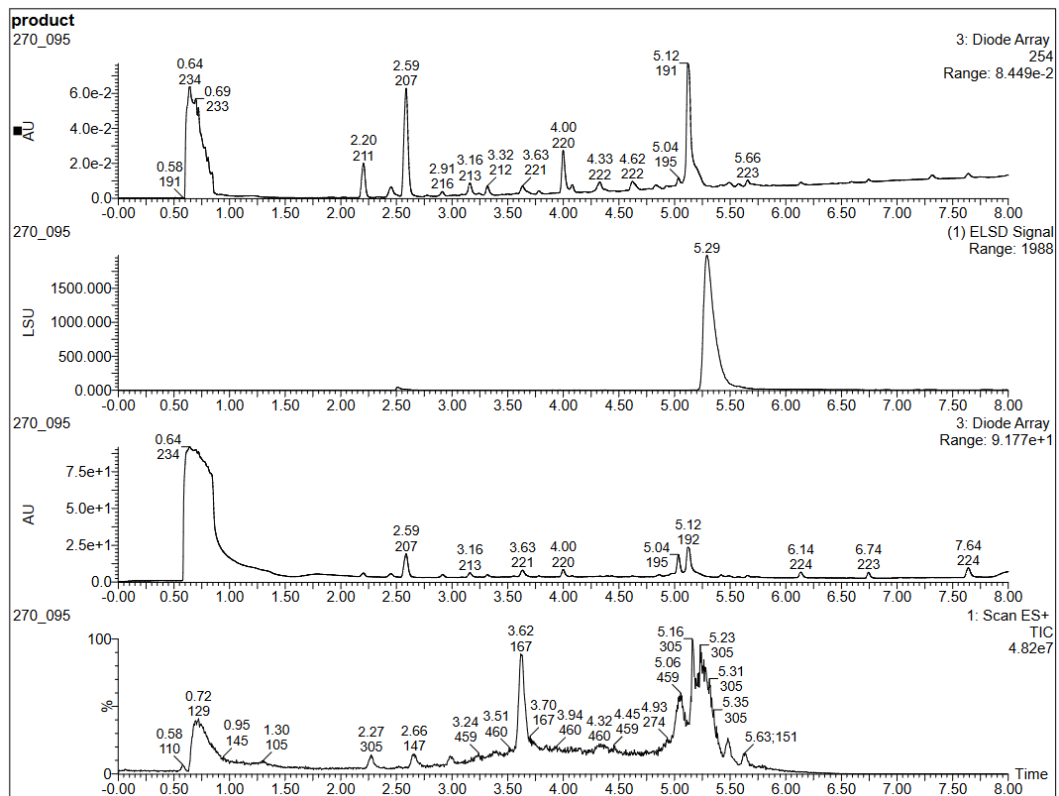


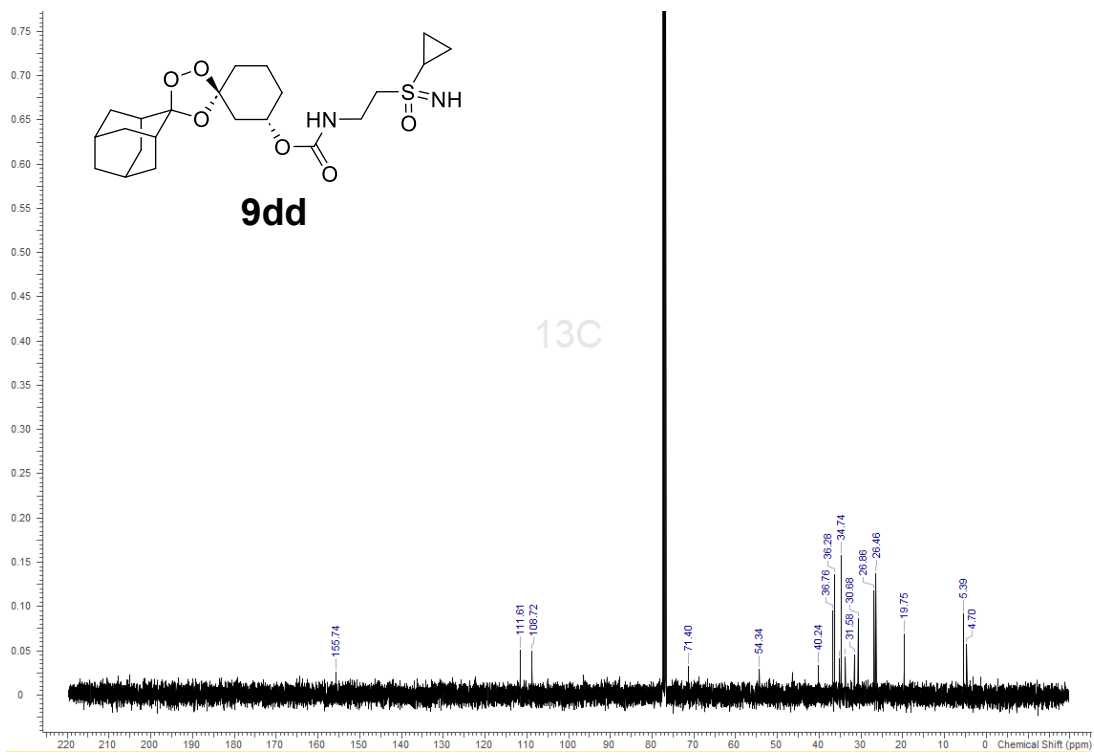
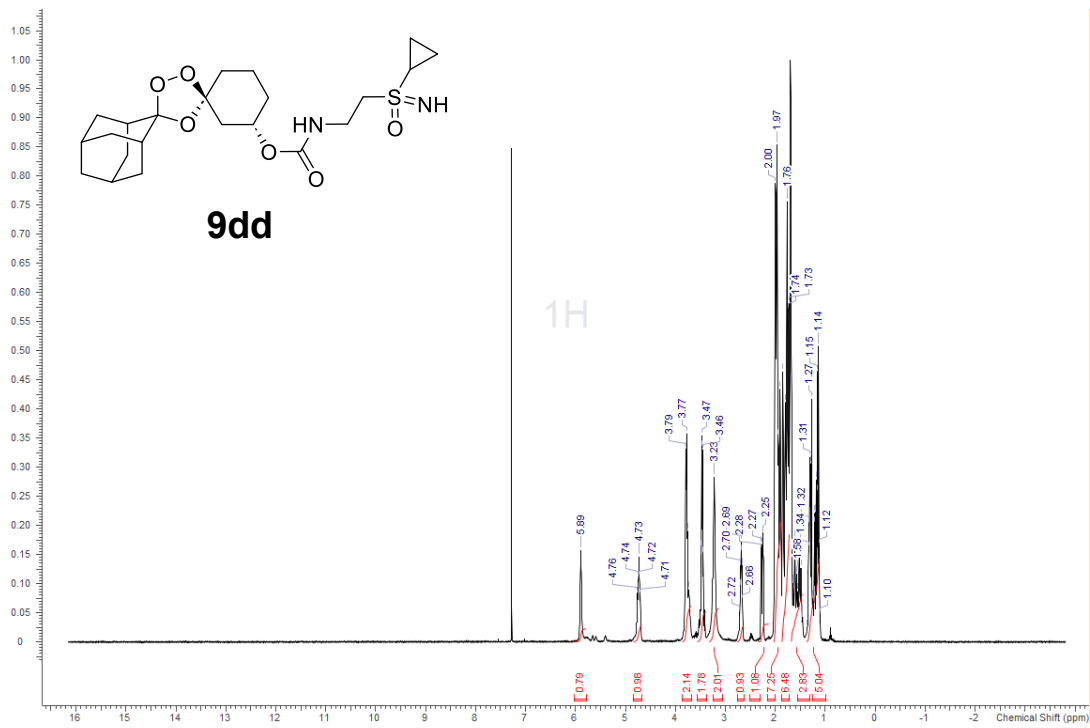


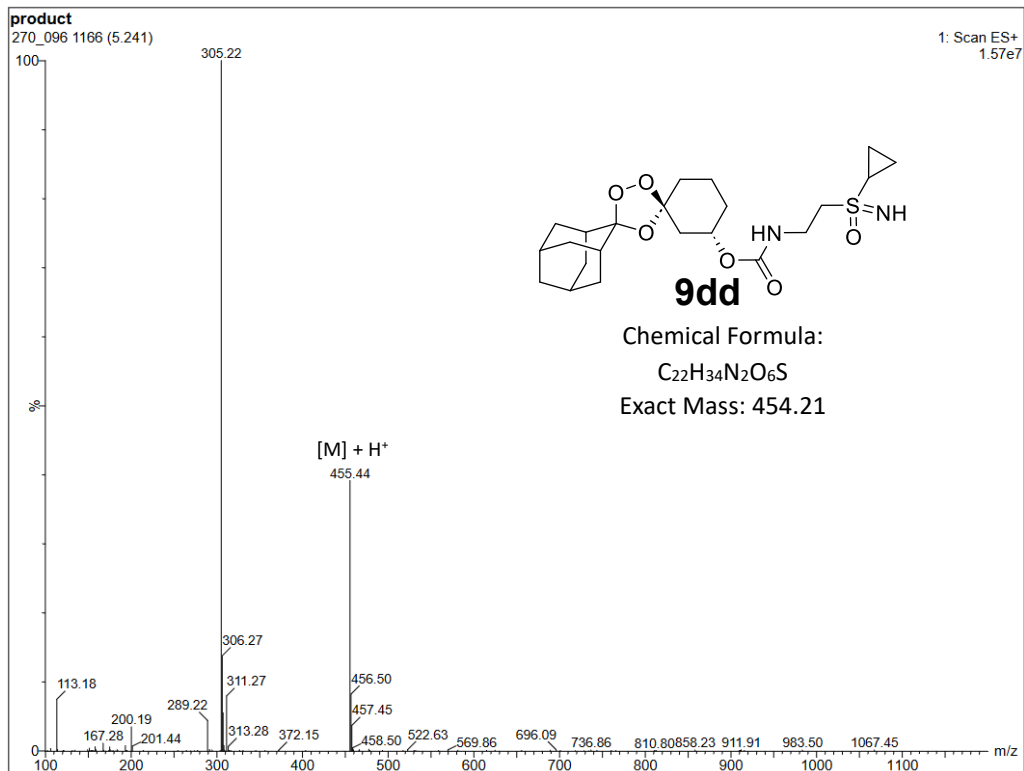
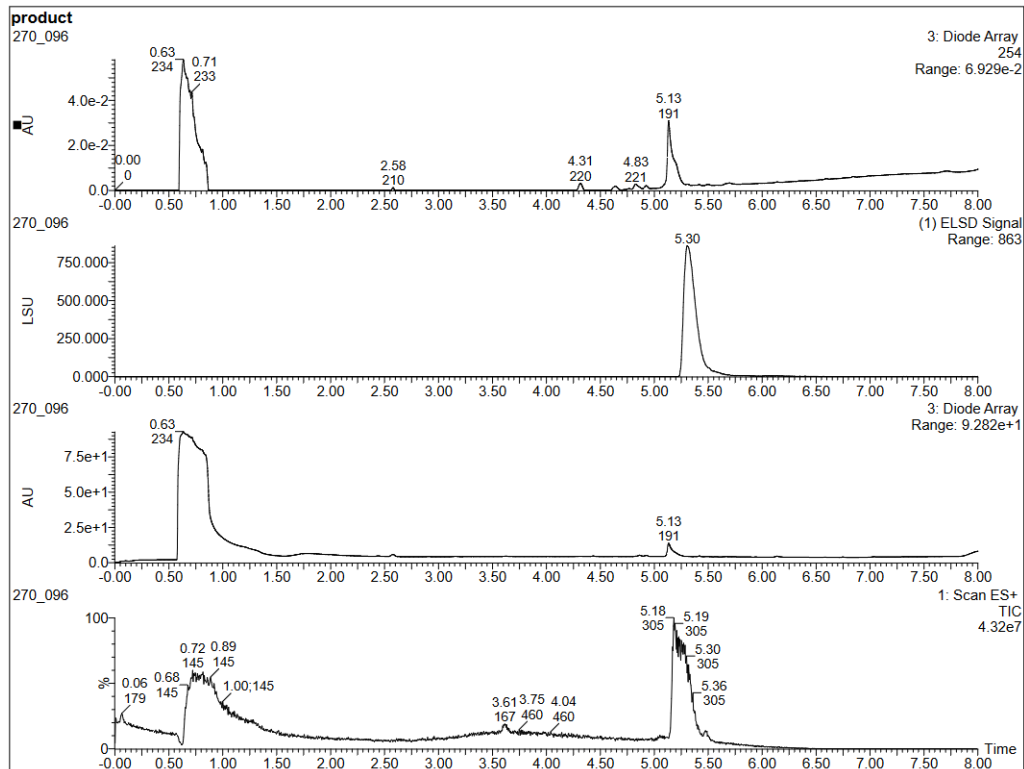












Chapter S3

Supporting Information for Chapter 3

Matthew T. Klope, Poulami Talukder, Brian R. Blank, Jun Chen, Priyadarshini Jaishankar, Ryan L. Gonciarz, Aswathy Vinod, Vineet Mathur, Juan Tapia, Jennifer Legac, Avani Narayan, Shaun D. Fontaine, Philip J. Rosenthal, Adam R. Renslo

Supplementary Figures

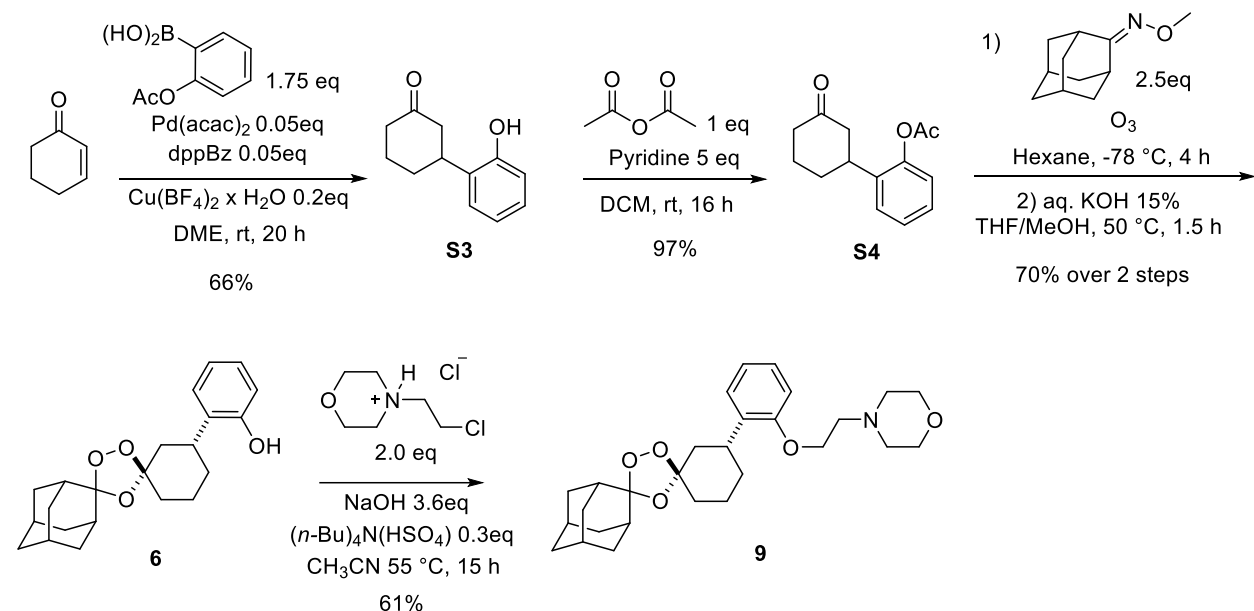


Figure S3-1. Synthesis of *ortho trans*-3' Artefenomel regioisomer

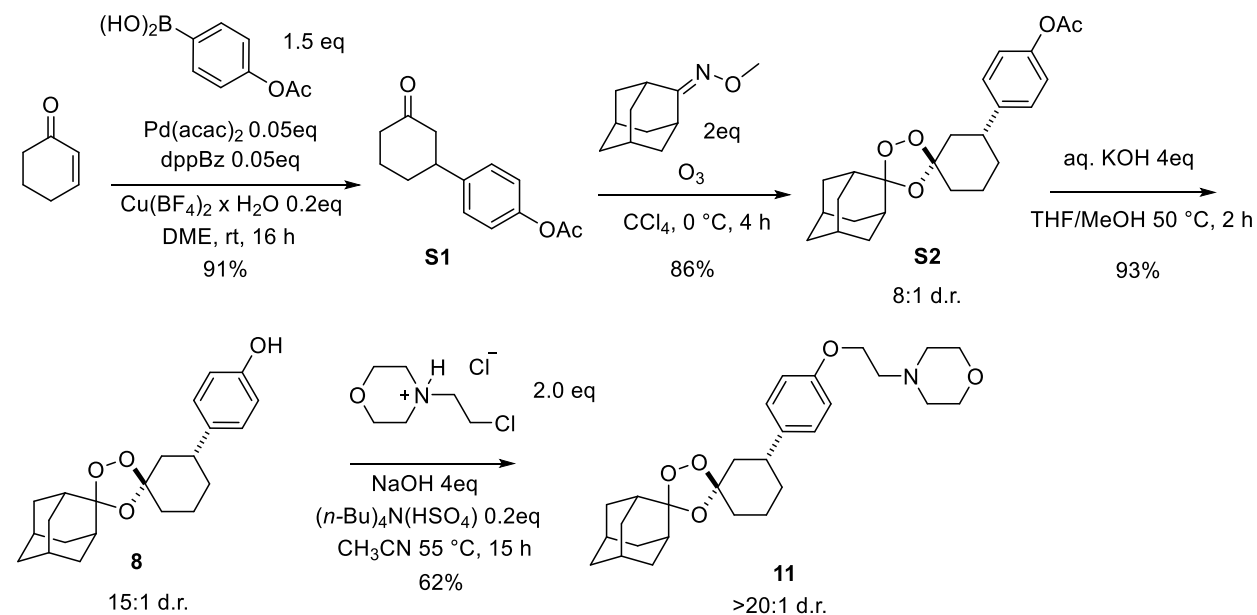


Figure S3-2. Synthesis of *para trans*-3' Artefenomel regioisomer

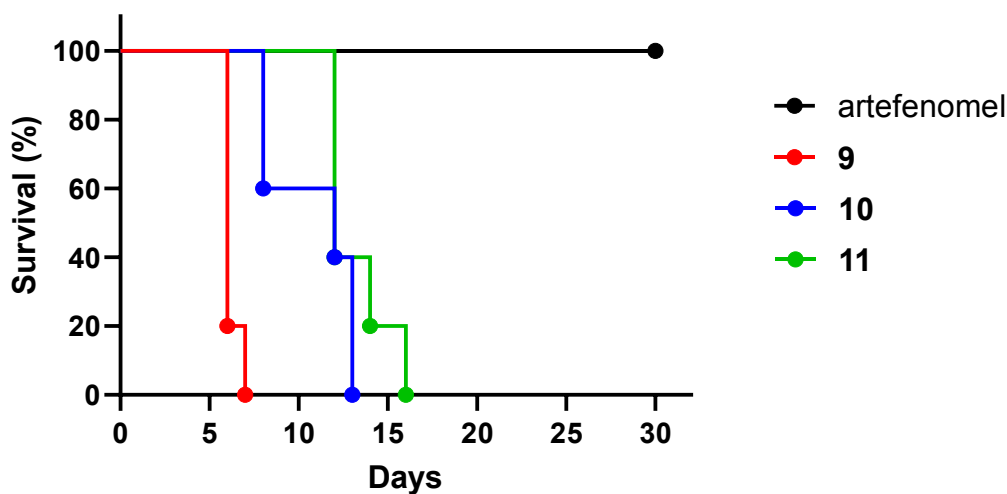


Figure S3-3. Artefenomel regioisomers versus Artefenomel in rodent *P. berghei* malaria model. Days survival in infected mice following a single 20mg/kg dose on day 0 (n=5 per group)

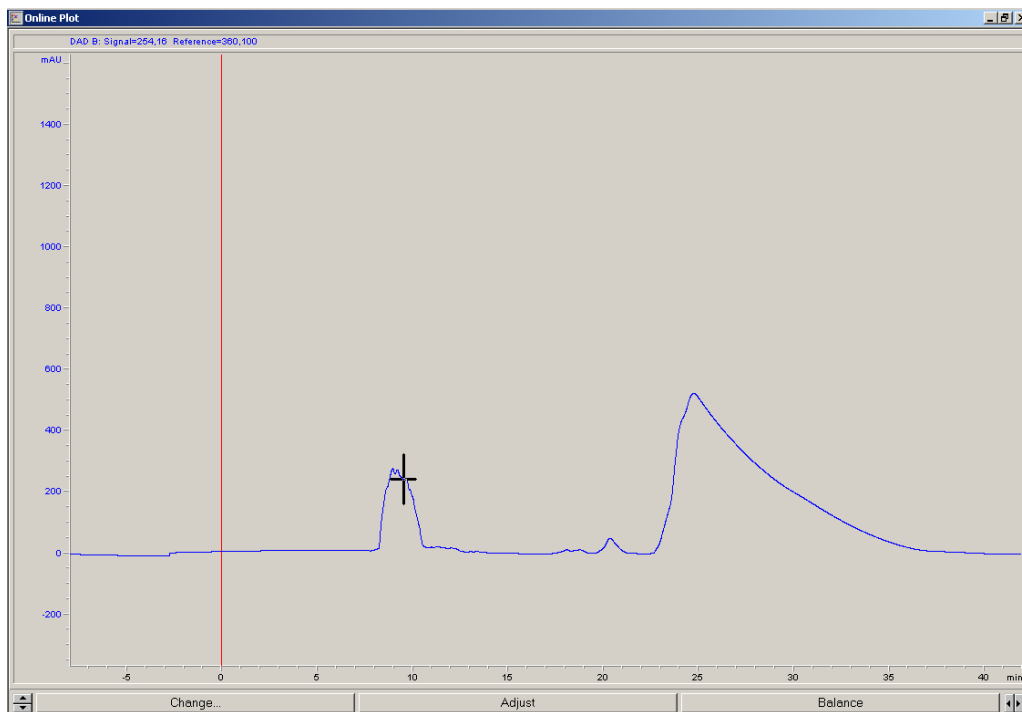


Figure S3-4A. HPLC (Agilent 1200 Series) trace of **17R** using a 5uM Cellulose-3 column (Phenomenex) with an isocratic mobile phase consisting of 40:60 20mM Ammonium Bicarbonate in Acetonitrile (with 0.1% Diethylamine). Solvent front at 10min. Retention time = 26min

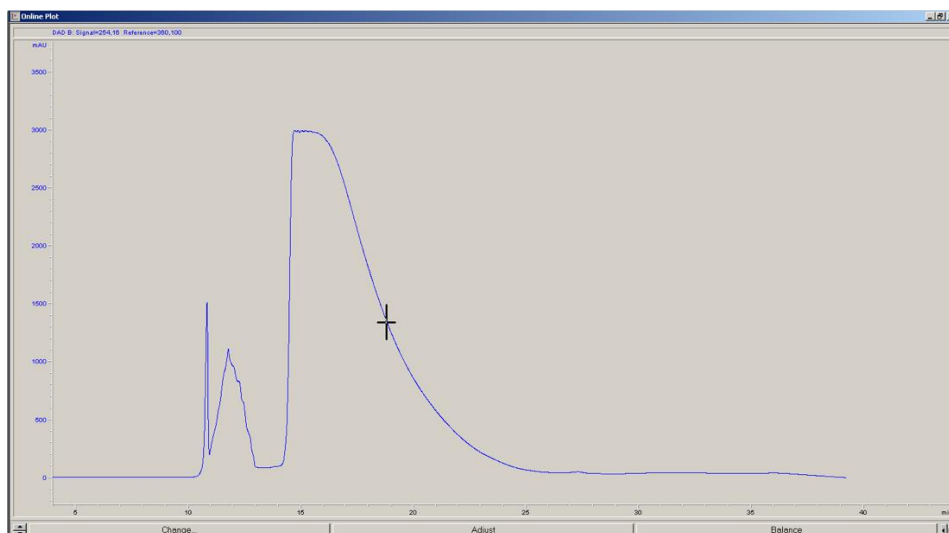


Figure S3-4B. HPLC (Agilent 1200 Series) trace of **17S** using a 5 μ M Cellulose-3 column (Phenomenex) with an isocratic mobile phase consisting of 40:60 20mM Ammonium Bicarbonate in Acetonitrile (with 0.1% Diethylamine). Solvent front at 12min. Retention time = 16min

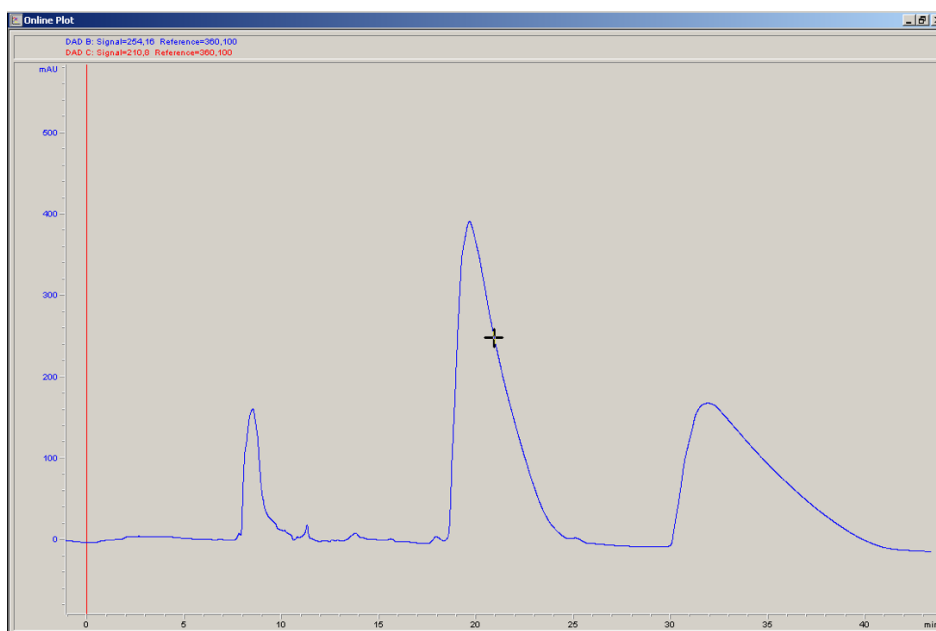


Figure S3-4C. HPLC (Agilent 1200 Series) trace of **17S** and **17R** coinjection using a 5 μ M Cellulose-3 column (Phenomenex) with an isocratic mobile phase consisting of 40:60 20mM Ammonium Bicarbonate in Acetonitrile (with 0.1% Diethylamine). Solvent front at 8min. P1 retention time = 19min P2 retention time = 32min

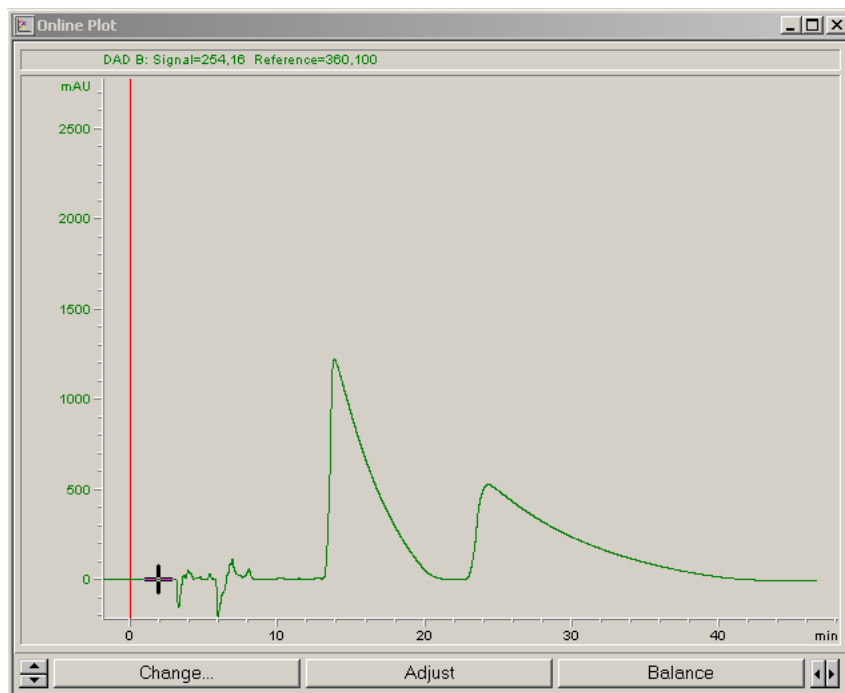


Figure S3-4D. HPLC (Agilent 1200 Series) trace of **17** (racemic) using a 5uM Cellulose-3 column (Phenomenex) with an isocratic mobile phase consisting of 40:60 20mM Ammonium Bicarbonate in Acetonitrile (with 0.1% Diethylamine). Solvent front at 8min. P1 retention time = 16min P2 retention time = 26min

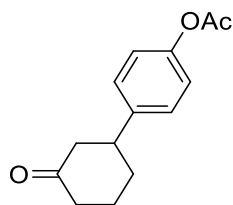
Supplementary Tables

Conditions	Aqueous Solubility (μM)
17 purified in 15:85 Methanol (0.1% Ammonia):DCM	3.5
17 purified in 40:60 20mM Ammonium Bicarbonate in Acetonitrile (with 0.1% Diethylamine)	11.5

Table S3-1. Measured aqueous solubility of **17** purified under original column conditions and chiral column conditions. Data generated for this study by Analiza, Inc., Cleveland, OH.

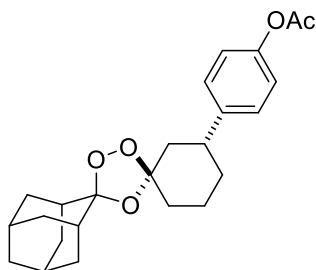
Synthetic Procedures

Para aryl intermediates and final compounds



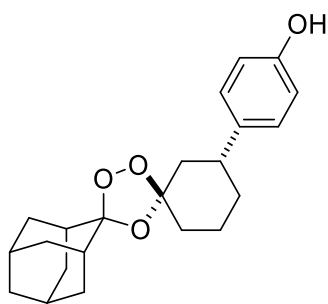
4-(3-oxocyclohexyl)phenyl acetate (S1).

To a solution of 4-acetoxyphenylboronic acid (2.79 g, 15.19 mmol) in anhydrous DME (60 mL) was added palladium(II) acetylacetonate (156 mg, 0.51 mmol), 1,2-bis(diphenylphosphino)benzene (231 mg, 0.51 mmol), H (484 mg, 2.02 mmol) and 2-cyclohexen-1-one (1 mL, 10.12 mmol). The reaction mixture was stirred at room temperature for 16 h under argon atmosphere. The solvent was removed in *vacuo*. The residue was purified by column chromatography (petroleum ether / ethyl acetate = 1/10) to afford 4-(3-oxocyclohexyl)phenyl acetate (2.1 g, 91% yield) as a white solid. ^1H NMR (400 MHz, CDCl_3) δ 7.22 (d, J = 8.5 Hz, 2H), 7.04 (d, J = 8.5 Hz, 2H), 3.08–2.93 (m, 1H), 2.64–2.55 (m, 1H), 2.55–2.42 (m, 2H), 2.42–2.32 (m, 1H), 2.29 (s, 3H), 2.19–2.03 (m, 2H), 1.90–1.70 (m, 2H); ^{13}C NMR (100 MHz, CDCl_3) δ 210.8, 169.6, 149.2, 141.8, 127.5, 121.7, 48.9, 44.1, 41.1, 32.7, 25.4, 21.1; LCMS: Calculated Exact Mass = 232.1, Found $[\text{M}+\text{H}]^+$ (ESI+) = 233.1



trans-4-(dispiro[adamantane-2,3'-[1,2,4]trioxolane-5',1''-cyclohexan]-3''-yl)phenyl acetate (S2)

To a solution of adamantane-2-one O-methyl oxime (3.23 g, 18.0 mmol) in CCl₄ (100 mL) was added 4-(3-oxocyclohexyl)phenyl acetate (2.1 g, 9.0 mmol) at room temperature. The solution was then cooled to 0 °C and bubbled with ozone for 4 h. After completion, the reaction was purged with nitrogen for 10 minutes to remove any dissolved ozone. The solvent was removed in *vacuo*. The residue was purified by column chromatography (petroleum ether / ethyl acetate = 20/1) to afford *trans*-4-dispiro[adamantane-2,3'-[1,2,4]trioxolane-5',1''-cyclohexan]-3''-yl)phenyl acetate (3.1 g, 86% yield) as a white solid. The diastereoselectivity of reaction was determined by ¹H NMR to be 8.1:1 in favor of the *trans* diastereomer. ¹H NMR (400 MHz, CDCl₃) δ 7.24–7.18 (m, 2H), 7.05–6.98 (m, 2H), 2.95 (tt, *J* = 12.7, 3.1 Hz, 1H, minor diastereomer), 2.81 (tt, *J* = 12.8, 3.3 Hz, 1H), 2.29 (s, 3H), 2.18–2.09 (m, 1H), 2.04–1.55 (m, 20H), 1.44–1.30 (m, 1H); ¹³C NMR (100 MHz, CDCl₃) δ 169.6, 148.9, 143.3 (minor diastereomer), 143.1, 127.7, 121.4, 111.8 (minor diastereomer), 111.3, 108.9, 46.9 (minor diastereomer), 42.1, 41.6 (minor diastereomer), 41.3, 41.0 (minor diastereomer), 39.2 (minor diastereomer), 36.7, 36.4, 36.3 (minor diastereomer), 35.0 (minor diastereomer), 34.9 (minor diastereomer), 34.8, 34.7, 34.1, 34.0 (minor diastereomer), 33.5 (minor diastereomer), 32.7, 27.4 (minor diastereomer), 26.9 (minor diastereomer), 26.8, 26.4, 23.5, 21.1. LCMS: Calculated Exact Mass = 398.2, Found [M+NH₄]⁺ (ESI+) = 416.2

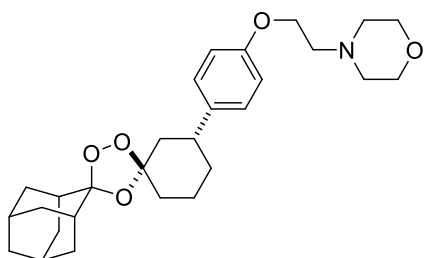


***trans*-4-(dispiro[adamantane-2,3'-[1,2,4]trioxolane-5',1''-cyclohexan]-3''-yl)phenol (8).**

To a solution of *trans*-4-(dispiro[adamantane-2,3'-[1,2,4]trioxolane-5',1''-cyclohexan]-3''-yl)phenyl acetate (3.1 g, 7.78 mmol) in THF (35 mL) and MeOH (70 mL) was added a solution of KOH (1.74 g, 31.2 mmol) in water (15 mL). The reaction mixture was stirred for

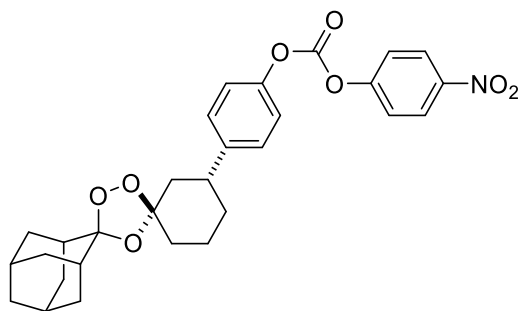
2 h at 50 °C. The solvent was removed in *vacuo*. The crude was diluted with water and extracted with EA (50 mL x 3). The combined organic layers were washed with brine, dried over Na₂SO₄, filtered and concentrated under reduced pressure. The residue was purified by flash chromatography (PE/EA = 7/1%) to afford *trans*-4-(dispiro[adamantane-2,3'-[1,2,4]trioxolane-5',1''-cyclohexan]-3''-yl)phenol (2.6 g, 93% yield) as an oil that was determined to be a ~15:1 mixture in favor of the *trans* diastereomer. ¹H NMR (400 MHz, CDCl₃) δ 7.12–7.02 (m, 2H), 6.81–6.72 (m, 2H), 4.95 (br s, 1H), 2.89 (tt, *J* = 12.6, 3.3 Hz, 1H, minor diastereomer), 2.74 (tt, *J* = 12.8, 3.3 Hz, 1H), 2.15–2.08 (m, 1H), 2.05–1.64 (m, 19H), 1.64–1.55 (m, 1H), 1.40–1.28 (m, 1H); ¹³C NMR (100 MHz, CDCl₃) δ 153.9, 138.0, 127.8, 115.2, 111.4, 109.1; 42.3, 41.8 (minor diastereomer), 41.0, 40.7 (minor diastereomer), 36.8, 36.4, 35.0 (minor diastereomer), 34.9 (minor diastereomer), 34.8, 34.7, 34.2, 33.0, 26.8, 26.5, 23.5, 21.1 (minor diastereomer);

LCMS: Calculated Exact Mass = 356.2, Found [M-H]⁻(ESI⁺) = 355.2



***trans*-4-(2-(4-(dispiro[adamantane-2,3'-[1,2,4]trioxolane-5',1''-cyclohexan]-3''-yl)phenoxy)ethyl)morpholine (11)**. To a solution of *trans*-4-(dispiro[adamantane-2,3'-[1,2,4]trioxolane-5',1''-cyclohexan]-3''-yl)phenol (100 mg, 0.281 mmol, 1.0 equiv) in dry CH₃CN (5 mL) was added tetrabutylammonium hydrogen sulfate (19.1 mg, 0.056 mmol, 0.2 equiv) and powdered NaOH (44.9 mg, 1.122 mmol, 4.0 equiv). This mixture was then allowed to stir at room temperature for 30 minutes, at which point 4-(2-chloroethyl)morpholine hydrochloride (104.4 mg, 0.561 mmol, 2.0 equiv) was added to the solution. The mixture was then placed in an oil bath preheated to 55 °C and was allowed to stir at this temperature for 14.5 hours after which the reaction was judged complete. After cooling, the mixture was diluted with EtOAc (20 mL) and H₂O (10 mL),

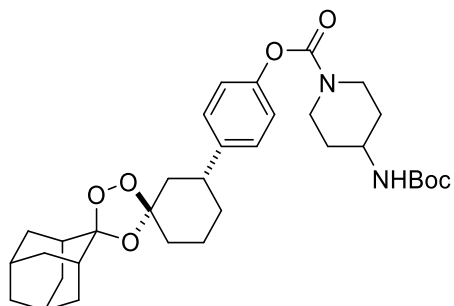
which served to dissolve all of the inorganic solids present. Following separation of the layers, the aqueous layer was extracted with EtOAc (20 mL) which resulted in the formation of an emulsion, to which brine (10 mL) was added to aid in separation of the organic phase. The combined organic layers were then washed with Brine (10 mL), dried over anhydrous Na₂SO₄, filtered, and concentrated under reduced pressure. The residue was then purified via flash column chromatography (25 g silica gel cartridge, 0–100% EtOAc/Hexanes) to yield **2** (82 mg, 62%) as a clear colorless oil that was a single diastereomer by ¹H NMR analysis. ¹H NMR (400 MHz, CDCl₃) δ 7.11 (d, *J* = 8.6 Hz, 2H), 6.84 (d, *J* = 8.6 Hz, 2H), 4.09 (t, *J* = 5.7 Hz, 2H), 3.74 (t, *J* = 4.7 Hz, 4H), 2.79 (t, *J* = 5.7 Hz, 2H), 2.79–2.68 (m, 1H), 2.58 (t, *J* = 4.5 Hz, 4H), 2.15–2.06 (m, 1H), 2.04–1.87 (m, 7H), 1.87–1.54 (m, 13H), 1.40–1.24 (m, 1H); ¹³C NMR (100 MHz, CDCl₃) δ 157.0, 138.1, 127.6, 114.5, 111.3, 109.0, 66.8, 65.7, 57.6, 54.0, 42.3, 41.0, 36.7, 36.4, 34.8, 34.7, 34.1, 32.9, 26.8, 26.4, 23.5; MS (ESI) calculated for C₂₈H₄₀NO₅ [M + H]⁺ *m/z* 470.29, found 470.09.



***trans*-4-(dispiro[adamantane-2,3'-[1,2,4]trioxolane-5',1''-cyclohexan]-3''-yl)phenyl (4-nitrophenyl) carbonate (14).**

To an oven-dried round bottom flask containing a magnetic stir bar under an Ar(g) atmosphere was added *trans*-4-(dispiro[adamantane-2,3'-[1,2,4]trioxolane-5',1''-cyclohexan]-3''-yl)phenol (0.150 mg, 0.42 mmol, 1.0 equiv) dissolved in dichloromethane (10 mL), *N,N*-diisopropylethylamine (0.22 mL, 1.26 mmol, 3.00 equiv), and 4-dimethylaminopyridine (0.062 g, 0.51 mmol, 1.2 equiv). The mixture was cooled to 0 °C while 4-nitrophenyl chloroformate (0.254 g, 1.26 mmol, 3.00 equiv) was added as a solid

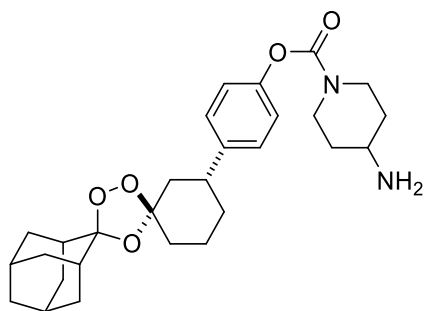
in one portion. The solution was allowed to stir at room temperature for 3 hours. The reaction was then diluted with H₂O (100 mL) and subsequently extracted with EtOAc (100 mL). The organic layer was washed repeatedly by potassium carbonate solution until the aqueous layer was colorless and no longer yellow (indicating that *p*-nitrophenol had been successfully removed from the organic layer). The organic layer was dried over anhydrous Na₂SO₄, filtered, and concentrated under reduced pressure to yield thick yellow oil. The residue was then purified through flash column chromatography (80 g silica gel cartridge, 0–25% EtOAc/Hexanes, product eluted during 10% EtOAc/Hex) to yield the desired intermediate (170 mg, 77%) as a colorless solid. ¹H NMR (400 MHz, CDCl₃-d) δ 8.29 - 8.34 (m, 2H), 7.49 (d, *J* = 9.01 Hz, 2H), 7.20 - 7.30 (m, 4H), 2.85 (tt, *J* = 3.01, 12.69 Hz, 1H), 2.16 (br d, *J* = 13.15 Hz, 1H), 1.91 - 2.05 (m, 7H), 1.65 - 1.88 (m, 13H), 1.37 - 1.45 (m, 1H); ¹³C NMR (100 MHz, CDCl₃) δ 155.4, 151.2, 149.0, 145.6, 144.3, 128.1, 125.4, 121.8, 120.7, 111.5, 108.9, 42.1, 41.4, 36.8, 36.5, 34.9, 34.8, 34.2, 32.8, 26.9, 26.5, 23.5. MS (ESI) calculated for C₂₉H₃₁NNaO₈ [M + Na]⁺ *m/z* 544.19, found 544.23.



***trans*-4-(dispiro[adamantane-2,3'-[1,2,4]trioxolane-5',1''-cyclohexan]-3''-yl)phenyl 4-((tert-butoxycarbonyl)amino)piperidine-1-carboxylate.**

To a solution of *trans*-4-(dispiro[adamantane-2,3'-[1,2,4]trioxolane-5',1''-cyclohexan]-3''-yl)phenol (2.6 g, 7.30 mmol) in dichloromethane (50 mL) was added DIEA (2.83 g, 21.9 mmol) and bis(4-nitrophenyl)carbonate (2.26 g, 7.45 mmol) at room temperature, and the mixture was stirred at room temperature for 2 h. Tert-butyl piperidin-4-ylcarbamate (2.20 g, 10.95 mmol) was added to the mixture. The reaction mixture was stirred for 2 h at room temperature. The mixture was poured into H₂O (50 mL) and extracted with dichloromethane (50 mL x 3). The combined organic layers were washed with brine (100

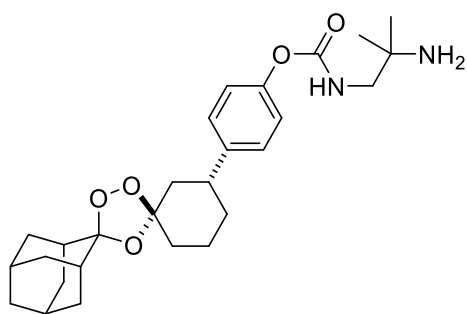
mL), dried over Na₂SO₄, filtered, and concentrated under reduced pressure. The residue was purified by column chromatography (PE/EA = 5/1) to afford *trans*-4-(dispiro[adamantane-2,3'-[1,2,4]trioxolane-5',1''-cyclohexan]-3''-yl)phenyl 4-((*tert*-butoxycarbonyl)amino)piperidine-1-carboxylate (1.2 g, 29% yield) as a white solid. ¹H NMR (400 MHz, CDCl₃) δ 7.16 - 7.20 (m, 2H), 6.99 - 7.03 (m, 2H), 4.61 (br d, *J* = 6.82 Hz, 1H), 4.13 - 4.25 (m, 2H), 3.66 (br s, 1H), 2.93 - 3.16 (m, 2H), 2.75 - 2.83 (m, 1H), 2.12 (br d, *J* = 13.39 Hz, 1H), 1.89 - 2.05 (m, 9H), 1.59 - 1.86 (m, 15H), 1.44 - 1.51 (m, 9H), 1.33 - 1.44 (m, 3H); ¹³C NMR (100 MHz, CDCl₃) δ 155.2, 153.8, 149.7, 142.6, 127.6, 121.6, 111.4, 109.0, 79.6, 47.7, 43.3, 43.2, 42.2, 41.3, 36.8, 36.5, 34.9, 34.8, 34.2, 32.9, 32.6, 28.5, 26.9, 26.5, 23.5. LCMS: Calculated Exact Mass = 582.3, Found [M+NH₄]⁺ (ESI+) = 600.5



***trans*-4-(dispiro[adamantane-2,3'-[1,2,4]trioxolane-5',1''-cyclohexan]-3''-yl)phenyl 4-aminopiperidine-1-carboxylate (17).**

To a solution of *trans*-4-dispiro[adamantane-2,3'-[1,2,4]trioxolane-5',1''-cyclohexan]-3''-yl)phenyl 4-((*tert*-butoxycarbonyl)amino)piperidine-1-carboxylate (1.2 g, 2.06 mmol) in MeOH (50 mL) was added dropwise acetyl chloride (3.21 g, 41.2 mmol) at 0° C, and the reaction mixture was stirred at room temperature for 4 h. After completion, the mixture was concentrated. The residue was poured into water and adjusted to pH = 10 with sat.aq. NaHCO₃. The mixture was extracted with CH₂Cl₂ (50 mL x 3). The combined organic layers were washed with brine, dried over Na₂SO₄, filtered and concentrated under reduced pressure. The residue was purified by column chromatography (MeOH containing 0.7N ammonia | dichloromethane = 1:10) to afford *trans*-4-(dispiro[adamantane-2,3'-[1,2,4]trioxolane-5',1''-cyclohexan]-3''-yl)phenyl 4-

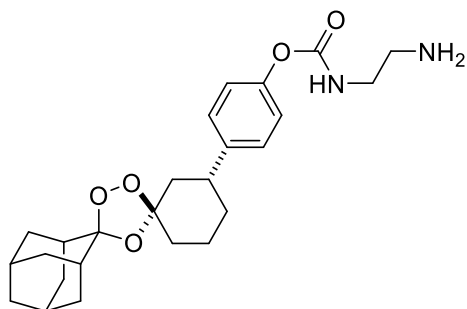
aminopiperidine-1-carboxylate (650 mg, 65% yield) as a white solid. ^1H NMR (400 MHz, CDCl_3) δ ppm 7.20 (d, $J = 8.52$ Hz, 2 H), 7.04 (d, $J = 8.77$ Hz, 2 H), 4.18 - 4.32 (m, 2 H), 2.99 - 3.14 (m, 3 H), 2.96 (br s, 2 H), 2.81 (tt, $J = 12.69, 3.26$ Hz, 1 H), 2.14 (br d, $J = 13.15$ Hz, 1 H), 1.90 - 2.07 (m, 9 H), 1.60 - 1.88 (m, 13 H), 1.44 - 1.56 (m, 2 H), 1.33 - 1.43 (m, 1 H) ^{13}C NMR (100 MHz, CDCl_3) δ 153.8, 149.7, 142.6, 127.6, 121.6, 111.4, 109.0, 48.7, 42.1, 41.3, 36.8, 36.4, 34.8, 34.8, 34.2, 32.9, 26.9, 26.5, 23.5. MS (ESI) calculated for $\text{C}_{27}\text{H}_{37}\text{N}_2\text{O}_5$ $[\text{M} + \text{H}]^+$ m/z 483.29, found 483.24.



***trans*-4-(dispiro[adamantane-2,3'-[1,2,4]trioxolane-5',1''-cyclohexan]-3''-yl)phenyl (2-amino-2-methylpropyl)carbamate (20).**

To a solution of *trans*-4-(dispiro[adamantane-2,3'-[1,2,4]trioxolane-5',1''-cyclohexan]-3''-yl)phenyl (4-nitrophenyl) carbonate (52.0 mg, 0.10 mmol, 1.0 equiv) in dichloromethane (2.0 mL) was added Et_3N (21 μL , 0.15 mmol, 1.5 equiv), followed by 2-methylpropane-1,2-diamine (16 μL , 0.15 mmol, 1.5 equiv) at room temperature. The bright yellow mixture was then allowed to stir at room temperature for 5 h, at which point, the reaction was judged complete by TLC and LCMS. The reaction was then diluted with H_2O (100 mL) and subsequently extracted with EtOAc (100 mL). The organic layer was washed repeatedly with potassium carbonate solution until the aqueous layer was colorless and no longer yellow (indicating successful removal of *p*-nitrophenol from the organic layer). The combined aqueous layers were then back extracted with EtOAc (30 mL). The combined organic layers were then washed with brine (20 mL), dried over anhydrous Na_2SO_4 , filtered, and concentrated under reduced pressure. The residue was then purified through flash column chromatography (12 g silica gel cartridge, 0–100% EtOAc/Hexanes, followed by 0–20% MeOH (containing 0.7 N NH_3)/ CH_2Cl_2 , and desired

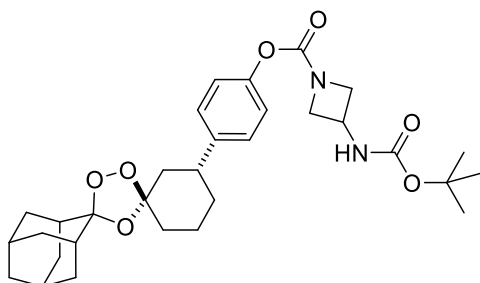
product eluted during 15% MeOH (containing 0.7 N NH₃)/ CH₂Cl₂], to yield the desired product (43.0 mg, 76%) as a white solid. ¹H NMR (400 MHz, CDCl₃) δ 7.14 - 7.19 (m, 2H), 7.09 - 7.14 (m, 2H), 3.34 (br s, 2H), 2.78 (br t, *J* = 12.66 Hz, 1H), 2.07 - 2.13 (m, 1H), 1.93 - 2.04 (m, 7H), 1.65 - 1.86 (m, 14H), 1.59 - 1.64 (m, 1H), 1.37 - 1.46 (m, 1H), 1.39 (s, 4H), 1.27 - 1.33 (m, 2H); ¹³C NMR (100 MHz, CDCl₃) δ 156.2, 149.4, 143.0, 127.9, 122.1, 115.4, 111.5, 109.1, 56.1, 42.5, 42.3, 41.4, 41.1, 36.5, 34.9, 34.3, 34.3, 33.2, 34.9, 27.0, 26.6, 23.7, 23.6. MS (ESI) calculated for C₂₉H₄₁N₂O₅ [M + H]⁺ *m/z* 471.29, found 471.27.



3-[*p*-(2-Aminoethylaminocarbonyloxy)phenyl]dispiro[cyclohexane-1,3'-[1,2,4]trioxolane-5',2''-tricyclo[3.3.1.1^{3,7}]decane] (30).

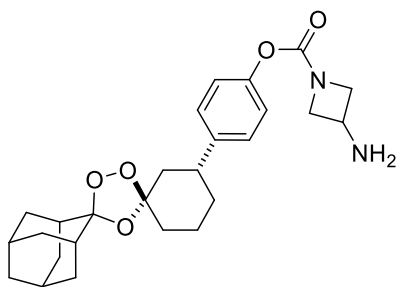
To a solution of PNP-carbonate **14** (52.0 mg, 0.10 mmol, 1.0 equiv) in dichloromethane (2.0 mL) was added Et₃N (21 μL, 0.15 mmol, 1.5 equiv), followed by ethylenediamine (12 μL, 0.18 mmol, 1.5 equiv) at room temperature. The bright yellow mixture was then allowed to stir at room temperature for 5 h, at which point, the reaction was judged complete by TLC and LCMS. The reaction was then diluted with DI H₂O (100 mL) and subsequently extracted with EtOAc (100 mL). The organic layer was washed repeatedly by potassium carbonate solution until the aqueous layer was colorless and no longer yellow (meaning that all of the *p*-nitrophenol had been successfully removed from the organic layer). The combined aqueous layers were then back extracted with EtOAc (30 mL). The combined organic layers were then washed with brine (20 mL), dried over anhydrous Na₂SO₄, filtered, and concentrated under reduced pressure. The residue was then purified through flash column chromatography (12 g silica gel cartridge, 0–100%

EtOAc/Hexanes, followed by 0–20% MeOH (containing 0.7 N NH₃)/ CH₂Cl₂, and desired product eluted during 20% MeOH (containing 0.7 N NH₃)/ CH₂Cl₂, to yield the desired product (43.0 mg, 76%) as a white foam. ¹H NMR (400 MHz, CHLOROFORM-d) δ 7.03 - 7.06 (m, 2H), 6.77 - 6.80 (m, 1H), 3.37 (br s, 1H), 2.93 - 3.01 (m, 1H), 2.66 - 2.83 (m, 1H), 2.08 - 2.15 (m, 1H), 1.90 - 2.03 (m, 8H), 1.76 - 1.87 (m, 6H), 1.56 - 1.75 (m, 8H), 1.30 - 1.39 (m, 1H); ¹³C NMR (100 MHz, CHLOROFORM-d) δ 154.9, 137.3, 127.8, 121.6, 115.5, 111.4, 109.3, 42.5, 41.1, 41.0, 36.9, 36.5, 34.9, 34.8, 34.3, 34.2, 33.1, 33.1, 27.0, 26.6, 23.6. MS (ESI) calculated for C₂₉H₄₁N₂O₅ [M + H]⁺ *m/z* 443.25, found 443.20.



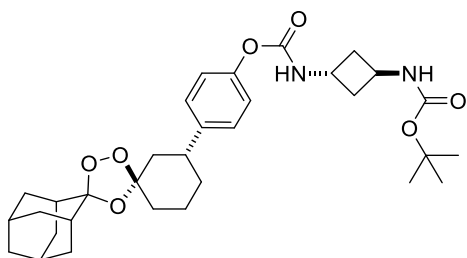
4-((1R,3S,3''S,5S,5'S,7S)-dispiro[adamantane-2,3'-[1,2,4]trioxolane-5',1''-cyclohexan]-3''-yl)phenyl 3-((tert-butoxycarbonyl)amino)azetidine-1-carboxylate

To a cooled (0° C) solution of 3-((1R,3S,3''R,5R,5'R,7R)-dispiro[adamantane-2,3'-[1,2,4]trioxolane-5',1''-cyclohexan]-3''-yl)phenyl (4-nitrophenyl) carbonate (50 mg, 0.096 mmol) in N,N'-dimethylformamide (1 mL) were added 3-N-Boc-amino azetidine (25 mg, 0.14 mmol) and triethylamine (0.02 mL, 0.14 mmol). After stirring at 35° C for 72 h, the reaction mixture was diluted with ethyl acetate and washed multiple times with 1N aqueous sodium hydroxide solution. The organic layer was washed with brine, dried over magnesium sulfate, concentrated under reduced pressure and purified by flash column chromatography (5-10% methanol/dichloromethane to obtained 11 mg (21% yield) of 4-((1R,3S,3''S,5S,5'S,7S)-dispiro[adamantane-2,3'-[1,2,4]trioxolane-5',1''-cyclohexan]-3''-yl)phenyl 3-((tert-butoxycarbonyl)amino)azetidine-1-carboxylate as yellow crystals. ¹H NMR (CHLOROFORM-d, 400 MHz) δ 7.19 (d, 2H, *J*=8.5 Hz), 7.04 (d, 2H, *J*=8.5 Hz), 4.99 (br s, 1H), 4.55 (br s, 1H), 4.44 (br s, 2H), 3.97 (br dd, 2H, *J*=1.5, 3.4 Hz), 2.77-2.84 (m, 1H), 1.97-2.15 (m, 8H), 1.65-1.86 (m, 13H), 1.49 (s, 9H), 1.30-1.36 (m, 1H).



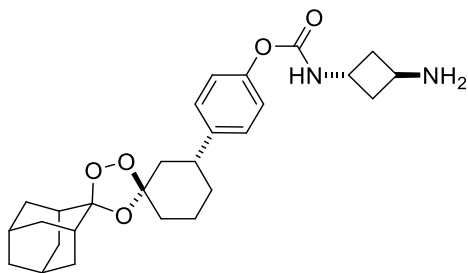
4-((1R,3S,3''S,5S,5'S,7S)-dispiro[adamantane-2,3'-[1,2,4]trioxolane-5',1''-cyclohexan]-3''-yl)phenyl 3-aminoazetidine-1-carboxylate (31)

To a cooled (0° C) solution 4-((1R,3S,3''S,5S,5'S,7S)-dispiro[adamantane-2,3'-[1,2,4]trioxolane-5',1''-cyclohexan]-3''-yl)phenyl 3-((tert-butoxycarbonyl)amino)azetidine-1-carboxylate (9.4 mg, 0.017 mmol) in methanol (0.5 mL), was added acetyl chloride (12 uL, 0.17 mmol). The reaction was then allowed to stir at room temperature for 48 h. The reaction mixture was concentrated azeotropically with toluene *in vacuo* and the residue was washed with diethyl ether to obtain 4-((1R,3S,3''S,5S,5'S,7S)-dispiro[adamantane-2,3'-[1,2,4]trioxolane-5',1''-cyclohexan]-3''-yl)phenyl 3-aminoazetidine-1-carboxylate (4.3 mg, 56%) as a white powdery hydrochloride salt. ¹H NMR (DMSO-d₆, 400 MHz) δ 8.55 (br s, 3H), 7.27-7.29 (m, 2H), 7.03-7.05 (m, 2H), 4.3-4.5 (m, 1H), 4.39 (br s, 1H), 4.18-4.20 (m, 2H), 4.03-4.06 (m, 2H), 2.68-2.71 (m, 1H), 1.65-1.93 (m, 18H), 1.20-1.60 (m, 4H). MS (ESI) calculated for C₂₆H₃₄N₂O₅ [M + H]⁺ *m/z* 455.25, found 455.25.



tert-butyl (4-((1R,3S,3''S,5S,5'S,7S)-dispiro[adamantane-2,3'-[1,2,4]trioxolane-5',1''-cyclohexan]-3''-yl)phenyl) ((1R,3s)-cyclobutane-1,3-diyl)dicarbamate

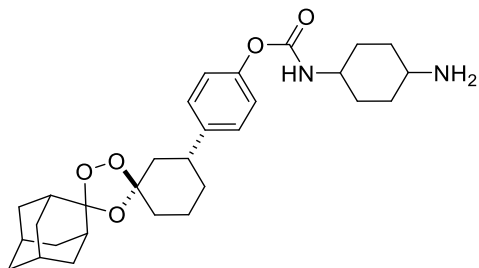
To a cooled (0° C) solution of 3-((1*R*,3*S*,3''*R*,5*R*,5'*R*,7*R*)-dispiro[adamantane-2,3'-[1,2,4]trioxolane-5,1''-cyclohexan]-3''-yl)phenyl (4-nitrophenyl) carbonate (20 mg, 0.038 mmol) in *N,N'*-dimethylformamide (0.5 mL), were added *tert*-butyl 3-aminocyclobutyl)carbamate (11 mg, 0.058 mmol) and triethylamine (8 μL, 0.058 mmol). After stirring at room temperature overnight, the reaction mixture was then diluted with ethyl acetate and washed with thrice with 1M aqueous sodium hydroxide solution. The organic layer was then washed with brine, dried over magnesium sulfate, filtered, and concentrated under reduced pressure. The residue was then purified by flash column chromatography (0-100% ethyl acetate/hexanes) to obtain 12 mg (55%) of *tert*-butyl (4-((1*R*,3*S*,3''*S*,5*S*,5'*S*,7*S*)-dispiro[adamantane-2,3'-[1,2,4]trioxolane-5',1''-cyclohexan]-3''-yl)phenyl) ((1*R*,3*s*)-cyclobutane-1,3-diyl)dicarbamate as a colorless oil. ¹H NMR (CHLOROFORM-*d*, 400 MHz) δ 7.20 (d, 2H, *J*=8.5 Hz), 7.04-7.08 (m, 2H), 5.27 (br d, 1H, *J*=6.6 Hz), 4.79 (br s, 1H), 4.24-4.32 (m, 2H), 2.80-2.84 (m, 1H), 2.36-2.40 (m, 4H), 2.13 (br d, 1H, *J*=13.4 Hz), 1.63-2.02 (m, 20H), 1.47 (s, 9H), 1.35-1.39 (m, 1H).



4-((1*R*,3*S*,3''*S*,5*S*,5'*S*,7*S*)-dispiro[adamantane-2,3'-[1,2,4]trioxolane-5',1''-cyclohexan]-3''-yl)phenyl ((1*R*,3*S*)-3-aminocyclobutyl)carbamate (32)

To a solution of *tert*-butyl (4-((1*R*,3*S*,3''*S*,5*S*,5'*S*,7*S*)-dispiro[adamantane-2,3'-[1,2,4]trioxolane-5',1''-cyclohexan]-3''-yl)phenyl) ((1*R*,3*s*)-cyclobutane-1,3-diyl)dicarbamate (49.5 mg, 0.09 mmol) in methanol (3.0 mL), was added acetyl chloride (186 μL, 2.61 mmol). The reaction was then allowed to stir at room temperature for 24 h. The reaction mixture was concentrated azeotropically with toluene under reduced pressure and the residue was washed with diethyl ether to obtain the desired product (32 mg, 79%) as a white powdery salt. ¹H NMR (CHLOROFORM-*d*, 400 MHz) δ 7.10 (br d,

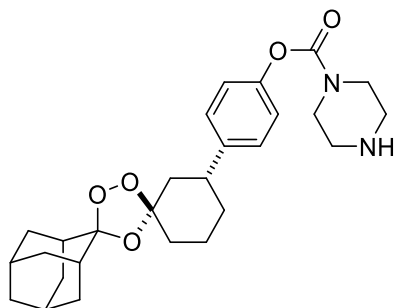
2H, $J=8.0$ Hz), 6.96-6.98 (m, 2H), 6.61 (br s, 1H), 4.48 (br s, 1H), 4.01 (br s, 1H), 3.75 (br s, 1H), 2.56-2.70 (m, 5H), 1.27-2.07 (m, 21H). MS (ESI) calculated for $C_{27}H_{37}N_2O_5$ [$M + H$]⁺ m/z 468.59, found 469.20.



3-[*p*-(4-Aminocyclohexylaminocarbonyloxy)phenyl]dispiro[cyclohexane-1,3'-[1,2,4]trioxolane-5',2''-tricyclo[3.3.1.1^{3,7}]decane] (33).

To a solution of PNP-carbonate **14** (58 mg, 0.11 mmol, 1.0 equiv) in dichloromethane (2.0 mL) was added Et₃N (24 μ L, 0.17 mmol, 1.5 equiv), followed by (1*r*,4*r*)-cyclohexane-1,4-diamine (19 mg, 0.17 mmol, 1.5 equiv) at room temperature. The bright yellow mixture was then allowed to stir at room temperature for 5 h, at which point, the reaction was judged complete by TLC and LCMS. The reaction was then diluted with DI H₂O (100 mL) and subsequently extracted with EtOAc (100 mL). The organic layer was washed repeatedly by potassium carbonate solution until the aqueous layer was colorless and no longer yellow (meaning that all of the *p*-nitrophenol had been successfully removed from the organic layer). The combined aqueous layers were then back extracted with EtOAc (30 mL). The combined organic layers were then washed with brine (20 mL), dried over anhydrous Na₂SO₄, filtered, and concentrated under reduced pressure. The residue was then purified through flash column chromatography (12 g silica gel cartridge, 0–100% EtOAc/Hexanes, followed by 0–20% MeOH (containing 0.7 N NH₃)/ CH₂Cl₂, and desired product eluted during 20% MeOH (containing 0.7 NH₃)/ CH₂Cl₂], to yield the desired product (43.0 mg, 76%) as a white solid. ¹H NMR (400 MHz, CHLOROFORM-*d*) δ 7.13 (br d, $J = 8.28$ Hz, 2H), 6.98 (br d, $J = 8.28$ Hz, 2H), 3.44 (br s, 1H), 2.96 (br s, 2H), 2.74 (br t, $J = 12.66$ Hz, 1H), 2.55 - 2.66 (m, 1H), 1.99 - 2.09 (m, 3H), 1.83 - 1.98 (m, 9H), 1.61 - 1.82 (m, 13H), 1.12 - 1.37 (m, 6H); ¹³C NMR (100 MHz, CHLOROFORM-*d*) δ 149.3,

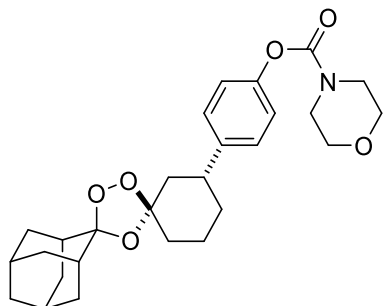
142.6, 127.6, 127.5, 121.5, 115.3, 111.4, 111.3, 109.0, 49.7, 49.5, 42.1, 41.3, 36.7, 36.4, 34.8, 34.7, 34.6, 34.1, 32.8, 31.7, 26.8, 26.5, 23.5. MS (ESI) calculated for C₂₉H₄₁N₂O₅ [M + H]⁺ *m/z* 497.30, found 497.28.



***trans*-4-(dispiro[adamantane-2,3'-[1,2,4]trioxolane-5',1''-cyclohexan]-3''-yl)phenyl piperazine-1-carboxylate (34).**

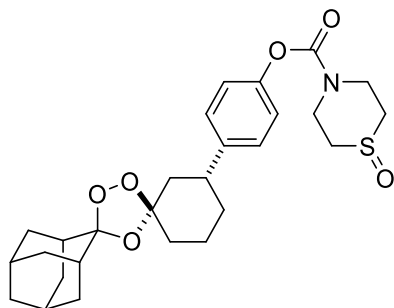
To a solution of intermediate *trans*-4-(dispiro[adamantane-2,3'-[1,2,4]trioxolane-5',1''-cyclohexan]-3''-yl)phenyl (4-nitrophenyl) carbonate (60 mg, 0.12 mmol, 1.0 equiv) in dichloromethane (2.0 mL) was added Et₃N (24 μL, 0.17 mmol, 1.5 equiv), followed by piperazine (18.0 mg, 0.19 mmol, 1.5 equiv) at room temperature. The bright yellow mixture was then allowed to stir at room temperature for 5 h, at which point, the reaction was judged complete by TLC and LCMS. The reaction was then diluted with H₂O (100 mL) and subsequently extracted with EtOAc (100 mL). The organic layer was washed repeatedly by potassium carbonate solution until the aqueous layer was colorless and no longer yellow (indicating successful removal of *p*-nitrophenol from the organic layer). The combined aqueous layers were then back extracted with EtOAc (30 mL). The combined organic layers were then washed with brine (20 mL), dried over anhydrous Na₂SO₄, filtered, and concentrated under reduced pressure. The residue was then purified through flash column chromatography (12 g silica gel cartridge, 0–100% EtOAc/Hexanes, followed by 0–20% MeOH (containing 0.7 N NH₃)/ CH₂Cl₂, and desired product eluted during 5% MeOH (containing 0.7 N NH₃) | CH₂Cl₂], to yield the desired product (43.0 mg, 76%) as a colorless solid. ¹H NMR (400 MHz, CDCl₃) δ 7.19 (d, *J* = 8.52 Hz, 1H), 7.03 (d, *J* = 8.52 Hz, 2H), 3.55 - 3.71 (m, 4H), 3.16 - 3.20 (m, 1H), 2.93 - 2.98 (m, 4H), 2.80 (tt,

$J = 3.10, 12.60$ Hz, 1H), 2.13 (br d, $J = 13.39$ Hz, 1H), 1.89 - 2.03 (m, 7H), 1.78 - 1.87 (m, 5H), 1.64 - 1.76 (m, 7H), 1.59 - 1.64 (m, 1H), 1.31 - 1.42 (m, 1H); ^{13}C NMR (100 MHz, CDCl_3) δ 153.8, 149.6, 142.7, 127.6, 121.6, 111.4, 109.0, 42.1, 41.3, 36.4, 34.8, 34.2, 34.8, 26.9, 26.5, 23.5. MS (ESI) calculated for $\text{C}_{27}\text{H}_{37}\text{N}_2\text{O}_5$ $[\text{M} + \text{H}]^+$ m/z 469.27, found 469.17.



***trans*-4-(dispiro[adamantane-2,3'-[1,2,4]trioxolane-5',1''-cyclohexan]-3''-yl)phenyl morpholine-4-carboxylate (35).**

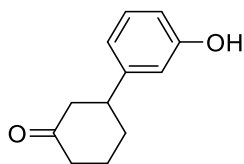
To a solution of *trans*-4-(dispiro[adamantane-2,3'-[1,2,4]trioxolane-5',1''-cyclohexan]-3''-yl)phenyl (4-nitrophenyl) carbonate (49 mg, 0.09 mmol, 1.0 equiv) in dichloromethane (2.0 mL), was added triethylamine (39 μL , 0.28 mmol, 3 equiv), followed by morpholine hydrochloride (17 mg, 0.14 mmol, 1.5 equiv). The bright yellow mixture was then allowed to stir at room temperature for 3 d, at which point, the reaction was judged complete by TLC and LCMS. The reaction was then diluted with dichloromethane (15mL) and subsequently extracted with 1M NaOH (20mL). The organic layer was then washed with brine (20 mL), dried over anhydrous MgSO_4 , filtered, and concentrated under reduced pressure. The residue was then purified through flash column chromatography (0–60% EtOAc/Hex), with the product eluting at 30% EtOAc/Hex to yield the desired product (40 mg, 90%) as a white powder. ^1H NMR (400 MHz, CDCl_3) δ 7.21 (d, $J = 8.6$ Hz, 2H), 7.05 (d, $J = 8.6$ Hz, 2H), 3.80 – 3.73 (m, 4H), 3.63 (d, $J = 37.4$ Hz, 4H), 2.88 – 2.75 (m, 1H), 2.18 – 1.55 (m, 18H), 1.44 – 1.27 (m, 4H). MS (ESI) calculated for $\text{C}_{27}\text{H}_{35}\text{NO}_6$ $[\text{M} + \text{Na}]^+$ m/z 492.58 found 492.20.



***trans*-4-(dispiro[adamantane-2,3'-[1,2,4]trioxolane-5',1''-cyclohexan]-3''-yl)phenyl thiomorpholine-4-carboxylate 1-oxide (36).**

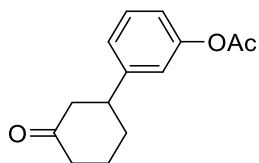
To a solution of *trans*-4-(dispiro[adamantane-2,3'-[1,2,4]trioxolane-5',1''-cyclohexan]-3''-yl)phenyl (4-nitrophenyl) carbonate (75mg, 0.14 mmol, 1.0 equiv) in DMF (0.5 mL) cooled to 0 °C in an ice bath, was added triethylamine (60 μ L, 0.43 mmol, 3.0 equiv), 1-oxide thiomorpholine hydrochloride (34mg, 0.22 mmol, 1.5 equiv) in DMF (2.0 mL) dropwise via micro syringe. The bright yellow mixture was then allowed to stir for 48 h under argon gas and allowed to warm up to room temperature, at which point, the reaction was deemed complete by TLC and LCMS. The reaction was then diluted with EtOAc (10 mL) and subsequently extracted with 1M NaOH (15 ml). The organic layer was washed three times, at which point the aqueous layer was colorless and no longer yellow (indicating the p-nitrophenol had been successfully removed from the organic layer). The organic layer was washed with brine (15 mL), dried over anhydrous MgSO₄ and concentrated under reduced pressure. The residue was then purified through silica gel flash column chromatography (0–15% MeOH/CH₂Cl₂), the product eluting around 7% MeOH/CH₂Cl₂ and yielding the desired product (45 mg, 62%) as a yellow crystal. ¹H NMR (400 MHz, CDCl₃) δ 7.23 (d, *J* = 8.5 Hz, 2H), 7.04 (d, 2H), 4.23 (t, 4H), 2.94 (t, 1H), 2.88 – 2.77 (m, 4H), 2.06 – 1.66 (m, 20H), 1.42 – 1.35 (m, 2H). MS (ESI) calculated for C₂₇H₃₅NO₆S [M + Na]⁺ *m/z* 524.64, found 524.06.

Meta aryl intermediates and final compounds



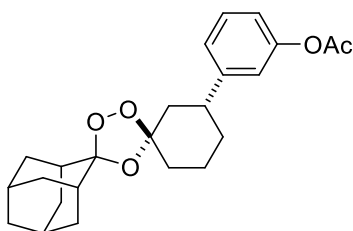
3-(3-hydroxyphenyl)cyclohexan-1-one (3).

To an oven-dried round bottom flask containing a magnetic stir bar under an Ar(g) atmosphere was added palladium(II) acetylacetonate (0.158 g, 0.52 mmol, 0.05 equiv), 1,2-bis(diphenylphosphino)benzene (0.232 g, 0.520 mmol, 0.05 equiv), copper(II) tetrafluoroborate hydrate (0.531 g, 2.081 mmol, 0.2 equiv), and 3-hydroxyphenylboronic acid (2.511 g, 18.21 mmol, 1.75 equiv). To the mixture of solid materials was added anhydrous dimethoxyethane (60 mL). To the stirring solution was then added 2-cyclohexen-1-one (1.0 g, 10.33 mmol, 1.0 equiv) via syringe at room temperature. The solution was allowed to stir at room temperature for 20 hours. Based on LCMS and TLC analysis, it was determined that the reaction was complete. The mixture was then concentrated under reduced pressure to yield a dark green oil. To this oil was added EtOAc (100 mL) followed by H₂O (50 mL). Following separation of the layers, the organic layer was washed with additional DI H₂O (50 mL). The organic layer was then filtered through a pad of Celite to remove all insoluble inorganic material. The pad was then rinsed with EtOAc (50 mL x 4). The aqueous layer was extracted with EtOAc, and the resulting organic solution was filtered through the same pad of Celite. The pad was then again rinsed with EtOAc (50 mL x 2). The clear yellow solution was concentrated under reduced pressure to yield a yellow oil. The residue was then purified through flash column chromatography (120 g silica gel cartridge, product eluted during 35–40% EtOAc/Hex) to yield **3a** (1.44 g, 73%) as a colorless oil. ¹H NMR (400 MHz, CDCl₃) δ 7.33 (s, 1H), 7.16 (t, *J* = 8.04 Hz, 1H), 6.72 - 6.77 (m, 3H), 2.88 - 2.97 (m, 1H), 2.43 - 2.61 (m, 3H), 2.32 - 2.41 (m, 1H), 2.08 - 2.15 (m, 1H), 2.02 (br d, *J* = 11.69 Hz, 1H), 1.67 - 1.84 (m, 2H); ¹³C NMR (100 MHz, CDCl₃) δ 213.6, 156.3, 146.0, 129.8, 118.5, 113.8, 113.7, 48.7, 44.6, 41.1, 32.5, 25.4; MS (ESI) calculated for C₁₂H₁₃O₂ [M - H]⁻ *m/z* 189.09, found 188.99.



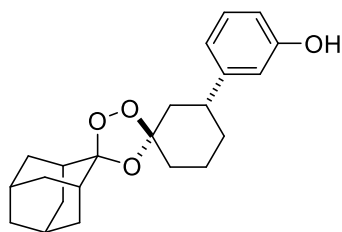
3-(3-oxocyclohexyl)phenyl acetate (4).

To an oven-dried round bottom flask containing a magnetic stir bar under an Ar(g) atmosphere was added 3-(3-hydroxyphenyl)cyclohexan-1-one (0.525 g, 2.76 mmol, 1.0 equiv), dichloromethane (7 mL), acetic anhydride (0.29 mL, 3.04 mmol, 1.1 equiv), and 4-dimethylaminopyridine (0.337 g, 2.76 mmol, 1 equiv). The solution was allowed to stir at room temperature for 2 hours. The reaction was then diluted with H₂O (100 mL) and subsequently extracted with EtOAc (100 mL). The organic layer was dried over anhydrous Na₂SO₄, filtered, and concentrated under reduced pressure to yield a thick yellow oil. The residue was then purified through flash column chromatography (80 g silica gel cartridge, 0–25% EtOAc/Hexanes, product eluted during 20% EtOAc/Hex) to yield **3b** (503 mg, 78%) as a white solid. ¹H NMR (400 MHz, CDCl₃) δ 7.15 - 7.24 (m, 1H), 6.97 - 7.02 (m, 1H), 6.87 - 6.92 (m, 2H), 2.85 - 2.94 (m, 1H), 2.40 - 2.51 (m, 2H), 2.23 - 2.35 (m, 2H), 2.17 - 2.20 (m, 3H), 1.90 - 2.02 (m, 2H), 1.57 - 1.75 (m, 2H); ¹³C NMR (100 MHz, CDCl₃) 210.5, 169.0, 150.5, 145.7, 129.2, 123.7, 119.4, 119.4, 48.1, 43.8, 40.6, 32.0, 24.9, 20.6; MS (ESI) calculated for C₁₄H₁₆NaO₃ [M + Na]⁺ *m/z* 255.10, found 255.04.



trans-3-(dispiro[adamantane-2,3'-[1,2,4]trioxolane-5',1''-cyclohexan]-3''-yl)phenyl acetate (5). A solution of adamantan-2-one *O*-methyl oxime (772 mg, 4.31 mmol, 2.0 equiv) and 3-(3-oxocyclohexyl)phenyl acetate (500 mg, 2.15 mmol, 1.0 equiv) in 50 mL carbon tetrachloride was cooled to 0 °C and subsequently sparged with O₂ for 10 minutes. The reaction was kept at 0 °C while ozone was then bubbled (2 L/min, 35% power). After

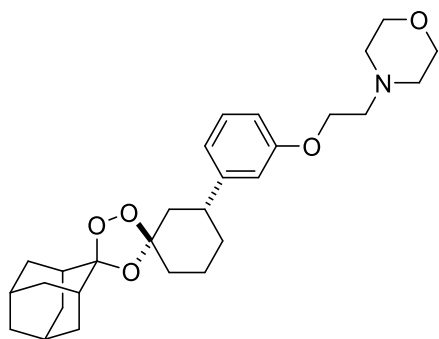
stirring for 2 hrs, the reaction was deemed to be incomplete based on LCMS analysis and additional oxime (193 mg, 1.08 mmol, 0.5 equiv) was added in a single portion to the reaction. Ozone was bubbled through the reaction for another 60 mins, at which point the reaction was found to be complete. The reaction was then purged with O₂ for 10 minutes to remove any dissolved ozone, followed by sparging with argon gas for 10 minutes to remove any dissolved oxygen. The solution was then concentrated under reduced pressure to provide an extremely viscous oil. The residue was purified through flash column chromatography (80 g silica gel cartridge, 0–10% EtOAc/Hexanes, product eluted during 8% EtOAc/Hex) to yield the desired product (724 mg, 84%) as a thick colorless oil, which solidified to a white solid under high vacuum. The material was determined to a 7.4:1 mixture in favor of the *trans* diastereomer. ¹H NMR (400 MHz, CDCl₃) δ 7.28 - 7.35 (m, 1H), 7.10 (d, *J* = 7.79 Hz, 1H), 6.93 - 6.96 (m, 2H), 2.98 (tt, *J* = 12.7, 3.1 Hz, 1H, minor diastereomer), 2.83 (tt, *J* = 12.8, 3.3 Hz, 1H), 2.30 - 2.32 (m, 3H), 2.14 - 2.20 (m, 1H), 2.07 - 2.12 (m, 1H), 1.90 - 2.05 (m, 7H), 1.61 - 1.89 (m, 12H), 1.39 (dq, *J* = 3.17, 12.42 Hz, 1H); ¹³C NMR (100 MHz, CDCl₃) δ 169.5, 169.5 (minor diastereomer), 150.9, 147.6 (minor diastereomer), 147.4, 129.4, 124.4, 124.3 (minor diastereomer), 120.0 (minor diastereomer), 120.0, 119.5, 111.9 (minor diastereomer), 111.4, 109.0 (minor diastereomer), 108.9, 47.0, 42.0, 41.7, 41.5, 41.4, 39.3, 36.8, 36.5, 36.5, 36.4, 35.1, 35.0, 34.8, 34.8, 34.2, 34.1, 33.4, 32.6, 27.5, 27.0, 26.9, 26.5, 23.5, 21.2; MS (ESI) calculated for C₂₄H₃₀O₅Na [M + Na]⁺ *m/z* 421.20, found 421.14.



***trans*-3-(dispiro[adamantane-2,3'-[1,2,4]trioxolane-5',1''-cyclohexan]-3''-yl)phenol (7).**

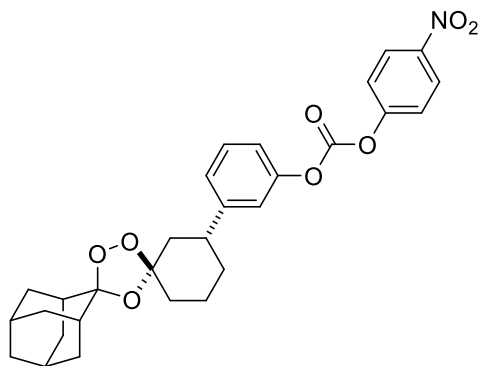
To a solution of *trans*-3-(dispiro[adamantane-2,3'-[1,2,4]trioxolane-5',1''-cyclohexan]-3''-yl)phenyl acetate (724 mg, 1.0 equiv) in anhydrous THF (7 mL) and MeOH (14 mL) was

added 15% aqueous KOH (3 mL, 4.5 equiv). The solution was then placed in an oil bath that had been preheated to 50 °C and was allowed to stir at this temperature for 1.5 hours, and the solution then allowed to cool to room temperature. The mixture was then concentrated under reduced pressure, to this was then added H₂O (30 mL). Citric acid was then added to this solution until pH ~ 4 and extracted with EtOAc (100 mL). The organic layer was then washed with brine, dried over anhydrous Na₂SO₄, filtered, and concentrated under reduced pressure, the residue was then purified through flash column chromatography (80 g silica gel cartridge, 0–50% EtOAc/Hexanes, product eluted during 30%) to yield the desired product (550 mg, 85%) as a thick colorless oil, which solidified to a white solid under high vacuum. This material was determined to be a 8.2:1 mixture in favor of the *trans* diastereomer. ¹H NMR (400 MHz, CDCl₃) δ 7.14 - 7.18 (m, 1H), 6.76 - 6.79 (m, 1H), 6.67 - 6.71 (m, 2H), 5.38 (br s, 1H), 2.98 (tt, *J* = 12.7, 3.1 Hz, 1H, minor diastereomer), 2.83 (tt, *J* = 12.8, 3.3 Hz, 1H), 2.10 - 2.16 (m, 1H), 1.89 - 2.04 (m, 7H), 1.65 - 1.86 (m, 12H), 1.58 - 1.65 (m, 1H), 1.30 - 1.41 (m, 1H); ¹³C NMR (100 MHz, CDCl₃) δ 155.8 (minor diastereomer), 155.8, 147.9 (minor diastereomer), 147.7, 129.7, 119.3, 113.9, 113.3, 113.3 (minor diastereomer), 112.0 (minor diastereomer), 111.6, 109.3, 42.1, 41.8, 41.6, 41.6, 36.9, 36.5, 35.1, 35.0, 34.9, 34.9, 34.8, 34.3, 34.2, 33.4, 32.7, 27.0, 27.0, 26.6, 23.6; MS (ESI) calculated for C₂₂H₂₇O₄ [M – H][–] *m/z* 355.19, found 355.13.



***trans*-4-(2-(3-(dispiro[adamantane-2,3'-[1,2,4]trioxolane-5',1''-cyclohexan]-3''-yl)phenoxy)ethyl)morpholine (10).**

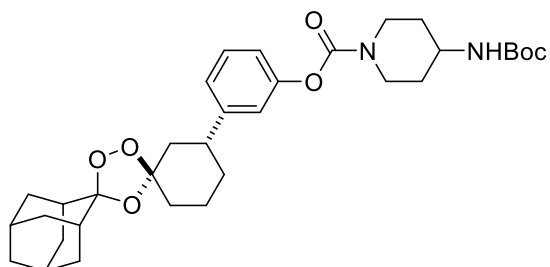
To a solution of *trans*-3-(dispiro[adamantane-2,3'-[1,2,4]trioxolane-5',1''-cyclohexan]-3'-yl)phenol (60.0 mg, 0.17 mmol, 1.0 equiv) in dry CH₃CN (4 mL) was added tetrabutylammonium hydrogen sulfate (16.0 mg, 0.05 mmol, 0.3 equiv) and powdered NaOH (24.0 mg, 0.60 mmol, 3.6 equiv). This mixture was then allowed to stir at room temperature for 30 minutes, at which point 4-(2-chloroethyl)morpholine hydrochloride (63.0 mg, 0.34 mmol, 2.0 equiv) was added to the solution. The mixture was then placed in an oil bath that had been preheated to 55 °C and was allowed to stir at this temperature for 14 hours. Following determination of reaction completion by TLC and LCMS analysis, the solution was then removed from the oil bath and allowed to cool to room temperature. Upon cooling, the mixture was diluted with EtOAc (20 mL) prior to the addition of H₂O (10 mL), which served to dissolve all of the inorganic solids present. Following separation of the layers, the aqueous layer was extracted with EtOAc (20 mL). The organic layer was then washed with brine (10 mL), dried over anhydrous Na₂SO₄, filtered, and concentrated under reduced pressure. The residue was then purified through flash column chromatography (12 g silica gel cartridge, 0–50% EtOAc/Hexanes, followed by 0–20% MeOH/CH₂Cl₂, and desired product eluted during 2% MeOH, to yield RLA-4741 (48.0 mg, 61%) as a light yellow oil. The material was observed to be solely the *trans* diastereomer within limits of NMR detection. ¹H NMR (400 MHz, CDCl₃) δ 7.18 - 7.24 (m, 1H), 6.72 - 6.83 (m, 3H), 4.09 - 4.14 (m, 2H), 3.71 - 3.79 (m, 4H), 2.73 - 2.85 (m, 3H), 2.56 - 2.65 (m, 4H), 1.89 - 2.15 (m, 9H), 1.78 - 1.87 (m, 5H), 1.65 - 1.75 (m, 6H), 1.56 - 1.65 (m, 1H), 1.32 - 1.44 (m, 1H); ¹³C NMR (100 MHz, CDCl₃) δ 158.8, 147.4, 129.5, 119.4, 113.4, 112.1, 111.4, 109.0, 73.2, 66.9, 65.6, 57.7, 54.1, 42.1, 42.0, 41.3, 36.8, 36.5, 35.8, 34.9, 34.8, 34.3, 32.7, 31.0, 26.9, 26.5, 25.9, 23.6; MS (ESI) calculated for C₂₈H₄₀NO₅ [M + H]⁺ *m/z* 470.29, found 470.22.



***trans*-3-((dispiro[adamantane-2,3'-[1,2,4]trioxolane-5',1''-cyclohexan]-3''-yl)phenyl (4-nitrophenyl) carbonate (13).**

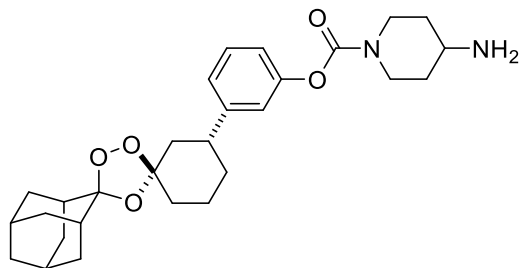
To an oven-dried round bottom flask containing a magnetic stir bar under an Ar(g) atmosphere was added *trans*-3-(dispiro[adamantane-2,3'-[1,2,4]trioxolane-5',1''-cyclohexan]-3''-yl)phenol (0.300 mg, 0.84 mmol, 1.0 equiv), dichloromethane (10 mL), N,N-diisopropylethylamine (0.48 mL, 2.74 mmol, 3.25 equiv), and 4-dimethylaminopyridine (0.123 g, 1.01 mmol, 1.2 equiv). The mixture was cooled to 0 °C while 4-nitrophenyl chloroformate (0.551 g, 2.74 mmol, 3.25 equiv) was added as a solid in one portion. The solution was allowed to stir at room temperature for 3 hours. The reaction was then diluted with DI H₂O (100 mL) and subsequently extracted with EtOAc (100 mL). The organic layer was washed repeatedly by potassium carbonate solution until the aqueous layer was colorless and no longer yellow (indicating successful removal of *p*-nitrophenol from the organic layer). The organic layer was dried over anhydrous Na₂SO₄, filtered, and concentrated under reduced pressure to yield a thick yellow oil. The residue was then purified through flash column chromatography (80 g silica gel cartridge, 0–25% EtOAc/Hexanes, product eluted during 8% EtOAc/Hex) to yield the desired intermediate (347 mg, 79%) as a colorless solid. ¹H NMR (400 MHz, CDCl₃) δ 8.31 - 8.36 (m, 2H), 7.49 - 7.53 (m, 2H), 7.35 - 7.41 (m, 1H), 7.12 - 7.19 (m, 3H), 3.01 (tt, *J* = 3.32, 12.63 Hz, 1H), 2.87 (tt, *J* = 3.32, 12.63 Hz, 1H), 2.15 - 2.21 (m, 1H), 1.77 - 2.05 (m, 13H), 1.65 - 1.75 (m, 5H), 1.59 - 1.65 (m, 1H), 1.39 - 1.46 (m, 1H); ¹³C NMR (100 MHz, CDCl₃) δ 155.4, 151.2, 150.9, 148.2, 148.0, 145.7, 129.8, 125.5, 125.4, 121.9, 119.2, 118.6, 112.0 (minor diastereomer), 111.6, 108.9, 42.0, 41.7, 41.5, 36.9, 36.5, 35.0, 34.9, 34.2, 33.5,

32.7, 27.0, 26.6, 23.5. MS (ESI) calculated for C₂₉H₃₁NNaO₈ [M + Na]⁺ *m/z* 544.19, found 544.02.



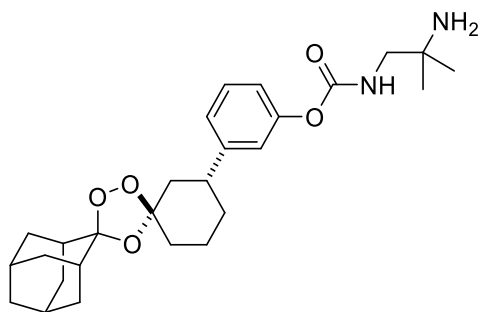
***trans*-3-(dispiro[adamantane-2,3'-[1,2,4]trioxolane-5',1''-cyclohexan]-3''-yl)phenyl 4-((*tert*-butoxycarbonyl)amino)piperidine-1-carboxylate.**

To a solution of 3-(*trans*-dispiro[adamantane-2,3'-[1,2,4]trioxolane-5',1''-cyclohexan]-3''-yl)phenyl (4-nitrophenyl) carbonate (87.4 mg, 0.15 mmol, 1.0 equiv) in dichloromethane (1.5 mL), was added 4-(*N*-Boc-amino)piperidine (48 mg, 0.24 mmol, 1.5 equiv), and triethylamine (34 μ L, 0.24 mmol, 1.5 equiv) at room temperature and was set to stir for 2 days. The reaction was deemed complete by LCMS and TLC, diluted with EtOAc (10 mL) and subsequently extracted with 1M NaOH (15 mL). The organic layer was washed with brine (12 mL), dried over anhydrous MgSO₄, filtered, and concentrated under reduced pressure to yield a clear oil. The residue was then purified through silica gel flash column chromatography (0-30% EtOAc/Hex), with the product eluting around 20% EtOAc/Hex to yield *trans*-3-(dispiro[adamantane-2,3'-[1,2,4]trioxolane-5',1''-cyclohexan]-3''-yl)phenyl 4-((*tert*-butoxycarbonyl)amino)piperidine-1-carboxylate (40 mg, 45%) as a colorless oil. ¹H NMR (400 MHz, Chloroform-*d*) δ 7.33 – 7.23 (m, 1H), 7.06 (d, *J* = 7.7 Hz, 1H), 6.97 – 6.91 (m, 2H), 4.53 (s, 1H), 4.22 (s, 1H), 4.14 (q, *J* = 7.1 Hz, 4H), 3.07 (d, *J* = 49.6 Hz, 2H), 2.81 (tt, *J* = 12.8, 3.5 Hz, 1H), 2.05 – 1.57 (m, 24H), 1.48 (s, 9H). MS (ESI) calculated for C₃₃H₄₆N₂NaO₇ [M + Na]⁺ *m/z* 605.73, found 605.33.



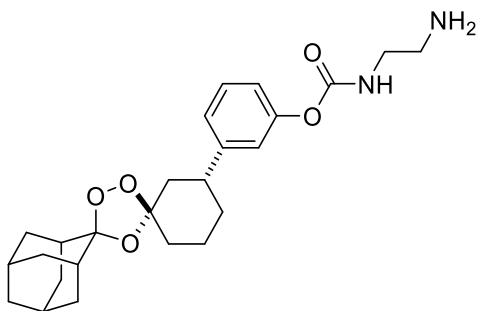
***trans*-3-(dispiro[adamantane-2,3'-[1,2,4]trioxolane-5',1''-cyclohexan]-3''-yl)phenyl 4-aminopiperidine-1-carboxylate (16).**

To a solution of *trans*-3-(dispiro[adamantane-2,3'-[1,2,4]trioxolane-5',1''-cyclohexan]-3''-yl)phenyl 4-((tert-butoxycarbonyl)amino)piperidine-1-carboxylate (29.1 mg, 0.05 mmol, 1.0 equiv) in methanol (1.5 mL), was added acetyl chloride (110 μ L, 1.5 mmol, 30 equiv) in methanol (0.7 mL). The reaction was then allowed to stir at 0° C, warmed up to room temperature and stirred for 3 days, at which point the reaction was judged complete by LCMS. The reaction mixture was concentrated to dryness and triturated with diethyl ether to yield the desired product (21.7 mg, 89.4%) as a hydrochloride salt, a white powder. ^1H NMR (400 MHz, DMSO- d_6) δ 7.33 – 7.26 (m, 1H), 7.11 (d, J = 7.6 Hz, 1H), 7.07 – 6.88 (m, 2H), 4.29 – 3.87 (m, 2H), 3.27-3.03 (m, 1H), 3.03 – 2.90 (m, 1H), 2.69 (m, J = 15.8, 12.2, 7.4, 4.6 Hz, 1H), 2.17-1.15 (m, 24H). MS (ESI) calculated for $\text{C}_{28}\text{H}_{38}\text{N}_2\text{NaO}_5$ [$\text{M} + \text{Na}$] $^+$ m/z 505.61, found 505.15.



***trans*-3-((dispiro[adamantane-2,3'-[1,2,4]trioxolane-5',1''-cyclohexan]-3''-yl)phenyl (2-amino-2-methylpropyl)carbamate (19).**

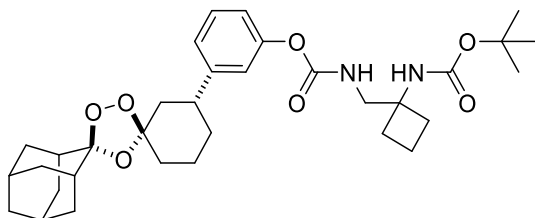
To a solution of 3-(*trans*-dispiro[adamantane-2,3'-[1,2,4]trioxolane-5',1''-cyclohexan]-3''-yl)phenyl (4-nitrophenyl) carbonate (87.4 mg, 0.15 mmol, 1.0 equiv) in dichloromethane (1.5 mL), was added 2-methylpropane-1,2-diamine (20 mg, 0.24 mmol, 1.5 equiv), and triethylamine (34 μ L, 0.24 mmol, 1.5 equiv) at room temperature and was set to stir for 2 days. The reaction was deemed complete by LCMS and TLC, diluted with EtOAc (10 mL) and subsequently extracted with 1M NaOH (15 mL). The organic layer was washed with brine (12 mL), dried over anhydrous MgSO₄, filtered, and concentrated under reduced pressure to yield a clear oil. The residue was then purified through silica gel flash column chromatography (0-30% EtOAc/Hex), the product eluting around 20% EtOAc/Hex to yield 3 *trans*-3-((dispiro[adamantane-2,3'-[1,2,4]trioxolane-5',1''-cyclohexan]-3''-yl)phenyl (2-amino-2-methylpropyl)carbamate (19.1 mg, 23%) as a white solid. ¹H NMR (400 MHz, DMSO-*d*₆) δ 7.29 (t, *J* = 7.9 Hz, 1H), 7.13 – 7.01 (m, 2H), 6.95 (dd, *J* = 8.1, 2.3 Hz, 1H), 3.08 (t, *J* = 5.1 Hz, 2H), 2.78 – 2.63 (m, 1H), 1.94 – 1.63 (m, 22H), 1.12 (t, *J* = 2.2 Hz, 6H). MS (ESI) calculated for C₂₇H₃₉N₂O₅ [M + H]⁺ *m/z* 471.61, found 471.30.



3-[*m*-(2-Aminoethylaminocarbonyloxy)phenyl]dispiro[cyclohexane-1,3'-[1,2,4]trioxolane-5',2''-tricyclo[3.3.1.1^{3,7}]decane] (21).

To a solution of PNP-carbonate **13** (60 mg, 0.12 mmol, 1.0 equiv) in dichloromethane (2.0 mL) was added Et₃N (24 μ L, 0.17 mmol, 1.5 equiv), followed by ethylenediamine (12 μ L, 0.17 mmol, 1.5 equiv) at room temperature. The bright yellow mixture was then allowed to stir at room temperature for 5 h, at which point, the reaction was judged complete by TLC and LCMS. The reaction was then diluted with DI H₂O (100 mL) and subsequently extracted with EtOAc (100 mL). The organic layer was washed repeatedly by potassium

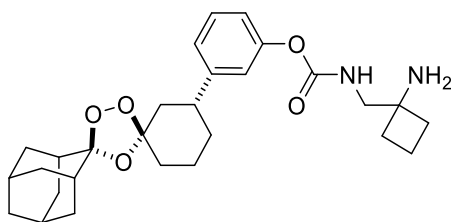
carbonate solution until the aqueous layer was colorless and no longer yellow (meaning that all of the *p*-nitrophenol had been successfully removed from the organic layer). The combined aqueous layers were then back extracted with EtOAc (30 mL). The combined organic layers were then washed with brine (20 mL), dried over anhydrous Na₂SO₄, filtered, and concentrated under reduced pressure. The residue was then purified through flash column chromatography (12 g silica gel cartridge, 0–100% EtOAc/Hexanes, followed by 0–20% MeOH (containing 0.7 N NH₃)/CH₂Cl₂, and desired product eluted during 20% MeOH (containing 0.7 N NH₃)/ CH₂Cl₂], to yield the desired product (38.0 mg, 75%) as a colorless oil. ¹H NMR (400 MHz, CHLOROFORM-*d*) δ 7.22 - 7.27 (m, 1H), 7.03 (br d, *J* = 7.55 Hz, 1H), 6.91 - 7.01 (m, 2H), 3.51 (br s, 2H), 3.13 (br s, 2H), 2.06 - 2.13 (m, 1H), 1.88 - 2.01 (m, 6H), 1.83 - 1.88 (m, 1H), 1.74 - 1.83 (m, 5H), 1.58 - 1.73 (m, 8H), 1.27 - 1.46 (m, 2H), 1.15 - 1.27 (m, 1H); MS (ESI) calculated for C₂₅H₃₅N₂O₅ [M + H]⁺ *m/z* 443.25, found 443.28.



***tert*-butyl (1-((((3-((1S,2S,3''R,5R,5'R,7S)-dispiro[adamantane-2,3'-[1,2,4]trioxolane-5',1''-cyclohexan]-3''-yl)phenoxy)carbonyl)amino)methyl)cyclobutyl)carbamate**

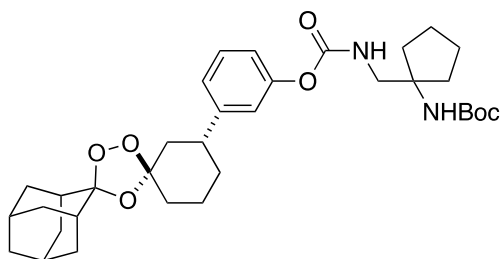
To a solution of 3-((1*R*,3*S*,3''*R*,5*R*,5'*R*,7*R*)-dispiro[adamantane-2,3'-[1,2,4]trioxolane-5',1''-cyclohexan]-3''-yl)phenyl (4-nitrophenyl) carbonate (101.8 mg, 0.20 mmol) in dichloromethane (2 mL), was added *tert*-butyl (1-(aminomethyl)cyclobutyl)carbamate (55 mg, 0.27 mmol), and triethylamine (38.3 μL, 0.27 mmol). After stirring at room temperature for 72 h, the reaction mixture was then diluted with ethyl acetate and washed with thrice with 1M aqueous sodium hydroxide solution. The organic layer was then washed with brine, dried over magnesium sulfate, filtered, and concentrated under reduced pressure. The residue was then purified by flash column chromatography (0-30% ethyl acetate/hexanes) to yield 35.8 mg (32%) of *tert*-butyl (1-((((3-((1S,2S,3''R,5R,5'R,7S)-

dispiro[adamantane-2,3'-[1,2,4]trioxolane-5',1''-cyclohexan]-3''-yl)phenoxy)carbonyl)amino)methyl)cyclobutyl)carbamate as a clear oil. ¹H NMR (CHLOROFORM-d, 400 MHz) δ 7.21 – 7.33 (m, 1H), 6.91-7.10 (m, 3H), 5.82-6.21 (m, 2H), 3.54-3.69 (m, 2H), 2.73-2.78 (m, 1H), 1.25-2.20 (m, 37H).



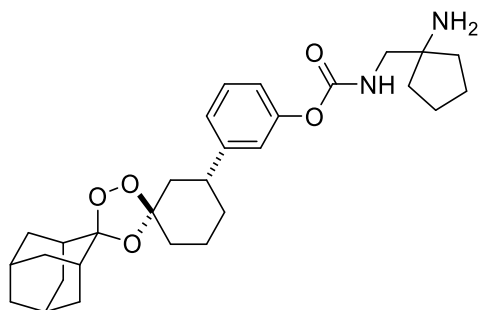
3-((1S,2S,3''R,5R,5'R,7S)-dispiro[adamantane-2,3'-[1,2,4]trioxolane-5',1''-cyclohexan]-3''-yl)phenyl ((1-aminocyclobutyl)methyl)carbamate (22)

To a cooled (0° C) solution of tert-butyl (1-(((3-((1S,2S,3''R,5R,5'R,7S)-dispiro[adamantane-2,3'-[1,2,4]trioxolane-5',1''-cyclohexan]-3''-yl)phenoxy)carbonyl)amino)methyl)cyclobutyl)carbamate (35.8 mg, 0.06 mmol) in methanol (1.5 mL), was added acetyl chloride (132 uL, 1.8 mmol). The reaction was then allowed to stir at room temperature for 72 h. The reaction mixture was concentrated azeotropically with toluene under reduced pressure and the residue was washed with diethyl ether to obtain 3-((1S,2S,3''R,5R,5'R,7S)-dispiro[adamantane-2,3'-[1,2,4]trioxolane-5',1''-cyclohexan]-3''-yl)phenyl ((1-aminocyclobutyl)methyl)carbamate 22.5 mg (70%) as a white powdery hydrochloride salt. ¹H NMR (METHANOL-d₄, 400 MHz) Shift 7.33 (t, 1H, J=7.9 Hz), 7.13 (d, 1H, J=7.8 Hz), 6.99-7.06 (m, 2H), 3.58 (s, 2H), 2.76-2.82 (m, 1H), 2.26-2.30 (m, 3H), 1.44-2.06 (m, 25H). MS (ESI) calculated for C₂₈H₃₉N₂O₅ [M + H]⁺ *m/z* 483.28, found 483.37.



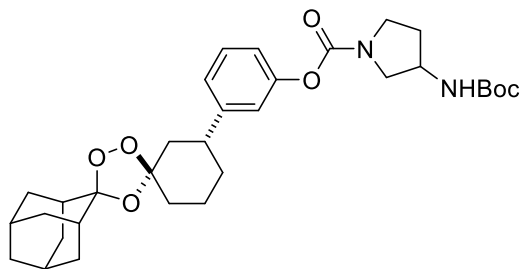
3-(*trans*-dispiro[adamantane-2,3'-[1,2,4]trioxolane-5',1''-cyclohexan]-3''-yl)phenyl ((1-((*tert*-butoxycarbonyl)amino)cyclopentyl)methyl)carbamate.

To a solution of 3-(*trans*-dispiro[adamantane-2,3'-[1,2,4]trioxolane-5',1''-cyclohexan]-3''-yl)phenyl (4-nitrophenyl) carbonate (80.4 mg, 0.15 mmol, 1.0 equiv) in dichloromethane (1.5 mL), was added *tert*-butyl (1-(aminomethyl)cyclopentyl)carbamate (52.1 mg, 0.24 mmol, 1.5 equiv), and triethylamine (34 μ L, 0.24 mmol, 1.5 equiv) at room temperature and was set to stir for 2 days. The reaction was deemed complete by LCMS and TLC, diluted with EtOAc (10 mL) and subsequently extracted with 1M NaOH (15 mL). The organic layer was washed with brine (12 mL), dried over anhydrous MgSO₄, filtered, and concentrated under reduced pressure to yield a clear oil. The residue was then purified through silica gel flash column chromatography (0-30% EtOAc/Hex), the product eluting around 20% EtOAc/Hex to yield 3-(*trans*-dispiro[adamantane-2,3'-[1,2,4]trioxolane-5',1''-cyclohexan]-3''-yl)phenyl ((1-((*tert*-butoxycarbonyl)amino)-cyclopentyl)methyl)carbamate (30.6 mg, 33%). ¹H NMR (400 MHz, CDCl₃) δ 7.28 (s, 1H), 7.12 (t, 1H), 6.91 (d, 1H), 6.81 (d, 1H), 6.45 (s, 1H), 5.25 (s, 1H), 3.43 (s, 1H), 3.07 (s, 1H), 2.65 (s, 1H), 2.07 – 1.08 (m, 39H).



***trans*-3-(dispiro[adamantane-2,3'-[1,2,4]trioxolane-5',1''-cyclohexan]-3''-yl)phenyl ((1-((*tert*-butoxycarbonyl)amino)-cyclopentyl)methyl)carbamate (23).**

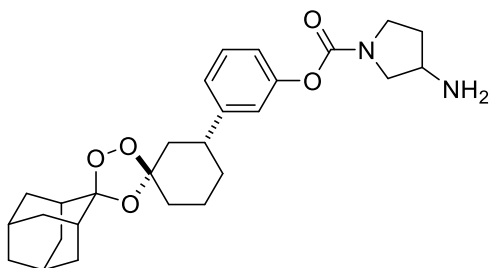
To a solution of 3-(*trans*-dispiro[adamantane-2,3'-[1,2,4]trioxolane-5',1''-cyclohexan]-3''-yl)phenyl ((1-((*tert*-butoxycarbonyl)amino)-cyclopentyl)methyl)carbamate (30.6 mg, 0.05 mmol, 1.0 equiv) in methanol (1.5 mL), was added acetyl chloride (110 μ L, 1.5 mmol, 30 equiv) in methanol (0.7 mL). The reaction was then allowed to stir at 0° C, warmed up to room temperature and stirred for 3 days, at which point, the reaction was judged complete by LCMS. The reaction mixture was concentrated to dryness and triturated with diethyl ether to yield the desired product (24.5 mg, 89.4%) as a hydrochloride salt, a white powder. ¹H NMR (400 MHz, DMSO) δ 8.16 – 8.00 (m, 3H), 7.29 (t, 1H), 7.16 – 6.96 (m, 3H), 3.32 – 3.27 (m, 2H), 2.77 – 2.65 (m, 1H), 1.76 (s, 31H). MS (ESI) calculated for C₂₉H₄₀N₂O₅ [M + H]⁺ *m/z* 496.65, found 497.38.



***trans*-3-(dispiro[adamantane-2,3'-[1,2,4]trioxolane-5',1''-cyclohexan]-3''-yl)phenyl 3-((*tert*-butoxycarbonyl)amino)pyrrolidine-1-carboxylate**

To a solution of 3-(*trans*-dispiro[adamantane-2,3'-[1,2,4]trioxolane-5',1''-cyclohexan]-3''-yl)phenyl (4-nitrophenyl) carbonate (87.4 mg, 0.15 mmol, 1.0 equiv) in dichloromethane (1.5 mL), was added 3-(Boc-amino)pyrrolidine (44.7 mg, 0.24 mmol, 1.5 equiv), and triethylamine (34 μ L, 0.24 mmol, 1.5 equiv) at room temperature and was set to stir for 2 days. The reaction was deemed complete by LCMS and TLC, diluted with EtOAc (10 mL) and subsequently extracted with 1M NaOH (15 mL). The organic layer was washed with brine (12 mL), dried over anhydrous MgSO₄, filtered, and concentrated under reduced pressure to yield a clear oil. The residue was then purified through silica gel flash column chromatography (0-30% EtOAc/Hex), the product eluting around 20% EtOAc/Hex to yield

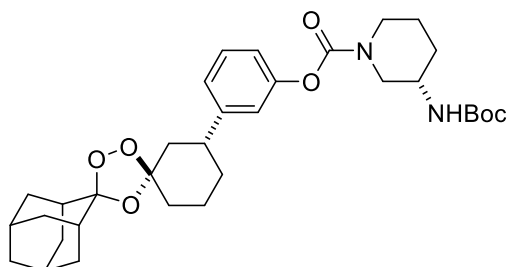
trans-3-(dispiro[adamantane-2,3'-[1,2,4]trioxolane-5',1''-cyclohexan]-3''-yl)phenyl 3-((*tert*-butoxycarbonyl)amino)pyrrolidine-1-carboxylate (55 mg, 65%) as a colorless oil. ¹H NMR (400 MHz, Chloroform-*d*) δ 7.29 (d, *J* = 2.7 Hz, 1H), 7.06 (d, *J* = 7.7 Hz, 1H), 7.04 – 6.92 (m, 2H), 4.71 (s, 1H), 4.30 (s, 1H), 3.93 – 3.70 (m, 1H), 3.67 – 3.55 (m, 2H), 3.40 (ddd, *J* = 27.0, 11.5, 4.5 Hz, 1H), 2.82 (tt, *J* = 12.9, 3.5 Hz, 1H), 2.04 – 1.54 (m, 24H), 1.49 (s, 9H). ¹³C NMR (100 MHz, CDCl₃) δ 153.27, 151.43, 147.14, 129.17, 123.74, 120.07, 119.58, 111.37, 108.98, 54.62, 44.74, 41.94, 41.65, 41.23, 39.28, 36.81, 36.66, 36.44, 35.77, 34.83, 34.19, 32.64, 30.96, 29.70, 26.89, 26.50, 25.85, 24.70, 23.50. MS (ESI) calculated for C₃₂H₄₄N₂NaO₇ [M + Na]⁺ *m/z* 591.70, found 591.48.



***trans*-3-(dispiro[adamantane-2,3'-[1,2,4]trioxolane-5',1''-cyclohexan]-3''-yl)phenyl 3-aminopyrrolidine-1-carboxylate (24).**

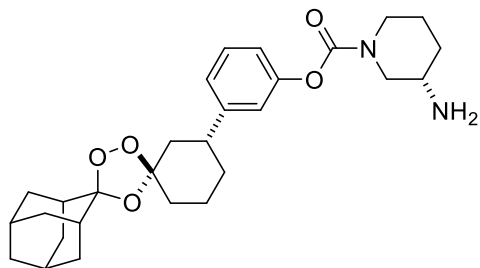
To a solution of *trans*-3-(dispiro[adamantane-2,3'-[1,2,4]trioxolane-5',1''-cyclohexan]-3''-yl)phenyl 3-((*tert*-butoxycarbonyl)amino)pyrrolidine-1-carboxylate (28.4 mg, 0.05 mmol, 1.0 equiv) in methanol (1.5 mL), was added acetyl chloride (110 μ L, 1.5 mmol, 30 equiv) in methanol (0.7 mL). The reaction was then allowed to stir at 0° C, warmed up to room temperature and stirred for 3 days, at which point, the reaction was judged complete by LCMS. The reaction mixture was concentrated to dryness and triturated with diethyl ether to yield the desired product (16.8 mg, 72%) as a hydrochloride salt, a white powder. ¹H NMR (400 MHz, Chloroform-*d*) δ 7.28 (s, 1H), 7.05 (dd, *J* = 7.6, 1.5 Hz, 1H), 7.00 – 6.96 (m, 2H), 4.72 (s, 1H), 4.30 (s, 1H), 3.86-3.74 (m, *J* = 11.6, 6.2 Hz, 1H), 3.67 (td, *J* = 6.8, 6.2, 1.8 Hz, 1H), 3.58 (td, *J* = 7.1, 2.6 Hz, 1H), 3.43-3.36 (m, *J* = 11.5, 4.4 Hz, 1H), 2.81 (tt, *J* = 12.9, 3.5 Hz, 1H), 2.05 – 1.27 (m, 24H). ¹³C NMR (100 MHz, CDCl₃) δ 155.24, 153.11, 151.32, 147.18, 129.20, 123.84, 119.99, 111.82, 108.99, 77.36, 52.24, 44.44,

41.93, 41.64, 36.80, 36.41, 34.82, 34.19, 34.07, 32.64, 32.09, 31.13, 30.94, 28.38, 26.88, 26.49, 23.49. MS (ESI) calculated for $C_{27}H_{36}N_2NaO_5$ $[M + Na]^+$ m/z 491.58, found 491.20.



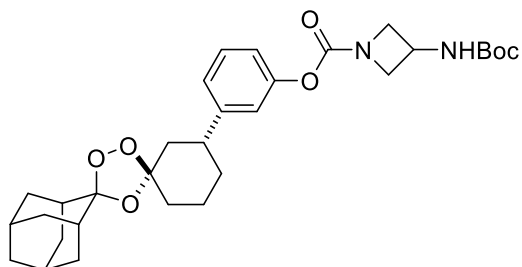
***trans*-3-(dispiro[adamantane-2,3'-[1,2,4]trioxolane-5',1''-cyclohexan]-3''-yl)phenyl 3-((tert-butoxycarbonyl)amino)piperidine-1-carboxylate**

To a solution of 3-(*trans*-dispiro[adamantane-2,3'-[1,2,4]trioxolane-5',1''-cyclohexan]-3''-yl)phenyl (4-nitrophenyl) carbonate (87.4 mg, 0.15 mmol, 1.0 equiv) in dichloromethane (1.5 mL), was added (s)-3-(Boc-amino)piperidine (48 mg, 0.24 mmol, 1.5 equiv), and triethylamine (34 μ L, 0.24 mmol, 1.5 equiv) at room temperature and was set to stir for 2 days. The reaction was deemed complete by LCMS and TLC, diluted with EtOAc (10 mL) and subsequently extracted with 1M NaOH (15 mL). The organic layer was washed with brine (12 mL), dried over anhydrous $MgSO_4$, filtered, and concentrated under reduced pressure to yield a clear oil. The residue was then purified through silica gel flash column chromatography (0-30% EtOAc/Hex), the product eluting around 20% EtOAc/Hex to *trans*-3-(dispiro[adamantane-2,3'-[1,2,4]trioxolane-5',1''-cyclohexan]-3''-yl)phenyl 3-((tert-butoxycarbonyl)amino)piperidine-1-carboxylate (50.8 mg, 56.8%) as a colorless oil. 1H NMR (400 MHz, Chloroform-*d*) δ 7.29 (d, J = 2.7 Hz, 1H), 7.06 (d, J = 7.7 Hz, 1H), 7.04 – 6.92 (m, 2H), 3.97-3.16(m,5H), 2.82 (tt, J = 12.9, 3.5 Hz, 1H), 2.04 – 1.54 (m, 28H), 1.49 (s, 9H). MS (ESI) calculated for $C_{33}H_{46}N_2O_7$ $[M + Na]^+$ m/z 582.33, found 605.22.



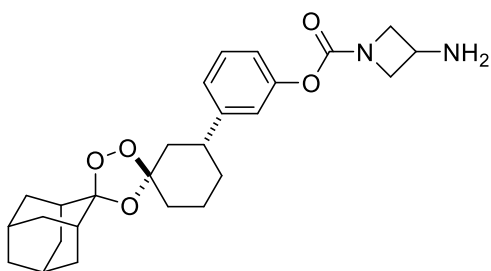
***trans*-3-(dispiro[adamantane-2,3'-[1,2,4]trioxolane-5',1''-cyclohexan]-3''-yl)phenyl 3-aminopiperidine-1-carboxylate (25).**

To a solution of *trans*-3-(dispiro[adamantane-2,3'-[1,2,4]trioxolane-5',1''-cyclohexan]-3''-yl)phenyl 3-((*tert*-butoxycarbonyl)amino)piperidine-1-carboxylate (54 mg, 0.11 mmol, 1.0 equiv) in methanol (1.5 mL), was added acetyl chloride (240 μ L, 3.3 mmol, 30 equiv) in methanol (1 mL). The reaction was then allowed to stir at 0° C, warmed up to room temperature and stirred for 3 days, at which point, the reaction was judged complete by LCMS. The reaction mixture was concentrated to dryness and triturated with diethyl ether to yield the desired product (20.1 mg, 38%) as a hydrochloride salt, a white powder. ¹H NMR (400 MHz, Chloroform-*d*) δ 7.28 (s, 1H), 7.05 (dd, *J* = 7.6, 1.5 Hz, 1H), 7.00 – 6.96 (m, 2H), 3.63-4.33 (m, 2H), 3.31-3.37 (dd, 2H), 3.16-3.25 (d, 1H), 2.81 (tt, *J* = 12.9, 3.5 Hz, 1H), 2.05 – 1.27 (m, 28H). ¹³C NMR (100 MHz, CDCl₃) δ 153.28, 151.44, 147.14, 129.17, 123.74, 120.07, 119.59, 111.37, 108.98, 54.63, 44.74, 41.94, 41.65, 39.28, 36.81, 36.66, 36.44, 35.77, 34.83, 34.19, 34.06, 32.64, 30.96, 26.89, 26.50, 25.85, 23.50. MS (ESI) calculated for C₂₈H₃₈N₂NaO₅ [M + Na]⁺ *m/z* 482.28, found 505.13.



***trans*-3-(dispiro[adamantane-2,3'-[1,2,4]trioxolane-5',1''-cyclohexan]-3''-yl)phenyl 3-((*tert*-butoxycarbonyl)amino)azetidine-1-carboxylate**

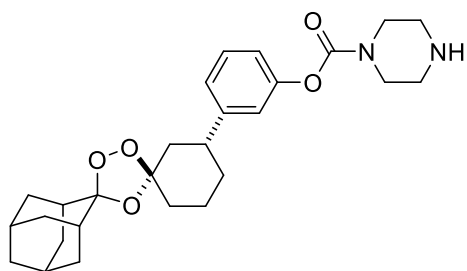
To a solution of 3-(*trans*-dispiro[adamantane-2,3'-[1,2,4]trioxolane-5',1''-cyclohexan]-3''-yl)phenyl (4-nitrophenyl) carbonate (87.4 mg, 0.15 mmol, 1.0 equiv) in dichloromethane (1.5 mL), was added *tert*-butyl azetidino-3-ylcarbamate (41.2 mg, 0.24 mmol, 1.5 equiv), and triethylamine (34 μ L, 0.24 mmol, 1.5 equiv) at room temperature and was set to stir for 2 days. The reaction was deemed complete by LCMS and TLC, diluted with EtOAc (10 mL) and subsequently extracted with 1M NaOH (15 mL). The organic layer was washed with brine (12 mL), dried over anhydrous MgSO₄, filtered, and concentrated under reduced pressure to yield a clear oil. The residue was then purified through silica gel flash column chromatography (0-30% EtOAc/Hex), the product eluting around 20% EtOAc/Hex to yield *trans*-3-(dispiro[adamantane-2,3'-[1,2,4]trioxolane-5',1''-cyclohexan]-3''-yl)phenyl 3-((*tert*-butoxycarbonyl)amino)azetidino-1-carboxylate (30.7mg, 37%) as a colorless oil. ¹H NMR (400 MHz, Chloroform-*d*) δ 7.28 (dt, *J* = 7.5, 4.6 Hz, 1H), 7.05 (dt, *J* = 7.7, 1.4 Hz, 1H), 6.97 (ddd, *J* = 5.3, 3.4, 1.4 Hz, 2H), 4.44 (t, *J* = 45.6 Hz, 2H), 3.97 (s, 1H), 3.75 – 3.60 (m, 1H), 3.09 – 2.92 (m, 1H), 2.81 (tt, *J* = 12.9, 3.5 Hz, 1H), 2.61 (d, *J* = 6.1 Hz, 1H), 2.26 – 1.54 (m, 22H), 1.52 – 1.37 (m, 9H). ¹³C NMR (100 MHz, CDCl₃) δ 154.88, 154.25, 151.15, 151.04, 147.24, 129.24, 123.93, 119.85, 119.37, 111.83, 111.39, 108.95, 62.86, 44.45, 41.92, 41.62, 41.36, 40.82, 36.79, 36.43, 34.82, 34.18, 32.62, 29.71, 28.34, 26.88, 26.49, 23.48. MS (ESI) calculated for C₃₁H₄₂N₂NaO₇ [M + Na]⁺ *m/z* 577.67, found 577.32.



***trans*-3-(dispiro[adamantane-2,3'-[1,2,4]trioxolane-5',1''-cyclohexan]-3''-yl)phenyl 3-aminoazetidino-1-carboxylate (26).**

To a solution of *trans*-3-(dispiro[adamantane-2,3'-[1,2,4]trioxolane-5',1''-cyclohexan]-3''-yl)phenyl 3-((*tert*-butoxycarbonyl)amino)azetidino-1-carboxylate (27.7 mg, 0.05 mmol, 1.0 equiv) in methanol (1.5 mL), was added acetyl chloride (110 μ L, 1.5 mmol, 30 equiv)

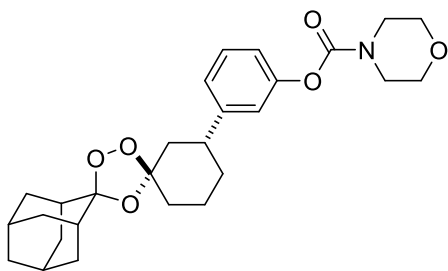
in methanol (0.7 mL). The reaction was then allowed to stir at 0° C, warmed up to room temperature and stirred for 3 days, at which point, the reaction was judged complete by LCMS. The reaction mixture was concentrated to dryness and triturated with diethyl ether to yield the desired product (12.7 mg, 56%) as a hydrochloride salt, a white powder. ¹H NMR (400 MHz, DMSO-*d*₆) δ 7.30 (qd, *J* = 7.6, 3.4 Hz, 1H), 7.13 (m, *J* = 13.5, 9.3, 4.0 Hz, 1H), 7.02 – 6.90 (m, 2H), 4.41-3.98 (m, 4H), 3.10 (d, *J* = 2.3 Hz, 1H), 2.68 (qd, *J* = 11.9, 5.7 Hz, 1H), 2.17 – 1.11 (m, 22H). MS (ESI) calculated for C₂₆H₃₄N₂NaO₅ [M + Na]⁺ *m/z* 477.56, found 477.25.



***trans*-3-((dispiro[adamantane-2,3'-[1,2,4]trioxolane-5',1''-cyclohexan]-3''-yl)phenyl)phenyl piperazine-1-carboxylate (27).**

To a solution of *trans*-3-((dispiro[adamantane-2,3'-[1,2,4]trioxolane-5',1''-cyclohexan]-3''-yl)phenyl)phenyl (4-nitrophenyl) carbonate (60 mg, 0.12 mmol, 1.0 equiv) in dichloromethane (2.0 mL) was added Et₃N (24 μL, 0.17 mmol, 1.5 equiv), followed by piperazine (18.0 mg, 0.19 mmol, 1.5 equiv) at room temperature. The bright yellow mixture was then allowed to stir at room temperature for 5 h, at which point, the reaction was judged complete by TLC and LCMS. The reaction was then diluted with H₂O (100 mL) and subsequently extracted with EtOAc (100 mL). The organic layer was washed repeatedly by potassium carbonate solution until the aqueous layer was colorless and no longer yellow (indicating successful removal of *p*-nitrophenol from the organic layer). The combined aqueous layers were then back extracted with EtOAc (30 mL). The combined organic layers were then washed with brine (20 mL), dried over anhydrous Na₂SO₄, filtered, and concentrated under reduced pressure. The residue was then purified through flash column chromatography (12 g silica gel cartridge, 0–100% EtOAc/Hexanes, followed by 0–20% MeOH (containing 0.7 N NH₃)/ CH₂Cl₂, and desired product eluted near 10% MeOH

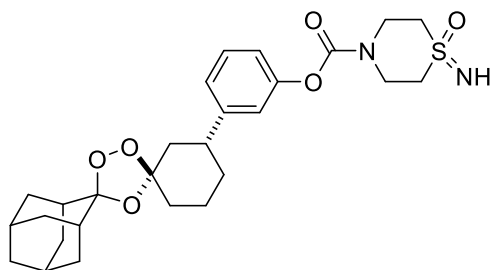
(containing 0.7 N NH₃)/ CH₂Cl₂, to yield the desired product (41.0 mg, 76%) as a colorless oil. ¹H NMR (400 MHz, CHLOROFORM-d) δ 7.22 - 7.32 (m, 1H), 7.04 (d, J = 7.79 Hz, 1H), 6.92 - 6.96 (m, 2H), 3.62 - 3.75 (m, 2H), 3.60 - 3.77 (m, 1H), 3.51 (br s, 2H), 3.44 - 3.58 (m, 1H), 2.97 - 3.06 (m, 3H), 2.80 (tt, J = 3.17, 12.66 Hz, 1H), 2.13 (br d, J = 13.39 Hz, 1H), 2.01 - 2.10 (m, 1H), 1.87 - 2.01 (m, 6H), 1.77 - 1.85 (m, 4H), 1.63 - 1.73 (m, 7H), 1.43 - 1.63 (m, 1H), 1.31 - 1.42 (m, 1H), 1.19 - 1.31 (m, 1H); ¹³C NMR (100 MHz, CDCl₃) δ 153.8, 151.5, 147.4, 129.4, 124.1, 120.1, 119.7, 111.5, 109.1, 45.3, 44.0, 42.0, 41.8, 36.9, 36.6, 36.5, 34.9, 34.9, 34.3, 32.8, 29.8, 27.0, 26.6, 23.6; MS (ESI) calculated for C₂₇H₃₇N₂O₅ [M + H]⁺ *m/z* 469.27, found 469.17.



***trans*-3-(dispiro[adamantane-2,3'-[1,2,4]trioxolane-5',1''-cyclohexan]-3''-yl)phenyl morpholine-1-carboxylate (28).**

To a solution of *trans*-3-((dispiro[adamantane-2,3'-[1,2,4]trioxolane-5',1''-cyclohexan]-3''-yl)phenyl (4-nitrophenyl) carbonate (60 mg, 0.12 mmol, 1.0 equiv) in dichloromethane (2.0 mL) was added Et₃N (24 μL, 0.17 mmol, 1.5 equiv), followed by morpholine hydrochloride (23 mg, 0.19 mmol, 1.5 equiv) at room temperature. The bright yellow mixture was then allowed to stir at room temperature for 5 h, at which point, the reaction was judged complete by TLC and LCMS. The reaction was then diluted with H₂O (100 mL) and subsequently extracted with EtOAc (100 mL). The organic layer was washed repeatedly by potassium carbonate solution until the aqueous layer was colorless and no longer yellow (indicating successful removal of *p*-nitrophenol from the organic layer). The combined aqueous layers were then back extracted with EtOAc (30 mL). The combined organic layers were then washed with brine (20 mL), dried over anhydrous Na₂SO₄, filtered, and concentrated under reduced pressure. The residue was then purified through

flash column chromatography (12 g silica gel cartridge, 0–100% EtOAc/Hexanes, followed by 0–20% MeOH (containing 0.7 N NH₃)/ CH₂Cl₂, and desired product eluted near 10% MeOH (containing 0.7 N NH₃)/ CH₂Cl₂, to yield the desired product (31.6 mg, 56.1%) as a colorless oil ¹H NMR (400 MHz, CHLOROFORM-d) δ 7.28 - 7.33 (m, 1H), 7.06 (d, J = 7.79 Hz, 1H), 6.94 – 6.98 (m, 2H), 3.75 - 3.8 (t, 4H), 3.55 - 3.73 (d, 4H), 2.80 (tt, J = 3.17, 12.66 Hz, 1H), 2.13 (br d, J = 13.39 Hz, 1H), 2.01 - 2.10 (m, 1H), 1.87 - 2.01 (m, 6H), 1.77 - 1.85 (m, 4H), 1.63 - 1.73 (m, 7H), 1.43 - 1.63 (m, 1H), 1.31 - 1.42 (m, 1H), 1.19 - 1.31 (m, 1H); ¹³C NMR (100 MHz, CDCl₃) δ 153.79, 151.34, 147.30, 129.28, 124.01, 120.02, 119.51, 111.40, 108.94, 66.61, 44.88, 41.94, 41.66, 41.36, 36.80, 36.43, 36.41, 34.81, 34.78, 34.19, 32.65, 26.88, 26.49, 23.48; MS (ESI) calculated for C₂₇H₃₅NO₆ [M + Na]⁺ *m/z* 469.25, found 492.1.

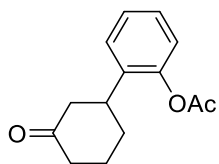


3-((1R,3S,3''R,5R,5'R,7R)-dispiro[adamantane-2,3'-[1,2,4]trioxolane-5',1''-cyclohexan]-3''-yl)phenyl 1-imino-116-thiomorpholine-4-carboxylate 1-oxide (29)

To a solution of 3-((1R,3S,3''R,5R,5'R,7R)-dispiro[adamantane-2,3'-[1,2,4]trioxolane-5,1''-cyclohexan]-3''-yl)phenyl (4-nitrophenyl) carbonate (30 mg, 0.058 mmol) in dichloromethane (3 mL) were added 1-imino-thiomorpholine 1-oxide hydrochloride (11 mg, 0.063 mmol) and triethylamine (0.016 mL, 0.12 mmol). After stirring at 35° C for 72 h, the reaction mixture was diluted with ethyl acetate and washed multiple times with 1N aqueous sodium hydroxide solution. The organic layer was washed with brine, dried over magnesium sulfate, concentrated *in vacuo* and purified by flash column chromatography (25% ethyl acetate/hexanes followed by 10% 0.7N ammonia in methanol/dichloromethane to obtained 10 mg (34% yield) of 3-((1R,3S,3''R,5R,5'R,7R)-dispiro[adamantane-2,3'-[1,2,4]trioxolane-5',1''-cyclohexan]-3''-yl)phenyl 1-imino-116-thiomorpholine-4-carboxylate 1-oxide as a colorless oil. ¹H NMR (400 MHz, CDCl₃) δ 1H

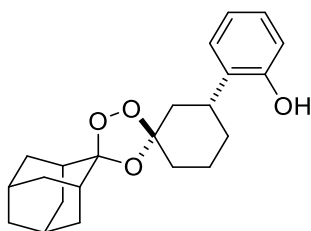
NMR (CHLOROFORM-d, 400 MHz) Shift 1H NMR (CHLOROFORM-d, 400 MHz) Shift 7.33 (t, 1H, J=7.0 Hz), 7.11 (d, 1H, J=7.8 Hz), 6.9-7.0 (m, 2H), 4.03-4.22 (m, 4H), 3.20 (br s, 4H), 2.84 (br s, 1H), 1.33-2.18 (m, 23H). MS (ESI) calculated for C₂₇H₃₇N₂O₆S [M + H]⁺ *m/z* 517.23, found 517.11.

Ortho aryl intermediates and final compounds



2-(3-oxocyclohexyl)phenyl acetate (S4).

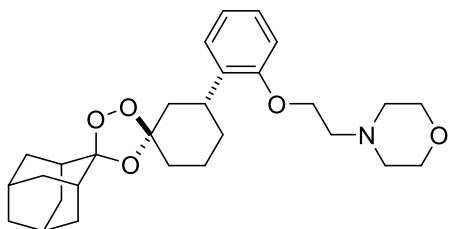
To a suspension of 3-(2-hydroxyphenyl)cyclohexan-1-one (2.7 g, 14.3 mmol, 1 equiv.) in 50 mL CH₂Cl₂ was added pyridine (5.8 mL, 71.5 mmol, 5 equiv.) and acetic anhydride (2.7 mL, 28.6 mmol, 1 equiv.) and the reaction mixture stirred at room temperature for 16 h. The reaction mixture was quenched by 1 M HCl aq. and extracted with CH₂Cl₂ three times. The resulting organic layers were combined, dried over MgSO₄ and concentrated. The residue was then purified through flash column chromatography (120 g silica gel cartridge, 0–100 % EtOAc/Hexanes) to yield the product (3.2 g, 97 %) as a white solid. ¹H NMR (400 MHz, CDCl₃) δ 7.35 – 7.28 (m, 1H), 7.28 – 7.23 (m, 2H), 7.08 – 7.00 (m, 1H), 3.11 (tt, *J* = 11.7, 3.9 Hz, 1H), 2.59 – 2.35 (m, 4H), 2.32 (s, 3H), 2.16 (ddq, *J* = 12.9, 6.6, 3.0 Hz, 1H), 2.05 – 1.98 (m, 1H), 1.90 – 1.69 (m, 2H). ¹³C NMR (100 MHz, CDCl₃) δ 210.5, 169.4, 148.0, 135.8, 127.5, 126.8, 126.4, 122.7, 47.8, 41.1, 38.0, 31.4, 25.5, 20.9. LRMS (ESI) calcd for C₁₄H₁₇O₃Na [M + Na]⁺ *m/z* 255.11, found 255.22.



trans-2-(dispiro[adamantane-2,3'-[1,2,4]trioxolane-5',1''-cyclohexan]-3''-yl)phenol (6).

To a 100 mL flask containing 40 mL hexane was added 2-(3-oxocyclohexyl) phenyl acetate (850 mg, 3.7 mmol, 1.0 equiv.) and adamantan-2-one O-methyl oxime (1.64 g, 9.2 mmol, 2.5 equiv.) The mixture was cooled to -78 °C and ozone was bubbled through

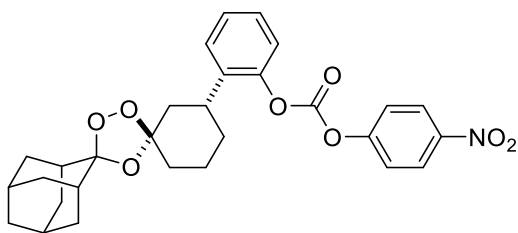
the solution. The O₂ flow rate was 1 liter/min, ozone gauge set to 3.5 (this setting amounts to ~ 6 g/hour ozone production). The reaction flask was wrapped with aluminum foil and the reaction mixture stirred at -78 °C for 4 hours, at which point the reaction was complete based on UPLC-MS. The reaction mixture was then bubbled with N₂ for 10 mins and concentrated. To the resulting crude trioxolane product in THF (7 mL) and MeOH (14 mL) was added 15% aqueous KOH (3 mL). The solution was then placed in an oil bath that had been preheated to 50 °C and was allowed to stir at this temperature for 1.5 hour, after which the solution then allowed to cool to room temperature. The mixture was then concentrated under reduced pressure. To the residue was then added H₂O (30 mL) and 1M HCl aq. until the solution reached pH ~ 4, and then extracted with EtOAc (100 mL). The organic layer was then washed with brine, dried over anhydrous Na₂SO₄, filtered, and concentrated under reduced pressure. The residue was then purified by flash column chromatography (80 g silica gel cartridge, 0–50 % EtOAc/Hexanes, product eluted around 30 %) to yield the product (0.9 g, 70 %) as a colorless oil. ¹H NMR (400 MHz, CDCl₃) δ 7.15 (dd, *J* = 7.7, 1.7 Hz, 1H), 7.08 (td, *J* = 7.7, 1.7 Hz, 1H), 6.90 (td, *J* = 7.5, 1.2 Hz, 1H), 6.77 (dd, *J* = 7.9, 1.2 Hz, 1H), 3.15 (tt, *J* = 12.9, 3.4 Hz, 1H), 2.15 – 1.62 (m, 21H), 1.44 (qd, *J* = 12.4, 3.4 Hz, 1H), ¹³C NMR (100 MHz, CDCl₃) δ 153.2, 131.5, 127.2, 127.1, 120.9, 115.7, 111.5, 109.5, 40.5, 39.4, 36.9, 36.5, 36.5, 35.2, 35.0, 34.9, 34.9, 34.5, 31.2, 27.0, 26.6, 23.7. LRMS (ESI) calcd for C₂₂H₂₈O₄Na [M + Na]⁺ *m/z* 379.20, found 379.19.



***trans*-4-(2-(2-(dispiro[adamantane-2,3'-[1,2,4]trioxolane-5',1''-cyclohexan]-3''-yl)phenoxy)ethyl)morpholine. (9).**

To a solution of *trans*-2-(dispiro[adamantane-2,3'-[1,2,4]trioxolane-5',1''-cyclohexan]-3''-yl)phenol (50.0 mg, 0.14 mmol, 1.0 equiv.) in dry CH₃CN (4 mL) was added tetrabutylammonium hydrogen sulfate (14.3 mg, 0.04 mmol, 0.3 equiv.) and powdered

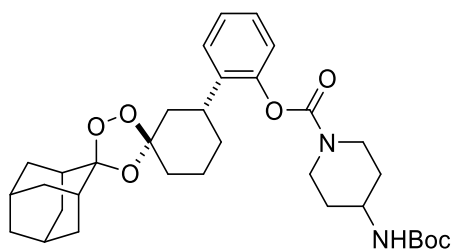
NaOH (20.2 mg, 0.51 mmol, 3.6 equiv.). This mixture was then allowed to stir at room temperature for 30 minutes, at which point 4-(2-chloroethyl)morpholine hydrochloride (42.0 mg, 0.28 mmol, 2.0 equiv.) was added to the solution. The mixture was then placed in an oil bath that had been preheated to 55 °C and was allowed to stir at this temperature for 14 hours. At this point the reaction was judged complete by TLC and LCMS analysis, and so the reaction mixture was allowed to cool to room temperature. The mixture was then diluted with EtOAc (20 mL) prior to the addition of H₂O (10 mL), which served to dissolve all of the inorganic solids present. The organic phase was separated and the aqueous layer extracted with EtOAc (20 mL). The combined organic phases were then washed with brine (10 mL), dried over anhydrous Na₂SO₄, filtered, and concentrated under reduced pressure. The residue was then purified through flash column chromatography (12 g silica gel cartridge, 0–10 % MeOH/CH₂Cl₂) to yield the product (40.2 mg, 61%). ¹H NMR (400 MHz, CDCl₃) δ 7.20 – 7.09 (m, 2H), 7.00 – 6.87 (m, 1H), 6.82 (d, *J* = 8.3 Hz, 1H), 4.15 (t, *J* = 5.4 Hz, 2H), 3.87 – 3.70 (m, 4H), 3.21 (t, *J* = 13.3 Hz, 1H), 3.01 – 2.82 (m, 2H), 2.70 (s, 4H), 2.61 (s, 2H), 2.20 – 1.17 (m, 22H); ¹³C NMR (100 MHz, CDCl₃) δ 155.9, 133.9, 127.2, 126.8, 121.0, 111.5, 111.3, 109.4, 66.8, 66.1, 57.9, 54.2, 41.1, 40.8, 36.9, 36.5, 35.0, 34.9, 34.5, 31.3, 27.0, 26.6, 23.9. LRMS (ESI) calcd for C₂₈H₄₀NO₅ [M + H]⁺ *m/z* 470.28, found 479.42.



***trans*-2-(dispiro[adamantane-2,3'-[1,2,4]trioxolane-5',1''-cyclohexan]-3''-yl)phenyl (4-nitrophenyl) carbonate (12).**

To a 20 mL vial with *trans*-2-(dispiro[adamantane-2,3'-[1,2,4]trioxolane-5',1''-cyclohexan]-3''-yl)phenol (230 mg, 0.65 mmol, 1 equiv.) dissolved in CH₂Cl₂ (5 mL) was added 4-nitrophenyl chloroformate (325 mg, 1.6 mmol, 2.5 equiv.), DIPEA (0.34 mL, 1.9 mmol, 3 equiv.), and DMAP (8.0 mg, 0.07 mmol, 0.1 equiv.) at 0 °C. The reaction mixture was

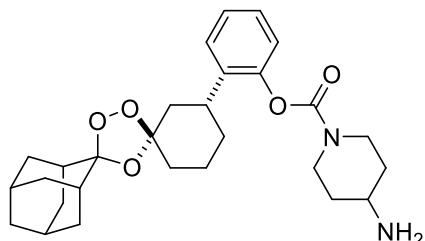
stirred at room temperature overnight and then treated with 1M NaOH aq. and diluted with CH₂Cl₂. The organic phase was washed with aq. NaHCO₃ thrice, brine, and then dried over MgSO₄ and concentrated. The crude residue was then purified by flash column chromatography (40 g silica gel cartridge, 0–80 % EtOAc/Hexanes) to yield the product (260 mg, 77 %) as a yellow oil. ¹H NMR (400 MHz, CDCl₃) δ 8.33 (d, *J* = 8.9 Hz, 2H), 7.57 (d, *J* = 8.8 Hz, 2H), 7.43 – 7.15 (m, 4H), 3.11 (tt, *J* = 12.5, 3.4 Hz, 1H), 2.26 – 2.13 (m, 1H), 2.06 – 1.65 (m, 20H), 1.58 – 1.42 (m, 1H). ¹³C NMR (100 MHz, CDCl₃) δ 155.6, 151.5, 148.2, 145.8, 137.1, 127.6, 127.4, 125.5, 122.2, 121.7, 111.7, 108.9, 41.4, 36.8, 36.5, 36.5, 35.0, 34.9, 34.9, 34.9, 34.9, 34.3, 31.5, 26.9, 26.5, 23.7. LRMS (ESI) calcd for C₂₉H₃₂NO₈ [M + H]⁺ *m/z* 522.21, found 522.91.



***trans*-2-(dispiro[adamantane-2,3'-[1,2,4]trioxolane-5',1''-cyclohexan]-3''-yl)phenyl 4-((*tert*-butoxycarbonyl)amino)piperidine-1-carboxylate.**

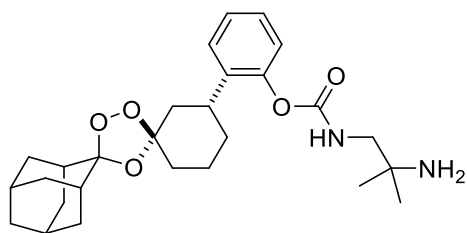
A 20 mL vial was charged with *trans*-2-(dispiro[adamantane-2,3'-[1,2,4]trioxolane-5',1''-cyclohexan]-3''-yl)phenyl (4-nitrophenyl) carbonate (15 mg, 0.03 mmol, 1.0 equiv.), *tert*-butyl 4-aminopiperidine-1-carboxylate (8.7 mg, 0.4 mmol, 1.5 equiv.) and 5 mL of CH₂Cl₂. Triethylamine (12.0 μL, 0.09 mmol, 3.0 equiv.) was then added to the reaction mixture slowly and the mixture stirred at room temperature overnight. After diluting the reaction mixture with CH₂Cl₂, the organic phase was washed with 1M NaHCO₃ aq. 3 times, and brine. The organic layer was then dried over MgSO₄, filtered and concentrated, and the residue purified by flash column chromatography (12 g silica gel cartridge, 0–20 % MeOH/CH₂Cl₂) to yield the product (6.4 mg, 38%). ¹H NMR (400 MHz, CDCl₃) δ 7.25 – 7.15 (m, 3H), 7.09 (d, *J* = 7.9 Hz, 1H), 5.12 (d, *J* = 7.7 Hz, 1H), 4.06 (s, 2H), 3.73 (s, 1H), 3.04 – 2.80 (m, 3H), 2.16 (d, *J* = 12.8 Hz, 1H), 2.03 – 1.47 (m, 32H), 1.29 – 1.22 (m, 2H); ¹³C NMR (100 MHz, CDCl₃) δ 154.9, 154.0, 148.5, 137.6, 127.1, 126.8, 126.1, 123.0,

111.6, 109.2, 79.8, 48.8, 41.5, 36.9, 36.6, 35.2, 35.1, 35.0, 34.8, 34.3, 32.3, 31.0, 28.6, 27.0, 26.6, 23.8. LRMS (ESI) calcd for C₃₃H₄₆N₂O₇Na [M + Na]⁺ m/z 605.33, found 605.38.



***trans*-2-(dispiro[adamantane-2,3'-[1,2,4]trioxolane-5',1''-cyclohexan]-3''-yl)phenyl 4-aminopiperidine-1-carboxylate (15).**

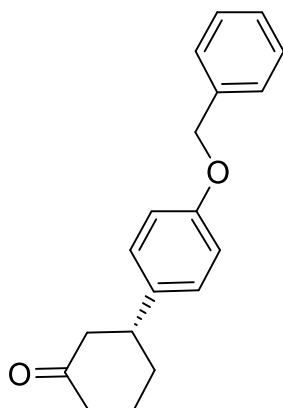
To a solution of *trans*-2-(dispiro[adamantane-2,3'-[1,2,4]trioxolane-5',1''-cyclohexan]-3''-yl)phenyl 4-((*tert*-butoxycarbonyl)amino)piperidine-1-carboxylate (62.4 mg, 107 μmol, 1.0 equiv.) in methanol (1.0 mL) cooled to 0 °C in an ice bath, was added acetyl chloride (228 uL, 3.2 mmol, 30 equiv.) dropwise via microsyringe. The solution was allowed to stir for 10 minutes at 0 °C, after which the solution was removed from the bath and allowed to warm to room temperature overnight. The reaction mixture was then quenched by NH₃ in MeOH (7M). The resulting solution was concentrated and purified by column chromatography (12 g silica gel cartridge, 0–20% of 10% NH₄OH in MeOH/CH₂Cl₂) to yield the product (11.1 mg, 21.5 %). ¹H NMR (400 MHz, MeOD) δ 7.40 – 7.30 (m, 1H), 7.29 – 7.18 (m, 2H), 7.09 – 7.00 (m, 1H), 4.46 (s, 1H), 4.24 (s, 1H), 3.31 – 3.17 (m, 2H), 3.14 – 2.87 (m, 2H), 2.30 – 1.40 (m, 28H), ¹³C NMR (100 MHz, MeOD) δ 155.3, 149.8, 138.7, 128.1, 127.4, 123.9, 112.5, 110.2, 43.4 (rotamer, m), 37.9, 37.8, 37.7, 36.4, 35.9, 35.8, 35.7, 35.2, 32.0 (rotamer, m), 28.3, 28.0, 24.8. LRMS (ESI) calcd for C₂₈H₃₉N₂O₅ [M + H]⁺ m/z 483.27, found 483.27.



***trans*-2-(dispiro[adamantane-2,3'-[1,2,4]trioxolane-5',1''-cyclohexan]-3''-yl)phenyl (2-amino-2-methylpropyl)carbamate (18).**

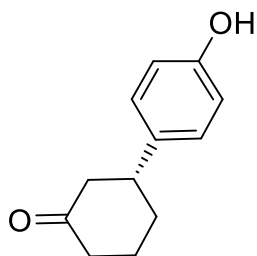
To a solution of *trans*-2-(dispiro[adamantane-2,3'-[1,2,4]trioxolane-5',1''-cyclohexan]-3''-yl)phenyl 4-((*tert*-butoxycarbonyl)amino)piperidine-1-carboxylate (35 mg, 0.07 mmol, 1.0 equiv.) in CH₂Cl₂ was added Et₃N (28 μL, 0.20 mmol, 3.0 equiv.) followed by 1,1-dimethyl-1,2-ethanediamine (11 μL, 0.1 mmol, 1.5 equiv.). The bright yellow mixture was allowed to stir at room temperature for 16 h and then quenched by the addition of NH₃ in MeOH (7M). The resulting solution was concentrated and purified by column chromatography (12 g silica gel cartridge, 0–20% of 10% NH₄OH in MeOH/CH₂Cl₂) to yield the product (10.8 mg, 34 %). ¹H NMR (400 MHz, CDCl₃) δ 7.26 – 7.13 (m, 3H), 7.13 – 7.03 (m, 1H), 5.69 (t, *J* = 6.3 Hz, 1H), 3.23 (dd, *J* = 13.5, 6.8 Hz, 1H), 3.12 (dd, *J* = 13.5, 5.8 Hz, 1H), 3.02 (tt, *J* = 12.6, 3.2 Hz, 1H), 2.17 (dq, *J* = 13.0, 3.7, 2.8 Hz, 1H), 1.98 – 1.65 (m, 20H), 1.47 – 1.38 (m, 1H), 1.19 (s, 6H). ¹³C NMR (100 MHz, CDCl₃) δ 155.5, 148.6, 137.6, 127.1, 126.8, 126.0, 123.0, 111.6, 109.2, 52.8, 50.6, 41.4, 36.9, 36.6, 36.5, 35.3, 35.0, 35.0, 34.9, 34.4, 31.1, 28.4, 28.3, 28.2, 27.0, 26.6, 23.8. LRMS (ESI) calcd for C₂₇H₃₉N₂O₅ [M + H]⁺ *m/z* 471.28, found 471.20.

Enantioselective synthesis of 17R and 17S



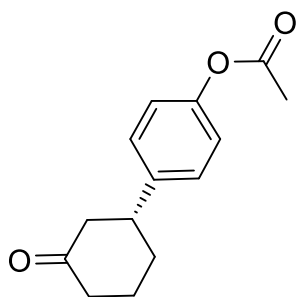
(3R)-3-[4-(benzyloxy)phenyl]cyclohexan-1-one

To a round bottom flask under inert atmosphere was added Acetylacetonatobis(ethylene)-rhodium(I) (160mg, 0.625mmol, 0.03equiv.) and dioxane (100mL). The flask was flushed with Argon, then R-BINAP (1.30g, 2.08mmol, 0.1equiv.), Potassium Hydroxide (1M solution, 10mL), and [4-(benzyloxy)phenyl]boronic acid (11.9g, 52.0mmol, 2.5equiv.) were added sequentially. The flask was stirred under Argon for 10 minutes. Cyclohex-2-en-1-one (2.00g, 20.8mmol, 1 equiv.) was added and the reaction flask was purged and back-filled with Argon three times. The reaction was heated to 100C and stirred overnight. Following consumption of starting material, the reaction was cooled to room temperature, filtered over celite, and concentrated. Purification via flash column chromatography (330g silica gel cartridge, isocratic 12% EtOAc:Hexanes elution) followed by concentration and lyophilization of product fractions yielded (3R)-3-[4-(benzyloxy)phenyl]cyclohexan-1-one (3.17g, 11.3mmol, 54.3%) as a white solid. ¹H NMR (CHLOROFORM-d, 400 MHz) δ 7.3-7.6 (m, 5H), 7.19 (d, 2H, J=8.5 Hz), 7.00 (d, 2H, J=8.5 Hz), 5.09 (s, 2H), 3.01 (tt, 1H, J=3.9, 11.7 Hz), 2.6-2.7 (m, 1H), 2.4-2.6 (m, 3H), 2.0-2.3 (m, 2H), 1.8-2.0 (m, 2H); ¹³C NMR (CHLOROFORM-d, 100 MHz) δ 211.2, 157.6, 137.1, 136.9, 128.7, 128.0, 127.6, 127.6, 115.0, 70.1, 49.3, 44.0, 41.2, 33.0, 25.6; MS (ESI) calc for C₁₉H₂₁O₂ [M+H]⁺: m/z 281.15 found 281.29



(3R)-3-(4-hydroxyphenyl)cyclohexan-1-one

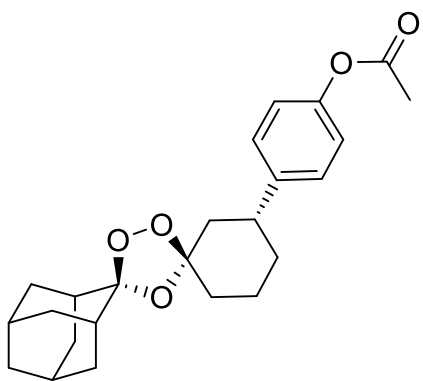
To a round bottom flask under inert Argon atmosphere was added 10% Palladium on Carbon (0.317g, 0.298mmol, 0.0264 equiv.) in ethyl acetate (50mL). (3R)-3-[4-(benzyloxy)phenyl]cyclo-hexan-1-one (3.17g, 11.3mmol, 1 equiv.) was added and the flask was evacuated and purged with Argon three times. The flask was again evacuated and backfilled with Hydrogen at 1atm. The solution was heated to 50C and stirred for 48 hours. Following completion, the reaction mixture was filtered over celite, rinsed with ethyl acetate, concentrated, and lyophilized to yield (3R)-3-(4-hydroxyphenyl)cyclohexan-1-one (1.97g, 10.4mmol, 91.6%) as a white powder. ¹H NMR (CHLOROFORM-d, 400 MHz) δ 7.10 (d, 2H, J=8.5 Hz), 6.83 (d, 2H, J=8.3 Hz), 2.97 (tdd, 1H, J=3.9, 7.9, 15.5 Hz), 2.4-2.6 (m, 4H), 2.0-2.2 (m, 2H), 1.7-1.9 (m, 2H); ¹³C NMR (CHLOROFORM-d, 100 MHz) δ 212.2, 154.5, 128.6, 127.7, 115.5, 49.3, 44.0, 41.2, 33.0, 25.5; MS (ESI) calc for C₁₂H₁₅O₂ [M+H]⁺: m/z 191.10 found 191.17



4-[(1R)-3-oxocyclohexyl]phenyl acetate

To a solution of (3R)-3-(4-hydroxyphenyl)cyclohexan-1-one (1.90g, 9.99mmol, 1 equiv.) in dichloromethane (50mL) was added triethylamine (2.02g, 20.0mmol, 2 equiv.). The solution was cooled to 0C, and acetic anhydride (3.06g, 30.0mmol, 3 equiv.) was added

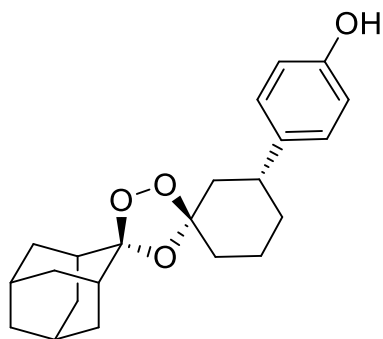
dropwise. The solution was allowed to return to room temperature and was stirred for 45 minutes. Following completion the solution was diluted with deionized water and the organic layer was extracted over water, saturated NaHCO₃, and brine. The organic fraction was dried over MgSO₄, concentrated, and lyophilized to yield 4-[(1R)-3-oxocyclohexyl]phenyl acetate (2.32g, 9.99mmol, 100%) as a white solid. Product was confirmed via UPLC/MS and used immediately in the next reaction. MS (ESI) calc for C₁₄H₁₇O₃ [M+H]⁺: m/z 233.11 found 233.23.



4-[(1''R,3''R)-dispiro[adamantane-2,3'-[1,2,4]trioxolane-5',1''-cyclohexan]-3''-yl]phenyl acetate.

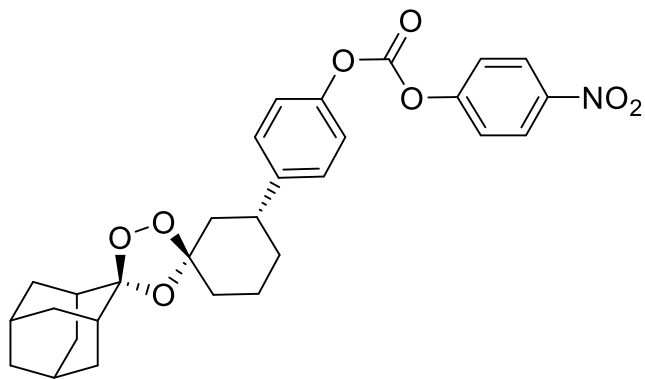
To an oven-dried round bottom flask was added 4-[(1R)-3-oxocyclohexyl]phenyl acetate (1.00g, 4.31mmol, 1 equiv.), N-methoxyadamantan-2-imine (2.00g, 11.2mmol, 2.59 equiv.) and carbon tetrachloride (50mL). The solution was cooled to 0C and sparged with O₂ for 10min. The reaction was maintained at 0C while ozone was bubbled (2L/min, 40% power) through the solution. Following 3.5 hours, the reaction was deemed complete via UPLC/MS and TLC. The reaction mixture was concentrated to yield a crude mixture as a viscous oil. The crude material was purified via flash column chromatography (220g silica gel cartridge, 5-15% EtOAc:Hex) and product fractions were concentrated and lyophilized to yield 4-[(1''R,3''R)-dispiro[adamantane-2,3'-[1,2,4]trioxolane-5',1''-cyclohexan]-3''-yl]phenyl acetate (1.146g, 2.876mmol, 66.8%) as a colorless solid. ¹H NMR (CHLOROFORM-d, 400 MHz) δ 7.22 (d, 2H, J=8.5 Hz), 7.03 (d, 2H, J=8.8 Hz), 2.82 (tt, 1H, J=3.4, 12.8 Hz), 2.31 (s, 3H), 2.1-2.2 (m, 1H), 1.9-2.0 (m, 7H), 1.7-1.9 (m, 12H),

1.5-1.6 (m, 1H), 1.2-1.5 (m, 1H); ¹³C NMR (CHLOROFORM-d, 100 MHz) δ 169.7, 148.9, 143.2, 127.8, 121.4, 111.4, 109.0, 42.2, 41.3, 36.8, 36.4, 34.8, 34.8, 34.2, 32.8, 26.9, 26.5, 23.5, 21.2; MS (ESI) calc for C₂₄H₃₀O₅Na [M+Na]⁺: m/z 421.20 found 421.29



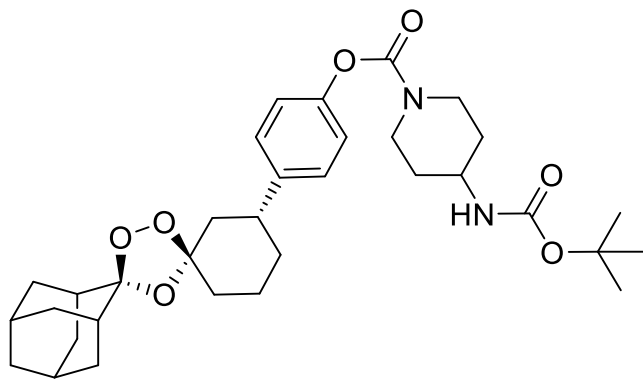
4-[(1''R,3''R)-dispiro[adamantane-2,3'-[1,2,4]trioxolane-5',1''-cyclohexan]-3''-yl]phenol

To an oven-dried round bottom flask was added 4-[(1''R,3''R)-dispiro[adamantane-2,3'-[1,2,4]trioxolane-5',1''-cyclohexan]-3''-yl]phenyl acetate (1.10g, 2.760mmol, 1 equiv.) in Tetrahydrofuran (20mL) and methanol (20mL). Lithium hydroxide (0.264g, 11.04mmol, 4 equiv.) was added as a 1M solution in DI water and the reaction was stirred overnight at room temperature. The reaction was quenched with 1M NH₄Cl and the aqueous layer was extracted 3 times with DCM. The combined organic fractions were dried over MgSO₄, concentrated, and lyophilized to yield 4-[(1''R,3''R)-dispiro[adamantane-2,3'-[1,2,4]trioxolane-5',1''-cyclohexan]-3''-yl]phenol (0.984g, 2.760mmol, 84.8%) as a white solid. ¹H NMR (CHLOROFORM-d, 400 MHz) δ 7.09 (br d, 2H, J=8.3 Hz), 6.79 (br d, 2H, J=8.5 Hz), 2.7-2.8 (m, 1H), 2.12 (br d, 4H, J=12.4 Hz), 1.9-2.0 (m, 7H), 1.7-1.9 (m, 8H), 1.5-1.7 (m, 2H), 1.2-1.5 (m, 2H); ¹³C NMR (CHLOROFORM-d, 100 MHz) δ 153.9, 138.0, 127.9, 115.2, 111.4, 109.2, 100.0, 42.4, 41.0, 36.8, 36.4, 34.8, 34.8, 34.2, 33.0, 26.9, 26.5, 23.6; MS (ESI) calc for C₂₂H₂₉O₄ [M-H]⁻: m/z 355.19 found 355.26



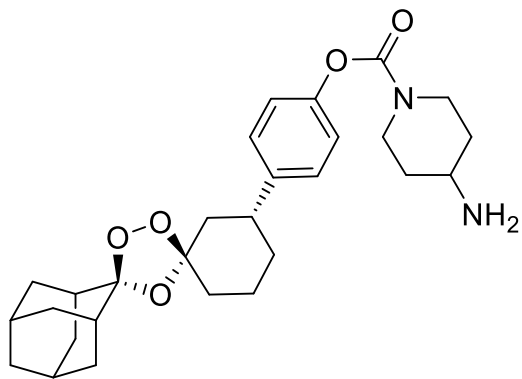
4-[(1''R,3''R)-dispiro[adamantane-2,3'-[1,2,4]trioxolane-5',1''-cyclohexan]-3''-yl]phenyl 4-nitrophenyl carbonate

To an oven-dried round bottom flask was added 4-[(1''R,3''R)-dispiro[adamantane-2,3'-[1,2,4]trioxolane-5',1''-cyclohexan]-3''-yl]phenol (0.834g, 2.34mmol, 1 equiv.) and dichloromethane (50mL). The solution was cooled to 0C, and DIPEA (0.907g, 7.02mmol, 3 equiv.) and DMAP (0.057g, 0.468mmol, 0.2 equiv.) were added. The solution was stirred at 0C for 10 minutes, following which p-Nitrophenol Chloroformate (1.41g, 7.02mmol, 3 equiv.) was added portionwise. Upon complete addition the reaction was allowed to return to room temperature and stirred overnight. The reaction was diluted with dichloromethane and 1M Na₂CO₃, and the organic layer was extracted repeatedly with 1M Na₂CO₃ until no yellow color was observed, indicating depletion of p-nitrophenol. The organic layer was dried over MgSO₄ and concentrated to yield a crude colorless oil. This crude product was purified via flash column chromatography (80g silica gel cartridge, 0-25% EtOAC:Hex elution) and the product fractions were combined, concentrated, and lyophilized to yield 4-[(1''R,3''R)-dispiro[adamantane-2,3'-[1,2,4]trioxolane-5',1''-cyclohexan]-3''-yl]phenyl 4-nitrophenyl carbonate (0.310g, 2.34mmol, 25%) as a white powder. NMR indicated the presence of some uncoupled product, which was carried through as an impurity. ¹H NMR (DMSO-d₆, 400 MHz) δ 8.37 (d, 1H, J=9.3 Hz), 7.71 (d, 1H, J=9.0 Hz), 7.3-7.4 (m, 4H), 2.5-2.8 (m, 1H), 1.8-2.1 (m, 8H), 1.7-1.8 (m, 9H), 1.6-1.7 (m, 4H), 1.3-1.6 (m, 3H); ¹³C NMR (DMSO-d₆, 100 MHz) δ 155.6, 151.3, 149.4, 145.9, 144.3, 128.5, 126.0, 123.2, 121.5, 111.1, 109.2, 41.7, 41.3, 38.9, 36.6, 36.3, 34.7, 33.9, 32.6, 26.7, 26.3, 23.6; MS (ESI) calc for C₂₉H₃₁NO₈Na [M+Na]⁺: m/z 544.19 found 543.94



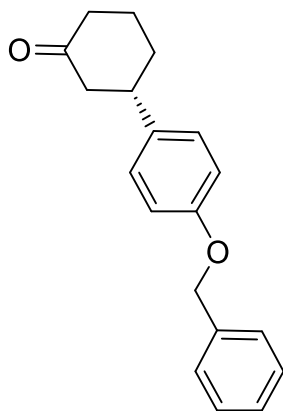
4-[(1^R,3^R)-dispiro[adamantane-2,3'-[1,2,4]trioxolane-5',1''-cyclohexan]-3''-yl]phenyl 4-tert-butylpiperidin-1-carboxylate

To an oven-dried round bottom flask was added 4-[(1^R,3^R)-dispiro[adamantane-2,3'-[1,2,4]trioxolane-5',1''-cyclohexan]-3''-yl]phenyl 4-nitrophenyl carbonate (0.300g, 0.575mmol, 1 equiv.) followed by tert-butyl piperidin-4-ylcarbamate (0.184g, 0.920mmol, 1.6 equiv.) and DMAP (0.014g, 0.115mmol, 0.2 equiv.). The reaction flask was evacuated and purged with argon. DMF (35mL) and DIPEA (0.223mg, 1.73mmol, 3 equiv.) were added and the reaction was stirred at room temperature overnight. Following completion, the reaction was diluted with Ethyl Acetate and the organic layer was extracted with 1M Na₂CO₃ until no yellow color was observed, indicating depletion of p-Nitrophenol. The organic layer was dried over MgSO₄ and concentrated to yield a crude colorless oil. The crude product was purified via flash column chromatography (40g silica gel cartridge, 0-25% EtOAc:Hex) to yield 4-[(1^R,3^R)-dispiro[adamantane-2,3'-[1,2,4]trioxolane-5',1''-cyclohexan]-3''-yl]phenyl 4-tert-butylpiperidin-1-carboxylate (0.226g, 0.389mmol, 67.5%) as a white powder. Product was confirmed via UPLC/MS and used immediately in the next reaction. MS (ESI) calc for C₃₃H₄₆N₂O₇Na [M+Na]⁺: m/z 605.32 found 605.52.



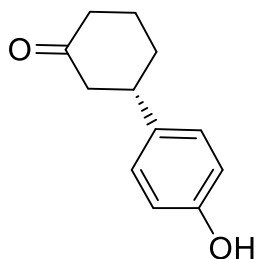
4-[(1''R,3''R)-dispiro[adamantane-2,3'-[1,2,4]trioxolane-5',1''-cyclohexan]-3''-yl]phenyl 4-aminopiperidine-1-carboxylate (17R)

A solution of 4-[(1''R,3''R)-dispiro[adamantane-2,3'-[1,2,4]trioxolane-5',1''-cyclohexan]-3''-yl]phenyl 4-[[tert-butoxy]carbonyl]amino}piperidine-1-carboxylate (290mg, 0.498 mmol, 1.0 equiv.) in methanol (5mL) and THF (5mL) was cooled to 0C using an ice bath. After purging the flask with inert atmosphere, acetyl chloride (389mg, 4.98mmol, 10equiv.) was added dropwise. The solution was stirred at 0C for 15 minutes, then allowed to return to room temperature for 16 hours. The reaction was diluted with dichloromethane, quenched with 1M Na₂CO₃, and the aqueous layer was extracted 3X with dichloromethane. The combined organic fractions were filtered, dried over MgSO₄, and concentrated to yield a crude product resembling a light yellow oil. The crude residue was purified in batches by HPLC (Agilent 1200 Series) using a 5uM Cellulose-3 column (Phenomenex) with an isocratic mobile phase consisting of 40:60 20mM Ammonium Bicarbonate pH 8.5 in Acetonitrile (with 0.1% diethylamine). Product peaks from each batch were combined, concentrated, and lyophilized to yield 4-[(1''R,3''R)-dispiro[adamantane-2,3'-[1,2,4]trioxolane-5',1''-cyclohexan]-3''-yl]phenyl 4-aminopiperidine-1-carboxylate (85.8mg, 0.178mmol, 36%) as a colorless solid. ¹H NMR (DMSO-d₆, 400 MHz) δ 7.27 (d, 2H, J=8.5 Hz), 7.02 (d, 2H, J=8.5 Hz), 3.9-4.2 (m, 2H), 3.1-3.3 (m, 1H), 3.10 (br s, 1H), 2.94 (br s, 1H), 2.5-2.8 (m, 2H), 1.8-2.0 (m, 8H), 1.6-1.8 (m, 12H), 1.4-1.5 (m, 3H); ¹³C NMR (DMSO-d₆, 100 MHz) δ 153.5, 149.9, 142.8, 128.0, 122.2, 111.0, 109.2, 47.7, 41.8, 41.3, 36.5, 36.2, 34.7, 33.9, 32.7, 26.7, 26.3, 23.7 ; MS (ESI) calc for C₂₈H₃₉N₂O₅ [M+H]⁺: m/z 483.28 found 483.51



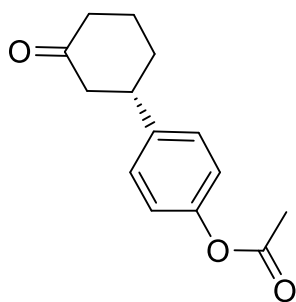
(3S)-3-[4-(benzyloxy)phenyl]cyclohexan-1-one (37).

To a round bottom flask under inert atmosphere was added Acetylacetonatobis(ethylene)-rhodium(I) (160mg, 0.625mmol, 0.03equiv.) and dioxane (100mL). The flask was flushed with Argon, then S-BINAP (1.30g, 2.08mmol, 0.1equiv.), Potassium Hydroxide (1M solution, 10mL), and [4-(benzyloxy)phenyl]boronic acid (11.9g, 52.0mmol, 2.5equiv.) were added sequentially. The flask was stirred under Argon for 10 minutes. Cyclohex-2-en-1-one (2.00g, 20.8mmol, 1 equiv.) was added and the reaction flask was purged and back-filled with Argon three times. The reaction was heated to 100C and stirred overnight. Following consumption of starting material, the reaction was cooled to room temperature, filtered over celite, and concentrated. Purification via flash column chromatography (330g silica gel cartridge, isocratic 12% EtOAc:Hexanes elution) followed by concentration and lyophilization of product fractions yielded (3S)-3-[4-(benzyloxy)phenyl]cyclohexan-1-one (1.948g, 6.95mmol, 33.4%) as a white solid. ¹H NMR (CHLOROFORM-d, 400 MHz) δ 7.4-7.6 (m, 5H), 7.19 (d, 2H, J=8.5 Hz), 7.00 (d, 2H, J=8.8 Hz), 5.09 (s, 2H), 3.00 (tt, 1H, J=3.8, 11.7 Hz), 2.6-2.7 (m, 1H), 2.4-2.6 (m, 3H), 2.0-2.3 (m, 2H), 1.7-2.0 (m, 2H); ¹³C NMR (CHLOROFORM-d, 100 MHz) δ 211.2, 157.6, 137.1, 136.9, 128.7, 128.0, 127.6, 127.5, 115.0, 70.1, 49.3, 44.0, 41.2, 33.0, 25.6; MS (ESI) calc for C₁₉H₂₁O₂ [M+H]⁺: m/z 281.15 found 281.24



(3S)-3-(4-hydroxyphenyl)cyclohexan-1-one (38).

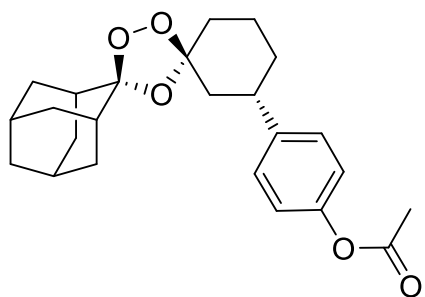
To a round bottom flask under inert Argon atmosphere was added 10% Palladium on Carbon (0.195g, 0.183mmol, 0.0264 equiv.) in ethyl acetate (50mL). (3S)-3-[4-(benzyloxy)phenyl]cyclo-hexan-1-one (1.948g, 6.948mmol, 1 equiv.) was added and the flask was evacuated and purged with Argon three times. The flask was again evacuated and backfilled with Hydrogen at 1atm. The solution was heated to 50C and stirred for 48 hours. Following completion, the reaction mixture was filtered over celite, rinsed with ethyl acetate, concentrated, and lyophilized to yield (3S)-3-(4-hydroxyphenyl)cyclo-hexan-1-one (1.15g, 6.04mmol, 87.0%) as a white powder. ¹H NMR (CHLOROFORM-d, 400 MHz) δ 7.09 (d, 2H, J=8.3 Hz), 6.83 (d, 2H, J=8.8 Hz), 2.97 (dt, 1H, J=3.9, 11.6 Hz), 2.4-2.6 (m, 4H), 2.0-2.2 (m, 2H), 1.7-1.9 (m, 2H); ¹³C NMR (CHLOROFORM-d, 100 MHz) δ 212.3, 154.5, 136.4, 127.7, 115.5, 49.3, 44.0, 41.2, 33.0, 25.5; MS (ESI) calc for C₁₂H₁₅O₂ [M+H]⁺: m/z 191.10 found 191.22



4-[(1S)-3-oxocyclohexyl]phenyl acetate (39).

To a solution of (3S)-3-(4-hydroxyphenyl)cyclohexan-1-one (1.10g, 5.78mmol, 1 equiv.) in dichloromethane (50mL) was added triethylamine (1.17g, 11.6mmol, 2 equiv.). The solution was cooled to 0C, and acetic anhydride (1.77g, 17.3mmol, 3 equiv.) was added

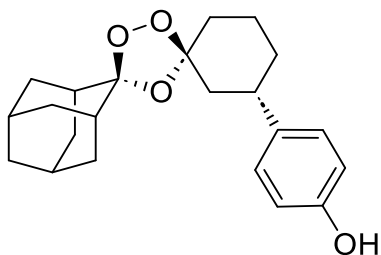
dropwise. The solution was allowed to return to room temperature and was stirred for 45 minutes. Following completion the solution was diluted with deionized water and the organic layer was extracted over water, saturated NaHCO₃, and brine. The organic fraction was dried over MgSO₄, concentrated, and lyophilized to yield 4-[(1S)-3-oxocyclohexyl]phenyl acetate (2.32g, 9.99mmol, 100%) as a white solid. Product was confirmed via UPLC/MS and used immediately in the next reaction. MS (ESI) calc for C₁₄H₁₇O₃ [M+H]⁺: m/z 233.11 found 233.23.



4-[(1''S,3''S)-dispiro[adamantane-2,3'-[1,2,4]trioxolane-5',1''-cyclohexan]-3''-yl]phenyl acetate (40).

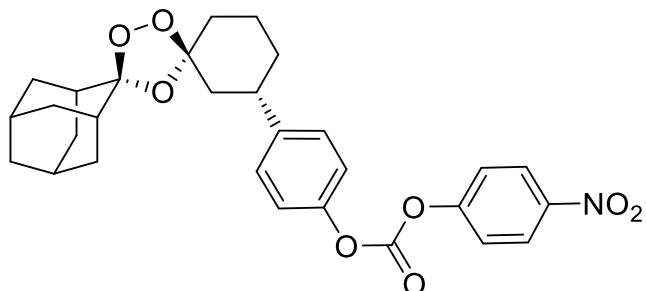
To an oven-dried round bottom flask was added 4-[(1S)-3-oxocyclohexyl]phenyl acetate (1.00g, 4.31mmol, 1 equiv.), N-methoxyadamantan-2-imine (2.00g, 11.2mmol, 2.59 equiv.) and carbon tetrachloride (50mL). The solution was cooled to 0C and sparged with O₂ for 10min. The reaction was maintained at 0C while ozone was bubbled (2L/min, 40% power) through the solution. Following 3.5 hours, the reaction was deemed complete via UPLC/MS and TLC. The reaction mixture was concentrated to yield a crude mixture as a viscous oil. The crude material was purified via flash column chromatography (220g silica gel cartridge, 5-15% EtOAc:Hex) and product fractions were concentrated and lyophilized to yield 4-[(1''S,3''S)-dispiro[adamantane-2,3'-[1,2,4]trioxolane-5',1''-cyclohexan]-3''-yl]phenyl acetate (0.714g, 4.31mmol, 41.6%) as a colorless solid. NMR Indicated presence of residual oxime and ketone starting materials in resultant product, which were carried through as an impurity. ¹H NMR (CHLOROFORM-d, 400 MHz) δ 7.23 (d, 2H, J=7.5 Hz), 7.02 (d, 2H, J=8.8 Hz), 2.40 (br s, 5H), 2.31 (s, 3H), 1.9-2.2 (m, 29H), 1.8-1.9 (m, 16H), 1.3-1.5 (m, 4H); ¹³C NMR (CHLOROFORM-d, 100 MHz) δ 169.7,

148.9, 127.7, 121.4, 111.4, 109.2, 109.0, 47.0, 42.2, 41.3, 39.3, 37.3, 36.8, 36.6, 36.4, 35.8, 35.0, 34.8, 34.8, 34.8, 34.2, 34.0, 33.8, 33.6, 33.2, 32.8, 32.3, 31.5, 31.0, 27.5, 27.2, 27.1, 27.0, 26.9, 26.5, 23.5, 21.2; MS (ESI) calc for C₂₄H₃₀O₅Na [M+Na]⁺: m/z 421.20 found 421.19



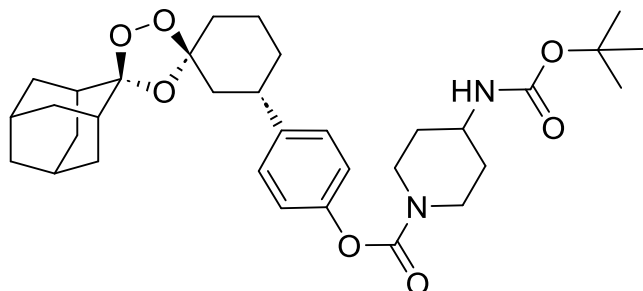
4-[(1''S,3''S)-dispiro[adamantane-2,3'-[1,2,4]trioxolane-5',1''-cyclohexan]-3''-yl]phenol (41).

To an oven-dried round bottom flask was added 4-[(1''S,3''S)-dispiro[adamantane-2,3'-[1,2,4]trioxolane-5',1''-cyclohexan]-3''-yl]phenyl acetate (0.700g, 1.76mmol, 1 equiv.) in Tetrahydrofuran (20mL) and methanol (20mL). Lithium hydroxide (0.168g, 7.03mmol, 4 equiv.) was added as a 1M solution in DI water and the reaction was stirred overnight at room temperature. The reaction was quenched with 1M NH₄Cl and the aqueous layer was extracted 3 times with DCM. The combined organic fractions were dried over MgSO₄, concentrated, and lyophilized to yield 4-[(1''S,3''S)-dispiro[adamantane-2,3'-[1,2,4]trioxolane-5',1''-cyclohexan]-3''-yl]phenol (0.560g, 1.57mmol, 89.4%) as a white solid. ¹H NMR (CHLOROFORM-d, 400 MHz) δ 7.09 (br d, 2H, J=8.3 Hz), 6.79 (br d, 2H, J=8.0 Hz), 2.75 (br t, 1H, J=12.7 Hz), 2.12 (br d, 2H, J=12.7 Hz), 1.9-2.1 (m, 9H), 1.7-1.9 (m, 9H), 1.5-1.7 (m, 3H), 1.2-1.5 (m, 2H); ¹³C NMR (CHLOROFORM-d, 100 MHz) Shift 153.9, 138.1, 127.9, 115.2, 111.4, 109.2, 42.4, 41.0, 39.3, 36.8, 36.4, 34.8, 34.8, 34.2, 33.0, 26.9, 26.5, 23.6; MS (ESI) calc for C₂₂H₂₉O₄ [M-H]⁻: m/z 355.19 found 355.31



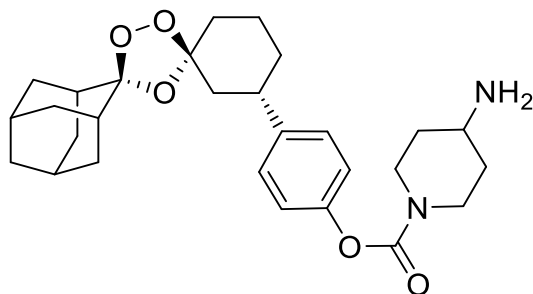
4-[(1^S,3^S)-dispiro[adamantane-2,3'-[1,2,4]trioxolane-5',1''-cyclohexan]-3''-yl]phenyl 4-nitrophenyl carbonate (42).

To an oven-dried round bottom flask was added 4-[(1^S,3^S)-dispiro[adamantane-2,3'-[1,2,4]trioxolane-5',1''-cyclohexan]-3''-yl]phenol (0.560g, 1.57mmol, 1 equiv.) and dichloromethane (50mL). The solution was cooled to 0C, and DIPEA (0.609g, 4.71mmol, 3 equiv.) and DMAP (0.038g, 0.314mmol, 0.2 equiv.) were added. The solution was stirred at 0C for 10 minutes, following which p-Nitrophenol Chloroformate (1.41g, 7.02mmol, 3 equiv.) was added portionwise. Upon complete addition the reaction was allowed to return to room temperature and stirred overnight. The reaction was diluted with dichloromethane and 1M Na₂CO₃, and the organic layer was extracted repeatedly with 1M Na₂CO₃ until no yellow color was observed, indicating depletion of p-nitrophenol. The organic layer was dried over MgSO₄ and concentrated to yield a crude colorless oil. This crude product was purified via flash column chromatography (80g silica gel cartridge, 0-25% EtOAC:Hex elution) and the product fractions were combined, concentrated, and lyophilized to yield 4-[(1^S,3^S)-dispiro[adamantane-2,3'-[1,2,4]trioxolane-5',1''-cyclohexan]-3''-yl]phenyl 4-nitrophenyl carbonate (0.339g, 0.65mmol, 41.4%) as a white powder. ¹H NMR (DMSO-d₆, 400 MHz) δ 8.37 (d, 2H, J=9.0 Hz), 7.71 (d, 2H, J=9.0 Hz), 7.3-7.4 (m, 4H), 2.5-2.8 (m, 1H), 1.9-2.0 (m, 7H), 1.6-1.8 (m, 13H), 1.3-1.6 (m, 3H); ¹³C NMR (DMSO-d₆, 100 MHz) δ 155.6, 151.3, 149.4, 145.9, 144.3, 128.5, 126.0, 123.2, 121.5, 111.1, 109.2, 41.7, 41.3, 38.9, 36.5, 36.3, 34.7, 33.9, 32.6, 26.7, 26.3, 23.6; MS (ESI) calc for C₂₉H₃₁NO₈Na [M+Na]⁺: m/z 544.19 found 544.14



4-[(1''S,3''S)-dispiro[adamantane-2,3'-[1,2,4]trioxolane-5',1''-cyclohexan]-3''-yl]phenyl 4-[[tert-butoxy]carbonyl]piperidine-1-carboxylate (43).

To an oven-dried round bottom flask was added 4-[(1''S,3''S)-dispiro[adamantane-2,3'-[1,2,4]trioxolane-5',1''-cyclohexan]-3''-yl]phenyl 4-nitrophenyl carbonate (0.320g, 0.614mmol, 1 equiv.) followed by tert-butyl piperidin-4-ylcarbamate (0.197g, 0.982mmol, 1.6 equiv.) and DMAP (0.015g, 0.123mmol, 0.2 equiv.). The reaction flask was evacuated and purged with argon. DMF (35mL) and DIPEA (0.238mg, 1.84mmol, 3 equiv.) were added and the reaction was stirred at room temperature overnight. Following completion, the reaction was diluted with Ethyl Acetate and the organic layer was extracted with 1M Na₂CO₃ until no yellow color was observed, indicating depletion of p-Nitrophenol. The organic layer was dried over MgSO₄ and concentrated to yield a crude colorless oil. The crude product was purified via flash column chromatography (40g silica gel cartridge, 0-25% EtOAc:Hex) to yield 4-[(1''S,3''S)-dispiro[adamantane-2,3'-[1,2,4]trioxolane-5',1''-cyclohexan]-3''-yl]phenyl 4-[[tert-butoxy]carbonyl]piperidine-1-carboxylate (0.315g, 0.540mmol, 88.0%) as a white powder. Product was confirmed via UPLC/MS and used immediately in the next reaction. MS (ESI) calc for C₃₃H₄₆N₂O₇Na [M+Na]⁺: m/z 605.32 found 605.32.



4-[(1^S,3^S)-dispiro[adamantane-2,3'-[1,2,4]trioxolane-5',1''-cyclohexan]-3''-yl]phenyl 4-aminopiperidine-1-carboxylate (17S).

A solution of 4-[(1^S,3^S)-dispiro[adamantane-2,3'-[1,2,4]trioxolane-5',1''-cyclohexan]-3''-yl]phenyl 4-[[tert-butoxy)carbonyl]amino]piperidine-1-carboxylate (300mg, 0.515 mmol, 1.0 equiv.) in methanol (5mL) and THF (5mL) was cooled to 0C using an ice bath. After purging the flask with inert atmosphere, acetyl chloride (402.6mg, 5.15mmol, 10equiv.) was added dropwise. The solution was stirred at 0C for 15 minutes, then allowed to return to room temperature for 16 hours. The reaction was diluted with dichloromethane, quenched with 1M Na₂CO₃, and the aqueous layer was extracted 3X with dichloromethane. The combined organic fractions were filtered, dried over MgSO₄, and concentrated to yield a crude product resembling a light yellow oil. The crude residue was purified in batches by HPLC (Agilent 1200 Series) using a 5uM Cellulose-3 column (Phenomenex) with an isocratic mobile phase consisting of 40:60 20mM Ammonium Bicarbonate pH 8.5 in Acetonitrile (with 0.1% diethylamine). Product peaks from each batch were combined, concentrated, and lyophilized to 4-[(1^S,3^S)-dispiro[adamantane-2,3'-[1,2,4]trioxolane-5',1''-cyclohexan]-3''-yl] (150.3mg, 0.311mmol, 61%) as a colorless solid. ¹H NMR (DMSO-d₆, 400 MHz) δ 7.26 (d, 2H, J=8.3 Hz), 7.01 (d, 2H, J=8.3 Hz), 3.8-4.2 (m, 2H), 2.9-3.1 (m, 2H), 2.8-2.9 (m, 1H), 2.6-2.8 (m, 1H), 1.8-2.0 (m, 7H), 1.6-1.8 (m, 15H), 1.3-1.6 (m, 3H); ¹³C NMR (DMSO-d₆, 100 MHz) δ 153.5, 150.0, 142.6, 127.9, 122.2, 111.0, 109.2, 48.1, 41.8, 41.3, 36.5, 36.2, 34.7, 33.9, 32.7, 26.7, 26.3, 23.7; MS (ESI) calc for C₂₈H₃₉N₂O₅ [M+H]⁺: m/z 483.28 found 483.56

Publishing Agreement

It is the policy of the University to encourage open access and broad distribution of all theses, dissertations, and manuscripts. The Graduate Division will facilitate the distribution of UCSF theses, dissertations, and manuscripts to the UCSF Library for open access and distribution. UCSF will make such theses, dissertations, and manuscripts accessible to the public and will take reasonable steps to preserve these works in perpetuity.

I hereby grant the non-exclusive, perpetual right to The Regents of the University of California to reproduce, publicly display, distribute, preserve, and publish copies of my thesis, dissertation, or manuscript in any form or media, now existing or later derived, including access online for teaching, research, and public service purposes.

DocuSigned by:

Matthew Klope

3C0D50A5495F472...

Author Signature

11/27/2023

Date